Springer Tracts in Advanced Robotics 106

Samer Mohammed
Juan C. Moreno
Kyoungchul Kong
Yacine Amirat *Editors*

Intelligent Assistive Robots

Recent Advances in Assistive Robotics for Everyday Activities

Springer Tracts in Advanced Robotics 106

Editors

Prof. Bruno Siciliano
Dipartimento di Ingegneria Elettrica
e Tecnologie dell'Informazione
Università degli Studi di Napoli
Federico II
Via Claudio 21, 80125 Napoli
Italy
E-mail: siciliano@unina.it

Prof. Oussama Khatib
Artificial Intelligence Laboratory
Department of Computer Science
Stanford University
Stanford, CA 94305-9010
USA
E-mail: khatib@cs.stanford.edu

More information about this series at http://www.springer.com/series/5208

STAR (Springer Tracts in Advanced Robotics) has been promoted under the auspices of EURON (European Robotics Research Network)

Samer Mohammed · Juan C. Moreno
Kyoungchul Kong · Yacine Amirat
Editors

Intelligent Assistive Robots

Recent Advances in Assistive Robotics for Everyday Activities

Springer

Editors
Samer Mohammed
University Paris-Est/UPEC LiSSi Laboratory
Vitry-sur-Seine
France
e-mail: samer.mohammed@upec.fr

Juan C. Moreno
Spanish National Research Council (CSIC)
Bioengineering Group (GBIO)
Madrid
Spain
e-mail: jc.moreno@csic.es

Kyoungchul Kong
Department of Mechanical Engineering
Robotic Systems Control Laboratory
Sogang University
Seoul
Korea
e-mail: kckong@sogang.ac.kr

Yacine Amirat
University Paris-Est/UPEC LiSSi Laboratory
Vitry-sur-Seine
France
e-mail: amirat@u-pec.fr

ISSN 1610-7438 ISSN 1610-742X (electronic)
Springer Tracts in Advanced Robotics
ISBN 978-3-319-12921-1 ISBN 978-3-319-12922-8 (eBook)
DOI 10.1007/978-3-319-12922-8

Library of Congress Control Number: 2014953944

Springer Cham Heidelberg New York Dordrecht London

Printed on acid-free paper

Springer International Publishing AG Switzerland is part of Springer Science+Business Media (www.springer.com)

Foreword

Robotics is undergoing a major transformation in scope and dimension. From a largely dominant industrial focus, robotics is rapidly expanding into human environments and vigorously engaged in its new challenges. Interacting with, assisting, serving, and exploring with humans, the emerging robots will increasingly touch people and their lives.

Beyond its impact on physical robots, the body of knowledge robotics has produced is revealing a much wider range of applications reaching across diverse research areas and scientific disciplines, such as: biomechanics, haptics, neurosciences, virtual simulation, animation, surgery, and sensor networks among others. In return, the challenges of the new emerging areas are proving an abundant source of stimulation and insights for the field of robotics. It is indeed at the intersection of disciplines that the most striking advances happen.

The *Springer Tracts in Advanced Robotics (STAR)* is devoted to bringing to the research community the latest advances in the robotics field on the basis of their significance and quality. Through a wide and timely dissemination of critical research developments in robotics, our objective with this series is to promote more exchanges and collaborations among the researchers in the community and contribute to further advancements in this rapidly growing field.

The volume by S. Mohammed, J.C. Moreno, K. Kong and Y. Amirat provides an edited collection on recent advances in assistive robotics. The growing challenges of using assistive robots in our everyday activities along with providing intelligent services are addressed. The emergence of novel technologies such as wearable and ubiquitous robotic systems with considerable reduction in size, cost and energy consumption, are becoming a privileged solution to provide assistive services to humans. The applications concern mainly healthcare and wellness such as helping elderly people, assisting dependent persons, habitat monitoring in smart environments, well-being, and security. Common threads across the seventeen chapters of the volume regard control theory, mechanical design, mechatronics, portability, acceptability, scalability, and security.

Rich of results by active research teams in the field, this volume constitutes a fine addition to STAR!

Naples, Italy
September 2014

Bruno Siciliano
STAR Editor

Foreword

Robotics is undergoing a phase of renaissance today where novel applications of robots are being sought for human assistance and functional rehabilitation following brain and other injuries. In conjunction with robots, human physiological data from the muscles and brain are being used to demonstrate the effectiveness of these new robotic interventions and to develop better insights into the interrelations of improved function and human physiology. Robots today are taking a leap from predominant use in the industry to this challenging arena of human health. As the percentage of elderly population rapidly grows today in our society, in the next 2-3 decades, robots will be ubiquitous companions in our daily life and in healthcare, working hand-in-hand with clinical caregivers.

This book *Intelligent Assistive Robotics* by Samer Mohammed, Juan C. Moreno, Kyoungchul Kong, Yacine Amirat compiles the current state-of-the-art from many prominent researchers in the field of assistive and rehabilitation robots. The book presents new technological developments in this field such as intelligent cane robots, lower-limb power-assist robots, wearable robots, actuated orthoses, smart walkers, and others. Novel control interfaces using physiological signals, such as EEG data from the brain and EMG data from the muscles, are the focus of some chapters. Clinic-based gait rehabilitation, robotic intervention of children with cerebral palsy, detecting human emotions, are comprehensively described in other chapters. Emerging social topics such as human-machine interaction in public spaces and ethical-legal issues of care robots add a new dimension to this book as we define the role of assistive technology in health care.

This seventeen-chapter collection is a comprehensive compilation of research in this field and offers a valued resource both for seasoned researchers and newcomers in this field. I want to congratulate the authors for this accomplishment and sincerely thank them for their efforts in bringing this book to our community.

Columbia University, New York City
September, 2014

Sunil K. Agrawal, PhD
Professor of Mechanical Engineering
and Rehabilitation Medicine

Preface

Assistive Robotics covers currently a broad spectrum of research axis, from intelligent robots acting as a servant, secretary, or companion to intelligent robotic functions such as autonomous wheelchair navigation, embedded robotics, ambient intelligence, or intelligent spaces. Various mechatronic technologies are steadily penetrating in our daily lives. We are surrounded by mechatronic products and interact with them in many ways. In particular, mechatronic devices may potentially improve the quality of life of elderly people and patients with impairments. Solutions to assist daily living require robust interfaces that allow for natural control. These interfaces may rely on diverse modalities information that can be related with the intention, preparation and generation of voluntary movement, either at mechanical or neural level. Assistive devices and robots can be designed to enhance not only physical but also cognitive skills of human users through mobility experiences. There has been tremendous progress in the engineering of learning mechanisms inspired by biology that can be applied for assistive robotics. This book intends to deal with the growing challenges of using assistive robots in our everyday activities along with providing intelligent assistive services. Applications concern mainly healthcare and wellness such as helping elderly people, assisting dependent persons, habitat monitoring in smart urban environments, well-being, security, etc. Several key technologies for effectively assisting humans are introduced in this book. These technologies include 1) development of hardware platforms in ergonomic approaches, 2) sensing technologies for identifying the intent of humans, 3) decision making algorithms to decide about the right amount of assistance, 4) actuation technologies to provide precise assistive forces, and 5) control algorithms for effectively assisting humans. In the design of mechatronic devices interacting with humans, the dynamic characteristics of the human body are an important issue. Furthermore, the compatibility between machines and humans must be optimized. If the assistive device is interacting with normal and healthy humans, the design may take advantage of the robust and intelligent controllability of the human brain system. In the case of assistive devices for the elderly and patients with physical impairments, such approaches may not be appropriate, and the mechanical and control systems are required to be precise, robust and intelligent. This book focuses also on the recent advances and challenges related to social interaction, smart spaces and mobility assistance.

In chapter [Vitiello et al.], authors reviewed three research activities carried out at the BioRobotics Institute of Scuola Superiore Sant'Anna in the past decade. i) the development of a robotic tactile stimulator for human active and passive touch studies, ii) the development of NEURARM, a new robotic model of the human arm which mimicked the dynamic properties of the human upper limb and iii) the development of NEUROExos, an elbow robotic exoskeleton with a biomimetic antagonistic actuation capable of changing its joint output impedance, in a human-like fashion.

Chapter [Low et al.] presents a review and comparison of existing gait rehabilitation robots. Based on the findings of gait rehabilitation in clinical aspects, a robotic overground gait rehabilitation system, *NaTUre-gaits*, is designed and built. The 14-DOFs gait rehabilitation robot, *NaTUre-gaits*, provides lower limb motion assistance in the sagittal plane, natural pelvic movement assistance, body weight support with no restriction on the pelvic movement, and overground walking. The modular and reprogrammable architecture of the developed system allows control strategy to be implemented and validated on the system with ease.

Chapter [Hortal et al.] discusses brain-computer interfaces, one of the important areas in neuroengineering research that has rapidly become an important option to communicate users with external assistive devices. The chapter provides a deep description and results of non-invasive interfaces with the human brain that rely on the detection of evoked potentials that are available to control assistive robotic devices.

In Chapter [Frizera et al.], the authors specifically cover the user-machine multimodal interaction for control of so-called smart walkers that can assist natural mobility in humans. Reviewed topics include the key features in most advanced smart walkers and the use of adaptive filtering strategies, fuzzy logic and robust inverse kinematic controllers to interpret user's postures and gestures during assisted walking.

Chapter [Raya et al.] provides a critical perspective about assistive robotic devices for infants with cerebral palsy, laying down the foundations that can be employed in such devices to support movement as a route to enhance the cognitive experience and cognitive interaction.

Chapter [Kose et al.] investigates the role of interaction and communication kinesics in human-robot interaction. The aim is to design a computational framework, which enables to motivate the children with communication problems to understand and imitate the signs implemented by the robot using the basic upper torso gestures and sound in a turn-taking manner. An exploratory study is done to investigate the effect of basic non-verbal gestures consisting of hand movements, body and face gestures expressed by a humanoid robot, and having comprehended the word, the child will give relevant feedback in Sign Language or visually to the robot, according to the context of the game.

Chapter [Aly et al.] presents the development of an online incremental learning system of emotions using Takagi-Sugeno fuzzy model in an assistive context. This chapter discusses also the understanding and generation of multimodal actions from the cognitive point of view. The main objective of this system is to detect whether the observed emotion needs a new corresponding multimodal action to be generated in case it constitutes a new emotion cluster not learnt before, or it can be attributed to one of the existing actions in memory in case it belongs to an existing cluster.

Chapter [Shimoda et al.] provides a description of how such natural learning mechanisms can be applied to generate unintentional behaviours. For that, the authors introduce a learning architecture that is based on biology. The chapter was written mainly for readers with background in physical sciences and engineering and includes a case report that illustrates the emergence of walking behaviour in a humanoid biped robot in a similar way as in humans.

In chapter [Glas et al.], authors developed a network robot system framework with the objective of enabling practical deployment of social robots to provide real-world services in everyday social environments. This framework addresses practical issues in social human-robot interaction by integrating ambient intelligence systems, networked data stores, human supervisors, and centralized planning. All of the elements of the system have been developed and tested in public and commercial spaces such as shopping malls, resulting in a flexible robot control architecture based on practical, real-world requirements.

Chapter [Kim et al.] presents the ubiquitous robots that integrates three forms of robots: Sobot, Embot and Mobot. Sobots, which are software-based virtual robots in virtual environments, can traverse space through physical networks. Embots, the embedded robots, are implanted in the environment or embedded in Mobot, for sensing, detecting, recognizing, and verifying the objects or the situation. The Ubibot system is seamless, calm, context aware in its ability to provide integrated services. Implementations, using software and hardware robots, demonstrated the significance of each category of robot intelligence.

Chapter [Chibani et al.] discusses the necessity to move beyond built-in monotonic semantic web based reasoning-architectures for endowing ubiquitous robots with cognitive capabilities, towards new architectures that combine different reasoning mechanisms to achieve better context awareness and adaptability in dynamic environments. Practical reasoning approaches developed for ambient intelligence and robotics applications are presented. This chapter discusses also the future directions that should be investigated to implement high-level cognitive capabilities that can be supported by cloud computing platforms as reasoning backend for robots and connected devices in smart spaces.

Chapter [Fukuda et al.] presents the design of an intelligent cane robot for aiding the elderly and handicapped people walking. The robot consists of a stick, a group of sensors and an omni-directional basis driven by wheels. Multiple sensors were used to recognize the user's walking intention, which is quantitatively described by a new concept called intentional direction. A novel intention-based admittance motion control scheme was proposed for the cane robot. The effectiveness of proposed fall detection method was also confirmed by experiments.

In Chapter [Oh et al.], signal processing algorithms for observing the physical state of an augmented system that consists of a human, an assistive system and associated control methods are introduced based on the use of a power-assisted wheelchair (PAW). This chapter gives details in the mathematical model of PAW and its derivation, the design of the signal processing and control algorithms, and extensive analyses of experimental results.

Chapter [Kiguchi et al.] introduces a high-level control algorithm that determines the motion and the amount of assistive torque for an assistive robot to generate. In particular, the methods used in this chapter are based on bio-signals and Electromyography (EMG). In order to extract meaningful information from the EMG signals, several effective signal-filtering methods are also introduced in this chapter.

Chapter [Mohammed et al.] presents the development of two rehabilitation approaches of the lower limb by means of the knee joint exoskeleton. The model of the exoskeleton is presented as well as a modified Hill-type muscular model of the wearer's lower limb. Two control techniques are proposed: the first one ensures the passive rehabilitation of the lower limb by means of bounded control laws and the second ensures the assistance-as-need of the wearer based on the human intention estimated by means of EMG electrodes fixed at some particular muscles.

Chapter [Kong et al.] investigates an actuator module and its robust control algorithm for an ideal force-mode actuation, which is required for improved safety and for minimal discomfort. To guarantee robust stability as well as robust performance in a harsh environment due to human-robot interaction, a disturbance observer, one of the most popular robust control methods, is utilized to compensate for changes in the human body dynamics as well as for mechanical disturbances in the actuators.

Chapter [Salvini et al.] intends to provide the reader with an overview of the main ethical, legal and societal challenges concerning the use of care robots, which, together with appropriate design procedures, may contribute to design better robots.

January 2015

Samer Mohammed
Vitry-sur-Seine, France

Juan C. Moreno
Madrid, Spain

Kyoungchul Kong
Seoul, Korea

Yacine Amirat
Vitry-sur-Seine, France

Contents

Neuro-robotics Paradigm for Intelligent Assistive Technologies

Nicola Vitiello[1], Calogero Maria Oddo[1], Tommaso Lenzi[2], Stefano Roccella[1], Lucia Beccai[3], Fabrizio Vecchi[1], Maria Chiara Carrozza[1], and Paolo Dario[1]

[1] The BioRobotics Institute, Scuola Superiore Sant'Anna, Viale Rinaldo Piaggio, 34, 56025, Pontedera, Pisa, Italy
[2] Northwestern University, Feinberg School of Medicine, Chicago, Illinois, USA
[3] Center for Micro-BioRobotics@SSSA, Istituto Italiano di Tecnologia, Viale Rinaldo Piaggio, 34, 56025, Pontedera, Pisa, Italy

1 Introduction to Neuro-robotics

The *neuro-robotics paradigm* is a design approach, mainly aimed *at the fusion of neuroscience and robotic competences and methods* to design better robots that can act and interact closely with humans, in several application fields: rehabilitation and personal assistance, prosthetics, urban services, surgery, diagnostics, and environment monitoring.

The neuro-robotics design paradigm relies on a strongly co-ordinated, multidisciplinary and interdisciplinary effort which involves three main scientific areas:

- *robotics*, with special reference to bio-mimetic, anthropomorphic systems and bionic components,
- *neuroscience,* with special reference to sensory-motor coordination;
- and *interfacing technology,* with reference to non-invasive and invasive interfaces to the peripheral nervous system (PNS) as well as to non-invasive interfaces to the central nervous system (CNS).

Mostly, the neuro-robotics paradigm applies in the research area of 'human augmentation' through 'hybrid bionic systems'. As suggested by E. Von Gierke, a pioneer of this discipline, the primary goal of *bionics* is "to extend man's physical and intellectual capabilities by prosthetic devices in the most general sense, and to replace man by automata and intelligent machines" (Von Gierke et al., 1970).

Hybrid Bionic Systems (HBSs) can be generically defined as systems that contain both technical (artificial) and biological components. They can include:

- *artificial systems* with *biological elements* or subsystems. In such a case, the biological system is a complementary or supplementary element to the technical system;
- *biological systems* with *artificial elements* or subsystems. The artificial subsystem, e.g. a robotic artefact, is a complementary or supplementary element to the biological system.

S. Mohammed et al. (eds.), *Intelligent Assistive Robots*,
Springer Tracts in Advanced Robotics 106, DOI: 10.1007/978-3-319-12922-8_1

In recent years, many scientific and technological efforts have been devoted to create HBSs that link, via neural interfaces, the human nervous system with electronic and/or robotic artefacts. In general, this research has been carried out with various aims: on the one hand, *to develop systems for restoring motor and sensory functionalities in injured and disabled people*; on the other hand, *for exploring the possibility of augmenting sensory-motor capabilities of humans in general*, not only of disabled people.

Examples of devices for the restoration of lost sensory-motor functions are: neuroprostheses for subjects with neurological disorders, such as those caused by spinal cord injury (SCI) or stroke/head injury (Stein et al., 1992; Popovic and Sinkjaer 2000; Lauer et al., 2000); robotic devices like the LOPES, Lokomat, HAL5, ReWalk, EKSO (Craelius, 2002; Veneman et al., 2006; Jezernik et al., 2003; Kawamoto and Sankai, 2005; Esquenazi et al., 2012; Mertz, 2012), active exoskeletons which can augment or replace muscular functions of the lower limbs, for example to assist motor-impaired individuals; or powered upper- and lower-limb prostheses (Edin et al., 2008; Carrozza et al., 2006; Velliste et al., 2008; Sup et al., 2008; Hargroveet al., 2013).

As for sensory functionalities, important results have been achieved in restoring hearing and sight capabilities. Some improvements in auditory performance of people with hearing loss can be obtained with cochlear implants (Simmons et al., 1965; Blume, 1999; Loizou, 1999; Spelman, 1999; Marsot-Dupuch et al., 2001). Retinal implants can be realized in the attempt to regain lost visual functionality (Eiber et al., 2013).

Examples of HBSs which aimed at augmenting capabilities of able-bodied persons were developed within the framework of the DARPA program called Exoskeletons for Human Performance Augmentation (EHPA). The goal of this program was to "increase the capabilities of ground soldiers beyond that of a human" and led to the development of three exoskeletons: the Berkeley Exoskeleton (BLEEX), the MIT Exoskeleton and SARCOS (Dollar and Herr, 2008).

2 The Strategic Alliance between Robotics and Neuroscience

George Bekey (2005) defined a robot as a "machine that senses, thinks, and acts", and which is "embodied and situated in the real world". Robots have physical dimensions, and they can exert forces on other objects. Robots are also subject to the world's physical laws, they have mass and inertia, their moving parts encounter friction and hence produce heat, measurements are corrupted by noise, and parts break. Robots also contain computers, which provide them with ever increasing speed and power for both signal processing and cognitive functions. In other terms, Robots "are an imitation of life". They "appear to move intelligently, they avoid obstacles, they interact with one another, and they accomplish tasks". Roboticists have the goal of enabling robots "to perform these and other actions".

Under this perspective, a grand challenge for robotics is to develop new robots with the capability to work for, and to interact effectively and friendly with, human beings. In order to achieve this goal robotics needs not only *new technology*, but also

more science. Investigating and taking inspiration from biological models (in particular from the human model) to design new robots is an approach increasingly adopted by the robotics research community. Neuroscience (whose goal is "to understand the mind, how we perceive, move, think and remember", as Eric R. Kandel, James H. Schwarts and Thomas M. Jessell pointed out in the book "Principles of Neural Science") is an excellent example of a scientific discipline that could provide knowledge, models and methodological tools for advancing robotics progress.

Starting from the robotics challenges and the neuroscience potentialities, the neuro-robotics design paradigm, which fuses robotics and neuroscience methodologies, tools and scientific knowledge, aims to be beneficial for the progress of both robotics and neuroscience. Indeed, on one hand, the neuro-robotics paradigm aims to enhance the development of *a new generation of robotic systems*, such as advanced HBSs for human assistance and augmentation. On the other hand, neuro-robotics aims at achieving new neural-scientific findings.

Under the neuro-robotics umbrella, roboticists and neuroscientists have three main "opportunities" for an effective cooperation.

One opportunity is that roboticists can provide advanced platforms to be used as a *tool for supporting neuroscience investigations.* For instance, the robotic device can be used either to measure and record specific parameters of neuroscientific interest, such as the position and velocity of the human hand (Burdet et al., 2000) or the impendence of the human arm during reaching movements (Gomi and Kawato, 1997), or to interact with a subject to analyze his/her responses to a specific external stimulus, such as the response to a tactile stimulus on the fingertip (Andrè et al., 2009), or the effect of a given force disturbance on the hand trajectory (Burdet et al., 2001). In both the above cases, the object of the scientific investigation is barely neuroscience-driven, e.g. the *behaviour of human within a certain scenario.* This is maybe the simplest way neuroscience and robotics can interact and cooperate.

Another possible opportunity is the development of *robotic models* (physical platforms) to test and validate neuroscience theories. In this case, the validation of a neuroscientific model or hypothesis is conducted through the experimental activities performed by means of a robotic model. Examples of robotic models are: the *salamander robot driven by a spinal cord model*, for the investigation of how a primitive neural circuit for swimming can be extended, by phylogenetically more recent limb oscillatory centers, to explain the ability of salamanders to switch between swimming and walking (Ijspeert et al., 2007); the lamprey-like robot (Dario et al., 2006; Stefanini et al, 2006; Manfredi et al., 2013) for the investigation of motion control strategies based on central pattern generators in lampreys (Ekeberg et al., 1995; Grillner et al., 1995; Grillner, 1985); the brachiation robot, aimed at the investigation of gorilla's brachiation (Fukuda and Soito, 1996); the snake robot (Hirose and Morishima, 1990) for the investigating of snake's locomotion. Other interesting examples of robotic models are related to the investigation of human behaviour, such as robotic arms and hands used to support the analysis of human arm motor control, visual-motor coordination and hand grasping and writing tasks. Among many, Schaal and Sternad used an anthropomorphic robotic arm for the investigation of mechanisms of rhythmic movements generation (Sternad and Schaal, 1999; Schaal and Sternad, 2001); Potkonjak

and colleagues used a 5-degree-of-freedom (DOF) anthropomorphic robotic arm to investigate the human multi-joint coordination in the demanding task of hand writing (Potkonjal et al., 1998); Zollo and colleagues used a platform consisting of the anthropomorphic robotic arm Dexter, of a robotic hand and of a visually-capable head to investigate different models of high-level sensory motor control (Zollo et al., 2008); Edin, Carrozza and their colleagues employed a highly sensorized artificial robotic hand to investigate the grasp-and-lift task (Edin et al., 2008; Carrozza et al., 2006). Using robotic models for neuroscience investigation is a key point of the neuro-robotics paradigm, which can lead to the development of new technologies (the ones necessary to develop the robotic models), and more generally to the development of a new generation of robotic artefacts.

Finally, the third way neuroscience and robotics can cooperate is when robotics takes inspiration from neuroscience for the development of a new robot, or a new human-robot interfacing system. In this case robotics is neither just a tool or a model: robotics benefits of neural science to generate artefacts that are revolutionary and pioneering. Examples of input from neuroscience are: *motion control theories, sensory-motor coordination frameworks, behavioural models and learning strategies.* This scenario is much likely the most interesting: it allows to imagine that *bio-inspiration* goes beyond the *usual biomimetic morphology*, and lead to new control strategies for *motion control and human-robot interfacing*.

It is worth noting that neuroscience and robotics can cooperate in a wide framework which is not limited to only one of the above opportunities. Indeed, rather than a limiting taxonomy, the description of these three opportunities represent a description of the potentiality of the strategic alliance between robotics and neuroscience.

3 Neuro-robotics is a Development Engine for New Assistive Devices

By moving from the potentialities of the neuroscience-robotics collaboration - in this chapter - we review the following three research activities (case studies) carried out at The BioRobotics Institute of Scuola Superiore Sant'Anna in the past decade.

- Case-study #1: development of *a robotic tactile stimulator for human active and passive touch studies*, to be used as precise *tool* to stimulate the human finger pad under repetitive and controlled stimulation conditions.
- Case-study #2: development of NEURARM, *a new robotic model of the human arm* which mimicked the dynamic properties (i.e. link masses, and joint inertia, damping and stiffness) of the human upper limb.
- Case-study #3: development of NEUROExos, an *elbow robotic exoskeleton with a biomimetic antagonistic actuation* capable of changing its joint output impedance, in a human-like fashion.

4 A Neuro-robotic Tactile Stimulation Platform to Enable Human and Artificial Touch Studies

4.1 Motivation, Design Requirements and State-of-Art Analysis

Passive- and active- touch are the main experimental paradigms used in the literature to study the neuronal mechanisms of the sense of touch in the human hand.

Various definitions of the passive- and active- paradigms are actually possible, and a simple one involves considerations on the energy flow associated to the dynamic phases of the tactile experience (Prescott, 2011). With such a definition, similarly to passive measurement instruments, in dynamic passive-touch the (kinetic) energy required to apply the relative motion between the sensory system and the tactile surface is provided via the surface under test. Conversely, in active-touch protocols the (kinetic) energy to achieve the dynamic tactile stimulation condition is provided by an actuated mechanism closely integrated with the (human or artificial) sensory system.

A possible application of such definition to dynamic-touch studies (either passive- or active-) results in the core of the tactile stimulation sequence being characterized by a tangential relative motion between the fingerpad and the (textured) surface. Therefore, in such case the difference between passive- and active- is in the body (i.e., fingertip or tactile stimulus) which actually moves with respect to a chosen reference frame. The relative motion can be obtained by sliding the tactile stimulus while the fingertip is still (passive- dynamic-touch) (Yoshioka et al., 2001), or by exploration via the finger (active- dynamic-touch) while the tactile stimulus is static (Lawrence et al., 2007).

While considering the deformation of skin tissues, established findings showed that passive- and active- passive protocols are equivalent (e.g., up to 4 N in Birznieks et al., 2001). In addition, one may wonder whether this is the same at perceptual level, considering that in passive-touch there is a lack of voluntary movement, while in active-touch the percept may be integrated by kinesthetic afferent sensory feedback or by efference copy associated to motion dynamics of the body part. However, with respect to this particular point, a dedicated study on the perception of roughness (Lederman, 1981) excluded relevant differences between passive- and active- touch protocols.

In both human and artificial passive-touch studies, the presentation of tactile stimuli should be replicated several times repeatably in the same conditions to infer models based on statistical analysis of acquired data (Johansson and Birznieks, 2004); also, the passive-stimulation operation should avoid to introduce spurious information by the system delivering the tactile surfaces.

To achieve standardization and repeatability, the passive-touch approach requires a robotic stimulator that enables detailed analyses of receptor response through controlled variation of stimulation parameters (e.g. stimulus spatial coarseness, materials and tribological properties) to make comparisons between sessions or participants, or to average over a large number of replications.

There are a number of particular requirements in the design of such a robotic tactile stimulation device.

First, to allow repeatable experiments with standardized conditions, accuracy and precision in the control of stimulation parameters, such as the contact force and the sliding velocity profile, is required.

Second, the device must guarantee a range of forces and movement velocities covering those that would naturally be used by humans in the exploration of textures, while both normal and tangential forces need to be recorded as they are fundamental quantities for human touch investigation. Studies on discriminative touch (Johnson and Yoshioka, 2001; Jones and Lederman, 2006) suggested:

- for the indentation force a range of at least 100 mN–5 N, with a control accuracy of about 5% of the reference force and sensing resolution within a few mN;
- 100 mm of stroke along the sliding direction and velocities up to 150 mm/s with μm position sensing resolution and steady state control accuracy.

Such requirements apply to both artificial and human touch studies but the latter ones present additional constraints due to the particular neurophysiological experimental methods while dealing with the biological system.

The third challenging requirement, given that some classes of tactile receptors are highly sensitive to vibration up to 400 Hz or more (Connor and Johnson, 1992), is in developing a stimulator that could get into contact with the human finger free from any spurious vibration that could interfere with the encoding of tactile stimuli.

Fourth, electrophysiological methods such as microneurography and EEG involve recording of signals in the μV range, and electromagnetic interference from the robotic system has to be minimized.

Fifth, these experiments can require the participant to sit in a natural position and to remain relaxed for hours. Hence, the subject's comfort puts stringent demands on the mounting of the device and on the control laws of each DoF so that it can be adapted in 3D space to the position of the subject's arm, hand and finger (Birznieks et al., 2001).

Finally, the programming operation by the experimenter to implement the targeted protocols has to be simple and flexible, and upgradeability of the platform should be possible.

The reviewed previous works span from platforms with flat or curve extended textured stimuli for studying the application of ridged or dotted surfaces to the fingerpad, to other devices with wide or pointed probes, to pinned stimulators for applying spatio-temporal indentation profiles with an array of contact locations. Some neurophysiological studies addressed the response of single afferents to the applied stimuli, while others took into account population of mechanoreceptors. Nevertheless, one of the major limitations of most of reviewed platforms is that they were developed for touch experiments in monkeys rather than humans, then presenting less demanding requirements since higher level of invasiveness is tolerated in animal model studies (Goodwin and Morley, 1987; LaMotte et al., 1998).

A considerable input was given in the 70's by the availability of digital controllers (Looft and Williams, 1979) which enabled the design of mechatronic platforms with customizable motion profiles to address specific experimental paradigms. This is confirmed by the fact that in the 80's a few platforms integrated complex mechanisms (Goodwin et al., 1985) for tuning the desired stimulation parameters. Furthermore, the analog circuitry was reduced as much as possible, remaining between the sensors and the controller only, and between the controller and the actuators or, at most, for implementing low-level force (or position) servo control (Byrne, 1975; Looft and Williams, 1979; LaMotte et al., 1983). As a matter of fact, almost all the reported tactile platforms employed digital processors for data storage at least, and for the generation of force and position references. In contrast to the almost standardized architecture for the control electronics, a greater variability could be found between the core mechanisms of the reported systems.

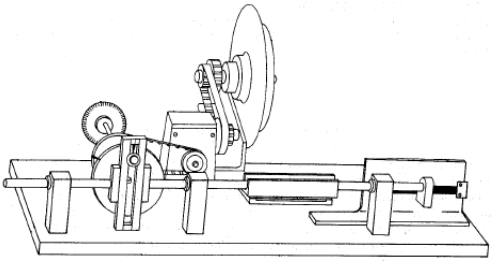

Fig. 1. From Goodwin et al. (Journal of Neuroscience Methods 1985). A schematic diagram of the scotch yolk stimulator (reprinted with permission from Elsevier).

In the class of devices that were built to study the neural coding and perception of texture, Goodwin and colleagues (1985) used a scotch yolk driven by a DC motor which rotated at constant speed for producing a sinusoidal motion (Fig. 1). The motion control was completely in open-loop, relying on the non-backdrivability of the mechanism in spite of subject-machine interaction. The advanced stimulator shown by LaMotte and colleagues (1983) controlled the sliding motion and the indentation position or load force of a selectable surface which, in turn, contacted and stroked the skin of the fingerpad in passive-touch studies. The stimulus could be selected among eight flat plates carrying textured surfaces. The user could select the motion profiles, allowing the definition of the horizontal and vertical displacements or the load force, and the displacement velocities, however it was very bulky to be easily oriented in 3D space and it relied on the early digital electronics available at the time.

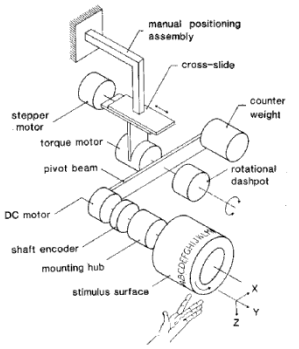

Fig. 2. From Johnson and Phillips (Journal of Neuroscience Methods 1988). An example system belonging to the class of rotating drum stimulators (reprinted with permission from Elsevier).

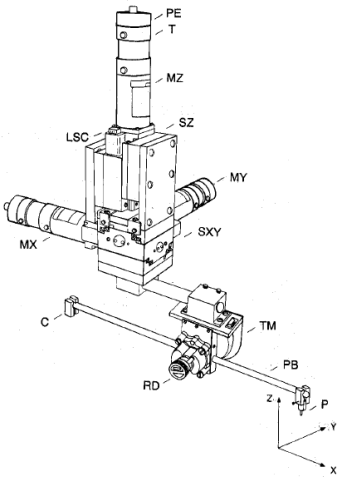

Fig. 3. From Romo et al. (Journal of Neuroscience Methods 1993). Design of the scanning probe stimulator suitable for indenting and sliding punctuated stimuli to the fingerpad (reprinted with permission from Elsevier).

A number of groups (Darian-Smith and Oke, 1980; Johnson and Phillips, 1988; Romo et al., 1993; Radwin et al., 1993; Wheat et al., 2004) utilized beams for the application of stimuli to the subjects. The devices shown by Darian-Smith and Oke (1980) and by Johnson and Phillips (1988), the latter being an improved version of the stimulator described by Johnson and Lamb (1981), had a rotating drum with embossed patterns mounted at one end of a pivot beam (Fig. 2). A major difference between the two rotating drum platforms regards the motion along the indentation direction. Darian-Smith and Oke (1980) chose an electronically controlled solenoid for enabling the counterweight to apply the desired force, while Johnson and Phillips (1988) used a torque motor driven in open loop mode for regulating the interaction

force. Both the rotating drums platforms used dampers, also applied to other devices (Romo et al., 1993; Wheat et al, 2004; Oddo et al., Mechatronics 2011), for minimizing any transient increase in the contact force at the onset of the stimulation, or to reduce the propagation of vibrations to the human subject (Fig. 3).

Another class of tactile stimulators is represented by pinned systems (Bliss et al., 1970; Gardner and Palmer, 1989; Killebrew et al., 2007). A noticeable number of such devices has been reported in literature (wideband devices were shown by Summers and Chanter, 2002 and by Kyung et al., 2006), being of great interest for pointed and distributed stimulation of the fingerpad stimulation, also allowing flexible experimental paradigms with a variety of spatio-temporal stimulation profiles (Vidal-Verdú and Hafez, 2007).

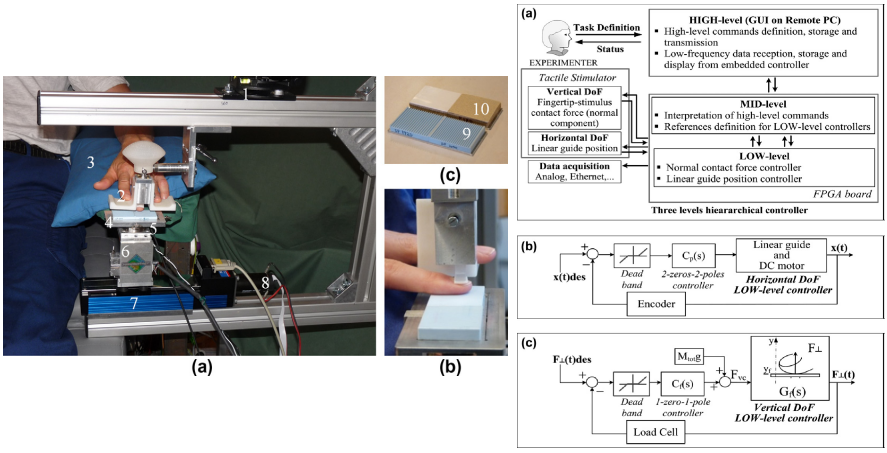

Fig. 4. Mechatronic tactile stimulation platform by Oddo et al. (Mechatronics, 2011). Left: (a) Experimental set-up during microneurography: frame hold by spherical joint (1), hand-finger support system (2), vacuum cast for arm support (3), carrier for stimuli (4), load cell (5), voice-coil actuator assembly for indentation of stimuli (6), linear guide for tangential sliding of stimuli (7), DC motor with encoder (8). (b) Fingerpad-stimulus interface with finger fixation system and free fingers support. (c) Examples of the used stimuli glued to a changeable aluminum plate: a couple of ridged stimuli (9), smooth plastic and rough sandpaper (10). Right: (a) Overview of the Dynamic Platform hierarchical controller. (b) Block diagram of the LOW-level closed-loop position controller along the sliding direction. (c) Block diagram of the LOW-level closed-loop force controller along the indentation direction (reprinted with permission from Elsevier).

4.2 Overview of the Robotic Platform

A 2-DOF mechatronic system (Oddo et. al, Mechatronics 2011) was dedicatedly developed to enable passive-touch protocols that are the core of this case study on neuro-robotic platforms for investigating the sense of touch. The developed platform fulfils all the requirements detailed above for passive-touch tactile stimulation and was replicated in five exemplars delivered to European research groups within the FP7 Nanobiotouch project, with customizations for electrophysiological,

psychophysical, and artificial touch studies and for tribological experiments on different tactile surfaces as well. It can be used to perform neurophysiological studies in humans with techniques such as microneurography and EEG (Beckmann et al., 2009) even in combination with psychophysical experimental paradigms. Also, it is suitable for tribological and artificial touch studies as well.

The platform could indent and slide sequences of textured stimuli (lodged in 77 mm x 32 mm changeable plates) to the fingerpad with feedback-controlled normal contact force and parametric sliding trajectories while recording (Smith et al., 2002; Libouton et al., 2010) the normal and tangential forces at finger-stimulus interface; a voice-coil actuator (NCC05-18-060-2X, H2W Tech.) applied the indentation force with a 12.7 mm stroke, and a linear guide (LTP 60.180.0804-02, SKF Multitec) driven by a DC motor (RE35, Maxon Motors) applied the sliding motion through a 4 mm pitch ball bearing screw, allowing a maximum velocity of 300 mm/s and a stroke of 110 mm. Linear Current Amplifier Modules (LCAM, Quanser), guaranteeing very low electromagnetic interference, were chosen for driving the actuators. Switching power devices were avoided since the typical (10–50 kHz) range for PWM carrier frequency is higher than half the microneurography sampling rate, but just outside the cutoff frequency of the bandpass filter preceding the sampling block. Hence, even introducing shielding techniques, a residual slight coupling between the PWM carrier frequency and μV range microneurography data could have been aliased at significant low frequencies, affecting the band of interest.

The robotic system has been devised with an open design approach since it is simple to command via a graphical user interface and is upgradable thanks to the FPGA control electronics. This design choice represented an advancement with respect to state of the art systems coherently with the trend showed in the literature of mechatronic tactile stimulators, which used digital controllers (Looft and Williams, 1979) for avoiding to integrate complex mechanisms such as in the scotch yolk stimulator (Goodwin et al., 1985) and reducing as much as possible the analog circuitry (LaMotte et al., 1983; Byrne et al., 1975; Schneider et al., 1995). Despite this design solution is promising, only a few mechatronic tactile stimulators were based on FPGA control electronics at the time of the platform development (Wagner et al., 2002; Pasquero et al., 2007).

For the platform presented by Oddo and colleagues (Mechatronics, 2011), this choice was operated for two main reasons: i) to allow future upgradeability of the architecture of control electronics (e.g. by instantiating on the same FPGA a number of additional parallel soft-core processors, peripherals, custom digital hardware modules, etc.); ii) to achieve, via hardware-software codesign, a multi-layered hierarchical controller (Fig. 4-right) allowing low-level parallel (Astarloa et al., 2009) scheduling of periodic routines implementing the motion control laws and of interruptions managing the communication (commands and platform data) functions. Therefore, the multi-layered hierarchical control architecture partitioned the tasks between a general purpose PC and the embedded FPGA hardware-programmable logics, which was interfaced to the sensors and power current drivers of the platform (Fig. 4-right a).

The HIGH-level layer ran a Graphical User Interface (GUI) to generate, save, load or execute buffers of HIGH-level commands and for displaying the received platform data. The MID-level layer was in charge of interpreting HIGH-level commands, of point-to-point trajectory generation for the linear guide LOW-level controller, of force target generation for the voice coil LOW-level controller, and of transmitting

the platform variables to the GUI for display purposes and to the acquisition systems for electrophysiological or artificial touch experiments.

The dimensioning of the 2-DOF LOW-level control laws took into account the mechanical characteristics of the fingertip (Serina et al., 1997; Pawluk and Howe, 1999; Nakazawa et al., 2000); both the controllers were in closed loop with integrator to reject disturbances (e.g. variable friction) or modifications of the boundary conditions (e.g. the inclination of the platform in 3D space for adapting it to the position of the subject during electrophysiological recordings); also, they had ad hoc dead bands (Fig. 4-right b) to prevent any steady-state vibration (Iskakov et al., 2007).

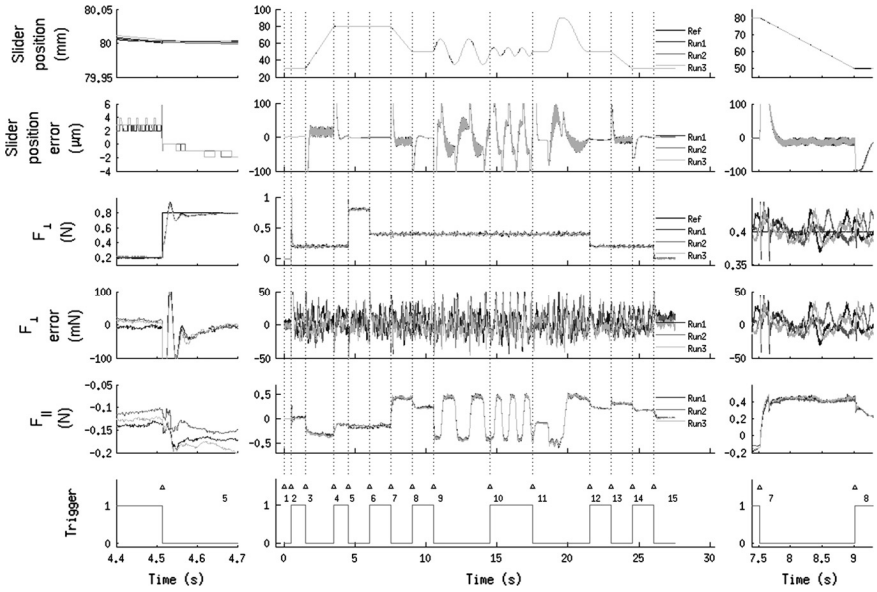

Fig. 5. From Oddo et al. (Mechatronics 2011). Sample protocols that can be implemented with the mechatronic platform. Three runs acquired at 5 kHz through Ethernet digital transmission, of the same sequence of commands are superimposed to show high repeatability. The plots represent, from the top: position of the translational slider (target and actual), error in tracking the reference slider position, indentation force at finger-stimulus interface (target and actual), error in tracking the reference indentation force, tangential force component along the direction of the sliding motion, Boolean channel switching each time a new high-level command is executed. Phases 2 and 15, at the beginning and at the end of the protocol, are the loading and unloading of the smooth aluminum stimulus to the finger. In phase 3 the stimulus is stroked for 50mm at 25 mm/s and normal contact force at 200 mN; phases 5 and 6 are normal contact force steps from 200 mN to 800 mN and then to 400 mN; from phase 7 to phase 11 the normal contact force is held at 400 mN, while the stimulus is stroked for 30 mm at constant speed of 20 mm/s (phase 7), while two (phase 9, 15 mm amplitude at 0.5 Hz) or three (phase 10, 5 mm amplitude at 1 Hz) sine waves are executed, or while a fifth order polynomial trajectory is followed (phase 11). Phase 13 is a position ramp from 50 mm to 30 mm in 1.5 s and normal contact force set to 200 mN. The left inset shows a zoom on the transitory between phase 4 and phase 5. The right inset shows a zoom on dynamic phase 7 (reprinted with permission from Elsevier).

4.3 Experimental Evaluation of the Robotic Platform

Traditional indices (tracking error along the 2 DOFs and confidence intervals to evaluate repeatability) were calculated for assessing the controllers of the 2 DOFs over repeated tactile stimulation runs. Such quantitative indexes confirmed adequate control performances (example protocols are shown in Fig. 5): the reference slider position is tracked with an error lower than 28 μm for ramps (phases 3, 7 and 13 in Fig. 5); reference sine waves (phases 9 and 10) having peak velocities up to 47.1 mm/s are followed with error lower than 68 μm; and 5th order polynomial trajectories (phase 11) present a Tracking Error lower than 43 μm. As regards the regulation of the indentation force, all the calculated parameters showed absolute Tracking Error lower than 20 mN, while the normalized error was comprised between 1.6% and 6.6%. As a further relevant result, the extremely reduced values of the confidence intervals (typically in the order of few permille points of the reference target) confirm that the developed mechatronic platform guarantees excellent repeatability in the presentation of tactile stimuli (Oddo et al., 2011).

This achievement is fundamental in touch studies: even if the tracking of the reference curves may get relatively worse in certain conditions, the actual trajectories under feedback control are almost coincident among different runs.

Apart for the particular design choices and results for traditional robotic assessment, the research work presented by Oddo and colleagues (Mechatronics 2011) also provided neuro-robotic methodological contributions on the possibility to use the human mechanoreceptors as instrumental sensors, to assess platform compatibility with the exacting demands of electrophysiological methods, specifically the lack of electromagnetic interference and absence of spurious vibrations.

The lack of significant electromagnetic interference coupling with the electrode for microneurography due to the platform was investigated by means of analysis of neural recordings from a SAI unit (left index finger), under three experimental conditions: i) Manual Stimulation (MS)-mode: while the platform was not actuated, the experimenter manually stimulated the finger of the subject (test subject) from which neural data was recorded; ii) Closed Loop (CL)-mode: a 1600 μm periodic ridged stimulus was indented and scanned across the fingertip of a second subject (control subject), in close proximity to the fingertip of the test subject (from which neural data was recorded), with 500 mN feedback controlled contact force, sliding distance of 20 mm and velocity set to 20 mm/s; iii) Open Loop (OL)-mode: to double check whether or not the time varying driving current (related to the indentation DoF actuator in feedback force control) affected the microneurography results, the same protocol of point ii) was operated apart for the fact that the indentation was in open loop by supplying a constant current to the voice-coil actuator, resulting in a normal contact force of about 750 mN before the onset of stimulus sliding motion. Noise amplitude distribution was evaluated in the three experimental conditions described above.

No relevant noise pickup was observed in the raw nerve signals (top plots of Fig. 6-right) recorded during platform movement or when the force control was engaged, as an effect of the selected linear power drivers for the actuators instead of switching ones. Fig. 6 depicts neural data from a SAI unit of the test subject in the

three MS-mode, CL-mode and OL-mode experimental conditions detailed above. Neural spikes are identified in MS-mode and marked with dots, corresponding to the phases during which the finger of the test subject was manually probed. The spike template applied for spike sorting in MS-mode was then used to evaluate whether or not neural spikes were elicited under the two other stimulation conditions due to electromagnetic interference by the platform (since the fingertip of the test subject was not mechanically stimulated in CL-mode and OL-mode, and a SAI unit is expected to be silent in that condition). Noticeably, no spikes could be identified in both the CL-mode and OL-mode, confirming that the platform did not induce vibrations resulting in spurious neural firing. As one could expect, the mechatronic platform had an effect in the background neural noise, confirmed by the higher amplitude of the CL-mode and OL-mode traces if compared to the spike-free regions of the MS-mode one. However, the overlap of the traces shows that the increase in noise was not enough to mask the spikes occurring while manually probing (MS-mode) the fingertip of the test subject.

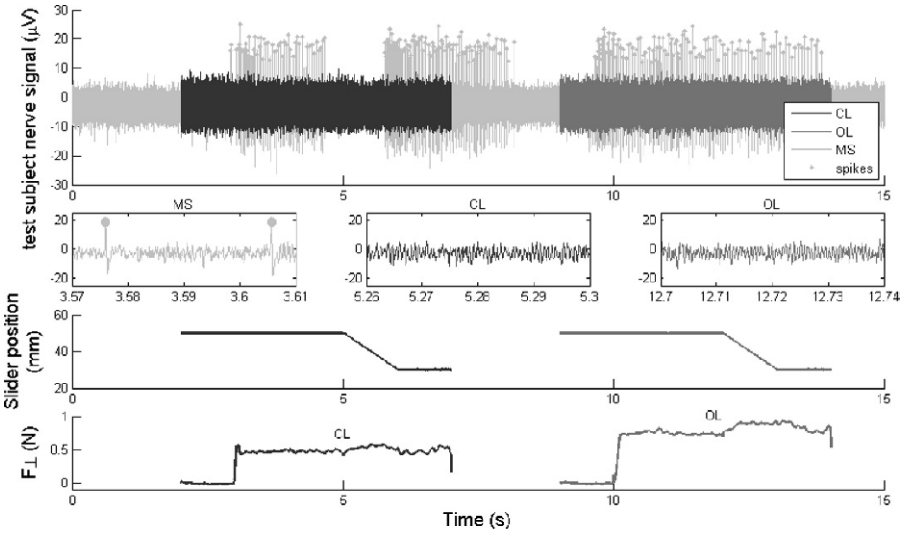

Fig. 6. From Oddo et al. (Mechatronics 2011). Neural recordings under the three MS-mode, CL-mode and OL-mode experimental conditions are depicted in the top plot for assessment of platform electromagnetic compatibility with the microneurographic technique. Left to right, the insets in the second row from the top show zooms on neural data recorded from the test subject with MS-mode, CL-mode and OL-mode. The position of the translational slider and the normal component of the indentation force are shown as well under both the CL-mode and OL-mode experiments (reprinted with permission from Elsevier).

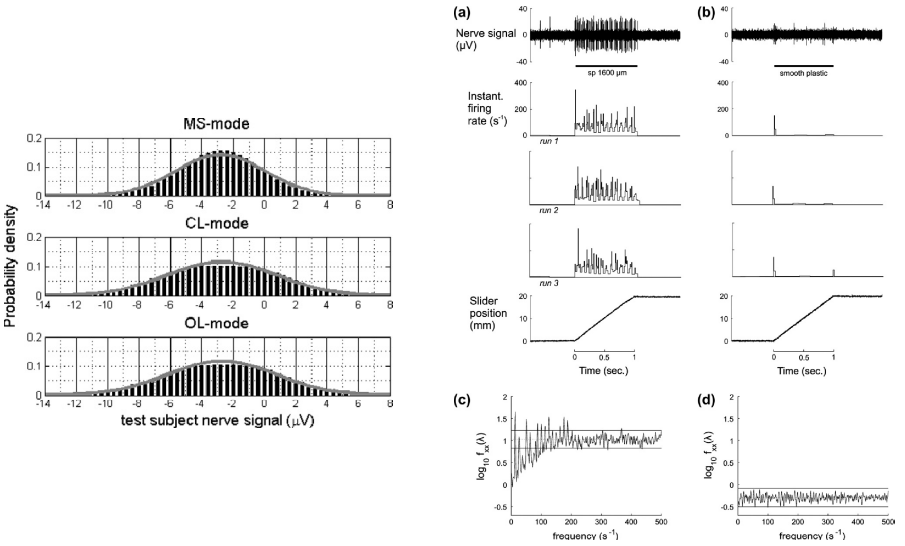

Fig. 7. From Oddo et al. (Mechatronics 2011). Left: Statistical neural noise analysis for each of the three MS-mode, CL-mode and OL-mode stimulation conditions. The probability that the neural signal belongs to a bin (width set to 0.4 lV) is evaluated based on amplitude levels experimentally occurring in 38 s of data at 12.8 kHz. The solid line shows Gaussian fitting of noise probability density. Right: Microneurographic recording from a RA (Meissner) tactile afferent unit. (a) Stimulation with a ridged grating. Records from top, recorded nerve signal, instantaneous rate of nerve discharges during three repeated runs of the same stimulus, slider position. (b) Stimulation with a smooth plastic surface on the same unit, records as in A. (c) Spectrum of nerve discharge during ridged grating stimulation. Solid lines show $p < 0.01$ confidence limits. (d) Spectrum for a smooth surface as in C (reprinted with permission from Elsevier).

A statistical noise analysis is presented in Fig. 7-left for each of the three MS, CL and OL stimulation conditions, where the probability that the neural signal belongs to a bin (width set to 0.4 μV) is evaluated based on amplitude levels experimentally occurring in 38 s of data at 12.8 kHz. A Gaussian fitting is shown as well in Fig. 7-left: platform activation causes a non-relevant increase in noise standard deviation from 2.82 μV (MS-mode) to 3.43 μV (OL-mode) and 3.48 μV (MS-mode), and had almost no effect in its mean value.

To directly assess the presence of biologically significant vibrations introduced by the platform, the spectra resulting from the point processes of identified neural spikes were calculated considering the firing of RA units during indentation and sliding motion of a smooth polypropylene plastic surface, in comparison to that occurring with periodic gratings having spatial period between 280 μm and 1920 μm.

As shown in Fig. 7-right b depicting a single RA afferent, after the expected short burst of impulses at the start of motion, this unit fired only sporadic impulses. The spectral signature of the firing for all the data from the same RA unit is shown in Fig. 7-right c for 1600 μm spatial period grating, meaningfully depicting the modulation of firing at the expected fundamental frequency (i.e. the ratio between the sliding velocity and the spatial period of the presented surface) of 12.5 Hz at a sliding

velocity of 20 mm/s, as well as significant modulation at harmonics up to 200 Hz. Therefore, the spatial period of the grating was revealed as a modulation of firing frequency as the ridges of the surface were sliding across the receptive field of the RA unit, confirming the high sensitivity in encoding the mechanical characteristics of the stimulating surface in this unit. In the frequency domain, the spectrum for all the data from stimulation with a smooth plastic surface in the same unit reveals no periodic firing or pickup of vibrations (Fig. 7-right d). To succeed in this objective, a relevant design choice was the introduction of custom dead bands (Fig. 4-right b and c) which allowed errors lower than specific thresholds to occur, thus avoiding vibrations produced by continuous sub-threshold error-correction control actions.

Human microneurography recordings also confirmed excellent repeatability (Fig. 7-right a), being mainly a consequence of the intrinsically reduced jitter in the scheduling of periodic control tasks by the implemented hierarchical control architecture (particularly, the hardware programmable FPGA logics for the embedded controller). Similar results were obtained in all recorded afferents.

The dedicated design of the platform allowed to implement a wide variety of passive- (Oddo et al., Sensors 2009; Oddo et al., IEEE RoBio 2009; Oddo et al., Sensors 2009; Muhammad et al., MNE 2011; Oddo et al., IEEE TRo 2011; Spigler et al., 2012) and active- (Oddo et al., IEEE TRo 2011) protocols in artificial touch studies, also supported by parallel human touch outcomes via the microneurographic technique (Oddo et al., Sensors 2011). Such studies are now contributing towards a more complete understanding of the human sense of touch and the implementation of an artificial sense and its interfacing with natural neural afferents in amputees.

5 NEURARM: A Robotic Model of the Human Arm

5.1 Background

Experiments addressing questions about how humans adapt their upper-limb impedance have been tested extensively in human and animal subjects, primarily by applying mechanical perturbations (impulses, vibrations, etc.) to the limb during natural movements and observing the corrective responses of the limb (Burdet et al., 2001). These methods have provided a wealth of insight into how the central nervous system (CNS) controls the mechanical behaviour of the limb, however they suffer from the fact that the applied perturbations may themselves change the stiffness characteristics of the arm. A possible way to overcome the measurement artefact problem consists of simulating the human arm movements using mathematical models describing the behavior of the muscle-skeletal system (Flash, 1987). This research methodology represents a powerful tool for neuroscience investigation. However, it is still affected by an important drawback: the “reality gap”. Indeed, mathematical models of complex physical phenomena, such as the interaction between the human arm and the external environment, always present a discrepancy with the real world. This could results in a divergence between the simulation result and real-world behavior, possibly reducing the usefulness of the model.

As a complement to mathematical analyses, the implementation of a given neuroscientific hypothesis on a real mechanical system can reveal the effects of unmodelled dynamics, overcoming the reality gap problem. This is the reason why it is necessary to have a robotic model of the human arm that replicates the key mechanical behaviour of the human neuromuscular system. As such, an accurate robotic model of the human arm could provide a tool under the full control of the experimenter, reproducing the main functional features of the human arm and being able to interact with the same physical environment of the human.

Based on the above analysis, over the past six years we developed the anthropomorphic 2-DOF planar robotic arm NEURARM, a robotic model of the human arm under the full control of the experimenter (Vitiello et al., 2007; Vitiello et al., 2008; Cattin et al., 2008; Vitiello et al., 2010; Lenzi et al., 2011).

Requirements for the design of the NEURARM originated from the investigation of some of the major works on the human motion control theories. In particular, we started from the fact that the motion control strategy used by the CNS to control our own body is still under debate (Hinder and Milner, 2003). Among the main theories, the 'equilibrium point hypothesis' (EPH) (Hogan, 1984; Hogan, 1985; Hogan et al., 1987; Bizzi et al., 1984; Polit and Bizzi, 1979), and the 'interior model hypothesis' (IMH) (Kawato, 1999; Wolpert et al., 1995; Wolpert et al., 1999; Flanagan and Wing, 1995), while being completely different, are of great interest.

According to the EPH, CNS can generate stable angular equilibrium postures, towards which the arm is attracted, by properly regulating the activation levels of antagonistic muscles and with no knowledge of the human arm dynamic behaviour. Conversely, according to IMH, CNS uses the muscle activation to directly control the joint torque taking into account a prior knowledge of the dynamic behaviour of the system.

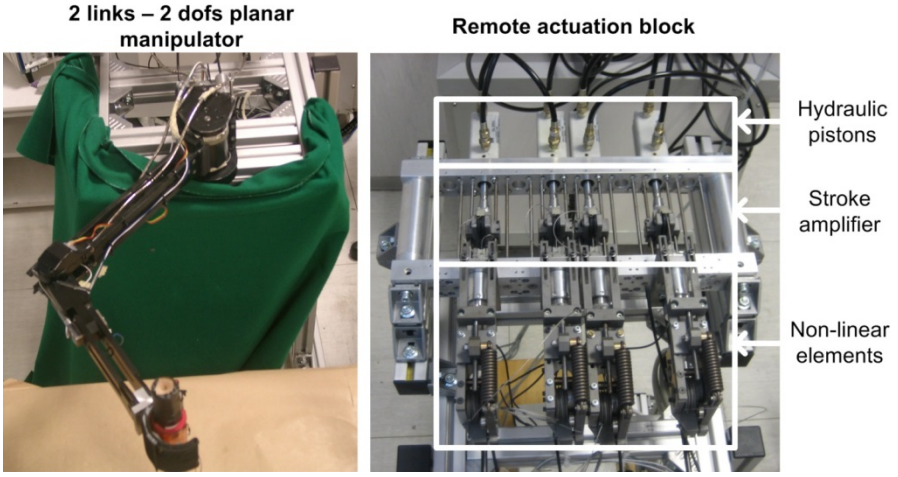

Fig. 8. From Lenzi et al. (Biological Cybernetics 2011). Overview of the NEURARM platform (with kind permission from Springer Science+Business Media).

In order to realize a robotic tool that could be used for addressing investigations with both the above strategies, the NEURARM design addressed two key requirements. First, the robot kinematic parameters and inertia should be similar to that of the human being. Second, the robot actuation should mimic the main physical features of the human actuator system, such as: (i) the use of tendons to transfer force; (ii) passive elasticity of muscles in absence of any neural feedback; (iii) implementation of antagonistic pairs of muscles; (iv) non-linearity of the elastic behaviour allowing modulation of net stiffness through co-activation of opposing muscles.

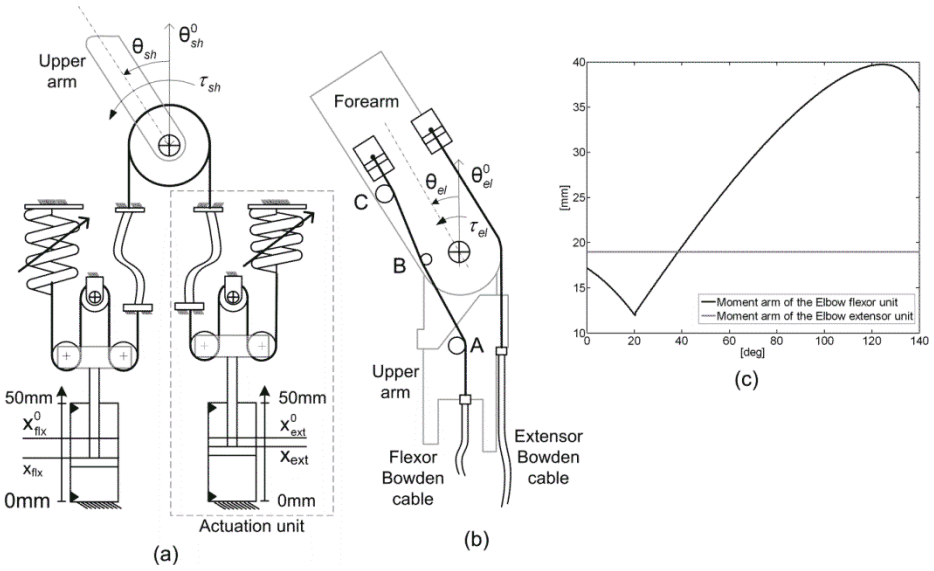

Fig. 9. From Vitiello et al. (Mechatronics 2010). NEURARM joints. (a) Shoulder joint. (b) Elbow joint. (c) Flexor moment art vs. joint angle of the NEURARM elbow joint (reprinted with permission from Elsevier).

5.2 Overview of the Robotic Platform

The NEURARM platform is a 2-link-2-DOF planar robotic arm with two revolute joints, the shoulder and the elbow, whose rotation axes are perpendicular to the motion plane, and two aluminium links, the upper arm and the forearm. The current setup of the NEURARM platform is shown in Fig. 8.

Both the NEURARM shoulder and elbow joints are driven by a pair of antagonist actuation units. However, the two joints have a different configuration. The shoulder, whose motion range is in the interval [-90°, 90°], consists of a pulley with a diameter of 60 mm, on which the antagonist cables reel and can generate a torque by means of a constant moment arm equal to 30 mm (Fig. 9-a). The elbow joint, thoroughly described in (Cattin et al., 2008), has a motion range in the interval [0°, 140°], is more complex and mimics the tendon routing of the human elbow (Kapandji, 1982; Fagg, 2000) (Fig. 9-b). The cables for the extension and flexion of the elbow are directly attached on the forearm. For the extensor rope, the elbow behaves like a pulley with a

constant radius equal to 19.5 mm. The flexor rope, because of its particular path around the rotating shaft A, and the two pins B and C, has a moment arm that is a non-linear function of the joint angle. The analytical model used to get the description of the non-linear function can be found in (Cattin et al., 2008). The function of the flexor moment arm vs. the elbow joint angle is shown in Fig. 9-c. For both the shoulder and elbow joints, the joint is flexing when the joint speed is positive, and it is extending when it is negative.

The NEURARM joint actuation system replicates the human musculoskeletal system configuration by means of two antagonist compliant actuators (Vitiello et al., 2010; Lenzi et al., 2011). As illustrated in Fig. 9-a, each antagonist actuation unit consists of three functional elements:

- a non-linear elastic element emulating the muscle's passive elastic behaviour;
- a linear hydraulic actuator combined with a stroke amplifier to mimic the contractile capability of the muscle. These two elements allow the regulation of the rest length of the non-linear elastic element. The hydraulic piston is the active component of the transmission system, while the stroke amplifier is used to transform a piston displacement into a four-time higher cable displacement This latter element satisfies the system requirement in terms of contraction velocity and force generation, and allows one to achieve performance similar to that of the human arm;
- a steel cable transmitting the force to the NEURARM joint by means of a Bowden cable.

Both the non-linear springs and the hydraulic actuators are located remotely from the robot. This solution satisfies the requirements for the mass and inertia of the links without affecting the system's capability to functionally emulate the human musculoskeletal system. This would not have been possible with an on-board actuation solution. Moreover, thanks to the low weight and high flexibility of the Bowden cables, the power is transferred to the joints without affecting the arm kinetics and kinematics.

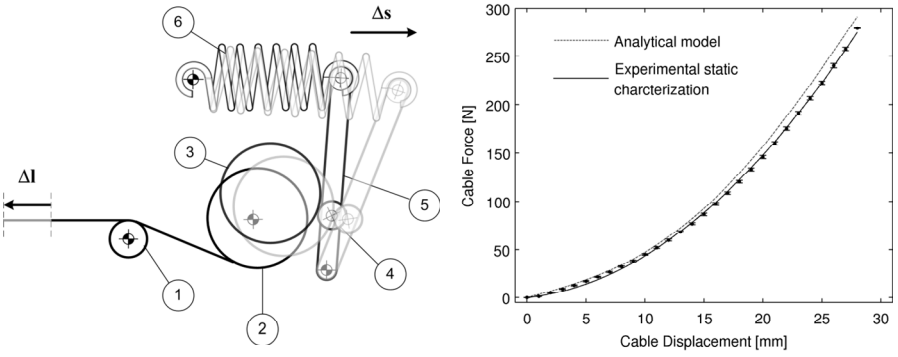

(a) (b)

Fig. 10. From Lenzi et al. (Biological Cybernetics 2011). (a) Schematic representation of the non-linear spring. (1) Idle pulley. (2) Reel. (3) Cam. (4) Idle wheel. (5) Bar. (6) Tension spring. (b) Comparison between numerical model and experimental data of the non-linear spring (with kind permission from Springer Science+Business Media).

5.3 The Non-Linear Elastic Element

The design of the non-linear elastic element was of crucial importance to mimic the human muscle characteristics. Its main design requirements were:

- the force (F) vs. elongation (Δl) characteristic should be well approximated by a quadratic polynomial curve $F(\Delta l) = a_1 \Delta l^2 + a_2 \Delta l$; such that the force increases with elongation and the stiffness ($dF/\Delta l$) increases with force;
- the linear stiffness of the spring, coupled with the tendon transmission around the joints should result in a joint stiffness range for the shoulder and the elbow joint of about 40 $N \cdot m \cdot rad^{-1}$, based on measured values of human arm stiffness in static position (Mussa-Ivaldi et al., 1985) or during movement (Gomi and Kawato, 1997; Burdet et al., 2000).

Starting from a linear tension spring, we designed a low-friction mechanism to obtain the non-linear elastic behavior. The mechanism works in a two-stage fashion. First, it establishes a non-linear relationship between the displacement of the cable (Δl), and the elongation of the linear tension spring (Δs). Second, the force exerted by the linear-tension spring $F_{\Delta s}$ is transformed into a force on the cable $F_{\Delta l}$ by a cam mechanism.

As illustrated in the schematic representation of Fig. 10-a, the mechanism consists of six elements and the working principle can be summarized in five steps: (i) the steel cable is deflected by an idle pulley (*body* 1) and then wrapped around a reel (*body* 2) which is fixed with a cam (*body* 3); (ii) the cam transmits the force and the movement to a bar (*body* 5) by means of an idle wheel (*body* 4), minimizing the friction; (iii) the bar is hinged down on the frame and is connected at its opposite extremity to the tension spring (*body* 6), which is hinged on the frame; (iv) a displacement Δl of the cable rotates the reel and consequently the cam; (v) the cam moves the bar via the idle wheel, and so the tension spring is stretched of Δs.

A detailed modelling of the non-linear elastic mechanism was presented in (Lenzi et al., 2011), while a detailed experimental characterization was given in (Vitiello et al., 2008). A comparison between the numerical model and the results from the experimental characterization are recapped in Fig. 10-b. Results pointed out that the non-linear force/elongation curve was well approximated by a second order polynomial function.

5.4 Control Strategies of the NEURARM

In order to use the NEURARM as a robotic model to explore both EPH- and IMH-based control hypotheses, we implemented two control strategies:

- an *independent control of the NEURAMR joint position and stiffness*, derived from the investigations on the EPH;
- a *sensorless joint torque control*, in this case the NEURARM joints were modelled as Antagonistic Driven Compliant Joints (ADCJ), a particular case of compliant joint.

Both the above control strategies relied on a lower-level closed-loop position controller of the four hydraulic pistons, each controlled by means of a three-land-four-way proportional electronic valve: the control signal being the reference of the spool

valve position, and actually fixing the piston velocity, as explained in (Vitiello et al., 2007; Vitiello et al., 2008). The hydraulic circuit was powered by a three-phase 1.1 kW AC motor (Parker-Hannifin Corp., OH, USA).

The control system runs on a real-time controller, a NI-PCI-8196 RT (National Instruments, Austin, Texas, US), endowed with three data acquisition cards M-series (National Instruments, Austin, Texas, US). Two digital incremental encoders (resolution of 0.05°) are used to measure the joints position and four linear potentiometers (resolution of 0.01 mm) for the measurement of the pistons position. Finally, the NEURARM end-effector can be equipped with a 6-axis load cell in order to measure the interaction force between the robotic arm and the environment.

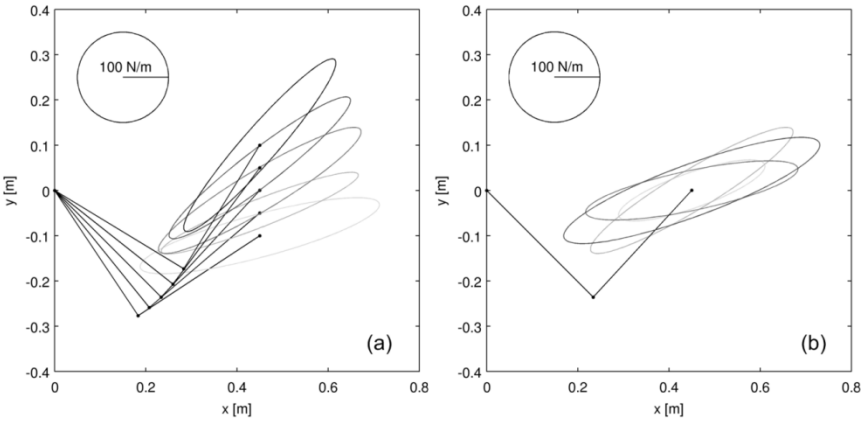

Fig. 11. From Lenzi et al. (Biological Cybernetics 2011). Estimates stiffness ellipses for: (a) different positions and fixed joint stiffness and, (b) different joint stiffness and fixed position (with kind permission from Springer Science+Business Media).

Independent Joint Position and Stiffness Control

The independent control of the joint position and stiffness relies on the following biomimetic concept. When two non-linear elastic springs are coupled to act around a single joint, the opposing torques generated by each elastic element will result in a convergent torque field around a virtual equilibrium position θ_{eq} (i.e. the static position that the arm would reach if no external loads are applied). The equilibrium point as well as the torque field slope (i.e. joint stiffness) will be directly determined by the positions of the two hydraulic pistons. By properly moving the pistons the joint equilibrium point and stiffness change. To show how it is possible to independently adjust the equilibrium position and the joint stiffness, a mathematical description of the actuation scheme working principle is given in (Lenzi et al., 2011). For instance, for the NEURARM shoulder the following equations for equilibrium position θ_{eq}^{sh} and stiffness K_{θ}^{sh} apply:

$$\theta_{eq}^{sh} = a_f\left(x_{ext}^{sh} - x_{flx}^{sh}\right)/2R \tag{1}$$

$$K_{\theta}^{sh} = -2R^2(a_2 - a_1 a_f(x_{ext}^{sh} + x_{flx}^{sh})) \tag{2}$$

where a_f is the stroke amplifier transmission ratio, x_{ext}^{sh} and x_{flx}^{sh} are the shoulder flexor and extensor piston positions, R is the shoulder pulley radius. From the above equations it is evident that the shoulder joint equilibrium position is proportional to the difference between the two piston positions, while the joint stiffness depends on their sum. Thereby, the joint position and stiffness can be regulated independently. Similar – but more complex, given the non-linear function between the flexor moment arm and the joint angle - equations can be written for the elbow joint, as it is well described in (Lenzi et al., 2011).

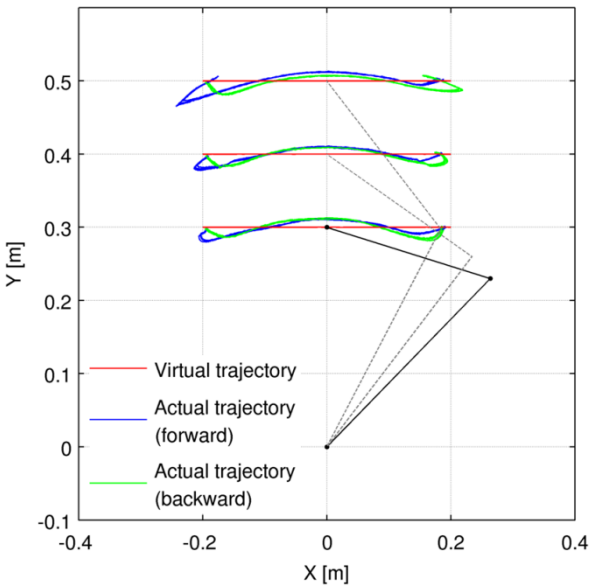

Fig. 12. From Lenzi et al. (Biological Cybernetics 2011). Cartesian space reaching tasks: three different end point virtual paths are tested by performing 10 iteration, back and forth for each trajectory (with kind permission from Springer Science+Business Media).

In the work (Lenzi et al., 2011) we also evaluated the performance of the independent joint position and stiffness control. In particular, performance can be summarized in the following main points.

- The static torque-angle characterization showed that the joint stiffness could be actively tuned in the range 6.5-21 N·m·rad^{-1} for the shoulder and 1.7-8.5 N·m·rad^{-1} for the elbow (Lenzi et al., 2011).
- The step response of the joints position controller - recorded for different stiffness levels – pointed out that the natural frequency of the shoulder joints increases from 1.1 Hz to 1.53 Hz (damping ratio increasing from 0.138 to 0.173) at the increase of the joint stiffness when the elbow joint is fully extended, and from 1.49 Hz to 2.13 (damping ratio increasing from 0.142 to 0.192) when the elbow joint is fully flexed.
- The experimental characterization of the end-point stiffness – that was addressed by applying a procedure similar to that used in the characterization of the human

arm spring-like behaviour (Mussa-Ivaldi et al., 1985) – showed that NEURARM could change in a bio-mimetic fashion the end-point stiffness ellipsoid (Fig. 11).
- NEURARM was capable to execute 40-cm rectilinear paths in the Cartesian space by sliding the equilibrium point along a virtual trajectory (i.e. the desired end-effector equilibrium position) with a bell shaped velocity profile, with a duration of 1 s (Fig. 12) with performance comparable to the numerical simulation performed in (Hogan 1984, Flash 1987) and consistent with direct observations on the human being (Gomi and Kawato, 1997).

Sensorless Torque Control

From an engineering view point, the research activities carried out for the development of a sensorless torque control are framed within the research field of robotic compliant joints. Compliant joints are receiving increasing attention in current robotics research, representing one of the best solutions to actuate robots involved in *cooperative tasks with humans*. It is current opinion that conventional robot technology, in which the robot actuators are designed primarily as rigid positioning devices or torque sources, is not able to match safety requirements in human-robot interaction. For instance, in collaborative tasks, a rigid robot could present great risks in case of a collision, as common software interaction controls require some time to react and adjust the compliance of the robot after the detection of the impact. On the other hand, the mechanical properties of hardware compliant robots, together with an appropriate control scheme, can make the robot safer (Van Damme et al., 2009). Moreover, compliant joints improve the robotic system robustness by making the overall system more tolerant to unpredictable changes in the models of the environment and of the robot, as well as in the dynamics of the human they are interacting with (Pfeifer et al., 2005; Filippini et al., 2008; Vanderborght et al., 2009).

These properties make the use of compliant joints appropriate for application in robots for personal assistance and rehabilitation (Vallery et al., 2008). Pratt and Williamson (1995) proposed one of the first examples of compliant joints, the Series Elastic Actuator (SEA). Following these studies, different examples have been conceived and tested exploiting various working principles and architectures (Collins and Ruina, 2005; Hurst and Rizzi, 2008; Mao et al., 2007; Van Ham et al., 2007).

The NEURARM joints can be classified as Antagonistic Driven Compliant Joint (ADCJ), one of the most studied configurations in the last years. This solution has two peculiar characteristics: (i) the joint is powered by two independent actuation units; (ii) each actuation unit works functionally as a non-linear elastic element with an adjustable resting position.

Several different engineering solutions based on the ADCJ configuration have been investigated. Schiavi et al. (2008) designed the variable stiffness actuator VSAII, using a 4-bar mechanism along with a linear spring as a non-linear element. Migliore et al. (2005) presented a tendon-driven ADCJ, in which the non-linear element consisted of a spring wrapped in a kinematic mechanism. Koganezawa et al. (2006) presented the Actuator with Non Linear Elastic System (ANLES), consisting of a DC motor rotating a guide shaft connected to the transmission board via a torsion spring. In this kind of actuators, the joint was controlled by means of two independent position-stiffness regulators. Pneumatic muscle actuators (pMA) were also exploited for developing ADCJ (Caldwell et al., 1995; Jutras and Bigras, 2006; Lilly, 2003; Tsagarakis and Caldwell, 2003; Tondu et al., 2005).

Majority of the algorithms exploited to control ADCJs are aimed at regulating the joint position and stiffness independently, as in the case of the *biological inspired joint stiffness control* presented by Migliore, or the independent joint position and stiffness control of the NEURARM. Nevertheless, there are some cases in which a direct control of the joint torque is required. For instance, for application in rehabilitation and assistive robotics, the robotic device (e.g. exoskeleton, Cartesian manipolandum) is often required to support the disabled person by providing a controllable force/torque (Vallery et al., 2008).

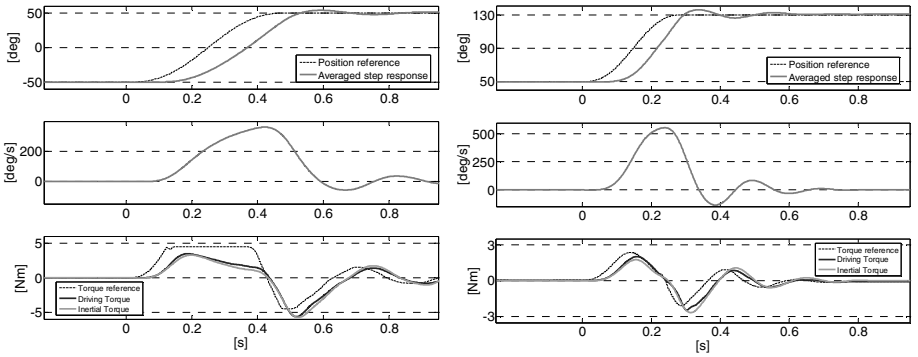

Fig. 13. From Vitiello et al. (Mechatronics 2010). Execution of the single-joint trajectories: (a) Shoulder joint. (b) Elbow joint. Top panel: desired and actual position. Middle panel: actual joint velocity. Bottom panel: desired driving torque, actual driving torque and inertial torque. Actual trajectories are averaged over 20 iterations (reprinted with permission from Elsevier).

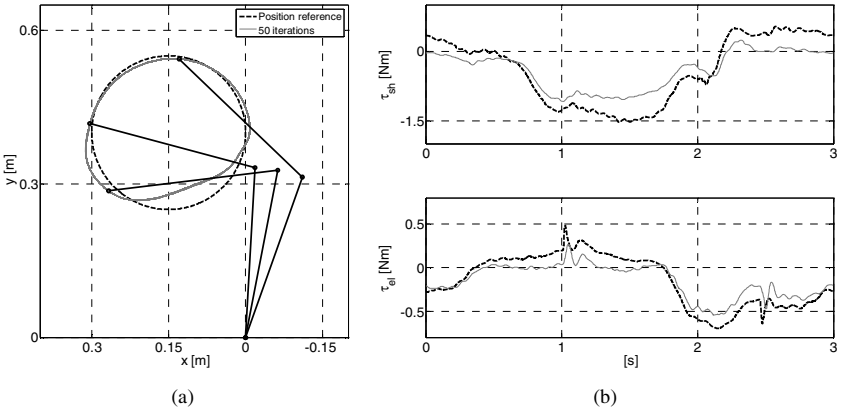

Fig. 14. From Vitiello et al. (Mechatronics 2010). Cartesian space multi-dof trajectories. (a) Desired and actual Cartesian trajectory. (b) Desired and actual driving torque. Top panel: shoulder torque. Bottom panel: elbow torque. Actual trajectories are averaged over 50 iterations (reprinted with permission from Elsevier).

Within this framework we developed a "sensorless" torque control strategy suitable for ADCJs based architectures. The proposed strategy does not require any additional force/torque sensors, and can be applied to all the ADCJs usually controlled through a position/stiffness regulator. The proposed sensorless torque control strategy can be explained as follows (Vitiello et al., 2010).

- An ADCJ is powered by a couple of independent actuation units, named flexor and extensor units. Each unit implements a non-linear spring whose resting position is controlled by a dedicated motor. The resulting torque τ acting on the joint depends on the forces applied respectively by the flexor F_{flx} and extensor F_{ext} actuation units, and, possibly, on the joint angular position θ: $\tau = h(F_{flx}, F_{ext}, \theta)$. For instance, in the case of an ADCJ consisting of a pulley-driven joint, the torque is simply dependent on the actuation units force difference, while in the case of a lever-driven joint, the force arms not being constant, the torque is also function of the joint angle (Vanderborght et al., 2009). Therefore, a suitable strategy to control the joint torque is to properly and independently control the force powered by each actuation unit.
- In order to control the actuation unit force, and consequently the joint torque, without using any force/torque sensor, a strategy to estimate these forces is needed. The proposed method relies on the actuation unit elastic property: because of this, each unit exerts a force F function of its elongation Δl: $F = f_{NL}(\Delta l)$, where f_{NL} is a generic non-linear function, and Δl depends on the joint angular position and the motor position x through a function g: $\Delta l = g(\theta, x)$.
- Since θ and x can be measured, the force F can be estimated if the functions f_{NL} and g are known. In particular, the function g can be obtained from kinematic considerations while f_{NL} from an experimental characterization. The experimental characterization is a key point of the proposed strategy because it is a reliable way to model in f_{NL} the effects of: (i) the undesired elastic action of flexible transmission means, such as tendon wires or belts; (ii) Coulomb friction introduced by high-friction transmission elements, such as Bowden cables.
- Assuming that the functions h, g and f_{NL} are known, it is then possible to exploit the indirect estimation of F to perform a closed-loop control of the force powered by each actuation unit, and consequently the resulting torque τ on the joint.

In the work (Vitiello et al., 2010) we actually employed the above strategy to develop a joint torque control for NEURARM. Performance of the proposed torque control strategy are summarized in the following main points.

- The torque control bandwidth was higher than 10 Hz for both shoulder and elbow joints; in the step response the control accuracy at the steady state was in the range 0.02-0.04 N·m.
- The developed torque control strategy was successfully benchmarked against the execution of both single- (Fig. 13) and multi-joint trajectories (Fig. 14), with a bell-shaped velocity profile with a peak of 300 deg·s^{-1} and 500 deg·s^{-1}, respectively for the shoulder and the elbow joints.

5.5 Remarks

The experimental activities carried out with the NEURARM had an immediate and strong impact on the design and development of the elbow exoskeleton NEUROExos, which is described in the following section. Indeed, for the actuation of the first prototype of NEUROExos we employed the same biomimetic antagonistic actuation we developed for the NEURARM. Thanks to this choice we could endow NEUROExos with an adaptive joint impedance, which is typical of the human arm. Furthermore, because of its variable impedance antagonistic actuation, NEUROExos can interact with human subjects with the appropriate joint output impedance. For instance NEUROExos can be "stiff" (and modulate its stiffness) when it is requested to drive the human motion or "transparent" when it has to constructively cooperate with humans. In other terms, thanks to its adjustable joint compliance NEUROExos can address the execution of both *robot-in-charge* and *patient-in-charge* rehabilitation exercises.

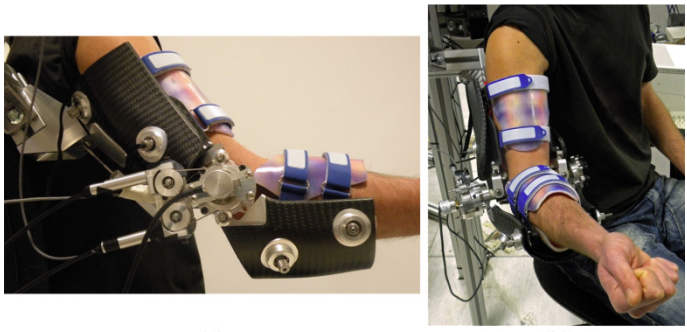

Fig. 15. Overview of the NEUROExos. (a) Lateral view. (b) Front view. © 2013 IEEE. Reprinted, with permission, from Vitiello et al. (IEEE Transactions on Robotics 2013).

6 NEUROExos: An Elbow Robotic Exoskeleton

6.1 Background

Robot-aided physical rehabilitation has been proposed to support physicians in providing high-intensity therapy, consisting of repetitive movements of post-stroke impaired limbs (Barreca et al., 2003; Feys et al., 1999; Kwakkel et al, 1999). The use of robots enable the patients to receive the benefits from the rehabilitation process, while the therapists can reduce their workload. Moreover, the robotic device offers an objective, reliable means of monitoring the patient progress.

State-of-the-art devices for upper limb robot-assisted therapy can be classified in: end-point manipulators (Krebs et al., 1998; Fasoli et al., 2003; Lum et al., 1999; Micera et al., 2006; Reinkensmeyer et al., 2001), cable suspensions (Mayhew et al., 2005; Stienen et al., 2007), and exoskeletons (Jia-Fan et al., 2008; Kiguchi et al., 2004; Perry et al., 2007; Frisoli et al., 2007; Frisoli et al., 2009; Tsagarakis and Caldwell, 2003; Carignan et al., 2007; Rocon et al., 2007; Nef et al., 2007; Mihelj et al.,

2007; Sanchez et al., 2006; Sanchez et al., 2007; Schiele and van der Helm, 2006; Stienen et al., 2009). Among these, the latter was proposed as a solution to the problem of control and measurement of angle and torque on each joint of the impaired limb (Stienen et al., 2009).

An exoskeleton for post-stroke physical rehabilitation is a nonportable mechanical device that is anthropomorphic in nature, is "worn" by the user, and fits closely to his or her body (Dollar and Herr, 2008). Given the close interaction with the user, comfort is a major concern. An exoskeletal robot for physical rehabilitation should be lightweight and take into account the user's joints range of motion (ROM), anthropometry, and kinematics (Schiele and van der Helm, 2006; Stienen et al., 2009). The physical human–robot interaction (pHRI) area should be large and should match the shape of the patient's limb to reduce the pressure on the user's skin (Rocon et al., 2007; Pons, 2010). Furthermore, the actuation and control of the robot should allow safe execution of rehabilitation exercises in two modes of operation: *robot-in-charge*, when the robot is driving the subject in doing the exercises, and *patient-in-charge*, when the subject is driving the robot that is only partially assisting the movement (Krebs et al., 1998).

The NEUROROBOTICS Elbow Exoskeleton (NEUROExos) was introduced in the state of the art with three innovative design solutions (Fig. 15): (i) a compact and light-weight mechanical structure with double-shelled links, with a wide pHRI area to minimize the pressure on the skin; (ii) a 4-DOF passive mechanism that unloads the elbow articulation from undesired loads by ensuring the alignment of human and robot joint axes; (iii) the biomimetic, remote antagonistic actuation unit developed for the robotic arm NEURARM (Lenzi et al., 2011; Vitiello et al., 2013).

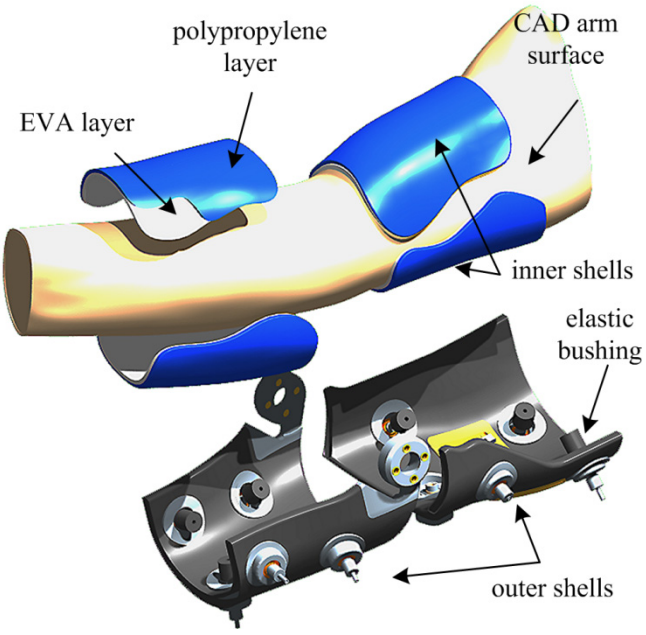

Fig. 16. Double-shelled structured links. © 2013 IEEE. Reprinted, with permission, from Vitiello et al. (IEEE Transactions on Robotics 2013).

6.2 System overview

The NEUROExos is a mechatronic device, constituted of the following four subsystems: (i) two double-shell structured links, (ii) a 4-DOF passive mechanism, (iii) a remote, antagonistic tendon-driven compliant actuation, (iv) a control system and a sensory apparatus.

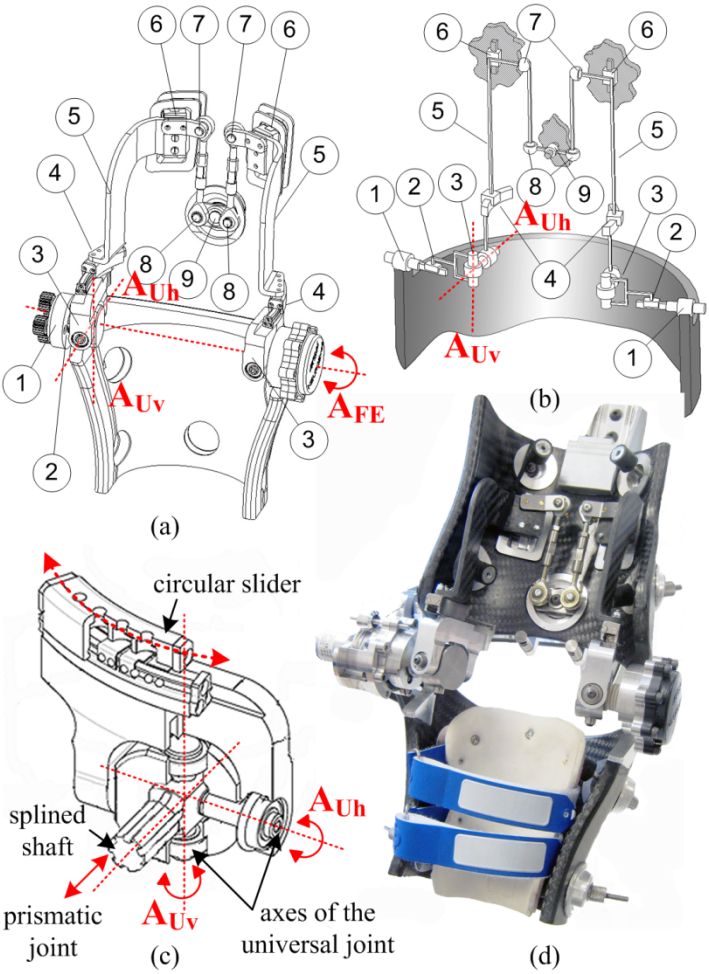

Fig. 17. 4-DOF passive mechanism. (a) CAD and (b) layout of the passive mechanism. (1) NEUROExos flexion–extension joint, axis A_{FE}. (2) Prismatic joint through splined shaft. (3) Universal joint. (4) Circular slider. (5) Carbon fiber link. (6) Linear slider. (7) Spherical joint. (8) Spherical joint. (9) Rotational joint. (c) Zoom on joints (1), (2), (3), and (4). A_{Uv} and A_{Uh} are the vertical and horizontal rotational axes of the universal joint; the splined shaft allows for the prismatic joint (2) whose axis coincides with A_{FE} (d) Implementation of the passive mechanism. © 2013 IEEE. Reprinted, with permission, from Vitiello et al. (IEEE Transactions on Robotics 2013).

Double-Shelled Links

The NEUROExos links were conceived in a way that the interaction force between the user and the robot should be distributed over a wide area, which should fit the shape of the human limb segments. Linkages were developed by taking into account the inter-subject variability and have low weight, inertia, and encumbrance, while ensure a good level of flexional stiffness to sustain the interaction torque.

The solution implemented for NEUROExos is depicted in Fig. 16. Each link is composed of two concentric shell-like structures.

Inner shells come in different sizes, and can be tailor-made on each subject (e.g., by thermo shaping a polypropylene layer). Each inner shell is made of two half-shells, to be coupled with the dorsal and ventral sides of the limb segment. Inner shells have a structure composed by two layers: a 3 mm-thick internal layer of ethylene vinyl acetate (555XEB/3, M.T.O., Italy), which is in contact with the skin of the patient and has properties of moisture draining and skin transpiration, and a 3 mm-thick outer layer of polypropilene (558/3, M.T.O., Italy).

Outer shells have a double-walled carbon fiber structure, which has a total height of 10 mm and thickness of 1.5 mm. Outer shells can be connected to inner shells of different shapes, and, therefore, enable the same exoskeleton links to be used by several users. Outer shells also house the aluminium frames of the 4-DOF passive mechanism, the gear box for the active flexion–extension DOF, and the inner–outer shell connecting elements. Connecting elements consist of an aluminium frame housed inside the carbon fiber structure and containing a passive spherical joint (GE 8C, SKF, Sweden) and an elastic bushing (Radialflex M4, Paulstra, France). Spherical joint and elastic bushing allow small relative motions between inner and outer shells and thus enhance comfort.

4-DOF Passive Mechanism

In order to guarantee the best kinematics matching between human and robot rotation axes, NEUROExos was equipped with a 4-DOF passive mechanism (Fig. 17). This mechanism is implemented by means of a closed-chain mechanism composed of 13 passive joints: 4 prismatic, 4 spherical, 2 circular sliders, 2 universal and 1 rotational joints. The flexion-extension axis A_{FE} is identified by means of the two axes of the prismatic joints (labeled as 2 in Fig. 17). These joints are implemented by means of two splined shaft-hole couplings having a range of motion (ROM) of 35 mm. Each splined shaft is attached to a universal joint (labeled as 3 in Fig. 17), whose ROM is 100° around the axis A_{Uh} and 24° around the axis A_{Uv}. Each fork housing one universal joint is then attached to a slider (joint number 4 in Fig. 17) moving along a circular trajectory having a diameter of 250 mm and an angular ROM of 42°. Through a carbon fiber link, the circular slider is connected to a linear slider (joint number 6 in Fig. 17, ROM of 30 mm). The linear slider is linked to the rotational joint labeled as 9 in Fig. 17 (ROM of 40°) by means of two spherical joints (male threaded, maintenance-free rod ends, SKF, Göteborg, Sweden) labeled as 7 and 8, connected by a bar with an adjustable length.

The passive mechanism provides A_{FE} with three passive DOFs, which allow the NEUROExos axis to trace the same double conic frustum traced by the human axis

(Bottlang et al., 1998; Bottlang et al., 2000; Duck et al., 2003). First, A_{FE} can rotate in the frontal plane of an angle $\gamma_f = \pm 15°$. Then, A_{FE} can rotate in the horizontal plane of an angle $\gamma_h = \pm 21°$. Finally, the NEUROExos forearm link can slide along the axis A_{FE}.

Finally, A_{FE} can translate onto the horizontal plane along the antero-posterior direction of a segment $\Delta = \pm 15$ mm. This translational DOF is fundamental to partly compensate for the undesired forces which are caused by the joint axes misalignment (Stienen et al., 2009).

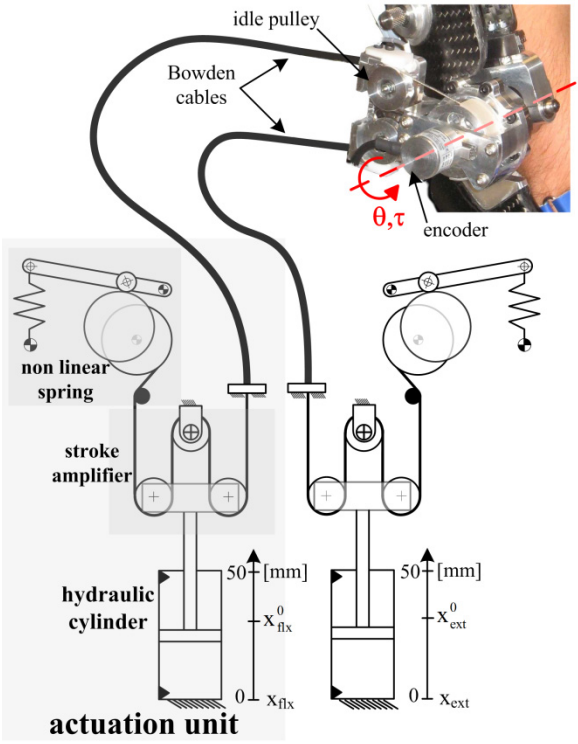

Fig. 18. Schematic drawing of the antagonistic tendon-driven compliant actuation and sensory system of the NEUROExos. Two remote antagonistic units, which are named flexor ("flx") and extensor ("ext"), power the NEUROExos active joint. © 2013 IEEE. Reprinted, with permission, from Vitiello et al. (IEEE Transactions on Robotics 2013).

Antagonistic Compliant Actuation

The layout of the actuation system of NEUROExos is depicted in Fig. 18. It consists of a pair of remote and independent antagonistic units, which are similar to those used for the actuation system of the anthropomorphic robotic arm NEURARM: in this case we used a tension spring of 80 $N \cdot mm^{-1}$ so that NEUROExos can achieve an actively adjustable passive joint stiffness in the range 20-60 $N \cdot m \cdot rad^{-1}$. This range is indeed comparable with the one of the human elbow.

Control and Sensory System

The actuation system of NEUROExos allows for the use of two alternative control strategies: the *passive-compliance control* and the *torque control*, respectively for the execution of robot-in-charge and patient-in-charge exercises.

The passive compliance control – as for the NEURARM – allows for an independent joint position and stiffness control by respectively setting the difference and the sum of the piston positions.

The torque control relies instead of the independent closed-loop control of the cable force powered by the each actuation unit. The desired torque τ_{des} is converted into two desired forces on the antagonistic cables. Then, the desired cable forces serve as input of two independent closed-loop force controllers.

Both the NEUROExos control algorithms run on a real-time control system (NI PXI-8196 RT, Austin, TX, USA) equipped with a data acquisition card (NI M-series, Austin, TX, USA). Cable force and pistons positions signals are sampled at 250 kHz, then low-pass filtered and down-sampled to 1 kHz.

NEUROExos is endowed with a 1024 ppr incremental optical encoder (2420, Kübler, Germany) assembled coaxially with the driving pulley (resolution of 0.022°). Two custom-made load cells were included in the design, to measure the force transmitted by the antagonist tendon cables (Accuracy 0.05 N). Two linear potentiometers (SLS095, Penny&Giles, Dorset, UK) are used for the measurement of the pistons positions with an accuracy of 0.01 mm.

6.3 System Performance and Perspectives

In the past years, in addition to the experimental characterization addressed within the work (Vitiello et al., 2013), NEUROExos was also employed in experimental trials that aimed at either exploring new human-machine interfaces (Ronsse et al., 2010; Ronsse et al., 2011; Lenzi et al., 2011b; Lenzi et al., 2012) or testing a novel wearable pressure-sensitive sensor to sense the physical human-robot distributed interaction (Lenzi et al., 2011c; De Rossi et al., 2010; De Rossi et al., 2011; Donati et al., 2013). From this extensive experimentation of the NEUROExos the following main results derived.

- Measurements on five healthy subjects proved that – thanks to the 4-DOF passive mechanism – the NEUROExos rotation axis actually moves along with the elbow flexion-extension, and thus it ensures a safe and comfortable human-robot interaction. Thanks to this result we were motivated to develop a theoretical framework for the design of passive mechanisms for human-robot joint axes self-alignment (Cempini et al., 2013), and to apply the same idea on a hand exoskeleton (Chiri et al., 2012; Cempini et al., 2013b).
- Under the passive-compliance control, the NEUROExos passive stiffness can be actively tuned in the range The torque control bandwidth was higher than 10 Hz for both shoulder and elbow joints; in the step response the control accuracy at the steady state was in the range 24-56 $N \cdot m \cdot rad^{-1}$; the equilibrium point can be changed with a -3-dB bandwidth of about 7 Hz.

- Under the action of the torque control, the NEUROExos joint is highly transparent: its output impedance increases across the spectrum, and it changes from 1 $N \cdot m \cdot rad^{-1}$, for 0.3 Hz motion, up to 1 $N \cdot m \cdot rad^{-1}$, for 3.2 Hz motion. The closed-loop torque control bandwidth is higher than 10 Hz.

Recently a new version of the NEUROExos was developed, which is endowed with a new actuation unit based on a compact, light-weight series-elastic actuator. This new version was early presented in a conference paper and is currently employed in an extensive clinical trial in the rehabilitation center "Auxilium Vitae", in Volterra, Italy.

References

André, T., Lefèvre, P., Thonnard, J.-L.: A continuous measure of fingertip friction during precision grip. Journal of Neuroscience Methods (2009)

Astarloa, A., Lazaro, J., Bidarte, U., Jimenez, J., Zuloaga, A.: FPGA technology for multiaxis control systems. Mechatronics 19(2), 258–268 (2009)

Barreca, S., Wolf, S.L., Fasoli, S., Bohannon, R.: Treatment interventions for the paretic upper limb of stroke survivors: a critical review. Neurorehabilitation and Neural Repair 17(4), 220–226 (2003)

Beckmann, S., Bjrnsdotter, M., Backlund-Wasling, H., Wessberg, J.: Brain decoding of texture processing using independent component analysis and support vector machines. In: Proc. 2009 IEEE International Symposium on Intelligent Signal Processing, Budapest, Hungary, pp. 287–292 (2009)

Bekey, G.: Autonomous Robots. From Biological Inspiration to Implementation and Control. The MIT Press, US (2005)

Birznieks, I., Jenmalm, P., Goodwin, A.W., Johansson, R.S.: Encoding of direction of fingertip forces by human tactile afferents. J. Neurosci. 21, 8222–8237 (2001)

Bizzi, E., Accornero, N., Chapple, W., Hogan, N.: Posture control and trajectory formation during arm movement. Journal of Neuroscience 4, 2738–2744 (1984)

Bliss, J.C., Katcher, H., Rogers, C.H., Shepard, R.P.: Optical-to-Tactile Image Conversion for the Blind. IEEE Transactions on Man-Machine Systems 11, 58–65 (1970)

Bonsignori, G., Stefanini, C., Scarfogliero, U., Mintchev, S., Benelli, G., Dario, P.: The green leafhopper, Cicadella viridis (Hemiptera, Auchenorrhyncha, Cicadellidae), jumps with near-constant acceleration. The Journal of Experimental Biology 216(7), 1270–1279 (2013)

Bottlang, M., Madey, S.M., Steyers, C.M., Marsh, J.L., Brown, T.D.: Factors influencing accuracy of screw displacement axis detection with a DC-based electromagnetic tracking system. Journal of Biomechanical Engineering 120(3), 431–435 (1998)

Bottlang, M., Madey, S.M., Steyers, C.M., Marsh, J.L., Brown, T.D.: Assessment of elbow joint kinematics in passive motion by electromagnetic motion tracking. Journal of Orthopaedic Research 18, 195–201 (2000)

Burdet, E., Osu, R., Franklin, D.W., Milner, T.E., Kawato, M.: The central nervous system stabilizes unstable dynamics by learning optimal impedance. Nature 414, 446–449 (2001)

Burdet, E., Osu, R., Franklin, D.W., Milner, T.E., Yoshioka, T., Milner, T., Kawato, M.: A method for measuring end-point stiffness during multi-joint arm movement. Journal of Biomechanics 33(12), 1705–1709 (2000)

Byrne, J.: A feedback controlled stimulator that delivers controlled displacements or forces to cutaneous mechanoreceptors. IEEE Trans. Biomed. Eng. 22, 66–69 (1975)

Caldwell, D.G., Medrano-Cerda, G.A.: Goodwin M, Control of pneumatic muscle actuators. IEEE Contr. Sys. Mag. 15(1), 40–48 (1995)

Carignan, C., Tang, J., Roderick, S., Naylor, M.: A Configuration-Space Approach to Controlling a Rehabilitation Arm Exoskeleton. In: Proc. IEEE International Conference on Rehabilitation Robotics (ICORR), Noordwijk, The Netherlands, pp. 524–531 (2007)

Carrozza, M.C., Cappiello, G., Micera, S., Edin, B.B., Beccai, L., Cipriani, C.: Design of a cybernetic hand for perception and action. Biological Cybernetics 95(6), 629–644 (2006)

Cattin, E., Roccella, S., Vitiello, N., Clemens, E., Sardellitti, I., Panagiotis, K.A., Vacalebri, P., Vecchi, F., Carrozza, M.C., Kyriakopulos, K., Dario, P.: Design and Development of a Novel Robotic Platform for Neuro-Robotics Applications: the NEURobotics ARM (NEURARM). Advanced Robotics, Special Issue on Robotics Platforms for Neuroscience 22, 3–37 (2008)

Cempini, M., De Rossi, S.M.M., Lenzi, T., Cortese, M., Giovacchini, F., Vitiello, N., Carrozza, M.C.: Kinematics and Design of a Portable and Wearable Exoskeleton for Hand Rehabilitation. In: Proceedings of the IEEE International Conference on Rehabilitation Robotics, ICORR (2013)

Cempini, M., De Rossi, S.M.M., Lenzi, T., Vitiello, N., Carrozza, M.C.: Self-Alignment Mechanisms for Assistive Wearable Robots: a KinetoStatic Compatibility Method. IEEE Transactions on Robotics 29(1), 236–250 (2013)

Chiri, A., Vitiello, N., Giovacchini, F., Roccella, S., Vecchi, F., Carrozza, M.C.: Mechatronic design and characterization of the index finger module of a hand exoskeleton for post-stroke rehabilitation. IEEE Transactions on Mechatronics 17(5), 884–894 (2012)

Collins, S., Ruina, A.: A bipedal walking robot with efficient and human-like gait. In: Proceedings of the IEEE International Conference on Robotics and Automation, pp. 1983–1988 (2005)

Connor, C.E., Johnson, K.O.: Neural coding of tactile texture: comparison of spatial and temporal mechanisms for roughness perception. J. Neurosci. 12(9), 3414–3426 (1992)

Craelius, W.: The bionic man: restoring mobility. Science 295(5557), 1018–1021 (2002)

Darian-Smith, I., Oke, L.E.: Peripheral neural representation of the spatial frequency of a grating moving across the monkey's finger pad. J. Physiol. 309, 117–133 (1980)

De Rossi, S.M.M., Vitiello, N., Lenzi, T., Ronsse, R., Koopman, B., Persichetti, A., Giovacchini, F., Vecchi, F., Ijspeert, A.J., van der Kooij, H., Carrozza, M.C.: Soft artificial tactile sen-sors for the measurements of human-robot interaction in the rehabilitation of the lower limb. In: Proc. of the 2010 Annual International Conference of the IEEE Engineering in Medicine and Biology Society (EMBC), Buenos Aires, Argentina, pp. 1279–1282 (2010)

De Rossi, S.M.M., Vitiello, N., Lenzi, T., Ronsse, R., Koopman, B., Persichetti, A., Vecchi, F., Ijspeert, A.J., van der Kooij, H., Carrozza, M.C.: Sensing pressure distribution on a Lower-Limb Exoskeleton Physical Human-Machine Interface. Sensors 11, 207–227 (2011)

Dollar, A., Herr, H.: Lower extremity exoskeletons and active orthoses: Challenges and state-of-the-art. IEEE Transactions on Robotics 24(1), 144–158 (2008)

Donati, M., Vitiello, N., De Rossi, S.M.M., Lenzi, T., Crea, S., Persichetti, A., Giovacchini, F., Koopman, B., Podobnik, J., Munih, M., Carrozza, M.C.: A Flexible Sensor Technology for the Distributed Measurement of Interaction Pressure. Sensors 13(1), 1021–1045 (2013)

Edin, B.B., Ascari, L., Beccai, L., Roccella, S., Cabibihan, J.-J., Carrozza, M.C.: Bio-inspired sensorization of a biomechatronic robot hand for the grasp-and-lift task. Brain Research Bulletin 75(6), 785–795 (2008)

Eiber, C.D., Lovell, N.H., Suaning, G.: Attaining higher resolution visual prosthetics: a review of the factors and limitations. Journal of Neural Engineering 10, 11002 (2013)

Ekeberg, Ö., Lansner, A., Grillner, S.: The neural control of fish swimming studied through numerical simulations. Adaptive Behavior 3, 363–384 (1995)

Esquenazi, A., Talaty, M., Packel, A., Saulino, M.: The ReWalk powered exoskeleton to restore ambulatory function to individuals with thoracic-level motor-complete spinal cord injury. American Journal of Physical Medicine and Rehabilitation 91(11), 911–921 (2012)

Fagg, A.H.: A model of muscle geometry for a two degree-of-freedom planar arm, Technical report, University of Massachusetts, [UMI order no: UM-CS- 2003-003] (2000)

Fasoli, S.E., Krebs, H.I., Stein, J., Frontera, W.R., Hogan, N.: Effects of Robotic Therapy on Motor Impairement and Recovery in Chronic Stroke. Archives of Physical Medicine and Rehabilitation 84(4), 477–482 (2003)

Feldman, A.G.: Functional tuning of the nervous system with control of movement or maintenance of steady posture, II: controllable parameters of the muscles. Biophisics 11, 565–578 (1966)

Feldman, A.G.: Once More on the Equilibrium-Point Hypothesis (λ Model) for Motor Control. Journal of Motor Behavior 18(1), 17–54 (1986)

Feys, H.M., De Weerdt, W.J., Selz, B.E., Cox Steck, G.A., Spichiger, R., Vereeck, C.E., Putman, K.D., Van Hoydonock, G.A.: Effect of a therapeutic intervention for the hemiplegic upper limb in the acute phase after stroke. A single-blind, randomized, controlled multicenter trial. Stroke 29(4), 785–792 (1999)

Filippini, R., Sen, S., Bicchi, A.: Toward Soft Robot You Can Depend On. IEEE Robotics and Automation Magazine 15(3), 31–41 (2008)

Flanagan, J.R., Wing, A.M.: The Role of Internal Models in Motions Planning and Control: Evidence from Grip Force Adjustments during Movements of Hand-Held Loads. The Journal of Neuroscience 17(4), 1519–1528 (1995)

Flash, T.: The Control of Hand Equilibrium Trajectories in Multi-Joint Arm Movement. Biological Cybernetics 57, 257–274 (1987)

Frisoli, A., Borelli, L., Montagner, A., Marcheschi, S., Procopio, C., Salsedo, F., Bergamasco, M., Car-boncini, M.C., Tolaini, M., Rossi, B.: Arm rehabilitation with a robotic exoskeleton in Virtual Reality. In: Proc. of IEEE International Conference on Rehabilitation Robotics, Noordwijk, The Netherlands, pp. 631–642 (2007)

Frisoli, A., Salsedo, F., Bergamasco, M., Rossi, B., Carboncini, M.C.: A force-feedback exoskeleton for upper-limb rehabilitation in virtual reality. Applied Bionics and Biomechanics 6(2), 115–126 (2009)

Fukuda, T., Saito, F.: Motion control of a brachiation robot. Robotics and Autonomous Systems 18(1), 83–93 (1996)

Gardner, E.P., Palmer, C.I.: Simulation of motion of the skin. I. Receptive fields and tem-poral frequency coding by cutaneous mechanoreceptors of OPTACON pulses delivered to the hand. J. Neurophysiol. 62, 1410–1436 (1989)

Gomi, H., Kawato, M.: Equilibrium-point control hypothesis examined by measured arm stiffness during multijoint movement. Science 272, 117–120 (1996)

Gomi, H., Kawato, M.: Human arm stiffness and equilibrium-point trajectory during multijoint movement. Biological Cybernetics 76, 163–171 (1997)

Goodwin, A., Morley, J.: Sinusoidal movement of a grating across the monkey's finger-pad: representation of grating and movement features in afferent fiber responses. J. Neurosci. 7, 2168–2180 (1987)

Goodwin, A.W., Morley, J.W., Clarke, C., Lumaksana, B., Darian-Smith, I.: A stimulator for moving textured surfaces sinusoidally across the skin. J. Neurosci. Methods 14, 121–125 (1985)

Grillner, S.: Neurobiological bases of rhythmic motor acts in vertebrates. Science 228(4696), 143–149 (1985)

Grillner, S., Deliagina, T., Ekeberg, O., El Manira, A., Hill, R., Lansner, A., Orlovski, G., Wallen, P.: Neural networks that coordinate locomotion and body orientation in the lamprey. Trends in Neurosciences 18, 270–279 (1995)

Hargrove, L., Simon, A.M., Young, A.J., Lipschutz, R.D., Finucane, S.B., Smith, D.G., Kuiken, T.A.: Robotic Leg Control with EMG Decoding in an Amputee with Nerve Transfers. The New England Journal of Medicine 369, 1237–1242

Hirose, S., Morishima, A.: Design and control of a mobile robot with an articulated body. The International Journal of Robotics Research 9(2), 99–114 (1990)

Hogan, N.: An organizing principle for a class of voluntary movements. Journal of Neuroscience 4, 2745–2754 (1984)

Hogan, N.: Impedance control: an approach to manipulation. Part I: Theory. ASME J. of Dynamic System and Control 107, 1–7 (1985)

Hogan, N.: Impedance control: an approach to manipulation. Part II: Implementation. ASME J. of Dynamic System and Control 107, 8–16 (1985)

Hogan, N.: Impedance control: an approach to manipulation. Part III: Application. ASME J. of Dynamic Systems and Control 107, 17–24 (1985)

Hogan, N., Bizzi, E., Mussa-Ivaldi, F.A., Flash, T.: Controlling multijoint motor behaviour. Exercise and Sport Sciences Reviews 15, 153–190 (1987)

Hurst, J.W., Rizzi, A.A.: Series compliance for an efficient running gait: lessons learned from the electric cable differential leg. IEEE Robot Autom. Mag. 15(3), 42–51 (2008)

Iskakov, R., Albu-Schaeffer, A., Schedl, M., Hirzinger, G., Lopota, V.: Influence of sensor quantization on the control performance of robotics actuators. In: Proc. 2007 IEEE/RSJ International Conference on Intelligent Robots and Systems, San Diego, CA, USA, pp. 1085–1092 (2007)

Jia-Fan, Z., Can-Jun, Y., Ying, C., Yu, Z., Yi-Ming, D.: Modeling and control of a curved pneumatic muscle actuator for wearable elbow exoskeleton. Mechatronics 18, 448–457 (2008)

Johansson, R.S., Birznieks, I.: First spikes in ensembles of human tactile afferents code complex spatial fingertip events. Nature Neuroscience 7(2), 170–177 (2004)

Johnson, K.O., Lamb, G.D.: Neural mechanisms of spatial tactile discrimination: Neural patterns evoked by Braille-like dot patterns in the monkey. J. Physiol. 310, 117–144 (1981)

Johnson, K.O., Phillips, J.R.: A rotating drum stimulator for scanning embossed patterns and textures across the skin. J. Neurosci. Methods 22, 221–231 (1988)

Johnson, K.O., Yoshioka, T.: Neural mechanisms of tactile form and texture perception. In: Nelson, R.J. (ed.) The Somatosensory System: Deciphering the Brain's Own Body Image, pp. 73–101. CRC Press LLC, Boca Raton (2001)

Jones, L.A., Lederman, S.J.: Tactile sensing. In: Jones, L.A., Lederman, S.J. (eds.) Human Hand Function, pp. 44–74. Oxford University Press, New York (2006)

Jutras, D., Bigras, P.: Control of an actuator made of two antagonist McKibben muscles via LMI optimization. In: Proceedings of the IEEE International Symposium on Industrial Electronic, pp. 3072–3077 (2006)

Kapandji, A.: The physiology of the joints – upper limb. Churchill Living-stone, Edinburgh (1982)

Kawamoto, H., Sankai, Y.: Power assist method based on phase sequence and muscle force condition for HAL. Advanced Robotics 19(7), 717–734 (2005)

Kiguchi, K., Tanaka, T., Fukuda, T.: Neuro-fuzzy control of a robotic exoskeleton with EMG signals. IEEE Transactions on Fuzzy Systems 12(4), 481–490 (2004)

Killebrew, J.H., Bensmaia, S.J., Dammann, J.F., Denchev, P., Hsiao, S.S., Craig, J.C., Johnson, K.O.: A dense array stimulator to generate arbitrary spatio-temporal tactile stimuli. J. Neurosci. Methods 161, 62–74 (2007)

Koganezawa, K., Ianba, T., Nakazawa, T.: Stiffness and Angle Control of Antagonistically Driven Joint. In: Proceedings of the IEEE International Conference on Biomedical Robotics and Biomechatronics, pp. 1007–1013 (2006)

Krebs, H.I., Hogan, N., Aisen, M.L., Volpe, B.T.: Robot-Aided Neurorehabilitation. IEEE Transactions on Rehabilitation Engineering 6(1), 75–87 (1998)

Kwakkel, G., Wagenaar, R.C., Twisk, J.W., Lankhorst, G.J., Koetsier, J.C.: Intensity of leg and arm training after primary middle-cerebral-artery stroke: a randomized trial. Lancet 354(9174), 191–196 (1999)

Kyung, K.U., Ahn, M., Kwon, D.S., Srinivasan, M.A.: A compact planar distributed tactile display and effects of frequency on texture judgment. Advanced Robotics 20, 563–580 (2006)

LaMotte, R.H., Friedman, R.M., Lu, C., Khalsa, P.S., Srnivasan, M.A.: Raised object on a planar surface stroked across the fingerpad: responses of cutaneous mechanoreceptors to shape and orientation. J. Neurophysiol. 80, 2446–2466 (1998)

LaMotte, R.H., Whitehouse, G.M., Robinson, C.J., Davis, F.: A tactile stimulator for controlled movements of textured surfaces across the skin. J. Electrophysiol. Tech. 10, 1–17 (1983)

Lauer, R.T., Peckham, P.H., Kilgore, K.L., Heetderks, W.J.: Applications of cortical signals to neuroprosthetic control: a critical review. IEEE Trans. Rehabil. Eng. 8, 205–208 (2000)

Lawrence, M.A., Kitada, R., Klatzky, R.L., Lederman, S.J.: Haptic roughness perception of linear gratings via bare finger or rigid probe. Perception 36, 547–557 (2007)

Lederman, S.J.: The perception of surface roughness by active and passive touch. Bulletin of the Phychonomic Society 18(5), 253–255 (1981)

Lenzi, T., De Rossi, S.M.M., Vitiello, N., Carrozza, M.C.: Proportional EMG control for upper-limb powered exoskeletons. In: Proc. of the 2011 Annual International Conference of the IEEE Engineering in Medicine and Biology Society (EMBC), Boston, USA, pp. 628–631 (2011)

Lenzi, T., De Rossi, S.M.M., Vitiello, N., Carrozza, M.C.: Intention-based EMG Control for Powered Exoskeletons. IEEE Transactions on Biomedical Engineering 59(8), 2180–2190 (2012)

Lenzi, T., De Rossi, S.M.M., Vitiello, N., Chiri, A., Roccella, S., Giovacchini, F., Vecchi, F., Carrozza, M.C.: The neuro-robotics paradigm: NEURARM, NEUROExos, HANDEXOS. In: Proc. of the International Conference of the IEEE Engineering in Medicine and Biology Society (EMBC 2009), Minneapolis, US, pp. 2430–2433 (2009)

Lenzi, T., Vitiello, N., De Rossi, S.M.M., Persichetti, A., GiovacchiniF, R.S., Vecchi, F., Carrozza, M.C.: Measuring Human-Robot Interaction on Wearable Robots: a Distributed Approach. Mechatronics 21(6), 1123–1131 (2011)

Lenzi, T., Vitiello, N., De Rossi, S.M.M., Roccella, S., Vecchi, F., Carrozza, M.C.: NEUROExos: A variable impedance powered elbow exoskeleton. In: Proc. of the 2011 IEEE International Conference on Robotics and Automation (ICRA), Shanghai, China, pp. 1419–1426 (2011)

Lenzi, T., Vitiello, N., McIntyre, J., Roccella, S., Carrozza, M.C.: A robotic model to investigate the human motor control. Biological Cybernetics 105(1), 1–19 (2011)

Libouton, X., Barbier, O., Plaghki, L., Thonnard, J.-L.: Tactile roughness discrimination threshold is unrelated to tactile spatial acuity. Behav. Brain Res. 208(2), 473–478 (2010)

Loizou, P.: Introduction to cochlear implants. IEEE Eng. Med. Biol. Mag. 18(1), 32–42 (1999)

Looft, F.J., Williams, W.J.: On-line receptive field mapping of cutaneous receptors. IEEE Trans. Biomed. Eng. 26, 350–356 (1979)

Lum, P.S., Burgar, C.G., Kenney, D.E., Machiel Van der Loos, H.F.: Quantification of Force Abnormalities During Passive and Active-Assisted Upper-Limb Reaching Movements in Post-Stroke Hemiparesis. IEEE Transactions on Biomedical Engineering 46(6), 652–662 (1999)

Manfredi, L., Assaf, T., Mintchev, S., Marrazza, S., Capantini, L., Orofino, S., AscariL, G.S., Wallén, P., Ekeberg, O., Stefanini, C., Dario, P.: A bioinspired autonomous swim-ming robot as a tool for studying goal-directed locomotion. Biological Cybernetics 107(5), 513–527 (2013)

Marsot-Dupuch, K., Meyer, B.: Cochlear implant assessment: imaging issues. European Journal of Radiology 40, 119–132 (2001)

Mayhew, D., Bachrach, B., Rymer, W., Beer, R.: Development of the MACARM-a Novel Cable Robot for upper Limb Neurorehabilitation. In: Proc. of the IEEE International Conference on Rehabilitation Robotics, Chicago, US, pp. 299–302 (2005)

Mertz, L.: The Next Generation of Exoskeletons: Lighter, Cheaper Devices Are in the Works. IEEE Pulse 3(4), 56–61 (2012)

Micera, S., Carrozza, M.C., Guglielmelli, E., Cappiello, G., Zaccone, F., Freschi, C., Colombo, R., Mazzone, A., Del Conte, C., Pisano, F., Minuto, G., Dario, P.: A Simple Robotic System for Neurorehabilitation. Autonomous Robots 19(3), 271–284 (2006)

Migliore, S.A., Brown, E.A., DeWeerth, S.P.: Biologically inspired joint stiffness control. In: Proceedings of the IEEE international Conference on Robotics and Automation, pp. 4508–4513 (2005)

Mihelj, M., Nef, T., Riener, R.: ARMin II – 7 DoF rehabilitation: mechanics and kinematics. In: Proc. of IEEE International Conference on Robotics and Automation (ICRA), pp. 4120–4125 (2007)

Muhammad, H.B., Recchiuto, C., Oddo, C.M., Beccai, L., Anthony, C.J., Adams, M.J., Carrozza, M.C., Ward, M.C.L.: A capacitive tactile sensor array for surface texture discrimination. Microelectron. Eng. 88, 1811–1813 (2011)

Mussa-Ivaldi, F.A., Hogan, N., Bizzi, E.: Neural, mechanical, and geometric factors subserving arm posture in humans. The Journal of Neuroscience 5, 2732–2743 (1985)

Nakazawa, N., Ikeura, R., Inooka, H.: Characteristics of human fingertips in the shearing direction. Biol. Cybern. 82(3), 207–214 (2000)

Nef, T., Mihelj, M., Riener, R.: ARMin: A robot for patient-cooperative arm therapy. Medical and Biological Engineering and Computing 45(9), 887–900 (2007)

Oddo, C.M., Beccai, L., Felder, M., Giovacchini, F., Carrozza, M.C.: Artificial roughness encoding with a bio-inspired MEMS-based tactile sensor array. Sensors 9, 3161–3183 (2009)

Oddo, C.M., Beccai, L., Muscolo, G.G., Carrozza, M.C.: A biomimetic MEMS-based tactile sensor array with fingerprints integrated in a robotic fingertip for artificial roughness encoding. In: Proc. 2009 IEEE Conference on Robotics and Biomimetics, Guilin, China, pp. 894–900 (2009)

Oddo, C.M., Beccai, L., Vitiello, N., Backlund Wasling, H., Wessberg, J., Carrozza, M.C.: A Mechatronic Platform for Human Touch Studies. Mechatronics 21, 604–613 (2011)

Oddo, C.M., Beccai, L., Wessberg, J., Backlund Wasling, H., Mattioli, F., Carrozza, M.C.: Roughness encoding in human and biomimetic artificial touch: spatiotemporal frequency modulation and structural anisotropy of fingerprints. Sensors 11, 5596–5615 (2011)

Oddo, C.M., Controzzi, M., Beccai, L., Cipriani, C., Carrozza, M.C.: Roughness Encoding for Discrimination of Surfaces in Artificial Active Touch. IEEE Trans. Robot. 27(3), 522–533 (2011)

Pasquero, J., Luk, J., Lévesque, V., Wang, Q., Hayward, V., MacLean, K.E.: Haptically enabled handheld information display with distributed tactile transducer. IEEE Trans. Multimedia 9(4), 746–753 (2007)

Pawluk, D.T.V., Howe, R.D.: Dynamic lumped element response of the human fingerpad. J. Biomech. Eng. 121, 178–183 (1999)

Perry, J.C., Rosen, J., Burns, S.: Upper-Limb Powered Exoskeleton Design. IEEE/ASME Transactions on Mechatronics 12(4), 408–417 (2007)

Pfeifer, R., Iida, F., Bongard, J.: New robotics: design principles for intelligent systems. Artif. Life 11, 99–120 (2005)

Polit, A., Bizzi, E.: Characteristics of motor programs underlying arm movements in monkeys. J. Neurophysiol. 42, 183–194 (1979)

Pons, J.L.: Wearable Robotics: Biomechatronic Exoskeletons. Wiley, New York (2008)

Pons, J.L.: Rehabilitation exoskeletal robotics. The promise of an emerging field. IEEE Engineering in Medicine and Biology Magazine 29, 57–63 (2010)

Popovic, D., Sinkjaer, T.: Control of movement for the physically disabled. Springer (2000)

Potkonjak, V., Popovic, M., Lazarevic, M., Sinanovic, J.: Redundancy Problem in Writing: From Human to Anthropomorphic Robot Arm. IEEE Transactions on Systems, Man, And Cybernetics-Part B: Cybernetics 28(6), 790–805 (1998)

Pratt, G., Williamson, M.M.: Series elastic actuators. In: Proceedings of the IEEE International Conference on Intelligent Robot and Systems, pp. 339–406 (1995)

Prescott, T.: Vibrissal behaviour in rodents and marsupials. Lecture at the Theo Murphy meeting on Active Touch Sensing. Chicheley Hall, Buckinghamshire (January 31, 2011)

Radwin, R., Jeng, O., Gisske, E.: A new automated tactility test instrument for evaluating hand sensory function. IEEE Transactions on Rehabilitation Engineering 1, 220–225 (1993)

Reinkensmeyer, D.J., Takahashi, C.D., Timoszyk, W.K., Reinkensmeyer, A.N., Kahn, L.E.: Design of robot assistance for arm movement therapy following stroke. Advanced Robotics 14(7), 625–637 (2001)

Rocon, E., Belda-Lois, J.M., Ruiz, A.F., Manto, M., Moreno, J.C., Pons, J.L.: Design and Validation of a Rehabilitation Robotic Exoskeleton for Tremor Assessment and Suppression. IEEE Transactions on Neural Systems and Rehabilitation Engineering 15(3), 367–378 (2007)

Romo, R., Ruiz, S., Crespo, P., Hsiao, S.S.: A tactile stimulator for studying motion processing in the somatic sensory system of primates. J. Neurosci. Methods 46, 139–146 (1993)

Ronsse, R., Vitiello, N., Lenzi, T., van den Kieboom, J., Carrozza, M.C., Ijspeert, A.J.: Human-robot synchrony: flexible assistance using adaptive oscillator. IEEE Transactions on Biomedical Engineering 58(4), 1001–1012 (2011)

Ronsse, R., Vitiello, N., Lenzi, T., van den Kieboom, J., Carrozza, M.C., Ijspeert, A.J.: Adaptive oscillators with human-in-the-Loop: Proof of concept for assistance and rehabilitation. In: Proc. of the 2010 3rd IEEE RAS and EMBS International Conference on Biomedical Robotics and Biomechatronics (BIOROB), Tokyo, Japan, pp. 668–674 (2010)

Sanchez, R.J., Liu, J., Rao, S., Shah, P., Smith, R., Rahman, T., Cramer, S.C., Bobrow, J.E., Reinkensmeyer, D.J.: Automating Arm Movement Training Following Severe Stroke: Functional Exercises With Quantitative Feedback in a Gravity-Reduced Environment. IEEE Transactions on Neural Systems and Rehabilitation Engineering 14(3), 378–389 (2006)

Sanchez, R.J., Wolbrecht, E., Smith, R., Liu, J., Rao, S., Cramer, S., Rahman, T., Bobrow, J.E., Reinken-meyer, D.J.: A Pneumatic Robot for Re-Training Arm Movement after Stroke: Rationale and Mechanical Design. In: Proc. of the IEEE International Conference on Rehabilitation Robotics (ICORR), pp. 500–504 (2005)

Schaal, S., Sternad, D.: Origins and violations of the 2/3 power law in rhythmic three-dimensional arm movements. Exp. Brain Res. 136, 60–72 (2001)

Schiavi, R., Grioli, G., Sen, S., Bicchi, A.: VSA-II: a novel prototype of variable stiffness actuator for safe and performing robots interacting with humans. In: Proc. of the IEEE International Conference on Robotics and Automation, pp. 2171–2176 (2008)

Schiele, A., van der Helm, F.C.: Kinematic Design to Improve Ergonomics in Human Machine Interaction. IEEE Transaction on Neural Systems and Rehabilitation Engineering 14(4), 456–469 (2006)

Schneider, W., Slugg, R.M., Turnquist, B.P., Meyer, R.A., Campbell, J.N.: An electromechanical stimulator system for neurophysiological and psychophysical studies of pain. J. Neurosci. Methods 60, 61–68 (1995)

Serina, E.R., Mote, C.D., Rempel, D.: Force response of the fingertip pulp to repeated compression – effects of loading rate, loading angle and anthropometry. J. Biomech. 30(10), 1035–1040 (1997)

Simmons, F.B., Epley, J.M., Lummois, R.C.: Auditory nerve: electrical stimulation in man. Science 148, 104–106 (1965)

Smith, A.M., Chapman, C.E., Deslandes, M., Langlais, J.-S., Thibodeau, M.-P.: Role of friction and tangential force variation in the subjective scaling of tactile roughness. Exp. Brain Res. 144, 211–223 (2002)

Spelman, F.A.: The past, present, and future of cochlear prostheses. IEEE Eng. Med. Biol. Mag. 18(3), 27–33 (1999)

Spigler, G., Oddo, C.M., Carrozza, M.C.: Soft-neuromorphic artificial touch for applications in neuro-robotics. In: Proc. 2012 IEEE RAS/EMBS International Conference on Bio-Medical Robotics and Biomechatronics, Roma, Italy, pp. 1913–1918 (2012)

Stefanini, C., Orlandi, G., Menciassi, A., Ravier, Y., La Spina, G., Grillner, S., Dario, P.: A Mechanism for Biomimetic Actuation in Lamprey-like Robots. In: Proc. of the IEEE/RAS-EMBS International Conference on Biomedical Robotics and Biomechatronics, pp. 579–584 (2006)

Stein, R.B., Peckham, P.H., Popovic, D.P.: Neural prosthesis. Oxford University Press (1992)

Sternad, D., Schaal, S.: Segmentation of endpoint trajectories does not imply segmented control. Exp. Brain Res. 124, 118–136 (1999)

Stienen, A., Hekman, E., Van der Helm, F., Prange, G., Jannink, M., Aalsm, A., Van der Kooij, H.: Freebal: Dedicated gravity compensation for the upper extremities. In: Proc. of the International Conference on Rehabilitation Robotics, Noordwijk, The Netherlands, pp. 804–808 (2007)

Stienen, A., Hekman, E., Van Der Helm, F.T.H., Prange, G., Jannink, M., Aalsma, A., Van Der Kooij, H.: Dampace: dynamic force-coordination trainer for the upper extremities. In: Proc. IEEE 10th Int. Conf. Rehabi. Robot, Noordwijk, pp. 820–826 (2007)

Stienen, A.H.A., Hekman, E.E.G., ter Braak, H., Aalsma, A.M.M., van der Helm, F.C.T., van der Kooij, H.: Design of a rotational hydro-elastic actuator for a powered exoskeleton for up-per-limb rehabilitation. IEEE Transactions on Biomedical Engineering, accepted for future publication (2009)

Stienen, A.H.A., Hekman, E.E.G., van der Helm, F.C.T., van der Kooij, H.: Self-Aligning Exoskeleton Axes Trough Decoupling of Joint Rotations and Translations. IEEE Transactions on Robotics 25(3), 628–633 (2009)

Summers, I.R., Chanter, C.M.: A broadband tactile array on the fingertip. J. Acoust. Soc. Am. 112, 2118–2126 (2002)

Sup, F., Bohara, A., Goldfarb, M.: Design and Control of a Powered Transfemoral Prosthesis. The International Journal of Robotics Research 27(2), 263–273 (2008)

Tondu, B., Ippolito, S., Guiochet, J., Daidie: A Seven-degree-of-freedom Robot-arm Driven by Pneumatic Artificial Muscle for Humanoid Robots. The International Journal of Robotic Research 24(4), 257–274 (2005)

Tsagarakis, N.G., Caldwell, D.G.: Development and Control of a 'Soft-Actuated' Exo-skeleton for Use in Physiotherapy and Training. Autonomous Robots 15, 21–23 (2003)

Vallery, H., Veneman, J., Van Asseldonk, E., Ekkelenkamp, R., Buss, M., Van Der Kooij, H.: Compliant actuation of rehabilitation robots. IEEE Robot. Autom. Mag. 15(3), 60–69 (2008)

Van Damme, M., Verrelst, B., Van Ham, R., Daerden, F., Lefeber, D.: Proxy-based sliding mode control of a planar pneumatic manipulator. Int. J. Robot. Res. 28, 266–284 (2009)

Van Ham, R., Vanderborght, B., Van Damme, M., Verrelst, B., Lefeber, D.: MACCEPA, the mechanically adjustable compliance and controllable equilibrium position actuator: design and implementation in a biped robot. Robot. Auton. Syst. 55(10), 761–768 (2007)

Vanderborght, B., Van Ham, R., Lefeber, D., Sugar, T.G., Hollander, K.: Comparison of mechanical design and energy consumption of adaptable, passive-compliant actuators. Int. J. Robot. Res. 28, 90–103 (2009)

Velliste, M., Perel, S., Spalding, M.C., Whitford, A.S., Schwartz, A.B.: Cortical control of a prosthetic arm for self-feeding. Nature 453, 1098–1101 (2008)

Velliste, M., Perel, S., Spalding, M.C., Whitford, A.S., Schwartz, A.B.: Cortical control of a prosthetic arm for self-feeding. Nature 453(7198), 1098–1101 (2008)

Veneman, J.F., Ekkelenkamp, R., Kruidhof, R., van der Helm, F.C.T., van der Kooij, H.: A Series Elastic- and Bowden-Cable-Based Actuation of Use Torque Actuator in Exoskeleton-Type Robots. The International Journal of Robotics Research 25(3), 261–281 (2006)

Vidal-Verdú, F., Hafez, M.: Graphical tactile displays for visually-impaired people. IEEE Transactions on Neural Systems and Rehabilitation Engineering 15, 119–130 (2007)

Vitiello, N., Cattin, E., Roccella, S., Giovacchini, F., Vecchi, F., Carrozza, M.C., Dario, P.: The NEURARM towards a Platform for Joint Neuroscience on Human Motion Control Theories. In: Proc. of the 2007 IEEE International Conference on Intelligent Robots and Systems (IROS 2007), San Diego, CA, USA, pp. 1852–1857 (2007)

Vitiello, N., Lenzi, T., De Rossi, S.M.M., Roccella, S., Carrozza, M.C.: A sensorless torque control for Antagonistic Driven Compliant Joints. Mechatronics 20, 355–367 (2010)

Vitiello, N., Lenzi, T., McIntyre, J., Roccella, S., Cattin, E., Vecchi, F., Carrozza, M.C.: Charac-terization of the NEURARM bio-inspired joint position and stiffness open loop controller. In: Proc. of the 2008 IEEE International Conference on Biomedical Robotics and Biomechatronics (BIOROB 2008), Scottsdale, Az, USA, pp. 138–143 (2008)

Vitiello, N., Lenzi, T., Roccella, S., De Rossi, S.M.M., Cattin, E., Giovacchini, F., Vecchi, F., Carrozza, M.C.: NEUROExos: A Powered Elbow Exoskeleton of Physical Rehabilitation. IEEE Transactions on Robotics 29(1), 220–235 (2013)

Von Gierke, H.E., Keidel, W.D., Oestreicher, H.L.: AGARD Conference Proceedings 44: Principles and Practice of Bionics. In: AGARD Conference Proceedings, Slough, U.K., vol. 44, pp. 371–387 (1970)

Wagner, C.R., Lederman, S.J., Howe, R.D.: A tactile shape display using RC Servomotors. In: Proc. 2002 IEEE Symposium on Haptic Interfaces for Virtual Environment and Teleoperator Systems, Orlando, USA, pp. 354–355 (2002)

Wheat, H.E., Salo, L.M., Goodwin, A.W.: Human ability to scale and discriminate forces typical of those occurring during grasp and manipulation. J. Neurosci. 24, 3394–3401 (2004)

Wolpert, D.M., Ghahramani, Z., Jordan, M.I.: An Internal Model for sensorimotor integration. Science 269(5232), 1880–1882 (1995)

Wolpert, D.M., Miall, R.C., Kawato, M.: Internal models in the cerebellum. Trends in Cognitive Sciences 2(9), 338–347 (1999)

Yoshioka, T., Gibb, B., Dorsch, A.K., Hsiao, S.S., Johnson, K.O.: Neural coding mechanisms underlying perceived roughness of finely textured surfaces. J. Neurosci. 21, 6905–6916 (2001)

Zollo, L., Eskiizmirliler, S., Teti, G., Laschi, C., Burnod, Y., Guglielmelli, E., Maier, M.A.: An anthropomorphic Robotic Platform for Progressive and Adaptive Sensorimotor Learning. Advanced Robotics 22, 91–118 (2008)

Recent Development and Trends of Clinical-Based Gait Rehabilitation Robots

Kin Huat Low

School of Mechanical and Aerospace Engineering, Nanyang Technological University
50 Nanyang Avenue, Singapore 639798, Singapore
mkhlow@ntu.edu.sg

1 Background

Loss of motor and sensory ability is frequently encountered by people with arthritis, stroke, trauma resulting in brain injuries or spinal cord injury (SCI), or other neurological diseases [1]. Walking impairments have an impact on subjects in terms of decreased self-independence and quality of life. Moreover, people with motor disabilities become a great burden on their families and healthcare units [2]. In order to regain normal lower-limb function as much as possible, gait rehabilitation such as locomotion training is commonly employed as therapy.

The key to gait recovery from a clinical perspective is neuroplasticity. Neuroplasticity is an adaptive change in brain structure in response to a change in environment over time with a consequent change in function [3-5]. For example, walking disabilities are commonly encountered after spinal cord injury (SCI) [6, 7]. These locomotion disorders are attributed to neuronal circuitry being cut off within the spinal cord [8]. Various gait recovery approaches via training programs have been proposed in recent years [9-13]. The correlations between environment, adaptation, and function are fundamental to recover gait function after injury. Table 1 summaries the major factors related to the gait disorders, training, and assessment.

Manual-assisted gait rehabilitation is commonly used to tackle the issues listed in Table 1. As shown in Figure 1, manual training procedures might require about three therapists to lift, support, and assist a subject. In addition to providing body-weight support to prevent the subject from falling, therapists need to manually facilitate the movement for the lower limb to simulate a walking pattern with a proper posture. The therapists have to concurrently support subject's body weight and facilitate propulsion of the legs. Therefore, the whole training session is labour-intensive. Moreover, the training procedures are exhausting for all concerned and the outcomes might be inconsistent. Due to high labor cost and the shortage of skilled therapists, few subjects can afford and benefit from such a manual-assisted therapy. Also, the number of clinical visits for gait rehabilitation training is limited and therefore insufficient for any effective rehabilitation training.

S. Mohammed et al. (eds.), *Intelligent Assistive Robots*,
Springer Tracts in Advanced Robotics 106, DOI: 10.1007/978-3-319-12922-8_2

Table 1. Brief Summary of Factors Related to Gait Rehabilitation [14]

	Major Factors
Common Gait Disorders	Hip-hiking, circumduction (swing leg out to the side), trunk lean to the side or back, foot drag/slap, knee-lock, flexed, shuffling, vaulting (to clear the weak leg), veering to one side, etc.
Major Causes of Gait Disorders	SCI, stroke, Parkinson's disease, etc.
Guideline for Effective Gait Training	Repetitive, intensive, goal-orientated, functional, massed, active.
Balance and Gait Assessment	Gait observation analysis, 6 mins walk, 10 meters walk, ambulation index (AI), dynamic gait index (DGI), time up and go (TUG), functional reach test, berg balance test (BBT), Tinetti gait and balance assessment.

(a)

(b)

(c)

Fig. 1. Clinical gait rehabilitation: (a) Subject walk with help of a walker [15]; (b) Physical therapists help subject to walk on a treadmill with a body weight support system for off-loading body weight burden [16]; (c) Therapists carefully help the subject with trunk control [17]

2 Gait Deficit of Stroke and SCI Subjects

The level of gait deficit depends on the severity of the muscle and sensory disability, and the lower limb muscle and sensory affected by the illness. In general, stroke subject usually suffers disability on one side of the body, either left or right side. As for complete SCI subjects, gait disabilities are usually symmetry for both lower limbs. Muscle and sensory of lower limb affected by SCI depends on the level of spinal cord

injured. Incomplete SCI may exhibit a complex gait deficit, depending on how much the spinal cord is injured.

As depicted in Figure 2, a clinical-based gait rehabilitation program normally covers five major functions: (1) enhancing muscle force, (2) maintaining balance control, (3) training of gait locomotion, including exercises for leg-propulsion and body weight support (BWS), (4) providing pelvic control, and (5) assisting locomotion activities of daily living (ADL) [18].

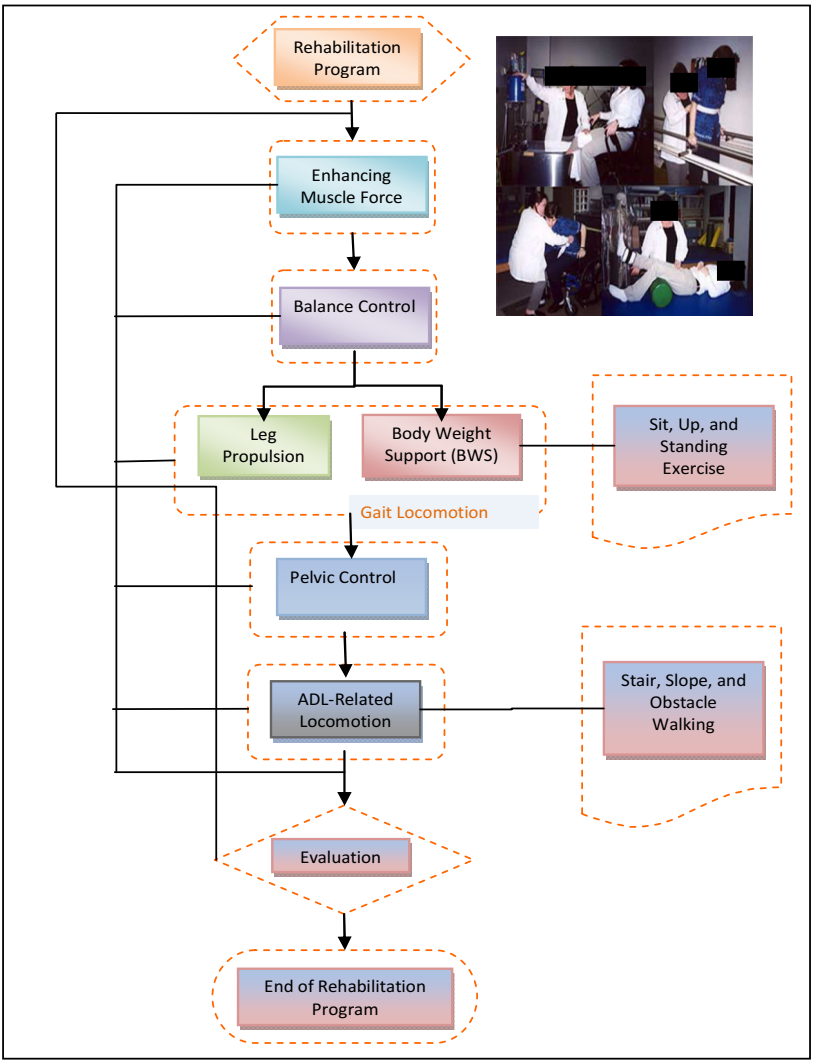

Fig. 2. Process of clinical-based gait rehabilitation [14]

The advances in robotics and sensor technology have helped in the development of robotics rehabilitation gait systems, which can contribute to the fields of neuro-rehabilitation [18-24]. There are various robotic therapies available to stimulate muscle activity pattern effectively with little supervision from therapists [25]. As shown in Figure 3, robotic-assisted gait rehabilitation covers four major fields of study: design of robotic system, generation of gait pattern, control strategy, and bio-feedback and clinical assessment. As a consequence, the research scope and requirement for OGW rehabilitation training for subject groups without trunk control [26] is shown in Figure 4.

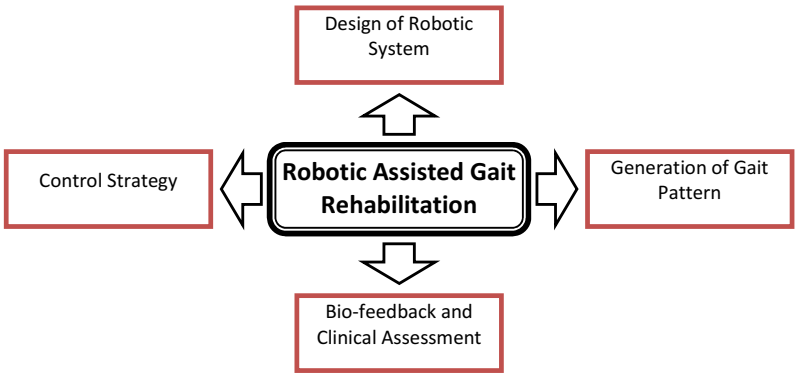

Fig. 3. Four major fields of study of robotic assisted gait rehabilitation [14, 27]

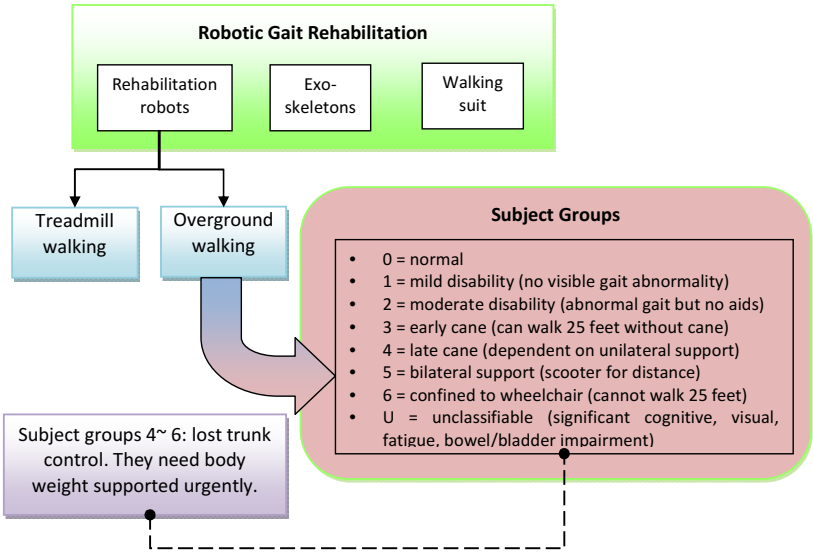

Fig. 4. Development of gait rehabilitation robots for various subject groups [14]

It is necessary to provide body weight supported and locomotion propulsion at the same time. The drawback of gait robots operated with partial body weight support on treadmill is that the majority of treadmills available commercially do not provide appropriate speeds for subjects [25]. Moreover, a stroke subject with hemi-paralysis might have time-variance gait as well as unequal step durations for left and right legs, which are impossible to be covered in treadmill training. Furthermore, the muscular activation pattern between overground walking (OGW) and treadmill walking are slightly different [28].

Only few studies [20] considered the control of pelvic motions [29]. However, doctors and therapists have emphasized the importance of pelvic posture and its role in coordinating normal walking. There is therefore a need to design an overground training robot with pelvic control and active assistance to the lower limb [30]. Possible research areas contributed to the overground gait training robots is presented in Figure 5.

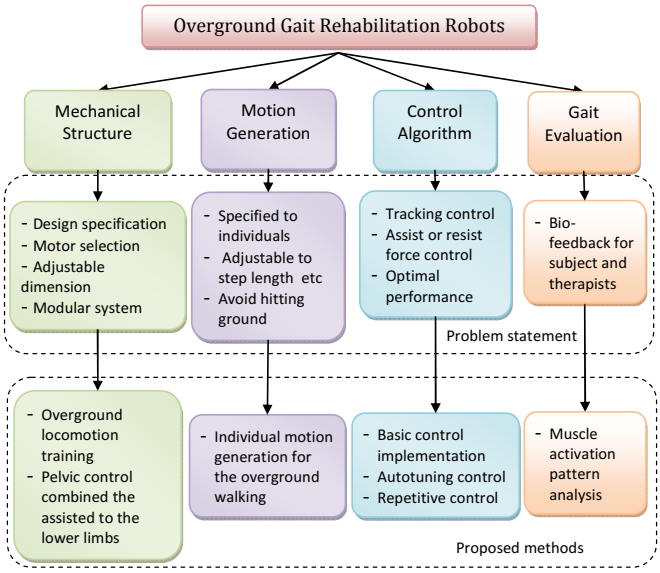

Fig. 5. Scope and requirement for the overground walking rehabilitation robots [14]

3 State-of-the-Art in Gait Robots

As previously mentioned, physical rehabilitation is essential for gait recovery. Unfortunately, limits of rehabilitation sessions and shortages of therapists cannot satisfy the demand of rehabilitation, which might result in compromising recovery. Robotics rehabilitation has recently been suggested to integrate with conventional manual rehabilitation to tackle the issues. In this regards, the rehabilitation robots can be

divided into two categories: treadmill-based rehabilitation robots and overground walking (OGW) rehabilitation robots.

Body weight supported treadmill training was first invented for walking training on a treadmill. Subsequently, there are other progression approaches on walking environment, footplate and overground, made available on robotic gait rehabilitation. The difference between overground and treadmill walking has been studied in many works. Some concluded that no clear different are found between overground and treadmill walking [31]. In contrast, some studies concluded that there is difference between overground and treadmill walking. Differences are found in term of spatial-temporal gait parameters [32], thorax and pelvis movement [33], joint kinematics, and muscle activation. In general, a faster cadence and shorter stride length tends to be used by normal subjects on the treadmill than during the overground walking [34]. The details of the comparison between overground and treadmill walking are available references [32-38]. There have been positive views on the acceptance of treadmill-based gait rehabilitation [31, 32]. Nevertheless, it is noteworthy that the ultimate goal of gait rehabilitation is to return the subject to overground walking, instead of walking on a treadmill. The treadmill-based rehabilitation may not be effective because the walking on a moving belt is not ecological [39]. Moreover, overground walking is the mode that a person moves from one location to another. A treadmill is a machine designed for walking while staying in one place. Practicing gait in functional overground contexts, as opposed to that on treadmills, is widely recommended [40].

Various types of gait robots have been developed for difference purposes. The robots include (a) Rehabilitation robots: Lokomat [24], LOPES [41], ALEX [42] providing treadmill walking training (see Figure 6); *NaTUre-gaits* [18], WalkTrainer [20], KineAssist [22] based on overground walking training (see Figure 7); (b) Performance-augmenting exoskeletons: BLEEX [43], NTU-LEE [44], HAL [19, 45] (see Figure 8); (c) Walking suits: e-Legs [46], ReWalk [47], REX [48], Honda Leg [49] (see Figure 9). A comparison on the parameters of these robotic devices is listed in Table 2.

Fig. 6. Treadmill-based rehabilitation robotst: (a) Lokomat system with subjects [24]; (b) LOPES [41]; (c) ALEX [42]

(a) (b) (c)

Fig. 7. Overground walking (OGW) rehabilitation robots: (a) a SCI subject walks with NaTUre-gaits [18]; (b) WalkTrainer [20]; (c) KineAssist [22]

(a) (b) (c)

Fig. 8. Performance-augmenting exoskeletons: (a) BLEEX [43]; (b) NTU-LEE [44]; (c) HAL-5 [45]

(a) (b) (c) (d)

Fig. 9. Walking suits: (a) eLegs [46]; (b) ReWalk [47]; (c) REX [48], (d) Honda leg [49]

Table 2. Comparisons of Rehabilitation Robots, Performance-augmenting Exoskeletons and Walking Suits [14]

		Parameters	Rehabilitation Robots					Performance-augmenting Exo-skeletons			Walking Suits				
	Joints	**Biological Limb**	***Loco co-mat***	***Nature-gaits***	***WalkTrainer***	***ALEX***	***LOPES***	***BLEEX***	***HAL-5***	***NTU-LEE***	***eLegs***	***MIT Medical Exoskeleton***	***ReWalker***	***REX***	***Honda Leg***
Degrees of freedom	Pelvis	6	N/A	5	N/A	3	N/A	N/A	N/A	N/A	N/A	N/A	N/A	N/A	N/A
	Hip	3	1	1	3	2	2	3	3	2	1	2	2	3	2
	Knee	2	1	1	1	1	1	1	1	1	1	1	1	1	1
	Ankle & Foot	4	N/A	3	3	1	N/A	4	1	1	1	1	N/A	2	3
Range of motion (deg)	Hip	140/15[a] 40/30-35[b] 15-30/60[c]	N/A	50/15	N/A	40/40[a]	60/30 15/15	121/10[a] 16/16[b] 35/35[c]	115 [a]	140/15[a] 40/30-35[b] 15-30/60[c]	N/A	N/A	N/A	N/A	N/A
	Knee	120-140/0-10[a]	N/A	80/0	N/A	45-60/0	90/0	121/0[a]	97 [a]		N/A	N/A	N/A	N/A	N/A
	Ankle & Foot	40-50/20[a] 30-35/15-20	N/A	10/20	N/A	N/A	N/A	45/45[a] 20/20	N/A	140/15[a]	N/A	N/A	N/A	N/A	N/A
Torque (Nm)	Hip	140/120[a]	N/A	31[a]	N/A	50[a]	65 30	150/120[a]	N/A	118	N/A	N/A	N/A	N/A	N/A
	Knee	140/15[a]	N/A	35.2[a]	N/A	50[a]	65	100/120[a]	N/A	118	N/A	N/A	N/A	N/A	N/A
	Ankle & Foot	165[a]	N/A	132[a]	N/A	N/A	N/A	200/150[a]	N/A	118	N/A	N/A	N/A	N/A	N/A

a. Flexion/Extension b. Adduction/Abduction c. Internal/External d. Inversion/Eversion

4 Engineering-Clinical Consideration: Gait Rehabilitation Systems

The previous section provides a general review of the robotic gait rehabilitation system. This section will discuss about the principles and features suggested for the robotic gait rehabilitation viewing from the clinical perspective.

4.1 Three Principles of Gait Rehabilitation and Robotic Gait Rehabilitation Systems

The principles of rehabilitation training are summarized and a comparison between manual-assisted and robotic-assisted gait rehabilitation are presented in Table 3, in which

Table 3. Comparisons of Manual-assisted and Robotic-assisted Gait Rehabilitation [14]

Principles of rehabilitation	*Manual-assisted Rehabilitation*	*Robotic-assisted Rehabilitation*
Intensity of practice	Low; due to physical limitation of therapists	High; since motorized machine do not get tired
Effect of participation	High; subject will participate actively	Low; if subject remain totally passive during training
Independence of participation	Low; therapist limit participation of subject for the sake of safety	High; wide range of motion (ROM) with body weight supported by mechanical structure
Specificity of training (*locomotion guidance*)	Less specifics; therapist not able to properly guide on the motion	High specific; machine can control the motion precisely
Assessment and evaluation	Less frequently conducts when charge in/out by experienced therapists	High frequently involved advanced sensory for more prompt and accurate biofeedback
Duration of training	Short training time; due to limited manpower	High; machine can insist repetitive training
Costs	High; paying therapist manpower hours	High; machine setup cost and usage cost
Risk of fall	Low; over-constrained manual assisted for body weight support	Low; with mechanical support of body weight

possible benefits for the robotics rehabilitation are demonstrated. The principles listed in Table 3 can further be grouped into three main goals; practice, specificity, and effort [41, 50]. These goals are also the principles of gait rehabilitation to verify and justify the effectiveness of robotic gait rehabilitation systems, with the therapist assisted body weight supported (BWS) treadmill training used as the benchmark.

Based on the principle on specificity, body weight supported robotic gait rehabilitation systems should be developed to facilitate the gait rehabilitation. As outlined in Figure 10, three elements are required for gait training: (1) balance, (2) reciprocal stepping, and (3) body weight shifting [17]. Balance and reciprocal stepping are the essential elements highlighted for gait locomotion [51, 52]. Balance requires maintaining the equilibrium during the entire walking process, reciprocal stepping consists of lower limb and pelvic motions, while body weight shifting is the shifting of body weight, from the previous supporting leg to next supporting leg, to facilitate the swing phase of supporting legs [53].

Figure 10 also compares therapist-assisted and robotic-assisted schemes in terms of the three principles of gait rehabilitation. For example, the robotic system is capable of executing pre-defined trajectories precisely. Therefore, the gait locomotion is able to be induced by robotic system precisely on the subject. In contrast, the gait locomotion provided by therapist has significant deviation [54], which is considered as poorly controlled. Pelvic motion is marked as limited control for robotic systems, due to the constraint of the pelvic motion by the body weight support apparatus. Body weight shifting is widely available on therapist assisted body weight supported gait rehabilitation.

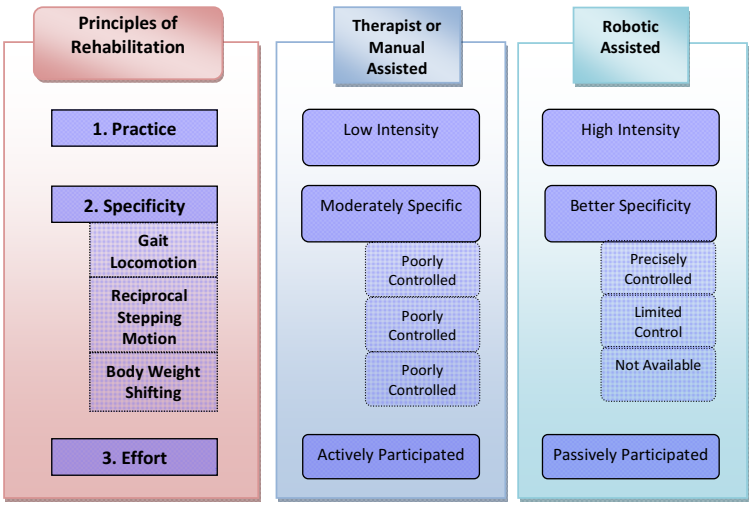

Fig. 10. Comparisons of therapist and robotic assisted body weight supported gait rehabilitation for three principles of gait rehabilitation [27, 55]

The major weakness of robotic system is the lack of interaction with the subject. The subject can remain totally passive during the process of robotic-assisted rehabilitation. The greatly reduced the effort of participation of the subject. In comparison, therapist is able to interact with the subject throughout the process of rehabilitation. Although the active participation is being considered in the research of robotic rehabilitation systems, but the therapist input and interaction in this area is not easily replaced and the total replacement is not desirable [56].

In order to gain an insight of the ability and limitation of the existing robotic gait rehabilitation systems in providing the functional walking, the three required elements for gait training are further discussed: (1) balance by maintaining equilibrium during locomotion, (2) reciprocal stepping, and (3) body weight shifting.

The balance of the subject during gait rehabilitation is maintained by the harness of body weight support apparatus suspending the subject [57]. The trunk of the subject is kept upright during gait rehabilitation by the harness. Alternatively, the balance can be actively controlled by keeping center of mass (COM) within the support polygon. As for the reciprocal stepping, it consists of lower limb and pelvic motion. Reciprocal stepping of the lower limb received the most attention in the field of robotic assisted gait rehabilitation.

Robotic lower limb orthosis is a module commonly required in robotic gait rehabilitation systems, provides the assistance to complete the reciprocal stepping of lower limb, while the pelvic motions are assisted by robotic gait rehabilitation system with the incorporation of pelvic mechanisms. The following section provides a brief review on the three common modules found in robotic gait rehabilitation systems. They are (i) lower limb orthosis for reciprocal stepping, (ii) unit to provide support body weight and balance control, and (iii) pelvic mechanism for pelvic motion assistance.

4.2 Lower Limb Orthosis (for Reciprocal Stepping)

Robotic lower limb devices have been developed to provide the reciprocal stepping assistance to the subject during the robotic assisted gait rehabilitation. Some examples of recent developed lower limb systems are shown in Figure 11 for treadmill-based systems and Figure 12 for overground systems.

Fig. 11. Robotic orthosis of treadmill-based systems, from left to right, ALEX [58], Lokomat [59], LOPES [60], and POGO [61]

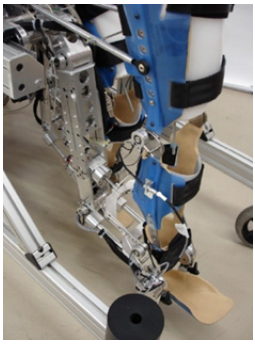

Fig. 12. Robotic orthosis, from left to right, WalkTrainer (overground-based system) [62], and footplate of Haptic Walker (footplate-based system) [63]

Among the treadmill based systems, ALEX is developed with DC motor actuated hip and knee joints (total of four degrees of freedom). Robotic orthosis of ALEX is equipped with more passive joints as compared to Lokomat. The robotics orthosis [64] provides passive movement for abduction and adduction of hip joint, plantarflexion and dorsiflexion of ankle joint, and limited inversion-eversion of ankle joint. Similarly, Lokomat uses DC motor to power their robotic orthosis, providing actuation to the hip and knee joints (total of four degrees of freedom). The actuation is provided in the sagittal plane. To prevent foot drop issue during swing phase, the subject's feet are suspended with elastic band. As for the lower extremity powered exoskeleton (LOPES), it consists of joints actuated with series elastic actuators. Actuator is detached from the exoskeleton, by transmitting the power of actuator to the intended joint via Bowden cable. LOPES has eight degrees of freedom [65], which include (1) forward/backward movement of the pelvis, (2) horizontal movement of the pelvis, (3) abduction and adduction of hip joint, (4) flexion and extension of hip joint, (5) flexion and extension of knee joint. Pneumatically operated gait orthosis (POGO) consists of two pneumatic cylinders for the motion assistance of one side of the leg. Flexion and extension of hip and knee joints are actuated [66]. It is designed to work in conjunction with Pelvic Assist Manipulator (PAM).

The WalkTrainer incorporates a pair of leg orthoses to provide lower limb motion assistance. The motion assistance is provided to thigh (flexion and extension of hip joint), shank (flexion and extension of knee joint), and foot (plantarflexion and dorsiflexion of ankle joint) in the sagittal plane [62]. Passive joint is made available for the inversion and eversion movement of the ankle joints. With a different approach, HapticWalker provide reciprocal stepping for rehabilitation using footplate. Instead of moving the thigh and shank of the subject, HapticWalker induces the gait locomotion through ankle. Two robotic arms, each with three degrees of freedom, are used to provide the desire motion for the footplates. The footplate can move in the sagittal plane, while rotates with respect to the axis perpendicular to the sagittal plane.

4.3 Units of Body Weight Support

The unit providing body weight support (BWS) is another essential module in gait rehabilitation system. As depicted in Figure 13, BWS methods in gait rehabilitation system can be classified as cable-harness body weight support (cBWS) and structural body weight support (sBWS). To offload the subject's body weight, the harness system is connected to a counterpoise system through cable. Cable-harness BWS is the common body weight support method found in most of the gait rehabilitation systems, for example, Lokomat [67], POGO [61], WalkTrainer [62], and Haptic Walker [63]. In contrast, the method of sBWS uses an extended holding framed mechanism to support the subject's body weight by holding either at the waist level or at the back. The concept of sBWS is less popular compared to cBWS. *NaTUre-gaits* [18] are KineAssist [40] are the rehabilitation systems applying the scheme of sBWS.

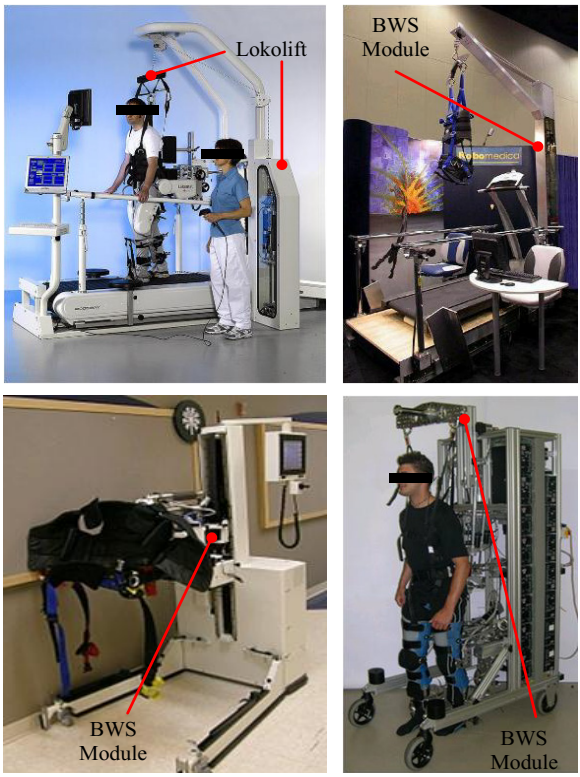

Fig. 13. Body Weight Support Module, from left to right, Lokolift [67], POGO (produced by Robomedica Inc., POGO is not shown in the photo) [68], KineAssist [69], and WalkTrainer [62]

4.4 Pelvis Motion Provision (with Pelvic Orthosis)

Being the mobile link between the two lower limbs, pelvic allows the swing to be initiated since the pelvic lateral displacement allows the center of mass and body mass to transfer to the stance foot, thus allowing the contra lateral foot to swing [70, 71]. In addition to allowing the transferring of forces from the lower extremities to the trunk, pelvic contributes to the forward progression of the body and to the vertical support of trunk [72]. The pelvic motion significantly affects human's gait. The lack of pelvic control on subject will result in alteration of gait pattern, which should be avoided [73].

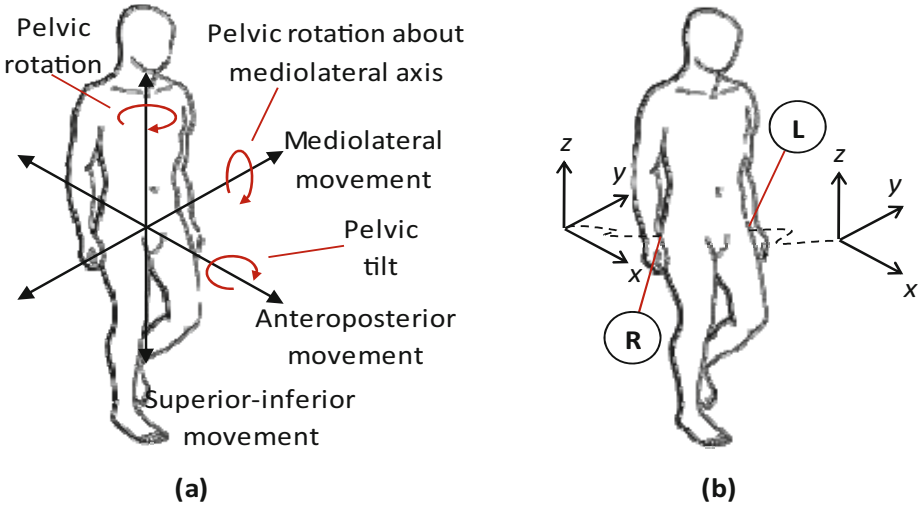

Fig. 14. (a) Movement definition of the pelvis, (b) Coordination assignment for left side (indicated by L) and right side (indicated by R) of the pelvis [27]

In general, pelvis can be modeled as a system with six DoFs, as depicted in Figure 14. The pelvic motion consists of translational and rotational movements: (1) three translational movements consist of mediolateral movement (left/right), anteroposterior movement (front/back), and superior-inferior (up/down) movement; (2) the rotational movements are pelvic rotation, pelvic tilt, and pelvic rotation about mediolateral axis. During gait locomotion, the pelvic rotates at transverse axis, tilts at frontal plane, and shifts laterally.

One of the useful considerations in gait rehabilitation research is the controllable pelvic motion for natural walking. Moreover, it is desired to provide unrestricted pelvic motion guidance, in order to encourage the training of body weight shifting. Therefore, there is a need to develop other body weight support approaches. Any body weight support approach should provide the pelvic movement as much as possible. As an alternate design, the method of overground walking provides a much more physiological resembled walking environment.

The implementation of natural pelvic control on the robotic gait system with cBWS is limited. For example, PAM and WalkTrainer provide the relatively complete DoFs to achieve pelvic movement for walking. However, the full potential of these systems are limited by the module of body weight support. LOPES provide partial actuated assistance and passive movement for pelvic movement. Alex, Lokomat, KineAssist, and HapticWalker do not provide any actuated assistance to the pelvic motion throughout the gait rehabilitation process.

5 Brief Review of Control Strategies for Robotic Gait Rehabilitation

Studies have also shown that passive guidance during practice of a voluntary motor task is less effective in enhancing motor learning than that by an unrestricted practice [74-76]. In addition, for subjects who are unable or too weak to perform voluntary movements, passive movements in functionally relevant contexts can be used to replace active training [75]. It is found from several studies [77-79] that passive movement activates the similar cortical regions compares to voluntary movement. Robotic assisted BWS training can be optimized as a gait rehabilitation strategy, which allows practice of correct kinematic gait patterns [80].

In recent developments of robotic gait rehabilitation, researches have been focused on active assistances for robotic gait rehabilitation. If a less severe subject is trained with passive assistance strategy, he or she tends to use reduced activity of muscles and metabolism. For example, subjects with incomplete SCI trained in a robotic gait training system with position control consume 60% less energy than in conventional therapist assisted therapy [81]. On the other hand, if subject attempts to walk actively with the robotic rehabilitation system providing passive assistance, the subject will work against the resistance of the system, which might result in abnormal muscle activation patterns [82].

To address the above-mentioned limitations of passive assistance strategy, the scheme of active assistance (also known as subject-cooperative control strategy) has been introduced by several research groups [64, 83-87]. The subject cooperative control strategy is developed to recognize the movement intention and muscle effort of the subject. The bio-feedback information will be displayed and available to the subject and therapist. The strategy will incorporate the subject's effort and be adjusted accordingly to robotic assistance during the rehabilitation training. Ideally, the control strategy for gait rehabilitation should perform the same task as that by an experienced therapist. The subject-cooperative control strategy will assist the subject movement only as much as needed and allow the subject to apply voluntary muscle efforts [88]. For on-line interaction, the subject cooperative control strategies are often combined with biofeedback. Figure 15 summarizes the findings of the above introduction, review, discussion, and comparisons.

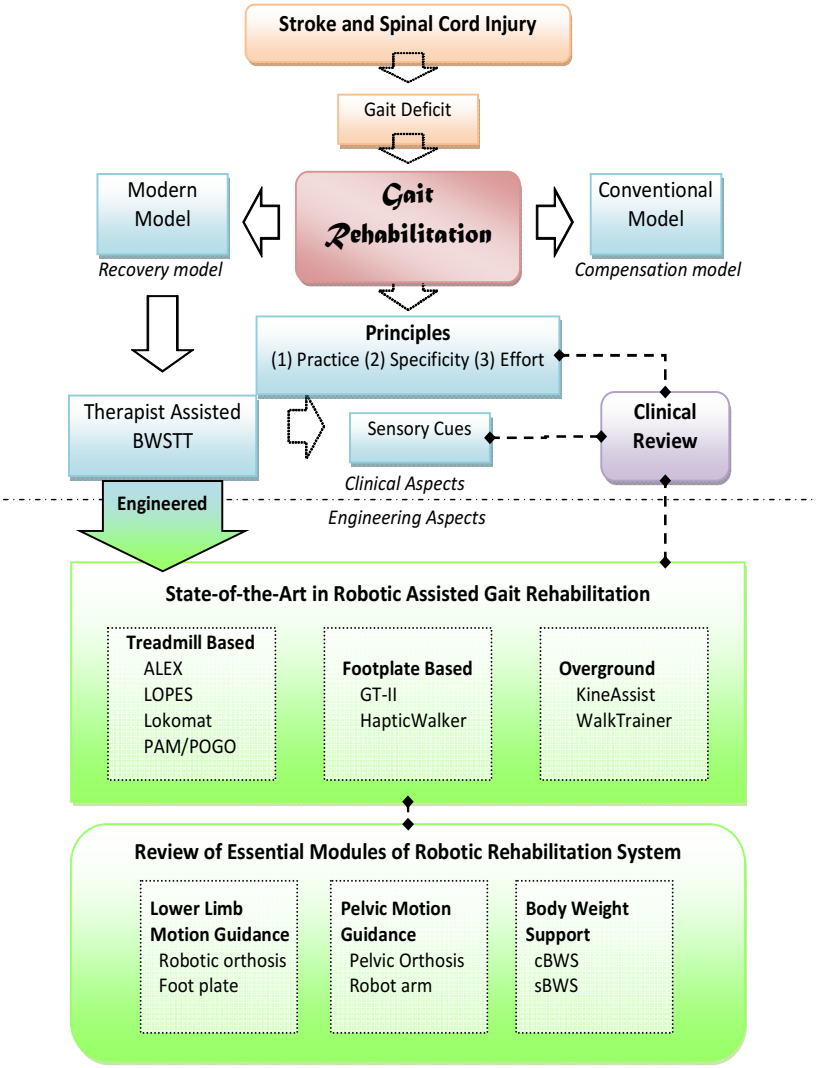

Fig. 15. Summary of Clinical-Engineering Approaches for Gait Rehabilitation [27]

6 Requirements of Robotics Gait Rehabilitation

The review presented in the previous sections on the clinical gait rehabilitation practice and robotics gait rehabilitation can be useful to the design and implementation of subject-oriented gait rehabilitation robots. In addition, the discussion and advices of doctor and therapist from a local rehabilitation centre are also found useful. Accordingly, four features are suggested for robotic assisted gait rehabilitation, as shown in Figure 16. The features are pelvic motion assistance, body weight support, overground walking, and lower limb motion assistance. As also indicated in the figure, the following modules are suggested to incorporate the specified features. A mobile platform (MP) is introduced to allow the robot to follow the subject during gait rehabilitation. A pair of robotic arms for pelvic assistance (PA) mechanism is attached on the mobile platform. To provide BWS and pelvic control, the end of the arm (or end effector) connects to the waist of subject. A lower limb robotic orthosis (RO) is attached to the end of the arm, which induces gait locomotion to the subject. The platform carries all other modules with it, so that the subject will not bear any undesired load.

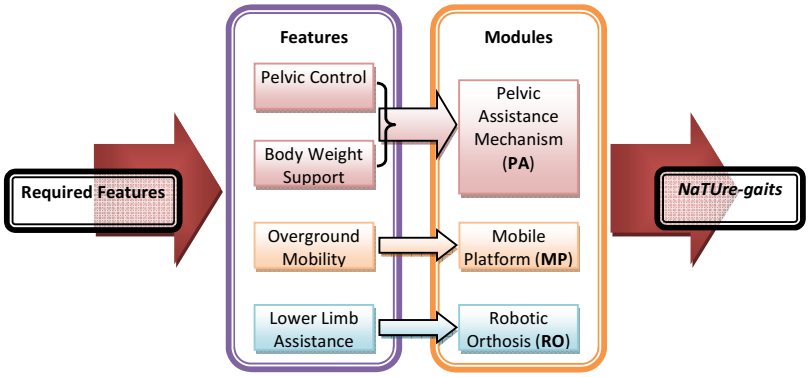

Fig. 16. Features of robotic gait rehabilitation and the required modules [14, 27]

7 Features of Developed *NaTUre-gaits*

A robotic gait rehabilitation system has been designed and developed based on the three elements of gait training: (reciprocal stepping, balance, and body weight shifting. Figure 17 shows the CAD model of the robotics system (known as *NaTUre-gaits*), while the incorporated features are presented in Figure 18.

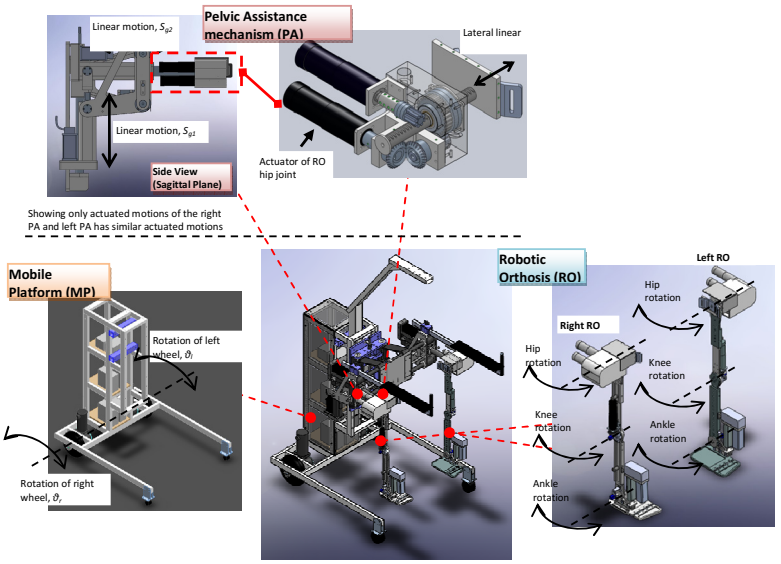

Fig. 17. CAD model of NaTUre-gaits and its main modules and corresponding 14 actuator joints [14]

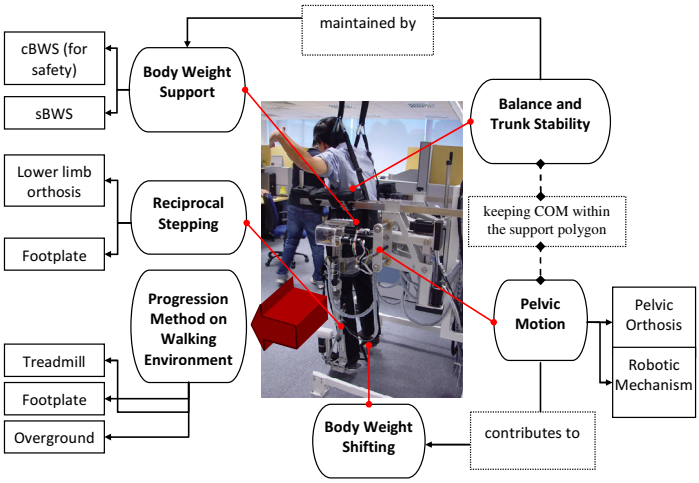

Fig. 18. Modules and features of the developed robotic overground gait rehabilitation [27]

8 Modules of Implemented Overground Gait Rehabilitation Robot

To provide body weight supported gait rehabilitation together with the assistance to hip and lower limb movement in the context of overground walking, the developed gait system *NaTUre-gaits* is assembled by the three modular units: robotic orthosis, mobile platform, and pelvic assistance mechanism. The features provided by *NaTUre-gaits* include the pelvic motion assistance and the body weight support with the pelvic assistance mechanism. As shown in Figure 19, a six-DoFs robotic orthosis is developed for the lower limb motion assistance. The mobile platform of *NaTUre-gaits* covers a large footprint (1.2m x 1m) for two reasons: increases the stability of the entire system and allows a larger space for the CoM of the subject to walk within the support polygon of the system. A smooth pelvic motion is induced by pelvic assistance mechanism by incorporating body weight shifting. The comparison of *NaTUre-gaits* with other existing gait systems is presented in Tables 4 and 5.

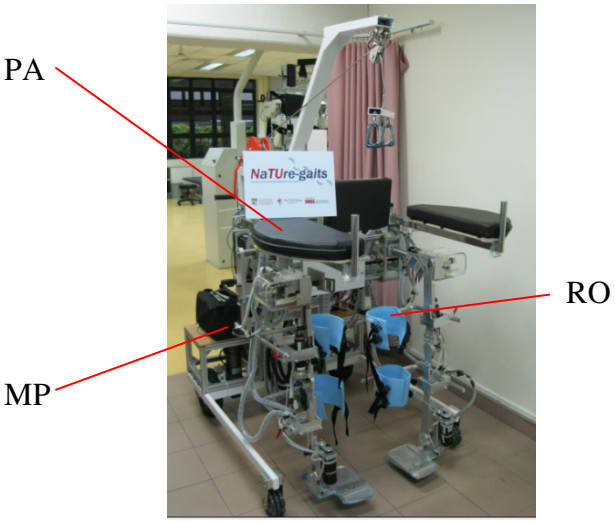

Fig. 19. Overview of NaTUre-gaits: Pelvic Arm (PA) to provide pelvis motion and body weight support (BWS); Robotic Orthosis (RO) for active assistance to hip/knee/ankle joints in the Sagittal plane; and Mobile Platform (MP) to allow the locomotion training [14]

Table 4. Pelvic Movement Assistance of *NaTUre-gaits* as Compared to Pelvic Movement Assistance Provided by Other Robotic Gait Rehabilitation Systems [27]

	Active Assistance				Passive Movement	
	NaTUre-gaits	***PAM***	***WalkTrainer***	***LOPES***	***Alex/ Lokomat***	***Kine-Assist***
Type of Actuator	DC motor	Pneumatic	DC motor	DC motor	NA	NA
BWS	sBWS	cBWS	cBWS	cBWS	cBWS	sBWS
Translational Pelvic Movement						
Mediolateral	Active	Active	Active	Active	Fixed	Passive
Antero-posterior	Active	Active	Active	Active	Fixed	Passive
Superior-inferior	Active	Active	Active	Passive	Passive	Fixed
Rotational Pelvic Movement						
Pelvic rotation	Active	Active	Active	Fixed	Fixed	Passive
Pelvic tilt	Active	Active	Active	Fixed	Fixed	Passive
Pelvic rotation about medio-lateral axis	Passive	Fixed	Active	Fixed	Fixed	Passive

Active – Actuated movement; Passive – Not actuated by free movement allowed; Fixed – No movement allowed

Table 5. Body Weight Support Feature of *NaTUre-gaits* as Compared to Other Gait Rehabilitation Systems [27]

	NaTUre-gaits	***Lokomat***	***WalkTrainer***	***KineAssist***
Unloading /Loading Capacity				
Static	120 kg	150 kg	-	159 kg
Dynamic	80 kg	80 kg	-	68 kg
Other Features				
Unloading Mechanism	Motor	Motor and Spring	Motor and Spring	Motor
Control System	Robust Control System	Robust Control System	Active Control System	-

Field marked with - indicates information is not available

8.1 Mobile Platform (MP)

The mobile platform in Figure 19 is the base of *NaTUre-gaits*. It also serves as the carrier of the robotic orthosis, pelvis assistance mechanism, controller, power source, and any other electronics components of *NaTUre-gaits*. Two motorized wheels are mounted at the rear of mobile platform. Each wheel is independently controlled. Therefore, it is possible for the mobile platform to follow straight or curved path.

The speed of the mobile platform is design and customized based on several considerations, such as comfortable normal walking speed of a subject. The average natural walking speed for a healthy adult is 1.5 m/s (aged 20 – 65 years) [89]. Based on the suggestions by doctor and therapist from a local rehabilitation centre, the subject usually admitted to rehabilitation center with average walking speed of 0.1 m/s. The information serves as the guideline for the operation of the gait system developed. The maximum speed of the mobile platform is designed to be 0.7 m/s, while the system operating speed will be around 0.2 m/s – 0.4 m/s.

8.2 Robotic Orthosis (RO)

The robotic orthosis is the module in *NaTUre-gaits* providing actuated assistance to perform the gait locomotion of the lower limb. The key function of RO is to hold the subjects leg, and move it to complete the desired gait locomotion during gait rehabilitation. Having discussed with clinical collaborators, the robotic orthosis is designed to provide actuated assistance only in the sagittal plane. The robotic orthosis has a total of six degrees of freedom (for hip, knee, and ankle joints), three on the right side and three on the left side. The length of the robotic orthosis for the thigh and shank can be

adjusted to cater to different subjects. The CAD model of the robotic orthosis is shown in Figure 20 together with the associated features. The range of motion (ROM) designed for each joint is listed in Table 6. Note that the ROM is limited by limiter switches for safety. The anthropometric data of the developed *NaTUre-gaits* is given in Table 7.

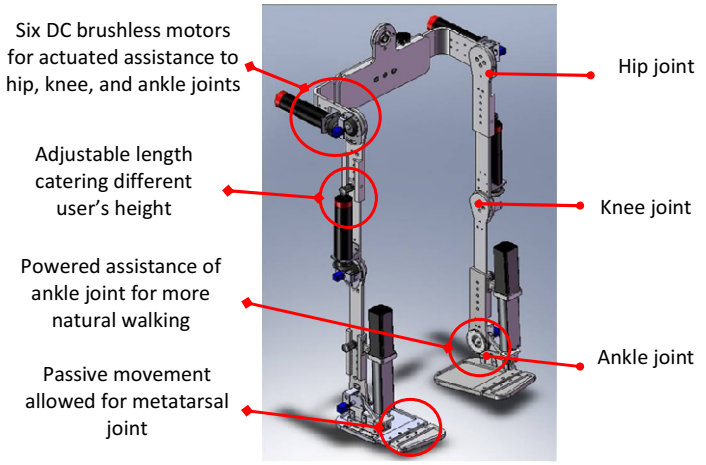

Fig. 20. CAD model of developed robotic orthosis for NaTUre-gaits [27, 55]

Table 6. Designed Range of Motion (ROM) for Robotic Orthosis (presented with permissible ROM of human and ROM of human during walking) [27, 55]

		Range of Motion (Sagittal plane)		
		Permissible [90]	***Walking*** [91]	***Designed***
Hip	Flexion	122°	20°	50°
	Extension#	10°	11°	15°
Knee	Flexion	134°	60°	80°
	Hyperextension	0°	0°	0°
Ankle	Dorsiflexion	13°	9°	10°
	Plantarflexion	56°	18°	20°

The permissible range of hip extension is 10° as recorded in reference [90]. As recorded in reference [92], the permissible range has a range of 10° to 30°. The discrepancies of the value could be due to measuring method. The designed ROM for hip extension is 15°.

Table 7. Design Requirement based on Anthropometric Data of Targeted User Groups [27]

	Minimum	***Maximum***
Body Weight	-	80 kg
Waist Height	840 mm	1000 mm
Shank Length	330 mm	400 mm
Thigh Length	330 mm	400 mm
Hip Breadth	250 mm	550mm

8.3 Pelvic Assistance (PA) Mechanism

Apart from eliminating the restriction of the body weight support apparatus, to provide the unrestricted and natural pelvic motion assistance during gait rehabilitation, the developed robotic mechanism is required to provide the necessary pelvic movement during walking. Although the pelvis has six movements (the description of the pelvic movements are made available in Figure 14), only three significant movements are provided by the developed PA mechanism: pelvic rotation, pelvic tilt, and translational mediolateral movement.

The PA mechanism is mounted on a mobile platform. The pelvic motion in the x-axis is provided by the combined motions of PA mechanism and mobile platform in the axis. As shown in Figure 21, actuators 1 and 2 in the sub-mechanism provides the motion of s_{g1} and s_{g2} in the sagittal plane. The third actuator is connected to the end effector of the sub-mechanism (see A3 in Figure 21(b)), provides the lateral shifting motion (motion along *y*-axis). The position of the end effector is given as

$$\mathbf{P}_{PA,g3} = \begin{bmatrix} x_{g3} & y_{g3} & z_{g3} \end{bmatrix}$$

The kinematic chain of the PA mechanism is depicted in Figure 21(a). The sagittal motion (x_{g3}, z_{g3}) of pelvic is provided by the linear motion of s_{g1} and s_{g2}, given that

$$s_{g2} = \sqrt{{x_{g3}}^2 + {z_{g3}}^2}$$

$$\theta_{g2} = \sin^{-1}\left(z_{g3} / s_{g2}\right)$$

$$s_{g1} = \sqrt{\left(x_{g2} - l\cos\theta_{g2} - x_{g0}\right)^2 + \left(z_{g2} - l\sin\theta_{g2} - z_{g0}\right)^2}$$

and $g = l, r$. The variables for PA at the right side is denoted by $g = r$, and the left side is denoted by $g = l$. As shown in Figure 21(b), the initial position of PA is at $\theta_{g1} = 90^{\circ}$ and $\theta_{g2} = 0^{\circ}$.

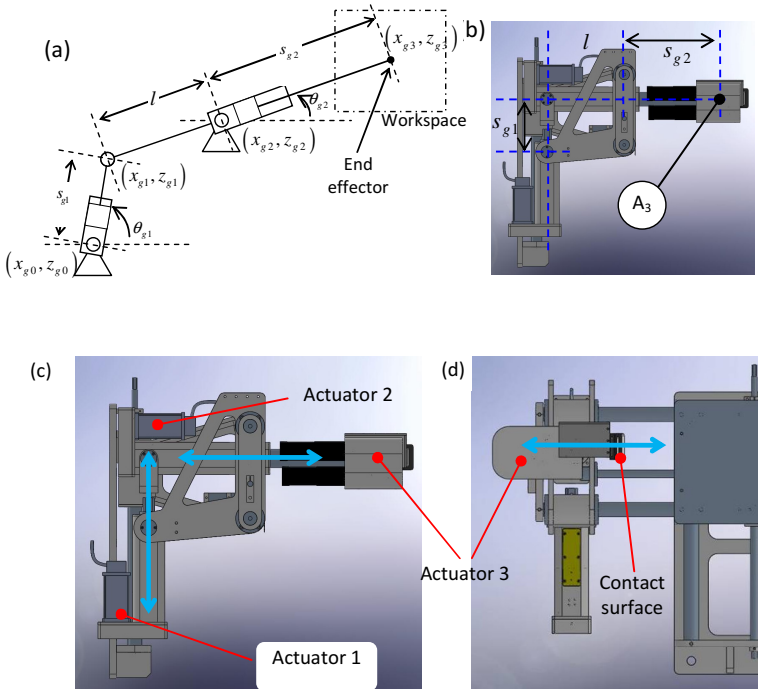

Fig. 21. PA mechanism; (a) Kinematic representation in x-z plane; (b) Initial position. (c) Robotic arm providing pelvic motion in sagittal plane (d) Lateral shift mechanism of the right side. (Arrows indicates the actuated motion) [27]

9 Coordination between Pelvic Assistance and Robotic Orthosis

Figure 22 shows the model of PA mechanism relative to the subject's lower extremities. The movement of end effector should be carefully defined because it is the contact and support position between subject and machine. Moreover, a natural gait-like trajectory planning for the end effector is required for the coordination of the two modules, PA and RO.

As illustrated in Figure 22, the pelvis of the subject is held by the pelvic assistance mechanism at the side. The pelvic motion is induced by the combined movements of the left and right modules of the pelvic assistance mechanism. As shown in Figure 22, the pelvic rotation and position (considering the center of the pelvis) can be controlled by the position of the two end effectors of the pelvic assistance mechanism, as given by

$$\theta_{tilt} = \tan^{-1}\left(\frac{z_{l3} - z_{r3}}{y_{l3} - y_{r3}}\right) \quad ; \qquad \theta_{rot} = \tan^{-1}\left(\frac{y_{l3} - y_{r3}}{x_{l3} - x_{r3}}\right) \quad ;$$

$$\mathbf{P}_{Pelvis} = \frac{1}{2}\begin{bmatrix} x_{r3} + x_{l3} \\ y_{r3} + y_{l3} \\ z_{r3} + z_{l3} \end{bmatrix}$$

in which θ_{tilt} is the angle of pelvic tilt, θ_{rot} is the angle of pelvic rotation, and $\mathbf{P}_{Pelvis}$ denotes the position vector of the center of the pelvis.

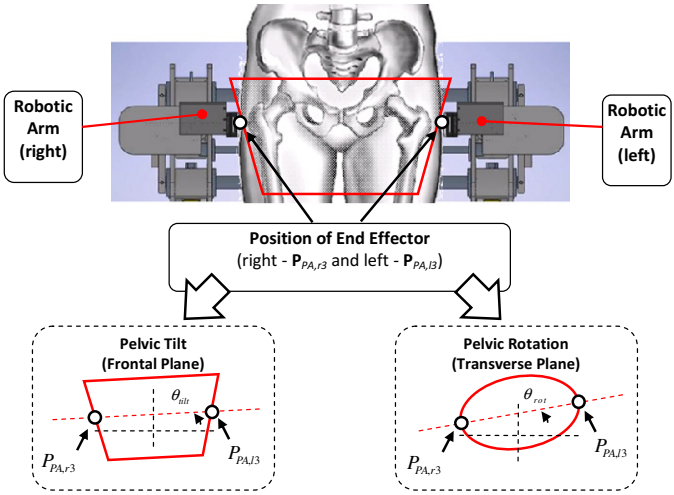

Fig. 22. Illustration of pelvic motion provided by the pelvic assistance mechanism in fontal (y-z) and transverse (x-y) planes [27, 55]

10 Motion Synchronization between Pelvic Assistance and Mobile Platform

The trajectories of the hip joint center and contact position of Pelvic Assistance (PA) mechanism are depicted in Figure 23, while the end-point position of PA in one gait cycle during human walking in sagittal plane is shown in Figure 24.

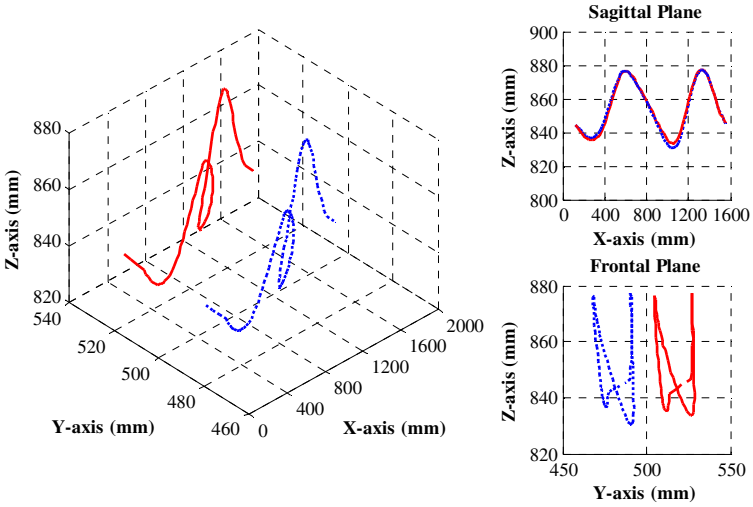

Fig. 23. Trajectories of hip joint center (dotted line) and contact point (solid line) of the pelvic mechanism in one walking gait cycle (only left side is shown) [55]

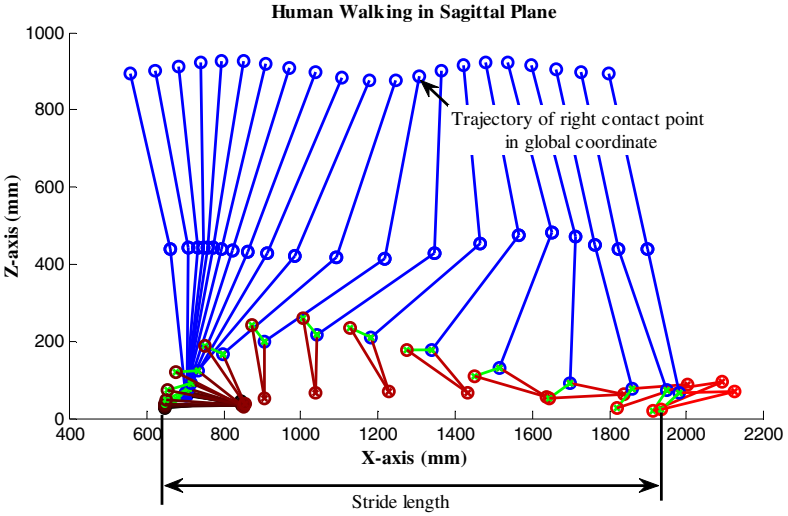

Fig. 24. Human walking in sagittal plane [55]

The motion planning for left end-effector has been computed by talking the right end effector with 50% phase lag. The motion of the pelvis in the *z-axis* is found to be always lower than the hip height of standing. The generated trajectories of pelvic motion in the respective axes for the play-back on PA mechanism of *NaTUre-gaits* are illustrated in Figure 25.

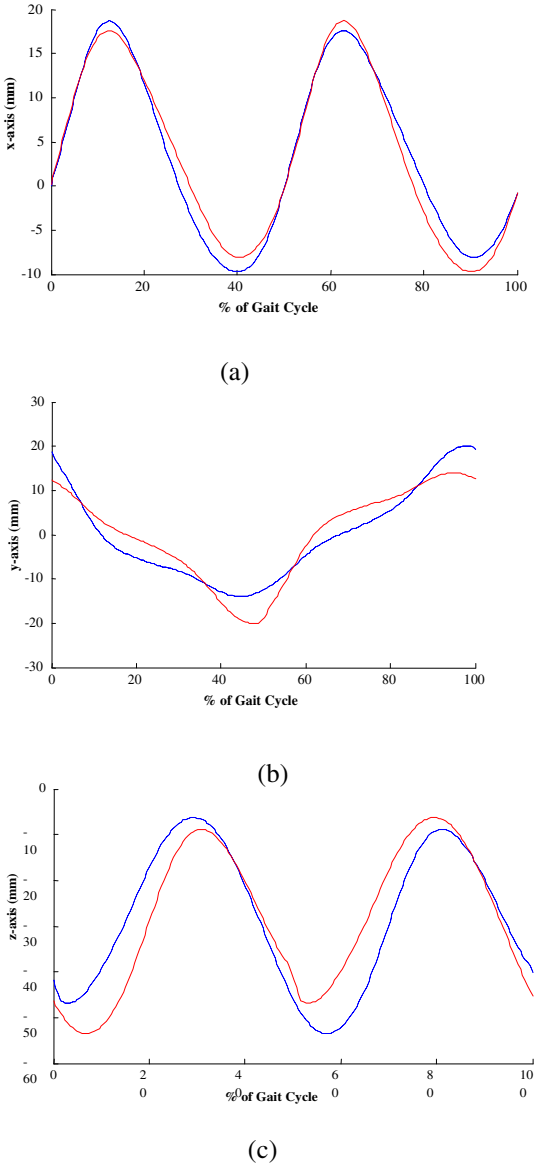

Fig. 25. Generated motion for PA mechanism in the respective axes (solid line – right side, dotted line – left side) [55]: (a) x-axis; (b) y-axis; (c) z-axis

The localized movement of PA mechanism in 3D space has also been analyzed and shown in Figure 26. The trajectory of the left and right end effectors in sagittal plane is the same. In frontal plane, the trajectories trace an "8". The results are agreed with the pelvic motion study in [89].

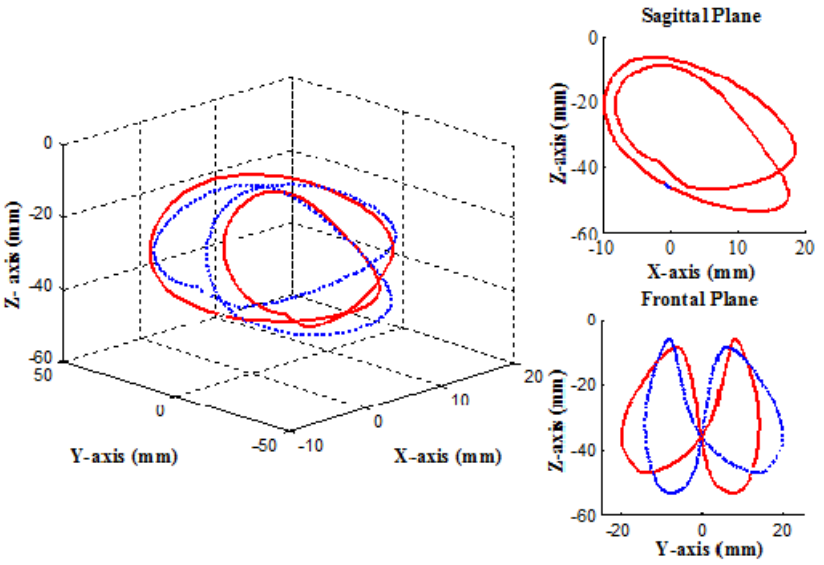

Fig. 26. Final constructed motion for PA mechanism in 3D space (solid line – right side, dotted line – left side) [55]

11 Control Architecture and Implementation

The control system for the three modules (PA, RO and MP) has been developed separately. For the operation of *NaTUre_gaits*, the communication to each other is done through wireless connections to a host computer. The control framework of the overall system is shown in Figure 27.

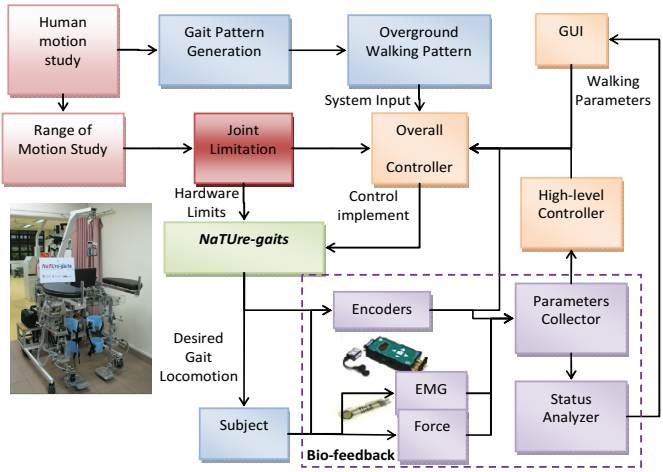

Fig. 27. Control framework of NaTUre-gaits [14]

12 Concluding Remarks

The review and comparison of the existing gait rehabilitation robots have first been presented in this chapter. Based on the findings of gait rehabilitation in clinical aspects, a robotic overground gait rehabilitation system, *NaTUre-gaits*, is designed and built. The 14-DOFs gait rehabilitation robot, *NaTUre-gaits*, provides lower limb motion assistance in the sagittal plane, natural pelvic movement assistance, body weight support with no restriction on the pelvic movement, and overground walking (OGW). The robotic mechanism together with the modulation of the structure is capable of providing a platform for verification of control strategy. The modular and reprogrammable architecture of the developed system allows control strategy to be implemented and validated on the system with ease.

After several rounds of in-house testing and evaluation by the doctor and therapist from a local hospital, three SCI/stroke subjects were recruited and participated in clinical trials on *NaTUre_gaits*. Every trial covered a continual 10-m walking with the system speed of 0.1 m/s, as required in the conventional rehabilitation gait training in clinics. The coordination of the system has been optimized to prevent the foot from being dragged over the ground. The clinical results show that the performance of overground walking with the rehabilitation gait system with minimum manual assistance is good and the system is able to provide smooth gait rehabilitation training. The research on the detection of abnormal muscle activations [93] and the individual-specific gait pattern prediction model by neural networks [94, 95] are worth exploring further for effective robotic gait rehabilitation.

Acknowledgements. The author claims no originality of the review, study, and results presented in this chapter. The contents presented are mainly compiled from the works done by the three ex-PhD students supervised or co-supervised by the author. The materials, including many figures and tables, in this chapter are obtained and modified from those in the respective theses (references 14, 27, and 55). Details of works presented in this chapter can be found in these theses. Therefore, the author would like to thank P. Wang, H. B. Lim, and T. P. Luu for their good works and the great contribution. Works and photos from many excellent articles and books on such meaningful fields are also acknowledged. The grants provided by Singapore's NMRC and the PhD scholarship provided by the NTU to the three ex-PhD candidates on the robotics rehabilitation research are greatly appreciated. The financial support by Lee Foundation on the gait device is also acknowledged. Thanks are also due to Adela Tow and P. H. Lim from the Tan Tock Seng Hospital and Alison McGregor from Imperial College for their clinical input, which are important and useful to the design, development and research on the developed gait rehabilitation robot. The support from TTSH Rehabilitation Centre and NTU Robotics Research Centre are also acknowledged. L. Li and many other research and final year project students contributed to this research project in different aspects, including L. Li's help in formatting this chapter, are appreciated. Last but not least, the author would like thank my colleagues, K. H. Hoon and X. Qu, for the support and the co-supervision to the respective students. The consent from participants in the in-house testing and clinical trials are also acknowledged.

References

1. Edgerton, V.R., Tillakaratne, N.J.K., Bigbee, A.J., de Leon, R.D., Roy, R.R.: Plasticity of the spinal neural circuitry after injury. Annual Review of Neuroscience 27, 145–167 (2004)
2. Wolf, S.L., Butler, A.J., Alberts, J.L., Kim, M.W.: Contemporary linkages between EMG, kinetics and stroke rehabilitation. Journal of Electromyography and Kinesiology 15, 229–239 (2005)
3. Shadmehr, R., Holcomb, H.H.: Neural Correlates of Motor Memory Consolidation. Science 277, 821–825 (1997)
4. Barnes, M.P., Dobkin, B.H., Bogousslavsky, J.: Recovery after stroke: Cambridge Univ. Pr. (2005)
5. A.R.: M ller, Neural plasticity and disorders of the nervous system: Cambridge Univ. Pr. (2006)
6. Anderson, K.D.: Targeting recovery: Priorities of the spinal cord-injured population. Journal of Neurotrauma 21, 1371–1383 (2004)
7. Dietz, V., Harkema, S.J.: Locomotor activity in spinal cord-injured persons. Journal of Applied Physiology 96, 1954–1960 (2004)
8. Yen, S.C., Schmit, B.D., Landry, J.M., Roth, H., Wu, M.: Locomotor adaptation to resistance during treadmill training transfers to overground walking in human SCI. Experimental Brain Research 216, 473–482 (2012)
9. Harkema, S.J.: Neural plasticity after human spinal cord injury: application of locomotor training to the rehabilitation of walking. The Neuroscientist 7, 455–468 (2001)
10. Dobkin, B., Apple, D., Barbeau, H., Basso, M., Behrman, A., Deforge, D., Ditunno, J., Dudley, G., Elashoff, R., Fugate, L., Harkema, S., Saulino, M., Scott, M., Grp, S.: Weight-supported treadmill vs overground training for walking after acute incomplete SCI. Neurology 66, 484–492 (2006)
11. Barbeau, H., Ladouceur, M., Norman, K.E., Pepin, A., Leroux, A.: Walking after spinal cord injury: Evaluation, treatment, and functional recovery. Archives of Physical Medicine and Rehabilitation 80, 225–235 (1999)
12. Wirz, M., Zemon, D.H., Rupp, R., Scheel, A., Colombo, G., Dietz, V., Hornby, T.G.: Effectiveness of automated locomotor training in patients with chronic incomplete spinal cord injury: A multicenter trial. Archives of Physical Medicine and Rehabilitation 86, 672–680 (2005)
13. Nooijen, C.F.J., ter Hoeve, N., Field-Fote, E.C.: Gait quality is improved by locomotor training in individuals with SCI regardless of training approach. Journal of Neuroengineering and Rehabilitation 6 (October 2009)
14. Wang, P.: Gait Locomotion Generation and Leg Muscle Evaluation for Overground Walking Rehabilitation Robots, PhD Thesis, School of Mechanical and Aerospace Engineering, Nanyang Technological University, Singapore (2012)
15. Ottenbacher, K.J.: Evaluating clinical change: Strategies for occupational and physical therapists. Lippincott Williams and Wilkins (1986)
16. Gordon, K., Ferris, D., Roberton, M., Beres, J., Harkema, S.: The importance of using an appropriate body weight support system in locomotor training. Soc. Neurosci., 160 (2000)
17. Behrman, A.L., Harkema, S.J.: Locomotor training after human spinal cord injury: A series of case studies. Physical Therapy 80, 688–700 (2000)
18. Wang, P., Low, K.H., Tow, A., Lim, P.H.: Initial System Evaluation of an Overground Rehabilitation Gait Training Robot (*NaTUre-gaits*). Advanced Robotics 25, 1927–1948 (2011)

19. Hayashi, T., Kawamoto, H., Sankai, Y.: Control method of robot suit HAL working as operator's muscle using biological and dynamical information. In: 2005 IEEE/RSJ International Conference on Intelligent Robots and Systems (IROS), Edmonton, Alberta, Canada, pp. 3455–3460 (2005)
20. Bouri, M., Stauffer, Y., Schmitt, C., Allemand, Y., Gnemmi, S., Clavel, R., Metrailler, P., Brodard, R.: The WalkTrainer (TM): a robotic system for walking rehabilitation. In: IEEE International Conference on Robotics and Biomimetics (ROBIO), Kunming, China, pp. 1616–1621 (2006)
21. Veneman, J.F., Kruidhof, R., Hekman, E.E.G., Ekkelenkamp, R., Van Asseldonk, E.H.F., Van der Kooij, H.: Design and evaluation of the LOPES exoskeleton robot for interactive gait rehabilitation. IEEE Transactions on Neural Systems and Rehabilitation Engineering 15, 379–386 (2007)
22. Peshkin, M., Brown, D.A., Santos-Munne, J.J., Makhlin, A., Lewis, E., Colgate, J.E., Patton, J., Schwandt, D.: KineAssist: a robotic overground gait and balance training device. In: IEEE 9th International Conference on Rehabilitation Robotics (ICORR), Chicago, IL, USA, pp. 241–246 (2005)
23. Mokhtarian, A., Fattah, A., Agrawal, S.K.: A novel passive pelvic device for assistance during locomotion. In: IEEE International Conference on Robotics and Automation (ICRA), Anchorage, Alaska, USA, pp. 2241–2246 (2010)
24. Frey, M., Colombo, G., Vaglio, M., Bucher, R., Jorg, M., Riener, R.: A novel mechatronic body weight support system. IEEE Transactions on Neural Systems and Rehabilitation Engineering 14, 311–321 (2006)
25. Norman, K.E., Pepin, A., Ladouceur, M., Barbeau, H.: A treadmill apparatus and harness support for evaluation and rehabilitation of gait. Archives of Physical Medicine and Rehabilitation 76, 772–778 (1995)
26. Morris, D.M., Taub, E.: Constraint-induced therapy approach to restoring function after neurological injury. Topics in Stroke Rehabilitation 8, 16–30 (2001)
27. Lim, H.B.: Study and Implementation of a Gait Rehabilitation System with Capability for Mobility and Gait Pattern Generation. PhD Thesis, School of Mechanical and Aerospace Engineering, Nanyang Technological University, Singapore (2012)
28. Nymark, J.R., Balmer, S.J., Melis, E.H., Lemaire, E.D., Millar, S.: Electromyographic and kinematic nondisabled gait differences at extremely slow overground and treadmill walking speeds. Journal of Rehabilitation Research and Development 42, 523–534 (2005)
29. Whittle, M.: Gait analysis: an introduction. Butterworth-Heinemann Medical (2002)
30. Low, K.H.: Robot-assisted gait rehabilitation: From exoskeletons to gait systems. In: Proceedings of the 2011 Defense Science Research Conference and Expo (DSR 2011), Singapore, 10 pages (August 2011), doi:10.1109/DSR.2011.6026886).
31. Warabi, T., Kato, M., Kiriyama, K., Yoshida, T., Kobayashi, N.: Treadmill walking and overground walking of human subjects compared by recording sole-floor reaction force. Neuroscience Research 53, 343–348 (2005)
32. Stolze, H., Kuhtz-Buschbeck, J.P., Mondwurf, C., Boczek-Funcke, A., Johnk, K., Deuschl, G., Illert, M.: Gait analysis during treadmill and overground locomotion in children and adults. Electroencephalography and Clinical Neurophysiology - Electromyography and Motor Control 105, 490–497 (1997)
33. Vogt, L., Pfeifer, K., Banzer, W.: Comparison of angular lumbar spine and pelvis kinematics during treadmill and overground locomotion. Clinical Biomechanics 17, 162–165 (2002)

34. Hesse, S., Konrad, M., Uhlenbrock, D.: Treadmill walking with partial body weight support versus floor walking in hemiparetic subjects. Archives of Physical Medicine and Rehabilitation 80, 421–427 (1999)
35. Song, J.L., Hidler, J.: Biomechanics of overground vs. treadmill walking in healthy individuals. Journal of Applied Physiology 104, 747–755 (2008)
36. Riley, P.O., Paolini, G., Della Croce, U., Paylo, K.W., Kerrigan, D.C.: A kinematic and kinetic comparison of overground and treadmill walking in healthy subjects. Gait and Posture 26, 17–24 (2007)
37. Brouwer, B., Parvataneni, K., Olney, S.J.: A comparison of gait biomechanics and metabolic requirements of overground and treadmill walking in people with stroke. Clinical Biomechanics 24, 729–734 (2009)
38. Alton, F., Baldey, L., Caplan, S., Morrissey, M.C.: A kinematic comparison of overground and treadmill walking. Clinical Biomechanics 13, 434–440 (1998)
39. Seo, K.H., Lee, J.J.: The development of two mobile gait rehabilitation systems. IEEE Transactions on Neural Systems and Rehabilitation Engineering 17, 156–166 (2009)
40. Patton, J., Brown, D.A., Peshkin, M., Santos-Munn, J.J., Makhlin, A., Lewis, E., Colgate, J.E., Schwandt, D.: KineAssist: Design and development of a robotic overground gait and balance therapy device. Topics in Stroke Rehabilitation 15, 131–139 (2008)
41. Ferris, D.P., Sawicki, G.S., Domingo, A.R.: Powered lower limb orthoses for gait rehabilitation. Topics in Spinal Cord Injury Rehabilitation 11, 34–49 (2005)
42. Banala, S.K., Kim, S.H., Agrawal, S.K., Scholz, J.P.: Robot assisted gait training with active leg exoskeleton (ALEX). IEEE Transactions on Neural Systems and Rehabilitation Engineering 17, 2–8 (2009)
43. Zoss, A.B., Kazerooni, H., Chu, A.: Biomechanical design of the Berkeley Lower Extremity Exoskeleton (BLEEX). IEEE/ASME Transactions on Mechatronics 11, 128–138 (2006)
44. Liu, X.P., Low, K.H.: Development and preliminary study of the NTU lower extremity exoskeleton. In: IEEE Conference on Cybernetics and Intelligent Systems, Singapore, pp. 1243–1247 (2004)
45. Kawamoto, H., Sankai, Y.: Comfortable power assist control method for walking aid by HAL-3. In: IEEE International Conference on Systems, Man and Cybernetics, Hammamet, Tunisia, vol. 4, p. 6 (2002)
46. Bionics, B. (June 2012), http://berkeleybionics.com/exoskeletons-rehab-mobility/
47. AGRO (June), http://www.argomedtec.com/
48. Bionics, R.: (June)
49. Ikeuchi, Y., Ashihara, J., Hiki, Y., Kudoh, H., Noda, T.: Walking assist device with bodyweight support system. In: IEEE/RSJ International Conference on Intelligent Robots and Systems (IROS), St. Louis, MO, USA, pp. 4073–4079 (2009)
50. Werner, C., Von Frankenberg, S., Treig, T., Konrad, M., Hesse, S.: Treadmill training with partial body weight support and an electromechanical gait trainer for restoration of gait in subacute stroke patients: A randomized crossover study. Stroke 33, 2895–2901 (2002)
51. Barbeau, H., Wainberg, M., Finch, L.: Description and application of a system for locomotor rehabilitation. Medical and Biological Engineering and Computing 25, 341–344 (1987)
52. Behrman, A.L., Lawless-Dixon, A.R., Davis, S.B., Bowden, M.G., Nair, P., Phadke, C., Hannold, E.M., Plummer, P., Harkema, S.J.: Locomotor training progression and outcomes after incomplete spinal cord injury. Physical Therapy 85, 1356–1371 (2005)

53. Lim, H.B., Luu, T.P., Hoon, K.H., Qu, X., Tow, A., Low, K.H.: Study of body weight shifting on robotic assisted gait rehabilitation with NaTUre-gaits. In: Proceedings of the 2011 IEEE/RSJ International Conference on Intelligent Robots and Systems (IROS2011), San Francisco, pp. 4923–4928 (September 2011)
54. Galvez, J.A., Kerdanyan, G., Maneekobkunwong, S., Weber, R., Scott, M., Harkema, S.J., Reinkensmeyer, D.J.: Measuring human trainers' skill for the design of better robot control algorithms for gait training after spinal cord injury. In: Proceedings of the 2005 IEEE 9th International Conference on Rehabilitation Robotics, Chicago, IL, vol. 2005, pp. 231–234 (2005)
55. Luu, T.P.: Individual-Specific Gait Pattern Planning and Locomotion Control Strategy for Robotic Gait Rehabilitation. PhD Thesis, School of Mechanical and Aerospace Engineering, Nanyang Technological University, Singapore (2014)
56. Hesse, S., Mehrholz, J., Werner, C.: Robot-assisted upper and lower limb rehabilitation after stroke. Roboter- und Gerätegestützte Rehabilitation Nach Schlaganfall: Gehen und Arm-/handfunktion 105, 330–336 (2008)
57. Hesse, S., Werner, C.: Connecting research to the needs of patients and clinicians. Brain Research Bulletin 78, 26–34 (2009)
58. Banala, S.K., Kulpe, A., Agrawal, S.K.: A powered leg orthosis for gait rehabilitation of motor-impaired patients. In: Proceedings of the IEEE International Conference on Robotics and Automation, Rome, pp. 4140–4145 (2007)
59. Our Technology, `http://www.warecentre.com/_images/_tech/lokomat.jpg` (accessed on July 2010)
60. Van Asseldonk, E.H.F., Veneman, J.F., Ekkelenkamp, R., Buurke, J.H., Van Der Helm, F.C.T., Van Der Kooij, H.: The effects on kinematics and muscle activity of walking in a robotic gait trainer during zero-force control. IEEE Transactions on Neural Systems and Rehabilitation Engineering 16, 360–370 (2008)
61. Aoyagi, D., Ichinose, W.E., Harkema, S.J., Reinkensmeyer, D.J., Bobrow, J.E.: A robot and control algorithm that can synchronously assist in naturalistic motion during body-weight-supported gait training following neurologic injury. IEEE Transactions on Neural Systems and Rehabilitation Engineering 15, 387–400 (2007)
62. Allemand, Y., Stauffer, Y., Clavel, R., Brodard, R.: Design of a new lower extremity orthosis for overground gait training with the WalkTrainer. In: Proceedings of the IEEE 11th International Conference on Rehabilitation Robotics, Kyoto, Japan, pp. 550–555 (2009)
63. Hussein, S., Schmidt, H., Hesse, S., Kruger, J.: Effect of different training modes on ground reaction forces during robot assisted floor walking and stair climbing. In: Proceedings of the 2009 IEEE International Conference on Rehabilitation Robotics, ICORR 2009, Kyoto, Japan, pp. 845–850 (2009)
64. Banala, S.K., Kim, S.H., Agrawal, S.K., Scholz, J.P.: Robot assisted gait training with active leg exoskeleton (ALEX). IEEE Transactions on Neural Systems and Rehabilitation Engineering 17, 2–8 (2009)
65. Vallery, H., Veneman, J., van Asseldonk, E., Ekkelenkamp, R., Buss, M., van Der Kooij, H.: Compliant actuation of rehabilitation robots. IEEE Robotics and Automation Magazine 15, 60–69 (2008)
66. Reinkensmeyer, D.J., Aoyagi, D., Emken, J.L., Galvez, J.A., Ichinose, W., Kerdanyan, G., Maneekobkunwong, S., Minakata, K., Nessler, J.A., Weber, R., Roy, R.R., De Leon, R., Bobrow, J.E., Harkema, S.J., Reggie Edgerton, V.: Tools for understanding and optimizing robotic gait training. Journal of Rehabilitation Research and Development 43, 657–670 (2006)

67. The Driven Gait Orthosis Lokomat, http://www.jneuroengrehab.com/content/4/1/1/figure/F1?highres=y (accessed on September 2010)
68. Robomedica, Inc., http://www.robomedica.com/ (accessed on July 2010)
69. KineAssist, http://www.kineadesign.com/ (accessed on July 2010)
70. Perry, J.: Gait Analysis - Normal and Pathological Function. SLACK Incorporated (1992)
71. Inman, V.T., Ralston, H., Todd, F.: Human Walking, 1st edn. Williams and Wilkins, Baltimore/London (1981)
72. Neptune, R.R., Kautz, S.A., Zajac, F.E.: Contributions of the individual ankle plantar flexors to support, forward progression and swing initiation during walking. Journal of Biomechanics 34, 1387–1398 (2001)
73. Veneman, J.F., Menger, J., van Asseldonk, E.H.F., van der Helm, F.C.T., van der Kooij, H.: Fixating the pelvis in the horizontal plane affects gait characteristics. Gait and Posture 28, 157–163 (2008)
74. Kaelin-Lane, A., Sawaki, L., Cohen, L.G.: Role of voluntary drive in encoding an elementary motor memory. Journal of Neurophysiology 93, 1099–1103 (2005)
75. Lotze, M., Braun, C., Birbaumer, N., Anders, S., Cohen, L.G.: Motor learning elicited by voluntary drive. Brain 126, 866–872 (2003)
76. Lippman, L.G., Rees, R.: Consequences of Error Production in a Perceptual-Motor Task. Journal of General Psychology 124, 133–142 (1997)
77. Weiller, C., Juptner, M., Fellows, S., Rijntjes, M., Leonhardt, G., Kiebel, S., Muller, S., Diener, H.C., Thilmann, A.F.: Brain representation of active and passive movements. NeuroImage 4, 105–110 (1996)
78. Carel, C., Loubinoux, I., Boulanouar, K., Manelfe, C., Rascol, O., Celsis, P., Chollet, F.: Neural substrate for the effects of passive training on sensorimotor cortical representation: A study with functional magnetic resonance imaging in healthy subjects. Journal of Cerebral Blood Flow and Metabolism 20, 478–484 (2000)
79. Mima, T., Sadato, N., Yazawa, S., Hanakawa, T., Fukuyama, H., Yonekura, Y., Shibasaki, H.: Brain structures related to active and passive finger movements in man. Brain 122, 1989–1997 (1999)
80. Hornby, T.G., Zemon, D.H., Campbell, D.: Robotic-assisted, body-weight-supported treadmill training in individuals following motor incomplete spinal cord injury. Physical Therapy 85, 52–66 (2005)
81. Israel, J.F., Campbell, D.D., Kahn, J.H., Hornby, T.G.: Metabolic costs and muscle activity patterns during robotic- and therapist-assisted treadmill walking in individuals with incomplete spinal cord injury. Physical Therapy 86, 1466–1478 (2006)
82. Hidler, J.M., Wall, A.E.: Alterations in muscle activation patterns during robotic-assisted walking. Clinical Biomechanics 20, 184–193 (2005)
83. Riener, R., Lunenburger, L., Jezernik, S., Anderschitz, M., Colombo, G., Dietz, V.: Patient-cooperative strategies for robot-aided treadmill training: First experimental results. IEEE Transactions on Neural Systems and Rehabilitation Engineering 13, 380–394 (2005)
84. Bernhardt, M., Frey, M., Colombo, G., Riener, R.: Hybrid force-position control yields cooperative behaviour of the rehabilitation robot LOKOMAT. In: Proceedings of the 2005 IEEE 9th International Conference on Rehabilitation Robotics, Chicago, IL, pp. 536–539 (2005)
85. Banala, S.K., Agrawal, S.K., Kim, S.H., Scholz, J.P.: Novel gait adaptation and neuromotor training results using an active leg exoskeleton. IEEE/ASME Transactions on Mechatronics 15, 216–225 (2010)

86. Dollar, A.M., Herr, H.: Lower extremity exoskeletons and active orthoses: Challenges and state-of-the-art. IEEE Transactions on Robotics 24, 144–158 (2008)
87. Vallery, H., Van Asseldonk, E.H.F., Buss, M., Van Der Kooij, H.: Reference trajectory generation for rehabilitation robots: Complementary limb motion estimation. IEEE Transactions on Neural Systems and Rehabilitation Engineering 17, 23–30 (2009)
88. Riener, R., Lunenburger, L., Colombo, G.: Cooperative strategies for robot-aided gait neuro-rehabilitation. In: Annual International Conference of the IEEE Engineering in Medicine and Biology - Proceedings, San Francisco, CA, vol. 26 VII, pp. 4822–4825 (2004)
89. Rose, J., Gamble, J.G.: Human Walking, 3rd edn. Lippincott Williams & Wilkins, Philadelphia (2006)
90. Boone, D.C., Azen, S.P.: Normal range of motion of joints in male subjects. Journal of Bone and Joint Surgery - Series A 61, 756–759 (1979)
91. Levangie, P.K., Norkin, C.C.: Joint Structure and Function: A Comprehensive Analysis, 4th edn. F A Davis Company (2005)
92. Winter, D.A.: The Biomechanics and Motor Control of Human Gait: Normal, Elderly and Pathological, 2nd edn. Waterloo Biomechanics, Ontario (1991)
93. Wang, P., Low, K.H., McGregor, A.H., Tow, A.: Detection of abnormal muscle activations during walking following spinal cord injury (SCI). Research in Developmental Disabilities 34, 1226–1235 (2013)
94. Luu, T.P., Low, K.H., Qu, X., Lim, H.B., Hoon, K.H.: An individual-specific gait pattern prediction model based on generalized regression neural networks. Gait and Posture 39, 443–448 (2014)
95. Luu, T.P., Low, K.H., Qu, X., Lim, H.B., Hoon, K.H.: Hardware Development and Locomotion Control Strategy for an Over-Ground Gait Trainer: NaTUre-Gaits. IEEE Journal of Translational Engineering in Health and Medicine 2014, 9 pages, doi:10.1109/JTEHM.2014.2303807

Brain-Machine Interfaces for Assistive Robotics

Enrique Hortal, Andrés Úbeda, Eduardo Iáñez, and José M. Azorín

Biomedical Neuroengineering Group in Miguel Hernández University of Elche, Spain
{ehortal,aubeda,eianez,jm.azorin}@umh.es

1 Introduction

Motor disability may be caused by many different conditions. The most common one is a cerebrovascular accident (CVA) which occurs when the blood supply to the brain stops [1]. If the length of this interruption is longer than several seconds, brain cells can die causing a permanent damage in the patient. When this damage occurs in the brain areas responsible for motor control, the patients may suffer permanent or temporal loss of mobility, coordination and control of their limbs. Another important cause of motor disability is due to spinal cord injury (SCI), which provokes the total loss of sensibility and movement capability below the level of the injury [2]. In this case, the patient assistance must be purely based on motor substitution, given that it is impossible to perform a rehabilitation procedure. Finally, less frequent illnesses and diseases may cause motor disfunctions, such as cerebral palsy, spina bifida, muscular dystrophy, amyotrophic lateral sclerosis (ALS) or central nervous system diseases such as Parkinson syndrome or Huntington disease.

In recent years, the interest for solving or, at least, reducing the limitations caused by motor problems of disabled people has been accompanied by a very important development of assistive technologies. These technologies can be defined as the use of any assistive, adaptive, and rehabilitative device that enables disabled people to perform tasks that they were formerly unable to accomplish. Focusing on the specific case of motor disability, the main goal is to either rehabilitate the motor capabilities of a patient with movement limitations or, if this is not possible, to replace the natural movement by a commanded action over a prosthesis or an orthosis. A more common way to improve the interaction between the subject and the environment consists of establishing alternative communication channels with external devices such as a computer or a robot through the so-called human-machine interfaces (HMI). Amongst these devices, there are a great number of possibilities such as ocular interfaces, voice control, adapted mechanical switches and many more. A particular case of this kind of devices, which will be explained in detail throughout the chapter, are brain-machine interfaces (BMI) which allow, through voluntary thoughts of the subject, interacting with the environment without the need for any actual motor activity or physical effort.

In this chapter we address the use of brain-machine interfaces as an assistive technology in the control of robots. With a brain-machine interface is possible to

S. Mohammed et al. (eds.), *Intelligent Assistive Robots*,
Springer Tracts in Advanced Robotics 106, DOI: 10.1007/978-3-319-12922-8_3

control the movement of a robot to perform, for example, reaching and grasping tasks with objects. As a result, motor disabled people will be capable of manipulating daily objects and improve their accesibility and the interaction with the environment. To illustrate this kind of technology, we show the use of two different BMIs. The first one consists of the control of a 6 degree of freedom robot arm through evoked potentials. The second one consists of the control of a planar robot through the classification of volitive mental states related to concentration and motor imagery tasks.

2 Brain-Machine Interfaces

A Brain-Machine Interface is a device that allows registering, processing and classifying the brain signals of a person to generate control commands [3]. In other words, a BMI allows a person to bypass the conventional neuromuscular pathways to interact with the environment. BMIs can use both invasive and non-invasive methods. The first ones make use of intracortical recordings of neuronal activity [4,5,6]. However, this methodology implies medical risks regarding surgery and subsequent complications in the implantation of arrays of electrodes directly on the brain cortex. On the other hand, non-invasive BMIs are based on the analysis and classification of brain patterns that appear in electroencephalographic (EEG) recordings from the scalp. These systems have experienced a great progress in less complex and constraint environments due to their simplicity and relatively short-term preparation [7,8]. BMI technology has a promising future in rehabilitating motor capabilities [9] or in restoring motor control of severely disabled patients [10]. It is also a hopeful way to assist people with a total motor loss, such as SCI patients or amputees [11].

The use of BMIs to support rehabilitation procedures has been recently explored with promising expectations [12]. The use of these systems during motor recovery is still in its early stages [9]. Nevertheless, according to Mak and Wolpaw, the application of BMI systems can augment the current rehabilitation therapies by reinforcing and increasing effective use of impaired brain areas and connections [13]. Furthermore, the progress made in the field has enabled SCI patients to grasp or manipulate objects without performing any physical movements. In some studies, the motor cortical activity of the monkeys was used to perform reaching and grasping activities with a robot arm [4], or to perform three dimensional movements that included force grasping for self-feeding using a mechanical device [6].

Brain-Machine Interfaces have been widely used to command communication and control systems [8]. Birbaumer and colleagues developed a spelling device system that could be operated by people suffering from ALS [14]. Other BMI-driven devices have been developed to work either synchronously [15] or asynchronously [16]. Some web browsers are based on evoked potentials such as P300 [17,18]. This kind of potentials have been also tested with ALS patients using a four odd-ball paradigm for task selection [19]. Another important application of brain interfaces are BMI-driven wheelchairs which enable quadriplegic patients to move around on their own [20,21].

We have seen how brain-machine interfaces have a wide range of applications for both the field of rehabilitation and motor substitution and the field of communication and control. This gives some idea of their great potential to support assistive technology. The main goal of this chapter is to address how the combination of BMIs with assistive robotics can help people with a severe motor disability to interact with the environment in a easy and intuitive way.

3 Evoked BMI for Assistive Robotics

Evoked BMIs are based on the extraction of a characteristic EEG signal pattern produced automatically in the brain as a response to some external stimuli [22]. One evoked potential widely explored in the field of BMI is the P300 [23]. P300 is a potential evoked by an awaited infrequent event and it is characterized by a positive deflection in the EEG signal approximately produced 300 milliseconds after receiving a visual stimulus. This paradigm was first used in 1998 to develop a speller application [22]. However, this paradigm has been used recently on other applications, such as controlling a wheelchair [20] or an Internet browser [17,24]. In these applications, in order to evoke the P300, subjects are given a sufficiently large number of options (e.g, letters of the alphabet or icons) from which they choose one by paying attention to the desired one. These option are pseudo-randomly flickering in a screen and it is possible to determine which choice the subject intended as a target, simply by selecting the stimulus that elicits the largest P300. Another evoked potential is the N2PC which is a negative deflection in the EEG approximately produced 200 milliseconds after a visual stimulus. This potential has been widely studied to prove its relationship with selective attention [25,26].

In this section, we describe a non-invasive BMI based on the P300 and N2PC paradigm that allows controlling devices and interacting with people without any motor muscular movement. A robot application has been developed in order to assist disabled people using the BMI. It allows controlling a robotic arm to manipulate objects (performing pick and place tasks). In this application, the traditional interfaces (i.e., keyboard, mouse and control console) have been replaced by virtual interfaces shown on the screen of a computer, which are controlled by the brain activity of the users. These interfaces show different options related to the application in a computer screen. The options are flickering pseudo-randomly to produce visual stimulation. In order to select a specific option, the user must focus on the desired option. The method used to obtain the desired option from the EEG signals is a SWLDA classifier. Different experiments with volunteers have been carried out in order to validate the application, and also to show the improvements achieved by using the combination of P300 and N2PC.

Event Related Potentials and Location. Two different event related potentials (ERP) or evoked potentials that can be registered using electroencephalography (EEG) are going to be used in the following experimental procedures.

- The first paradigm used is P300, that it is characterized by a positive deflection in the EEG signal approximately produced 200 ms after receiving a visual stimulus [23]. The presence, amplitude, topology and delay of this signal is normally used to measure cognitive functions and detect neural desorders [27], but it is also used in BMI applications [22]. The "odd-ball" technique is normally used to evoke the P300 on the brain [28]. In this technique, a target stimulus is presented among other background stimulus. The subject must pay attention only to the target stimulus and ignore the rest. The P300 signal has been widely used to develop Brain-Machine Interfaces [23].
- The second paradigm used is the N2PC, which is also a visual evoked potential that can be produced using the odd-ball paradigm. The N2PC wave is characterized by a negative deflection of the EEG over the visual cortex and its typical latency is 200 ms after a visual stimulus [29]. The N2PC has been widely studied to determine its relationship with selective attention to locate stimulus in certain area of the visual field, giving as a result, stronger deflection amplitudes in the opposite area of the visual cortex where the stimuli is located [25,26].

The P300 signal is usually registered placing electrodes over the central areas of the scalp (Cz, Fz, Pz and around) [17,30]. This response is extended to almost all the brain cortex, but with less amplitude. In the case of the N2PC, its typical location is around the electrodes PO4 and PO3 [25], depending on the placement of the attended stimuli. The placement of the electrodes in the 10/10 International System [31] was chosen according to previous studies [32,33] as follows: Fz, C3, Cz, C4, CP3, CP4, P5, P3, Pz, P4, P6, PO7, PO3, PO4, PO8, Oz, ground on Fpz and reference on the right ear lobe (common reference for all the electrodes). These electrodes include the typical placement used for registering both potentials. Figure 1 shows the placement of the electrodes and their relationship with the channels of the amplifier used.

Hardware and Software. The hardware used is based on the commercial amplifier g.USBamp from g.tec. The EEG signals are registered using 16 electrodes that are connected to this amplifier which has 16 channels. An EEG cap is used to place the electrodes on the scalp of the person as commented before. A special abrasive and conductive gels are used to improve the contact skin/electrode reducing impedances.

Two computers have been used during the experimental tests: one shows the BMI applications developed (user screen), while the other shows the configuration options for the controller (controller screen). Figure 2 shows the hardware of the BMI.

The BCI2000 software has been used for sampling, processing and classify of the EEG signals [34]. This open source software platform for general purpose consists on a series of independent modules (each of them is responsible of a concrete function). During this research a new application module has been developed to design the BMI.

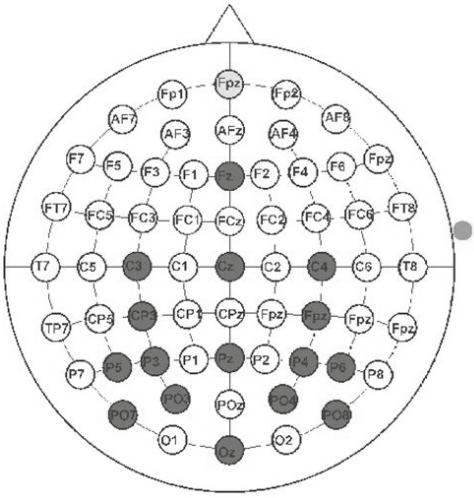

Sensors & Channels			
Fz	1	*Pz*	9
C3	2	*P4*	10
Cz	3	*P6*	11
C4	4	*Po7*	12
Cp3	5	*Po3*	13
Cp4	6	*Po4*	14
P5	7	*Po8*	15
P3	8	*Oz*	16

Fig. 1. Placement of the electrodes used in the study

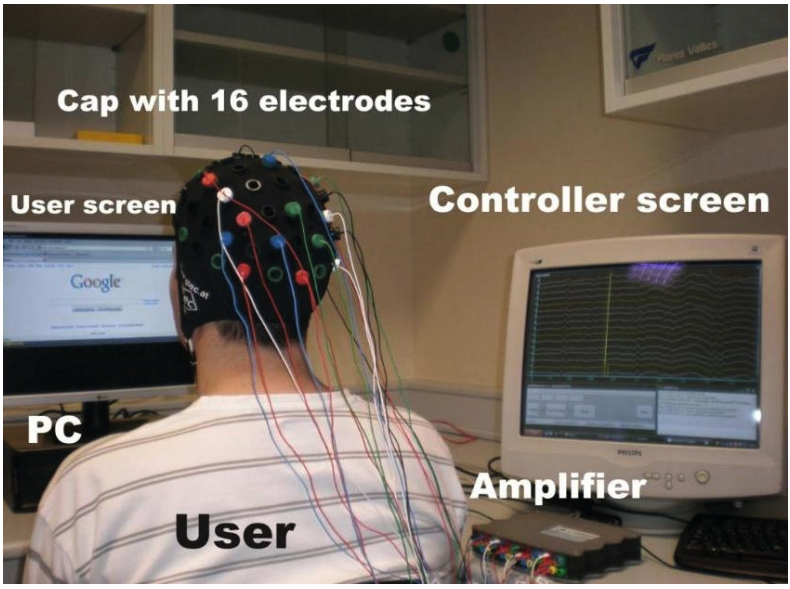

Fig. 2. Hardware used in the Brain-Machine Interface

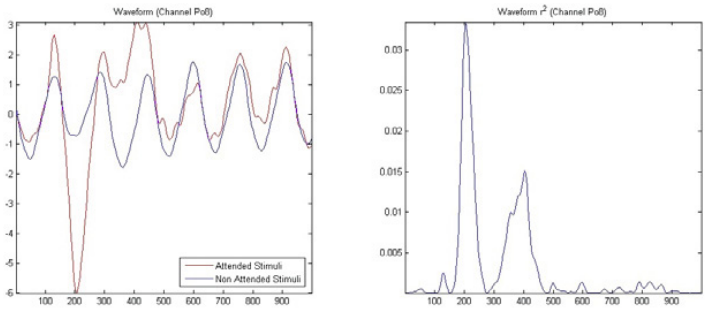

Fig. 3. N2PC signal in the electrode PO8 (20 averages) produced by attended stimulus, compared to the signal produced by non-attended stimulus (left), and the r^2 value of the signals (right)

Processing of the EEG Signals: Features Extraction Algorithm. The EEG signals are amplified and digitalized with a sample frequency of 256 Hz using 8 bits per sample. Afterwards, a band-pass Butterworth IIR filter has been applied between 0.1 and 30 Hz. The EEG signals of the users are registered while the user is paying attention to a certain stimulus and not paying attention the rest of stimulus. Then, a temporal filtering is applied to the signal produced after each visual stimulus. The evoked potentials are time variant but bounded, so the filter is configured to consider the first 600 ms as study time. After each series of visual stimuli corresponding to a decision, the average of all the segments of 600 ms for each stimulus is calculated, removing the background activity, possible artifacts and isolating repetitive patterns.

The new signal is the result of this average and it is composed of 153 samples by channel. Afterwards the signals are decimated at 20 Hz. After this decimation, there are a total of 192 samples, from which finally the 60 most significative samples are statistically chosen by the program used to train the system (P300 Classifier) as characteristics for the classifier. This way, approximately 4 characteristics (or samples) are used per channel.

Figures 3 and 4 show the signals before the decimation. The red signal shows an attended stimulus and the blue one the non-attended stimulus. Figure 3 shows the electrode PO8, one of the most important electrodes in the case of the N2PC, while in Figure 4 the electrode is Cz, the most important in the case of the P300 evoked potential. The repetitive pattern is visible because of the averages done, while the background noise is attenuated.

Classification. The classifier is responsible for distinguishing between the waveform produced by an attended or a non-attended stimulus. In this study, the Stepwise Linear Discriminant Analysis (SWLDA) has been used as classifier [30]. This algorithm is widely used for the classification of evoked potentials and previous studies prove its high performance for this kind of signals [32].

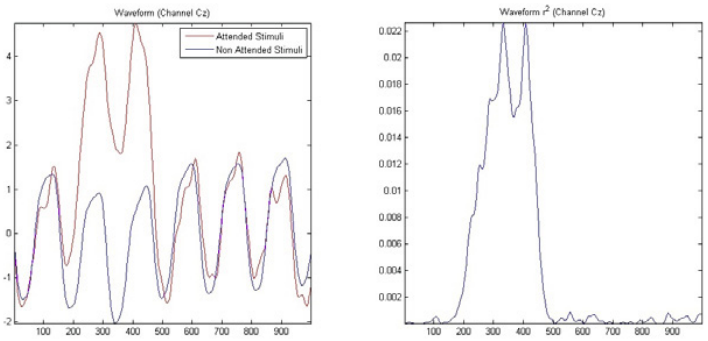

Fig. 4. P300 signal in the electrode Cz (20 averages) produced by attended stimulus, compared to the signal produced by non-attended stimulus (left) and the r^2 value of the signals (right)

This classifier performs a linear transformation, i.e. a matrix multiplication of a classification matrix with the input signal matrix (the output of the temporal filter). The classifier looks for the optimal discriminant function adding features (in this case, consisting on samples from each channel) to a linear equation, obtaining the maximum variability and optimal separation between two classes. The classification matrix consists of a matrix of 60 coefficients obtained from the training signals of each volunteer. These coefficients were extracted by using the P300 classifier (a BCI2000 contribution) [34].

3.1 Robot Control Application

The application designed using the BMI allows disabled people to control a robotic arm of 6 degrees of freedom in order to help them to manipulate objects (performing pick and place tasks). The Fanuc LR Mate 200iB robot has been used in this application (right of Figure 5). It is a commercial robotic arm for general purpose with a pneumatic gripper attached at the end effector to pick objects.

Figure 5 shows the architecture of the brain-based robot control system. This architecture is divided in two parts: the local environment, where the BMI is located, and the remote environment, where the robotic arm is placed. The user receives visual feedback from the robot using an IP camera placed in the remote environment.

The application consists of various selection menus that show the available options. The user has to concentrate his/her attention on the desired option to execute an action while rows and columns are randomly flickering. To have a complete control of the robotic arm, three menus have been developed:

– Actions menu (4x3 matrix) (Figure 6 left): It has several options to move the robot end-effector in the 3D space and to open/close the gripper placed at the robot end-effector. The robot is controlled using Cartesian coordinates.

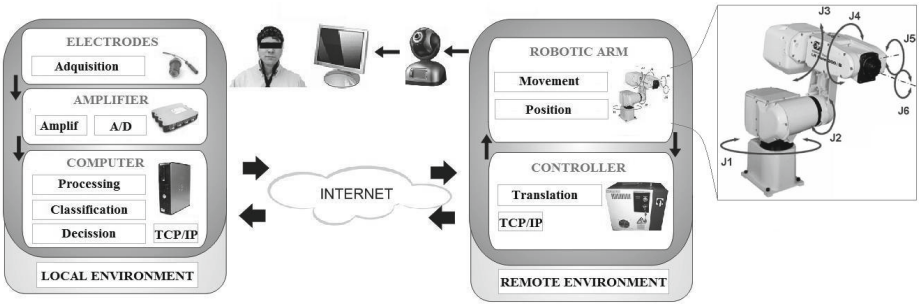

Fig. 5. Architecture of the robot control system and detail of the joints of the robotic arm (right)

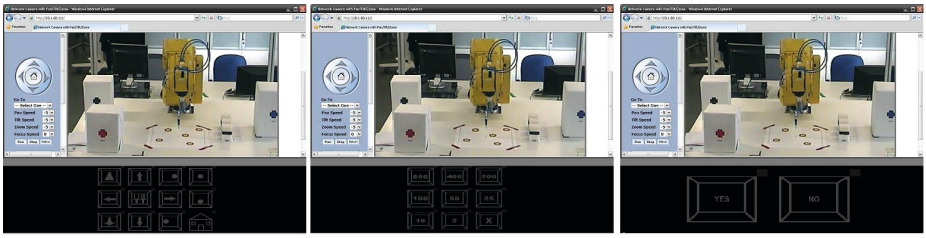

Fig. 6. Graphical interface of the robot control system: Action menu (left), Distance selection (center) and Confirmation menu (right)

- The basic options to move the robot are: up/down, left/right, and forward/backward (all of them represented by arrows).
- Other options allow changing the orientation of the end-effector. Four orientations have been considered: front, table, right and left (represented by options that show a ball in different places inside a square). These options maximize the workspace of the robotic arm. This way the robot can reach any object inside that workspace.
- The "Home" option moves the robot to the default position with the tool in the table position.
- The option to close/open the tool of the robot in order to pick objects is represented in the center of the matrix.

– Distance control menu (3x3 matrix) (Figure 6 center): After selecting a basic movement option using the actions menu, the user uses this menu in order to select the distance that the robot has to be moved. There are 9 options with different distances of movement, from 5 mm to 800 mm. The "X" option, cancel the decision and allows returning to the actions menu without any movement.
– Confirmation menu (Figure 6 right): Some options must be confirmed before being done. This is the case of changing the orientation of the end-effector, go to home position or interact with the gripper. Once selected one of these

options, the confirmation menu is shown. Finally the user must confirm to execute an action, or cancel to avoid an incorrect decision.

A control software module of the robot has been developed. This control software allows that the robot executes the option selected by the user using the BMI. The control software interacts with the BMI using a TCP/IP protocol. When the user concentrates on one of the characters or options that are flickering on the screen, the system starts the features extraction of the signal and average the signals produced by each symbol. When all the options have flashed 12 times (6 per row and 6 per column) the classifier determine the desired option and the application executes the action associated.

Figure 7 shows the states machine of the application. The application starts showing the actions menu ("Waiting Action" state). At that time the robot is in the "Home" position. If the user selects a basic option of movement, the application will show the distance control menu ("Waiting Interval" state). Once the distance is selected, the robotic arm will be moved and the actions menu will be shown again. The options to open/close the tool, to move the robot to "Home" or to change the orientation of the end-effector of the robot need an additional confirmation before being executed. This confirmation is selected by the user using the third menu that only shows the options Yes/No.

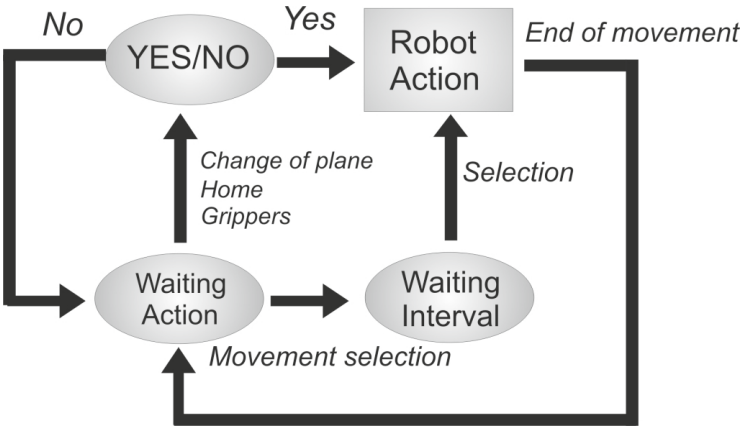

Fig. 7. States machine diagram of the BMI system for controlling a robotic arm

3.2 Experimental Results

Different experiments with volunteers have been carried out in order to validate the usability and viability of the applications. All the volunteers were informed about the requirements of the experiments and all of them gave their consent.

Before performing the experiments, the volunteers must perform a previous training with the BMI. This training allows establishing the coefficients of the

classifier (SWLDA) for each volunteer. The registered information is also going to be used to study the combination of the two evoked potentials: P200 y N2PC. The training is composed by several trials where the volunteers must concentrate on the letters of two specific words using the Copy Spelling function of BCI2000 [34]. In this training, a 6x6 matrix made up of characters that reproduces the "odd-ball" paradigm of Farwell and Donchin [22] is used. The rows and columns are randomly flashing with a stimulus time of 31.25 ms and a time between stimuli of 125 ms. Each character flashed 20 times and afterwards the user had to concentrate on the next one. The volunteers must focus on the indicated letter in order to complete the specified word. During the training, the volunteers performed two trials, using the "COMPUTER" and "SCIENCE" words, respectively. After these trials the performance of each training is tested, doing a cross validation of the classifier.

The tests were done by 3 volunteers. Each one lasted 4.5 minutes, giving as a result 160 attended stimuli and 560 non attended stimuli. After doing these tests with the volunteers, the averages of the two groups of signals were done in each electrode, obtaining two signals per electrode, which lasted one second. This way, both signals (attended and non-attended) can be compared. To compare both groups, a correlation analysis was done in each electrode. The correlation was obtained by using the determination coefficient r2 (square of the correlation coefficient) .The calculus was done by using temporal windows.

This analysis can be topographically represented as a map of the scalp in the 10/10 International System. As it is shown in the Figure 8, around the electrodes P5, P3, P4, P6, PO7, PO3, PO4 and PO8, and near 200 ms, the colors are warmer. This means that the difference between the attended signal and non-attended signal is stronger in the parietal/occipital cortex, being this the N2PC contribution. Progressing in the time evolution, at 300 ms it is highly remarkable the contribution of the P300, visible on the central area (Fz, Cz, C3, C4 and Pz). Finally, at 400 ms there are no evoked potentials and the graph returns to the initial status. By checking the scales, in the case of the 200 and 300 ms it is detectable that the contribution of the N2PC is stronger than the contribution of the P300.

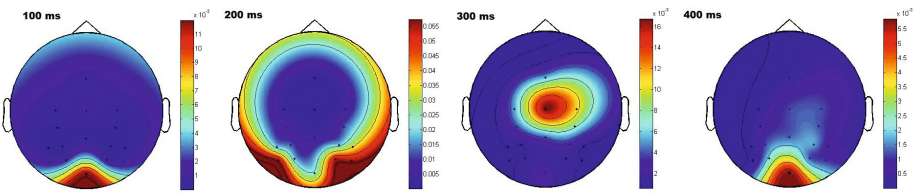

Fig. 8. Evolution of the contribution of visual evoked potentials in the topographic map of the scalp

Table 1. Hit rate obtained using P300, N2PC and the combination of both

	P300 5 Electrodes	N2pc 8 Electrodes	P300+N2pc 16 Electrodes
User 1	60%	95%	100%
User 2	75%	71%	86%
User 3	93%	86%	100%

During this study we have used the N2PC in combination with the P300 paradigm. For BMI applications, based on evoked potentials, it is normally used only the P300 potentials, placing electrodes mainly in the central areas of the scalp. In order to increase the hit rate of the system, both evoked potentials were used in these applications. A negative aspect of the N2PC potential is that it is located at the opposite hemisphere where attended stimulus are placed, this means that for using the N2PC it is mandatory to use two groups of electrodes.

To verify the improvements obtained by the use of both potentials in the BMI, a comparison was done using the training trials and checking in cross validation the hit rate obtained in each case. This study compares the results obtained by using:

- The 5 most representative electrodes in the case of the P300: Fz, Cz, C3, C4 and Pz (see Figure 1).
- The 8 most important electrodes for the N2PC: P5, P3, P4, P6, PO7, PO3, PO4 and PO8 (see Figure 1), distributed in two groups of four electrodes each.
- The 16 electrodes which uses the combination of both potentials (see Figure 1).

Table 1 shows the results obtained by three of the healthy volunteers. The results obtained indicate that it is possible to develop a BMI application by only using the N2PC potentials. The hit rate using this potential is almost the same, or even better in some cases than the hit rate obtained using the P300. However the drawback is that the number of electrodes is higher. On the other hand, the results obtained using both potentials are better than by using only one of them. Therefore the combination of both potentials is a useful tool for increasing the hit rate of the BMI.

Robot Control Application. Three healthy users, with ages between 24 and 29 years old, without gender restriction or laterality, performed some experiments in order to validate the robot control application. A setup with 3 small boxes and 3 big boxes was used in the experiments (Figure 9). Each box is identified by a color (blue, red and black). The aim of the experiment is that the user controls the robot to pick every small box and place it on the top of the big box with the same color. Figure 10 shows a volunteer doing an experiment with the robot control application.

Table 2. Experimental results with the robot control application

	First object		**Second object**		**Third object**		**Hit rate**
	Pick	Place	Pick	Place	Pick	Place	
User 1	1'22"	4'07"	1'04"	2'00"	2'27"	4'21"	98%
User 2	1'41"	3'37"	4'10"	5'30"	2'30"	3'14"	97%
User 3	2'17"	6'36"	3'20"	7'48"	4'15"	5'46"	75%
Average	6'30"		7'55"		7'06"		90%
Standard deviation	±1'38"		±3'30"		±1'48"		

The results of the experiments are shown in Table 2. In the results, the required time to pick the small box and place it on the top of the box with the same color is shown. In addition, the hit rate obtained with a cross validation of the trained classifier is shown. It can be verified that the hit rate was quite high, around 90%. A lower hit average means more time for doing the tasks, which happens to the user 3. In case of a wrong movement selection, this has to be canceled or corrected. The best time average for picking and placing an object was approximately 6 minutes and 30 seconds (first object). This was considered satisfactory according to the task (several basic movements, changes of orientation and opening/closing actions of the tool were required to control the robot). In these experiments, the application provided a selection speed of 8.5 selections/minute for the "action menu" and 10 selections/minute for the distance control menu.

4 Spontaneous BMI for Assistive Robotics

Spontaneous BMIs have a great advantage when using applications where performing voluntary commands is necessary. In these systems, the user performs a volitive cognitive action, i.e., thinks of a particular mental task, generating a command willingly. This approach has been used to control a robot arm [35,15] or a virtual keyboard [36]. Motor imagery consists of the imagination of real motor movement performed by the user. According to Decety and Lindgren, the mental activity of an actual and an imagined motor movement follows the same pattern [37]. The analysis of the activity in regions destined to motion action may allow the detection of different mental tasks such as motor imagery. Moreover, other kind of mental activity (concentration tasks) can be studied in order to obtain a better differentiation between mental tasks. The use of these EEG signals can allow patients with mobility impairments to control systems that provide an improvement in their quality of life.

In this section, the differentiation of two mental tasks is performed to control a planar robot in the horizontal plane. Mental tasks differentiation can be based on different techniques for both the extraction of the features used for classification and the classification method itself. Typically, electrical signals acquired from the scalp of the user are processed to extract the frequency components of these signals. This processing is performed to facilitate the work to the next stage,

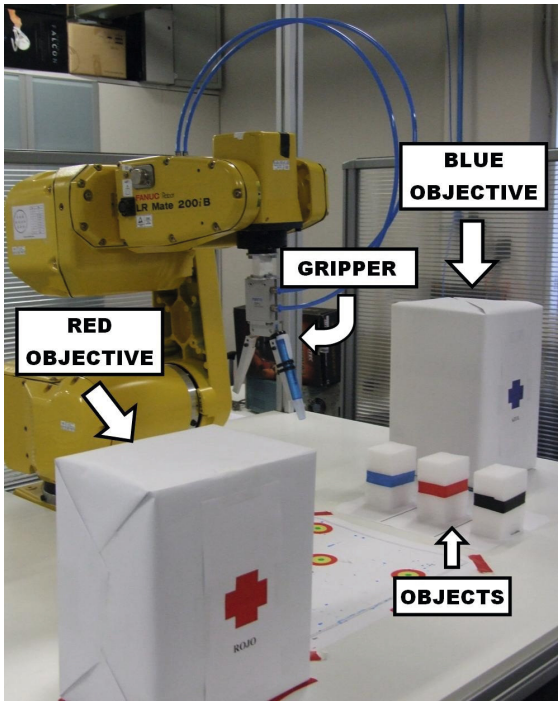

Fig. 9. Experimental set up for controlling the robotic arm

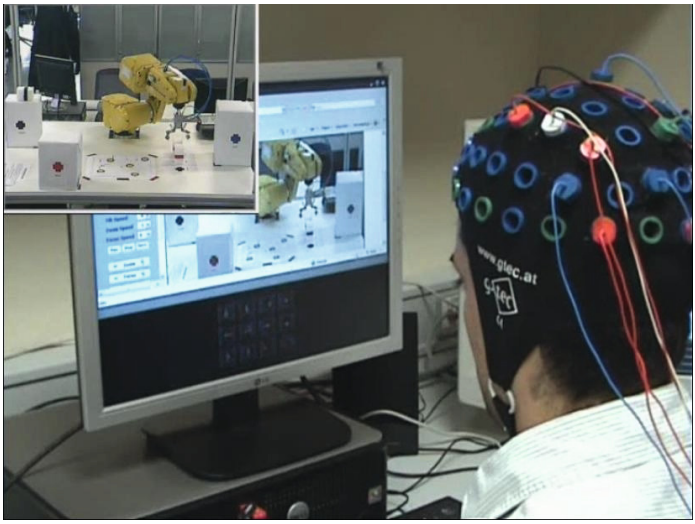

Fig. 10. Volunteer doing one of the tasks controlling the robotic arm with the BMI

the classification of the signals to distinguish the mental tasks performed. In this part there are multiple options such as the use of artificial neural networks or other methods like Bayesian classifiers or systems based on Support Vector Machine (SVM) [38,39]. Two mental tasks will be used to control the movement of a robot in the horizontal plane. To that end, a SVM-based system is used. This kind of classifier is often used to detect motor imagery tasks [40,41]. This system allows, through two different strategies (hierarchical and directional), the robot motion control in two axes. The aim of this approach is to verify the accuracy of the system, evaluating the time required to perform different tasks of achieving goals. The tests have been performed by 2 users in 2 different sessions. On each session, the user has to reach 4 targets twice (once for each control strategy).

4.1 Methodology

Signal Acquisition. The electrical activity of the brain is measured over the scalp using the equipment g.GAMMAcap by the company g.tec. This cap allows a quick placement of the electrodes. In this case, 16 active electrodes are used. The electrodes are the g.LADYbird model by g.tec. g.LADYbird electrodes are sintered Ag/AgCL crown with a 2-pin safety connector. These 16 electrodes follow a uniform distribution over the interesting areas of the brain. According to the International 10/10 System, their positions are the following: Fz, FC5, FC1, FCz, FC2, FC6, C3, Cz, C4, CP5, CP1, CP2, CP6, P3, Pz and P4. Moreover, two extra electrodes are used as a ground and reference. The ground electrode is placed on the AFz position and a monoauricular reference is used. The placement of the electrodes is shown in Figure 11.

After their acquisition, the EEG signals are filtered and amplified using a g.USBamp by the company g.tec. This amplifier allows sampling of the 16 channels to 256 Hz. Additionally, the amplifier is able to apply some internal filters. A notch filter in 50 Hz is used in order to eliminate the perturbations produced by the electrical network. Furthermore, with the purpose of reducing the DC component of the signals and the artifacts which can be generated by the user, a band-pass filter is also applied. This filter is configured between 0,5 and 100 Hz.

Signal Processing. Owing to the relevant motor and concentration information of the electrical activity of the brain is located in the alpha (8 to 12 Hz) and beta (14 to 30 Hz) frequency bands, another band-pass filter is applied. In this case, the filter gets the frequencies between 8 to 40 Hz. This filter is applied in the EEG signals using one-second long windows of the acquired data. To enhance the quality of the signal, a Laplacian filter is also applied to all the channels.

Classification Method. There are some kind of classifiers which are generally used to classify the cerebral activity of the users. One of the more commons

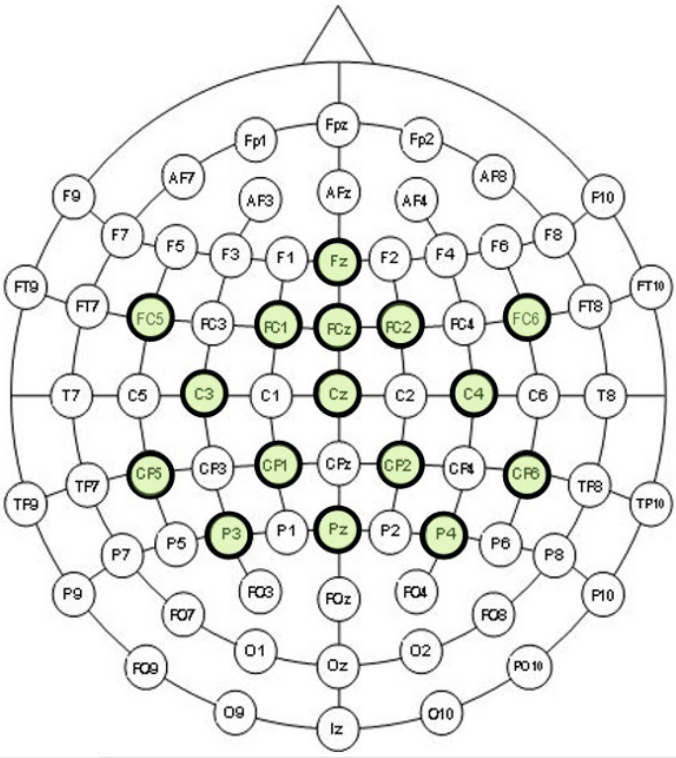

Fig. 11. Electrodes placement according to International 10/10 System

types are the classifiers based on Support Vector Machine. This learning machine, originally introduced by Vapnik and co-workers [42], is based on the use of separated hyperplanes. For cases in which no linear separation is possible, this system can work in combination with the technique of 'kernels', that automatically perform a non-linear mapping to a feature space. This technique is used to classify the data processed. SVM makes use of a hyperplane or a set of hyperplanes in a high (or even infinite) dimensional space by maximizing the margin between the classes to be distinguished.

SVM has different available kernels as linear, polynomial, Gaussian, Radial Basis Function (RBF) or sigmoid. The accuracy of the SVM-based systems depends directly on the kernel and the value of some of their parameters. In EEG signal classification RBF and Gaussian kernels are the most commonly used. In the current case, a RBF kernel is selected. The main parameters which determine the behavior of this kernel are C and γ. The C factor represents the parameter of regulation and it is established as C=512. The size of the kernel is determined by the γ parameter and its value is γ=0,002. These values are selected taking into account the analysis done in a previous work.

In order to obtain an online classification of the data, a previous model is needed. The data obtained in an offline session are used as the training set of data to create this model. Afterward, this model is applied in the SVM-based system to classify the data. It allows the prediction of the performed mental task in the online sessions. The model is created using the features of the signals extracted from the training set of data obtained with the periodogram.

Finally, an extra procedure is seeking to the predicted mental tasks. This procedure is applied to reduce the number of wrong classifications and therefore the erroneous final decisions (i.e. control commands). For this purpose the mental task predicted by the system is not directly used. A group composed of the five last predictions are used to take a decision. Only if, at least four of these predictions are equal, the mental task is considered as a final decision. Otherwise the classification is consider as uncertainty and the system does not react. Due to the fact that the classifier provides a prediction every 500 ms, the system starts to move at least two seconds after the beginning of the change of mental task performed. This fact involves a slight delay in the system. Nevertheless, this delay implies an important benefit reducing the wrong classifications but barely affects the correct ones [43].

4.2 Experimental Procedure

The behavior of the system described above is evaluated using it in the control of a planar robot. This planar robot (named PupArm) is controlled using two different interfaces. With each interface, four goals have to be reached. Five minutes are established as a limit to reach each one. If the user is able to reach the target in the established time, the test finishes and a message is shown to confirm the user that the test has been completed successfully. If the time is consumed, a message warns the user of this fact and two extra opportunities are provided to the user to reach every target. After the user reaches the current target (or the three opportunities are unsuccessfully finished), the next target is asked. During the test, the necessary time to reach the targets is saved to compare the results between sessions and users and to compare the usability of both control strategies.

Experimental Environment. Through a graphical interface the users control two different strategies which enable the generation of commands to move the planar robot. The movements of this assistive planar robot are limited to the horizontal plane. The user is placed in front of the robot and the computer which manages the graphical interface. Another computer is in charge of the control of the robot. In the working zone, four targets are placed as goals. In Figure 12 all these parts of the experimental environment along with the BMI system (the amplifier and the cap of electrodes) are shown. In order to move the robot, the control commands are sent, the current position is updated and the torque command is generated, moving the robot to the desired direction.

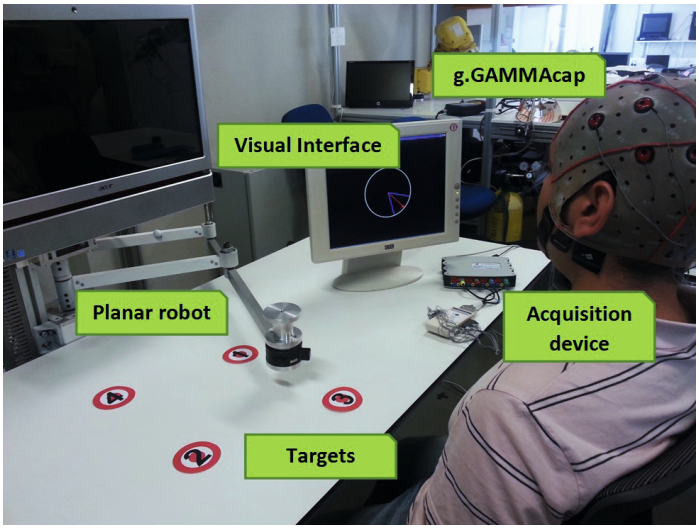

Fig. 12. Experimental environment. Targets are placed in four different positions over the table

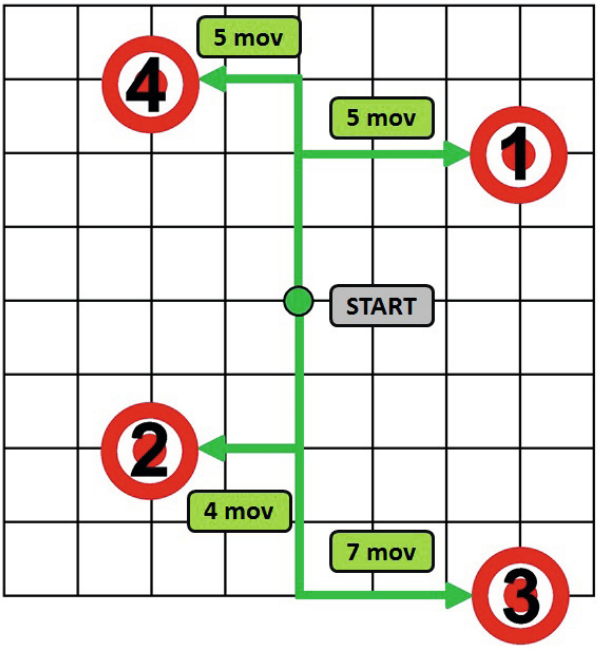

Fig. 13. Schematic distribution of the targets that shows the minimum number of the movement needed to reach each target with the hierarchical control

Planar Robot. The planar robot used in the tests is a PupArm. This force-controlled planar robot was designed and developed by the nBio research group at the Miguel Hernández University of Elche (Spain). The characteristics of the PupArm robot are described below.

As actuator for each two joints, pneumatic swivel modules with angular displacement encoder (DSMI-25-270 of Festo) have been used. This kind of actuators can exert enough driving power despite being lightweight and having a small size because the ratio of its output power to its weight is large. The semi-rotative drives are controlled by two proportional pressure valves (MPPE manufactured by Festo) to achieve a maximum torque of 5 Nm at 6 bar and a maximum swivel angle of 270°. The valve MPPE is designed so that pressure output is proportional to voltage input through a proportional electromagnet. With this configuration (two proportional valves and a pneumatic actuator), the pressure of the two chambers of the pneumatic drive can be regulated to get a desired output force.

The control of the PupArm is done by Simulink using a real time scheme. This robot is connected through USB to the computer. Four analog outputs are used to control each pneumatic actuator through two proportional pressure valves. The feedback of the position of the end effector and the pressure of the valves is obtained using 6 analog inputs.

Control Strategies. In order to control the robot, two different methods are used (see Figure 14). One of them is a hierarchical menu and the other one is a directional control. Both strategies are similar to the methods analyzed in a previous work [44]. These strategies are widely described below.

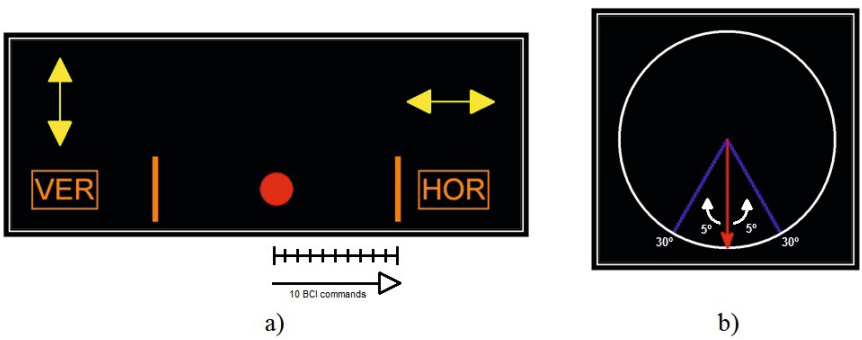

Fig. 14. Hierarchical interface (left). Directional interface (right)

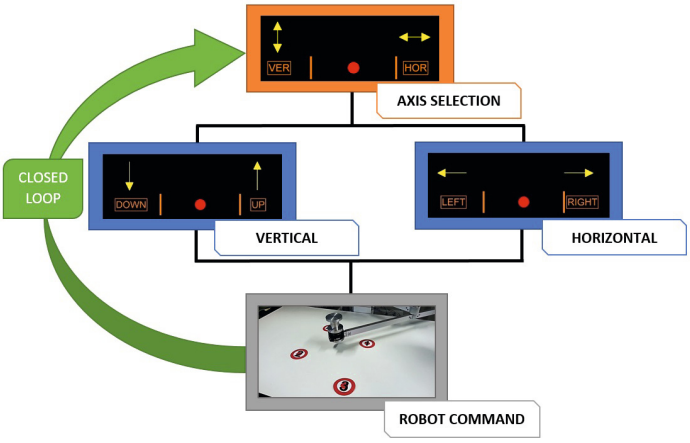

Fig. 15. Hierarchical control menus

– *Hierarchical control*:
This control is based on established movements controlled by a hierarchical menu. The movements of the robot are limited to 2 axis (in an horizontal plane) and these movements are done in predefined 50 mm steps. The distances between the initial position and the targets set up as goals are established to allow a perfect approach. The workspace is composed of a grid of 400x400 mm. The initial position of the robot is placed on the middle of the grid. At the beginning of every test the end effector is placed automatically in this position. In Figure 13 the positioning of the targets is shown.
The movement of the end effector is controlled by the BMI making use of the protocol shown in Figure 15. As it is shown there, in order to move the end effector, two decisions are necessary. Firstly, the user chooses the axis that he/she wants to use (horizontal or vertical). After that, the direction in this axis has to be selected. These decisions are taken by controlling the movement of a cursor in the graphical interface. Every axis or direction is selected when the cursor reaches the limit of the menu. In order to select every option, 10 movements in the menu are needed (see Figure 14-a). This method is used to reduce the probability of obtaining errors in the mental task detection are translated into wrong selections in the menu. Since a new decision is taken every 500 ms, at least five seconds are necessary to reach the limits of the menu. Moreover, and extra time is added to this time. This extra time is due to an initial uncertainty when changing the interface used to assure a better control of the decisions taken, as it is explained in Section 4.1. This extra time is 2 seconds long.
Once an option is selected, the control command is sent to the robot control computer via UDP. This computer controls the planar robot via a Simulink scheme. The output command from the BMI is translated to the corresponding absolute position by increasing the X and Y positions to obtain

a movement of 50 mm in the desired direction. Afterward, this position is sent to the robot controller where the current position is updated and the torque command is generated. This hierarchical strategy has been designed to allow a precise control of the position of the end effector. This precision can be very useful in future applications like grasping tasks.

– *Directional control*:
The directional control allows a more continuous control than the hierarchical one. By using two mental tasks, the users can change the direction of the next movement of the planar robot. Every five seconds, a new control command is generated and the planar robot is moved 25 mm in the selected direction. In order to choose the direction of the movement, the wheel shown in Figure 14-b is used.
The users control the position of the arrow which determines the direction of the next movement. This arrow changes its position every 500 ms when a mental task is detected. Depending on the mental task performed, a 5° right or left rotation of the arrow is generated. In each period of five seconds, a limit of 30° to the at right and left of the final position of the arrow in the previous cycle is established. If the user is able to reach this limit, the robot is moved in this direction immediately and a new cycle begins. At the beginning of the test, the direction of the arrow is located downwards. As in the hierarchical control, the decisions are sent via UDP to the control computer to update the position of the robot.
The directional strategy allows a faster and less constraint control of the end effector. Contrary to the hierarchical control, there is no uncertainty. Every five seconds a decision is taken and the robot is moved. In Figure 16 an example of a complete session test is shown.

4.3 Results

In a previous work [43], the models used for each user to classify the data in these tests were previously checked. Antecedently, every user made online sessions with a visual feedback in order to know if the behavior of the system was correct and the success rate was enough to control these strategies. These tests are similar to the method described in [44]. Two users took part in the experiments. The success rate in these sessions was very high for both users. User A had a average of 88.4±4% and user B had a 84.9±10%. The tests applied were made using the same models.

In each test session, the users try to reach four targets by making use of both strategies. As it is mentioned above, the working space consists of a 400x400 mm square. During the test, if the limits of this working space are reached in any direction, the subsequent movements in this direction will be ignored. The targets are placed into this square in different positions in order to check several directions and changes of the axis used to reach them. The targets are located in the following positions:

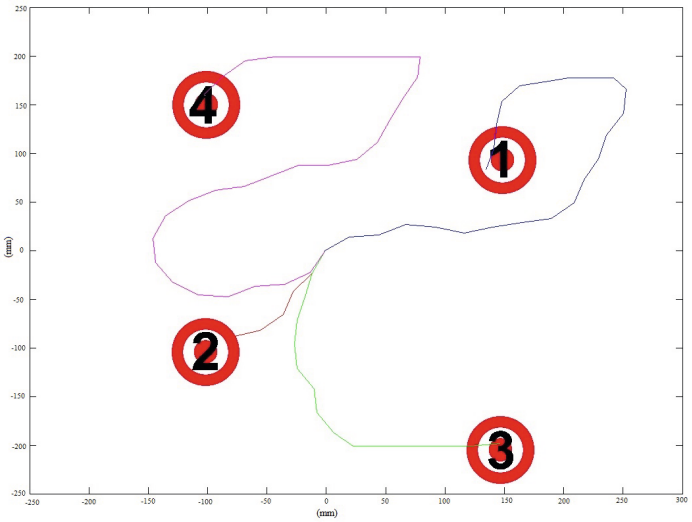

Fig. 16. Example of trajectories followed to reach the targets with the directional control

- Target 1: +150 mm in X-axis and +100 mm in Y-axis
- Target 2: -100 mm in X-axis and -100 mm in Y-axis
- Target 3: +150 mm in X-axis and -200 mm in Y-axis
- Target 4: -100 mm in X-axis and +150 mm in Y-axis

The results of the tests performed are shown in Table 3. In the first column (*User*), the user who takes part in the experimental session is shown. After that, the number of the session (*Test*) and the target established as goal for the run (*Target*) is presented. For each user, two different sessions (1 and 2) are performed. Each session consists of reaching four targets with the two control strategies. The rest of the columns are grouped into two classes, according to the control used. Firstly, three columns belonging to the hierarchical control are shown. Afterward, the data from the directional control are divided into two columns. The *Trials* columns represent the number of trials needed to reach the relevant target. The column *E/M* (Errors/Movements) represents the number of errors and movements (decisions of the BMI-based system) necessary to move the robot to the relevant goal. Finally, the columns *Test time (s)* show the required time to reach the target. By using the hierarchical control, the precise position of the targets are easily achievable. However, when the user uses the directional control, there is an error margin. If the end effector is moved to a position located less than 25 mm away from the target, this position is taken as successful reach. In the cases when the users needed several trials to reach the relevant goal, the values in the columns *Test time (s)* and *E/M* represent the values for the successful trial.

Table 3. Experimental results for both control strategies

User	Test	Target	Hierarchical control			Directional control	
			Trials	E/M	Test time (s)	Trials	Test time (s)
A	1	1	2	0/5	93	2	189
		2	1	5/14	269	2	128
		3	1	1/9	221	1	58
		4	1	2/9	206	1	165
Total time (s)					**789**		**540**
A	2	1	1	1/7	180	1	97
		2	1	0/4	76	1	32
		3	1	0/7	114	1	67
		4	1	0/5	106	2	251
Total time (s)					**476**		**447**
B	1	1	2	0/5	116	1	105
		2	1	0/4	27	1	108
		3	1	1/9	52	2	243
		4	2	0/5	238	1	88
Total time (s)					**433**		**544**
B	2	1	1	1/7	179	1	217
		2	1	2/8	111	1	27
		3	1	0/7	173	1	77
		4	1	0/5	148	1	152
Total time (s)					**611**		**473**

According to these results, it can be concluded that the number of trials necessary to reach the goals is improved in the second session in both users. The number of trials needed in the first session of the user A is 11 and in the second one it is reduced to 9. For user B, the number of trials is decreased from 11 to 8. This user reaches all the targets in the first trial of the second session. In Table 3 the total time need to conclude the whole sessions is also shown. Typically, these times are reduced in the second session. Moreover, the time to move the robot to each target is generally reduced.

5 Conclusions

In this chapter, we have described two different approaches in assistive robotics using Brain-Machine Interfaces. The first approach is a BMI based on evoked potentials to control a 6 degrees of freedom robotic arm. The BMI uses the P300 and N2PC paradigm, registering the EEG signals through 16 electrodes over the scalp. The application allows controlling a robotic arm in order to manipulate objects. This application provides autonomy to disabled people and allows performing complex tasks in an integrated single system. The second approach is a SVM-based system used to command two different control strategies. The handling of a planar robot using these methods is analyzed in order to check the usefulness of the system to reach several targets. The strategies studied are a

hierarchical menu and a directional control. The first one consists of the control of a discrete movement using two axis. Firstly, the desired axis is selected and afterward, the direction is chosen. The directional control consists of controlling the direction of the robot in established periods of time.

Brain-Machine Interfaces are a promising tool for assistive robotics as a more natural way to communicate with prosthetics devices and are particularly suitable for people with a severe motor disability who might even suffer from other limitations. Other systems, such as ocular or voice recognition interfaces are a good alternative. However, they have certain limitations depending on the patient's limitations who are sometimes not able to speak or move their eyes properly.

Regarding the presented BMIs, some improvements can be done to achieve an optimal solution for motor disabled people. The robot control and environment can be enhanced to make more adequate environments for physically handicapped people. For example, by adding a gripper to the planar robot and including some supplementary control, it would be possible to increase the accuracy of movement and grasping of objects in the environment. An interesting system can be a method based on the use of RFID targets which contain information about the objects placed on the table. This mechanism avoids the drawback of the obligation of reaching the specific location. This kind of approach has already been undertaken in previous work of our group with an spontaneous BMI [45] and with an electrooculographic interface [46]. Also, visual interfaces can be adapted to different applications, not always related to assistive robotics, such as a web browser or basic needs communication system [18].

Acknowledgments. This research has been funded by the Commission of the European Union under the BioMot project - Smart Wearable Robots with Bioinspired Sensory-Motor Skills (Grant Agreement number IFP7-ICT- 2013-10-611695), by the Spanish Ministry of Economy and Competitiveness as part of the project DPI2011-27022-C02-01, and by Conselleria d'Educació, Cultura i Esport of Generalitat Valenciana of Spain through grant VALi+d ACIF/2012/135.

References

1. Chung, C.S., Caplan, L.R.: Stroke and other Neurovascular Disorders. In: Textbook of Clinical Neurology, 3rd edn., ch. 45. Elsevier (2007)
2. Ling, G.S.F.: Traumatic Brain Injury and Spinal Cord Injury. In: Goldmans Cecil Medicine, 24th edn., ch. 406. Elsevier (2011)
3. Nicolelis, M.A.L.: Actions from thoughts. Nature 409, 403–407 (2001)
4. Carmena, J.M., et al.: Learning to control a brain-machine interface for reaching and grasping by primates. PLoS Biology 1(2), E42 (2003)
5. Hochberg, L.R., et al.: Neuronal ensemble control of prosthetic devices by a human with tetraplegia. Nature 442, 164–171 (2006)
6. Velliste, M., Perel, S., Spalding, M.C., Whitford, A.S., Schwartz, A.B.T.: Cortical control of a prosthetic arm for self-feeding. Nature 453, 1098–1101 (2008)

7. del R. Millan, J., et al.: Combining brain-computer interfaces and assistive technologies: state-of-the-art and challenges. Frontiers in Neuroscience 4, 161 (2010)
8. Wolpaw, J.R., Birbaumer, N., McFarland, D.J., Pfurtscheller, G., Vaughan, T.M.: Brain-computer interfaces for communication and control. Clinical Neurophysiology 113, 767–791 (2002)
9. Daly, J.J., Wolpaw, J.R.: Brain-computer interfaces in neurological rehabilitation. Lancet Neurology 7, 1032–1043 (2008)
10. Birbaumer, N., Cohen, L.G.: Brain-computer interfaces: Communication and restoration of movement in paralysis. J. Physiology 579, 621–636 (2007)
11. Müller-Putz, G.R., Scherer, R., Pfurtscheller, G., Rupp, R.: Brain-computer interfaces for control of neuroprostheses: from synchronous to asynchronous mode of operation. Biomedizinische Technik 51, 57–63 (2006)
12. Pfurtscheller, G., Müller-Putz, G.R., Scherer, R., Neuper, C.: Rehabilitation with brain-computer interface systems. Computer 41(10), 58–65 (2008)
13. Mak, J.N., Wolpaw, J.R.: Clinical applications of brain-computer interfaces: Current state and future prospects. IEEE Rev. Biomed. Eng. 2, 187–199 (2009)
14. Birbaumer, N., Ghanayim, N., Hinterberger, T., Iversen, I., Kotchoubey, B., Perelmouter, J., Taub, E., Flor, H.: A spelling device for the paralysed. Nature 398, 297–298 (1999)
15. Obermaier, B., Müller, G.R., Pfurtscheller, G.: Virtual keyboard controlled by spontaneous EEG activity. IEEE Trans. Neural Syst. Rehabil. Eng. 11, 422–426 (2003)
16. Müller, K.-R., Blankertz, B.: Toward noninvasive brain-computer interfaces. IEEE Signal Process. Mag. 23, 125–128 (2006)
17. Mugler, E., Bensch, M., Halder, S., Rosenstiel, W., Bogdan, M., Birbaumer, N., Kübler, A.: Control of an internet browser using P300 event-related potential. Int. J. Bioelectromagn. 10, 56–63 (2008)
18. Sirvent, J.L., Iáñez, E., Úbeda, A., Azorín, J.M.: Visual evoked potential-based brain–machine interface applications to assist disabled people. Expert Systems with Applications 39(9), 7908–7918 (2012)
19. Sellers, E.W., Donchin, E.: A P300-based brain-computer interface: Initial tests by ALS patients. Clinical Neurophysiology 117(3), 538–548 (2006)
20. Iturrate, I., Antelis, J.M., Kubler, A., Minguez, J.: A noninvasive brain-actuated wheelchair based on a P300 neurophysiological protocol and automated navigation. IEEE Transactions on Robotics 25(3), 614–627 (2009)
21. Carlson, T., del R. Millán, J.: Brain-controlled wheelchairs: a robotic architecture. IEEE Robotics and Automation Magazine 20(1), 65–73 (2013)
22. Farwell, L.A., Donchin, E.: Talking off the top of your head: Toward a mental prosthesis utilizing event-related brain potentials. Electroenceph. Clin. Neurophysiol. 70, 510–523 (1998)
23. Allison, B.Z., Pineda, J.A.: ERPs evoked by different matrix sizes: Implications for a brain computer interface (BCI) system. IEEE Trans. Neural Sys. Rehab. Eng. 11, 110–113 (2003)
24. Bensch, M., Karim, A.A., Mellinger, J., Hinterberger, T., Tangermann, M., Rosenstiel, W., Birbaumer, N.: Nessi: An EEG-controlled web browser for severely paralyzed patients. Computational Intelligence and Neuroscience (2007)

25. Eimer, M.: The N2pc component as an indicator of attentional selectivity. Electroencephalography and clinical Neurophysiology 99, 225–234 (1996)
26. Kiss, M., Van Velzen, J., Eimer, M.: The N2pc component and its links to attention shift and spatially selective visual processing. Psychophysiology 45(2), 240–249 (2008)
27. Purves, D., Augustine, G., Fitzpatrick, D., Hall, W., LaMantia, A.S., McNamara, J., Williams, S.: Neurociencia, 3rd edn. Editorial Medica Panamericana (2006)
28. Touyama, H., Hirose, M.: Non-target photo images in oddball paradigm improve EEG-based personal identification rates. In: Engineering in Medicine and Biology Society, pp. 4118–4121 (2008)
29. Luck, S.J., Heinze, H.J., Mangun, G.R., Hillyard, S.A.: Visual event-related potentials index focused attention within bilateral stimulus arrays. Functional Dissociation of P1 and N1 components. Electroencephalography and clinical Neurophysiology 75, 528–542 (1990)
30. Johnson, G.D., Krusienski, D.J.: Ensemble SWLDA classifiers for the P300 speller. In: Jacko, J.A. (ed.) HCI International 2009, Part II. LNCS, vol. 5611, pp. 551–557. Springer, Heidelberg (2009)
31. American Electroencephalographic Society: American Electroencephalography Society guidelines for standard electrode position nomenclature. Journal of Clinical Neurophysiology 8(2), 200–202 (1991)
32. Krusienski, D.J., Sellers, E.W., Cabestaing, F., Bayoudh, S., McFarland, D.J., Vaughan, T.M., Wolpaw, J.R.: A comparasion of classification tecniques for the P300 Speller. Journal of Neural Engineering 3, 299–305 (2006)
33. Mirghasemi, H., Fazel-Rezai, R.: Analysis of P300 classifiers in brain computer interface speller. Engineering in Medicine and Biology Society 1, 6205–6208 (2006)
34. Schalk, G., McFarland, D.J., Hinterberger, T., Birbaumer, N., Wolpaw, J.R.: BCI2000: A general-purpose brain-computer interface (BCI) system. IEEE Transactions on Biomedical Engineering 51(6), 1034–1040 (2004)
35. Iáñez, E., Azorín, J.M., Úbeda, A., Ferrández, J.M., Fernández, E.: Mental tasks-based brain–robot interface. Robotics and Autonomous Systems 58(12), 1238–1245 (2010)
36. Inoue, S., Akiyama, Y., Izumi, Y., Nishijima, S.: The development of BCI using alpha waves for controlling the robot arm. IEICE Transactions on Communications 91(7), 2125–2132 (2008)
37. Decety, J., Lindgren, M.: Sensation of effort and duration of mentally executed actions. Scandinavian Journal of Psychology 32, 97–104 (2001)
38. Lotte, F., Congedo, M., Lcuyer, A., Lamarche, F., Arnald, B.: A review of classification algorithms for EEG-based Brain-Computer Interfaces. Journal of Neural Engineering 4(2), 1–13 (2013)
39. Bashashati, A., Fatourechi, M., Ward, R.K., Birch, G.E.: A survey of signal processing algorithms in brain-computer interfaces based on electrical brain signals. Journal of Neural Engineering 4(2), 35–57 (2001)
40. Wang, L., Xu, G., Wang, J., Yang, S., Wang, J.: Motor imagery BCI research based on sample entropy and SVM. In: International Conference on Electromagnetic Field Problems and Applications, pp. 313–316 (2001)
41. Arbabi, E., Shamsollahi, M.B., Sameni, R.: Comparison between effective features used for the Bayesian and the SVM classifiers in BCI. In: IEEE Engineering in Medicine and Biology 27th Annual Conference, pp. 5365–5368 (2001)
42. Vapnik, V.: Statistical Learning Theory. Ed. Wily, New York (1998)

43. Hortal, E., Úbeda, A., Iáñez, E., Planelles, D., Azorín, J.M.: Online classification of two mental tasks using a SVM-based BCI system. In: Neural Engineering Conference 2013, pp. 1307–1310 (2013)
44. Úbeda, A., Iáñez, E., Badesa, F.J., Morales, R., Azorín, J.M., García, N.M.: Control strategies of an assistive robot using a Brain-Machine Interface. In: IEEE/RSJ International Conference on Intelligent Robots and Systems, pp. 3553–3558 (2012)
45. Úbeda, A., Iáñez, E., Azorín, J.M.: Shared control architecture based on RFID to control a robot arm using a spontaneous brain-machine interface. Robotics and Autonomous Systems 61(8), 768–774 (2012)
46. Iáñez, E., Úbeda, A., Azorín, J.M., Perez-Vidal, C.: Assistive robot application based on an RFID control architecture and a wireless EOG interface. Robotics and Autonomous System 60(8), 1069–1077 (2012)

Smart Walkers: Advanced Robotic Human Walking-Aid Systems

Anselmo Frizera Neto[1], Arlindo Elias[2], Carlos Cifuentes[1], Camilo Rodriguez[1], Teodiano Bastos[1,2], and Ricardo Carelli[3]

[1] Electrical Engineering Department, Federal University of Espirito Santo, Av. Fernando Ferrari 514, 29075-910, Brazil
[2] Biotechnology Department - RENORBIO, Federal University of Espirito Santo, Av. Fernando Ferrari 514, 29075-910, Brazil
[3] Institute of Automatics, National University of San Juan, Av. San Martin Oeste 1112, 5400, San Juan, Argentina
{anselmo,teodiano,carlos.garcia}@ele.ufes.br, arlindo.elias@ufes.br, camiloard@gmail.com, rcarelli@inaut.unsj.edu.ar

Abstract. In this book chapter, the authors present the Smart Walkers as robotic functional compensation devices for assisting mobility dysfunctions and empowering the human gait. First, general concepts of locomotion, mobility dysfunctions and assistive devices are presented. A special attention is given to the walkers, considering not only the large number of users, but mainly the rehabilitation and functional compensation potential of empowering the natural mobility. Following, robotic versions of wheeled-walkers for assisting locomotion dysfunctions are presented. In this context, the UFES Smart Walker is presented as an example of a robotic device focused on the user-machine multimodal interaction for obtaining a natural control strategy for the robotic device. Two developments are discussed: (i) an adaptive filtering strategy of the upper-body interaction forces is used in a Fuzzy-Logic based control system to generate navigation commands, and (ii) a robust inverse kinematics controller based on users-motion is presented as a new solution for controlling the Smart Walker motion. Finally, conclusions and future works in the field of walker-assisted gait is presented in the last section.

1 Introduction

1.1 Locomotion, Mobility Dysfunctions and Assistive Devices

Mobility is one of the most important human faculties and can be defined as the ability of an individual to move freely through multiple environments and perform daily personal tasks with ease [1]. Different types of pathologies, such as poliomyelitis, spinal cord injuries, multiple sclerosis or trauma, affect human mobility at different levels causing partial or total loss of such faculty. Recent evidences also show that mobility restrictions are associated to cognitive and psychosocial disturbances, which further impair the quality of life of the individual [2]. In addition, it is known that mobility decreases gradually with age as a consequence of neurological, muscular and/or osteoarticular deterioration.

S. Mohammed et al. (eds.), *Intelligent Assistive Robots*,
Springer Tracts in Advanced Robotics 106, DOI: 10.1007/978-3-319-12922-8_4

Although most gait/mobility disturbances are well recognized, only a small number of such conditions can be fully reversed by surgical procedures or rehabilitation approaches. Therapeutic alternatives in such cases include the selection and prescription of assistive devices to provide adequate functional compensation and to stop the progression of the disability and improve the overall quality of life of the affected subjects [3].

The choice of the most appropriate model of assistive device requires careful analysis and interpretation of the clinical features associated with the subject's residual motor capacity, including cognitive function, vision, vestibular function, muscle force (trunk and limbs), degenerative status of lower and upper limb joints, overall physical conditioning of the patient and also additional characteristics of the environment in which the patient lives and interacts. Severe dysfunctions in one or more of such features can compromise the safe use of the device and increase the risk of falls or energy expenditure [4].

Based on the levels of mobility restriction, the patients can be classified into two broad functional groups:

1. Individuals with total loss of the mobility capacity
2. Individuals with partial loss of mobility, presenting different levels of residual motor capacity.

Individuals belonging to the first group have completely lost the ability of move by themselves and are at high risk of confinement in bed and, consequently, to suffer the effects of prolonged immobility. Examples of subjects in this functional group include patients with complete spinal cord injury, advanced neurodegenerative pathologies, severe lower limb osteoarthritis and fractures of the spine/lower limb bones. In such cases, however, the motion can be performed by assistive technology known as alternative devices. Without the use of such equipment, the locomotion may become an impossible task for these patients, even through small spaces [5]. Some examples of alternative devices are robotic wheelchairs and special vehicles, including adapted scooters.

The mobility provided by the alternative devices can help patients to gain a certain amount of independence during daily tasks and may have positive impact on self-esteem and social interaction. However, the prolonged use of such devices do not prevent immobility-related adaptations in spine and lower limbs, characterized by loss of bone mass, circulatory disorders, pressure ulcers and other physiological impairments [6].

The second functional group is composed by individuals that present some level of residual motor capacity, which can be empowered by an assistive device. In other words, the use of such augmentative devices aims to empower the user's natural means of locomotion, taking advantage of the remaining motor capabilities. This second group of rehabilitation devices can be classified into wearable orthoses and prostheses or external devices, such as canes, crutches and walkers. In the last decade, researches in the field of intelligent augmentative devices have increased, with focus on the implementation of advanced robotic solutions for people with disability.

1.2 Walker-Assisted Ambulation: Benefits and Limitations

Conventional walkers are important examples of assistive devices because of its structural simplicity, low cost and rehabilitation potential. Walkers are usually prescribed for patients in need of gait assistance, to increase static and dynamic stability and also to provide partial body weight support during functional tasks [7]. Such devices are classified as augmentative because empower the residual motor capacity of the user, allowing a natural way of locomotion and preventing immobility-related changes. Additionally, evidence also shows that walker-assisted gait is related to important psychological benefits, including increased confidence and safety perception during ambulation.

The standard frame is the most common configuration of a passive walker, based on a metal frame with four rigid legs that must contact the ground simultaneously during each step. It is considered the most stable model, but requires a slow and controlled gait pattern, since the user must lift the device completely off the ground and move it ahead before taking a step forward [4].

Critics regarding the use of standard frames arise from evidence that shows increased force levels exerted by the upper limbs during locomotion [8]. The gait pattern imposed by the device also increases the user's energy expenditure by 217% during level walking when compared to unassisted or wheeled walker-assisted gait. Such findings restrict the prescription of standard walkers for patients presenting severe levels of metabolic, cardiac or respiratory dysfunctions [9]. Patients with cognitive disorders are also not among the scope of potential users of standard frames. This recommendation is mainly based on the results of Wright and Kemp (1992), which reported that gait assisted by standard walkers requires higher levels of attention when compared to canes or other walker models to avoid the risk of falls.

The reported adverse effects that may arise with standard frame assisted-gait suggest that the device prescription must be based on a detailed clinical assessment of the patient and the potential restrictions. To overcome such problem, other walker models were developed to provide better adaptation to the patient needs.

The two-wheeled walkers are another variation of conventional walkers. Although similar to standard frames in many aspects, these versions are characterized by the presence of two wheels mounted on the front legs (front-wheeled walkers). Such models are recommended for more active subjects or patients that have a hard time in lifting the device from the ground. The wheels allow the performance of a more natural gait pattern, but evidence shows that dynamic stability during walking is lower than standard frame assistance, and the energy expenditure is 84% higher when compared to normal ambulation [3] [4].

Rollator walkers are the evolution of the two-wheeled models and present four wheels attached to the legs of the walker. These models are faster and allow the performance of a natural gait pattern during locomotion, with lower energetic expenditure compared to other walker models. However, rollators are considered the most unstable walker version and the risk of falls is significantly increased in situations that require full body-weight support of the user, due to

uncontrolled displacement of the device. In a clinical setting, rollators may be recommended for patients that require a broad walking base without the need of continuous body-weight support. The design of such models allow great number of adaptations, like braking system at the handles (to increase static stability), varied wheel sizes, robust frames, attached seat cushions, among other different gadgets [9] [3].

1.3 Smart Walkers

General Concepts. In the field of robotic technologies for gait assistance, there are several ongoing projects regarding robotic versions of canes, walkers and other guidance devices. In this context, a new category of walkers have arised, integrating robotic technology, electronics and mechanics, known as "robotic walkers", "intelligent walkers" or simply "smart walkers" [10]. Such devices present a great number of functionalities and are capable of providing mobility assistance at different functional levels, better adjusted to the individual needs of the user [11] [10].

Robotic walkers are usually mounted over a rollator framework. This configuration takes advantage of the versatility of the four wheels and the ability to maintain approximate natural patterns of walking. Stability issues are dealed with special security mechanisms to prevent falls and undesirable movement intentions from the user [11]. Several other special features can be integrated in the system, allowing the implementation of different control strategies and monitoring mechanisms.

Functional Classification of Smart Walkers. Each model of robotic walker described in the literature presents an unique set of features that complicates the classification of such systems into homogenous groups based on the overall set of functions. A classification strategy was proposed by Elias et al [11], based on the allocation of the features implemented in robotic walker systems into four functional domains (Table 1).

A review of the main robotic walker models described in the literature are provided in the following sections, in the context of each defined functional domain.

Stability and motion support. Robotic walkers are able to provide physical stability and motion support in active or passive modalities [10] [12]. In passive systems, the user has to provide the pushing energy to propel the device and the system framework tends to be lighter and simpler to assemble. It can also be equipped with several security mechanisms, like obstacle avoiding and special braking capabilities [13] [14]. Patients using this type of walker must have a postural control and walking ability [15]. Such devices are suitable for use in later stages of rehabilitation programs and domiciliary functional compensation.

Conversely, active walkers are capable of automatic propelling power and navigation, providing better control of overall motion characteristics, like speed,

Table 1. Feature-based classification of smart walkers

Classification	Functions	Features
Physical stability	Propelling power	Passive
motion support	Motor task assistance	Active
	Motion detection	Hybrid systems
		Walking
		Multitask assistance
		Force sensors
Navigation and	Intelligent navigation	Installed maps
localization components	Localization assistance	Obstacle avoidance
		Environment interaction
		Embedded GPS
		Visual and voice feedback
		Automatic return to selected location
Biomechanical and	Functional monitoring	Gait and/or specific motor tasks
bioelectrical monitoring	Physiological monitoring	biosignal monitoring
Safety measures	Fall prevention	Braking
	Emergency braking	Involuntary movement detection
		User-device distance
		Gravity compensation

direction and slope negotiation [10] [12]. The device tends to be safer and suitable for patients in early stages of rehabilitation programs (lower limbs or spine surgery) or for those presenting a high degree of frailty. However, the construction of this type of walker is more complex than a passive system, and the need of extra electronic components may be reflected in higher costs [15].

Hybrid systems are also described in the literature, in which both types of control can co-exist in the device [12] [16]. This feature is especially interesting for rehabilitation purposes, since recovery protocols can be progressed from early stages, where more active control features are required, to advanced training strategies based on passive control to improve patient's proprioception and walking abilities.

Besides assisting in user's locomotion, some robotic walkers are also capable to assist other functional tasks, like sit-to-stand or stand-to-sit transfers [17] [18] [19]. The versatility of these multifunctional systems may have a positive impact in several clinical scenarios where upright postural training or stimulation are needed, such as inpatient rehabilitation following orthopaedical surgical procedures, elderly with poor postural control or lower limb weakness and patients presenting pathological gait patterns.

Several models of robotic walkers are equipped with force sensors in the handles of the device [20]. Such sensors are used to detect the subject's intents of movement, and it enhances the cognitive human-machine interaction. Force signals are converted into guidance commands through filtering and classification strategies [21]. In addition, involuntary movements of the user can also be detected and classified, avoiding undesirable motion commands.

An innovative forearm support was developed for the Simbiosis walker which was also used to detect force interactions patterns during motion level walking and to identify user's intent of movement [10] [21]. The detection of force patterns, both in handles or alternative supports, can also be used to identify altered gait patterns that can be corrected by a feedback intervention by the physical therapist.

Navigation and Localization Components. Navigation systems are a common feature of robotic walkers. The main objective of such hardware is to increase locomotion safety, since the embedded sensors are able to detect and automatically avoid obstacles, negociate an alternative route and also notify the user about the shape and location of the obstacle. This feature is of special interest for people with severe visual disturbances [22] [23] and may act in conjunction with active systems to drive the user safely throughout a closed environment.

This function can be accomplished by previous knowledge of the environment's map [23], or by real time obstacle detection and negotiation [24]. The first mode is suitable for closed environments, such as homes or clinical scenarios. The later mode is indicated for open or dynamic environments, being suitable for patients with more active lifestyle. In either way, these features may give more confidence to the patient in early stages of rehabilitation programs, and gait training can be safely done in either ambulatory or hospital settings, or even at home.

The devices can also communicate with the user via visual or voice feedbacks, informing the presence of obstacles and giving direction options [12] [23].

Autonomous localization features are relevant for patients with cognitive disturbance, sensory degradation and loss of memory that are associated with neuro-degenerative diseases such as Alzheimer or Parkinson. GPS devices can be installed in robotic walkers in order to keep track of the patient in a particular environment or outsides [10].

Modern systems are also able to interact with specific sensors in the environment, supplying the patient with direction options and localization via visual feedback [25].

Biomechanical and Bioelectrical Monitoring. Besides movement and navigation assistance, smart walkers present monitoring features that are of significant relevance for rehabilitation programs. Recent studies investigating gait parameters detected by smart walkers have shown the potential and versatility of this type of assistive device in treatment planning and progression. This feature also adds the possibility of out-of-the-clinic monitoring.

In a clinical setting, several gait parameters can be monitored by therapists in a treatment session using robotic walkers, including speed of movement, total distance traveled, gait patterns, total amount of force/torque exerted in the handles during gait, movement acceleration/deceleration, stride to stride distance and several others [26] [27] [28] [29] [30].

The detection of dysfunctional gait patterns during training sessions with smart walkers can provide additional clinical data that can be used by the clini-

cian to improve the overall treatment program and progression, which can reflect in increased precision and quality of the intervention.

In addition to biomechanical and bioelectrical data analysis acquisition, the monitoring of other physiological signals through smart walkers is also possible and can be used to keep track of associated co-morbidities of the user. The PAMM system, developed by MIT, was the first to present an embedded electrocardiogram monitor system. Modern walkers are also able to monitor blood oxygenation through photoplethysmography sensor located in the handles of the device [27] [28].

All this information can be used to record a medical and/or functional history of the user and can also be sent via a remote terminal to the professional staff responsible for the rehabilitation program [10] [29] [31].

Safety Measures. Safety is a major concern of robotic walker systems, since the user must rely on the support provided by the device to perform the necessary tasks of rehabilitation programs or daily activities.

Several strategies to prevent falls and to help stabilize the user's gait pattern are described in the literature. The main features associated with such function are emergency braking capabilities, jerky movement detection, gravity compensation and user-walker distance monitoring.

Emergency braking are often associated with obstacles and stairs detections, acting together with navigation components [14] [15] [24]. Gravity compensation is another feature that makes use of intelligent navigation, allowing the recognition and proper negotiation of terrain irregularities, such as slopes [15].

Irregular or jerky movements are indicative of postural imbalance and can be detected by force sensors in either handles or forearm support [10], braking the device to provide enough support for postural recovery [21].

A remarkable feature of some systems is related to the placement of rear sensors in the device. The objective is the constant monitoring of the distance between the user and the walker. Increasing of this distance is detected by the rear sensor and, thus, emergency braking is performed, allowing the user to re-establish the correct, and safer, distance [14]. A recent model presented an innovative step-by-step technology that enabled the walker to keep the same pace of the user by monitoring the user's footsteps [12].

Braking the device is also important to provide support for sit-to-stand and stand-to-sit assistance, avoiding slipping or undesired movement of the walker that could increase the chance of falls [15] [23].

Following, the full development of the UFES Smart Walker, a robotic system built at Federal University of Espirito Santo, is presented to illustrate the main features and rehabilitation potentials of such assistive devices.

2 UFES Smart Walker. System Overview

In this section, the UFES Smart Walker is presented (Fig. 1). The device focuses on enhancing safety and stability during assisted gait by means of partial body

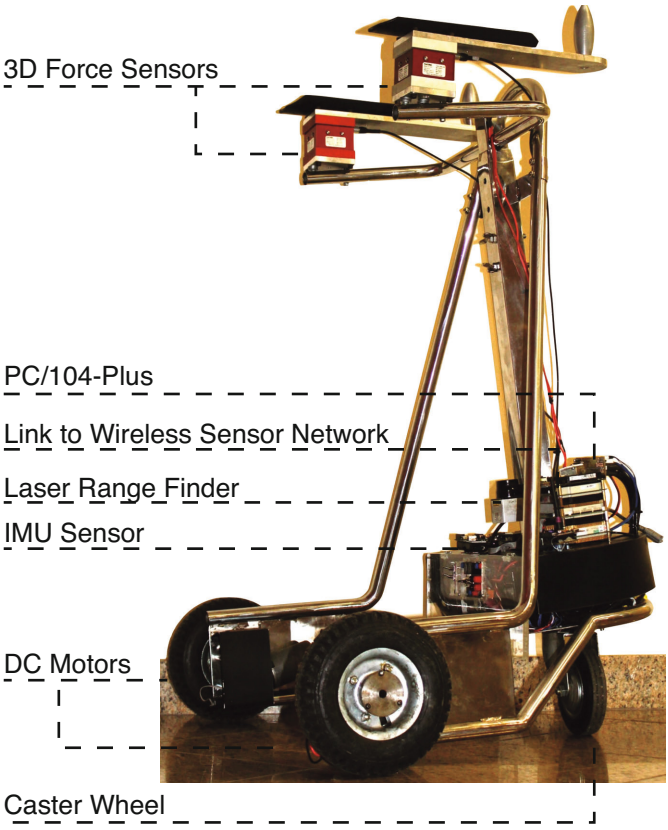

Fig. 1. The UFES Smart Walker and its subsystems

weight support and the use of advanced control strategies. The control system relies on a human machine interface (HMI) responsible for the acquisition and interpretation of user's postures and gestures during gait. Both upper and lower limbs information are combined in order to command the device's motion.

The robotic walker developed under the framework of the research project presents three sensor subsystems designed for the acquisition of gait parameters and for the characterization of the human-robot interaction during gait. First, the *upper-body force interaction subsystem* is based on two tridimensional force sensors (Futek MTA400) installed under the forearm supporting platforms. The forces signal acquisition is performed by an acquisition module installed on the embedded computer described below.

The second subsystem is based on a laser range finder (LRF) sensor (Hokuyo URG-04LX) to measure the user's feet evolution during the assisted gait. The LRF sensor is mounted on the walker framework at the legs height and the legs location is estimated in real-time by means of a processing board based on the

Microchip dsPIC33F micro-controller. A full scan, which provides the position of each leg, is performed by the laser sensor every 100 ms.

Finally, wireless inertial measurement units (IMU), developed in previous research project [32], are integrated into the system architecture. One of them is installed in the walker's structure, as shown in Fig. 1. Other IMUs can be integrated into the real-time architecture by means of the wireless link for biomechanical monitoring and to provide kinematic information to be used in the control strategies. All IMUs are linked using ZigBee protocol setting up a wireless sensor network that communicate via serial interface with the embedded computer. In the application presented in this chapter (see section 3.2), the IMU information is used to get walker and human orientation and human angular velocity to provide information to the controllers. IMU information is sampled every 20 ms.

An embedded computer based on the PC/104-Plus standard performs control and processing tasks and integrates the previously presented subsystems. It is based on a 1.67 GHz Atom N450, 2 GB of flash memory and 2 GB of RAM. The application is integrated into a real-time architecture based on Matlab Real-Time xPC Target. A laptop computer is used for programming the real-time system and to save the data from the experiments. It is connected to the PC/104-Plus by UDP protocol. If data recording is not necessary, the robotic system is able to operate without the laptop computer.

Fig. 1 summarizes the system architecture and subsystems installed on the walker's structure.

Regarding the feature-based classification of smart walkers, the UFES Smart Walker integrates functions related to:

- Physical stability and motion support. The device integrates forearm supporting platforms to allow partial body weight support. Additionally, the traction motors installed on the device's rear wheels offer an assistance to the propelling power. Finally, the sensors subsystems are also used for extracting the user's navigation intentions.
- Biomechanical monitoring. As it will be presented in section 3.2, gait parameters, such as cadence and step length, can be extracted by combining the data obtained from the LRF and IMU sensors. By using additional IMU sensors placed on the user's lower limbs, joint kinematics can also be measured.
- Safety measures. Considering the safety measures, a set of rules regarding the interaction forces and user-walker distance parameters are integrated into the device control architecture (see section 3.1). Emergency braking is performed in the case of unsafe situations. Involuntary interaction forces are also canceled in real-time during the operation of the device. The DC motors used for traction also automatically brake in cases of power failure or overheating of the motor electronic drivers.

3 Development of Controllers Based on User-Machine Interaction During Assisted Gait

In this section, two control strategies are presented. First, in section 3.1, an adaptive filtering strategy of the upper-body interaction forces is fed into a Fuzzy-Logic based controller. Section 3.2 addresses a robust inverse kinematics controller in which the navigation commands are obtained from the user's motion measured using the laser range finder and the inertial measurement units.

3.1 Adaptive Filtering of Force Interaction for the Identification of Guidance Intentions

On a previous research project that was the framework to the development of the Simbiosis Walker [33], a study regarding the force interaction during assisted gait led to the identification of three main components. The typical force data acquired on the y axis (F_y in Fig. 2) of one of the force sensors is presented in Fig. 3.

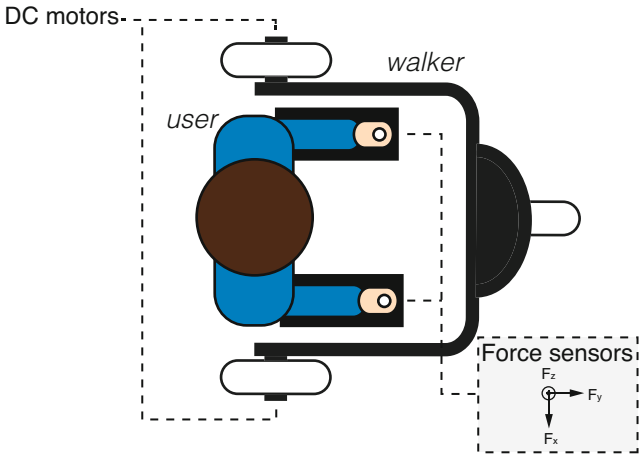

Fig. 2. The human-walker model used for the force interaction controller

The high frequency component is caused by the vibrations introduced by the floor/walker wheels imperfections and should be eliminated. The second component is due to the oscillations of the user's trunk during gait. This second component contains important information related to the user's gait (cadence, heel-strike and toe-off instants) and the evolution of the center of gravity (CoG) during the locomotion [34]. Nevertheless, this component does not reflect the user's locomotion intentions and, therefore, should be filtered. Finally, the voluntary components related to the user's navigational commands are the focus of interest in this approach.

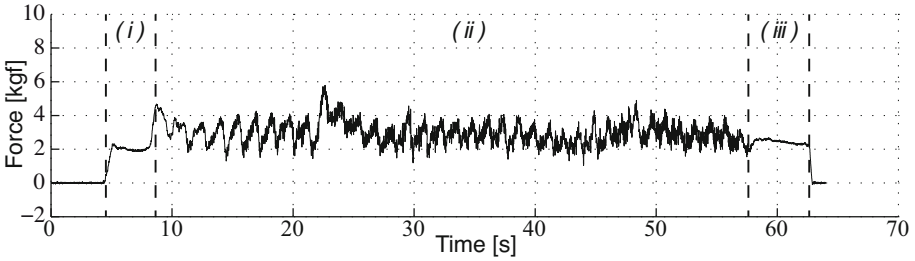

Fig. 3. Typical force signal (y axis) obtained experimentally. Areas (i) and (iii) indicate the periods that the user is supported by the device and is not walking. Area (ii) indicate the walking part of a sample experiment.

These voluntary components are also found within the force sensor data presented in Fig. 3 and can be seen as transient components that must be properly extracted in order to generate commands that drive the walker's motion.

The presence of the three force components led to the development of a technique for obtaining and characterizing such components in order to extract the user's commands to control the device [35]. This filtering technique will be addressed in the following sections.

Cancellation of the Vibrations Components Introduced by Floor/ Walker Wheels Imperfections. Irregularities on the ground or imperfections on the device's wheels cause mechanical vibrations in higher frequencies, where no gait or user's commands components are found. Classical low-pass filters can be generally used for the cancellation of high-frequency components of the force signals. Nevertheless, such approach would also introduce an important phase shift between input and outputs signals causing a temporal delay on the filtered signal. Such situation is undesirable in real-time applications once delay can affect the natural interaction between both agents (walker and user).

Therefore, to avoid the undesirable delays and considering the nature of the vibration signals, a filtering strategy with prediction would be a suitable approach. Architectures based on particle filters or Kalman algorithms could be an good alternative for such situations, but their use can imply in higher computational cost.

To overcome such limitation, a filtering architecture for the cancellation of such vibration components based on *g–h filters* was chosen. G–h filters are simple recursive filters that estimate future position and velocity of a variable based on first order model of the process. Measurements are used to correct these predictions, minimizing the estimation error.

G–h filters are closely related to Kalman filters and to linear state observers, but can be seen as a simpler approach as they do not require a detailed system model. Kalman filtering requires the time-dependent estimate of the state covariance to be

updated automatically, in order to calculate the Kalman gain matrix terms. G–h filters gains, alternatively, are manually selected and (usually) static.

Traditional applications of g–h filters are radar tracking and aeronautics [36]. The general form of a g–h filter is described in equations (1), (2), (4) and (5).

Equations 1 and 2 are known as update equations. These equations provide an updated estimate of the present target position and velocity based on the present measurement of target position (y_k) as well as on prior measurements. These equations are also called the filtering equations. Confidence on measures is weighted by the gains g_k and h_k.

Thus, $x^*_{k,k}$ is called the *filtered estimate* of x_k at the present time based on the use of the present measurement (y_k) and the past measurements. $x^*_{k,k-1}$ is the *prediction estimate* of x_k based on past measurements.

$$x^*_{k,k} = x^*_{k,k-1} + g_k(y_k - x^*_{k,k-1}) \tag{1}$$

$$\dot{x^*}_{k,k} = \dot{x^*}_{k,k-1} + \frac{h_k}{T_s}(y_k - x^*_{k,k-1}) \tag{2}$$

$$\tag{3}$$

Equations 4 and 5, or prediction equations, provide a prediction of future position and velocity, $x^*_{k+1,k}$, $\dot{x^*}_{k+1,k}$, based on the first order dynamic model of the variable. Thus, these equations allow to predict what the target position and velocity will be at the time $k+1$ and to repeat the entire update process previously described in equations (1) and (2). As it can be observed, $x^*_{k+1,k}$ and $\dot{x^*}_{k+1,k}$ are calculated with the filtered estimate of the current position and velocity ($x^*_{k,k}$ and $\dot{x^*}_{k,k}$, respectively).

As g–h trackers consider a constant velocity model, the predicted velocity $\dot{x^*}_{k+1,k}$ is equal to the current one, $\dot{x^*}_{k,k}$.

$$x^*_{k+1,k} = x^*_{k,k} + T_s\dot{x^*}_{k,k} \tag{4}$$

$$\dot{x^*}_{k+1,k} = \dot{x^*}_{k,k} \tag{5}$$

The assumption of constant speed is reasonable in the proposed application, considering that human movements are slow and present small accelerations [37], especially taking into account that data are sampled at much higher rates ($f_{sampling} = 1kHz$ for this study).

It is also possible to combine equation (1) with (4) and equation (2) with (5) to obtain the *g–h prediction-filtering equations* presented in equations 6 and 7.

$$x^*_{k+1,k} = x^*_{k,k-1} + T_s\dot{x^*}_{k+1,k} + g_k(y_k - x^*_{k,k-1}) \tag{6}$$

$$\dot{x^*}_{k+1,k} = \dot{x^*}_{k,k-1} + \frac{h_k}{T_s}(y_k - x^*_{k,k-1}) \tag{7}$$

Tuning g–h filters consists of selecting appropriate values for g_k and h_k. Thus, an important class of g–h filters are those for which g and h are fixed, as the

computations required for processing are very simple, [36]. This is especially important in the proposed robotic application, considering that it consists on a embedded real-time system.

From previous experience [35], the Benedict-Bordner Filter (BBF), an approach for selecting the values of g_k and h_k, presented excellent results. BBF minimizes the total transient error, defined as the weighted sum of the total transient error and the variance of prediction error due to measurement noise errors [38]. BBF is the constant g-h filter that satisfies:

$$h = \frac{g^2}{2-g} \tag{8}$$

As g and h are related by Equation 8, the BBF approach has only one degree of freedom. Additionally, g_k and h_k are constant (g and h), which implies a great simplification on the filtering architecture. Fig. 4 presents an example of a force signal filtered with the proposed technique.

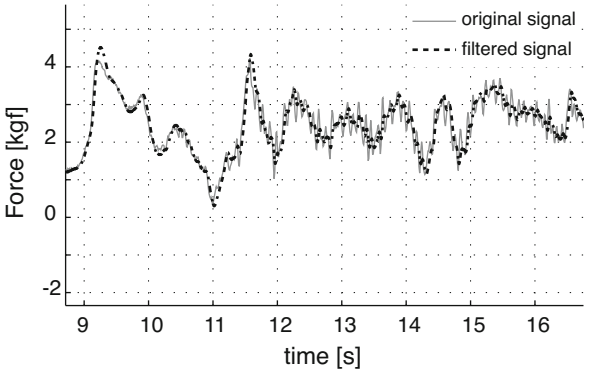

Fig. 4. Result of the filtering architecture for the cancellation of vibrations components introduced by floor or walker wheels imperfections

Estimation of Gait-Related Force Components and Extraction of Navigation Commands. This section presents a methodology for the estimation of the force component related to the user's gait. As previously commented, this component occurs due to the motion of the user's trunk during gait, which causes an oscillatory behavior on the measured forces.

For that purpose, taking advantage of the periodicity of the signals and its close relation with the gait cadence, an adaptive filter based on the *Fourier Linear Combiner* (FLC) was chosen for this filtering stage.

It is important to mention that the frequency of the gait related force components is very close to the voluntary components that contain the user's commands. This way, the use of low pass filtering could eliminate the voluntary components and, therefore, jeopardizing the proper functioning of a natural interaction.

FLC is an adaptive algorithm used for continuous estimation of quasi-periodical signals based on a M harmonics dynamic Fourier model (Equation 9). Using frequency and the number of harmonics as inputs for the model, the algorithm adapts amplitude and phase for each harmonic at the given frequency.

$$s = \sum_{r=1}^{M} [w_r sin(r\omega_0 k) + w_{r+M} cos(r\omega_0 k)] \tag{9}$$

The adaptation of the coefficients w_k is performed based on the least-mean-square (LMS) recursion, a descend method based on a special estimate of the gradient [39], which ensures inherent zero phase. The equations for the FLC algorithm are described below.

$$x_{r_k} = \begin{cases} \sin(r\omega_0 k), & 1 \leq r \leq M \\ \cos((r-M)\omega_0 k), & M+1 \leq r \leq 2M \end{cases} \tag{10}$$

$$\varepsilon_k = y_k - \mathbf{W}_k^{\mathrm{T}} \mathbf{X}_k \tag{11}$$

$$\mathbf{W}_{k+1} = \mathbf{W}_k + 2\mu\varepsilon_k \mathbf{X}_k, \tag{12}$$

where:

- y_k is the input signal;
- $\mathbf{W}_k$ is the adaptive weight vector that generates a linear combination of the harmonic orthogonal sinusoidal components of the reference input vector;
- $\mathbf{X}_k$ is the reference input vector;
- M is the number of the harmonics used in the model;
- μ represents the amplitude adaptation gain used for the LMS recursion.

As mentioned before, the FLC algorithm needs a frequency input for the correct estimation of the gait related force component. This frequency information is the gait cadence that is directly obtained by the laser range finder (LRF) sensor that measures the user's feet evolution during assisted gait.

Fig. 5 shows the complete filtering scheme for obtaining the user's navigation commands and the effect of the filtering architecture in a sample force signal. The filtered force signals (red line in Fig. 5) contain the user's navigation commands and serve as input signals to the controller presented in the following section.

Identification of User's Commands and Fuzzy-Logic Controller. The control strategy based on force interactions is presented in Fig. 6. The force signals filtered with the presented algorithm were used to drive the walker's motors through a controller based on fuzzy logic. y and z force components (see Fig. 1) from right and left sensors are filtered individually using the filtering architecture previously presented (Fig. 5).

F_y components are divided by the F_z components (when $F_y \neq 0$) in order to obtain force signals that are proportional to the amount of body weight applied in each armrest. This operation corrects asymmetrical supports caused by an

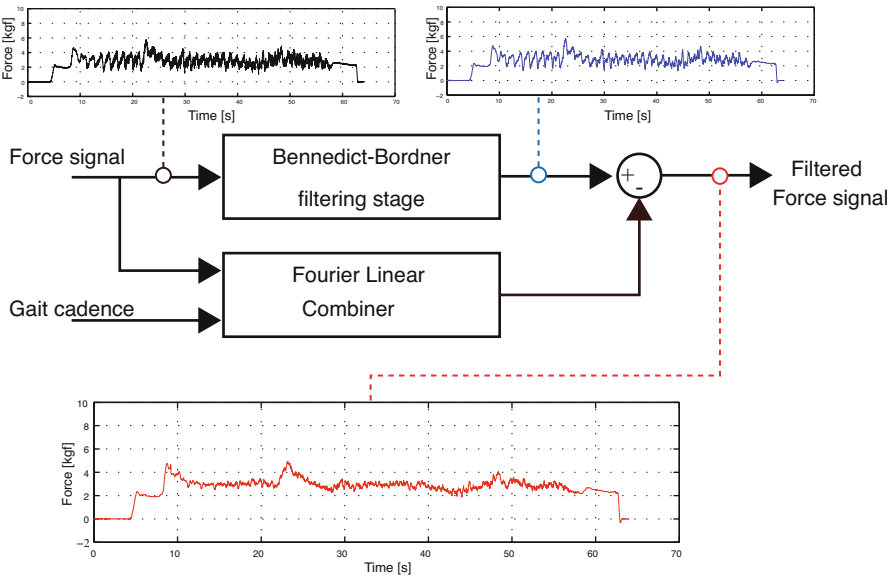

Fig. 5. Filtering architecture and the effects on a sample force signal

unilateral affection on the gait. Then, signals are conditioned to input the fuzzy logic classifier. The conditioning process consists of applying a *gain*, to adjust to the correct range of inputs; a *saturation function*, to avoid values over the input limits of the fuzzy classifier; and a *dead-zone*, to prevent motor commands in cases of signals very close to zero and, thus, not high enough to move the device.

The main element of the control scheme (Fig. 6) is the fuzzy logic block. It is built upon the information obtained experimentally from the tests performed with healthy subjects. It combines information of right and left sensors to generate motor commands. The filtered and conditioned force signal inputs can vary from -1 to $+1$ and are grouped into four classes:

– *Negative*, *Z-shaped* function with $a = -0.8$ and $b = 0$, Equation (13).

$$zmf(x) = \begin{cases} 1, x \leq a \\ 1 - 2 \cdot (\frac{x-a}{b-a})^2, a \leq x \leq \frac{a+b}{2} \\ 2 \cdot (b - \frac{x}{b-a})^2, \frac{a+b}{2} \leq x \leq b \\ 0, x \geq b \end{cases} \tag{13}$$

– *Zero*, Gaussian symmetrical function with $\sigma = 0.2045$ and $c = 0$, Equation (14).

$$gaussmf(x) = e^{\frac{-(x-c)^2}{2\sigma^2}} \tag{14}$$

– $Positive_{low}$, Gaussian symmetrical function with $\sigma = 0.1173$ and $c = 0.4$.
– $Positive_{high}$, *S-shaped* function with $a = 0.3148$ and $b = 0.8$, Equation (15).

$$smf(x) = \frac{1}{1 + e^{-a(x-b)}} \tag{15}$$

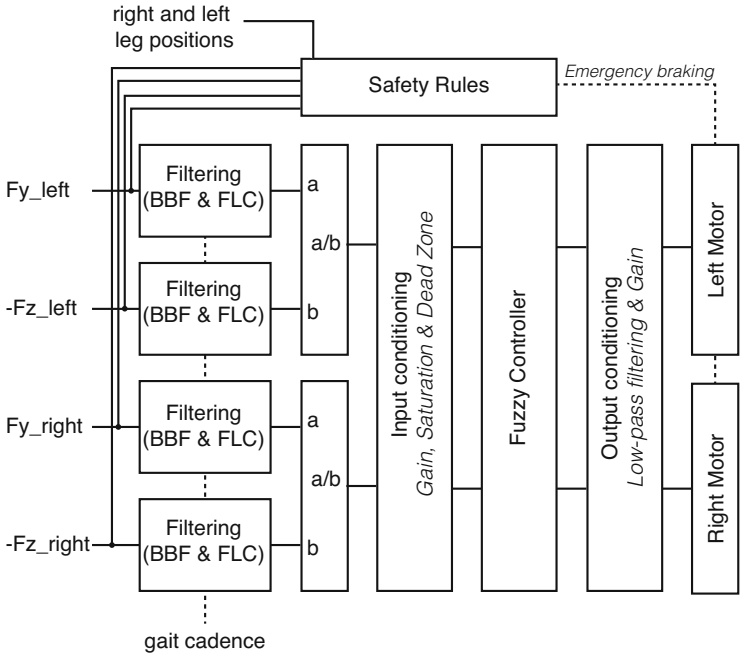

Fig. 6. Control strategy based on the user-walker interaction forces

Three functions were defined to the outputs:

- *Zero*, *Z-shaped* function with $a = -0.2$ and $b = 0.5$.
- $Positive_{low}$, Gaussian symmetrical function with $\sigma = 0.1944$ and $c = 0.5$.
- $Positive_{high}$, *S-shaped* function with $a = 0.5$ and $b = 0.8$.

A set of sixteen rules were implemented in the fuzzy logic architecture as presented in [40].

After the fuzzy logic block, the signals are passed through the output conditioning block that performs two functions: (i) low pass filtering to avoid eventual abrupt changes in control signals and, thus, ensuring comfortable navigation to the user; and (ii) signal adjustments (offset corrections and gains) to the analog range of inputs of the motor control board.

It is important to mention that, due to safety reasons, no backward motion was allowed. This will be implemented in the future and will only be active in special situations determined by the patient's needs.

Finally and also regarding safe navigation, it is important to mention that some safety rules were implemented into the system. These are simple rules that automatically brake the device's motors, presenting the highest priority in the control scheme. The UFES Smart Walker automatically brakes if:

- If both F_y components are negative (the system associates this with the intention to brake),

- If any of the F_z components is smaller than a certain value (forearm not placed on the armrests),
- If there is an excessive separation between user's legs and the device (user is left behind),
- If there is not enough separation between the user's legs and the device (user too close with not enough space to walk).

Under normal operation, none of these rules are activated and the proposed control scheme acts on the device's DC motors.

The developed filtering and control strategy were implemented into the device's firmware and the system was taken for clinical validation as it is discussed in the following section.

Results and Discussion. This first implementation of the control strategy is similar to the one integrated in a preceding research project that originated the Simbiosis Walker [33]. This section presents a short description of the clinical validation of the control scheme at the Biomechanical Unit of Spinal Cord Injury Hospital of Toledo (HNPT).

The trial experimentation consisted of walking in a U-shaped track, from point 1 to point 2 and back to point 1, as presented in Fig. 7. No instructions or training were provided in order to prepare the subjects for the proposed task and no adjustments of the controller was performed to adjust the device to the subject. The authors suggested that if the proposed interface and interaction strategy are supposed to be natural, no training should be required.

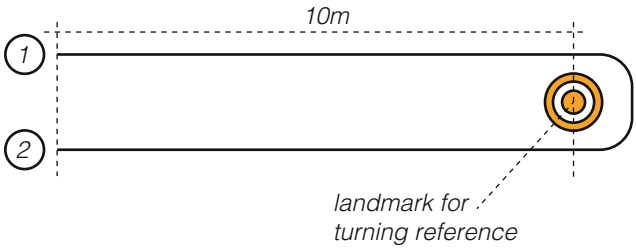

Fig. 7. U-shaped track used in the clinical validation of the control strategy

A total number of eight (incomplete spinal cord injury) patients were selected by the clinical staff taking into consideration inclusion factors such as: preserved cognitive functions, capacity of maintaining a standing position, capacity of grasping and being able to walk with or without the assistance of an assistive device.

The subjects were fitted into three subcategories:

- Two subjects presented severe impairment of the locomotion system. The objective here is to observe if the control scheme can be used in rehabilitation

scenarios. Notice that the subjects use almost exclusively wheelchairs as their assistive devices.
- Four patients that use the wheelchair as their main locomotion assistance, but can walk for short periods of time with the assistance of a device. The most common complain in this case is that existent technical aids do not provide a satisfactory experience and the risks of fall are important, causing the subject (or therapist) to choose the wheelchair as a safety measure. The aim is to evaluate the developed system as a functional compensation device.
- Two patients with the least affections in gait. Both of them were users of conventional two-wheeled walker at some point in their rehabilitation process. This small group can offer important feedback and comparison of the developed strategy versus the use of conventional / passive walkers.

All patients were able to use the device and walk the proposed track with self selected speed. The adaptive filtering scheme provided a mean amplitude cancellation of 73.18% of the cadence related force components and fuzzy logic control strategy offered smooth and responsive navigation. Fig. 8 shows an example of raw and filtered F_y signals and the velocity signal of the motorized wheels during a sample experiment.

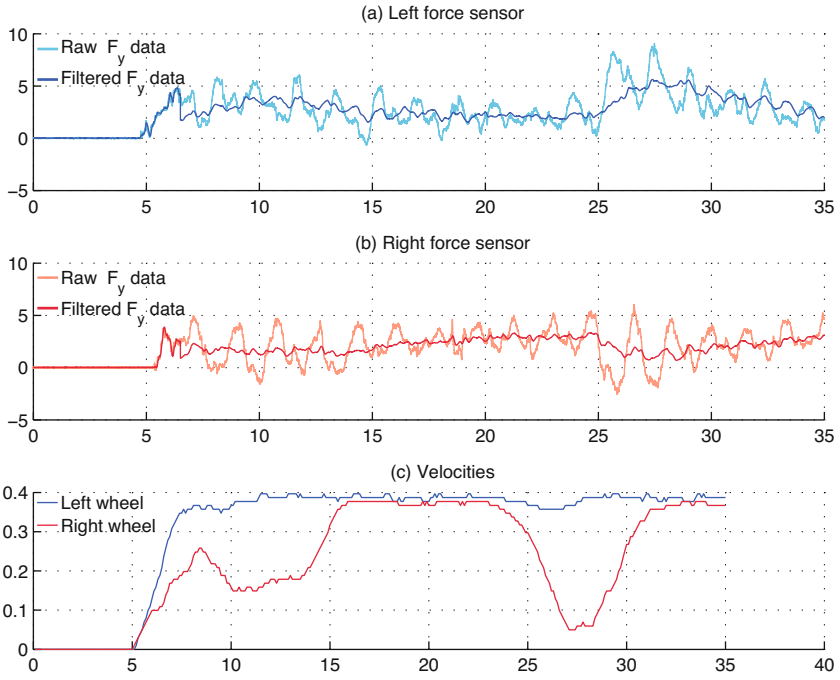

Fig. 8. Sample of clinical validation data: (a) raw and filtered left F_y data; (b) raw and filtered right F_y data; and (c) left and right wheel velocities

3.2 Inverse Kinematics Controller Based on Feet Evolution

The filtering and control strategy presented in the previous section showed good results in the clinical validation, assisting the user's gait at the same time that partial body weight support was performed. Information obtained from the laser range finder (LRF) was only used in order to provide cadence information and, therefore, the subsystem was not used to its full potential. Additionally, the inertial measurement unit (IMU) placed on the user's pelvis could provide important insights regarding the user's intentions and locomotion commands.

This section presents an implementation of a multimodal interaction scheme to be used in a control strategy for walker-assisted locomotion, using a LRF for tracking the human legs, and an IMU for capturing the human movement during the gait.

Proposal of Control Strategy. The human-walker interaction model is shown in Fig. 9. The variables and parameters used in the presented model are: human linear velocity (v_h), human angular velocity (ω_h), human orientation (ψ_h), walker linear velocity (v_w), walker angular velocity (ω_w) and walker orientation (ψ_w). The interaction parameters were defined as the angle ϕ between v_h and $\overline{WH}$ (named Human-Walker Line), the angle θ between $\overline{WH}$ and $\overline{WC}$ segments, and d, the length of $\overline{WH}$. Finally, the parameter a defines the distance between the controller reference point (W) and the walker center of rotation (C).

The control proposal is based on the inverse kinematics and the control variables are the angle ϕ and the distance d. The control law of this system aims to achieve a desired human-walker distance ($d = d_d$) and a ϕ angle that con-

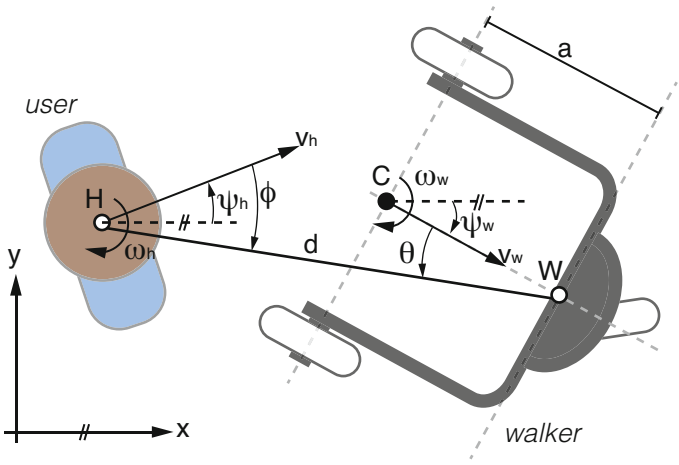

Fig. 9. The human-walker interaction model used for the inverse kinematics controller

verges asymptotically to zero. Direct kinematics is shown in (16), where $\tilde{d}$ is the difference between the desired and measured distances.

$$\begin{pmatrix} \dot{\tilde{d}} \\ \dot{\tilde{\phi}} \end{pmatrix} = \begin{pmatrix} \cos(\theta) & -a\sin(\theta) \\ -\frac{\sin(\theta)}{d} & -a\frac{\cos(\theta)}{d} \end{pmatrix} \overbrace{\begin{pmatrix} v_w \\ \omega_w \end{pmatrix}}^{u} + \begin{pmatrix} -v_h\cos(\phi) \\ \omega_h + v_h\frac{sin\phi}{d} \end{pmatrix} \tag{16}$$

The inverse kinematics controller, obtained from the kinematic model presented in (16), is shown in (17) and (18).

$$v_w = \cos(\theta) \left[-k_d\tilde{d} + v_h\cos(\phi) \right] - dsin(\theta) \left[-k_\phi\tilde{\phi} - \omega_h - \frac{v_h}{d}\sin(\phi) \right] \tag{17}$$

$$\omega_w = -\frac{\sin(\theta)}{d} \left[-k_d\tilde{d} + v_h\cos(\phi) \right] - \frac{d}{a}\cos(\theta) \left[-k_\phi\tilde{\phi} - \omega_h - \frac{v_h}{d}\sin(\phi) \right] \tag{18}$$

It could be demonstrated that the control system is exponentially and asymptotically stable, thus obtaining (19) and (20).

$$\tilde{d}(t) = \tilde{d}(0)\, e^{-k_d t} \tag{19}$$

$$\tilde{\phi}(t) = \tilde{\phi}(0)\, e^{-k_\phi t} \tag{20}$$

The proposed control strategy was simulated with different human locomotion patterns (straight lines, circle-shaped paths, eight-shaped paths, etc.) in order to observe whether the walker correctly follows the user. Fig. 10 shows one of the proposed simulations in which the human path performing an eight-shape curve (input) and the walker path following the human in front (controller output) are shown. Distance and angular errors are also kept withing low values. Therefore, the proposed controller is expected to keep the walker continuously following the human during gait while maintaining itself positioned in front of the user.

As the system architecture is based on Matlab Real-Time xPC Target, the implemented equations used for the simulations can be directly applied to the walker control architecture, avoiding the possibility of implementation errors.

It is possible to state that a good real-time implementation of the method proposed in this section relies on robust and precise measurement or estimation of the parameters used in the control scheme (see equations 17 and 18). This way, the next sections present the methods used to obtain all these parameters in real-time along with the experimentation, results and discussions of the proposed control proposal.

Estimation of Interaction Parameters. As previously discussed, the quality of the control approach relies on the correct estimation of the interaction parameters. Such parameters represent the link between the user and the walker in the control strategy. The method to obtain the parameters of the proposed model is described as follows:

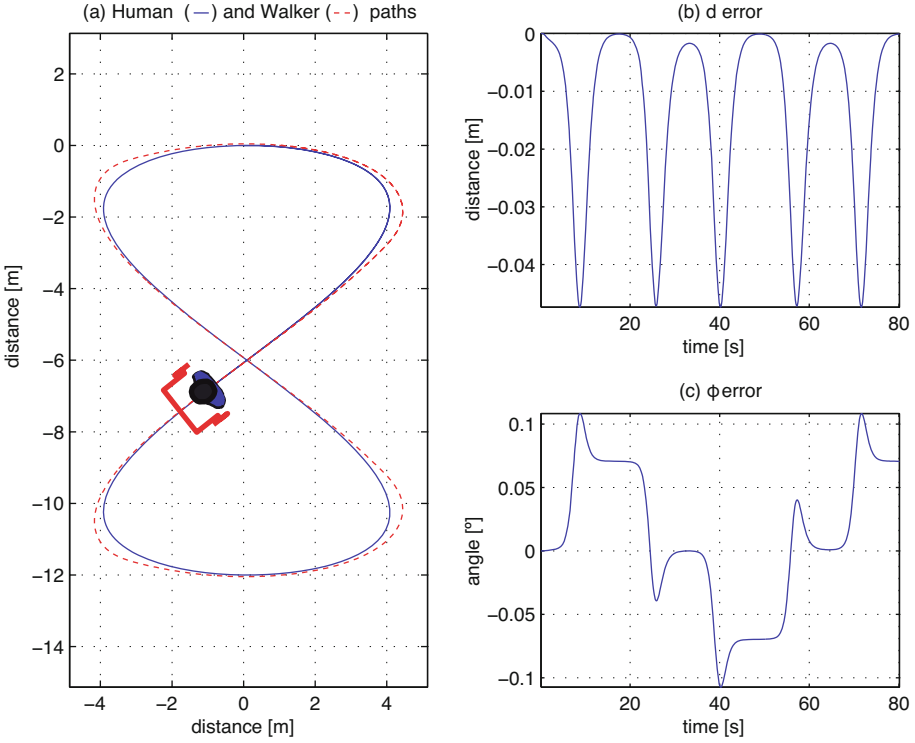

Fig. 10. Simulation of the proposed control strategy

θ and d. These parameters are measured directly using the LRF sensor after the legs detection process is performed. The leg detection algorithm consists of four steps. First, the area of interaction is reduced (in distance and aperture angle) to avoid the detection of legs of other individuals that are not driving the device. Note that the LRF can measure up to $4m$ of distance and 240 deg of aperture. Second, transitions in the distance vector are found to identify possible leg candidates. The third step is to use the transitions to classify the data into possible leg postures (separate, overlapped or together). Transitions that do not fulfill width and separation criteria are discarded. Finally, the coordinates of right and left legs are obtained. θ and d are obtained directly by averaging the left and right legs' coordinates.

v_h. The human linear velocity is obtained through the product of gait cadence ($steps/s$) and step amplitude ($m/step$). For that purpose, LDD, defined as the difference between the distances of left and right legs to the walker is fed into an adaptive filtering architecture. The filtering architecture that offers a real-time estimation of cadence and step amplitude will be addressed in the next section of this chapter

ω_h *and* ψ_h. Human angular velocity and orientation are obtained from the IMU placed on the human pelvis. The gyroscope integrated on the IMU offers a direct measurement of ω_h. ψ_h is obtained after the IMU orientation algorithm is performed [41]. In the same manner as previously performed to the force signals, cadence related components are also filtered using the Fourier Linear Combiner algorithm, canceling the influence of pelvic rotations during gait, and offering a more stable measurement of ψ_h.

ψ_w. Walker orientation is measured by the onboard IMU using the same IMU orientation algorithm [41].

ϕ. This angle represents the orientation difference between v_h and segment $\overline{WH}$. Fig. 9 shows that $\phi = \theta + \psi_h - \psi_w$. Also, ϕ is only defined if the magnitude of v_h is greater than zero.

Adaptive Estimation of Human Linear Velocity. As previously discussed, human linear velocity is obtained through the product of gait cadence and step amplitude. LDD, previously defined as the difference between the distances of left and right legs, can be used to obtain both parameters as it is shown in this section (Fig. 11).

The gait cadence can be defined as the rhythm of a person's walk, usually expressed in steps per minute (steps/min) [42]. This way, the frequency of the LDD signal yields cadence information. Additionally, the amplitude of the LDD signal (Fig. 11 *a* and *b*) is a direct measurement of the user's step length.

Considering the oscillatory nature of gait, a Weighted-Fequency Fourier Linear Combiner (WFLC) algorithm was proposed to obtain the frequency of LDD and, thus, the gait cadence. This information was also used as the gait cadence input to the controller presented in Section 3.1 (Fig. 6).

The WFLC is an extension of the FLC noise canceler, previously presented, that also tracks the frequency of an input signal based on a least-mean-square (LMS) recursion, a descend method based on a special estimate of the gradient [39]. Thus, it adapts, in real-time, its amplitude, frequency and phase to the reference signal [43]. The algorithm is based on a standard for fitting sine waves to noisy discrete-time observations, IEEE-STD-1057. The LMS recursion ensures inherent zero phase, thus allowing for real-time implementation.

The WFLC recursion minimizes the error ε_k between the input s_k and the signal harmonic model, as presented in (21). It assumes that the distance signal (LDD) can be mathematically modeled as a pure sinusoidal signal of frequency ω_{0_k} plus M harmonics [44].

$$\varepsilon_k = s_k - \sum_{r=1}^{M} \left[w_{r_k} \sin\left(r\omega_{0_k} k\right) + w_{r+M\,k} \cos\left(r\omega_{0_k} k\right) \right] \tag{21}$$

The WFLC provides an estimate of instantaneous frequency, as shown in (23).

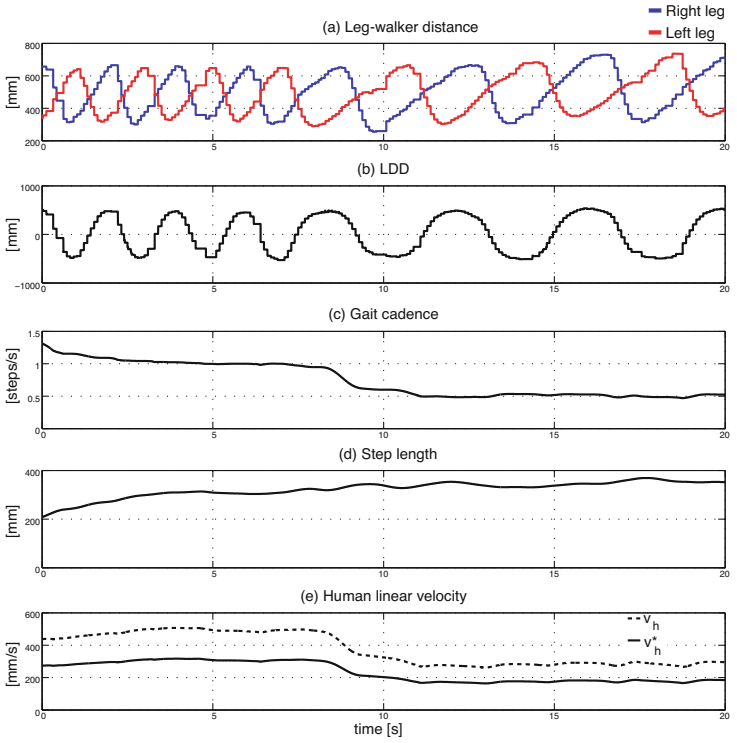

Fig. 11. (a) Leg to walker distances; (b) LDD signal obtained from the leg distances; (c) estimated gait cadence; (d) estimated step length; (e) human linear velocity obtained from the estimation of cadence and step length

$$\omega_{0_{k+1}} = \omega_{0_k} - 2\mu\varepsilon_k \frac{\partial \varepsilon_k}{\partial \omega_{0_k}} \tag{22}$$

$$\frac{\partial \varepsilon_k}{\partial \omega_{0_k}} = -k \sum_{k=1}^{M} \left[w_{r_k} \cos\left(r \sum_{t=1}^{k} \omega_{0_t} \right) - w_{r_k+M} \sin\left(r \sum_{t=1}^{k} \omega_{0_t} \right) \right] \tag{23}$$

The WFLC is formulated as follows:

- Equation (24) represents the sinusoidal signal model, which consists of M harmonics of the fundamental frequency, ω_{0_t}.
- Equation (25) describes the error which the algorithm uses to adapt itself to the input signal.
- Equations (26) and (27) express, respectively, the frequency and amplitude weights update based on the LMS algorithm [39].

$$x_{r_k} = \begin{cases} \sin\left(r \sum_{t=1}^{k} \omega_{0_t}\right), & 1 \leq r \leq M \\ \cos\left((r-M) \sum_{t=1}^{k} \omega_{0_t}\right), & M+1 \leq r \leq 2M \end{cases} \tag{24}$$

$$\varepsilon_k = s_k - \mathbf{W}_k^{\mathrm{T}} \mathbf{X}_k - \mu_b \tag{25}$$

$$\omega_{0_{k+1}} = \omega_{0_k} + 2\mu_0 \varepsilon_k \sum_{r=1}^{M} r \left(w_{r_k} x_{M+r_k} - w_{M+r_k} x_{r_k}\right) \tag{26}$$

$$\mathbf{W}_{k+1} = \mathbf{W}_k + 2\mu_1 \varepsilon_k \mathbf{X}_k \tag{27}$$

The algorithm has 5 parameters to be tuned [45]. M is the number of harmonics of the model which is fixed to 1. The instantaneous frequency at initialization is represented by $\omega_{0,0}$. Amplitude and frequency update weights are expressed by μ_0 and μ_1. Finally, μ_b is used to to compensate for low frequency drifts (bias weight).

As the WLFC is designed to adapt to the dominant-frequency component in a signal [46], it is important to perform a previous stage of band-pass filtering (compatible with gait cadence frequencies) for the correct performance of the WFLC (see Fig. 11 *c*). The band-pass filtering allows the WFLC to robustly adapt to the values of gait cadence.

Although this filtering stage can cause undesirable time delay in the filtered signals, here the WFLC algorithm is used only for cadence estimation. Considering the acquisition frequency, instantaneous temporal changes in gait cadence (WFLC's frequency output) are minimal, not affecting the performance of the proposed method. For amplitude estimation of the LDD signal, a FLC branch is used, operating on the raw input (Fig. 12), ensuring zero-phase amplitude estimation (see Fig. 11 *d*). Thus, the combination of WLFC and FLC presents great advantages [44].

Finally, as the LRF sensor is placed on a plane above the ground to allow robust detection of the users legs, a simple correction factor is applied to the signal $v_h = k * v_h^*$. Fig. 11 *e* shows the human linear velocity calculated by the product of *gait cadence* and *step length* before and after the correction factor is applied (solid and dashed line, respectively). Notice that in this sample experiment, the user was asked to walk at $500mm/s$ on the first half of the experiment and, then, slow down to $250mm/s$. Gait speed was indicated to the user by ground marks (to ensure step length) and a metronome (for indicating cadence). Step lengths were maintained constant at $500mm$ as gait cadence varied from 1 $step/s$ to 0.5 $step/s$.

Results and Discussion. The inverse kinematic interaction strategy proposed in this section was validated in the Intelligent Automation Laboratory (LAI) at Federal University of Espirito Santo, Brazil. Considering that the proposed controller relies only on LRF and IMU information, this stage of validation required no physical contact between user and walker. Based on this requirement, no experiments could be performed with patients suffering from gait disorders, as physical support would be required to assist gait.

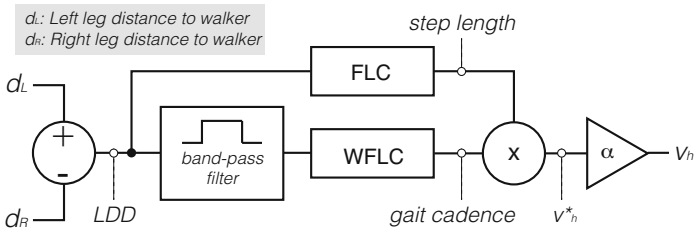

Fig. 12. Adaptive estimation architecture to obtain human linear velocity

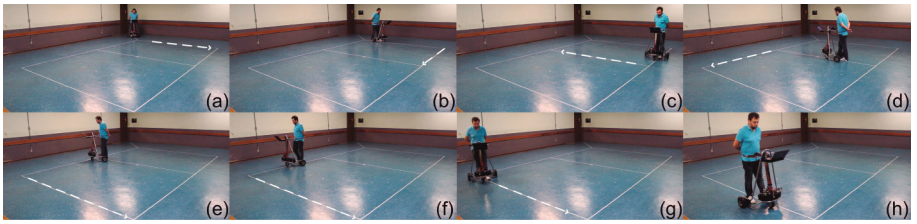

Fig. 13. 8-shaped path performed on the validation experiments

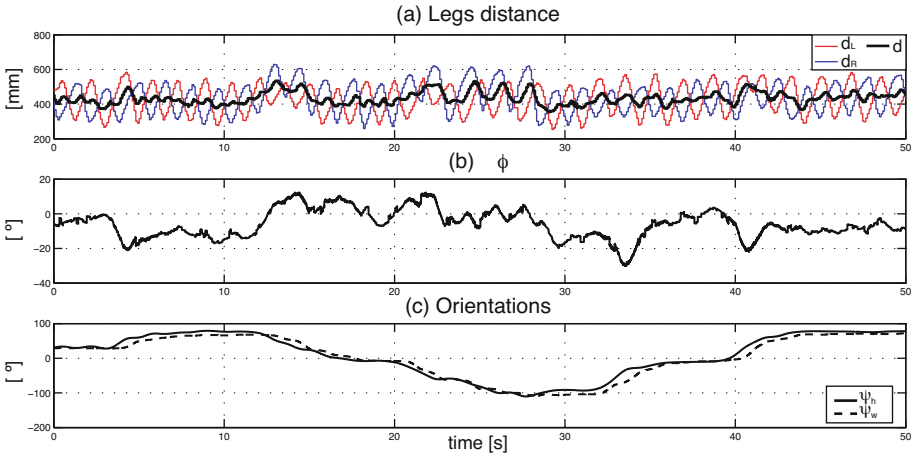

Fig. 14. Data obtained from a sample experiment: (a)The leg detection algorithm outputs (d_L and d_R) and user-walker distance d; (b) ϕ angle; and (c) user and walker orientation angles

A sample experiment of an 8-shaped path performed during the validation experiments with healthy subjects is presented in Fig. 13. It is possible to observe that the user keeps his upper-limbs behind his back at all moments, avoiding any physical interaction with the device.

Fig. 14 shows the results of a sample experiment. The leg detection algorithm outputs (d_L and d_R) are presented in Fig. 14 *a*. The user-walker distance (d) is obtained by averaging d_L and d_R. The control law aims to achieve a desired human-walker distance ($500mm$ in this experiment) and an ϕ angle equals to zero. The ϕ angle is presented in Fig. 14 *b*. Finally, user and walker orientation angles are also presented to illustrate that the robotic walker is always correctly orientated to the user during the performed 8-shaped path.

4 Conclusions and Future Work

This chapter presented the robotic walker developed at the Federal University of Espirito Santo (UFES), Brazil. After a brief description of the general concepts involved in locomotion, mobility dysfunctions and assistive devices, a functional classification of the Smart Walkers was presented.

The UFES Smart Walker was introduced as a system focused on user-machine multimodal interaction for obtaining a natural control strategy for the robotic device. Past experiences and current developments were addressed, especially considering interaction and control strategies to drive the robotic device. First, an adaptive filtering strategy of the upper-body interaction forces was presented. In this case, a Fuzzy-Logic based control system was developed to generate the navigation commands to the device.

A second approach based on a robust inverse kinematics controller was introduced in section 3.2. The navigation commands were obtained from the user's motions obtained by a laser range finder and a wearable inertial measurement unit, also developed at UFES, Brazil.

Currently, the authors are working on the fusion of both control methods aiming at obtaining a robust and safe interaction strategy to assist patients suffering from locomotion disorders. Once a reliable fusion strategy is conceived, the device will be validated with osteoarthritis and cerebrovascular accident (CVA) patients at the Center of Physical Rehabilitation of Espirito Santo (CREFES), Brazil.

Acknowledgments. This research is supported by the Brazilian National Council for Scientific and Technological Development (CNPq), Process # 471804/2012-6.

References

1. Winter, D.: Biomechanics and motor control of human movement. John Wiley & Sons (2009)
2. Buchman, A., Boyle, P., Leurgans, S., Barnes, L., Bennet, D.: Cognitive function is associated with the development of mobility impairments in community-dwelling elders. The American Journal of Geriatric Psychiatry 19(6), 571–580 (2011)
3. Van Hook, F.W., Demonbreun, D., Weiss, B.D.: Ambulatory devices for chronic gait disorders in the elderly. American Family Physician 67(8), 1717–1724 (2003)

4. Lam, R.: Practice tips: choosing the correct walking aid for patients. Canadian Family Physician Médecin de Famille Canadien 53(12), 2115–2116 (2007)
5. Ceres, R., Pons, J., Calderón, L., Mesonero-Romanos, A., Jiménez, A., Sánchez, F., Abizanda, P., Saro, B., Bonivardo, G.: Andador activo para la rehabilitación y el mantenimiento de la movilidad natural. In: IMSERSO, pp. 3–8 (2004)
6. Gross, K.D.: Device use: walking AIDS, braces, and orthoses for symptomatic knee osteoarthritis. Clinics in Geriatric Medicine 26(3), 479–502 (2010)
7. Bateni, H., Maki, B.E.: Assistive Devices for Balance and Mobility: Benefits, Demands, and Adverse Consequences. Archives of Physical Medicine and Rehabilitation 86(1), 134–145 (2005)
8. Haubert, L.L., Gutierrez, D.D., Newsam, C.J., Gronley, J.K., Mulroy, S.J., Perry, J.: A comparison of shoulder joint forces during ambulation with crutches versus a walker in persons with incomplete spinal cord injury. Archives of Physical Medicine and Rehabilitation 87(1), 63–70 (2006)
9. Priebe, J.R., Kram, R.: Why is walker-assisted gait metabolically expensive? Gait & Posture 34(2), 265–269 (2011)
10. Frizera, A., Ceres, R., Pons, J.L., Abellanas, A., Raya, R.: The Smart Walkers as Geriatric Assistive Device. The SIMBIOSIS Purpose. In: Proceedings of the 6th International Conference of the International Society for Gerontechnology, pp. 1–6 (2008)
11. Elias, A., Frizera, A., Bastos, T.: Robotic walkers from a clinical point of view: feature-based classification and proposal of a model for rehabilitation programs. In: XIV Reunión de Trabajo en Procesamiento de la Información y Control, pp. 1–5 (2011)
12. Yu, H., Spenko, M., Dubowsky, S.: Omni-Directional Mobility Using Active Split Offset Castors. Journal of Mechanical Design 126(5), 822 (2004)
13. MacNamara, S., Lacey, G.: A smart walker for the frail visually impaired. In: Proceedings 2000 ICRA. Millennium Conference. IEEE International Conference on Robotics and Automation. Symposia Proceedings, pp. 1354–1359. IEEE (2000)
14. Hirata, Y., Muraki, A., Kosuge, K.: Motion control of intelligent passive-type Walker for fall-prevention function based on estimation of user state. In: Proceedings of IEEE International Conference on Robotics and Automation, ICRA 2006, pp. 3498–3503 (May 2006)
15. Hirata, Y., Muraki, A., Kosuge, K.: Standing Up and Sitting Down Support Using Intelligent Walker Based on Estimation of User States. In: 2006 International Conference on Mechatronics and Automation, pp. 13–18. IEEE (June 2006)
16. Morris, A., Donamukkalat, R., Kapuria, A., Steinfeldt, A., Matthews, J.T., Dunbar-Jacob, J., Thrunti, S.: A Robotic Walker That Provides Guidance. In: Proceedings of the 2003 IEEE lnternational Conference on Robotics & Automation, pp. 25–30 (2003)
17. Rentschler, A.J., Cooper, R.A., Blasch, B., Boninger, M.L.: Intelligent walkers for the elderly: performance and safety testing of VA-PAMAID robotic walker. Journal of Rehabilitation Research and Development 40(5), 423–431 (2003)
18. Chugo, D., Asawa, T., Kitamura, T., Takase, K.: A moving control of a robotic walker for standing, walking and seating assistance. In: 2008 IEEE International Conference on Robotics and Biomimetics, pp. 692–697. IEEE (February 2008)
19. Chugo, D., Kitamura, T., Takase, K.: A rehabilitation walker with standing and walking assistance. In: 2008 IEEE/RSJ International Conference on Intelligent Robots and Systems, pp. 260–265. IEEE (September 2008)

20. Médéric, P., Pasqui, V., Plumet, F., Bidaud, P.: Design of a walking-aid and sit to stand transfer assisting device for elderly people 2 Disturbances induced by some particular. In: Proceedings of ROMAN 2004-15th CISM-IFToMM Symposium on Robot Design, Dynamics and Control, pp. 5–12 (2004)
21. Abellanas, A., Frizera, A., Ceres, R., Raya, R.: Assessment of the laterality effects through forearm reaction forces in walker assisted gait. Procedia Chemistry 1(1), 1227–1230 (2009)
22. Lacey, G., Namara, S.M., Dawson-Howe, K.M.: Personal adaptive mobility aid for the infirm and elderly blind. In: Mittal, V.O., Yanco, H.A., Aronis, J., Simpson, R.C. (eds.) Assistive Technology and AI. LNCS (LNAI), vol. 1458, pp. 211–220. Springer, Heidelberg (1998)
23. Rodriguez-Losada, D., Matia, F., Jimenez, A., Lacey, G.: Guido, the Robotic SmartWalker for the frail visually impaired. In: First International Conference on Domotics, Robotics and Remote Assitence for All - DRT4all, pp. 1–14 (2005)
24. Graf, B.: An Adaptive Guidance System for Robotic Walking Aids. Journal of Computing and Information Technology 1(1), 109–120 (2008)
25. Kulyukin, V., Kutiyanawala, A., LoPresti, E., Matthews, J., Simpson, R.: iWalker: Toward a Rollator-Mounted Wayfinding System for the Elderly. In: 2008 IEEE International Conference on RFID, pp. 303–311 (April 2008)
26. Zong, C., Chetouani, M., Tapus, A.: Automatic gait characterization for a mobility assistance system. In: 11th International Conference in Control, Automation, Robotics and Vision, pp. 473–478 (2010)
27. Chan, A.D.C., Green, J.R.: Smart Rollator Prototype. In: 2008 IEEE International Workshop on Medical Measurements and Applications, pp. 97–100. IEEE (May 2008)
28. Alwan, M., Wasson, G., Sheth, P., Ledoux, A., Huang, C.: Passive derivation of basic walker-assisted gait characteristics from measured forces and moments. In: Conference Proceedings: ... Annual International Conference of the IEEE Engineering in Medicine and Biology Society. IEEE Engineering in Medicine and Biology Society, vol. 4, pp. 2691–2694 (January 2004)
29. Dubowsky, S., Genot, F., Godding, S., Kozono, H., Skwersky, A., Yu, H., Yu, L.S.: PAMM - A Robotic Aid to the Elderly for Mobility Assistance and Monitoring: A “Helping-Hand" for the Elderly. In: Proceedings of the IEEE Conference on Robotics and Automation - ICRA (2000)
30. Henry, J., Aharonson, V.: Gait monitoring for the elderly using a robotic walking aid. In: IEEE 26th Convention of Electrical and Electronics Engineers in Israel, pp. 392–394 (2010)
31. Spenko, M., Yu, H., Dubowsky, S.: Robotic personal aids for mobility and monitoring for the elderly. IEEE Transactions on Neural Systems and Rehabilitation Engineering: A Publication of the IEEE Engineering in Medicine and Biology Society 14(3), 344–351 (2006)
32. Frizera, A., Cifuentes, C.A., Bastos, T.F.: Motion Capture System Based on the Integration of 3D Accelerometer in a Wireless Inertial Measurement Unit. In: Accelerometers: Principles, Structure and Applications, vol. 1, pp. 57–76. Nova Science Publishers, Inc. (2013)
33. Frizera, A., Ceres, R., Rocon, E., Pons, J.L.: Empowering and Assisting Natural Human Mobility: The Simbiosis Walker 8(3), 34–50 (2011)
34. Abellanas, A., Frizera, A., Ceres, R., Gallego, J.: Estimation of gait parameters by measuring upper limb-walker interaction forces. Sensors and Actuators A: Physical 162(2), 276–283 (2010)

35. Frizera Neto, A., Gallego, J.A., Rocon, E., Pons, J.L., Ceres, R.: Extraction of user's navigation commands from upper body force interaction in walker assisted gait. BioMedical Engineering Online 9(37), 1–16 (2010)
36. Brookner, E.: Tracking and Kalman Filtering Made Easy. John Wiley and Sons, Inc. (1998)
37. Mann, K., Werner, F.W., Palmer, A.K.: Frequency spectrum analysis of wrist motion for activities of daily living. Journal of Orthopedic Research 7(2), 304–306 (1989)
38. Benedict, T.R., Bordner, G.: Synthesis of an optimnal set of radar track-while-scan smoothing equations. IRE Transactions on Automatic Control 7(4), 27–32 (1962)
39. Widrow, B., Stearns, S.D.: Adaptive signal processing. Prentice Hall (1985)
40. Frizera, A.: Interfaz multimodal para modelado, estudio y asistencia a la marcha humana mediante andadores robóticos. PhD thesis, Universidad de Alcalá (2010)
41. Braidot, A., Cifuentes, C., Frizera Neto, A., Frisoli, M., Santiago, A.: Zigbee wearable sensor development for upper limb robotics rehabilitation. Latin America Transactions, IEEE (Revista IEEE America Latina) 11(1), 408–413 (2013)
42. Frizera, A., Elias, A., del Ama, A., Ceres, R., Bastos, T.: Characterization of spatio-temporal parameters of human gait assisted by a robotic walker. In: 2012 4th IEEE RAS EMBS International Conference on Biomedical Robotics and Biomechatronics (BioRob), pp. 1087–1091 (2012)
43. Riviere, C.N., Rader, R.S., Thakor, N.V.: Adaptive canceling of physiological tremor for improved precision in microsurgery. IEEE Transactions on Biomedical Engineering 45(7), 839–846 (1998)
44. Riviere, C., Khosla, P.: Augmenting the human-machine interface: improving manual accuracy. In: IEEE International Conference on Robotics and Automation, vol. 4, pp. 3546–3550 (1997)
45. Riviere, C.: Adaptive suppression of tremor for improved human-machine control. PhD thesis, Johns Hopkins University (1995)
46. Riviere, C.N., Thakor, N.V.: Modeling and canceling tremor in human-machine interfaces. IEEE Engineering in Medicine and Biology 15(3), 29–36 (1996)

Assistive Robots for Physical and Cognitive Rehabilitation in Cerebral Palsy

Rafael Raya, Eduardo Rocon, Eloy Urendes, Miguel A. Velasco, Alejandro Clemotte, and Ramón Ceres

Bioengineering Group, Spanish National Council for Science Research, (GBIO-CSIC) Crta. Campo Real Km 0.2 Arganda del Rey, Madrid, Spain
rafael.raya@csic.es

1 Introduction

Cerebral palsy (CP) is one of the most severe disabilities in childhood and makes heavy demands on health, educational, and social services as well as on families and children themselves. The most frequently cited definition of CP is a disorder of posture and movement due to a defect or lesion in the immature brain, [1]. The prevalence of CP is internationally 2-3 cases per 1000 births. Only in the United States 500,000 infants are affected by CP, [2]. In Europe these figures are even higher, [3]. The current definition of CP covers a heterogeneous range of clinical presentations and degrees of impairment. Therefore, individuals with CP are normally categorized into classes or groups. Traditional classification schemes focus on the affected limbs (hemiplegia, diplegia and tetraplegia), with an added modifier that describes the predominant type of movement abnormality (spasticity, dyskinesia, ataxia, or mixed), [1]. However, it has become apparent that additional characteristics must be taken into account in novel classification scheme that contributes substantively to the understanding and management of this disorder. Clinical decisions and medical research depend upon the ability to link clinically observable signs and symptoms to the underlying pathophysiology.

As cure for CP, which means a repair of the underlying brain damage, is not currently available, the management for children with CP usually focuses on maintaining and improving both quality of life and function, and on preventing secondary complications. Patients with CP are at high risk of develop musculoskeletal problems that are mainly related to physical growth, abnormal muscle tone, weakness, lack of mobility, poor balance and loss of selective motor control. Gait limitations are usual in children with CP. The Gross Motor Function Classification System (GMFCS) classifies CP into five levels according to the disability level in lower extremities, [4]. Additionally, people with CP often suffer difficulty with motor skills of upper limbs, such as reaching, grasping and manipulating objects with their hands. MACS scale, [5], classifies into five levels the upper extremity function, that means, the users capability for manipulating objects.

On the other hand, the motor disorders of CP are often accompanied by disturbances of sensation, cognition, communication, perception, and/or behavior, and/or by a seizure disorder. It is during early stages of development that

S. Mohammed et al. (eds.), *Intelligent Assistive Robots*,
Springer Tracts in Advanced Robotics 106, DOI: 10.1007/978-3-319-12922-8_5

fundamental abilities and skills are developed, [6]. Thus, it is essential to give infants with CP an opportunity to interact with the environment for an integral development (physical and cognitive).

The main therapies focused on the rehabilitation of people with CP are: (1) Physical and occupational therapy; (2) Oral medications; (3) Orthotics; (4) Botulinum toxin; (5) Casting; (6) Multilevel orthopedic surgery; (7) Neurosurgical procedures; (8) Partial bodyweight-supported treadmill training (PBWSTT) and constraint-induced movement therapy (CIMT); and (9) Gait robot-aided therapy.

Recent publications have demonstrated that robot-assisted therapies may be an effective tool to compensate and/or rehabilitate the function skills of people with CP, [7]. Most of the devices were previously designed for people with other disorders, such as stroke and spinal cord injury. Current trends in robotic rehabilitation are focused on validating these devices beyond these disorders and extend the benefits for people with CP.

In this chapter, we will present a bibliography review about assistive robotic devices for people with cerebral palsy, both rehabilitation and functional compensation. We will focus on devices designed to support users locomotion (lower limb) and manipulation (upper limb). Additionally, we will propose a holistic strategy (physical and cognitive) based on a playful robot, called PALMIBER, which will aim to enhance physical and cognitive users skills through mobility experiences. Finally, we will present an ambulatory robot for gait rehabilitation after multilevel surgery, called CPWalker.

2 Robot-Assisted Rehabilitation for People with Cerebral Palsy

Robot-assisted therapy is a form of physical therapy that uses a robotic device to help a person with an impaired functional ability learns to recover the function. The robotic device usually proposes a goal-directed task, which encourages the patient. This approach has interesting advantages compared to traditional therapy, because robotic therapy integrates functional tasks instead of repetitive movements without goal. As a result, it is usual to increase the number of sessions, frequency and intensity and finally the positive impact of the treatment. Additionally, these devices usually integrate assessment system to objectively measure the progress of the therapy. Sections 2.1 and section 2.2 present a review of robot-assisted therapies for cerebral palsy, for lower (ambulation) and upper limbs (manipulation) respectively.

2.1 Ambulation: Robot Assisted Rehabilitation for Lower Limbs

There are basically two groups of assistive devices to help people with mobility problems: the alternative devices and the empowering (or augmentative) devices. These solutions are selected based on the degree of disability of the user. In the

case of total incapacity of mobility (including both bipedestation and locomotion), alternative solutions are used. These devices are usually wheelchairs or solutions based on autonomous especial vehicles.

People who have reduced mobility commonly use augmentative devices by using their residual capabilities. In particular, walkers and exoskeleton robots are augmentative devices to assist in standing, balance and locomotion. Walkers are intended to help users navigation. Smart Walkers are robotic devices based on walkers optimised to improve human-machine interaction and as a result to improve the acceptance and functionality of these systems in rehabilitation. As walkers take advantage of the users remaining locomotion capability, they also help avoid the early and deteriorative use of alternative devices, most commonly, the wheelchairs. The PAMM system (Personal Aids for Mobility and Monitoring),[8], and the GUIDO system, an advanced walker for people with visual and/or mental deficiency, [9], are illustrative examples of this technology. The SIMBIOSIS Project introduced an implementation of a smart robotic walker, [10], specifically aimed at functional compensation of gait, differently from its counterparts, principally oriented at guiding assistance.

Exoskeleton Robots are mechatronic devices of which segments and joints correspond to some extend to these of the human body and the system is externally coupled to the person, (fig. 1). In rehabilitation applications, exoskeletons should be able to replicate with a patient the movements performed with a therapist during the treatment. In the case of functional compensation, exoskeletons are designed to support the execution of activities of daily living by assisting the user in the basic motor functions. The exoskeletons have been intended to provide either joint support by means of brakes or clutches, [11], [12], [13], [14], or actively add power to the joints, thus providing a mean to control and complete joint movements, [15], [16], [17], [18]. In addition, the sensors attached to the exoskeleton can assess forces and movements of the patient. This would give to the therapist quantitative feedback on the recovery of the patients and would imply a more efficient rehabilitation process. Therefore, the exoskeleton could act as tool for the measurement of the performance and the evolution of the treatment, [19]. In the REHABOT project, [20], the proposers have put through and developed the idea of functional restoration of walking in spinal cord injury patients through a synergistic strategy, in which both exoskeletal robots and motor neuroprostheses (MNP) are combined to improve functional recovery. MNPs constitute an approach to restoring function by means of artificially controlling human muscles or muscle nerves with functional electrical stimulation (FES). These hybrid approaches have demonstrated their capability to improve overall motor substitution outcome, as each individual component helps overcome the technological limitations of the counterpart. These effects are particularly critical in the case of unbalanced activity of agonist antagonist muscles, typically found in CP.

An interesting hybrid (exoskeleton and walker) approach was proposed by Stauffer et al.,[18]. They presented the WalkTrainer, a combined exoskeleton and FES systems in hybrid configuration with a smart walker. While the WalkTrainer

Fig. 1. Example of an exoskeleton robot: lower limb orthotic exoskeletons

exoskeleton controls hip, knee and ankle joints, and the pelvis movement, the deambulator supports the exoskeleton and the user, via a weight bearing system, similar to treadmill training systems. A closed-loop control of FES applies muscle stimulation, relying on the estimation of the interaction forces between the user and the exoskeleton.

The NF-Walker (made for movement) is a hybrid device for people with CP that combines dynamic standing and walking support. NF-Walker comprises two main parts: a base (similar to a walker) and the braces. The braces are fixed to the base allowing to stimulate an adequate gait pattern. The base pressures towards the ground through the wheels. Weight support of the user is taken up inside the shoes (independent from the pressure towards the ground). The Lokomat, manufactured by Hocoma, is a driven gait orthosis that automates locomotion therapy on a treadmill and improves the efficiency of treadmill training.

Partial body weightsupported treadmill training (PBWSTT) and constraint-induced movement therapy (CIMT) are therapies based on current theories of motor learning. They promote a normalized pattern of gait involving the sensory information and the reflex components of gait. This has been demonstrated to be useful to obtain patterns of gait in spinal cord injury patterns. However, for other types of pathologies it has been demonstrated the need to involve actively the user in the training as well as allowing some kind of error to promote the mechanisms of motor learning. This has lead to approaches such as assist as needed or error enhancement in which the amount of support to the patients is dynamically changed, usually as a factor of the number of sessions.

Meyer-Heim et al, [21], described the current state of the robot-assisted and computer-enhanced therapies for children with cerebral palsy. According to the Gross Motor Function Classification System (GMFCS), especially mildly affected children with GMFCS level I and II profited more from the intervention in contrast to those with GMFCS levels III and IV. Remarkably, one study

demonstrated that the improvements in gait capacity induced by 12 sessions of robot-assisted gait training were maintained for 6 months, [22]. Motivation as an emotional process is recognized as being an important factor in the rehabilitation process and therapy outcomes,[23], [24]. For instance, the therapist can provide verbal encouragement and verbal feedback for selective muscular training and raise the childs awareness to correct gait patterns and posture. Some works have demonstrated that robot-assisted therapy in combination with virtual reality could increase the user involvement and, as a consequence, enrich the treatment. Therapies based on goal-oriented tasks can be easily configured using virtual scenarios, [25].

A few of the assisted-mobility systems described in the literature address the particular problems of children affected by neuromotor disorders attending to cognitive rehabilitation through mobility experiences. One outstanding case worthy of mention is the Communication Aids for Language and Learning (CALL) center that developed a smart wheelchair specifically for children with mobility impairment. In this case, a standard wheelchair was instrumented and adapted in terms of the users interfaces. The Gobot is a special vehicle that enables mobility for children with CP created by the Hospital of Lucile Packard Stanford (US). It moves easily from a horizontal to a vertical position. Tray, hip, lateral supports and full foam knee supports are also simple to adjust. The Magellan Pro Robot is a commercial robot made by the IRobot Corporation. Researchers from the Delaware University (US) used it for rehabilitation of children with CP, [26],[27]. The robot was equipped with an on-board computer and odometry. Their results demonstrated that young infants independently move themselves via a mobile robot. Their data do provide indirect evidence that infants were not simply focused on moving the joystick but were associating joystick activation with their motion.

Although these devices are focused specifically for children with CP, they are based on standard or commercial devices. In this work, we propose two assistive platforms, called PALMIBER and CPWalker, designed specifically for alternative mobility of children with CP, in which the cognitive aspects are also considered as main part of the therapy.

2.2 Manipulation: Robot Assisted Rehabilitation for Upper Limbs

There are currently a limited number of robotic systems targeting the upper extremity that have been applied to children with CP, [21]. These devices propose goal-directed tasks and reaching movement to rehabilitate the hand and arm function.

The InMotion2 robot, is an end-effector robot, a commercial version of MIT-MANUS, which is capable of continuously adapting to and challenging each patients ability. This device aims to improve the range of motion, coordination, strength, movement speed and smoothness. It demonstrated functional improvements in the Quality of Upper Extremity Skills test (QUEST) and the Fugl-Meyer upper limb subtest, [28].

The HapticMaster is a 3 degrees of freedom, force-controlled haptic interface. It provides the user with a crisp haptic sensation and the power to closely simulate the weight and force found in a wide variety of human tasks. The programmable robot arm utilizes the admittance control (force control) paradigm, giving the device unique haptic specifications. People with CP used it in combination with virtual scenarios to improve the shoulder and elbow movements. The patients with in this study, [29], improved in measures of motor activity in the Melbourne Assessment.

The ARMEO system (based on T-WREX system) proposes a rehabilitative exercise that allows early rehabilitation of motor abilities and provides adaptive arm support in a 3D workspace. It is focused on patients with not sufficient strength to move their arm and hand against gravity, [30], [31]. There is a lack of clinical trials using this system with people with cerebral palsy. However, interesting results with patients who suffer stroke suggest promising result for people with CP.

In the case of children with CP is especially important the motivational aspect. For this reason these type of devices are usually designed in combination with playful scenarios such as videogames, which promote motivating and challenging tasks for a prolonged time.

According to some authors, [21], these approaches need to be refined and critically analyzed to determine their functional benefit for children with different levels of sensory-motor or cognitive impairment or both. Additionally, the current level of evidence regarding the efficacy of new technologies in the rehabilitation process still remains scarce. It would be necessary well-designed randomized clinical trials with better description and meaningful number of subjects. Furthermore, it would necessary to study the functional improvements for a prolonged time after the therapy.

3 A Mobile Robot for Physical-Cognitive Rehabilitation: The PALMIBER Vehicle

3.1 The Importance of Mobility and Interaction

The motivation of this work arises from the limitations caused by CP in the fundamental areas of human being: mobility, communication, manipulation, orientation and cognition. On the one hand, self-produced locomotion is essential for child development at the early ages. Independent mobility plays a crucial role in this exploration, leading to the child physical, cognitive and social development, [32]. According to the state of the art of mobility devices for people with CP, most devices are more focused on mobility than the integral development.

On the other hand, human-machine interaction is a critical factor. The posture and motor disorders associated to unable users with CP to control assistive devices. According to the state of the art of person-computer interfaces for people with CP, there is a wide diversity of solutions. However, authors assert that the usability decreases dramatically when users have a severe motor disability.

We propose a playful robotic vehicle to promote the interaction between the child with CP and his/her environment through mobility experiences. The vehicle has been designed under the assist as needed paradigm. Different driving modes with gradual intervention of the user are proposed. Additionally, different interfaces (driving console, switches and head-mounted interface) to drive the vehicle are proposed.

3.2 The PALMIBER Vehicle

The PALMIBER (figure 2) is a pre-industrial robotic vehicle designed and built with the main objective of providing severely disabled children the ability to explore the environment through independent mobility and be engaged in the same type of activities as their non-disabled peers. A multidisciplinary team participated in this project following a holistic approach in order to create a useful assistive device, which allows independent mobility in severely disabled children.

Fig. 2. Two children driving the PALMIBER vehicle with different interfaces (console of directions and single switch)

The objectives defined by the team of researchers led to the definition of the following technical requirements for the vehicle:

- A wide range of driving modes, adaptable to the various levels of cognitive performance of the potential users
- The capability to be used with several human machine interfaces as a function of the end user motor capabilities
- Monitoring functions for self-evaluation to help estimate the appropriate driving mode and the achieved progress;
- Playful aesthetics to attract child attention;
- Robust, safe, ergonomic and reasonable cost.

The vehicle is open and flexible so that it can be adapted to varying cognitive and physical performance levels. There are five levels implemented (figure 3):

- Level 0. Automatic. The vehicle detects and avoids obstacles without user intervention using an ultrasonic system.

- Level I. Cause-Effect. The child presses any key and the vehicle moves. The vehicle stops when it finds an obstacle.
- Level II. Training directions. The vehicle stops after detecting an obstacle (a crashing noise and alarm light warn of the eventual crash). The child must press the correct button proposed by the vehicle otherwise the vehicle does not move. If response is not obtained from the child, he is invited to do so by a verbal message. There are two partial modes: a) forward and backward keys alternatively and b) right and left keys alternatively.
- Level III. Deciding directions. The user decides and presses the driving buttons, but the vehicle automatically stops if any obstacle is detected. Verbal commands are generated. At this level, the children start deciding on a navigation target.
- Level IV. Fully guided. The vehicle is fully driven by the user; ultrasonic sensors are not active in this operation mode.

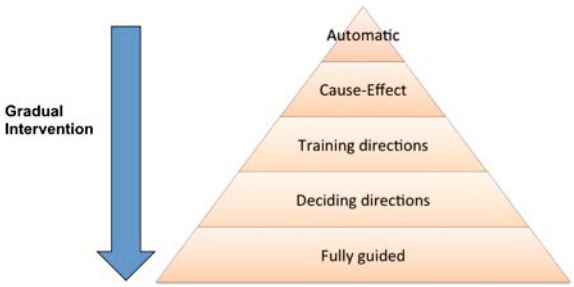

Fig. 3. Driving modes of the PALMIBER vehicle to adapt the system to the user cognitive skills

3.3 Human-Machine Interaction for People with CP

People with CP often have severe limitations using conventional human-machine interfaces, thus diminishing their opportunities to communicate and learn through computers, [33]. Therefore, the selection of the usable human-machine interfaces for driving the vehicle or another assitive device (as computer) is a key factor in order to reduce the barriers of manipulation and control due to motor disorders that affect upper limbs.

Davies et al. presented a systematic review of the development, use and effectiveness of devices and technologies that enable or enhance self-directed computer access by individuals with CP, [34]. They divided HMI into five categories: 1) pointing devices, 2) keyboard modifications, 3) screen interface options, 4) speech and gesture recognition software and 5) algorithms and filtering mechanisms.

Eye and face tracking interfaces are powerful pointing devices for people with motor disorders. They often succeed in improving human-computer interaction, [35]. They have the potential to be a very natural form of pointing, as people tend to look at the object they wish to interact with. However, they often present low performance with people with severe motor disorders.

As regards keyboard-based solutions, some studies have demonstrated that keyboard adaptations improve speed and accuracy, [36], [37]. The category screen interface includes the interfaces that scan through screen icons or dynamically change the icon position. Children with significant physical impairments (who are unable to point) use visual scanning and switches to select symbols. Symbol prediction software is a method of access that involves highlighting a specific symbol within an array on the basis of an expected or predicted response, [38]. The prediction software reduces the response time required for participants but there is a trade-off between speed and accuracy.

Some devices are voice-based human-computer interfaces in which a set of commands can be executed by the voice of the user. Speech-recognition software is difficult to customize for users with CP who have dysarthria. Finally, algorithms and filtering mechanisms are focused on improving the accuracy of computer recognition of keyboard input or tracking of the pointer motion.

Access solutions for individuals with CP are in the early stages of development and future work should include assessment of end-user comfort, effort and performance, as well as design features, [34]. A fundamental conclusion is that there is a wide diversity of solutions but their authors frequently assert that usability decreases dramatically when users have a severe motor disability.

The PALMIBER project proposes to use three types of interfaces for driving the vehicle:

- A console that consists of membrane keys to select the directions, (figure 4)
- A single switch and scanning methods (sequential activation of buttons and the user must press the switch when the desired direction is highlighted),
- The ENLAZA interface (figure 4) is a head-mounted interface, which transmits commands of control using the head movements. The interface integrates algorithms for discriminating, predicting and evaluating the normal and abnormal motor behavior of the user and his/her functional limitations and abilities. The ENLAZA interface integrates filtering techniques to reduce the effect of the involuntary movements on the control of the device. As a result, users who are unable to control conventional interfaces can access to the computer or other devices (e.g. PALMIBER vehicle).

This vehicle intends to follow the universal design approach. That means that the vehicle proposes different channels of interaction for people with different capabilities.

3.4 Experiments and Results

The vehicle proposed has been validated experimentally with users with cerebral palsy. A multidisciplinary team has participated during the different phases of

Fig. 4. Interfaces for driving the vehicle: console of direction, ENLAZA, an inertial head-mounted interface for driving the vehicle and control the computer

the work from the study of the users needs to the construction and validation of the devices. More than twenty users participated in different phases of the experimentation, [39], [40], with different levels of physical and cognitive capabilities. Depending the user capabilities, he/she worked with and specific driving mode, from automatic to fully guide mode.

According to the results, the PALMIBER device adapts efficiently to the particular users skills through the different driving modes (cognitive skills) and different interfaces (physical skills). This vehicle expands the current therapeutically approach to treat infants and adults with CP, by providing an autoadaptive therapy that enhance their fundamental abilities. According to the studies the vehicle improves the executive function of children unable to walk. The child learns to manage decisions, plans and predict the effect of his/her actions through mobility experiences.

Regarding to human machine interaction, users with manipulation capabilities are able to use the mechanical interfaces, as console of directions and switches. The lights and the mechanical feedback from the interface is essential to motivate children through physical stimuli. That means that keys based on capacity membranes were found less usable than mechanical switches, which provide mechanical feedback to the user. Additionally, some users with severe motor disorders in upper limbs participated. These users were unable to control conventional interfaces, console of directions and switches. Although all areas of the motor function can be limited, limbs are usually more affected than the head motion in infants with severe CP. The ENLAZA was demonstrated to be an effective human-computer interface to control the vehicle for those users unable to control the switch or the console of directions. The interface reduces the time between action planning and action execution, promoting the cause-effect process in an effective way. Additionally, the relation between movement direction and the arrow symbols on the console of directions requires mental abstraction, which can result difficult for these users. As a conclusion, the control with the head movement is a more intuitive method of control compared with pressing a key.

PALMIBER and ENLAZA have been validated technically and functionally for short-time periods. Currently, the Bioengineering group is carrying out longitudinal experiments (one year) to measure the impact of the PALMIBER vehicle on the physical-cognitive rehabilitation. ASPACE Cantabria, a specialized

center, is collaborating to test these devices and measure the changes on motor and cognitive skills of the user.

At this time, nine users (age 2-10 years) are participating in the experiments. All participants started with the automatic mode, and after four months five users have achieved the level Cause-Effect and four users achieved the level of Training directions. The Bioengineering Group is registering all the data related to the driving exercise and will correlate the objective metrics with functional and subjective skills to measure more precisely the effect of the therapy.

The integration of PALMIBER and ENLAZA constitutes a powerful platform to analyze both approaches and gain a deeper knowledge on the dynamics of learning, due to the interrelationship between physical and cognitive aspects related with cerebral palsy. This approach relies on the hypothesis that the therapies based on the vehicle and the interface will create a positive spiral of physical/cognitive rehabilitation, that is to say, the improvements on physical capacities of the patients will enable them to live new experiences, for instance, to interact with the cognitive therapies. On the other way around, improvements in patients cognitive capacities will result in improvement of their motor control.

4 Robotic Platform for Gait Rehabilitation after Multilevel Surgery: CPWalker

The main objective of CPWalker is to develop and validate a robotic platform to support novel therapies for CP rehabilitation. This platform (Smart Walker + exoskeleton + neuroprosthesis) will be controlled by a multimodal interface to establish the interaction of CP infants with robot-based therapies. The objective of these therapies is to improve the physical skills of infants with CP and similar disorders. CPWalker concept will promote the earlier incorporation of CP patients to the rehabilitation therapy and increase the level of intensity and frequency of the exercises, which will enable the maintenance of therapeutic methods in daily basis, lead to significant improvements in the treatment outcome. Three research groups participate in this project: the Bioengineering Group of CSIC (GBIO-CSIC), the Biomechanic Institute of Valencia (IBV) and the Jesus Child Hospital, national reference of cerebral palsy treatment.

4.1 Robotic Rehabilitation after Multilevel Surgery

In some cases, the development of secondary musculoskeletal pathology contributes to loss of function, gait impairments, fatigue, activity limitations, and participation restriction. Orthopaedic surgeries are considered one of the best treatments for significant musculoskeletal problems in CP, and thereby minimizing the subsequent impairments and activity limitations,[41]. One of the main techniques is the Multilevel orthopedic surgery, [42], which focuses on correcting all deformities and to improve gait. It is often referred to as Single-Event Multilevel Surgery (SEMLS) when is performed in a patient without previous

surgeries. SEMLS has shown benefits in the treatment of musculoskeletal problems of children with CP by reducing the effort and the appearance of walking, [43], improving GMFM, [44], [45], kinematic parameters,[46], gait speed, [47], and Gillette Gait Index score, [48]. Godwin et al. described that children categorized preoperatively at GMFCS levels II, III and IV showed greater change (trend toward lower GMFCS) compared with children classified as GMFCS levels I and V, [49]. After this procedure, a period up to 2 years is often required to get a functional plateau level, although there is a lack of published recommendations about the more efficient post-surgical rehabilitation program. New strategies are needed to help to promote, maintain, and rehabilitate the functional capacity, and thereby diminish the dedication and assistance required and the economical demands that this condition represents for the patient, the caregivers and the society,[50].

Most of the therapies for rehabilitation after surgery are peripherally driven and are based on motor control reorganization triggered by peripheral physical therapy. However, CP affects primarily brain structures. This suggests that both Peripheral Nervous System (PNS) and Central Nervous System (CNS) should be integrated in a physical and cognitive rehabilitation therapy. This is exactly the approach of CPWalker. It is important to highlight the plasticity of the target patients of this study, young children present increased brain plasticity compared to an adult, and is more likely to have a change in motor patterns following an intervention.

The main objective of CPWalker is to develop and validate a robotic platform to support novel therapies for CP rehabilitation after SEMLS surgery. The goal is to reduce the period of rehabilitation after surgery. This will be achieved by developing a robotic platform (Smart Walker + exoskeleton + neuroprosthesis) controlled by a multimodal interface to establish the interaction of CP infants with robot-based therapies.

4.2 The CPWalker Concept

CPWalker proposes the use of a robotic platform through which the infant can start experiencing autonomous locomotion in a rehabilitation environment. This robotic platform will consist of a smart walker with body weight and autonomous locomotion support and a wearable exoskeleton robot + motor neruprosthesis for joint range of motion support. The load on the human skeleton define the bone development, as a result, the pathological gaits typical of CP infants induce bones deformities. CPWalker will provide the infant with a structure that will rehabilitate his/her gait to physiological patterns, which will prevent deformation of their bones.

The interaction between the infant and the robotic platform will take place through a Multimodal Human-Robot Interface (MHRI) consisting of an (1) Electroencephalographic (EEG) acquisition unit; (2) an Inertial measurement unit (IMU), (3) wireless Electromyography (EMG) system for measuring residual movement and activation strategies, and (4) force sensors to measure the interaction between the user and the robotic platform. The rationale of this

multimodal interface is to allow integrated PNS and CNS physical and cognitive interventions. MHRI interaction with therapeutically selected tasks will be based on volitional motor planning, the aim being promoting reorganization of motor planning brain structures and thus integrating CNS in the therapy. Figure 5 depicts the overview of the CPWalker concept.

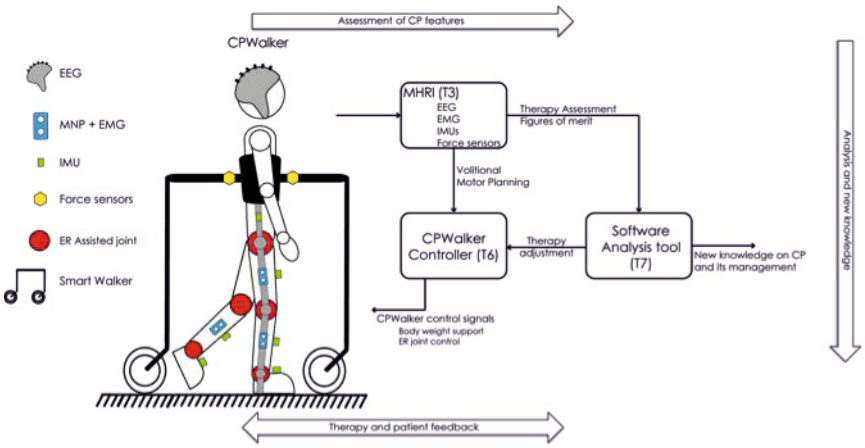

Fig. 5. Overview of CPWalker concept

Summarizing, CPWalker methodology will unify and standardize technological, biomechanical, neurophysiological and clinical concepts that will culminate in the development of the following instruments:

- A smart walker with body weight support to promote the autonomous locomotion,
- An exoskeleton + neuroprosthesis able to apply forces to lower limbs joints,
- A multimodal human-robot interface to promote the integration of the patient into the therapy,
- A software analysis and capture tool to quantify the rehabilitation progress in three domains: kinematic, physiological and functional.

4.3 Strategies for Gait and Body Weight Support

As decribed in previous sections, there are different gait training devices based on PBWS in the market. However, most of them do not propose ambulatory training and present difficult procedures to transfer the user from the wheelchair to the standing position. It is required for the therapist or caregiver to do important physical effort. In general, these devices seem to have promising results for rehabilitation, according to the literature, but present some limitations such as heavy weight, complex set-up and non-ambulatory mobility or poor maneuverability in

the case of mobile devices, making them inappropriate for small interior spaces with narrow doorways.

The CPWalker project is involved in the framework of a research line to design ambulatory devices for rehabilitation and functional compensation in the Bioengineering group of CSIC. These devices are the evolution of the classical walkers, which play an important role when the user has residual capabilities to push the system. However, the usability decreases when the user suffers severe motor impairment, as a patient after a multilevel surgery. This is the context where smart or robotic walkers are emerging as a feasible solution. Some works related to the CPWalker project have been previously developed by the authors and their colleagues. The SIMBIOSIS project proposed a smart walker, which analyzed dynamically the user gait adapting the active support according to user needs, [10], (fig. 6). The SIMBIOSIS measures the forearm forces to improve human-machine interaction. This walker embodies several innovative aspects, such as: i) enhanced user unloading by means of forearm support, ii) augmented stability in static and dynamic conditions, iii) improved guiding control skills based on detection of users intention and iv) accurate safety-oriented strategies.

Fig. 6. The SIMBIOSIS Smart Walker

An interesting result was extracted in the clinical validation of the SIMBIOSIS device in spinal cord injury (SCI) patients. The user unloading is crucial to improve the functionality of these systems in rehabilitation due to the lack of motor control and muscle tone in the lower limbs. Therefore, it is recommendable to implement body weight support to modulate the user unloading improving assisted ambulation and reducing the high metabolic energy expenditure required.

In this context, the HYBRID project, developed by GBIO-CSIC, tries to solve these issues. This system considers the use of a bilateral lower limb robotic exoskeleton integrated with an external ambulatory and active structure with electric traction, REMOVI (fig. 7), which provides support and stabilization to the user through a harness in real ambulatory scenario. This system is proposed as a device to develop rehabilitation exercises for patients with SCI or

other pathologies, who present serious mobility problems. The patient wears an integral harness in order to perform the elevation process from wheelchair to standing-up position. Two electrically actuated lifting arms or bars, placed on a superior plane, elevate the user by means of the harness. This motor sets the level of unloading. Finally, two tractor motors with encoders are mechanically coupled to the system allowing overground training.

Fig. 7. The REMOVI device

Preliminary studies with healthy subjects have been carried out with 0%, 30%, 50% and 70%. It was observed that the range of motion and the heel contact decreases as a function of the height support but the PBWS does not influence on the cadence or the step length, [51].

This background has been partially applied to the CPWalker concept. The design of the device is based on the framework of the NF Walker system, (Movement for Movement). The NF Walker is widely used as a very effective mobility aid for some users with CP, thereby, the CPWalker project will use the framework of this device to include elements that supports the gait and weight actively. Fig. 8 depicts a CAD design of the device. The design includes to DC motor for the gait support and a linear actuator for the weight support. Additionally, the system will include a pediatric exoskeleton, [52], which consists of an external structure that assists the natural skeleton of the user. The exoskeleton is composed of three parts, which are articulated by three joints and adjusted to the body by means of several belts. This exoskeleton is based on the devices designed from previous adult version develped in the context of the EU projects Hyper, [53] and Gait, [54], [55].

4.4 Multimodal Human Robot Interface

One of the main contribution of the CPWalker is to take into account the cognitive processes of the user to guide the device actively. The CPWalker includes a

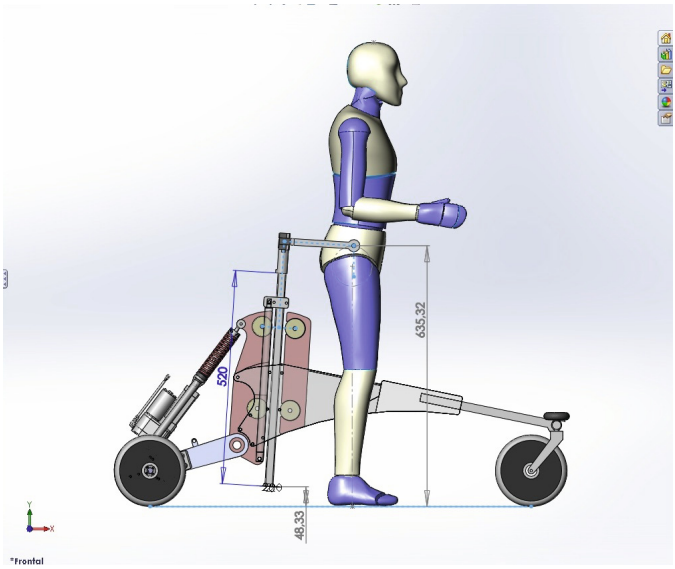

Fig. 8. CAD design of the CPWalker device

Multimodal Human Robot Interface (MHRI), which is a novel type of interface that integrates information from the central nervous system (CNS), and the peripheral nervous system (PNS) in order to characterize the full state of the user. MHRIs are topics of research in many contexts, and have proven, for example, to be able to characterize concomitant voluntary and pathological components of movement in tremor patients, [56]. MHRIs appear as an upgrade of traditional brain-computer interfaces (BCIs) and brain-machine interfaces (BMIs), which have been used for a large number of problems, e.g. wheelchair control, [57], spelling systems, [58,59], restore hand grasp, [60], or to improve upper or lower limb rehabilitation [61,62].

The rationale for using MHRIs in the CPWalker project is that by integrating the PNS one can obtain a more detailed representation of the behaviour of the CNS. This arises from the fact that the motor units that compose the muscles (and hence the PNS) are the smallest transductor of the commands generated at the brain, and muscle activation is responsible for the actual movement. Therefore, concurrent recording of these data provides with a richer and better characterization of the mechanisms of motor control. MHRIs are implemented using different technologies that range from highly invasive interfaces to record very localized neural ensembles, [63,64], to their noninvasive counterparts, electroencephalography (EEG) and surface electromyogrpahy (sEMG). The MHRI here proposed is aimed at integrating the CNS and PNS into the rehabilitaiton therapy, in order to optimize it according to the users skills.

In more detail, the CPWalker MHRI will comprise EEG, sEMG and inertial sensors (based on results obtained from ENLAZA project) in order to character-

ize both the generation, planning and execution of movement, and the users state during the therapy. This will be achieved based on: i) a previous characterization of the strategies that underlie volitional motion planning, [65], in CP affected children, ii) the neural drive to muscles (defined in terms of activation patterns, central pattern generators, [66], and muscle synergies) and iii) the kinematics of the actual movement, [67].

Movement parameters will also be exploited by the controller of the CPWalker to adjust certain features such as walking speed or initiation of gait. Furthermore, the MHRI data will serve to assess the outcome of the CPWalker therapy in terms of reorganization of the neural structures, which will be assessed by analysing the raw neural drive to muscles and the muscle synergies. This will in turn permit elucidating the neural mechanisms that mediate the recovery, such as the normalization of the muscle synergies or the correction of their activation and combination, [68], which will constitute a major neuophysiologic finding.

The CPWalker MHRI constitutes a novel means to integrate the CNS and PNS into the robotic therapy. First, online characterization of the level of attention (at the CNS) and of the neural drive to muscle (at the PNS) will permit optimizing the therapy, in terms of intensity and duration, for each user. Second, the reorganization of the muscle activation patterns will be investigated (at the CNS and PNS) as a means to objectively assess the outcome of the therapy, and also elucidate the neural mechanisms that mediate such recovery. Fig. 9 depicts an user with CP using the experimental MRI at the Jesus Child Hospital (Madrid) where the experiments took place.

Fig. 9. Experiments of an user with CP using the MRI device

4.5 Current and Expected Results

Currently, the CPWalker project has concluded the conceptual design of the platform and the definition of user needs. Additionally, the control and mechan-

ical architecture have been designed. At this time, CPWalker expects to achieve the following results:

- Description of the users needs (children with CP) for the different subtypes of CP, the functional level (GMFCS) and the special aspects of this still growing population,
- Description of the special features and actual difficulties in the current rehabilitation process,
- Definition of musculoskeletal models through the gait in CP to select and to draw up a plan for adaptive control strategy of the CPWalker,
- Establishment of the pathological kinematic pattern and the central pattern generators (muscle synergies) of children affected with CP,
- Evaluate the long-term benefits obtained with the CPWalker concept, alone or in combination with pharmacotherapy, in a group study. This evaluation will be carried out during continuous periods of use, while patients under traditional and robotic-based therapy.
- Definition of objective figures of merit that will assess the status of the disorder and its evolution. Such metrics will provide the clinician and the patient with feedback on the CP.

As a conclusion, we propose to create a prototype of pediatric sized and adapted wearable exoskeleton becoming the main device in the CPWalker technology. The equipment will support and assist the walking process, and will count in with modifing options to customize the therapy to the necesities of every user.

5 Conclusions

This chapter presented the state of the art of robot-assisted rehabilitation for people with cerebral palsy. According to the review, numerous devices for the rehabilitation of gait exist. Robotic exoskeletons to support the human gait have become very popular because they propose interesting strategies to increase the frequency and intensity of the sessions. Some of these devices, which were designed for spinal cord injury or stroke, have been recently adapted for people with cerebral palsy. On the other hand, robot systems for the rehabilitation of upper limbs are scarce. However, some studies demonstrate that robotic therapy may provide new opportunities for improving upper limb coordination, strength and functions, such as reaching and grasping. Generally, a lack of longitudinal and randomized clinical trials (RCT) exists. This fact makes difficult to evaluate the impact of the robotic device after the robotic training.

Recent studies suggest that the users motivation and cognitive aspects, e.g. (attention) is essential to achieve the maximum impact on physical skills. That means that the combination of the physical and cognitive aspects will lead to better results of the rehabilitation. In this context, the design of virtual scenarios (e.g. videogames) in combination with robotic devices is providing promising results. This aspect is particularly important in the children with cerebral palsy

cases, because their cognitive, social and perceptive skills are often more affected respect to other pathologies such as stroke or spinal cord injury.

In this chapter, we presented the PALMIBER vehicle, a robot platform to promote the integral development of children with cerebral palsy through mobility experiences. The vehicle is based on the fact that fundamental skills are developed at early ages when the brain plasticity is higher. The PALMIBER integrates different driving modes with gradual user intervention (from Cause-effect to Fully-guided mode) in order to adjust the robotic therapy the different cognitive levels of the child. Additionally, the vehicle includes a group of human-computer interfaces to adjust the driving task to the user manipulation skills. A head-mounted interface called ENLAZA allows users with severe motor disability to control the vehicle with head motion. The inertial interface is an effective channel to reduce the barriers between the user and the vehicle. Additionally, the interface is an intuitive method to drive the vehicle and learn spatial concepts, because the head movement is translated to the vehicle displacement. On the other hand, inertial technology provides a new opportunity for analysis and extraction of kinematic patterns of voluntary and pathological movement. The impact of therapies will be evaluated with objective parameters as complement to the functional and subjective evaluation of the therapists. According to the state of the art, virtual and playful applications (e.g. video games) will increase the interest and motivation of us-ers, which will have a positive impact in rehabilitation. In this context, motion capture systems and virtual representation allows users to encourage the exercise therapy by biofeedback methods. The ENLAZA interface, through head movements, allows the user with CP to control the vehicle but also it may be use for the computer.

The PALMIBER vehicle and the ENLAZA interface propose an auto-adaptive physical-cognitive and dual therapies, which will promote active participation of the infant with CP, implementing a gradual intervention tailored to his/her functional physical and cognitive limitations and abilities. Additionally, these devices provide objective metrics that assess the status of the user based on this multimodal information, which will be employed to provide support to the therapist, and to establish definite, personalized, criteria to assess the outcome of the rehabilitation, and guidelines for it. The final outcome of these robotic devices is a framework for the integrative (i.e. physical and cognitive) assessment and rehabilitation of infants with CP.

Additionally, we present the CPWalker project, which proposes an ambulatory robotic platform for gait rehabilitation after surgery. CPWalker platform includes a smart walker for weight support, an exoskeleton for support the joint range of motion, a human-machine interface and assessment software to generate objective outcomes metrics of the therapy progress. The main contribution of the project is to include the cognitive dimension into the physical therapy. The CPWalker Human Machine Interface constitutes a novel means to integrate the central neural system and peripheral neural system into the robotic therapy. Online characteriza-tion of the level of attention (at the CNS) and of the neural

drive to muscle (at the PNS) will permit optimizing the therapy, in terms of intensity and duration, for each user.

The results and problems that these developments faced suggest a field of work that must be addressed in future. One of the interesting factors to consider is to analyze how physical and cognitive learning affects the device control. Therefore, there will be carried out a long term planning experimentation.

The work presented in this chapter has given rise to new challenges to be addressed within a line of research with a commitment to find new solutions for people with CP. The state of the art shows that new Assistive Technologies and, specifically, robot-assisted therapies designed specifically for people with PC are taking up the interest of numerous research groups. This fact will lead to more efficient devices, auto-tailored to the particular users cognitive and physical needs and, finally, improve the autonomy of people with cerebral palsy.

References

1. Bax, M., Frcp, D.M., Rosenbaum, P., Dan, B., Universitaire, H., Fabiola, R., Bruxelles, U.L.D., Goldstein, M., Pt, D.D.: Review Proposed definition and classification of cerebral palsy, April 2005 Executive Committee for the Definition of Cerebral Palsy. Neurology 47, 571–576 (2005)
2. Winter, S., Autry, A., Boyle, C., Yeargin-Allsopp, M.: Trends in the prevalence of cerebral palsy in a population-based study. Pediatrics 110(6), 1220–1225 (2002)
3. Johnson, A.: Prevalence and characteristics of children with cerebral palsy in Europe. Developmental Medicine and Child Neurology 44(9), 633–640 (2002)
4. Palisano, R., Rosenbaum, P., Walter, S., Russell, D., Wood, E., Galuppi, B.: Development and reliability of a system to classify gross motor function in children with cerebral palsy. Developmental Medicine & Child Neurology 39(4), 214–223 (2008)
5. Eliasson, A.C., Krumlinde-Sundholm, L., Rösblad, B., Beckung, E., Arner, M., Ohrvall, A.M., Rosenbaum, P.: The Manual Ability Classification System (MACS) for children with cerebral palsy: scale development and evidence of validity and reliability. Developmental Medicine and Child Neurology 48(7), 549–554 (2006)
6. Shonkoff, J., Meisels, S. (eds.): Handbook of Early Childhood Intervention, 2nd edn. Cambridge University Press, Cambridge (2000)
7. Krebs, H.I., Ladenheim, B., Hippolyte, C., Monterroso, L., Mast, J.: Robot-assisted task-specific training in cerebral palsy. Developmental Medicine and Child Neurology 51(suppl. 4), 140–145 (2009)
8. Spenko, M., Yu, H., Dubowsky, S.: Robotic personal aids for mobility and monitoring for the elderly. IEEE Transactions on Neural Systems and Rehabilitation Engineering 14(3), 344–351 (2006)
9. Rodriguez-Losada, D., Matia, F., Jimenez, A., Galan, R., Lacey, G.: Implementing Map Based Navigation in Guido, the Robotic SmartWalker. In: Proceedings of the 2005 IEEE International Conference on Robotics and Automation, pp. 3390–3395. IEEE (2005)
10. Frizera Neto, A., Gallego, J.A., Rocon, E., Pons, J.L., Ceres, R.: Extraction of user's navigation commands from upper body force interaction in walker assisted gait. Biomedical Engineering Online 9, 37 (2010)

11. Kangude, A., Burgstahler, B., Kakastys, J., Durfee, W.: Single channel hybrid FES gait system using an energy storing orthosis: preliminary design. In: Conference Proceedings: ... Annual International Conference of the IEEE Engineering in Medicine and Biology Society. IEEE Engineering in Medicine and Biology Society Conference, vol. 2009, pp. 6798–6801 (January 2009)
12. Gharooni, S., Tokhi, M., Heller, B.: The use of elastic element in a hybrid orthosis for swing phase generation in orthotic gait. ... of the 5th Annual Conference on the ... (2000)
13. Farris, R.J., Quintero, H.A., Withrow, T.J., Goldfarb, M.: Design and simulation of a joint-coupled orthosis for regulating FES-aided gait. In: 2009 IEEE International Conference on Robotics and Automation, pp. 1916–1922. IEEE (May 2009)
14. Durfee, W., Goldfarb, M.: Design of a controlled-brake orthosis for regulating fes-aided gait. ... in Medicine and Biology Society (1992)
15. Popovic, D.: Hybrid assistive system-the motor neuroprosthesis. IEEE Transactions on ... (1989)
16. Obinata, G., Fukada, S., Matsunaga, T., Iwami, T., Shimada, Y., Miyawaki, K., Hase, K., Nakayama, A.: Hybrid control of powered orthosis and functional neuromuscular stimulation for restoring gait. In: Conference Proceedings: ... Annual International Conference of the IEEE Engineering in Medicine and Biology Society. IEEE Engineering in Medicine and Biology Society. Conference, vol. 2007, pp. 4879–4882 (January 2007)
17. Schmitt, C., Métrailler, P.: A study of a knee extension controlled by a closed loop functional electrical stimulation. Proceedings of the 9th An. ... (2004)
18. Stauffer, Y., Allemand, Y., Bouri, M., Fournier, J., Clavel, R., Metrailler, P., Brodard, R., Reynard, F.: The WalkTrainer–a new generation of walking reeducation device combining orthoses and muscle stimulation. IEEE Transactions on Neural Systems and Rehabilitation Engineering: A Publication of the IEEE Engineering in Medicine and Biology Society 17(1), 38–45 (2009)
19. Krebs, H., Hogan, N., Aisen, M., Volpe, B.: Robot-aided neurorehabilitation. IEEE Transactions on Rehabilitation Engineering 6(1), 75–87 (1998)
20. Moreno, J., Pons, J., Koutsou, A.: The Rehabot-Knee Project Approach for Recovery of Neuromuscular Control of the Knee With Controllable Braces. International Journal of ... (2009)
21. Meyer-Heim, A., van Hedel, H.J.A.: Robot-assisted and computer-enhanced therapies for children with cerebral palsy: current state and clinical implementation. Seminars in Pediatric Neurology 20(2), 139–145 (2013)
22. Borggraefe, I., Kiwull, L., Schaefer, J.S., Koerte, I., Blaschek, A., Meyer-Heim, A., Heinen, F.: Sustainability of motor performance after robotic-assisted treadmill therapy in children: an open, non-randomized baseline-treatment study. European Journal of Physical and Rehabilitation Medicine 46(2), 125–131 (2010)
23. Sandlund, M., McDonough, S., Häger-Ross, C.: Interactive computer play in rehabilitation of children with sensorimotor disorders: a systematic review. Developmental Medicine and Child Neurology 51(3), 173–179 (2009)
24. Maclean, N., Pound, P.: A critical review of the concept of patient motivation in the literature on physical rehabilitation. Social Science & Medicine 50(4), 495–506 (1982, 2000)
25. Reid, D.T.: Benefits of a virtual play rehabilitation environment for children with cerebral palsy on perceptions of self-efficacy: a pilot study. Pediatric Rehabilitation 5(3), 141–148

26. (Cole) Galloway, J.C., Ryu, J.C., Agrawal, S.K.: Babies driving robots: self-generated mobility in very young infants. Intelligent Service Robotics 1(2), 123–134 (2008)
27. Lynch, A., Ryu, J.C., Agrawal, S., Galloway, J.C.: Power mobility training for a 7-month-old infant with spina bifida. Pediatric Physical Therapy: The Official Publication of the Section on Pediatrics of the American Physical Therapy Association 21(4), 362–368 (2009)
28. Fasoli, S.E., Fragala-Pinkham, M., Hughes, R., Hogan, N., Krebs, H.I., Stein, J.: Upper limb robotic therapy for children with hemiplegia. American Journal of Physical Medicine & Rehabilitation / Association of Academic Physiatrists 87(11), 929–936 (2008)
29. Fluet, G.G., Saleh, S., Ramirez, D., Adamovich, S., Kelly, D., Parikh, H.: Robot-assisted virtual rehabilitation (NJIT-RAVR) system for children with upper extremity hemiplegia. In: 2009 Virtual Rehabilitation International Conference, pp. 189–192. IEEE (June 2009)
30. Sanchez, R.J., Liu, J., Rao, S., Shah, P., Smith, R., Rahman, T., Cramer, S.C., Bobrow, J.E., Reinkensmeyer, D.J.: Automating arm movement training following severe stroke: functional exercises with quantitative feedback in a gravity-reduced environment. IEEE Transactions on Neural Systems and Rehabilitation Engineering: A Publication of the IEEE Engineering in Medicine and Biology Society 14(3), 378–389 (2006)
31. Rudhe, C., Albisser, U., Starkey, M.L., Curt, A., Bolliger, M.: Reliability of movement workspace measurements in a passive arm orthosis used in spinal cord injury rehabilitation. Journal of Neuroengineering and Rehabilitation 9(1), 37 (2012)
32. Azevedo, L.: A Model Based Approach to Provide Augmentative Mobility to Severely Disabled Children through Assistive Technology. PhD thesis, Universidad del País Vasco (2006)
33. Man, D.W.K., Wong, M.S.L.: Evaluation of computer-access solutions for students with quadriplegic athetoid cerebral palsy. The American Journal of Occupational Therapy: Official Publication of the American Occupational Therapy Association 61(3), 355–364 (2007)
34. Davies, T.C., Mudge, S., Ameratunga, S., Stott, N.S.: Enabling self-directed computer use for individuals with cerebral palsy: a systematic review of assistive devices and technologies. Developmental Medicine and Child Neurology 52(6), 510–516 (2010)
35. Mauri, C., Granollers, T., Lorés, J., García, M.: Computer vision interaction for people with severe movement restrictions (2006)
36. Lin, Y.-L., Chen, M.-C., Yeh, C.-C., Yeh, Y.-M., Wang, H.-P.: Assisting an adolescent with cerebral palsy to entry text by using the chorded keyboard. In: Miesenberger, K., Klaus, J., Zagler, W.L., Karshmer, A.I. (eds.) ICCHP 2008. LNCS, vol. 5105, pp. 1177–1183. Springer, Heidelberg (2008)
37. McCormack, D.J.: The effects of keyguard use and pelvic positioning on typing speed and accuracy in a boy with cerebral palsy. The American Journal of Occupational Therapy: Official Publication of the American Occupational Therapy Association 44(4), 312–315 (1990)
38. Stewart, H., Wilcock, A.: Improving the communication rate for symbol based, scanning voice output device users. Technology and Disability (2000)
39. Ceres, R., Pons, J., Calderon, L., Jimenez, A., Azevedo, L.: A robotic vehicle for disabled children. IEEE Engineering in Medicine and Biology Magazine 24(6), 55–63 (2005)

40. Raya, R., Rocon, E., Ceres, R., Pajaro, M.: A mobile robot controlled by an adaptive inertial interface for children with physical and cognitive disorders. In: 2012 IEEE International Conference on Technologies for Practical Robot Applications (TePRA), pp. 151–156 (April 2012)
41. Bache, C., Selber, P., Graham, H.: (ii) The management of spastic diplegia (2003)
42. McGinley, J.L., Dobson, F., Ganeshalingam, R., Shore, B.J., Rutz, E., Graham, H.K.: Single-event multilevel surgery for children with cerebral palsy: a systematic review. Developmental Medicine and Child Neurology 54(2), 117–128 (2012)
43. Nene, A.V., Evans, G.A., Patrick, J.H.: Simultaneous multiple operations for spastic diplegia. Outcome and functional assessment of walking in 18 patients. The Journal of Bone and Joint Surgery. British Volume 75(3), 488–494 (1993)
44. Thomason, P., Baker, R., Dodd, K., Taylor, N., Selber, P., Wolfe, R., Graham, H.K.: Single-event multilevel surgery in children with spastic diplegia: a pilot randomized controlled trial. The Journal of Bone and Joint Surgery. American Volume 93(5), 451–460 (2011)
45. Koca, K., Yıldız, C., Yurttaş, Y., Balaban, B., Hazneci, B., Bilgiç, S., Başbozkurt, M.: Outcomes of multilevel orthopedic surgery in children with cerebral palsy. Eklem Hastalıkları ve Cerrahisi = Joint Diseases & Related Surgery 22(2), 69–74 (2011)
46. Gough, M., Eve, L.C., Robinson, R.O., Shortland, A.P.: Short-term outcome of multilevel surgical intervention in spastic diplegic cerebral palsy compared with the natural history. Developmental Medicine and Child Neurology 46(2), 91–97 (2004)
47. Zwick, E.B., Saraph, V., Strobl, W., Steinwender, G.: Single event multilevel surgery to improve gait in diplegic cerebral palsy - a prospective controlled trial. Zeitschrift für Orthopädie und ihre Grenzgebiete 139(6), 485–489
48. Thompson, N., Stebbins, J., Seniorou, M., Wainwright, A.M., Newham, D.J., Theologis, T.N.: The use of minimally invasive techniques in multi-level surgery for children with cerebral palsy: preliminary results. The Journal of Bone and Joint Surgery. British Volume 92(10), 1442–1448 (2010)
49. Godwin, E.M., Spero, C.R., Nof, L., Rosenthal, R.R., Echternach, J.L.: The gross motor function classification system for cerebral palsy and single-event multilevel surgery: is there a relationship between level of function and intervention over time? Journal of Pediatric Orthopedics 29(8), 910–915 (2009)
50. Parkes, J., Caravale, B., Marcelli, M., Franco, F., Colver, A.: Parenting stress and children with cerebral palsy: a European cross-sectional survey. Developmental Medicine and Child Neurology 53(9), 815–821 (2011)
51. Urendes, E., Ceres, R., Calderón, L.: Definition of the main parameters during the lifting and walking process of a gait trainer. In: Summer School on Neurorehabilitation (2011)
52. Pons, J.L., Torricelli, D., Pajaro, M. (eds.): Converging Clinical & Engi. Research on NR. Biosystems & Biorobotics, vol. 1. Springer, Heidelberg (2013)
53. DelAma, A., Bortole, M., Garza, A., Moreno, J., Gil-Agudo, A., Pons, J.L.: Actuadores multimodales para la compensación de la marcha de personas con patología neurológica. In: University, V. (ed.) XXXIII Jornadas de Automática, Vigo (2012)
54. Cullell, A., Moreno, J.: Biologically based design of an actuator system for a knee-ankle-foot orthosis. ... and Machine Theory (2009)
55. Moreno, J., Brunetti, F., Pons, J.: An autonomous control and monitoring system for lower limb orthosis: the gait project case. Engineering in Medicine and ... (2004)

56. Gallego, J.A., Ibanez, J., Dideriksen, J.L., Serrano, J.I., del Castillo, M.D., Farina, D., Rocon, E.: A Multimodal Human-Robot Interface to Drive a Neuroprosthesis for Tremor Management. IEEE Transactions on Systems, Man, and Cybernetics, Part C (Applications and Reviews) 42(6), 1159–1168 (2012)
57. Galán, F., Nuttin, M., Lew, E., Ferrez, P.W., Vanacker, G., Philips, J., Millán, J.D.R.: A brain-actuated wheelchair: asynchronous and non-invasive Brain-computer interfaces for continuous control of robots. Clinical Neurophysiology: Official Journal of the International Federation of Clinical Neurophysiology 119(9), 2159–2169 (2008)
58. Neuper, C., Müller, G.R., Kübler, A., Birbaumer, N., Pfurtscheller, G.: Clinical application of an EEG-based brain-computer interface: a case study in a patient with severe motor impairment. Clinical Neurophysiology: Official Journal of the International Federation of Clinical Neurophysiology 114(3), 399–409 (2003)
59. Neuper, C., Müller-Putz, G.R., Scherer, R., Pfurtscheller, G.: Motor imagery and EEG-based control of spelling devices and neuroprostheses. Progress in Brain Research 159, 393–409 (2006)
60. Pfurtscheller, G., Müller, G.R., Pfurtscheller, J., Gerner, H.J., Rupp, R.: 'Thought'–control of functional electrical stimulation to restore hand grasp in a patient with tetraplegia. Neuroscience Letters 351(1), 33–36 (2003)
61. Müller-Putz, G.R., Scherer, R., Pfurtscheller, G., Rupp, R.: EEG-based neuroprosthesis control: a step towards clinical practice. Neuroscience Letters 382(1-2), 169–174
62. Pfurtscheller, G., Muller-Putz, G., Scherer, R., Neuper, C.: Rehabilitation with Brain-Computer Interface Systems. Computer 41(10), 58–65 (2008)
63. Lebedev, M.A., Nicolelis, M.A.L.: Brain-machine interfaces: past, present and future. Trends in Neurosciences 29(9), 536–546 (2006)
64. Farina, D., Yoshida, K., Stieglitz, T., Koch, K.P.: Multichannel thin-film electrode for intramuscular electromyographic recordings. Journal of Applied Physiology (Bethesda, M.: 1985) 104(3), 821–827 (2008)
65. Ivanenko, Y.P., Poppele, R.E., Lacquaniti, F.: Five basic muscle activation patterns account for muscle activity during human locomotion. The Journal of Physiology 556(Pt. 1), 267–282 (2004)
66. Calancie, B., Needham-Shropshire, B., Jacobs, P., Willer, K., Zych, G., Green, B.A.: Involuntary stepping after chronic spinal cord injury. Evidence for a central rhythm generator for locomotion in man. Brain: A Journal of Neurology 117(Pt. 5), 1143–1159 (1994)
67. Winter, D.A.: Biomechanics and Motor Control of Human Movement. Wiley
68. Cheung, V.C.K., Piron, L., Agostini, M., Silvoni, S., Turolla, A., Bizzi, E.: Stability of muscle synergies for voluntary actions after cortical stroke in humans. Proceedings of the National Academy of Sciences of the United States of America 106(46), 19563–19568 (2009)

iSign: An Architecture for Humanoid Assisted Sign Language Tutoring

Hatice Kose*, Neziha Akalin, Rabia Yorganci, Bekir S. Ertugrul,
Hasan Kivrak, Semih Kavak, Ahmet Ozkul,
Cemal Gurpinar, Pinar Uluer, and Gökhan Ince

Faculty of Computer and Informatics, Istanbul Technical University, Istanbul, Turkey
{hatice.kose,akalinn,rabia.yorganci,bsertugrul,hkivrak,
semih.kavak,ahmet.ozkul,gurpinarcemal,pinar,gokhan.ince}itu.edu.tr

Abstract. This paper investigates the role of interaction and communication kinesics in human-robot interaction. It is based on a project on Sign Language (SL) tutoring through interaction games with humanoid robots. The aim of the study is to design a computational framework, which enables to motivate the children with communication problems (i.e., ASD and hearing impairments) to understand and imitate the signs implemented by the robot using the basic upper torso gestures and sound in a turn-taking manner. This framework consists of modular computational components to endow the robot the capability of perceiving the actions of the children, carrying out a game or storytelling task and tutoring the children in any desired mode, i.e., supervised and semi-supervised. Visual (colored cards), vocal (storytelling, music), touch (using tactile sensors on the robot to communicate), and motion (recognition and implementation of gestures including signs) based cues are proposed to be used for a multimodal communication between the robot, child and therapist/parent. We present an empirical and exploratory study investigating the effect of basic non-verbal gestures consisting of hand movements, body and face gestures expressed by a humanoid robot, and having comprehended the word, the child will give relevant feedback in SL or visually to the robot, according to the context of the game.

Keywords: Humanoid Robots, Interaction games, Non-verbal communication, Sign Language.

1 Introduction

Sign Language (SL) is a visual language that is an essential way of communication for hearing impaired people. SL is composed of upper body (including arms, hands and fingers) head, and face gestures. Since language acquisition is very important for brain development and intelligence, hearing impaired children have

* This work was supported by the Scientific and Technological Research Council of Turkey under the contract TUBITAK KARIYER 111E283, and partially supported by Istanbul Technical University Scientific Research Projects Foundation under the contract BAP 37255.

S. Mohammed et al. (eds.), *Intelligent Assistive Robots,*
Springer Tracts in Advanced Robotics 106, DOI: 10.1007/978-3-319-12922-8_6

to learn this language as their native language even before they learn written language on condition that their parents are hearing impaired as well. Given that, existence of sufficient native sign language materials is of great importance for the training of children with communication impairments.

Several computational solutions have been developed for the hearing-impaired people so far [1]. Among these studies, CopyCat is a vision-based interactive game to help in teaching American Sign Language [2]. The ICICLE (Interactive Computer Identification and Correction of Language Errors) project [3], aimed to establish an instructive system for the hearing-impaired children in order to provide them with individual lectures and guidelines by computer-aided commands. A comprehensive research is being held in Turkey for teaching Turkish Sign Language (TSL) and recognition of sign language performed by people through videos [4,5].

Various studies have been carried out for the recognition of different sign languages via face, hand, upper torso and finger actions. Staner et al [6], presents a system that recognizes 40 words in American Sign Language, with 90% precision. Another study states 80% success rate for recognizing 95 words taken from the Australian Sign language [7]. [8] describes a system based on the Japanese Sign Language, where, a total of 52 words, 42 of which are represented by the finger-alphabet, are identified. In another study, 19 words from American Sign Language are recognized by utilizing Hidden Markov Models (HMM) [9]. These words are expressed by the movements of the head and the two hands. The participant wears two different colored gloves so that the hands can be identified by the system. A success rate of 99% has been reported for the recognition of words expressed solely by hands and a success rate of 85% is achieved for the classification of words performed both by hands and the head. Various other studies on sign languages such as the recognition of hand shapes and movements or the classification of facial gestures have been carried out by the same research group in order to analyze and help teach sign languages [10,11]. Moni and Ali used a Matrox camera to recognize words expressed by hands in Bahasa Melayu Sign Language [12]. HMM and variations are used widely for hand gesture recognition. Comparison of the performances of several HMM variations were presented in [13], discarding their speed.

Since 1977, robotic devices including robotic hands that are able to spell words by utilizing the manual alphabet have been constructed to assist hearing-impaired individuals [14,15]. A study on the humanoid robot called Dinsow, which recognizes Thai sign language with the aid of its cameras to help hearing impaired people, is presented in [16]. Several studies on different sign languages via avatars are presented in [17,18]. Many cutting edge humanoid robots including ASIMO and HUBO demonstrated words from sign language with their hands and arms [19,20].

Our long-term project aims to utilize socially interactive humanoid robots to assist sign language tutoring for children due to the incompetency of 2-D instructional tools developed for this goal and the lack of sufficient educational material. In our proposed system, it is intended that a child-sized humanoid

robot should perform and recognize various elementary sign language words in order to assist teaching these words to participants, especially children with communication disabilities. This will be achieved through interaction games based on non-verbal communication, turn-taking and imitation that are designed specifically for robot and child to play together. There are several successful user studies on non-verbal communication through imitation based interaction games with humanoid robots and human participants [21,22]. A specially designed non-verbal interaction game based on drumming entitled as *drum-mate* with gestures provided by the robot to motivate successful turn-taking and interaction were studied in [22]-[24].

Within the framework of this sign language project, first several surveys have been carried out to evaluate the success of robot tutors within the video based studies. A subset of sign language words, which can be implemented by the Nao H25 robot were chosen, and for each word selected, a video which displays the robot performing the sign language expression has been prepared. The corresponding videos of sign language representations by human teachers are available within the TSL tutoring software [25]. For the test study, following the demonstration of the robot's and human teacher's performances of several selected words from TSL by videos, participants have been asked to give feedback via written questionnaires regarding the success of the robot's performance in matching to the correct human implementation. The survey was applied to several groups of participants of different age groups and test environments, such as class studies with adult participants, who were not familiar with sign language, adults who knew sign language, teenagers and preschool children having the test as a web based game [26,27].

Our main research interest was using the physical robot within *interactive games*. As a preliminary step, we designed a tale-telling based interaction game with Nao robot. In one study, the robot verbally told a story including some words in sign language (words were selected from the ones tested in the previous video-based study [26]). The children were asked to assist the robot by showing the color flashcards matching the signs. The performance of the children was evaluated through the play cards they filled after the tests, demonstrating if they have learned the sign language words or not. This study was tested on 106 preschool children with normal development and 6 preschool children with hearing disability [28,29].

This interactive story based study was extended with basic upper torso moves and action recognition mechanism to give relevant action feedback to children, as well as the feedback system with flashcards. In this game, the child was able to actively communicate with the robot by realizing the signs. This game was evaluated by several therapists and children with autism [30]-[32].

The aim of this paper is not to propose one single game for all children, but rather than that develop a multi-modal interactive platform, which enables the therapists/teachers/parents to design different games with different scenarios using different modules available in the platform. Every child/participant has different needs and different level of learning capability from different modalities,

therefore enriching the system with these inputs and outputs is vital for improvement of the learning and imitation performance and motivation of the children.

In order to achieve this aim, we prepared different scenarios to test the tutoring of same words in different contexts based on the same architecture, which will be described in details in the following subsections. Also different parameters, i.e., number of words taught in one test setup, are evaluated in this concept. We presented two example studies from this framework. In the first one, a story-telling based interaction game scenario is used to teach selected words from TSL. First 5 words are tested with preschool children. Then 10 words including the first 5 are tested with adults. We also included abstract words (i.e., "very", and "nice") as well as simple daily words (i.e., "car", and "table"). Usign a story-telling concept enables the experimenter/therapist to use the words within sentences to teach the semantics of abstract words as well. In this game, the interaction is achieved through colored flashcards. In the second game, action recognition is included to motivate the child to be an active learner. Unlike the first game, this second game focuses on teaching the imitation of the signs, and turn-taking, rather than the semantics. This game is designed especially for children with autism.

The rest of the article is organized as follows: In Section 2, we discuss the motivation behind this study and the research questions. Section 3 describes the proposed system and briefly summarizes the computational architecture of the sign language project. Section 4 investigates robot perception in detail. In Section 5, we explain sign selection procedure of the robot, while Section 6 elaborates the imitation-based motion generation scheme. In Section 7, we investigate two gaming modes: story telling interaction game and sign imitation game within the framework of game coordination module. Conducted experiments and consecutive results are presented in Section 8. The last section gives a conclusion and future work.

2 Motivation and Research Questions

The main contribution of the *Robotic Sign Language Tutor* project is to design an assistive and social robotic system for children with communication impairments to be used with/by the human therapist/tutor/parent as a part of Turkish Sign Language tutoring. In the project, humanoid robot is employed as a teacher/peer in order to improve their interaction ability.

In the previous studies within the project participants' subjective and objective evaluations through different test setups were tested [26]-[28] as such:

- Test environment:
  - Classroom, web-based and social media (Facebook)-based)
- Demonstrators/tutors:
  - Human tutors
    - Virtual (video of the human) or physical

    (note: human avatar will not be tested within the scope of this project)

  - Robot platforms
    - Virtual (avatar) robot, video of the physical robot, physical robot
- Participants
  - Preschool children, primary school children, teenagers, university students, adults
  - People, who are not familiar with sign language and people with sign language acquaintances
  - People without hearing impairment, and people with different levels of hearing impairment

In [26] the signs were taught directly to the participants (without the games). The study showed that children had difficulty recognizing the signs from the virtually embodied robot (or graphics generator), and lose motivation if the signs were taught directly in class studies/online studies instead of interaction games. Based on the findings of our previous studies in the sign language tutor project, we made several hypotheses, tested and verified them:

- H1: Participants, especially children's performance improves with the asistance of the **physically embodied** robot.
- H2: Children's performance and motivation improves if the signs are taught within **interaction games** with the robot
- H3: **Imitation based turn-taking** interaction games with robot for sign language tutoring, also improves imitation, turn-taking, communication, sensory-motor and interaction skills for children, i.e., for children having hearing impairement and autism.

In this paper, we come up with two additional hypotheses to be tested:

- H4: **The number of words** taught in one test can affect the performance. In [33], 15 words are taught in one scenario, and this decreased the performance. In [34], using 10 words in both Nao and R3 robots resulted in a better performance. In [28] 5 words were taught in the game, and the results are quite successfull. In this study we aimed to test 5 words and 10 words in the same concept , to see if the performances decrease with the increasing number of words.
- H5: It is easily possible to teach **abstract sign language words** within a story-telling based concept. To test this, we use colored flashcards to teach the signs but had difficulty in teaching abstract words, i.e., "nice", and "very". In this study we added these words to a child story we created and aimed to teach both the imitaiton and semantics of these words within this story based framework.

3 System Overview

To the best of our knowledge, this is the first project on the usage of humanoid robots in both producing and recognizing gestures for sign language tutoring

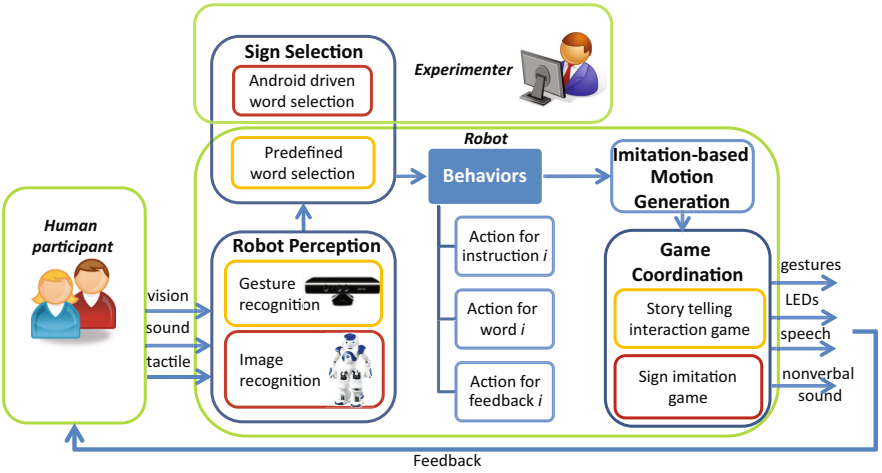

Fig. 1. Interactive game model of the project

within interaction games. In Fig. 1, the computational architecture of the whole *sign language project* is presented.

We present the overall system by partitioning it to its subsystems and introduce some modules of mutually exclusive possibilities to achieve an adaptive setup for the optimal sign language learning experience of the students. These modules can be selected based on the physical conditions of the learning room as well as physical and cognitive capabilities of the students.

In this research, the subsystems of special interest are 1. Robot perception, 2. Sign selection, 3. Motion generation, and 4. Game coordination:

1. We introduce two different modules to recognize the response of the student: camera based recognition of shown cards; and recognition of the signs directly from human motions.
2. The robot selects the signs in two modes: The supervised selection is performed using an interface developed on an Android-based device. In this mode, the experimenter is provided a set of motions to choose from and alter the scenario of the game instantly. In the second mode, the robot behaves according to a predefined scenario dictated by a hard-coded sequence of the motions and responses.
3. We propose to use a human inspired imitation of signs on robot platforms to generate motions.
4. The game coordination regulates the pattern of the outputs of the robot. Two interaction games with the robot were designed. The first game is based on story-telling. Children passively learn the signs from the robot and give feedback with colored flashcards. In the second game, the child can also actively communicate with the robot using the signs/upper torso gestures, as well as the cards therefore two modalities of feedback were employed

within the game. Also music is used to make the setup similar to the regular therapies used within autism.

In the following sections, we will describe all modules used in our long-term sign language tutor project in detail.

4 Robot Perception

The following two modules are used to generate the necessary features to be sent to the sign selection module in our proposed architecture. Visual, auditory and tactile cues coming from the students are observed.

4.1 Card Recognition

Hand gesture recognition has an important role in the problem of natural human-computer interaction. However, the effects of lighting conditions on vision, to access a third dimension requiring more than one camera and a particular arrangement of cameras prevented the spread of hand movement recognition. Camera based recognition of shown cards is also motivated by the fact that the physical and cognitive capabilities of the students can differ for every individual. Thus, just selecting a card and bringing it to the view angle of the robot's camera can be preferred by the student, as well as by the tutor occasionaly.

Technical implementation of the procedure to recognize the cards relies on the vision recognition module[1] of Nao developed by Aldebaran robotics. We also enhanced this module by using an image recognition software, which is implemented to recognize the flashcards within the game. OpenCV [2] is used for the technical implementation of this module. SURF was chosen for feature extraction and object detection. After image representations had been obtained with the Bag of Words (BoW) approach, SVM supervised learning was used for classification [30].

4.2 Gesture Recognition

In this section, we describe a method for capturing and recognizing Sign Language gestures performed using hands, arms and torso. Recently, development of cheap sensors that can detect depth with the method of infrared lasers has allowed the researchers to solve hand motion tracking and recognition problems regardless of the lighting conditions as opposed to Sec. 4.1. The upper body pose of the human participant is detected by a motion sensing input device sensor over time. With the captured upper body pose, we perform a vision based gesture recognition task that involves pose estimation and classification tasks [30,31,32]. This system is described below in Fig. 2.

[1] `http://www.aldebaran-robotics.com/documentation/naoqi/vision/alvisionrecognition.html`

[2] opencv.org

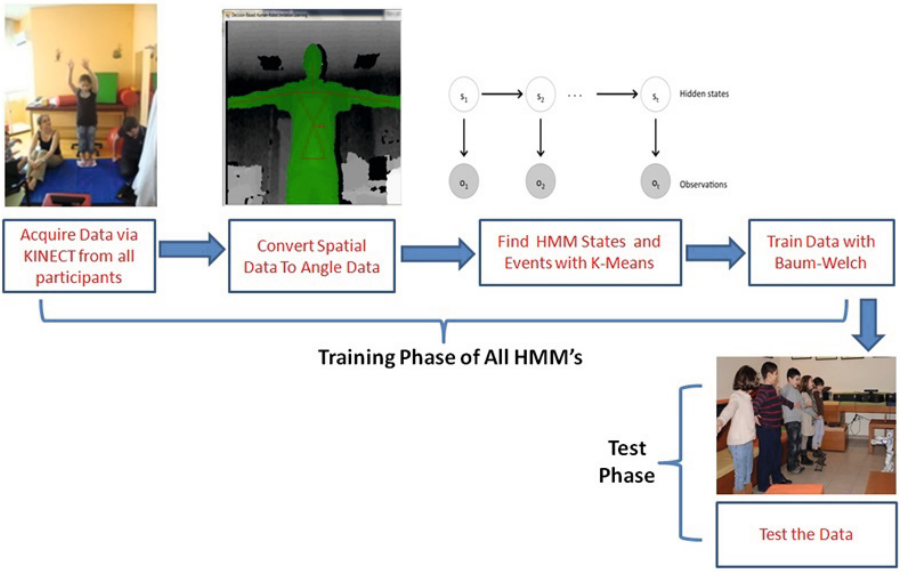

Fig. 2. Overview of the gesture recognition system

Our motion sensor, Kinect, provides the spatial data of 20 different joints of the human body. From these joints, only the spatial data (x, y, z) of 10 joints in the upper body (3 joints for left shoulder, 1 joint for left elbow, 1 joint for left wrist, 3 joints for right shoulder, 1 joint for right elbow, 1 joint for right wrist) are used. The coordinates of human body parts obtained from the *human pose detection* module yields 3D coordinates of the joints with respect to the camera. While the obtained coordinates give an accurate description of the users pose in the sign space, any translation effect caused by a change of the user's position prevents robust gesture recognition. For that reason, it is more convenient to use the data converted into angle values (Roll, Pitch, Yaw) for giving better results, instead of using spatial data obtained by Kinect. Therefore, 10 angle values in exchange for 10 joint values are acquired. To avoid any problems arising from varying frame lengths due to performing the gestures in different speeds, we propose to train a Hidden Markov Model (HMM)-based recognition system as shown in Fig. 2.

Firstly, the angular data regarding a particular training motion from different people are gathered and stored. This data collection procedure is repeated for all training motions corresponding to the gestures. The next step is creating a single HMM for every gesture. We used discrete HMMs for sign recognition. Every hidden state in HMM, which models the hand motion, is responsible for a specific part of given symbol sequence. In homogeneous HMMs, the durations of segments are modeled with geometric distribution. These durations for every

state are independent from each other. This constraint becomes important while types of hand movement and the number of different user increase.

In HMMs [35], there are states and events that can be coming up in every state. In order to determine the states and events of the HMM model for every gesture automatically and eliminate the necessity of human-based annotation, Customized K-Means Algorithm [36] is used. In an HMM-based recognition system, the number of states and events need to be specified before creating an HMM model, which is the same as the number of clusters of the K-Means algorithm. Thus, the centroid of the every cluster represents the states. The biggest difference between normal K-Means and Customized K-Means algorithm is that every time executing Customized K-Means algorithm on the same data file, it creates the same clusters. However, normal K-Means creates different clusters every time and the centroids represent the events in the model.

After finding the states and events needed for HMM, system begins the training phase using Baum-Welch Algorithm. In the Baum-Welch algorithm, the parameters of the HMM algorithm, which are the start probabilities (π), transition probabilities (a), and the emission probabilities (b), are recalculated until they do not change anymore. Since there are many probability multiplication in the formulas, underflow is inevitable in the results. To prevent this unwanted event, scaling is applied to the probabilities, which involves usage of loglikelihoods of the probabilities. Finally, an HMM model is created for all the gestures.

In the test phase, the recognizer cycle is started to provide recognition of this gesture so that recognized gesture patterns (SL words) are adaptively transferred to the humanoid robot. In order to recognize the gesture, it generates a dynamic model for every distinct behavior (gesture). According to the clustered data coming from the K-Means algorithm, it determines hidden states (node) and observable variables (output labels). In the training section, data as a target vector (a collection of observation sequences) seeds into recognizer cycle to perform supervised training algorithm (e.g., Baum-Welch). Finally, recognizer model throws a unique distinct behavior as a label (related SL word/ gesture).

5 Sign Selection

5.1 Predefined Sequence of Actions

Making a robot follow a fixed pattern of actions is mostly desired by the tutors. Such a study can be found in [28]. The robot implements a story-telling activity, both verbally and with sign actions within the predefined order. The feedback is gived using flashcards, which enables the robot to continue its predefined order of actions. In [33] and [34] the order is defined and initiated by the flashcards. The tactiles of the robot are used to start the game and in some experiments enable the robot to dance, to motivate and entertain the participants between the tests.

5.2 Android-Based Robot Control

Robot's tactile sensors, colored cards, motional or vocal cues were employed to initiate robot's actions and communicate with the robot. As suggested by the experts in autism therapy, designing individual games for each child is essential, since every child has different needs. The therapists need to form different schedules for each child, set the difficulty levels of the games and, choose gestures and parameters individually. Therefore, the same game with fixed parameters and actions for every child is not usable in the long term. To overcome this, we introduced a user-friendly interface for our games, to be used by the therapists, and care takers to form individual game patterns for each child, from the database of predefined action patterns and behavior sets. The therapists do not need to be experts in robotics or have programing skills but need an easy way to access the robot and game parameters, and change them without causing any damage to the robot or any harmful action for the children.

Smart phones and tablets are widely used in households, and schools, as well as in special schools as a part of therapy. We develop mobile applications compatible with these devices to be used within our system. The behavior patterns, developed for SL tutoring and autism game, are carried to Android-based smart phones to be used in therapies. By this means, the smart phone, or tablet which is already in use daily, is converted to a powerful tool to control and communicate with the robot (Fig. 3). Currently, our system is implemented on Android based smart phones, but we are working on the integration of the system to iOS devices [31].

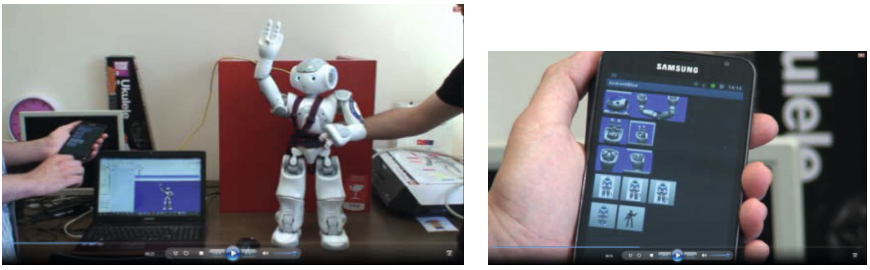

(a) Robotic environment (b) Handheld device

Fig. 3. Android based robot control system [31]

In this client-server system, on the client side, which is an Android smart phone, when the user clicks an icon of the selected behavior, the server gets which behavior/action is chosen. Once the server gets this data, it responds as intended, and sends the data to the operating system of the robot (Naoqi for Nao). As the behavior is shown on the simulator, it is also implemented on the physical robot at the same time. On the other side, Naoqi sends back a message to the server which acknowledges that the data is received and the behavior is

implemented, and this information is sent to the Android device by the server. On the Android device toastmessage is printed to the screen, which shows that the system works with success [31]. The steps of the system are displayed as such (Fig. 4):

1. Request for input
2. Response
3. Transmitting data to simulation
4. Transmitting from simulation to Nao
5. Acknowledgement
6. Acknowledgement
7. Output

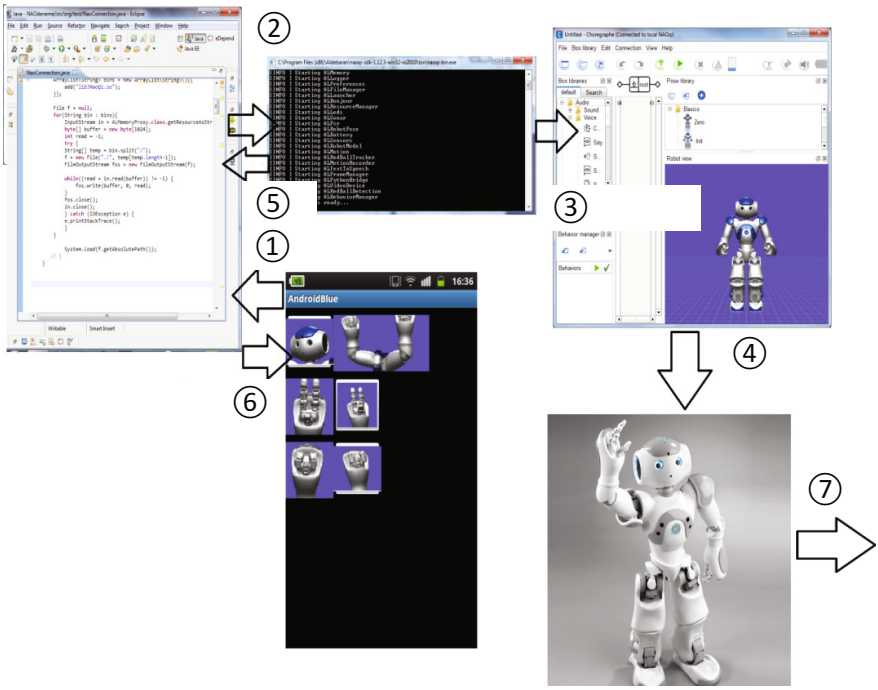

Fig. 4. Client-server system implementation [31]

6 Imitation-Based Motion Generation

This section summarizes our efforts to transfer the sign language actions of human teacher to robot by making use of motion recognition sensor [37]. This approach will decrease the time and effort to model and implement the SL words on robot, which is otherwise done manually. Since the Nao skeletal model and

human skeletal model do not match due to the number of joints and limb lengths, this transfer can not be done directly. For simple actions such as putting the arms forward, down, and sides the problem is less visible, but for more complex actions, the human joint values can be lost, or mismatched, therefore may not be interpreted on the robot perfectly. The ultimate aim is to translate the human action to the robot with the minimum information loss, maximum safety, and robustness.

This module is used to model and implement different sign language gestures using two probabilistic methods, Gaussian Mixture Model (GMM) and Gaussian Mixture Regression (GMR) [38]. The results from these models are performed on a humanoid robot. Using the first method (GMM), important features of the gestures are extracted. Secondly, generalized trajectory was retrieved by GMR. Finally, the reproduction of the gesture trajectory is implemented on virtual Nao humanoid robot using the Choregraphe simulation environment and tested whether humanoid robot is imitating the gestures well according to human gestures. Proposed learning model is illustrated at Figure 5.

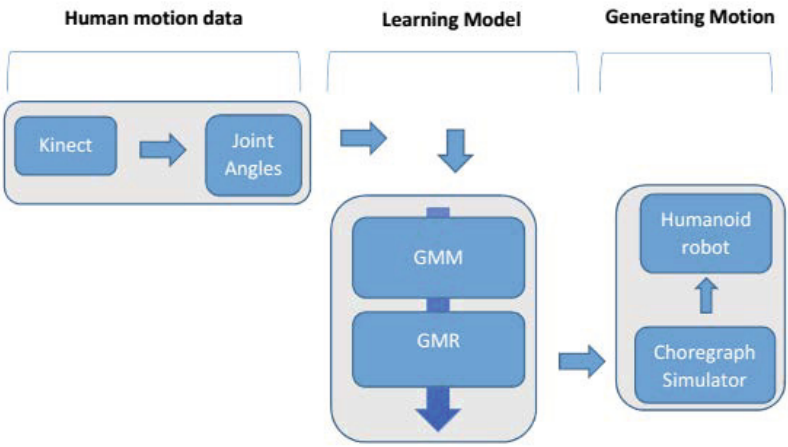

Fig. 5. Motion generation model

The main challenge in determining Gaussian mixture regression function is the estimation of the density of mixture. While you are converging to local optima using the maximum likelihood estimation, the number of components, defining the complexity of model, should be selected properly. Optimum number of components, namely number of component of regression function will not be known initially. It should be determined according to the data originally worked on [39]. For each gesture optimum number of mixture density of gaussian mixture regression function is determined as plotting dataset and making different trials.

7 Game Coordination

7.1 Coordination for Story Telling Interaction Game

In this gaming mode, the robot is telling an interactive story verbally, and implementing some of the words of the story using TSL signs without pronouncing the word verbally. The participating children are encouraged to assist the robot using special flashcards illustrating the signs of TSL in the story. A test including the signs in the story follows the story telling as well, to evaluate the children's learning performances within the game. Story telling robots were used in the literature before to model human-like gaze behaviour [40]. As stated in [23], this gaming mode allows us to observe a positive effect of the physical embodiment of the robot within a social interaction context, on the performance, and interaction of the children [28], compared to the video based studies [26].

The detailed game flow is displayed in Table 1. The game consists of two phases. In the first phase the robot tells a short story verbally. The children can also follow the story from the story cards which include the written story. Some of the words in the story were displayed by colored pictures. We have colored flashcards of same pictures. Whenever the robot reaches these points in the story, it implements the sign of these pictures, without any verbal clue and waits for a response from the participant (child). The participant is expected to show the matching flash card of this sign (if they do not know sign language, experimenter helps them with finding the matching card). This phase is the learning phase. If the flashcard was not the one that the robot expected to see, the robot's eyes turn from green to red, then they become green again, and robot waits for the child to guess again and give the right answer. In case the flash card is correct, the robot says the name of the flash card and continues the story until the next sign is done, or the story finishes.

We designed a story which is simple, and easy to understand and remember, yet interesting for preschool children. Also the story was specially arranged so that every special word appears exactly twice in the story, mostly at the beginning of the sentence (these make it easier to detect signs from the story it is required in our parallel study, which includes detection of sign language by the robot, as well). No more than two signs were used per sentence. At the time of the design, Nao did not have Turkish text-to-speech feature (by 2013 Nao robots have Turkish text-to-speech, and Turkish speech recognition support), we were unable to find a natural sounding Turkish text-to-speech program that is suitable with the robot's childlike appearance, hence we asked a 6 years old child to read the story loudly and use her voice on the robot. Hearing the story from a child's voice had a very positive effect on the children [28].

After the story is demonstrated by the robot, the experimenters explain the children that the robot would play a game with the children. In this second phase, the robot repeats the signs/gestures introduced in the first phase in a random order without any verbal clue. After each sign is repeated twice by the robot, the robot waits for the child to answer the question and continues with the next word. The child answers each question by putting the relevant colored

Table 1. Game flow chart

Order of action	*Reason*	*Actor*	*Action*	*Implementation*
1	Motivating and giving feedback to the participants verbally	Robot	Verbal story telling	Audio playing/text-to-speech
2	Teaching the implementation of the signs to the children	Robot	Non-verbal Sign implementation	Manual implementation of the selected signs on the Robot (action implementation module)
3	Child is motivated to follow the story from the story card, match the implemented gesture with the colored flashcard and gives visual feedback to the robot	Child	Choosing and showing the related Flashcard to robot	Paper based colored unique flashcards are used for each gesture.
4	Feedback to child	Robot	If the card is correctly matched to the implemented sign, eyes change to green color, and robot verbally says the word (name of the sign), else eyes become red, and robot waits for the correct card, until the correct card is shown. Robot continues to tell the story verbally until the next sign (action 1).	The robot is trained with the colored flash cards before, and can recognize them (vision recognition module). Feedback is given with LEDs in the eyes, name of the word is displayed by audio/text-to-speech,
5	Testing	Robot	After the story is finished, The robot verbally tells the child they will do a test now, and implements every action twice, without verbal cue. It waits shortly between the actions to let the child answer the question	Audio playing, and gesture implementation
6	Testing	Child	Child is motivated to put the colored sticker with the picture of the sign currently implemented to the selected place in the story card, he/she used to follow the story.	

(a) A child listens to the robot's story [28]

(b) Child interactively play with robot to complete the story [28]

Fig. 6. Screenshots from the story telling game

sticker of the implemented sign to the boxes placed on the story cards. The pictures on the stickers are exactly the same with the pictures used for each colored flashcard, only smaller in size.

In this stage, the robot realizes the signs one by one and the children are asked to put the sticker of the relevant word to their story cards. There are also slots for their names and picture of a boy and a girl which they can choose according to their gender for demographic information. Since most of the preschool children do not know how to read and write we have to simplify the questionnaire and test instructions as much as possible.

7.2 Coordination for Sign Imitation Game

Autism Spectrum Disorder (ASD) involves communication impairments, limited social interaction, and limited imagination. Researchers are interested in using robots in treating children with ASD [41]-[46]. Many children with ASD show interest in robots and find them engaging. Robots can act as a social tool for interaction between the child and teacher, and robot based interaction games play an important role in encouraging the children to carry the interaction skills they gain from the dyadic interaction with the robot to the interaction with their environment. Every child with autism has different needs. Robot behavior needs to be changed to accommodate individual children's needs and as each individual child makes progress.

The sign imitation game is an extention of the story telling game described in Sec. 7.1; it involves signs from American Sing Language (ASL) and TSL, and basic upper torso gestures, i.e., opening the arms sides, up, forward, waving hand, etc., as well. The basic upper torso gestures will act as a preliminary step to eliminate the bias when the children interact with the robot for the first time. This game was developed to teach the children to recognize and imitate the gestures/signs, within a turn-taking interaction game [30,31]. The robot will act as a demonstrator and the therapist will be able to manually assist the child, when the child fails to imitate the action demonstrated by the robot successfully.

Within this game it is possible to locate many of the tasks and exercises, which are already being used as a part of the autism therapy.

The game consists of three stages. In the first stage, the children will learn how to imitate the gestures one by one, the sequence and the quantity of the gestures were chosen by the therapist or the child. The robot's actions are initiated by the therapist/children using colored flashcards of the signs/gestures. When they show the flashcard with the picture of the selected gesture to the robot, the robot realizes the gesture and waits for the child to repeat the action. Using a RGB-D (Kinect) camera based system (as described in Sec. 4.2), child's actions are recognized, and evaluated. The system returns a feedback about how good the imitation is, to the robot. If the actual action matches the observed action of the robot, so as to say, if the child can repeat the action successfully, the robot gives a verbal feedback to the child, such as *you did the action good* (The experts suggested us that we have to praise the action of the child, it is not enough to say *its good* or *congratulations*), and action feedback with the green colored eye LEDs. Also robot nods the head in a positive manner. These feedback gestures, which are interpreted as praising and positive gestures in our culture, are suggested by the experts and are also used in the daily therapy routine of the children.

If the child fails to imitate the action, the robot asks the child to repeat the action and the above procedure is repeated. Through this stage, whenever child performs the wrong action, the therapist helps the child manually to correct the gesture. The experts we worked with in this experiment suggested this approach, which will not let the child complete the action wrong, but support the child to learn it correctly, otherwise the action will be learned wrong.

In the second stage, the game is like a sports work out, each action/gesture is repeated one after another several times without the need to initiate every action with flashcards and the therapist gets involved less (but still asists the child when the child fails to imitate or needs help).

In the third stage, we turned the game into a musical play. Robot sings a song related to the actions, and do the actions one by one; and the child is expected to repeat the sequence of actions in a rhytmic way like a dance (Fig. 7).

The robot will record the success rate of the child's imitation (from the feedback of the Kinect-based sign recognition system) and also the experimenter will record the therapist's corrections and the number of gestures completed by the child without the therapist's intervention. Also it is important to note how long the child plays, and which activities encourage the child to play more. The success rate related to each gesture also gives a good feedback to the researcher.

These games were usually played with the therapist, or the video of the therapist, or another autistic child as in Fig. 8. The robot will act as a play mate in these games.

The game was demonstrated for the therapists working in ASD, and positive feedback was achieved [26]. We also demonstrated a limited version of the game (only the first stage) in a special school for children with ASD using 4 children of 6-8 years old. One child attended the game with the asistance of her therapist.

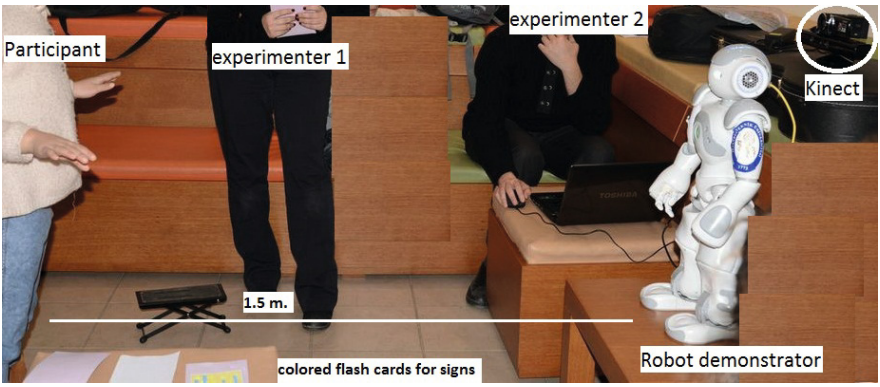

Fig. 7. Sign imitation game setup [26]

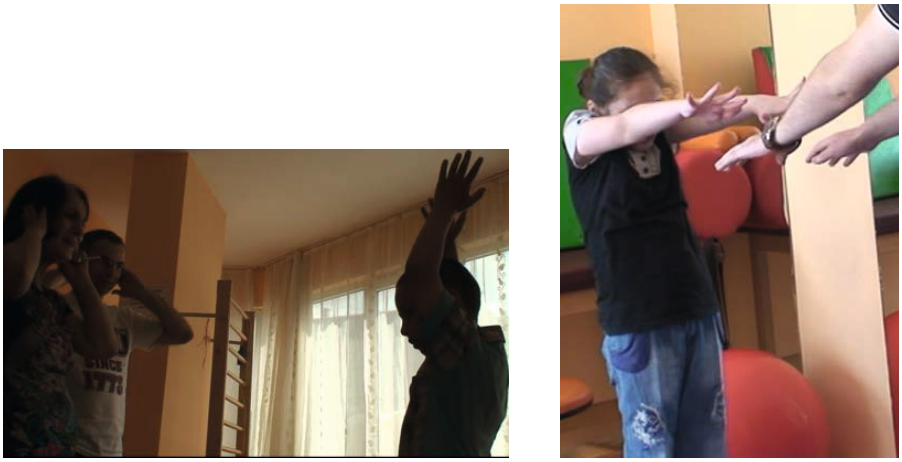

(a) Gesture for touching the ears (b) Gesture for leaning forward

Fig. 8. Therapists help children in the first stage of the game [31]

She was happy and got motivated with the game. The actions in the game were demonstrated to the children by the therapists. We plan to test all the three stages of the game with children, in a collaborative special school for ASD to verify the hypothesis H3 in the short term.

8 Experiments on Story Telling Interaction Game

The main aim of this study is to study the effect of interaction game context in the physical robot assisted sign language tutoring. Therefore, an interactive turn-taking game based on story telling using both words and signs from TSL is designed and implemented. The game is based on the same set of 5 TSL words used in the video based studies in [26], and was implemented on physically embodied Nao H25 robot. Then the story is extended with additional 5 words, and the new 10-word story is also tested within the same test setup. These games enable us to study the effect of using a physical robot within the project and interaction game context as well.

8.1 Participants

The 5-word story telling game was first tested with 106 preschool children (6 years old) within the nursery of our university. The experiment took place in the big atrium of the nursery as a demo event rather than a strictly controlled laboratory experiment due to the restrictions and limitations caused by the age and quantity of the children. None of the children who attended the demo session were hearing impaired and they were not familiar with any sign language. This work is one of the biggest robotic events in the world with this age group to the best of our knowledge. Our previous robotic experiment based on interaction games with a drumming robot included 68 primary school children of 7-11 age group in UK [23]. Then the game was demonstrated in a pilot preschool class in a special school for hearing impaired children with 6 children of age group 6-8. In the second phase of our project, 22 university students from Istanbul Technical University, Computer Engineering Department (age average 26.32) attended both 5-word and 10-word tests.

8.2 Robot Platform

The H-25 Nao robots is be used for this research in the user-studies, as they have hands and fingers to implement most of the sign language words, and appropriate to use in interactive children games due to its expressive face, small size, compact shape and toy-like appearance. The Nao robot, which has a height of 0.57 m. and a weight of 4.5 kg., is a system with 21-25 degrees of freedom, 500 MHz processor, two cameras, sonar sensors and force-sensitive resistors [47]. Aldebaran Robotics offer several software tools for use with the NAO robot, such as Choregraphe for face detection, face recognition, speech, speech recognition, walking, recognizing special marks and dances, and individual control

of the robot's joints. Choregraphe needs to be used with a robot proxy, real or simulated. The simulated proxy can be NAOqi or a sophisticated simulator such as NaoSim [48].

A subset of the most appropriate words from ASL and TSL that can be demonstrated by a Nao H25 robot have been chosen for the experiments. The physical limitations of the Nao robot makes it hard to implement some of the words. One of the reasons for this is the fact that the Nao robot has only 3 dependent fingers while most of the words from the i.e., TSL are performed by using 5 fingers (mostly independent, i.e one pointing a part of the face and other 4 are curled). Our current experiments are duplicated on a humanoid platform with 5 fingers and more DOF on the arms (a modified R3) to overcome these limitations [34].

8.3 Game Setup

The children were sitting around the robot and the robot was placed on a small table. Robot was assisted by two researchers, and the children who were directly playing with the robot were assisted by an additional researcher(Fig. 9). The other children watching the event were assisted by their own classroom teachers. We prepared special survey papers with the story where the special words were shown with flashcard pictures. Visual directions and instructions were chosen so that even if the children can not read and write they can still follow the study and express their written feedback.

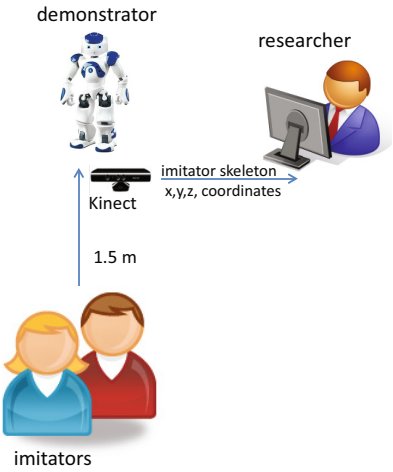

Fig. 9. Interaction game test setup

8.4 Tests and Results

First we had a demo with one of the experimenters. Then one of the children was chosen to play with the robot (Fig. 6(a)). The robot starts telling a short story. Whenever the robot does the sign, the child was expected to hold the relevant flashcard to the robot (Fig. 6(b)). The game continues as described in Sec. 7.1 in details. After these demo sessions we had the test session with all of the students. Due to the high number of students, we could not get more one-to-one sessions with children, and could not get the completed story cards immediately. But the teachers of each class were asked to help children to fill out the cards and return them as soon as possible. We also recorded the robot's telling the story, all the instructions and the test at the end as video. We included the video of the story told by one of the experimenters and several dance videos of the robot, which we promise to show to the children as a reward. We handed them to all classes, and the teachers told us they would show them to children again, in case some children might not see all the details due to crowdedness, and hand out the completed story cards for feedback, afterwards.

The demo and the game was demonstrated with 106 children of 6 years. Due to the high number of children and their small age, one class was chosen as pilot class and the detailed results of that class was reported by their teachers. The report suggested that, out of 20 children who attended the event, 18 children (9 boys and 9 girls) completed the play cards with 100% success, and the other two children had 80% success. The children showed much interest and were successful compared to their age group in terms of similar skills. Moreover the children liked the event, and although none of them knew sign language before they started to imitate signs after the robot. Although both girls and boys showed same success, the teachers reported that boys were more interested on the robot. They even asked to take the play cards to their homes to show to their parents. The teachers and the school gave promising and positive feedback and asked if they can use the videos and video based tests in other age groups and the following semesters as a part of their activity schedule [28].

The reader should note that, although the success rate is quite high, the test was not so trivial. The children attending the story-telling game were asked same signs as the adults including the sign language professionals, preschool children of same age group and teenagers, where teenagers, and children in these web-based studies showed a poor performance compared to the adults [26]. In comparison to these web-based studies, the high success rate of this study is an important step to verify the hypothesis H1 (Fig. 10). Moreover, in this experiment we saw that if the words are taught within a relevant story/context than their identification /recognition increases. This is a very important gain for us, which verifies the hypothesis H2.

In this game, verbal storytelling as well as visual and sign cues are used because the linguists, who are experts especially in TSL reported that children have different levels of hearing, some children could not hear anything, whereas some children had cochlear implant and could have limited hearing. Therefore, it will be convenient to give verbal support as well as signs and colored pictures, so

Fig. 10. The game was also performed in public demos within Robocup (obtained from press)

that the child can learn verbal communication, too. We have also demonstrated the game in a pilot preschool class in TIV (Turkish Hearing impaired Foundation) special school with 6 children of age group 6-8 and got positive feedback. Hearing impaired children were very engaged and motivated with the robot and the game and were managed to understand and answer most of the questions correct (appx. 70%). They were so excited that they could not wait until the end of the test, and wanted to play with the robot, and asked questions about the robot, therefore the written tests for feedback could not be completed. But as a preliminary work, the comments and positive attitude towards the play cards and robot were very promising.

In the second phase of our project, this 5-word story telling test is extended to a 10-word test keeping the same test setup in order to verify H4. At first, 6 people took the original 5-word test only, which will be called Experiment 1 (Exp.1). In Exp.2., other set of participants consisting of 16 people coming from the same educational background and age group took the test with 10 words, which includes the first 5 words implicitly. The profiles of the test subject participating in Exp.1 and Exp.2 are given in Tables 2 and 3.

Table 2. Exp.1: Profiles of the participants and their score

Gender	**Total Number**	**Full score**	**Prior experience on Sign Language**	**Prior experience on Robots**
Women	3+4	5	0	1
Men	13+2	11	3	0

Table 3. Exp.2: Profiles of the participants and their score

Gender	Total Number	Full score	Prior experience on Sign Language	Prior experience on Robots
Women	3	2	0	1
Men	13	9	2	0

The words used in the sign set and the corresponding scores are presented in Tables 4 and 5.

Table 4. Exp.1: Word set and success rates

Turkish Word	English Meaning	Referred in the Text as	Correct	Wrong	Empty
Masa	Table	Word 2	20	1	1
Üç	Three	Word 4	21	0	1
Araba	Car	Word 5	21	0	1
Arkadaş	Friend	Word 7	17	4	1
Baba	Dad	Word 9	22	0	0

The results of the Exp.2 were similar for the first 5 words (Exp.1), which are common in both tests, yet as the number of words increase, the number of overall mislabelling increases due to the similarity of the generation of some of the words (Fig. 11 and 12). Several people mislabelled same words such as"friend". One test subject out of six (the 5-word test group) got 2 mistakes in 5-words test. Others had 100% success rate in this group.

8.5 Discussion

The results show the success of the system with the Nao humanoid robot. The important fact is that, the participants had no difficulty in remembering even the abstract concepts when used in a text/story. This will be helpful in teaching abstract concepts to especially children using sign language, where it is difficult to teach via illustrations or physical examples (Hypothesis H5). For example, to teach an apple showing the picture of an apple or a real apple vs. to teach "nice", "accept", or "very". The reader should note that the usage of another robot platform with more physical capabilities such as having five fingers and longer limbs to demonstrate the actions in more detail will increase the success rate even more [34]. Figures 13 and 14 illustrate the improved capability of R3 robot in sign generation compared to Nao in one of the common words used in this study and [34].

Table 5. Exp.2: Word set and success rates

Turkish Word	English Meaning	Referred in the Text as	Correct	Wrong	Empty
Ev	House	Word 1	16	0	0
Masa	Table	Word 2	14	1	1
Güzel	Nice	Word 3	15	1	0
Üç	Three	Word 4	16	0	0
Araba	Car	Word 5	16	0	0
Çok	Very	Word 6	14	1	1
Arkadaş	Friend	Word 7	11	4	1
Küçük	Little	Word 8	15	1	0
Baba	Dad	Word 9	16	0	0
Kabul etmek	Accept	Word 10	16	0	0

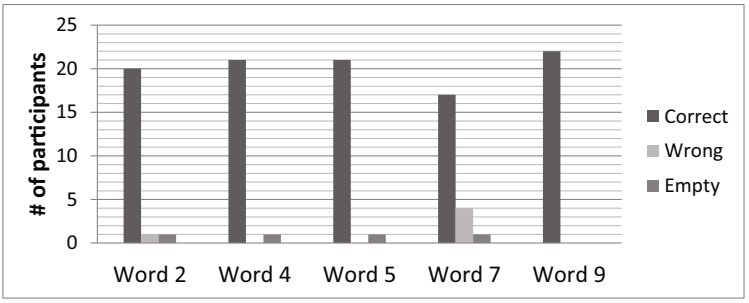

Fig. 11. Exp.1: Interaction game results

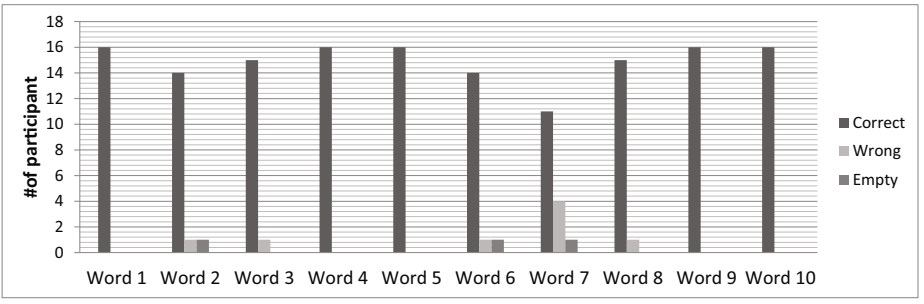

Fig. 12. Exp.2: Interaction game results

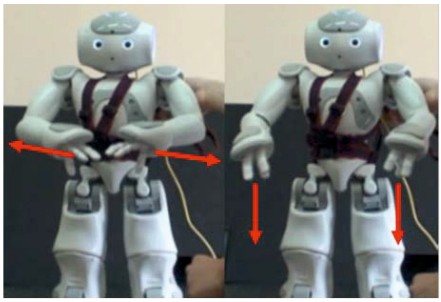

Fig. 13. Nao performing the "Table" sign: 87.5% succes rate achieved on 16 participants

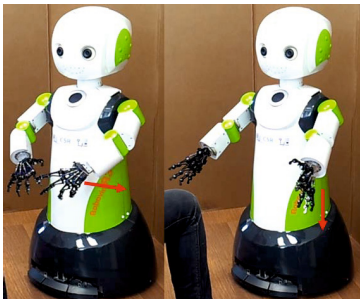

Fig. 14. R3 performing the "Table" sign. 98% succes rate achieved on 21 participants

For adults with no hearing disability, we use written texts and verbal instructions, in the games. For children especially with hearing difficulties or ASD, the instructions and some of the feedback in the game are given using flash cards. The words and their illustrations are presented with the flashcards in the games with children. We are careful about not using signs or any clue related to the signs in the illustrations (unless the sign is iconic itself like "throwing", or "me"). Therefore we tried to eliminate the participants getting extra clue about the action of the sign from the illustration. These cards are specially used for children of small age groups who can not read and get benefit from written instructions. Also this gives the children a non-verbal way to communicate with the robot (robot "understands" the message given by the cards). The cards are taken from a child game which aimed to teach preschool children words in written language, and especially in the early stage of the learning phase, it also encourages and motivates the children in the game.

In a pilot study conducted by Kose et al. in 2014 (unpublished data), 29 hearing impaired primary school students were tested using Nao robot in a classroom based study. The word-based game was used in the study, and the evaluations were taken by paper based tests including both written and visual instructions

used in the previous studies with hearing children. The children were asked 10 words similar in the tests conducted with the university students, and the success rate of recognizing the signs performed by the robot was in the range of 88%-100%. These results were similar to the results obtained in this paper. Furthermore, the children were eager to work with the robot; they asked their teachers to keep the robot in their school as part of their daily education. Several teachers, who are experts in Turkish Sign Language attended the session, and helped the students, who needed further instructions by communicating in sign language (i.e., "the robot will repeat every word twice, if you do not understand a word, please continue with the following question", etc.). The study will be repeated with student groups of 1-2 with different word sets, in the long term.

9 Conclusion and Future Work

In this paper, we developed a multi-modal interactive platform, which enables the therapists/teachers/parents to design different games with different scenarios using different modules available in the platform for teaching children sign language by means of interaction games with humanoid robots. We also introduced several studies from our long-term project. The first study is a tale-telling Nao Humanoid robot with both verbal and sign language, with visual feedbacks from the child. From the studies with children we verified our hypotheses on motivating and increasing the performance of children learning sign language within interaction games with robots. We showed that the number of words taught in one session can be up to 10 words without losing the accuracy of the teaching process. We also demonstrated that it is easily possible to teach abstract sign language words within a story-telling based scenario.

The main aim of this interdisciplinary study is to build a bridge between the technical know-how and robotic hardware with the know-how from different disciplines to produce useful solutions for children with communication problems. Moreover we would like to increase the awareness among families and public.

NAO H-25 humanoid robot is used during the field studies, since it is a small size humanoid robot which is suitable to implement basic signs in the ASL and TSL, robust and safe to work with children. For further studies a bigger size humanoid robot platform with 5 fingers and more DOF on arms will be used within the project. The extended version of this study is another multi-modal interaction game, which includes action recognition feedback, and also being used with children with autism in teaching non-verbal communication skills, imitation and turn-taking.

References

1. Adamo-Villani, N.: A Virtual Learning Environment for Deaf Children: Design and Evaluation. IJASET - International Journal of Applied Science, Engineering, and Technology 16, 18–23 (2006)

2. Weaver, K.A., Hamilton, H., Zafrulla, Z., Brashear, H., Starner, T., Presti, P., Bruckman, A.: Improving the Language Ability of Deaf Signing Children through an Interactive American Sign Language-Based Video Game. In: 9th International Conference of the Learning Sciences, pp. 306–307 (2010)
3. Greenbacker, C., McCoy, K.: The ICICLE Project: An Overiew. In: First Annual Computer Science Research Day, Department of Computer & Information Sciences, University of Delaware (2008)
4. Aran, O., Keskin, C., Akarun, L.: Sign Language Tutoring Tool. In: European Signal Processing Conference, EUSIPCO 2005, Antalya, Turkey (2005)
5. Gürel, T.C.: Turkish Sign Language Animation With Articulated Body Model. MSc. Thesis, Bogazici University (2010)
6. Staner, A.T., Pentland, A.: Real-Time American Sign Language Recognition from Video using Hidden Markov Models. Technical Report TR-306, Media Lab, MIT (1995)
7. Kadous, W.: GRASP: Recognition of Australian Sign Language Using Instrumented Gloves. MSc. Thesis, University of New South Wales (1995)
8. Murakami, K., Taguchi, H.: Gesture Recognition Using Recurrent Neural Networks. In: SIGCHI Conference on Human Factors in Computing Systems, pp. 237–242 (1991)
9. Aran, O., Akarun, L.: A Multi-class Classification Strategy for Fisher Scores: Application to Signer Independent Sign Language Recognition. Pattern Recognition 43(5), 1776–1788 (2010)
10. Aran, O., Ari, I., Benoit, A., Campr, P., Carrillo, A.H., Fanard, F., Akarun, L., Caplier, A., Rombaut, M., Sankur, B.: Signtutor: An Interactive System for Sign Language Tutoring. IEEE Multimedia 16(1), 81–93 (2009)
11. Caplier, A., Stillittano, S., Aran, O., Akarun, L., Bailly, G., Beautemps, D., Aboutabit, N., Burger, T.: Image and Video for Hearing-impaired People. Journal on Image and Video Processing, Special Issue on Image and Video Processing for Disability 2007(5), 2:1–2:14 (2007)
12. Moni, M.A., Ali, A.B.M.S.: HMM Based Hand Gesture Recognition: A Review on Techniques and Approaches. In: 2nd Conference on Computer Science and Information Technology, pp. 433–437 (2009)
13. Rabiner, L., Juang, B.: An Introduction to Hidden Markov Models. IEEE Acoustic Speech Signal Processing Magazine 3(1), 4–16 (1986)
14. Jaffe, D.: Evolution of Mechanical Fingerspelling Hands for People who are Deaf-Blind. Journal of Rehabilitation Research and Development 31, 236–244 (1994)
15. Hersh, M.A., Johnson, M.A. (eds.): Assistive Technology for the Hearing-impaired Deaf and Deaf Blind. Springer (2003)
16. http://www.cmu.ac.th/images/uploadfile/engnewsfile-100715102721.doc
17. Kipp, M., Heloir, A., Nguyen, Q.: Sign Language Avatars: Animation and Comprehensibility. In: Vilhjálmsson, H.H., Kopp, S., Marsella, S., Thórisson, K.R. (eds.) IVA 2011. LNCS, vol. 6895, pp. 113–126. Springer, Heidelberg (2011)
18. http://www.sign-lang.uni-hamburg.de/esign/
19. http://spectrum.ieee.org/automaton/robotics/humanoids/honda-robotics-unveils-next-generation-asimo-robot
20. Park, I., Kim, J., Lee, J., Kim, M., Cho, B., Oh, J.: Development of Biped Humanoid Robots at the Humanoid Robot Research Center, Korea Advanced Institute of Science and Technology (KAIST). In: Hackel, M. (ed.) Humanoid Robots, Human-Like Machines, pp. 43–64 (June 2007)

21. Shen, Q., Saunders, J., Kose-Bagci, H., Dautenhahn, K.: An Experimental Investigation of Interference Effects in Human-Humanoid Interaction Games. In: 18th IEEE International Symposium on Robot and Human Interactive Communication (RO-MAN), pp. 291–298. IEEE Press, New York (2009)
22. Kose-Bagci, H., Dautenhahn, K., Nehaniv, C.L.: Emergent Dynamics of Turn-Taking Interaction in Drumming Games with a Humanoid Robot. In: 18th IEEE International Symposium on Robot and Human Interactive Communication (RO-MAN), pp. 346–353. IEEE Press, New York (2008)
23. Kose-Bagci, H., Ferrari, E., Dautenhahn, K., Syrdal, D.S., Nehaniv, C.L.: Effects of Embodiment and Gestures on Social Interaction in Drumming Games with a Humanoid Robot. Advanced Robotics, Special issue on Robot and Human Interactive Communication 24(14), 1951–1996 (2009)
24. Kose-Bagci, H., Dautenhahn, K., Syrdal, D.S., Nehaniv, C.L.: Drum-mate: Interaction Dynamics and Gestures in Human-Humanoid Drumming Experiments. Connection Science 22(2), 103–134 (2010)
25. Turkish Sign Language Dictionary v1.0, `http://www.cmpe.boun.edu.tr/pilab/tidsozlugu`
26. Kose, H., Yorganci, R., Algan, H.E., Syrdal, D.S.: Evaluation of the Robot Assisted Sign Language Tutoring using Video-based Studies. International Journal of Social Robotics, Special issue on Measuring Human-Robot Interaction 4(3), 273–283 (2012)
27. Kose, H., Yorganci, R., Algan, H.E.: Evaluation of the Robot Sign Language Tutor using Video-based Studies. In: 5th European Conference on Mobile Robots (ECMR 2011), pp. 109–114 (2011)
28. Kose, H., Yorganci, R.: Tale of a Robot: Humanoid Robot Assisted Sign Language Tutoring. In: 11th IEEE-RAS International Conference on Humanoid Robots (HUMANOIDS 2011), pp. 105–111 (2011)
29. Kose, H., Yorganci, R., Itauma, I.I.: Humanoid Robot Assisted Interactive Sign Language Tutoring Game. In: IEEE International Conference on Robotics and Biomimetics (ROBIO), pp. 2247–2249 (2011)
30. Ertugrul, B.S., Gurpinar, C., Kivrak, H., Kulaglic, A., Kose, H.: Gesture Recognition for Humanoid Assisted Interactive Sign Language Tutoring. In: 6th International Conference on Advances in Computer-Human Interactions (ACHI), pp. 135–140 (2013)
31. Ertugrul, B.S., Kivrak, H., Daglarli, E., Kulaglic, A., Tekelioglu, A., Kavak, S., Ozkul, A., Yorgancı, R., Kose, H.: iSign: Interaction Games for Humanoid Assisted Sign Language Tutoring. In: International Workshop on Human-Agent Interaction, iHAI 2012 (2012)
32. Ertugrul, B.S., Gurpinar, C., Kivrak, H., Kose, H.: Gesture Recognition for Humanoid Assisted Interactive Sign Language Tutoring. In: 21st Signal Processing and Communications Applications Conference (SIU), pp. 1–4 (2013)
33. Akalin, N., Uluer, P., Kose, H., Ince, G.: Humanoid Robots Communication with Participants Using Sign Language: An Interaction Based Sign Language Game. In: IEEE Workshop on Advanced Robotics and its Social Impacts (ARSO), pp. 181–186 (2013)
34. Uluer, P., Akalin, N., Yorganci, R., Kose, H., Ince, G.: A New Robotic Platform as Sign Language Tutor. In: ASROB 2013 Workshop of IEEE. Int. Conf. on Intelligent Robots and Systems, IROS (2013) (to appear)
35. Rabiner, L.: A Tutorial on Hidden Markov Models and Selected Applications in Speech Recognition. Proceedings of IEEE, 257–286 (1989)

36. Aggarwal, N., Aggarwal, K.: A Mid-Point based k-mean Clustering Algorithm for Data Mining. International Journal on Computer Science and Engineering (IJCSE) 4 (2012)
37. Kivrak, H.: Learning, and Implementation of Sign Language Gestures By Iimitation in a Humanoid Robot, Istanbul Technical University, Ms Thesis (September 2013)
38. Calinon, S., Guenter, F., Billard, A.: On Learning, Representing and Generalizing a Task in a Humanoid Robot. IEEE Transactions on Systems, Man and Cybernetics, Part B 37(2), 286–298 (2007)
39. Sung, H.G.: Gaussian Mixture Regression and Classification, PhD Thesis, Rice University, Texas (2004)
40. Wang, S.B., Quattoni, A., Morency, L., Demirdjian, D.: Hidden Conditional Random Fields for Gesture Recognition. In: IEEE Computer Society Conference on Computer Vision and Pattern Recognition, pp. 1521–1527 (2006)
41. Wainer, J., Ferrari, E., Dautenhahn, K., Robins, B.: The Effectiveness of using a Robotics Class to Foster Collaboration among Groups of Children with Autism in an Exploratory Study. Pers. Ubiquit. Comput. 14, 445–455 (2010)
42. Davis, M., Dautenhahn, K., Nehaniv, C.L., Powell, S.D.: Guidelines for Researchers and Practitioners Designing Software and Software Trials for Children with Autism. Journal of Assistive Technologies 4(1), 38–48 (2010)
43. Billard, A., Robins, B., Dautenhahn, K., Nadel, J.: Building Robota, a Mini-Humanoid Robot for the Rehabilitation of Children with Autism. Assistive Technology Journal 19(1), 37–49 (2007)
44. Robins, B., Dautenhahn, K., Boekhorst, R., te, B.A.: Robotic Assistants in Therapy and Education of Children with Autism: Can a Small Humanoid Robot Help Encourage Social Interaction Skills? Special Issue "Design for a More Inclusive World" of the International Journal Universal Access in the Information Society (UAIS) 4(2), 105–120 (2005)
45. Dautenhahn, K., Werry, I.: Towards Interactive Robots in Autism Therapy: Background, Motivation and Challenges. Pragmatics and Cognition 12(1), 1–35 (2004)
46. Kozima, H., Nakagawa, C., Yasuda, Y.: Children-robot Interaction: A Pilot Study in Autism Therapy. Progress in Brain Research 164, 385–400 (2007)
47. Aldebaran Robotics, `http://www.aldebaran-robotics.com/en/`
48. Aldebaran Robotics Choregraphe, `http://www.aldebaran-robotics.com/en/programmable`

An Online Fuzzy-Based Approach for Human Emotions Detection: An Overview on the Human Cognitive Model of Understanding and Generating Multimodal Actions

Amir Aly and Adriana Tapus

ENSTA ParisTech, Robotics and Computer Vision Lab,
828 Boulevard des Maréchaux, 91120 Palaiseau, France
{amir.aly,adriana.tapus}@ensta-paristech.fr
http://cogrob.ensta-paristech.fr

Abstract. An intelligent robot needs to be able to understand human emotions, and to understand and generate actions through cognitive systems that operate in a similar way to human cognition. In this chapter, we mainly focus on developing an online incremental learning system of emotions using Takagi-Sugeno (TS) fuzzy model. Additionally, we present a general overview for understanding and generating multimodal actions from the cognitive point of view. The main objective of this system is to detect whether the observed emotion needs a new corresponding multimodal action to be generated in case it constitutes a new emotion cluster not learnt before, or it can be attributed to one of the existing actions in memory in case it belongs to an existing cluster.

Keywords: Plutchik model, Takagi-Sugeno (TS) fuzzy model, Potential calculation, Cluster centers.

1 Introduction

The fast developing human-robot interaction (HRI) applications require the robot to be capable of dealing appropriately with different and varying situations as human does. This objective necessitates the robot to have high level cognitive functions that can make it able to detect the emotional state of the interacting human in order to generate a corresponding action. The robot's ability to generate an appropriate action requires an understanding of the context, of the environment, and of human intentions and performed actions combined with its own accumulated experience.

Physical action understanding in human's brain is considered to be achieved through mirror neurons, which have been discovered first in the premotor and parietal cortices (the F5 and PF areas) of macaque monkeys [1,2]. Afterwards, different neuroscience studies found evidences that an equivalent mirror neurons system exists in human's brain (in the inferior frontal gyrus, including the Broca's area [3], which has a major contribution to speech production) [4,5,6].

S. Mohammed et al. (eds.), *Intelligent Assistive Robots*,
Springer Tracts in Advanced Robotics 106, DOI: 10.1007/978-3-319-12922-8_7

Mirror neurons get activated when the observer performs a physical action, and when he/she detects others doing the same action. This process requires the observed action to have a goal, so that the observer could estimate the intention of the person performing the action in order to reproduce the same physical action in other similar situations. This discovery had offered a great help towards explaining different high level cognitive phenomena, including understanding physical actions [7,8], and mind reading [9]. Besides, it had led to the "broken mirrors" theory, which revealed some clues that may help researchers develop new approaches to better diagnose autism [10]. Moreover, the Wernicke's area located in the superior temporal gyrus of human's brain, is involved in understanding written language through associating the structure of the written words to their equivalent representations in memory, and similarly with spoken language [11].

On the other hand, physical action generation is based generally on two learning strategies: *imitation*, in which the observer copies the demonstrator's behavior in order to reach the same result [12,13,14], and *emulation*, in which the observer achieves the same result using his own behavior [15,16,17]. Whiten in [18] distinguished two main subcategories of emulation: (1) end-state result learning (i.e., re-creation of the end of an action sequence by any behavioral means), and (2) affordance learning (e.g., learning about the operating and physical properties of objects through the observation of others when interacting with them, which makes the achievement of similar goals easier, without employing imitation). The selection between these two learning strategies (i.e., imitation and emulation) depends mainly on the context. Emulation could be a more convenient strategy than imitation in some contexts due to its flexibility and generality (e.g., when all important causal relationships are clear to the observer - i.e., relationships between causes and effects). Meanwhile, imitation could be more appropriate when these causal relationships are not totally recognized, or when high-fidelity action reproduction is required [19,20,21]. On the other hand, speech production associated with the generated physical actions by imitation or emulation, implies intercommunication between different areas in human's brain based on the selected strategy for generating speech; like repeating a sentence that the observer heard or read, using an existing expression in memory, or formulating a new expression or a group of words based on the accumulated linguistic experience. Repeating a sentence that the observer heard, for example, requires the primary auditory cortex to process the spoken words, then the information travels to the Wernicke's area in order to understand its content, then to the Broca's area in order to formulate the equivalent spoken content of information, and finally to the primary motor cortex, which translates it back into spoken words by controlling the movement of muscles [11]. Similarly, repeating a sentence read by the observer, requires the primary visual cortex to process the written words, afterwards the processed information travels to the Wernicke's area, then to the Broca's area, and finally to the motor cortex.

On the way for a complete computational cognitive model for understanding multimodal actions, Buchsbau et al., in [22] discussed an action segmentation ap-

proach that segments a sequence of observed body behavior into significant physical actions, through a Bayesian analysis that investigates the inference between causes and effects during action segmentation. Another approach for understanding physical actions was illustrated in [23], in which low-level video features were used for the segmentation process. Neural networks have also been employed for action understanding inspired by the human mirror neurons system, and for action generation [24,25]. Understanding natural language was- and still is- a challenging topic. It has the objective of extracting all possible information from speech, which necessitates defining the meaning of words and sentences, in addition to precising the corresponding representation of each defined meaning, which makes language understanding as a task-oriented process. Issar and Ward in [26] used a flexible frame-based parser in the development of the CMU's language understanding system. The advantage of this system is that it can deal with the grammatically incorrect formulated sentences, repetitions, etc. Consequently, the system gets able to segment the informative parts of speech in order to directly understand the expressed meaning through semantic analysis. An information retrieval system was discussed in [27], in which a speech recognizer, a semantic analyzer, and a dialog manager were employed. The semantic analyzer performs a case-frame analysis in order to understand the meaning of the processed information. A concept-based approach for understanding language was discussed in [28,29], in which language understanding could be considered as a mapping from a sequence of words composing a sentence to a sequence of concepts, where a concept is defined as the smallest meaning-unit.

On the other hand, language generation could be mainly realized whether through predefined language templates that include sentences and words, in addition to some variables that can change the verbosity of the generator's output according to the task, the communicative goal, and the human's profile, or through rule-based approaches that use grammatical rules and linguistic constraints in order to calculate the most appropriate verbal output of the system. A common example for the template-based language generation is the weather forecast generator illustrated in [30]. The main problem associated with the template-based approach is that the generated language is limited linguistically within the prescribed templates of a certain task without big variability [31,32], however it is simple to develop. Unlike the template-based approach, the rule-based approach presents a wider linguistic scope for the generated language, so that the linguistic knowledge of the generator could be used for different tasks, even in different languages. However, its relative generality could be a negative point in case the task requires precise information to be given in a certain style [33,34]. Similarly, action generation has also faced difficulties in synthesizing a physical behavior relevant to the context of interaction [35]. Kozima et al., in [36] proposed a human-inspired system for goal emulation, so that it can emulate a goal by its own based on its previous experience. Rudolph et al., in [37] employed a Bayesian network structure in order to store actions as a representation of the resulting effects, which can be used in imitating a physical action, or emulating its goal.

Human's emotional states detection has been a rich research topic during the last decade. Traditional approaches are based on constructing a finite database with a specific number of classes, and on performing a batch (offline) learning of the constructed database. However, the associated problems with the batch learning show the importance of processing data online for the following reasons: (1) avoiding storage problems associated with huge databases, and (2) input data comes as a continuous stream of unlimited length, which creates a big difficulty in front of applying the batch learning algorithms. The absence of online learning methods can make the robot unable to cope with different situations in an appropriate way, due to an error in classifying a new emotion as being one of the previously learnt emotions, while its content constitutes a new emotional state category.

Many approaches are present in the literature for the detection of human affective states from voice signal. The significance of prosody in conveying emotions is illustrated in [38,39]. The authors discussed a comparative study about the variation of some relevant parameters (such as pitch and voice quality) in case of different emotional states. Moreover, Cahn in [39] explained the emotionally driven changes in voice signal's features under physiological effects in order to understand how the vocal (i.e., tonal) features accompanying emotions could differ. Roy and Pentland in [40] illustrated a spoken affect analysis system that can detect speaker's approval versus speaker's disapproval in child-directed speech. Similarly, Slaney and McRoberts in [41] proposed a system that can recognize prohibition, praise, and attentional bids in infant-directed speech. Breazeal and Aryananda in [42] investigated a more direct scope for affective intent recognition in robotics. They extracted some vocal characteristics (i.e., pitch and energy), and discussed how they can change the total recognition score of the affective intent in robot-directed speech. A framework for human emotion recognition from voice through gender differentiation was described in [43]. Generally, the results of the offline recognition of emotions in terms of the above mentioned vocal characteristics, are reasonable. On the other hand, emotion-based applications became more and more important. In computer-based applications, the system can recognize human emotions in order to generate an adapted behavior so as to maintain maximum engagement with human [44]. Similarly, emotion-based applications appear in different areas with robots, like: entertainment, education, and general services [45,46].

On the other hand, the importance of using fuzzy logic in modeling complex systems has been increased gradually in the last decade. It imitates human logic by using a descriptive and imprecise language in order to cope with input data. Zadeh in [47,48] put the first theory of fuzzy sets after observing that the traditional mathematical definition of object classes in real world is neither sufficient nor precise, because these classes may have imprecise criteria of membership. This observation remains valid for emotion classes; so that the emotion class "anger" may have clear membership criteria in terms of its vocal (i.e., tonal) characteristics with respect to the emotion class "sadness". However, it can have ambiguous membership criteria when compared to the emotion class "happiness"

because of the vocal characteristics' similarity of the two emotional states. One of the main reasons behind this ambiguity is that people show different amounts of spoken affect according to their personal and cultural characteristics. This validates the necessity of modeling emotional states using fuzzy sets and linguistic *if-then* rules in order to illustrate the existing fuzziness between these sets. Fuzzy inference is the process of mapping an input to a corresponding output using fuzzy logic, which formulates a basis for taking decisions. The literature of fuzzy inference systems reveals two major inference models: Mamdani [49] and Sugeno [50]. Mamdani in [49] stated the first fuzzy inference system designed for controlling a boiler and a steam engine using a group of linguistic control rules stated by experienced human operators. Meanwhile, Sugeno in [51,50] proposed another fuzzy inference system known as TS fuzzy model, which can generate fuzzy rules from a given input-output dataset. Clearly, TS fuzzy model is the model adopted in this study, because we have an initial database of emotion labeled states constituting the input-output data necessary for defining the initial TS model. The relationship between these emotional states is represented by fuzzy sets. When new data arrives, whether a new TS model is constructed corresponding to a newly created cluster, or one of the existing TS models is updated according to the cluster to which the new data is attributed.

On the way for an online recognition system of human's emotional states, clustering algorithms have proven their importance [52,53]. Clustering implicates gathering data vectors based on their similarity. It generates specific data points "cluster centers" that construct the initial TS fuzzy rules indicated above. K-means algorithm defines the membership of each data vector as being related to one cluster only, in addition to not belonging to the rest of the clusters. Fuzzy C-means algorithm, which was first proposed by Dunn [54], then improved by Bezdek [52], is an extension of the K-means algorithm that considers the fuzziness existing within a dataset. Consequently, it indicates the membership degrees of data vectors to all the existing clusters. However, both the dataset and number of clusters are required to be defined a priori, which makes it not applicable for our online recognition approach. Gustafsson and Kessel in [55] developed the classical Fuzzy C-means algorithm by using an adaptive distance norm in order to define clusters of different geometrical shapes within a dataset. However, similarly to the Fuzzy C-means algorithm, the number of clusters is required to be defined a priori. Furthermore, Gath and Geva in [56] described an unsupervised extension of the algorithm illustrated in [55] (which takes both the density and size of clusters into account), so that a priori knowledge concerning the clusters' number is no longer required. However, this methodology suffers from other problems, such as: (1) the algorithm can get easily stuck to the local minima with increasing complexity, and (2) it is difficult to understand the linguistic terms defined through the linear combination of input variables.

Other algorithms were proposed in order to overcome the drawbacks of the previously mentioned clustering algorithms. For example, the mountain clustering algorithm [57,58] tries to calculate cluster centers using a density measure (mountain function) of a grid over the data space, in which cluster centers are

the points with the highest density values. However, even if this algorithm is relatively efficient, its computational load increases exponentially with the dimensionality of the problem. The subtractive clustering [59] solved this problem by considering data points as possible candidates for cluster centers, instead of constructing a grid each time when calculating a cluster center, as in the mountain clustering. In this work, we chose to use the subtractive clustering algorithm in order to identify the parameters of the TS fuzzy model [59,50].

The rest of the chapter is structured as following: Section 2 presents an overview for the cognitive system, Section 3 illustrates a general overview for the basic and complex emotions, Section 4 discusses the offline detection of human's emotional states, Sections 5 and 6 overview the subtractive clustering and Takagi-Sugeno fuzzy model, Section 7 describes the online updating of Takagi-Sugeno fuzzy model, Section 8 provides a description of the results, and finally Section 9 concludes the chapter.

2 Cognitive System Overview

The human cognitive model illustrated in Figure (1), is composed of two stages. Stage 1 represents the stage of emotional states detection, in which an observer decodes and analyzes the contained information in human speech, reaching to an estimation for his possible emotional emotional state, upon which the observer will generate a corresponding multimodal action. In this chapter, we will focus on this stage, and we will try to develop a computational model with the same functionality based on fuzzy logic. On the other hand, Stage 2 represents an overview of human cognitive architecture for understanding and generating multimodal actions. An observer learns the context and goal of each observed multimodal action in the surrounding environment. He/she tries to reproduce it by sending the processed information to the synchronization phase for multimodal temporal alignment, then to the motor cortex that controls the responsible muscles of both speech and gesture generation processes. Thereupon, the aligned multimodal actions get stored in the action memory. After accumulating enough multimodal interaction experience, and in a moment when an action (i.e., the output of Stage 1) is required to be generated, the action memory will synthesize a multimodal behavior corresponding to the analyzed information in Stage 1, and will send the necessary information to the motor cortex for multimodal action generation. Similarly, the action memory is important during the learning process, so that it can offer a base for the emulation process, and same for the Broca's area during speech generation.

A preliminary proposed computational model for understanding and generating multimodal actions (i.e., the equivalent computational model to Stage 2 of the human cognitive architecture discussed above), is illustrated in Figure (2). The observed multimodal actions in the environment are captured through appropriate audio and video channels. After parsing the text of the dictated speech, semiotic and linguistic analyses are implemented in order to extract the contained pragmatic information (i.e., speech acts [60,61]) and the semantic

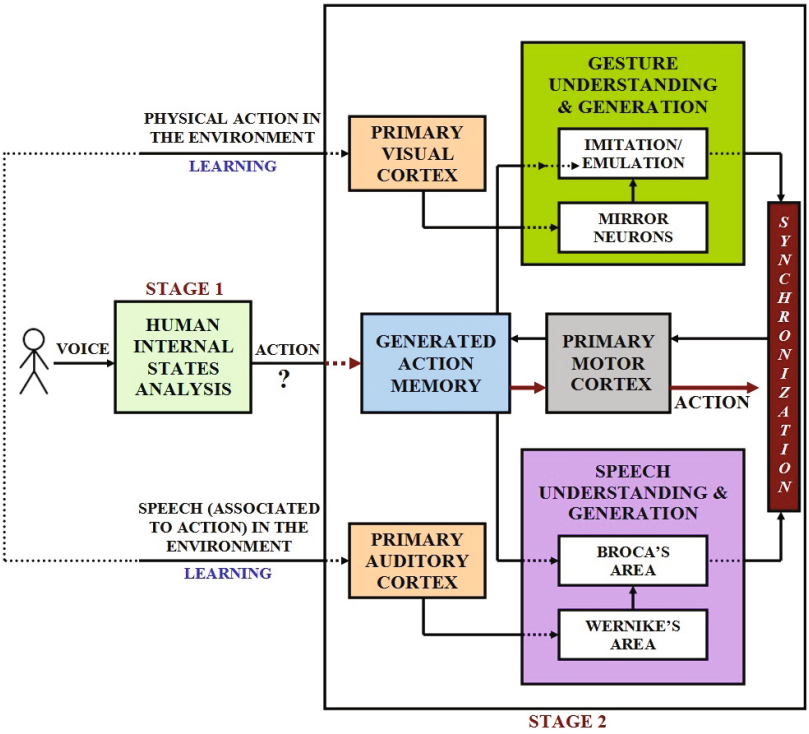

Fig. 1. Cognitive model for understanding multimodal actions of people in the surrounding environment, and generating multimodal actions corresponding to detected emotional states.

information (i.e., the meanings of words and sentences), and to calculate the interacting human's profile (i.e., personality traits [62,63]). Afterwards, the dialog manager can generate a similar text to the dictated one after understanding its content in the previous step, or it can generate a different text but expressing the same idea, goal, and context. This process represents the learning phase of the contained information in speech. On the other hand, action grammars are employed in order to understand the goal of the captured actions [64,65]. Thereupon, the observed action could be learnt by imitation or by emulating its goal. The synchronization phase uses a TTS (text-to-speech) engine in order to calculate the estimated duration of the generated text so as to align it temporally to the generated action. The aligned multimodal actions (learnt by the system) are stored in the action memory, so that the system gets ready for synthesizing a multimodal behavior when an action is required to be generated. This stage is composed of multi-complex sub-processes, and is considered as a future direction for the current research focusing on Stage 1.

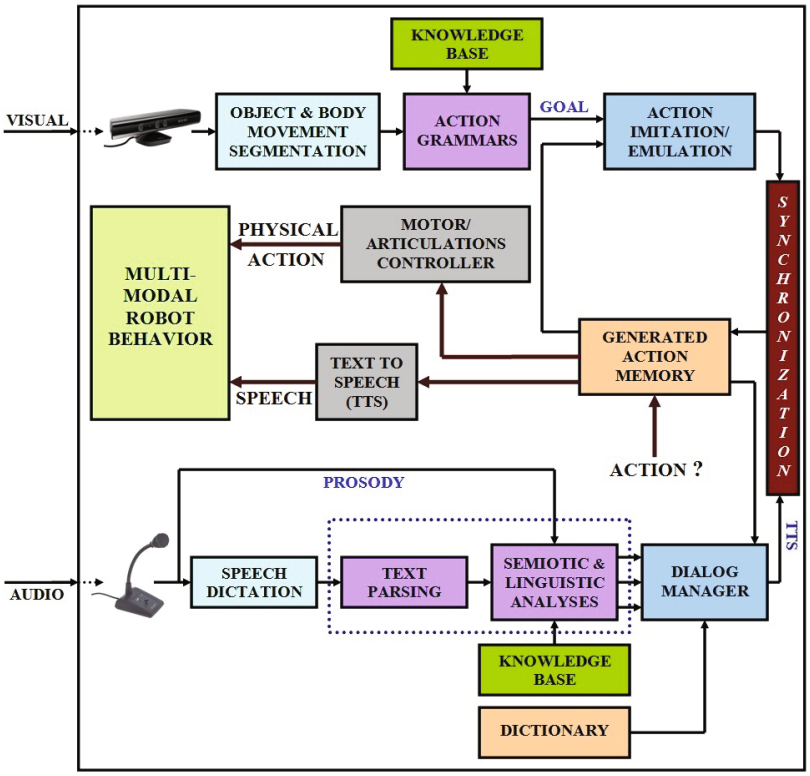

Fig. 2. Computational model for understanding and generating multimodal actions (Stage 2)

3 Basic and Complex Emotions

Emotion is one of the most controversial issues in human-human interaction nowadays, in terms of the best way to conceptualize and interpret its role in life. It seems to be centrally involved in determining the behavioral reaction to social environmental and internal events of major significance for human [66,67]. One of the main difficulties behind studying the objective of emotion is that the internal experience of emotion is highly personal and is dependent on the surrounding environment circumstances. Besides, many emotions may be experienced simultaneously [67].

Different emotion theories identified relatively small sets of fundamental or basic emotions, which are meant to be fixed and universal to all humans (i.e., they can not be broken down into smaller parts). However, there is a deep opinion divergence regarding the number of basic emotions. Ekman in [68,69] stated a group of 6 fundamental emotions (i.e., anger, happiness, surprise, disgust, sadness, and fear) after studying cross-cultural facial expressions, collected from a lot of media pictures for individuals from different countries. However, Ekman

in his theory, had not resolve the problem discussed in the research of Izard [66], which is the fact that it is not possible, or at least not easy, to unify basic universal facial expressions through processing media pictures only, because there are a lot of populations who have no access to media (like some populations in Africa). Consequently, there is no considerable database for their facial expressions to study. Thereafter, Izard in [70] devised a list of 10 primary emotions (i.e., anger, contempt, disgust, distress, fear, guilt, interest, joy, shame, and surprise), each one has its own neurobiological basis and pattern of expression (usually denoted by facial expressions), and each emotion is experienced uniquely. Tomkins in [71] proposed a biologically-based group of pan-cultural 9 primary emotions (i.e., anger, interest, contempt, disgust, distress, fear, joy, shame, and surprise). More theories exist in the literature of emotion modeling, similarly to the previously stated theories. However, they do not consider the evolutionary and combinatory nature of emotion, which may lead to a new advanced category of complex emotions that could be considered as mixtures of primary emotions based on cultural or idiosyncratic aspects.

Plutchik proposed an integrative theory based on evolutionary principles [67]. He created a three-dimensional (i.e., intensity, similarity, and polarity) circumplex wheel of emotions that illustrates different compelling and nuanced emotions based on a psychological-biological research study, as indicated in Figure (3). The 8 sectors of the wheel indicate that there are 8 primary emotions (i.e., anger, fear, disgust, trust, sadness, joy, surprise, and anticipation) arranged in four opposite pairs (different polarity; i.e., joy versus sadness). The circles represent emotions of similar intensity; the smaller circle contains the emotions of highest intensity in each branch, while the second circle contains extensions of the first circle's emotions, but in lighter intensity, and so on. The blank spaces represent the primary dyads, which are mixtures of two adjacent primary emotions. However, the secondary dyads are mixture of two non-adjacent primary emotions with one primary emotion in-between (e.g., $anger + joy = pride$, or $fear + sadness = desperation$). Meanwhile, tertiary dyads are mixtures of two non-adjacent primary emotions with two primary emotions in-between (e.g., $fear + disgust = shame$ or $anticipation + fear = anxiety$). Plutchik model is, therefore, the most appropriate model for this research.

4 Offline Detection of Emotional States

In this research, we investigated the performance of the offline classification system using the Support Vector Machine (SVM) algorithm [72], with 15 primary and complex emotions. Afterwards, we created a fuzzy classification system and we trained it offline on 6 primary emotions, in addition to the neutral emotion (i.e., anger, disgust, happiness, sadness, surprise, fear, and neutral). However, the online test phase contained 5 complex emotions (anxiety, shame, desperation, pride, and contempt), in addition to 3 primary emotions (i.e., interest, elation, and boredom).

Three databases (including more than 1000 voice sample) have been employed in training and testing the classification system. These databases are: (1) German

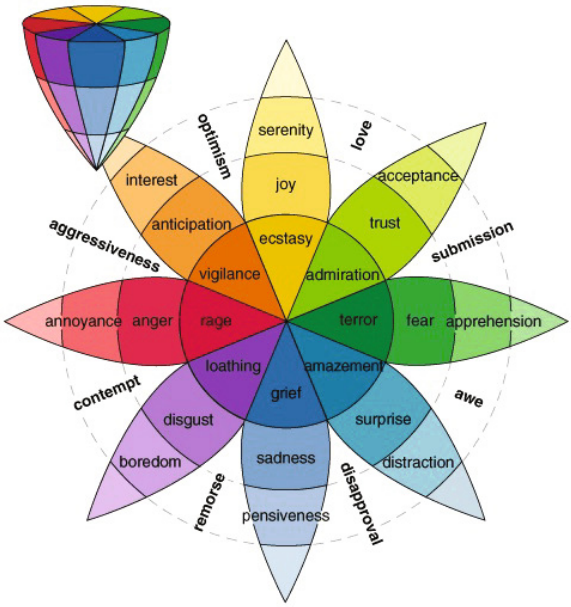

Fig. 3. Plutchik's primary and mixture emotions presented in a 2D wheel, and in a 3D cone [67].

emotional speech database (GES) [73], (2) Geneva vocal emotion expression stimulus set (GVEESS) [74] [1], and (3) Spanish emotional speech database (SES) [75]. [2] An important remark about the emotion classes of the total database is that they do not have all the same intensity, in addition to the existing emotion extension in two cases: boredom-disgust, and elation-happiness. This is due to the encountered difficulty to obtain well known databases with specific emotion categories that exactly match Plutchik model's emotion categories.

Relevant characteristics (i.e., pitch and energy [3]) have been calculated for all the samples of the databases [42] in order to find out their possible effects on characterizing emotional states. The emotional state detection system, normally, includes three different subprocesses: speech signal processing (Section 4.1), features extraction (Section 4.2), and classification (Section 4.3), as indicated in Figure (4).

[1] The stimulus set used is based on research conducted by Klaus Scherer, Harald Wallbott, Rainer Banse and Heiner Ellgring. Detailed information on the production of the stimuli can be found in [74].

[2] The SES database is a property of Universidad Politecnica de Madrid, Departamento de Ingenieria Electronica, Grupo de Tecnologia del Habla, Madrid (Spain).

[3] We use the terms energy and intensity interchangeably.

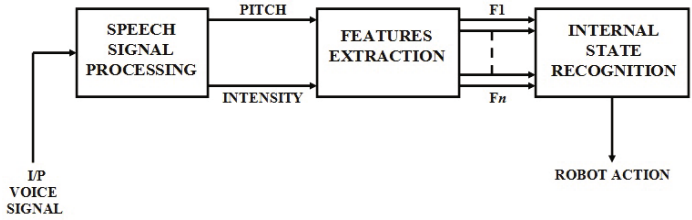

Fig. 4. Emotional state detection system

4.1 Speech Signal Processing

Talkin in [76] defined the pitch as the auditory percept of tone, which is not directly measurable from a signal. Moreover, it is a nonlinear function of the signal's temporal and spectral distribution of energy. Instead, another vocal (i.e., tonal) characteristic, which is the fundamental frequency $F0$, is calculated as it correlates well with the perceived pitch.

Voice processing systems that estimate the fundamental frequency $F0$ often have three common processes: (1) signal conditioning, (2) candidate periods estimation, and (3) post processing. The signal conditioning process tries to clear away interfering signal components, such as any unnecessary noise by using low pass filtering, which removes any loss of periodicity in the voiced signal's spectrum at high frequencies, and by using high pass filtering when there are DC or very low frequency components in the signal. The candidate periods estimation step tries to estimate the candidate voiced periods from which the fundamental frequency $F0$ could be calculated. Talkin [76] developed the traditional Normalized Cross Correlation (NCC) method [77,78] in order to estimate reliably the voicing periods and the fundamental frequency $F0$ by considering all candidates simultaneously in a large temporal context in order to avoid the variation of the glottal excitation periods through the signal. This methodology uses a two pass normalized cross correlation (NCC) calculation for searching the fundamental frequency $F0$, which reduces the overall computational load with respect to the traditional (NCC) methodology. Finally, the post processing step uses median filtering in order to refine the calculated fundamental frequency $F0$ and ignore isolated outliers, as indicated in Figure (5). On the other hand, voice signal's energy could be directly calculated from squaring the amplitude of signal's points.

4.2 Features Extraction

Rong et al., in [79] presented a detailed study concerning the common vocal (i.e., tonal) characteristics used in the literature of emotion recognition, and their significance. After testing different tonal characteristics in the offline classification phase, we found that the most important characteristics are: pitch and energy, upon which the recognition score highly depends. Meanwhile, other characteristics (e.g., duration and rhythm) did not have the same significant effect on the

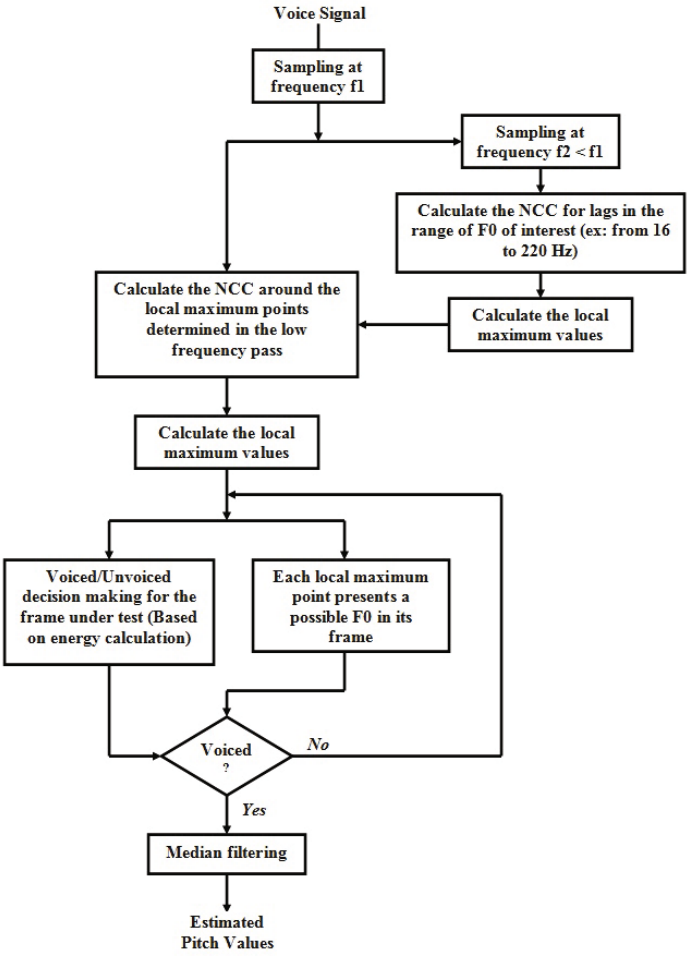

Fig. 5. Pitch tracking

recognition score. Relevant statistical measures of pitch and energy were calculated in order to create characteristic vectors used in constructing the database. The final features used in this work are: (1) Pitch mean, (2) Pitch variance, (3) Pitch maximum, (4) Pitch minimum, (5) Pitch range, (6) Pitch mean derivative, (7) Energy mean, (8) Energy variance, (9) Energy maximum, and (10) Energy range.

4.3 Classification

Voice samples were classified using the SVM algorithm with a quadratic kernel function [80,81], and the results were cross validated. Table (1) indicates the obtained recognition scores of 15 different emotions. The mean values of the

recognition scores indicated in Table (1), reflect the high precision of our classification system with respect to similar systems discussed in the literature. In [73], the mean value of the emotion recognition scores was 86.1%. Meanwhile, in [74], the mean value of the obtained scores was 60%. However, in [75], the mean value of the obtained scores was 85.9%.

Table 1. Recognition scores of different emotional states. Empty spaces are emotions not included in these databases.

Emotion	GES	GVEESS	SES	All 3 DB mixed
Anger	80.8%	88.7%	79.8%	81.7%
Boredom	85.4%	87.1%	-	90.1%
Disgust	92.1%	91.7%	-	93.5%
Anxiety	87.3%	86.5%	-	87.5%
Happiness	86.9%	88.5%	75.1%	86.1%
Neutral	83.7%	-	89.5%	87.8%
Sadness	86.9%	90.1%	94.1%	85.7%
Surprise	-	-	95.7%	96.3%
Interest	-	89.3%	-	90.4%
Shame	-	90.7%	-	91.9%
Contempt	-	91.3%	-	90.6%
Desperation	-	87.7%	-	89.2%
Elation	-	89.9%	-	87.5%
Pride	-	86.9%	-	87.3%
Fear	-	85.7%	-	89.7%
Mean Value	86.2%	88.8%	86.8%	89%

The calculated recognition scores of emotions depend mainly on the individuals performing the emotions, and on the amount of spoken affect they show. This may lead to a problem in real human-robot interaction scenarios if the expressed emotion to the robot is different (in terms of tonal features) from the trained emotion in the database. Consequently, two scenarios may exist: (1) if the expressed emotion is intended to belong to one of the prescribed emotion classes in the database, it is probable that the robot misclassifies it. This depends totally on the performance of the recognition system, and (2) if the expressed emotion does not belong to any of the existing emotion classes in the database, and the robot attributes it to the nearest existing emotion class (instead of constituting a new emotion class), it may lead the robot to behave in an inappropriate manner. Therefore, in order to avoid any improper robot's behavior, it is important for the robot to understand whether the online expressed emotion constitutes a new emotional state class or not. This allows the robot to perform a neutral action different from the corresponding prescribed actions to the learnt emotions so as to not make the performed action seems to be out of context to the interacting human (developing autonomously an appropriate multimodal robot's affective behavior is lightly discussed in this work a future research orientation).

5 Subtractive Clustering

Subtractive Clustering [59] is a fast algorithm used for calculating cluster centers within a dataset. It uses data points as possible candidates for cluster centers, and then it calculates a potential function for each proposed cluster center, which indicates to what extent the proposed cluster center is affected by the surrounding points in the dataset. Suppose a cluster composed of k normalized data points $\{x_1, x_2, ..., x_k\}$ in an M-dimensional space, where each data point has a potential P that could be represented as following (Equation 1):

$$P_d = \sum_{u=1}^{k} e^{-\frac{4}{r^2}\|x_d - x_u\|^2}; \qquad d \in \{1 \cdots k\} \tag{1}$$

where r is the neighborhood radius that is fixed to 0.3, at which the calculation of cluster centers is optimally precise. After choosing the first cluster center (which is the data point with the highest potential value), the potential of the other remaining data points will be recalculated with respect to it.

Assume x_n^* is the location of the n^{th} cluster center of potential P_n^*, consequently the potential of each remaining data point could be reformulated as following (Equation 2, where r_b is a positive constant):

$$P_d \Leftarrow P_d - \underbrace{P_n^* e^{-\frac{4}{r_b^2}\|x_d - x_n^*\|^2}}_{X} \tag{2}$$

From the previous equation, it is clear that the potential of each remaining data point is subtracted by the amount X, which is a function of the distance between the point and the last defined cluster center. Consequently, a data point near to the last defined cluster center will have a decreased potential, so that it will be excluded from the selection of the next cluster center. In order to avoid having close cluster centers, the value of r_b should be chosen greater than the value of the neighborhood radius r (r_b=1.5r) [59]. After calculating the reduced potential of all data points with respect to the last defined cluster center according to Equation (2), the next cluster center is chosen as the new highest potential value. This process is repeated until a sufficient number of centers is attained.

Chiu in [59] proposed a criterion for accepting and rejecting cluster centers in order to define the final sufficient number of clusters. This criterion defines two limiting conditions: lower ($\underline{\varepsilon} P_1^*$) and upper ($\overline{\varepsilon} P_1^*$) boundaries (where $\overline{\varepsilon}$ and $\underline{\varepsilon}$ are small threshold fractions). A data point is selected to be a new cluster center if its potential is higher than the upper threshold, and is rejected when its potential value is lower than the lower threshold. If the potential of the data point is between the upper and lower thresholds, a new decisive rule is used for accepting new cluster centers (Equation 3):

$$\frac{d_{min}}{r} + \frac{P_n^*}{P_1^*} \geq 1 \tag{3}$$

where d_{min} is the shortest distance between x_n^* and the locations of all the previously calculated cluster centers. Otherwise, the data point is rejected.

According to Chiu in [59], the upper threshold ($\overline{\varepsilon}$) is fixed to 0.5, while the lower threshold ($\underline{\varepsilon}$) is fixed to 0.15. This approach is used for calculating the antecedent parameters of the fuzzy model. It depends on the fact that each cluster center represents a characteristic fuzzy rule for the system.

6 Takagi-Sugeno (TS) Fuzzy Model

Takagi-Sugeno (TS) fuzzy model employs fuzzy rules, which are linguistic statements ($if - then$), involving fuzzy logic, fuzzy sets, and fuzzy inference. The fuzziness in the input sets is characterized by the input membership functions, which could have varying shapes (triangular, Gaussian, etc) according to the nature of the modeled process.

Considering a set of n cluster centers $\{x_1^*, x_2^*, ..., x_n^*\}$ produced from clustering the input-output data space; each vector x_i^* is decomposed into two component vectors y_i^* and z_i^*, which contain the cluster center's coordinates in the input and output spaces in order (i.e., the number of input and output membership functions is determined by the number of cluster centers).

Suppose that each cluster center x_i^* is a fuzzy rule, therefore for an input vector y= $[y_1, y_2, ..., y_m]$, the firing degree of the input vector's component y_j to the input membership function corresponding to the j^{th} input component and the i^{th} fuzzy rule y_{ji}^* is defined as following (Equation 4) [82]:

$$\mu_{ji} = e^{(-\frac{4}{r^2}\|y_j - y_{ji}^*\|^2)}; \quad i \in \{1 \cdots n\}, \;\; j \in \{1 \cdots m\} \tag{4}$$

Consequently, the total degree of membership of rule i with respect to the whole input vector could be defined as following (Equation 5):

$$\tau_i = \mu_{1i}(y_1) \times \mu_{2i}(y_2) \times \cdots \times \mu_{mi}(y_m) = \prod_{j=1}^{m} \mu_{ji}(y_j) \tag{5}$$

The previous model could be reformulated in terms of linguistic *if-then* fuzzy rule as following (Equation 6):

$$\begin{aligned} &\text{If } y_1 \text{ is } y_{1i}^* \text{ and } \cdots\cdots \text{ and } y_m \text{ is } y_{mi}^* \\ &\text{Then} \quad z_i^* = b_{0i} + b_{1i}y_1 + \cdots + b_{mi}y_m \end{aligned} \tag{6}$$

where z_i^* is the corresponding linear output membership function to rule i.

The input membership functions represent generally a linguistic description of the input vector (e.g., small, big, etc). Therefore, the first antecedent part of the rule (y_1 is $y_{1i}^* \cdots$) represents the membership level of the input y_1 to the

function y_{1i}^*. The output vector z could be represented in terms of the weighted average of rules contributions as following (Equation 7):

$$z = \sum_{i=1}^{n} \frac{\tau_i z_i^*}{\sum_{l=1}^{n} \tau_l} = \sum_{i=1}^{n} \gamma_i z_i^* \tag{7}$$

The learning parameters of the consequent part of the rule could be estimated by the recursive least squares approach. Suppose $\lambda_i = [b_{0i}, b_{1i}, \cdots, b_{mi}]$, $Y = [1, y_1, \cdots, y_m]^T$, so that the previous equation could be reformulated in terms of all fuzzy rules as following (Equation 8):

$$z = \chi\varphi \tag{8}$$

where:

$$\chi = \begin{bmatrix} \lambda_1 \\ \lambda_2 \\ \vdots \\ \lambda_n \end{bmatrix}, \qquad \varphi = [\gamma_1 Y, \gamma_2 Y, \cdots, \gamma_n Y]$$

In our context, for an existing human emotion cluster, the given set of input-output data is used to define a cost function, from which the parameters set χ could be calculated by minimizing that function (Equation 9, where k is the number of data points within a cluster):

$$J = \sum_{d=1}^{k} (z_d - \chi\varphi_d)^2 \tag{9}$$

Equation (9) could be reformulated as following (Equation 10, where the matrices Z, η are functions in z_d and φ_d):

$$J = (Z - \chi\eta)^T (Z - \chi\eta) \tag{10}$$

The least square estimation of χ, could be finally defined as following (Equation 11):

$$\hat{\chi} = (\eta\eta^T)^{-1}\eta Z \tag{11}$$

A typical fuzzy modeling of a human's emotional state is illustrated in Figure (6), in which each vocal feature is mapped to a corresponding group of input membership functions equal to the number of rules. The output of the model is represented by the value of z calculated in Equation (7). When the vocal features of a test voice sample are calculated, they get evaluated through the fuzzy model of each existing emotion. The decisive criterion of the emotional state's class to which the voice sample is attributed, could be defined as following (Equation 12, where α is the total number of the existing clusters):

$$Class = \arg\max_{p=1}^{\alpha}(z_p) \tag{12}$$

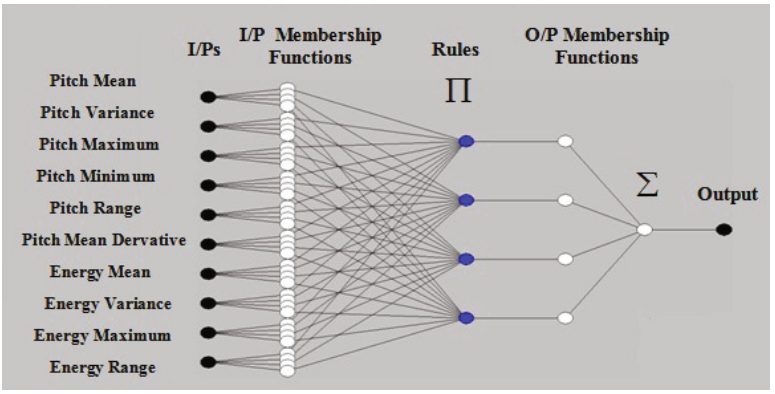

Fig. 6. TS fuzzy modeling of a human's emotion cluster

7 TS Fuzzy Model Online Updating

The online updating of the constructed TS fuzzy model is essential for continuous data streams. This requires an incremental calculation for the informative potential of the online incoming data [82] in order to decide whether the new data confirms the contained information in one of the existing data clusters, or it constitutes a new cluster (Figure 7). When a new data element arrives, it gets attributed to one of the existing clusters according to Equation (12), which leads to one of the three scenarios below:

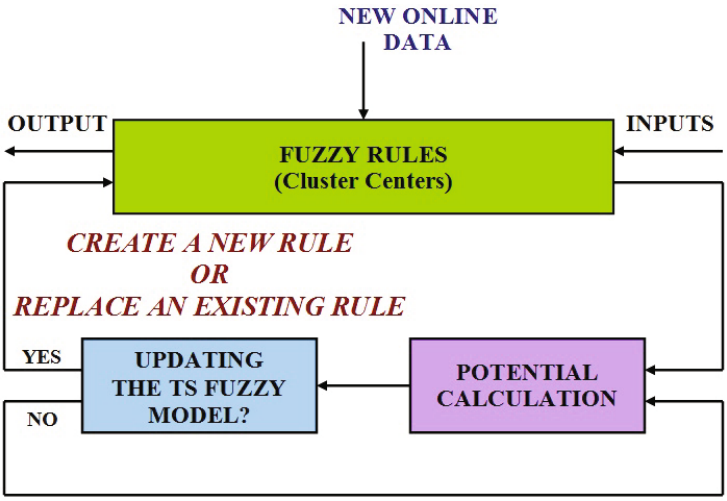

Fig. 7. TS fuzzy model updating whether by creating a new rule, or by replacing an existing rule.

7.1 Scenario 1

A new data element is attributed with a good score to an existing emotion cluster, so that the robot implements the associated action with the winner class. Considering the emotion recognition scores shown in Table (1), and the possible variation in the spoken affect shown by humans in real interaction experiments, we considered this score to be $> 80\%$ in order to assure a relatively high confidence in recognizing emotions. On the other hand, the fuzzy model of the winner class should keep updated in order to get ready for the arrival of any new element to the model (Figure 7). The procedures of updating the TS model are summarized in the following pseudo code (where n is the number of cluster centers):

1: **if** $(P_{NEW} > P_l^*)$, $\forall\ l \in \{1 \cdots n\}$ and the new data point is near an old cluster center, so that the following inequality is fulfilled: $\frac{P_{NEW}}{max P^*_{l \in \{1 \cdots n\}}}$ - $\frac{d_{min}}{r} \geq 1$ **then** the new data point will replace the old rule center.
go to: Scenario 3.
2: **else if** $(P_{NEW} > P_l^*)$, $\forall\ l \in \{1 \cdots n\}$ **then** the new point will be considered as a new cluster center x^*_{NEW}, thus a new fuzzy rule will be created.
go to: Scenario 3.
3: **else** The new data point does not possess enough descriptive potential to update the model, neither by creating a new rule, nor by replacing one of the existing rules.
4: **end if**

For the steps 1 and 2 of the pseudo code, the consequent parameters of the TS model should be estimated recursively, as indicated in Equations (7 to 11). Similarly, for all the steps 1, 2, and 3, the potential of all cluster centers needs to be calculated recursively. This is due to the fact that potential calculation measures the density level of groupings in the data space, consequently this measure will be reduced for a given cluster center in case the data space gets increased by acquiring more data elements of different patterns (Equation 2). Typically, the potential of a new acquired data point P_{NEW} will be increased, when other new data points of similar patterns group with it [82].

7.2 Scenario 2

In case the recognition score of the existing clusters for a new data element does not reach the predefined threshold (i.e., $< 80\%$), an uncertainty factor would be

considered. Consequently, the new data element will be attributed temporarily to all the existing clusters at the same time with a specific label in order to distinguish it from the normal data elements of each cluster. Thereupon, the robot will implement a prescribed neutral action (different from the normal neutral action associated with the "neutral" emotion class), until its cognitive awareness increases and gets ready to synthesize its own multimodal action according to the context, as referred to earlier. The main reason behind attributing temporarily the new data element X_{NEW} to all the existing clusters, is that when the potential of this new element is recursively calculated, it gets increased gradually when other uncertain data elements get attributed, in a similar manner, to all clusters, provided that they have a similar data pattern as X_{NEW}. Meanwhile, the potential of clusters' original centers will be reduced (Equation 2). Consequently, a new cluster will be created (with an associated neutral action, until the robot gets able to synthesize an alternative action by its own), if the potential of X_{NEW} gets greater than the potential of all the original centers in each cluster, as indicated in the following pseudo code (where α is the number of the existing clusters, and n is the number of cluster centers):

1: **if** $(P_{P_{NEW}} > P^*_{p,l}), \forall\ l \in \{1 \cdots n\},\ \ p \in \{1 \cdots \alpha\}$
then all the copies of the uncertain new data elements with similar patterns will be removed from all clusters, and only one group of them will create the new cluster.
and $\alpha := \alpha{+}1$
and A new TS fuzzy model will be created for the new cluster.
go to: Scenario 1.
2: **end if**

In case a new element gets attributed to a specific cluster with a confident score as in Scenario 1, the existence of temporarily uncertain data elements in this cluster will not affect the potential calculation of the new data element with respect to the original cluster centers. Therefore, they will not participate (in this case) in updating the TS fuzzy models of the clusters in which they exist, which explains the reason behind being labeled differently.

7.3 Scenario 3

During Scenario 2, it is possible that one of the uncertain data elements was belonging originally to one of the existing clusters, and got classified as an element of uncertain emotional content though, due to lack of experience. This results from fact that people show emotional affect in different ways even for the same expressed emotion, which may create a problem that is the necessity to train the classifier on unlimited emotion patterns for each cluster. Consequently, it is probable that the previous learning experience of the classifier was not sufficient

enough to recognize the new data element with a confident score. In order to avoid this problem, at each moment when a cluster is updated by a new element recognized with a confident score as in Scenario 1, a revision on the uncertain elements of this cluster will be performed by re-calculating the recognition scores of the updated cluster's fuzzy model for the uncertain elements. If any uncertain element is recognized with a confident score by the fuzzy classifier of the updated cluster, this element will join the updated cluster, and its copies will be eliminated from the uncertain data spaces of all other clusters, as indicated in the following pseudo code (where ω is the number of cluster's uncertain data points, S denotes the recognition score, and k is the number of the cluster's certain data points):

1: **do** Scenario 1 (steps 1 and 2)
2: **if** $(S_{P,u} > 80\%), \forall\ u \in \{1 \cdots \omega\},\ \ p \in \{1 \cdots \alpha\}$
then the uncertain data point $x_{p,u}$ will join the correct cluster, and will be removed from all the other clusters.
and $k_P := k_P + 1$
go to: Scenario 1.
3: **end if**

8 Results

The fuzzy classification system was trained on 7 emotions (i.e., anger, disgust, happiness, sadness, surprise, fear, neutral), and the results were cross validated (Table 2). The calculated scores are less than the previously obtained scores through the offline learning process using the SVM algorithm (Table 1), because the SVM algorithm deals directly with the data space, meanwhile the fuzzy classification system deals with the data space through an approximate TS model, however they remain acceptable results.

Table 2. Recognition scores of the fuzzy system's training emotions

Emotion	Recognition Score
Anger	83.76%
Disgust	75.60%
Happiness	76.92%
Sadness	69.57%
Surprise	80.28%
Fear	77.08%
Neutral	82.14%
Mean Value	77.91%

The online test database included voice samples covering simple and complex emotions from the three databases referred to earlier (Section 4), in addition to some other voice samples (for the same emotions), expressed by other actors in a noisy environment in our laboratory. These 8 emotions are: anxiety, shame, desperation, pride, contempt, interest, elation, and boredom. Table (3) illustrates the results of attributing the test clusters' data elements to the existing old clusters, upon which the system was trained on. A small part of the test data elements was attributed with a confident score (i.e., $> 80\%$) to the existing clusters, which is unavoidable and depends totally on the patterns of the test data elements, and on the actors' performance. However, the results of classification are not totally out of context, like the elements of the "anxiety" class that were attributed to the "fear" class, and the elements of the "elation" class that were attributed to the "happiness" class.

Table 3. Confusion matrix for the classification of the new data elements as being uncertain-emotion elements or as being a part of the existing clusters

New Data	Uncertain New Data (Scenario 2)	New Data Belonging to Old Data Clusters (Scenario1)						
		Anger	Disgust	Happiness	Sadness	Surprise	Fear	Neutral
Anxiety	81.6%	0	0	0	2.5%	0	15.9%	0
Shame	73.3%	0	13.3%	0	0	6.7%	0	6.7%
Desperation	68.75%	0	12.5%	0	6.25%	0	12.5%	0
Pride	73.3%	0	0	0	6.7%	6.7%	0	13.3%
Contempt	62.5%	6.25%	0	0	6.25%	0	18.75%	6.25%
Interest	75%	0	0	0	6.25%	6.25%	6.25%	6.25%
Elation	68.75%	6.25%	0	12.5%	0	0	0	12.5%
Boredom	69.8%	0	0	0	5.2%	0	23.9%	1.1%

The part of the new data attributed to the existing clusters (Table 3), was assigned for the validation of Scenario 1 (Section 7). The main encountered problem was that the new data elements attributed to the existing clusters were generally too few to update the fuzzy models of clusters easily. Unlike the elements attributed to the "fear" class, which were sufficiently descriptive to update the fuzzy model, so that two new elements satisfied the steps 1 and 2 of Scenario 1. On the other hand, the uncertain part of the new data (Table 3), was assigned for the validation of Scenario 2 (Section 7). Two new clusters were successfully constructed in case of the "anxiety" and "boredom" emotions. To the contrary, the number of elements in the other classes (i.e., shame, desperation, pride, contempt, interest, elation), was not sufficient to fulfill Scenario 2. Therefore, the elements of these classes were considered as uncertain data elements, until more data elements of similar patterns were acquired, then Scenario 2 was re-checked.

A video showing our system working in a simple interaction experiment with NAO robot (Figure 8) developed by Aldebaran Robotics [4] is available at: `http://www.ensta-paristech.fr/~tapus/HRIAA/media/videos/`. The video is composed of four scenes recognizing three emotions belonging to the existing clusters in the database (Figure 9), in addition to one new emotion not included in the database. These emotions are: surprise, anger, boredom, and shame. The voice signal was acquired through a wireless ear microphone (hidden from the angle of the video camera).

Fig. 8. Test-bed: Nao robot

The "surprise" and "anger" emotions were recognized successfully due to their distinguished vocal patterns. Meanwhile, the "boredom" emotion was confused with the "sadness" emotion due to the similarity between their vocal patterns, which made their recognition scores close to each other. Last but not least, the "shame" emotion was recognized correctly as a new emotion (i.e., not included in the database), after some confusion with one of the previously learnt emotions "anxiety". In the beginning, the expressed "shame" emotion to the robot was not attributed with a confident score to any of the existing classes. However, the "anxiety" class was the nearest winner class, but the attained score was less than 80%. Therefore, Scenario 2 (Section 7) was implemented. The expressed emotion was attributed to all the existing clusters, to which some data elements from the "shame" emotion class had been added, as if they represent the previously attributed uncertain data to all the existing clusters. The objective was to find out to what extent the algorithm would be able to detect the new emotion and to construct a new cluster.

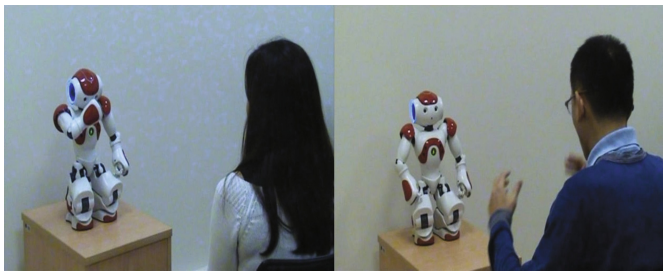

Fig. 9. Two participants are interacting with the robot. Each one expressed an emotion and the robot tried to recognize it. This recognition represents an action that the robot could generate corresponding to the expressed emotion.

9 Conclusion

This research illustrates the need for artificial cognitive functions that can allow the robot to understand and generate actions, in addition to understanding the emotional state of human so as to behave in a suitable way as human does. Mirror neurons and the Wernicke's area in human's brain play an important role in understanding the perceived multimodal actions in the surrounding environment. On the other hand, imitation and emulation are considered the most credible learning strategies in human's brain, because they provide the ability to generate an action according to the context. Moreover, the Broca's area in human's brain is believed to be responsible for speech production. The human cognitive model (Section 2), which interconnects between different brain areas and cognitive functions that organizes understanding and generating multimodal actions, represents a real challenge in front of the serious efforts towards creating a complete artificial cognitive model of similar functionality.

The major part of this research discusses an online learning approach for human's emotional states. Our approach is based on the subtractive clustering algorithm that calculates the cluster centers of a data space. These centers represent the rules of the TS fuzzy models that characterize emotion clusters separately. Decisive criteria based on a recursive potential calculation for the new data decide whether the new elements constitute a new cluster, or they belong to one of the existing clusters. In case a new cluster is set up, a corresponding TS fuzzy model will be created. Meanwhile, in case the new data is attributed to one of the existing clusters, it may update the TS model of the winner cluster whether by creating a new rule, or by replacing one of the existing rules according to its descriptive power.

When an uncertain-emotion data element is detected, or a new cluster is created, the robot performs a neutral action at the beginning in order to avoid any

[4] Nao is a 25 degrees of freedom robot equipped with two cameras, an inertial sensor, a sonar sensor, and many other sensors that allow it to perceive its surrounding with high precision and stability. `http://www.aldebaran-robotics.com/`

inconsistency in the context of interaction. Progressively, the robot's experience and awareness will increase, which helps it create autonomously a behavior from its own system by studying all the previous actions and interaction scenarios in order to propose autonomously new relevant actions. However, this last point is a future scope for this work.

Acknowledgments. This work is supported by the French National Research Agency (ANR) through Chaire d'Excellence program 2009 (Human-Robot Interaction for Assistive Applications). The project's website is accessible at: `http://www.ensta-paristech.fr/~tapus/HRIAA/`. This paper is an extension of our previous research [83], with more elaborated discussion and analysis.

References

1. Fogassi, L., Ferrari, P., Gesierich, B., Rozzi, S., Chersi, F., Rizzolatti, G.: Parietal lobe: From action organization to intention understanding. Science 308, 662–667 (2005)
2. Gallese, V., Fadiga, L., Fogassi, L., Rizzolatti, G.: Action recognition in the premotor cortex. Brain 119, 593–609 (1996)
3. Schaffler, L., Luders, H., Dinner, D., Lesser, R., Chelune, G.: Comprehension deficits elicited by electrical stimulation of broca's area. Brain 116, 695–715 (1993)
4. Gazzola, V., Keysers, C.: The observation and execution of actions share motor and somatosensory voxels in all tested subjects: Single-subject analyses of unsmoothed fmri data. Cerebral Cortex 19, 1239–1255 (2009)
5. Iacoboni, M., Woods, R., Brass, M., Bekkering, H., Mazziotta, J., Rizzolatti, G.: Cortical mechanisms of human imitation. Science 286, 2526–2528 (1999)
6. Ramachandran, V.: Mirror neurons and imitation learning as the driving force behind "the great leap forward" in human evolution. Edge 69 (2000)
7. Rizzolatti, G., Fogassi, L., Gallese, V.: Neurophysiological mechanisms underlying the understanding and imitation of action. Nature Reviews Neuroscience 2, 661–670 (2001)
8. Rizzolatti, G., Arbib, M.: Language within our grasp. Trends in Neurosciences 21, 188–194 (1998)
9. Gallese, V., Goldman, A.: Mirror neurons and the simulation theory of mind reading. Trends in Cognitive Sciences 2, 493–500 (1998)
10. Ramachandran, V., Oberman, L.: Broken mirrors: A theory of autism. Scientific American 295, 62–69 (2006)
11. Ojemann, G., Ojemann, J., Lettich, E., Berger, M.: Cortical language localization in left, dominant hemisphere: An electrical stimulation mapping investigation in 117 patients. Neurosurgery 71, 316–326 (1989)
12. Whiten, A., Ham, R.: On the nature and evolution of imitation in the animal kingdom: Reappraisal of a century of research. Advances in the Study of Behavior 21, 239–283 (1992)
13. Whiten, A., Custance, D., Gomez, J., Teixidor, P., Bard, K.: Imitative learning of artificial fruit processing in children (homo sapiens) and chimpanzees (pan troglodytes). Comparative Psychology 110, 3–14 (1996)
14. Whiten, A.: Imitation of sequential and hierarchical structure in action: Experimental studies with children and chimpanzees. In: Cambridge, M.P. (ed.) Imitation in Animals and Artifacts, MA, USA, pp. 191–209 (2002)

15. Tomasello, M., Davis-Dasilva, M., Camak, L., Bard, K.: Observational learning of tool use by young chimpanzees and enculturated chimpanzees. Human Evolution 2, 175–183 (1987)
16. Tomasello, M.: Emulation learning and cultural learning. Behavior and Brain Science 21, 703–704 (1998)
17. Wood, D.: Social interaction as tutoring. In: Bornsten, M.H., Bruner, J. (eds.) Interaction in Human Development, Hillsdale, NJ, USA, pp. 59–80 (1989)
18. Whiten, A.: The scope of culture in chimpanzees, humans and ancestral apes. Philosophical Transactions of the Royal Society 366, 935–1187 (2011)
19. Galef, B.: The question of animal culture. Human Nature 3, 157–178 (1992)
20. Heyes, C.: Imitation, culture and cognition. Animal Behavior 46, 999–1010 (1993)
21. Tomasello, M., Savage-Rumbaugh, E., Kruger, A.: Imitative learning of actions on objects by children, chimpanzees and enculturated chimpanzees. Child Development 64, 1688–1705 (1993)
22. Buchsbaum, D., Griffiths, T., Gopnik, A., Baldwin, D.: Learning from actions and their consequences: Inferring causal variables from continuous sequences of human action. In: Proceedings of the 31st Annual Conference of the Cognitive Science Society (2009)
23. Buchsbaum, D., Canini, K., Griffiths, T.: Segmenting and recognizing human action using low-level video. In: Proceedings of the 33rd Annual Conference of the Cognitive Science Society (2011)
24. Tani, J.: Learning to generate articulated behavior through the bottom-up and the top-down interaction processes. Neural Networks 16, 11–23 (2003)
25. Tani, J., Ito, M., Sugita, Y.: Self-organization of distributedly represented multiple behavior schemata in a mirror system: Reviews of robot experiments using rnnpb. Neural Networks 17, 1273–1289 (2004)
26. Issar, S., Ward, W.: Cmu's robust spoken language understanding system. In: Proceedings of the 3rd European Conference on Speech Communication and Technology, EUROSPEECH (1993)
27. Bennacef, S., Bonnea-Maynard, H., Gauvain, J., Lamel, L., Minker, W.: A spoken language system for information retrieval. In: Proceedings of the 3rd International Conference on Spoken Language Processing, ICSLP (1994)
28. Miller, S., Bobrow, R., Schwartz, R., Ingria, R.: Statistical language processing using hidden understanding models. In: Proceedings of the Human Language Technology Workshop, NJ, USA (1994)
29. Levin, E., Pieraccini, R.: Concept-based spontaneous speech understanding system. In: Proceedings of the 4th European Conference on Speech Communication and Technology, EUROSPEECH (1995)
30. Goldberg, E., Driedger, N., Kittredge, R.: Using natural language processing to produce weather forecasts. IEEE Intelligent Systems and their Applications 9, 45–53 (1994)
31. Busemann, S.: Ten years after: An update on tg/2 (and friends). In: Proceedings of the European Natural Language Generation Workshop (2005)
32. Mcroy, S., Channarukul, S., Ali, S.: An augmented template-based approach to text realization. Natural Language Engineering 9, 381–420 (2003)
33. Bateman, A.: Enabling technology for multilingual natural language generation: The kmpl development. Natural Language Engineering 3, 15–55 (1997)
34. Lavoie, B., Rambow, O.: A fast and portable realizer for text generation. In: Proceedings of the 5th Conference on Applied Natural-Language Processing, ANLP (1997)

35. Gergely, G.: What should a robot learn from an infant? mechanisms of action interpretation and observational learning in infancy. Connection Science 15, 191–209 (2003)
36. Kozima, H., Nakagawa, C., Yano, H.: Emergence of imitation mediated by objects. In: Proceedings of the 2nd International Workshop on Epigenetic Robotics (2002)
37. Rudolph, M., Muhlig, M., Gienger, M., Bohme, H.: Learning the consequences of actions: Representing effects as feature changes. In: Proceedings of the International Symposium on Learning and Adaptive Behavior in Robotic System (2010)
38. Murray, I., Arnott, J.: Toward the simulation of emotion in synthetic speech: A review of the literature on human vocal emotion. Journal of the Acoustical Society of America 93, 1097–1108 (1993)
39. Cahn, J.: Generating expression in synthesized speech. In Master's thesis, MIT Media Lab, USA (1990)
40. Roy, D., Pentland, A.: Automatic spoken affect analysis and classification. In: Proceedings of the 2nd International Conference on Automatic Face and Gesture Recognition, Vermont, USA (1996)
41. Slaney, M., McRoberts, G.: Baby ears: A recognition system for affective vocalizations. In: Proceedings of the 1998 International Conference on Acoustics, Speech, and Signal Processing (ICASSP), Seattle, USA (1998)
42. Breazeal, C., Aryananda, L.: Recognition of affective communicative intent in robot-directed speech. Autonomous Robots Journal 12, 83–104 (2002)
43. Vogt, T., Andre, E.: Improving automatic emotion recognition from speech via gender differentiation. In: Proceedings of the Language Resources and Evaluation Conference, LREC 2006 (2006)
44. Voeffra, C.: Emotion-sensitive human-computer interaction (hci): State of the art. In: Seminar Emotion Recognition (2011), http://diuf.unifr.ch/main/diva/teaching/seminars/emotion-recognition
45. Pierre-Yves, O.: The production and recognition of emotions in speech: features and algorithms. Human-Computer Studies 59 (2003)
46. Jones, C., Deeming, A.: Affective human-robot interaction. In: Peter, C., Beale, R. (eds.) Affect and Emotion in Human-Computer Interaction: From Theory to Applications, pp. 175–185 (2008)
47. Zadeh, L.: Fuzzy sets. Information and Control 8, 338–353 (1965)
48. Zadeh, L.: Outline of a new approach to the analysis of complex systems and decision processes. IEEE Transactions on Systems, Man, and Cybernetics 3, 28–44 (1973)
49. Mamdani, E., Assilian, S.: An experiment in linguistic synthesis with a fuzzy logic controller. International Journal of Man-Machine Studies 7, 1–13 (1975)
50. Takagi, T., Sugeno, M.: Fuzzy identification of systems and its application to modeling and control. IEEE Trans. on Systemsm Man, and Cybernetics 15, 116–132 (1985)
51. Sugeno, M.: Industrial applications of fuzzy control. Elsevier Science Pub. Co. (1985)
52. Bezdek, J.: Pattern recognition with fuzzy objective function algorithms. Plenum Press, New York (1981)
53. Vapnik, V.: Statistical learning theory. In: Haykin, S. (ed.) Adaptive and Learning Systems. John Wiley and Sons (1998)
54. Dunn, J.: A fuzzy relative of the isodata process and its use in detecting compact well-separated clusters. Journal of Cybernetics 3, 32–57 (1973)
55. Gustafsson, D., Kessel, W.: Fuzzy clustering with a fuzzy covariance matrix. In: Proceedings of the IEEE CDC, San Diego, CA, USA, pp. 761–766 (1979)

56. Gath, I., Geva, A.: Unsupervised optimal fuzzy clustering. IEEE Trans. on Pattern Analysis and Machine Intelligence 11, 773–781 (1989)
57. Yager, R., Filev, D.: Approximate clustering via the mountain method. In Technical Report MII 1305, Machine Intelligence Institute, Iona College, New Rochelle (1992)
58. Yager, R., Filev, D.: Learning of fuzzy rules by mountain clustering. In: Proceedings of SPIE Conference on Applications of Fuzzy Logic Technology, Boston, MA, pp. 246–254 (1993)
59. Chiu, S.: Fuzzy model identification based on cluster estimation. Journal of Intelligent and Fuzzy Systems 2, 267–278 (1994)
60. Searle, J.: Austin on locutionary and illocutionary acts. The Philosophical Review 77, 405–424 (1968)
61. Searle, J.: Speech acts: An essay in the philosophy of language. Cambridge University Press (1969)
62. Goldberg, L.: An alternative description of personality: The big-five factor structure. Personality and Social Psychology 59, 1216–1229 (1990)
63. Aly, A., Tapus, A.: A model for synthesizing a combined verbal and nonverbal behavior based on personality traits in human-robot interaction. In: Proceedings of the 8th ACM/IEEE International Conference on Human-Robot Interaction, HRI (2013)
64. Summers-Stay, D., Teo, C., Yang, Y., Fermuller, C., Aloimonos, Y.: Using a minimal action grammar for activity understanding in the real world. In: Proceedings of the IEEE/RSJ International Conference on Intelligent Robots and Systems, IROS (2012)
65. Pastra, K., Aloimonos, Y.: The minimalist grammar of action. Philosophical Transactions B 367, 103–117 (2012)
66. Izard, C.: Face of emotion. Appleton, New York (1971)
67. Plutchik, R.: The nature of emotions. University Press of America, Lanham (1991)
68. Ekman, P.: Emotion in the human face: Guidelines for research and an integration of findings. Pergamon Press, New York (1972)
69. Ekman, P., Friesen, W., Ellsworth, P.: What emotion categories or dimensions can observers judge from facial behavior? In: Ekman, P. (ed.) Emotion in the Human Face. Cambridge University Press, New York (1982)
70. Izard, C.: Human emotions. Plenum Press, New York (1977)
71. Tomkins, S.: Affect theory. In: Scherer, K., Ekman, P. (eds.) Approaches to Emotion, pp. 163–195. Erlbaum, Hillsdale (1984)
72. Cortes, C., Vapnik, V.: Support-vector networks. Machine Learning 20, 273–297 (1995)
73. Burkhardt, F., Paeschke, A., Rolfes, M., Sendlmeier, W., Weiss, B.: A database of german emotional speech. In: Proc. of Interspeech, Germany (2005), `http://database.syntheticspeech.de`
74. Banse, R., Scherer, K.: Acoustic profiles in vocal emotion expression. Journal of Personality and Social Psychology 70, 614–636 (1996)
75. Montero, J., Gutierrez-Arriola, J., Palazuelos, S., Enriquez, E., Aguilera, S., Pardo, J.: Emotional speech synthesis: from speech database to tts. In: Proceedings of the International Conference on Spoken Language Processing 1998, pp. 923–925 (1998)
76. Talkin, D.: A robust algorithm for pitch tracking. In: Kleijn, W.B., Paliwal, K. (eds.) Speech Coding and Synthesis, pp. 497–518. Elsevier (1995)
77. Sondhi, M.: New methods of pitch extraction. IEEE Trans. Audio and Electroacoustics 16, 262–266 (1968)

78. Rabiner, L., Atal, B., Sambur, M.: Lpc prediction error: Analysis of its variation with the position of the analysis frame. IEEE Trans. on Systems Man, and Cybernetics 25, 434–442 (1977)
79. Rong, J., Li, G., Chen, Y.P.: Acoustic feature selection for automatic emotion recognition from speech. Information Processing and Management 45, 315–328 (2008)
80. Cristianini, N., Shawe-Taylor, J.: Introduction to support vector machines. Cambridge University Press (2000)
81. Platt, J.: Fast training of support vector machines using sequential mininal optimization. In Microsoft Research Technical Report MSR-TR-98-14 (1998)
82. Angelov, P.: Evolving rule-based models: A tool for design of flexible adaptive systems. STUDFUZZ, vol. 92. Springer, Heidelberg (2002)
83. Aly, A., Tapus, A.: Towards an online real time fuzzy modeling for human internal states detection. In: Proceedings of the 12th IEEE International Conference on Control, Automation, Robotics and Vision, ICARCV (2012)

Tacit Learning – Machine Learning Paradigm Based on the Principles of Biological Learning

Shingo Shimoda

Autonomous Behavioral Control unit, RIKEN, BSI-TOYOTA collaboration center, 2271-130,
Anagahora, Shimo-shidami, Moriyama-ku Nagoya, Aichi, 463-0003, Japan
shimoda@brain.riken.jp

1 Introduction

Adaptations to unpredictable environmental changes enable living organisms to survive in their natural environments and are therefore the highest-priority tasks for all of them. In the long history of evolution, living organisms have developed regulatory systems that can adapt their activities to the environment and, as a result have been able to extend their activity fields to almost all places on the earth.

One of the most curious features of biological regulatory systems is the method of computations for the regulations. All the computations in biological systems are carried out by the activities of homogeneous computational media, and networks of these computational media deal with all environmental inputs relevant to an organism's survival. Neurons in a brain[1][2], protein-protein interactions in intracellular regulations[3], and T- and B- cell activities in adaptive immune systems[4] are prominent examples of computational media.

The most important feature of these regulatory systems is that the accumulation of the local activities of the computational media can adapt the global activity of their network to the environment without any supervising signals from the global point of view. Let us take behavior control by the brain as an example. The brain is a network of neurons whose activity rules are genetically defined. The neurons modify their synaptic connections, the amount of neurotransmitters they release, the conductances of their ion channels, and so on according to their innate rules. Behaviors are gradually changed to ones more adapted to the environment as a result of the accumulation of each neuron's activities even though nothing is supervising the behavior adaptation from the global point of view.

Another important feature of these biological regulation systems is that the control and the adaptation progress without an explicit distinction between them[5]. The environmental information taken into the controller through the behavior control is used to tune the behaviors. This feature of biological regulatory systems makes it possible to adapt behaviors to the continuously changing natural environment in everyday life. Figure 1 is a conceptual image of the regulation-by-brain system. When a living organism moves, a feedback loop including the environment, the body, and the brain is constructed. The inputs from

S. Mohammed et al. (eds.), *Intelligent Assistive Robots*,
Springer Tracts in Advanced Robotics 106, DOI: 10.1007/978-3-319-12922-8_8

the environment stimulate the neurons in the brain through the sensors, and the activities of the neurons create behaviors that influence the environment. In this feedback loop, behaviors are gradually adapted to the environment in parallel with behavior creations by accumulating the activities of the neurons even though each neuron does not recognize the state of the whole environment.

Although recent studies have succeeded in clarifying the details of biological computational media[6]–[8] and their network structures[9][10], the process of organizing the activities of computational media and creating global behaviors adapted to the environment remains an attractive research topic. Some attempts have been made to associate the activities of computational media with the global functions of their networks[11]–[17]. These analyses, however, have clarified only a few functions of biological regulations in static environments or in environments with controlled changes.

The construction of artificial controllers that are capable of adapting to unpredictable changes is an interesting approach useful for understanding the adaptation process because adaptation processes in artificial systems can be easily analyzed than those in biological systems[18]. Recent advances in artificial learning and adaptive methods for robot control, however, have not reached the level of adaptability of biological systems[19]–[32]. One of the most critical problems with conventional approaches is the way of specifying goals of learning. The goals of learning in many cases are specified in advance by using supervising signals such as teaching signals in neural networks[19]–[21], cost functions in genetic algorithm[25][26], and reference signals in adaptive control[27][28], that are not changed during learning even though the environments have changed. It would be difficult to adapt to environmental changes in learning that was supervised by fixed signals. Nowadays, these is a rapidly growing social demand for robots as real partners of human beings in role such as caring for the elderly, disaster rescue and rehabilitation assistance, which obviously require high levels of adaptability. The development of artificial controllers with high levels of adaptability is now an imminent problem facing the field of robotics, not just for understanding biological systems.

In this chapter we discuss this problem in the context of the novel learning algorithm called *Tacit Learning*[33][34]. Tacit learning is an unsupervised learning scheme based on the above features of biological regulatory systems. One of the most important points of tacit learning is that the learning process and the behavior control process progress in parallel. Roughly defined motions are modified into sophisticated behaviors adapted to the environment through body/environment interactions. All computations for behavior modifications by tacit learning are governed by the autonomous activities of the artificial computational media.

Another feature of tacit learning is the definition of the behavior target. In tacit learning, the behavior target is defined as the constraint conditions that should be achieved independent of the environmental situations. *Survival* is the ultimate constraint condition of tacit learning because all living organisms must achieve this condition independent of the environmental situation. In the case of

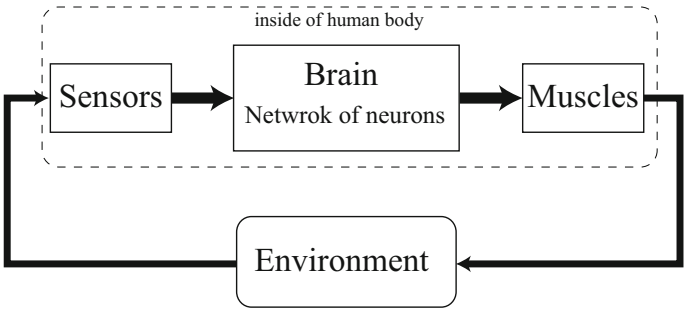

Fig. 1. Conceptual image of biological control loop

the learning of bipedal walking by tacit learning [34], the motions of the swing leg are used as the constraint conditions that could correspond to walking reflexes observed as the instinctive behaviors of newborn babies[35]. The target behavior in tacit learning is therefore strongly related to our instinctive behaviors. The way of specifying the instinctive behaviors for tacit learning is discussed in the following sections.

This chapter is organized as follows: Section 2 explains the features of tacit learning and the way of specifying target behaviors. Section 3 provides typical examples of tacit learning with experimental results obtained using a 2DOF manipulator and discusses the process of acquiring the environmental information based on the precise models of the manipulator and the networks. Section 4 presents the adaptability of tacit learning in terms of the energy consumption, walking rhythm tuning and robustness through the bipedal walking experiments using a 36DOF humanoid robot. Section 5 concludes this chapter.

2 Tacit Learning

The basic idea of tacit learning is the learning of robot behaviors adapted to the environment through body-environment interactions. The robot initially has roughly defined motions consisting of reflexive actions and instinctive behaviors, and tacit learning modifies these motions into sophisticated behaviors adapted to the environment.

2.1 Features of Tacit Learning

The fundamental idea of tacit learning is derived from the features of biological regulatory systems in which all regulations result from the spatial and temporal integration of simple and homogeneous computational media. Based on this characteristic of biological systems, tacit learning is characterized by four features. First, the controller for tacit learning is a network of homogeneous computational media. Learning progresses through accumulating the individual

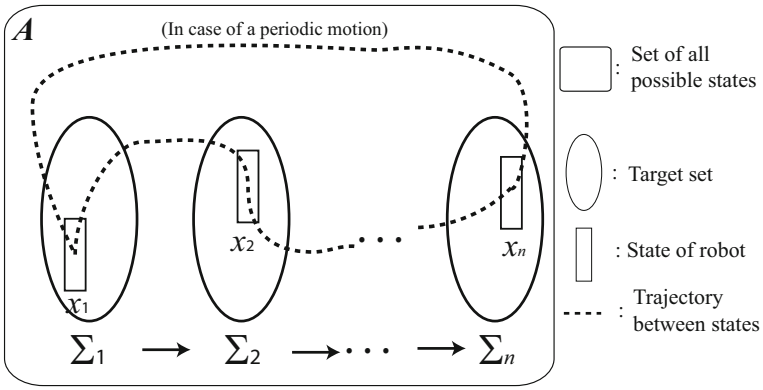

Fig. 2. Conceptual image of a task and its execution

activities of computational media that operate according to innate rules. Second, the sensor-motor connections in the network are organized such that sensor inputs are reduced by motor actions. These innate connections create reflexive actions through body-environment interactions. The combination of these reflexive actions generates primitive motions taking the environmental information into the network. Third, the target behavior is embedded in the network as the constraint conditions that should be achieved independent of the environment. Fourth, no supervising signal is used in the learning process. The learning progresses by accumulating the environmental information inside the network by the activities of the computational media. This learning strategy makes it possible for the behavior control and the behavior adaptation to progress in parallel.

2.2 Definition of Target Behavior for Tacit Learning

Tacit learning should be discussed with specified target behaviors because tacit learning is the way of tuning roughly defined behaviors to sophisticated ones. In the learning of bipedal walking discussed in [36], the specified target behavior was the part of walking locomotion that swung the legs forward alternately. Balance and walking rhythm emerged through tacit learning depending on the condition of the walking surface and the weight of the robot.

We can rigorously define the way of specifying target behaviors as *task* for tacit learning. Let $\boldsymbol{x}$ denote the vector representing the state of a plant to be controlled such that the behavior is described by a transition of $\boldsymbol{x}$ from an initial state to a specified state. For example, the motions of an n-DOF arm are described by the transition of the state of the joint space, $\boldsymbol{x} = [\theta_1\ \theta_2\ \cdots \theta_n]^T$, where, θ_i denotes the angle of Joint i. The target behavior is transition of $\boldsymbol{x}$ from an initial state to a specified state in the state space. These specified states are called *target states*.

State space is usually very large especially in the learning of devices with many degree of freedoms, while the target states frequently involve only a handful of degree of freedoms. Let us take as an example the learning of the motion of picking up an object by using a redundant arm. One of the target states in the motion should be the posture in which the end-effector of the arm reaches the object, which is not unique to redundant arms. In such cases, the target state can be expressed as the set in which every states $\boldsymbol{x}$ can reach to the object. The posture can be chosen from the set depending on the environment such as the position of obstacles. We call the set of the target states a *target set*.

The task for tacit learning is defined as a series of target sets. Figure 2 is a conceptual image illustrated the definition of the task. $\boldsymbol{A}$ and $\boldsymbol{\Sigma_i}$ denote a set of all possible states of $\boldsymbol{x}$ and the target sets, respectively. In the case of bipedal walking, the target sets are defined by the motions of the swing leg. The motions of the supporting leg and other joints are chosen from the target sets. The behaviors of the plant to be controlled are created by choosing trajectories that connect the target sets, and the behaviors may be ones adapted to the environment when appropriate trajectories are chosen. As mentioned in the previous section, we use tacit learning to choose the trajectories for creating adapted behaviors by acquiring environmental information through the reflexive actions.

3 Behavior Learning of 2DOF Manipulator by Tacit Learning

3.1 Network Structures for Tacit Learning

Tacit learning is executed through accumulating the activities of computational media. We proposed artificial computational media [36] whose activities were fundamentally governed by the classical McCulloch-Pitts neuron model[37], which has two states, firing denoted by 1 and rest denoted by 0. The difference between our model and the original McCulloch-Pitts model is the threshold modification to maintain the firing frequency in an appropriate range. That is, our neurons are variable-threshold neurons (VTNs), and each neuron's threshold is increased when the neuron fires and decreased when it rests. The neuron model is described as follows:

$$X(t) = \mathbb{1}(s(t) - \theta(t)) \tag{1}$$

$$\mathbb{1}(u) = \begin{cases} 1 & u \geq 0 \\ 0 & u < 0 \end{cases} \tag{2}$$

$$\theta(t+1) = \theta(t) + \overline{\Delta\theta} X(t) + \underline{\Delta\theta}(X(t) - 1) \tag{3}$$

where $X(t)$, $s(t)$, $\theta(t)$, $\overline{\Delta\theta}$, and $\underline{\Delta\theta}$ denote, respectively, the neuron state at time t, the input to the neuron, the threshold of the neuron, and the values for threshold tuning after firing and rest.

Another activity rule of VTNs is a way of changing the connection weight between them. We extend the Hebbian rule[38] to increase the stability of the

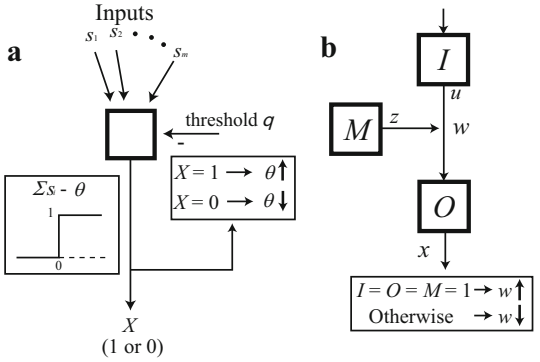

Fig. 3. Activity rules of variable-threshold neuron

network connections. According to the Hebbian rule, the connection weight between two VTNs, I and O, connected as illustrated in Fig. 3 **b** would increase if they fired simultaneously and decrease if they fired separately. We extend this rule by introducing another VTN called a *mediator* (M) so that the connection weight increases if I, O and M are simultaneously fired, otherwise decreases. The extended hebbian rule is described as follows:

$$w(t+1) - w(t) = \overline{\Delta w} x(t)u(t)z(t) + \underline{\Delta w}(x(t)u(t)z(t) - 1) \tag{4}$$

where $x(t)$, $u(t)$, and $z(t)$ correspond, respectively, to the states of O, I and M at t. If both $\overline{\Delta w}$ and $\underline{\Delta w}$ are positive, Eq. (4) is called *potentiation*, and if they are negative, it is called *inhibition*. We take the convention of using a bar to indicate a mediator action of inhibition. Note that both $\overline{\Delta\theta}$ and $\underline{\Delta\theta}$ are positive, while $\overline{\Delta w}$ and $\underline{\Delta w}$ can be negative.

A network of VTNs has strong computational power such as four arithmetic operations, conditioned reflexes, and input accumulation by selecting appropriate threshold patterns[36]. We have developed two networks based on these computational powers. One is an output regulation network, that can find the appropriate threshold pattern of VTNs to constrain the state of an unknown plant to a specified reference, and the other is a self-reference generation network, that can find the threshold pattern that can reduce the quantity of input to the plant by creating a control reference through body-environment interactions.

Block diagrams of the overall network configurations are shown in Fig. 4, where controller C is a network of VTNs that is composed of a serise of VTNs and is called a *cluster* (Fig. 5 **a**). The output from the cluster is the number of firing VTNs. The initial values of all thresholds in the cluster are set such that they are equally distributed in a single band of width $\alpha + \beta$. Here, α and β respectively denote the values for threshold incremental step $\overline{\Delta\theta}$ and decremental step $\underline{\Delta\theta}$ in Eq. (3). Under this assumption on the thresholds, the output from the cluster becomes 0 when the input is smaller than any of the thresholds, and all the VTNs fire when the input is larger than all the thresholds. Actually, the

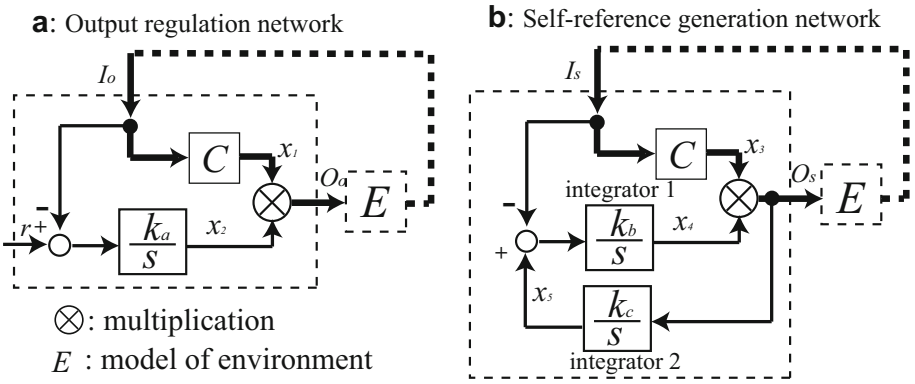

Fig. 4. Block diagrams of **a** output regulation network and **b** self-reference generation network

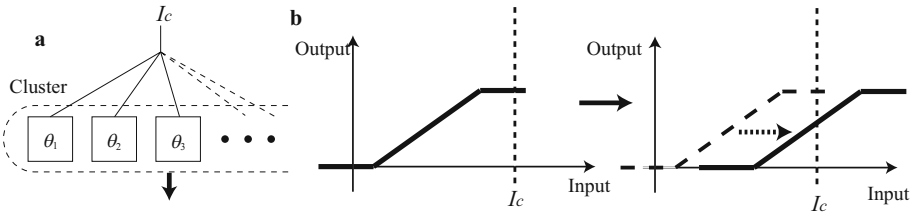

Fig. 5. Features of cluster: **a** Cluster is a group of VTNs that have same inputs. Output from a cluster is the number of firing VTNs. **b** Output reaches a saturation value. Tuning VTN thresholds moves the non-saturated area toward the input.

output from the cluster becomes the saturation system described in Fig. 5 **b**. An interesting feature of the cluster activity is that the non-saturated area moves depending on the output from the cluster to bring the non-saturated area closer to the input value. Tuning the thresholds of VTNs accroding to the rules Eqs. (1)-(3) results in the non-saturated area converging to the value appropriate to the environment. The mathematical expression for the activity of the cluster is given in the Appendix.

As described in Fig. 4 **a**, the output regulation network's output O_o is the value obtained by multiplying the cluster output x_1 by the integrator output x_2, which is the integral value of the difference between the reference r and the input I_o. At the equilibrium state of the output regulation network, the input I_o converges to the reference r and the cluster finds the appropriate threshold patterns in the environment. The control loop shown by the thick lines acts as a reflexive response. The role of this loop is discussed, along with the experimental results, in the next subsection.

In the self-reference generation network, the reference signal in the output regulation network is replaced by the result of integrating output O_s. The O_s should be 0 at the equilibrium state, otherwise the output x_5 from the integrator continues changing. Thus the self-reference generation network can find the appropriate threshold pattern that tunes the output from the network to 0 if the environment allows this. The mathematical expressions of these network activities are given in the Appendix.

3.2 Posture Control of 2DOF Manipulator by Tacit Learning

To experimentally demonstrate the process of creating behaviors by tacit learning, we gave the 2DOF manipulator shown in Fig. 6 **a** the task of making a specified angle in the upper joint, called Joint 2, from the vertically standing posture as shown in Fig. 6 **b** and **c**. In this task, the angle of the lower joint (Joint 1) was not specified but was chosen from the target set by tacit learning. The target set $\boldsymbol{\Sigma}$ of this task is described as follows:

$$\boldsymbol{\Sigma} = \{(\theta_1,\ \theta_2) \mid \forall\theta_1,\ \theta_2 = \theta_d\}, \tag{5}$$

which can be expressed as a line in the Cartesian space of θ_1 and θ_2 illustrated in Fig. 7. Here, θ_1 and θ_2 denote the angles of Joints 1 and 2, and θ_d denotes the desired angle of Joint 2.

As described in Fig. 8 we used the self-reference generation network to control Joint 1 and the output regulation network to control Joint 2. The plant in this configuration can be described as follows:

$$\boldsymbol{M}\begin{bmatrix}\ddot{\theta}_1\\ \ddot{\theta}_2\end{bmatrix} + \boldsymbol{B} = \boldsymbol{U} \tag{6}$$

$$\boldsymbol{Y} = \boldsymbol{C}\boldsymbol{\theta} \tag{7}$$

$$\boldsymbol{M} = \begin{bmatrix} I_1 + m_1a_1^2 + l_1^2m_2 + \zeta + 2\xi\cos\theta_2 & \zeta + \xi\cos\theta_2 \\ \zeta + \xi\cos\theta_2 & \zeta \end{bmatrix} \tag{8}$$

$$\boldsymbol{B} = \begin{bmatrix} -\xi(2\dot{\theta}_1 + \dot{\theta}_2)\dot{\theta}_2\sin\theta_2 + k_1\cos\theta_1 + k_2\cos(\theta_1 + \theta_2) \\ \xi\dot{\theta}_1^2\sin\theta_2 + k_2\cos(\theta_1 + \theta_2) \end{bmatrix} \tag{9}$$

$$\boldsymbol{U} = \begin{bmatrix} u_1\ u_2 \end{bmatrix}^T \tag{10}$$

$$\boldsymbol{Y} = \begin{bmatrix} y_1\ y_2 \end{bmatrix}^T \tag{11}$$

$$\boldsymbol{C} = \begin{bmatrix} 1.0\ 0.1\ 0.0\ 0.0 \\ 0.0\ 0.0\ 1.0\ 0.1 \end{bmatrix} \tag{12}$$

$$\boldsymbol{\theta} = \begin{bmatrix} \theta_1\ \dot{\theta}_1\ \theta_2\ \dot{\theta}_2 \end{bmatrix}^T \tag{13}$$

$$\zeta = I_2 + m_2a_2^2 \tag{14}$$

$$\xi = l_1m_2a_2 \tag{15}$$

$$k_1 = (m_1a_1 + m_2l_1)g \tag{16}$$

$$k_2 = m_2a_2g \tag{17}$$

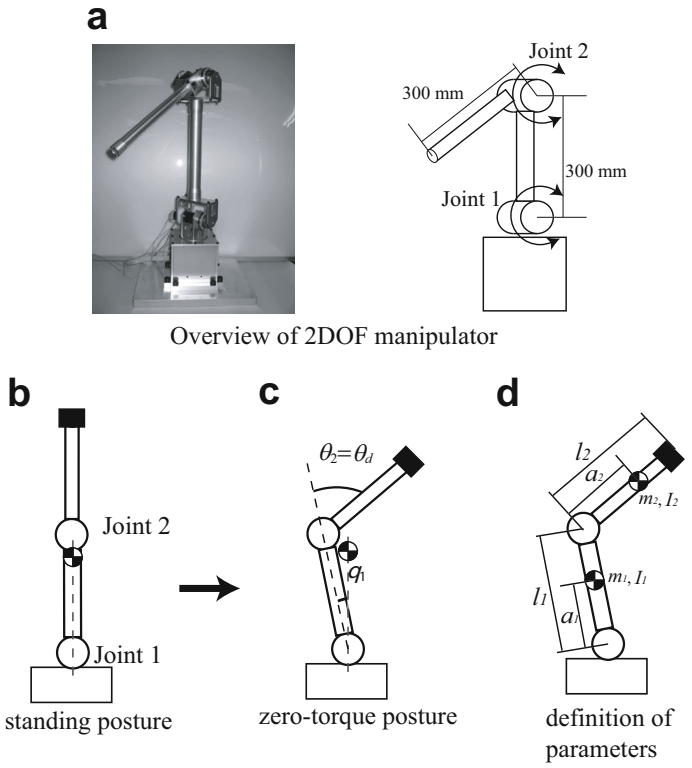

Fig. 6. 2DOF manipulator:**a** Overview of 2DOF manipulator **b** Posture of manipulator standing vertically **c** When the angle of the upper joint is specified and lower joint remains free to be adapted to the environment, the posture in which the center of mass of the manipulator is on a vertical line passing through the attachment point of the lower joint is called the zero-torque posture. **d** Definition of parameters

I_i : Inertia moment of each arm (See Fig.6)
l_i : Length of arm
a_i : Length from joint to center of gravity
m_i : Mass of arm (m_2 includes mass of payload.)

The most interesting feature of this experiment is how the self-reference generation network for Joint 1 finds its values during learning. Figure 9 illustrates the experimental results. A payload with amass of 360g was attached to the top of the manipulator in this experiment. The angle of Joint 2 smoothly converged to the pre-defined reference, which was $\pi/4$ rad in this experiment. Joint 1 was first rotated in the positive direction because the balance of the manipulator was disrupted by the motion of Joint 2. The reflexive action that was mainly

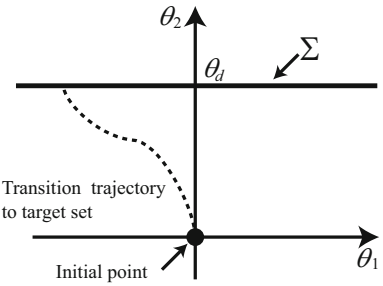

Fig. 7. Representation of target set $\boldsymbol{\Sigma}$ in Cartesian space. The state in $\boldsymbol{\Sigma}$ and the trajectory to the state were chosen through body-environment interaction.

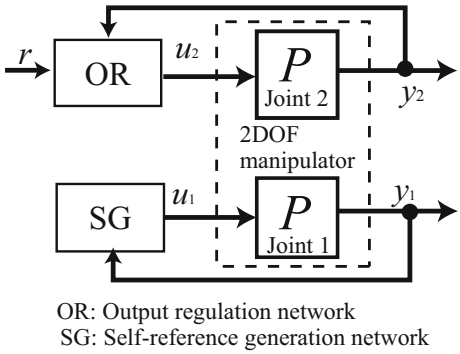

Fig. 8. Controller configuration for 2DOF manipulator control: The output regulation network was used to control the upper joint (Joint 2) and the self-reference generation network was used to control the lower joint (Joint 1).

controlled by the loop shown by the thick lines in Fig. 4 **b** appeared immediately after this rotation of Joint 1. The reflexive action of Joint 1 stimulated other network loops in Fig. 4 **b**. As shown in Fig. 9 **c**, the angle of Joint 1 finally converged to -0.26 rad, where the manipulator could be kept balanced without applying torque to Joint 1 . Through tacit learning, the self-reference generation network worked to find a *zero-torque posture* in which no torque was applied to Joint 1.

The equilibrium point of the self-reference generation network is described as follows:

$$y_1(t) = x_5(t),\ x_4(t) = 0.0,\ u_1(t) = 0.0,\ x_3(t) = \frac{N\beta}{\alpha + \beta}, \tag{18}$$

where N denotes the number of VTNs in the cluster. The details on the derivation of the equilibrium point can be found in the Appendix. Under the mechanical limitation of Joint 1 which was $-\pi < \theta_1 < \pi$, the angle of Joint 1 at the

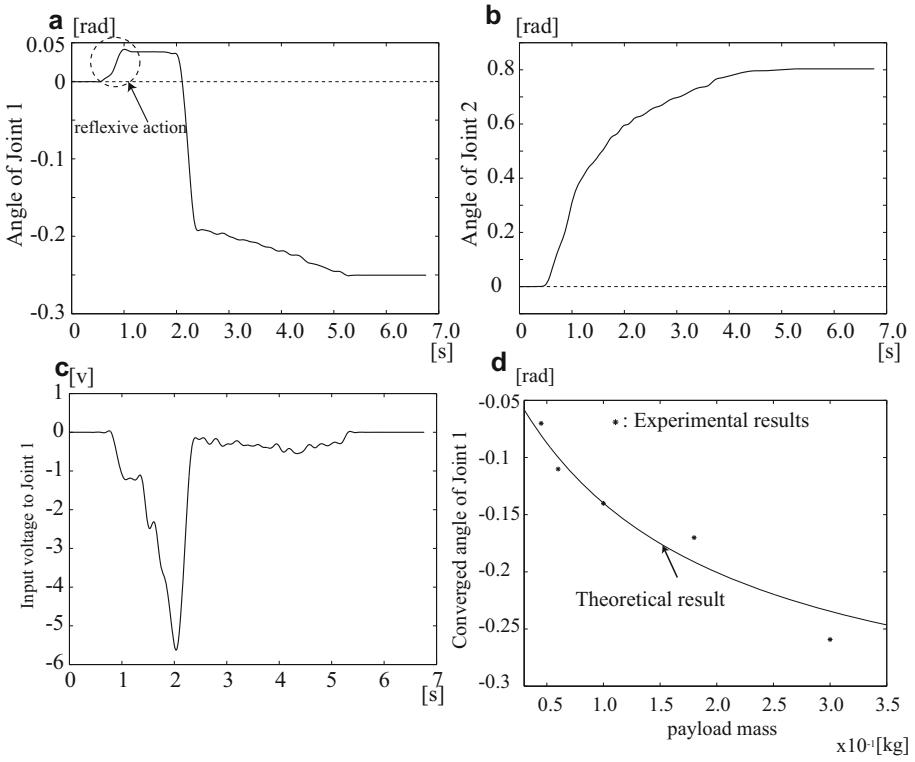

Fig. 9. Experimental results:**a** time history of angle of Joint 1 **b** time histories of angle of Joints 2 **c** time history of voltage working on Joint 1 **d** converged angle of Joint 1 as a function of payload mass

equilibrium point becomes

$$\theta_1 = \tan^{-1}\left(\frac{k_2 \cos\theta_d + k_1}{k_2 \sin\theta_d}\right), \tag{19}$$

which corresponds to a zero-torque posture. The reflexive action led the angle of Joint 1 to the above equilibrium angle, which was determined by the environment, the body parameters of the manipulator, and the specified angle of Joint 2.

The reflexive action of Joint 1 was created by body-environment interaction, which in this case was the loss of balance caused by gravitational force acting on the manipulator body. Thus when the body parameters were changed, the motion of Joint 1 automatically changed. $*$ in Fig. 9 **d** shows the converged angles of Joint 1 obtained with various payload masses. Without information to the network about the changes, the angle of Joint 1 converged to the neighborhood of the equilibrium point calculated using Eq. (18) (solid line in Fig. 9 **d**).

3.3 Emergence of Reciprocating Motion

Next, we gave alternative θ_d to Joint 1, $\theta_1 = 0$ and $\theta_d = \pi/4$ as described in Fig. 6 **b** and **c**. The target sets of these two postures are defined as follows:

$$\boldsymbol{\Sigma}_1 = \{(\theta_1,\ \theta_2) \mid \theta_1 = 0.0,\ \theta_2 = 0.0\} \tag{20}$$

$$\boldsymbol{\Sigma}_2 = \{(\theta_1,\ \theta_2) \mid \forall\theta_1,\ \theta_2 = \pi/4\} \tag{21}$$

Here, the target set Σ_1 is reduced to a single point representing the standing posture without applying torques to both joints. When the manipulator was moved from Σ_1 to Σ_2, the controllers described in Fig. 4 were used. When it moved in reverse from Σ_2 to Σ_1, both joints were controlled by the output regulation networks. The control direction was switched when the states of the manipulator were sufficiently close to Σ_1 and Σ_2.

Experimental results obtained with a 306 g payload are shown in Fig. 10. The periodic motion appeared after several reciprocating motions, in which zero-torque postures in Σ_2 were chosen. This result implies that the periodic motion was created between the equilibrium points in Σ_1 and Σ_2.

4 Learning of Bipedal Walking by Tacit Learning

This section describes experiments in which we applied tacit learning to a much more complex bipedal walking problem and investigated how well the behaviors created by tacit learning were adapted to the environment.

4.1 Definition of Task for Bipedal Walking

We used the 36DOF humanoid robot described in Fig. 11 in the experiments. As discussed in Section 2, the motions of putting the legs forward alternately were used . Actually, we took as the target sets four postures in one step (Table 1). In target set, we specified the desired angles of some joints on the swing leg and didn't specify the motion of the supporting leg like Joint 1 in the 2DOF manipulator experiments. The output regulation networks were used to control the specified joints and the self-reference regulation networks were used for the other joints.

4.2 Experiments on Bipedal Walking

The reference values for the specified joints in the experiments are summarized in Table 1. The target set was switched to the next one when the specified angles converged to the references. To create periodic motion, Σ_8 and Σ_1 were connected.

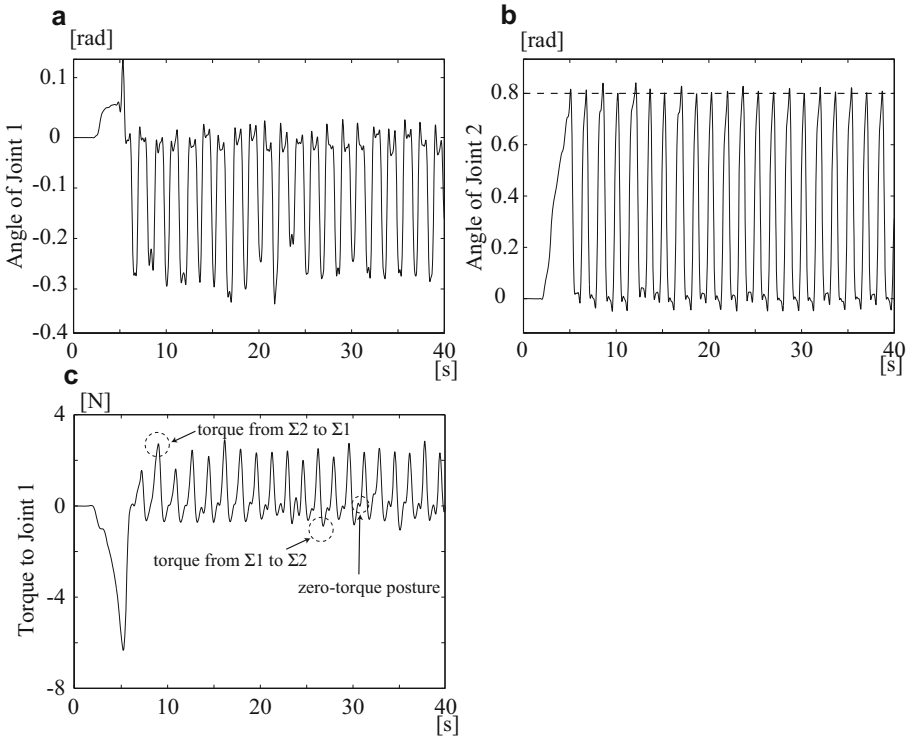

Fig. 10. Experimental results of 2DOF manipulator posture control:**a**, **b** and **c** show time histories of the angles of Joints 1 and 2 and of the torque applied to Joint 1, respectively. Direction of the trajectory was switched when the state converged to the constraint conditions.

Movies of the experiments are on [39]. In the initial state, the robot fell down at the initial state even though its legs moved forward. After about 10 minutes, the motion of the supporting leg was tuned and the robot kept walking. Figure 12 describes the lateral angle of the hip joint (Jr 6 in Fig. 11) before and after walking was learned. The motion of the joint that rotated randomly during the initial couple of minutes gradually became periodic, and eventually periodic motion emerged after 10 minutes.

Figure 13 describes the trajectories of Jr 6 when the state moved from $\boldsymbol{\Sigma_2}$ to $\boldsymbol{\Sigma_3}$. The broken lines represent the trajectories that were used before learning was complete. These lines appeared in the first 3 minutes. The solid lines are the trajectories after the robot became able to walk continuously, which occurred in the final 2 minutes. The trajectory modification from the broken to the solid lines happened during the process of searching for the equilibrium point through the reflexive actions, which was the same process as that for Joint 1 in the 2DOF manipulator experiments discussed in the previous section. We observed similar convergences of trajectories for other unspecified joints.

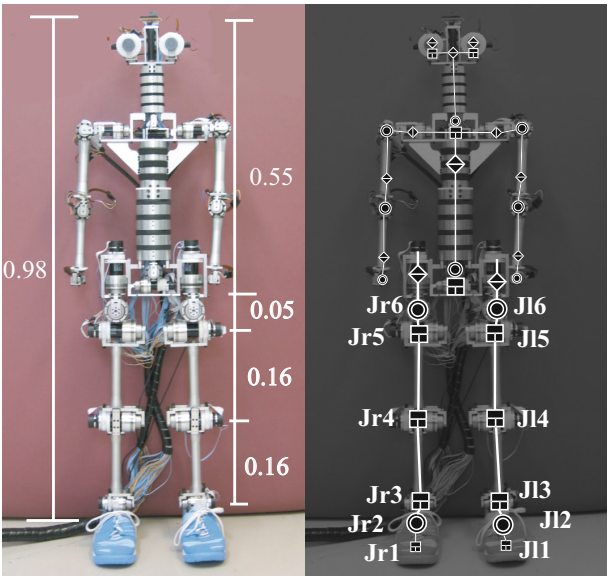

Fig. 11. Overview of 36DOF humanoid robot (distance are specified in meters)

Table 1. Target posture for walking and specified angles

Target set (key frame)	Description	Specified DOF (Value in experiment [rad])
$\sum_1$	Balance on Right Leg	Jr 6 (0.08) Jl6 (-0.08)
$\sum_2$	Left Leg Up	Jl4 (0.4) Jl5 (0.2)
$\sum_3$	Left Leg Down	Jl4 (0.0) Jl5 (0.2)
$\sum_4$	Waiting after Left Leg Step	-
$\sum_5$	Balance on Left Leg	Jr6 (-0.08) Jl6 (0.08)
$\sum_6$	Right Leg Up	Jr4 (-0.4) Jr5 (-0.2)
$\sum_7$	Right Leg Down	Jr4 (0.0) Jr5 (-0.2)
$\sum_8$	Waiting after Right Leg Step	-

4.3 Adaptability of Bipedal Walking to Environment

Our interest is how well the created walking gait was adapted to the environment, and here we discuss the following three aspects of this question.

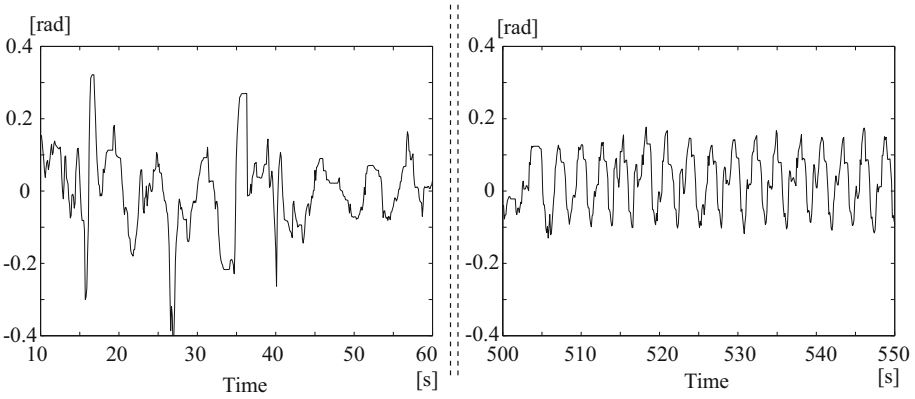

Fig. 12. Time histories of joint Jr6: In the first 60 s the trajectories rotated randomly and caused the robot to fall down. After 500 s from the start of the learning, however, regular rhythm appeared and the robot kept walking.

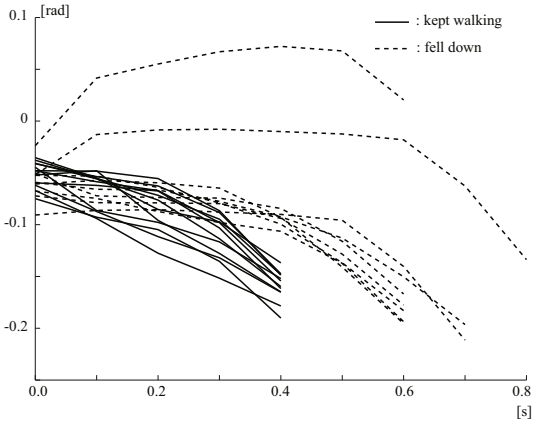

Fig. 13. Trajectories of joint Jr6 when the state moves from $\boldsymbol{\Sigma_2}$ to $\boldsymbol{\Sigma_3}$: The broken lines are the trajectories that caused the robot to fall down after the state moved on the trajectories. The solid lines are the trajectories where the robot kept walking. Because of the data sampling time during the experiments, 0.1 s, all the solid lines are stopped at 0.4 s. This implies that the error in walking pace is within 0.1 s.

The first is the efficiency of the walking gait, which is one of the most important indexes of a walking gait's adaptation to the environment[40]. It is natural to think that better efficiency implies a waking gait more adapted to the environment. We use the following index to evaluate efficiency[41]:

$$walkingsurfacesE = \frac{\text{energy comsumption}}{(\text{mass of the robot}) \times (\text{traveled distance})}. \qquad (22)$$

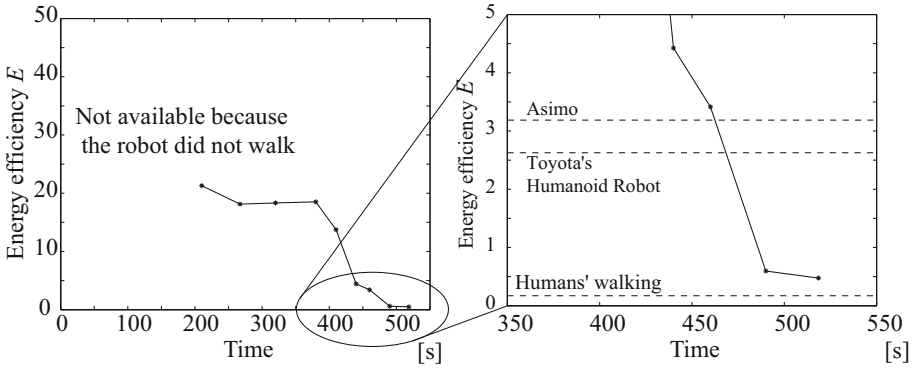

Fig. 14. Time history of energy efficiency E described in Eq. (22) during learning bipedal walking: At around 300s from the start learning, the energy efficiency was much worse than that for the fully controlled humanoid robot. However, around 500s, when walking rhythm appeared, efficiency improved greatly and the robot walked with efficiency near that of humans

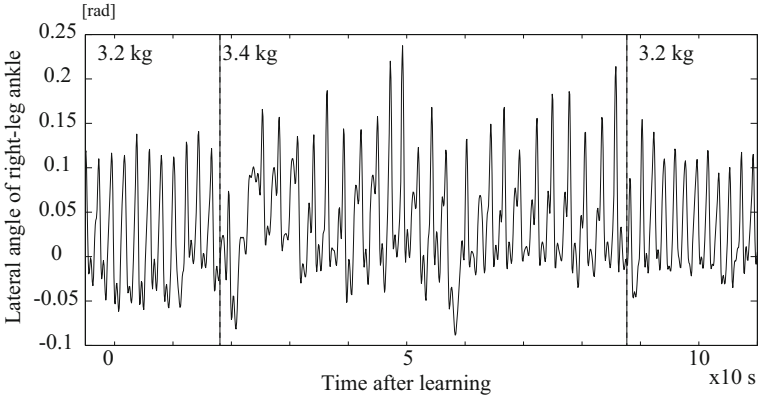

Fig. 15. Changes in walking rhythm depending on weight: The rhythm was tuned slower when the weight increased and *vice versa* without any explicit information about the change in weight.

Figure 14 describes the time history of this index during the learning of walking. The efficiency of a human's walking and of two other fully controlled humanoid robot's walking is also illustrated in Fig. 14[41][42]. The results demonstrate that the efficiency of our robot improved as the learning progressed. At the final stage of learning, it became less than one-fifth of that of other fully controlled humanoid robots and was almost the same value as that of a human walking. This remarkably high level of efficiency was achieved by reducing power consumption by maintaining balance without torque during walking. This walking style is

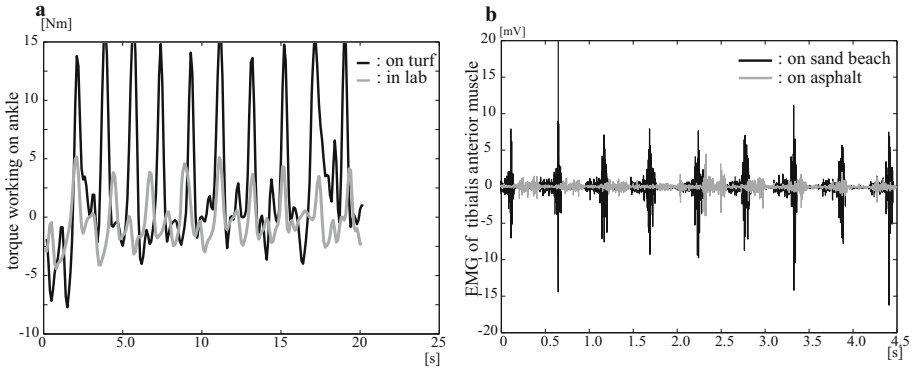

Fig. 16. Walking-surfaces-dependent difference in torque working on the ankle: **a** Much larger torque to the ankle joint was used when the robot walked on turf than on a hard flat surface. **b** Myoelectric potential of the tibialis anterior muscle becomes larger when human walks on a sandy beach that on asphalt.

similar to that of humans and corresponds to the zero-torque posture in the 2DOF manipulator experiments.

The second aspect we discussed here is the autonomous changes in the walking rhythm. We did not set any time-dependent parameters in the experiment: the periodic walking rhythm emerged through body-environment interactions. Thus when the body parameters and/or the environment were changed, the rhythm was automatically changed as described in Fig. 15, which shows what happened when the weight of the robot was changed abruptly after it had learned the walking. Without any explicit information about the change in weight, the rhythm was tuned slower when the weight increased and *vice versa*. These modifications are reasonable adaptation to the weight changes.

The final aspect we consider here is how the torque working on the ankle differs depending on the walking surface. As we can see from the movies on [39], our method succeeded in creating walking on natural turf, not just on the flat and hard surface in the laboratory. Figure 16 **a** describes the time histories of the torque working on the ankle after the learning of the walking. The results indicate that the controller required much larger torque for walking on turf than for walking in the laboratory. We can observe similar changes of torque in our walking. Figure 16 **b** shows electromyogram (EMG) data from the tibialis anterior muscle, which controls the angle of the ankle, obtained when a human walked on asphalt and on a sandy beach. As seen in Fig. 16 **b**, we empirically know that we use much more power to keep balance while walking on a sandy beach than on asphalt. Thus, the emergence of appropriate torque depending on the surface conditions in our experiments implies that body-environment interactions created a walking gait that was adapted to the environment.

The observations on the above three aspects imply that the behaviors created by tacit learning are not just adapted to the environment but also share many features with biological behaviors. We believe that these similarities were derived from the features of the activity rules of VTNs in the network, which changed their thresholds to reduce their outputs when the environmental inputs increased. In tacit learning, the environmental information was analyzed according to these features. The processes that can reduce the outputs carrying out a specified task tend to save energy in the environment. This would also be important for biological systems to increase the chance of survival in a natural environment.

5 Conclusion

The notion of tacit learning has been introduced to develop artificial control systems with remarkable adaptability to unpredictable environmental changes. The fundamental computational algorithm for tacit learning is based on the feature of biological regulatory systems in which all regulations result from the spatial and temporal integration of homogeneous computational media that act subject to innate rules. A network of the homogeneous computational media that connects the sensors and motors in proper ways is of great advantage in orchestrating the flow of heterogeneous environmental information. We developed networks of artificial computational media and used them to control a humanoid robot.

The experimental results demonstrated that the reflexive actions originating from the innate sensor-motor connections in the network changed primitive motions into sophisticated behaviors adapted to the environment. Even small changes in the environment influenced the learning results because the reflexive actions were caused by body-environment interactions. The three observations using 36DOF humanoid robot discussed in Section 4 verified the high adaptability of tacit learning in terms of gait generation, power consumption, and robustness.

The environmental information taken into the network through the reflexive actions played the roles of supervising signals for learning. This learning scheme is strongly associated with the notion of *affordance*[43], which is recognized as the key factor in cognition and intelligence. In our case, the environmental information was mainly used to create the motions of the joints without concrete references and led to the adapted behaviors. The creation of meaningful behaviors from purposeless actions by using the environmental information should be an essential process to establish adaptation and intelligence in man-made machines. This feature of tacit learning could open up innovative fields that can accomplish high levels of adaptability and artificial intelligence, and can provide a better understanding of biological systems.

The analysis of the tacit learning process in this chapter is limited to several behaviors. To the learning of multiple behaviors, we need further theoretical analysis to clarify the role of the computational media, reflexive actions, and the process of searching equilibrium to extend tacit learning . The way of the specification of the target sets, which in this chapter were given by the specified angles

of some joints, also warrants further discussion. To create behaviors that enable robots to act as real partners of human beings, behavioral objectives should be much more abstract like the eventual goal of all living organisms, *survival*. We are now on the way to creating multiple behaviors through interactions with more complicated environments.

Appendix: Mathematical expression of proposed computational media and controllers

The cluster described in Fig. 5 **a** is composed of a series of VTNs with a common input. The output from the cluster is the number of firing VTNs. When the input to the cluster is sufficiently large or small, all VTNs fire or none do. Thus, the cluster becomes the saturation system. Under some assumption on the distribution of the thresholds, we can prove the following input/output relationship of the cluster[33]:

$$O(t) = \mathrm{SAT}_{N,\gamma}(\eta(t)) \tag{23}$$

$$\Theta(t) = \Theta(t-1) + \frac{\gamma}{N} O(t-1) - \beta \tag{24}$$

$$\eta(t) = I(t) - \Theta(t) \tag{25}$$

$$\gamma = \alpha + \beta \tag{26}$$

Here, $O(t)$, N, $\Theta(t)$, $I(t)$, α, and β denote the output from the cluster, the number of VTNs in the cluster, the average of the thresholds of all VTNs, the input to the cluster, the value for the threshold incremental step $\overline{\Delta\theta}$, and that for the decremental step $\underline{\Delta\theta}$ in Eq. (3), respectively. $\mathrm{SAT}_{a,b}(x)$ is the saturation function described as follows:

$$\mathrm{SAT}_{a,b}(x) = \begin{cases} a & x > \frac{b}{2} \\ \left[\frac{a-1}{b}\left(x + \frac{b}{2}\right)\right] - 1 & |x| \le \frac{b}{2} \\ 0 & x < -\frac{b}{2} \end{cases} . \tag{27}$$

Here, $[*]$ denotes the floor function that expresses the next smallest integer of $*$.

When the input is a constant value, the output from the cluster converges to the following value that is independent of the input value:

$$O(t) = \frac{N\beta}{\gamma}. \tag{28}$$

By using these equations, the output regulator and the self-reference generator described in Fig. 4 are described by the following hybrid systems:

Output regulator:

$$O_o(t) = x_1(t)x_2(t) \tag{29}$$

$$x_1(t) = \mathrm{SAT}_{N,\gamma}(\eta_o(t)) \tag{30}$$

$$x_2(t) = -k_a \int_0^t (I_o(\tau) - r)d\tau \tag{31}$$

$$\Theta_o(t) = \Theta_o(t-1) + \frac{\gamma}{N} x_1(t-1) - \beta \tag{32}$$

$$\eta_o(t) = I_o(t) - \Theta_o(t) \tag{33}$$

Self-reference generator:

$$O_s(t) = x_3(t)x_4(t) \tag{34}$$

$$x_3(t) = \mathrm{SAT}_{N,\gamma}(\eta_s(t)) \tag{35}$$

$$x_4(t) = -k_b \int_0^t (I_s(\tau) - x_5(\tau))d\tau \tag{36}$$

$$x_5(t) = k_c \int_0^t O_s(\tau)d\tau \tag{37}$$

$$\Theta_s(t) = \Theta_s(t-1) + \frac{\gamma}{N} x_3(t-1) - \beta \tag{38}$$

$$\eta_s(t) = I_s(t) - \Theta_s(t) \tag{39}$$

x_i : Signals in controller (See Fig.4)
I_o and O_o : Inputs and outputs of plants in Output Regulator
I_s and O_s : Inputs and outputs of plants in Self − reference Generator
Θ_o and Θ_s : Average of thresholds in clusters

From the above equations, the values of parameters at equilibrium states are derived as follows:

$$x_1 = \frac{N\beta}{\gamma},\ I_o = r,\ I_s(t) = x_5(t),\ x_4(t) = 0.0,$$
$$u_1(t) = 0.0,\ x_3(t) = \frac{N\beta}{\alpha + \beta} \tag{40}$$

The values of x_2, O_o, I_s depend on the environment in which these controllers are used.

In the experiments in this chapter, we used the following values:

$$N = 100,\ \alpha = 1.0 \times 10^{-2},\ \beta = 1.0 \times 10^{-3}, \Theta_i(0) = -0.7,$$

$$k_a = 1.0 \times 10^{-2}, k_b = 1.0 \times 10^{-2}, k_c = 1.0 \times 10^{-3}. \tag{41}$$

References

1. Bear, M.F., Connors, B.W., Paradios, M.A.: Neuroscience: Exploring the brain, 3rd edn. Lippincott Williams and Wilkinse (2006)
2. Keener, J.: Mathematical Physiology. Springer (1998)
3. Tanaka, R.J., Kimura, H.: Mathematical classification of regulatory logics for compound environmental changes. Journal of Theoretical Biology 251, 363–379 (2008)
4. Janeway, C.A., Travers, P., Walport, M., Shlomchik, M.J.: Immunobiology: The Immune System in Health and Disease, 5th edn. Garland Science, New York (2001)
5. Shimoda, S., Yoshihara, Y., Fujimoto, K., Yamamoto, T., Maeda, I., Kimura, H.: Stability analysis of tacit learning based on environmental signal accumulation. In: Proceedings of the 2012 IEEE/RSJ International Conference on Intelligent Robots and Systems (2012)
6. Hodgkin, A.L., Huxley, A.F.: Currents carried by sodium and potassium ions through the membrane of the giant axon of *loligo*. Journal of Physiology 116, 449–472 (1952)
7. Markram, H., Tsodyks, M.: Redistribution of synaptic efficacy between neocortical pyramidal neurons. Nature 382, 807–810 (1996)
8. Phares, G.A., Antzoulatos, E.G., Baxter, D.A., Byrne, J.H.: Burst-Induced Synaptic Depression and Its Modulation Controbute to Information Transfer at Aplysia Sensorimotor Synapses: Empirical and Computational Analyses. The Journal of Neuroscience (23), 8392–8401 (2003)
9. Shepherd, G.M.: The synaptic organization of the brain. Oxford University Press (2003)
10. Jacob, F., Monod, J.: Genetic regulatory mechanisms in the synthesis of proteins. Journal of Molecular Biology 3, 318–356 (1961)
11. Abbott, L.F., Varela, J.A., Sen, K., Nelson, S.B.: Synaptic Depression and Control Gain Control. Science (275), 220–224 (1997)
12. Cook, D.L., Schwindt, P.C., Grande, L.A., Spain, W.L.: Synaptic depression in the localization of sound. Nature 421, 66–70 (2003)
13. Fortune, E.S., Rose, G.J.: Short-term synaptic plasticity as a temporal filter. Trends in Neurosciences 24(7), 381–385 (2001)
14. Castro-Alamancos, M.A.: Different temporal processing of sensory inputs in the rat thalamus during quiescent and information processing states in vivo. Journal of Physiology (539), 567–578 (2002)
15. Eytan, D., Bernner, N., Marom, S.: Selective adaptation in networks of cortical neurons. Journal of Neuroscience (23), 9349–9356 (2003)
16. Castellucci, V.F., Pinsker, H., Kupfermann, I., Kandel, E.R.: Neuronal mechanisms of habituation and dishabituation of the gill-withdrawal reflex in Aplysia. Science 167, 1745–1748 (1970)
17. Grade, L.A., Spain, W.J.: Synaptic Depression as a Timing Device. Physiology (20), 201–210 (2005)
18. Kawato, M., Furukawa, K., Suzuki, R.: A hierarchical network model for motor control and learning of voluntary movement. Biological Cybernetics 57, 169–185 (1987)
19. Minsky, M.L., Papert, S.A.: Perceptron. MIT Press (1969)
20. Rumelhart, D.E., Hinton, G.E., Williams, R.J.: Learning representations by back-propagating errors. Nature 323(9) (1986)
21. Kuniyoshi, Y., Yorozu, Y., Suzuki, S., Sangawa, S., Ohmura, Y., Terada, K., Nagakubo, A.: Emergence and development of embodied cognition: A constructivist approach using robots. Progress in Brain Research 164, 425–445 (2007)

22. Barto, A.G., Sutton, R.S., Anderson, C.W.: Neuronlike adaptive elements that can solve difficult learning control problems. IEEE Transactions on Systems, Man, and Cybernetics 13, 834–846 (1983)
23. Doya, K.: Reinforcement learning in continuous time and space. Neural Computation 12, 219–245 (2000)
24. Tedrake, R., Zhang, T.W., Seung, H.S.: Stochastic policy gradient reinforcement learning on a simple 3d biped. In: IEEE/RSJ International Conference on Intelligent Robots and Systems (2004)
25. Holland, J.H.: Adaptation in natural and artificial systems. MIT Press (1992)
26. Wang, H., Yang, S., Ip, W.H., Wang, D.: Adaptive primal-dual genetic algorithms in dynamic environments. IEEE Transactions on Systems, Man, and Cybernetics Part B 39, 1348–1361 (2009)
27. Astrom, K.J., Wittenmark, B.: Adaptive control. Addison Wesley (1989)
28. Slotine, J.E., Li, W.: Applied Nonlinear Control. Prentice Hall (1991)
29. Brooks, R.A.: A robust layered control system for a mobile robot. IEEE Journal of Robotics and Automation 2, 12–23 (1986)
30. Brooks, R.A.: New approaches to robotics. Science 253, 1227–1232 (1991)
31. Zadeh, L.A.: Outline of a new approach to the analysis of complex systems and decision processes. IEEE Transactions on Systems, Man, and Cybernetics SMC-3, 28–44 (1973)
32. Juang, J.G.: Fuzzy neural network control CMAC of a biped walking robot. IEEE Transactions on Systems, Man, and Cybernetics Part B 30(4), 594–601 (2000)
33. Shimoda, S., Kimura, H.: Bio-mimetic Approach to Tacit Learning based on Compound Control. IEEE Transactions on Systems, Man, and Cybernetics-Part B 40(1), 77–90 (2010)
34. Shimoda, S., Yoshihara, Y., Kimura, H.: Adaptability of tacit learning in bipedal locomotion. IEEE Transactions on Autonomous Mental Development 5(2), 152–161 (2013)
35. Forssberg, H.: Ontogeny of human locomotor control. I. Infant stepping, supported locomotion and transition to independent locomotion. Exp. Brain Res. 57(3), 480
36. Shimoda, S., Kimura, H.: Neural Computation Scheme of Compound Control: Tacit Learning for Bipedal Locomotion. SICE Journal of Control, Measurement, and System Integration 1(4), 275–283 (2008)
37. McCulloch, W.S., Pitts, W.: A logical calculus of the idea immanent in nervous activity. Bull. Math. Biophys. 5, 115–133 (1943)
38. Hebb, D.O.: The organization of behavior. Wiley, New York (1949)
39. `http://btcc.nagoya.riken.jp/biologic/movies.html`
40. Sockol, M.D., Raichlen, D.A., Pontze, H.: Chimpanzee locomotor energetics and the origin of human bipedalism. PNAS 104(30), 12265–12269 (2007)
41. Collins, S., Ruina, A., Tedrake, R., Wisse, M.: Efficient bipedal robots based on passive-dynamic walkers. Science 307, 1082–1085 (2005)
42. `http://workd.honda.com/asimo/`
43. Gibson, J.J.: The ecological approach to visual perception (new edition). Psychology Press (1986)

Human-Robot Interaction in Public and Smart Spaces

Dylan F. Glas, Koji Kamei, Takayuki Kanda,
Takahiro Miyashita, and Norihiro Hagita

ATR Intelligent Robotics and Communication Laboratories, Kyoto, Japan 619-0288
{dylan,kamei,kanda,miyasita,hagita}@atr.jp
http://www.irc.atr.jp/en/

Abstract. We have developed a "network robot system" framework with the objective of enabling practical deployment of social robots to provide real-world services in everyday social environments. This framework addresses practical issues in social human-robot interaction by integrating ambient intelligence systems, networked data stores, human supervisors, and centralized planning. All of the elements of the system have been developed and tested in public and commercial spaces such as shopping malls, resulting in a flexible robot control architecture based on practical, real-world requirements. We describe several elements of the system and demonstrate examples of its use in five years of real-world field deployments and research. Finally, we present the Ubiquitous Network Robot Platform (UNR-PF), an internationally-standardized high-level architecture for service robots based on our framework.

Keywords: network robot systems, human-robot interaction, ambient intelligence, cloud robotics, ubiquitous computing.

1 Social Robots in the Real World

Among the many fields of robotics, perhaps no application captures the public imagination like social robots – robots which are a part of our everyday lives, taking the role of social peers, interacting with people conversationally using speech, gaze, and gesture. Yet social robotics is also one of the youngest fields in robotics. Research has been progressing steadily in fields like computer vision, speech processing, and motion planning for safety, and a number of inspiring studies have demonstrated that social robots can be used as museum guides [4, 31], as receptionists for assisting visitors [11], and as peer-tutors in schools [16]. However, today's reality is that most demonstrations of social robotics are still confined to laboratory trials.

Many of the reasons for the continued absence of robots in our everyday social spaces stem from the fact that the noise and unpredictability of the real world and the complexity of social interactions provide enormous challenges for recognition and planning. In a busy shopping mall, school, or train station, a robot needs to localize itself in a world where products and furniture are

S. Mohammed et al. (eds.), *Intelligent Assistive Robots,*
Springer Tracts in Advanced Robotics 106, DOI: 10.1007/978-3-319-12922-8_9

constantly moved around; recognize and track people moving through changing lighting conditions in crowded, unstructured spaces; determine the intentions of people around it; and ultimately to interact with people, identify who it is talking to, perform speech recognition for natural language amid significant noise, and in the end provide a useful service.

With advances in algorithms and improved hardware, many of these recognition and planning problems may be solved in the near (or not-so-near) future. However, by augmenting the limited on-board capabilities of standalone robots using ambient intelligence systems and networked resources, it is possible to accelerate the development of social robots despite the limitations of today's technology.

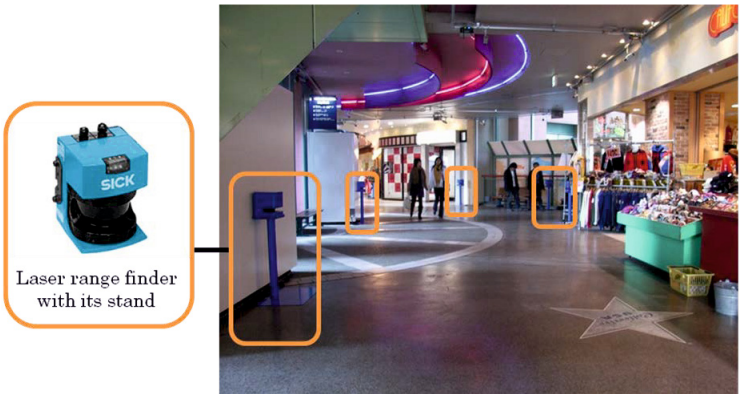

Fig. 1. Shopping arcade and laser range finders

By embedding sensor systems in the environment as shown in Figure 1, we are able to use networked resources to provide recognition, planning, and coordination between robots, extending their capabilities far beyond the limitations of standalone robots. Combining these ambient intelligence systems with networked data sources and human operators available in the network to occasionally assist with difficult recognition and planning tasks, we have been able to demonstrate prototype robot systems to provide a variety of services in long-term deployments in real shopping malls and other social spaces.

The work presented in this chapter spans about five years of research and field studies aimed towards deploying social robots in public and commercial spaces. We will present an overview of the systems we have developed, as well as some of the practical problems we have faced in the process.

In a world where humans are becoming more and more connected through wireless networks and mobile devices, it is our belief that the "network robot system" approach [25], using environmental sensor systems, is the inevitable future direction of robot system architectures. We hope that the contributions of our work provide a framework for future systems to provide ubiquitous coverage

Fig. 2. Example scenes using our Network Robot System framework. (a) helping a customer with shopping, (b) collaboration between heterogeneous robots.

of social robot services, and ultimately to enhance the quality, enjoyment, and humanity of our lives.

This framework has been successfully used by our research group (Fig. 2 (a)) and in collaboration with others (Fig. 2 (b)) in several field deployments, and we will present many examples of robot services we have implemented in the field using this framework.

Most importantly, the lessons learned throughout our development process have been distilled into a generalizable architecture called the Ubiquitous Network Robot Platform (UNR-PF), which is recognized by international standards organizations. These standards describe an architecture which will connect robots with sensor networks and mobile devices, and enable high-level robot services to be developed independently and executed on a wide variety of robotic platforms, including those based on popular software frameworks such as ROS and RT-Middleware.

2 Human Tracking

A cornerstone of much of our research is a system we have developed for simultaneously tracking the position and body orientation of large numbers of pedestrians, in order to support the spatial perception of robots for navigational interactions. Our technique combines data from a network of laser range finders mounted at torso height. In the tracking algorithm, an individual particle filter is created to estimate the position and velocity of each human over time, and a parametric shape model representing the person's cross-sectional contour is fit to the observed data at each step.

This section will provide an overview of our tracking system. Details of the algorithms used and measures of performance can be found in [9]. This tracking system has been used throughout six years of experiments and field trials, and it has been made into a commercial product called ATRacker[1] which has been used both for robotic and non-robotic applications.

[1] ATRacker is sold by ATR-Promotions. `http://www.atr-p.com/HumanTracker.html`

2.1 Related Work

Much of the human-tracking research to date has been based on leg tracking, for both mobile robotics [27, 37] and environmental monitoring [2, 5, 39]. This has historically been motivated in part by the fact that many robots use laser sensors for obstacle avoidance, and for that reason already have laser sensors mounted near the ground. However, their visibility is often limited by those same obstacles, making floor-level sensors a good choice for on-board robot systems but less so for wide-area environment monitoring in cluttered spaces.

In our work, the laser sensors constitute an essential part of a ubiquitous sensor network used exclusively for human tracking in real environments. For this reason, it is important for the sensors to be mounted higher, above furniture and ground clutter. Thus the sensors in our system are mounted on poles at a height of 85-90 cm, where the arms and torso can be clearly observed, as shown in Figure 3:

Fig. 3. The ATRacker system features Hokuyo laser range finders mounted on portable poles which can easily be placed in public spaces

Placing the sensors at this height does have the drawback that small children cannot be tracked. This may be acceptable in scenarios where adults are the primary targets of services, provided that the robots are capable of using on-board sensors to detect nearby children for safety reasons.

2.2 Tracking

State Model. The state vector tracked by the particle filter consists of four variables: x, y, v, and θ. The variables x and y represent the position of the human being tracked. Although the speed v, and direction θ of motion could be calculated *a posteriori* from the position data, these variables are included in the state and updated at every step to enable the person's position to be projected forward through time for more accurate tracking. These variables are used in the motion model, described below.

Motion Model. At every update of the particle filter, each particle is propagated according to a motion model. The purpose of this motion model is to approximate the probability of a state $\mathbf{x}_t$ based on the previous state $\mathbf{x}_{t-1}$. To capture the balance between randomness and predictability in human motion, a Gaussian noise component is added to each particle's v and θ values. We then propagate the (x, y) motion linearly according to the resultant v and θ values of the particle.

Likelihood Model. The purpose of the likelihood model is to approximate the value of $p(z_t|\mathbf{x}_t^{[m]})$ based on sensor measurements. In this case, the measurement vector z is an array of raw sensor range data. An effective likelihood model must provide a robust likelihood estimate in spite of noisy sensor data, partial and full occlusions, and the irregular and varying shapes of human bodies.

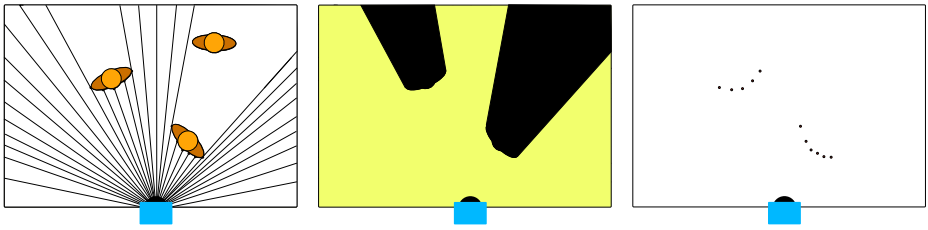

Fig. 4. A typical single-sensor laser scan. (Left) The positions of humans relative to the scanner can be seen. (Center) Occupancy information. (Right) Edge information.

Laser scan data provides two qualitatively distinct types of information useful for estimating human positions: *occupancy information*, indicating whether a certain point is occupied or empty, and *edge information*, indicating a contour which may correspond with the edge of a detected object. Fig. 4 illustrates the distinction between these two kinds of information.

To determine likelihood values from the raw sensor data, it is first necessary to create a background model. Our system uses an adaptive background model which is updated over time to determine the best estimate of the true background distance. Occupancy likelihood is then determined by dividing the world into three regions: "open", "shadow", and "unobservable". The "unobservable" region is beyond the background model for that sensor, and thus can contribute no information. The "open" region has been observed by the sensor to be unoccupied, and the remaining space is considered "shadow". Note also that every "shadow" region lies behind an "edge".

The likelihood model used to compute $p(z_t|\mathbf{x}_t^{[m]})$ is expressed in Eq. 1 and 2 and includes components reflecting both occupancy and edge information.

$$p(z_t|\mathbf{x}_t^{[m]}) = \frac{1}{n_{sensors}} \sum_{i=1}^{n_{sensors}} p_i(z_t|\mathbf{x}_t^{[m]}) - p_{collocation} \quad (1)$$

$$p_i(z_t|\mathbf{x}_t^{[m]}) = \begin{cases} p_{shadow} + p_{edge}(z_t|\mathbf{x}_t^{[m]}) & \text{in a shadow region} \\ p_{open} & \text{in an open region} \end{cases} \quad (2)$$

For a point in a shadow region (strictly speaking, we consider only those regions wide enough to contain a human), the likelihood in Eq. 2 is calculated as the sum of a constant value p_{shadow} and a likelihood $p_{edge}(z_t|\mathbf{x}_t^{[m]})$, calculated as a normal distribution centered upon a point located one approximate human radius behind the observed edge. (In our calculations a value of 25cm was used.) This reflects the fact that people are highly likely to be found just behind an observed edge, yet can plausibly exist anywhere in a shadow region (*e.g.* the occluded person in Fig. 4).

For a point in an open region (or in a shadow region too narrow to contain a human), the likelihood is theoretically zero, but for reasons described below is set to a small but nonzero constant value p_{open}. In this case, edge information is irrelevant.

Finally, in Eq. 1, these likelihood values are averaged across all $n_{sensors}$ sensors for which the proposed point lies within the sensor's "open" or "shadow" range, *i.e.* not "unobservable" to that sensor. To prevent two particle filters from tracking the same human, a value $p_{collocation}$ is subtracted from this result. Its value is calculated as a sum of normal distributions surrounding each of the other humans, based on the list of human positions from the previous time step.

Body Shape Model. After each update of the particle filter, we update a shape model to find a best fit to the torso and arm positions of each pedestrian. Although variations in clothing, backpacks, objects being carried, and individual body size and walking style make it difficult to develop a precise, yet generalizable, model, we found a simple three-circle model to be effective for tracking body orientation.

Our model is illustrated in Figure 5. A central, large circle represents the person's torso, and two smaller circles represent the arms. This model has six parameters which can be varied to best match a subject's cross-sectional body contour.

The update procedure for fitting the shape model to observed data is based on fitting the observed contour of the body to an empirically-derived probability distribution. The details of this procedure are presented in [9]. After these parameters have been adjusted, it is possible to estimate the direction in which a person is facing, even if they are standing still.

2.3 Tracking Results

The tracking accuracy of this system is highly dependent upon several factors, including the placement geometry and number of sensors and the degree of

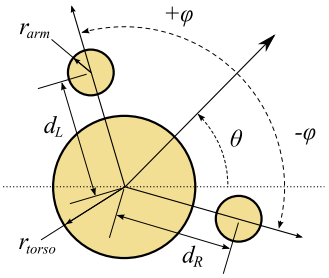

Parameter	Description
θ	Body orientation
φ	Arm separation angle
	$\varphi_L = \theta + \varphi$ for left arm
	$\varphi_R = \theta - \varphi$ for right arm
d_L	Distance of left arm from body
d_R	Distance of right arm from body
r_{arm}	Arm radius
r_{torso}	Torso radius

Fig. 5. Our three-circle model, with the six variable parameters indicated

crowding in the space. Our measurements in laboratory tests have shown accuracy as good as 4.6 cm ± 2.7 cm [9], and users in the field have reported accuracy ranging from 6 cm to 15 cm. Body direction tracking was found to be 8.2 ± 13.8 degrees in our laboratory studies, with occasional 180 deg reversals due to the nearly-symmetrical shape of the human body.

Shape Model Matching. To illustrate the quality of the shape model matching, Figure 6 shows raw data from five frames taken during the course of a single stride, overlaid with the model-based estimates for those time frames. Note that the swinging of the arms is clearly visible from the data, and that the model follows this movement closely.

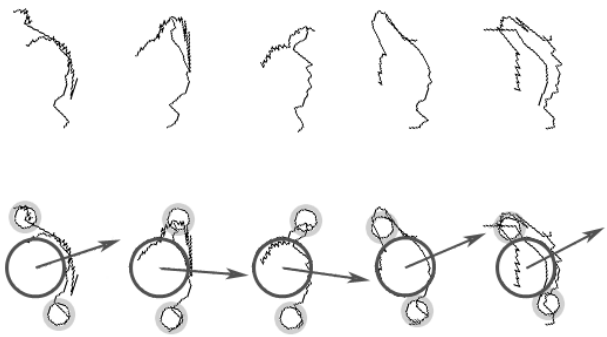

Fig. 6. Example of arm and torso movement during a single stride. Top: Five frames of raw data from laser scanners taken at 320ms intervals. Bottom: Corresponding human shape model positions for each frame.

3 Abstracting and Anticipating Trajectories

Once a high-precision pedestrian tracking system is available in an environment, the next step is to extract socially meaningful knowledge from the data. This section will present an overview of a series of techniques for abstraction of people's trajectories and a service framework for using these techniques to enhance the services provided by mobile social robots. The details of our algorithms and evaluation results for this system can be found in [15].

For a robot providing services to people in public spaces such as shopping malls, it is important to distinguish potential customers, such as window shoppers, from other people, such as busy commuters. The framework presented here enables a designer to make a robot proactively approach customers who exhibit some target local behavior, e.g. walking idly or stopping. This technique was used in a field trial to offer shop recommendations to visitors [28].

The techniques proposed in this section also enable information about the use of space and people's typical global behaviors to be automatically extracted from pedestrian trajectory data. This information enables the robot to anticipate spatial areas in which people are likely to perform the target behaviors, as well as anticipating the probable local behaviors of specific individuals a few seconds in the future. If slow-moving robots can anticipate a person's future behavior, they can start moving early to approach potential customers [26].

3.1 Abstraction Techniques

We use a series of three abstraction techniques for people's trajectories: local behavior, use of space, and global behavior. We define the term **local behavior** to refer to basic human motion primitives, such as walking, running, going straight, and so on. The observation of these local behaviors can then reveal information about the **use of space**, that is, general trends in people's behavior in different areas of the environment. Finally, for more insight into the structure of people's behaviors, we look at **global behavior,** that is, overall trajectory patterns composed of several local behaviors in sequence, such as "entering through the north entrance, walking across a street, and stopping at a shop." Global behaviors are highly dependent on the specific environment.

In addition, since timing is highly critical for social interactions, we also focus on the problem of anticipating the motion and behavior of customers, to determine where the robot should move and which customers the robot should approach. For example, if a robot is designed to invite customers to a shop, it should approach people who are walking slowly and possibly window-shopping. To approach those customers, two anticipation techniques are presented: **location-based anticipation**, based on aggregate behavior patterns observed in the environment, and **behavior-based anticipation**, based on anticipating the specific behavior of an individual person.

3.2 Robot Application Scenario

We conducted our experiments at Universal CityWalk Osaka, a popular entertainment and shopping arcade located by the entrance to Universal Studios Japan, a major theme park. We operated the robots within a 20 m subsection of the arcade, with shops selling clothing and accessories on one side and an open balcony on the other. Within this space, our objective was to enable robots to approach people and offer shop-recommendation services or entertain people. Since many people walking through the space were in a hurry and not interested in talking with the robot, one of our goals was to avoid those busy people and target instead people who appeared to be leisurely window-shopping.

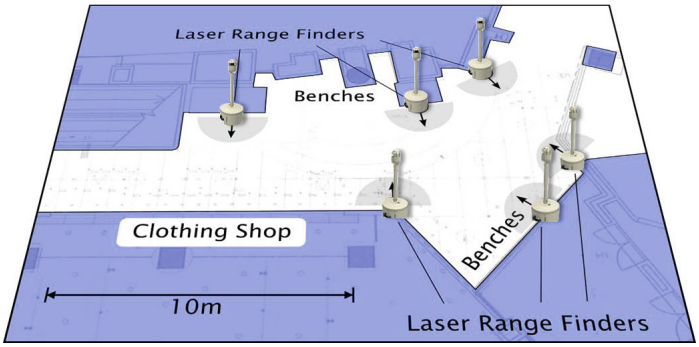

Fig. 7. Placement of laser range finders at the Universal CityWalk Osaka site

The motion of people through this area was monitored using the tracking platform presented in Section 2. Six SICK LMS-200 laser range finders were mounted around the perimeter of the trial area at a height of 85 cm (Figure 7).

3.3 System Design

Figure 8 shows how the sensor information is used to assist with providing robot services. In our framework, data from the position tracking system is abstracted into local behaviors and global behaviors in the recognition system. This information is then used to anticipate the robot's optimal position and generate a roaming path for the robot or to approach a specific individual.

Data Collection. Pedestrian motion data was first collected for a week in the shopping-arcade environment, from 11am-7pm each day, including 5 weekdays and 2 weekend days. We chose this time schedule because the shops open at 11am, and the number of visitors drops after 7pm, after the theme park closes in the evening.

In this environment, the major flow consisted of customers crossing the space from the left to the upper right or vice versa, generally taking about 20 seconds

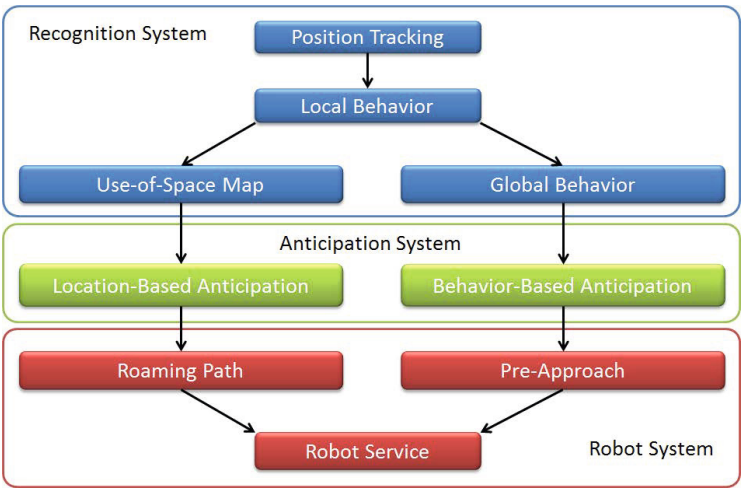

Fig. 8. Service framework

to go through. We removed trajectories shorter than 10 seconds, in order to avoid noise from false detections in the position tracking system. In all, we gathered 21,817 visitor trajectories.[2]

3.4 Local Behavior

As defined earlier, "local behaviors" represent basic human motion primitives. We began our analysis with a classification system which uses SVM (support vector machine) to categorize trajectories based on their velocity, direction, and shape features.

Trajectories were first normalized by rotating them to fit their starting points to the origin and its longest direction to the x axis. A set of 32 features was then extracted describing the shape and size of each trajectory. These features included x-coordinates, y-coordinates, and tangent angles of points sampled along each third of the trajectory, along with min, max, and average x and y values for the overall trajectory shape and a number of angles calculated within the trajectory.

A subset of the trajectories were then manually labeled as belonging to a specific "style" category, describing the trajectory's shape, (walking straight, turning left, turning right, etc.), and a "speed" category, describing the walking speed. This was performed for 5-second and 2-second trajectories, and around 200 trajectories were used for each category.

[2] In this study, we obtained approval from shopping mall administrators for this recording under the condition that the information collected would be carefully managed and only used for research purposes. The experimental protocol was reviewed and approved by our institutional review board.

We then combined these data sets and aggregated the detailed behavior classes into the following four local behavior categories: *fast-walk* (walking quickly in one direction), *idle-walk* (walking more slowly in one direction), *wandering* (turning in one direction or the other, or making a U-turn), and *stop*. Figure 9 shows examples of these local behaviors.

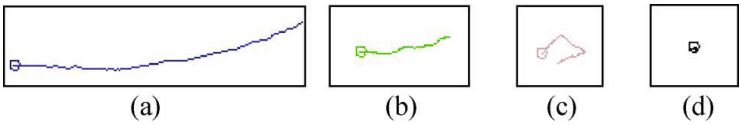

Fig. 9. Example trajectories for local behaviors: (a) fast-walk, (b) idle-walk, (c) wandering, (d) stop

We define the position P_t^n of visitor n at time t to include the x-y coordinates (x, y) as well as Boolean variables indicating the presence or absence of local behavioral primitives $P_{fast-walk}$, $P_{idle-walk}$, $P_{wandering}$, and P_{stop}.

Each trajectory has a sequence of local behaviors represented by these Boolean variables at each time step t. These values are computed by sending the most recent 2-second and 5-second trajectory segments to the SVM classifiers at each time step.

Analysis of Accumulated Trajectories. We then performed an analysis of the local behaviors to obtain a higher-level understanding of the use of space and people's global behaviors. This analysis constitutes the foundation for the robot's ability to anticipate people's local behaviors.

Use of Space (Map). The first analysis task was to identify how the space was used, and how the use of space changed over time. We applied the ISODATA clustering method [1] to achieve this. First, we partitioned the time into one-hour segments categorized as weekday or weekend. We then partitioned the space into a 25cm grid, mapping the environment into 2360 grid elements, and we clustered together the elements with similar local behavior frequencies.

Figure 10 shows a visualized output of the analysis for 40 spatial partitions and 4 temporal partitions of the space. The partitions are color-coded according to the dominant local behavioral primitive in each area.

In some areas, the use of space was very clearly observed to change as a function of time. For example, in Figure 10 (a), *busy-walk* is the dominant primitive in most of the space during weekdays in the daytime, whereas on weekends and evenings, *idle-walk* is more common. The map also provides insight into the spatial distribution of these behaviors, wherein it is clear that people *stop* at the rest spaces and the bench, or slow down in front of a map of the shopping arcade. Customers sometimes slowed down, stopped, and looked at this map.

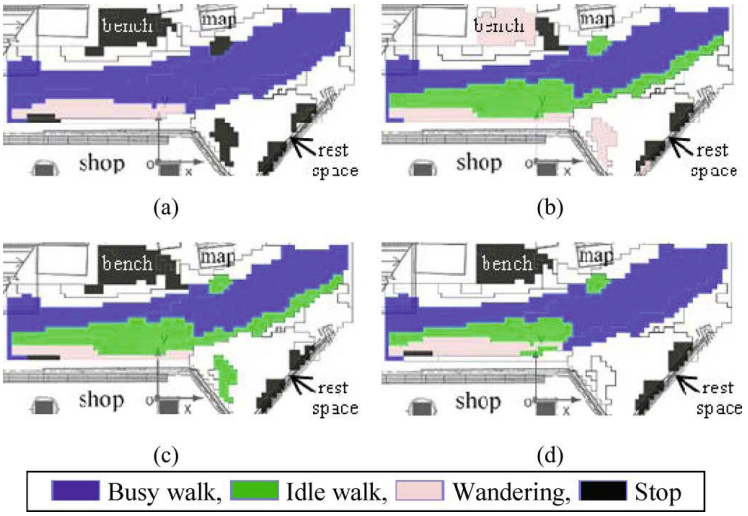

Fig. 10. Analysis of the use of space. (a)Weekday 11am-5pm, weekend 12-1pm (b)Weekday 5-6pm (c)Weekday 6-7pm (d)Weekend 11am-12pm, 1-7pm

The statistical analysis clearly revealed this phenomenon as defining a distinct behavioral space.

The areas where the *wandering* primitive was dominant are colored with pink (or very light gray). All maps in Figure 10 show the space immediately in front of the shop as having this property.

To summarize, we have demonstrated that through this analysis technique, we can separate space into semantically meaningful areas such as the corridor, the space in front of the shop, the area in front of the map, and the rest space. It also reveals how usage patterns change over time, such as the change of dynamics in the space in front of the shop.

3.5 Global Behavior

Global behaviors represent the overall spatiotemporal sequence of local behaviors performed by a pedestrian across a full trajectory. Here we will introduce a method of extracting clusters of global behaviors which represent the typical overall behavior patterns of people in the space.

State Chain Models. We analyzed trajectories based on the *state chain* model illustrated in Figure 11. That is, we converted P_t^n, which is represented in x-y coordinates, to a sequence of states, $S^i = \{s_{t0}^i, s_{t1}^i, \ldots\}$ based on spatial partitioning. s_t^i is defined as $s_t^i = \{n \in N | p_t^i \in A_n\}$ where A_n is the partition the point in trajectory p belongs to. In the example in Figure 11, the trajectory starting from partition 1, stayed in partition 1 for 3 time steps, then entered briefly into

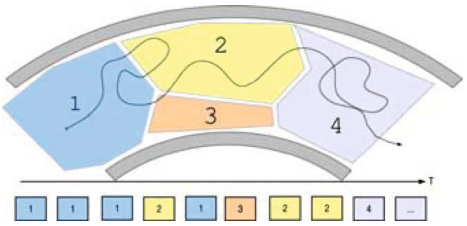

Fig. 11. State chain model

partition 2, and moved back to the partition 1 . . . , which is represented as the sequence of states 1, 1, 1, 2, 1, . . .

Distance between trajectories. We calculate the distance between two state chains, S^i and S^j, by using a dial pulse (DP) matching method (widely used in many research domains, e.g. [24]), which is identical to the comparison of strings known as the Levenshtein distance. Figure 12 illustrates this trajectory comparison technique. Here, we set the distance between partitions as the distance between the centers of the partitions. The cost for "insert" and "delete" operations is calculated as this partition distance plus a constant parameter, which represents the tradeoff cost between time and space.

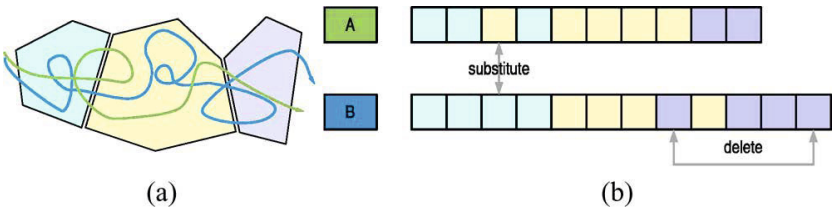

Fig. 12. Comparison of trajectories based on DP matching. (a) Two trajectories. (b) Comparison of state chains of trajectories.

The trajectories are segmented into 500 ms time steps, and they are compared with each other based on the physical distance between them at each time step. To this is added a cost function, based on "insert" and "delete" operation costs in the DP matching, where we defined the cost of a single insertion or deletion to be 1.0 m.

Clustering and Visualization. We then grouped trajectories using k-means clustering to identify typical visiting patterns. The distance between trajectories was provided from DP matching method mentioned above.

Figure 13 shows a visualization of the global behaviors at k=6. For this visualization, we separated the space into 50 similarly-sized partitions by the k-means method [19], although the actual computation used 2360 partitions. In this visualization, each area is colored according to its dominant local behavior primitive, and transitions between adjacent areas are shown as arrows. For example, blue represents *fast-walk*, and green represents *idle-walk*. Solid colors indicate a frequency of occurrence of at least one standard deviation above average, and lighter tints represent weaker dominance, down to white if the frequency is at least one standard deviation below average.

The transitions between adjacent areas are computed for each pair of adjacent areas by counting the transitions in the state chains of the trajectories that belong to each global behavior. Frequent transitions between adjacent areas are shown by arrows.

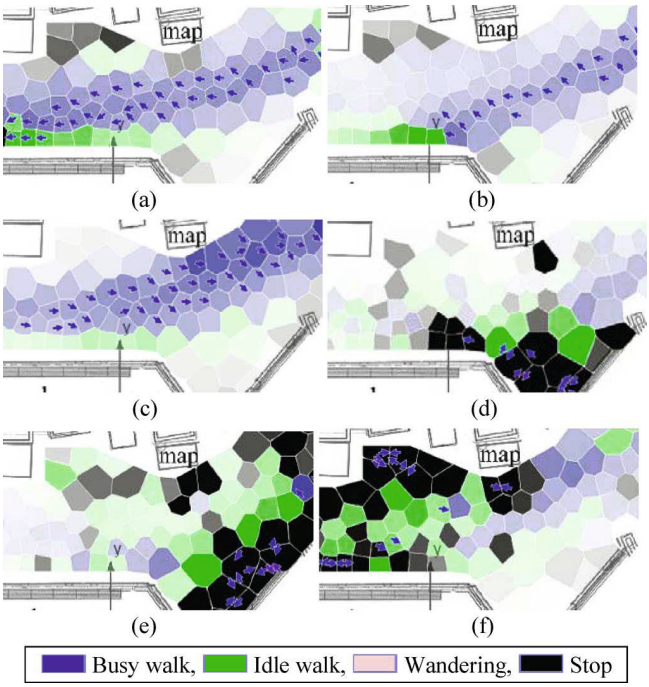

Fig. 13. Six typical patterns of global behavior. (a) From right to left. (b) From right and stop at the shop. (c) From left to right. (d) Rest at the rest space. (e) Around the rest space and right. (f) Around the shop and bench.

We can interpret about six typical global behaviors from Figure 13:

1. Pass through from right to left (7768 people)
2. Come from the right, and stop at the shop (6104 people)
3. Pass through from left to right (7123 people)

4. Rest at the rest space (213 people)
5. Around the rest space and right (275 people)
6. Around the shop and bench (334 people)

In this space, the train station was located to the left and the theme park to the right, so it is possible to interpret the meaning of several of these global behaviors. For example, people often came to stop at the shop while returning from the theme park, but not when coming from the train station.

In summary, this analysis technique has enabled us to extract typical global behavior patterns. These results show that most people simply pass through this space while a smaller number of people stop around the rest space or the map area. People tend to stop at the shop more often when they come from the right, a result which makes intuitive sense, as the shopping arcade is designed mainly to attract people coming back from the theme park.

3.6 Anticipation of Behaviors

Robots differ from other computing systems in that they are mobile, and it takes some time for a robot to reach a person in need of its service. Thus, the ability to anticipate people's actions is important, as it enables the robot to proactively pre-position itself so it can provide service in a timely manner.

We assume here that the robot's service is targeted towards people who are performing some particular local behavior, such as *stop* or *idle-walk*. The robot system uses the results of the analysis about the use of space and global behavioral primitives to anticipate the occurrence of this "target behavior". At the same time, the robot system tries to avoid people who are performing particular local behaviors, such as *fast-walk*, which we refer to as "non-target behavior". To anticipate local behaviors, we use two mechanisms: location-based anticipation and behavior-based anticipation.

Location-Based Anticipation. The robot uses the use-of-space information shown in Figure 10 to estimate the locations in which people will be statistically likely to perform the target behavior and unlikely to perform non-target behaviors. Figure 14 shows an example anticipation map. The darker areas represent areas where the system anticipates both a high likelihood of the target behavior and a low likelihood of the non-target behavior.

The robot roams through this high-likelihood area looking for people. At each time slice t, the system updates the roaming path, $\boldsymbol{P_x}$, to maximize the roaming value calculated from candidates of all possible straight-line paths from 1m to 5m in length on the 25cm-grid.

Usage Example. In one scenario, the robot's task might be to invite people to visit a particular shop. In this case, selecting *idle-walk* as the target behavior and *fast-walk* as the non-target behavior might be appropriate, since the robot wants to attract people who have time and would be likely to visit the store. Figure 14 (a) is the anticipation map for this scenario, calculated for the behavior

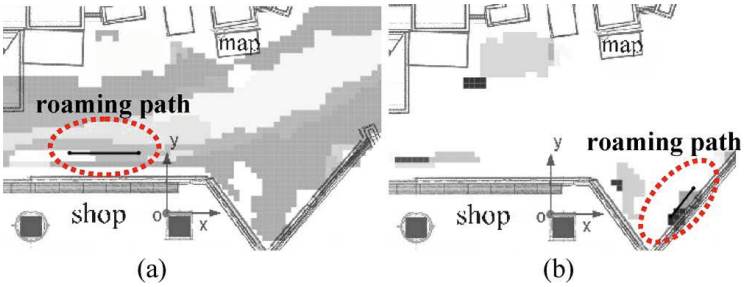

Fig. 14. Example of anticipation map. (a) Weekday 11am-5pm, idle-walk. (b) Weekday 11am-5pm, stop.

patterns observed on weekdays between 11am and 5pm. Several areas away from the center of the corridor are colored, and the roaming path is set in front of the shop. Note that the best path in this case is slightly below the line shown in the figure, but this area is very close to the boundary of the observed map. The robot's final path was translated about 50cm away from the edge for safety reasons.

In a different scenario, the robot's task might be to entertain idle visitors who are taking a break or waiting for friends. Particularly because this shopping arcade was situated near a theme park, this is quite a reasonable expectation. In this case, it would be more appropriate to select *stop* as the target behavior and *fast-walk* as the non-target behavior. Figure 14 (b) is the anticipation map for this second scenario. In this case, only a few areas are colored. The roaming path is set to the bottom-right area.

Note that since the roaming path was automatically calculated based on the anticipation map, no additional knowledge about the space was provided by designers.

3.7 Behavior-Based Anticipation

The second technique used for anticipating local behaviors is to estimate the global behaviors of people currently being observed, and then to use that information to predict their expected local behaviors a few seconds in the future.

For this analysis, we used only trajectories from our dataset that were at least 20 seconds in length, resulting in a set of 11,063 trajectories. We clustered these trajectories into 300 global behavior patterns, and for each cluster we identified a representative trajectory at the center of that cluster.

To predict the global behavior of a new trajectory which has been observed for T seconds, the system compares the new trajectory with the first T seconds of the center trajectories of each of the 300 clusters, using the same DP matching technique applied earlier for deriving the global behaviors. The cluster with the minimum distance from the new trajectory is considered to be the best-fit global behavior for that trajectory.

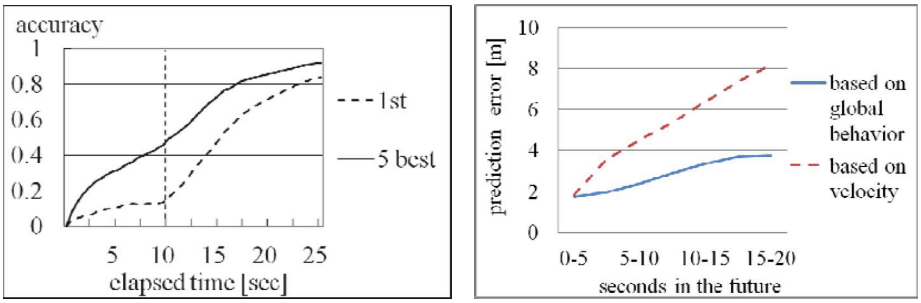

(a) (b)

Fig. 15. (a) Global behavior prediction accuracy. (b) Prediction error for position.

Figure 15 (a) shows the prediction accuracy for observed trajectories from 0 to 25 seconds in length. We used 6 of the 7 days of data to create the prediction model, and tested its ability to predict the remaining one day of the accumulated data. The prediction is counted to be successful if the predicted global behavior matches the classification result after observing the whole length of the trajectory.

The result labeled "1st" shows the case where the best-fit global behavior at time T was correct, and the result labeled "5 best" shows the result if we define success to mean that correct global behavior falls within the top 5 results.

We found that prediction accuracy increases with time as more information is available, and performance levels off after 20 seconds. Since there are 300 global behaviors, we believe that a success rate after 10 seconds of 45% and after 15 seconds of 71% for "5 best" represents fairly good performance.

Likewise, we computed the ability of our technique to predict a person's future position based on an average of the 5 best global behaviors. Figure 15 (b) compares our method with position prediction based on simple projection of the person's velocity over the last second. As the velocity method cannot account for motions like following the shape of the corridor, our method is about twice as accurate.

3.8 Conclusion

Here we have reported a series of abstraction techniques for retrieving information about people's behavior from their trajectories. Based on a set of over twenty thousand trajectories accumulated using robust tracking with multiple laser range finders, we were able to determine statistical patterns of local behaviors and use clustering to reveal typical global behavior patterns in the environment. These results enable us not only to identify human behavior and target

robot services appropriately, but also to anticipate people's future behavior, enabling robots to more effectively approach fast-walking pedestrians in dynamic environments.

4 The Network Robot System

Aside from these frameworks for robust pedestrian tracking and trajectory analysis, a number of other components are necessary for deploying social robot teams in real public environments. In this section, we will present our overall robot control framework, which provides coordination between robots operating in the same environment, manages the assignment and scheduling of robot services, allows human operators to assist the robots in difficult recognition tasks, and enables structured knowledge sharing between system elements.

The framework we have developed is based on a "Network Robot System" (NRS) design philosophy, in which the robots themselves are merely the visible component of a network which integrates environmental sensor systems, central planning servers, cloud-based knowledge resources, and human users and supervisors. These elements will be summarized here. A detailed report of the requirements and components used to build this system, together with empirical results from field experiments, can be found in [10].

Although the studies we have conducted with this framework focus on tasks such as guiding customers in a shopping mall, our intention is to share a general approach which can be useful in service robot deployment scenarios like those explored by other groups, e.g. trash collection [21], pedestrian guidance [6], and assisting people in hospitals [22], supermarkets [36], and offices [34].

4.1 System Overview

The high-level elements of our system are shown in Fig. 16. These include a **sensing framework**, several **information registries**, a **coordination module** for navigational coordination and path planning, a system for **service allocation**, and support from a **human supervisor**. Table 1 summarizes these elements.

In this section we will present a general description of each module of our system as well as specific instances of these modules from our implementations.

4.2 Sensing Framework

The sensing framework used in this system has already been described. Its role is to perform precise tracking, trajectory analysis, and behavior anticipation for pedestrians in the environment.

Another important function is identification of individuals, as it enables personalization of robot services. In our work, we have used techniques such as RFID [29, 18], visual face recognition using OKAO Vision[3] software, and Wi-Fi-based identification using smartphones for this task. By combining these results

[3] OKAO Vision, OMRON Corporation, `http://www.omron.com/r_d/coretech/vision/okao.html`

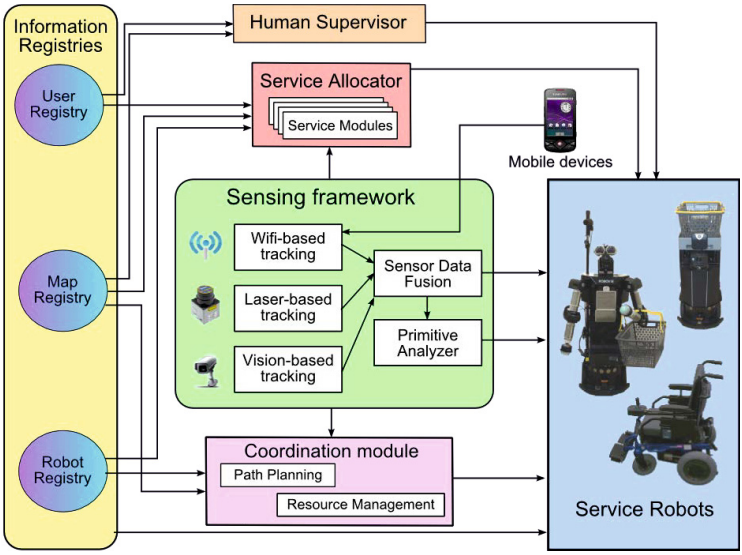

Fig. 16. Overall architecture of our Network Robot System framework

with the high-precision position information available from the position tracking systems, we can locate known individuals with high precision.

In addition to these functions, the human tracking system is often used to assist with robot localization [7], because maps of public spaces often change dramatically from day to day or during the day, as shown in Figure 17. In such environments, fixed sensors provide a better absolute reference than changing features such as product displays.

In fact, we have found precise localization to be quite important for human-robot interaction, as inconsistencies between the coordinate frames of different robots can cause a number of coordination problems. In the example shown in Fig. 18 (left), robots R1 and R2 have slight localization errors, perceiving their own poses to be R1' and R2'. Both robots believe they have identified separate people in need of help, but they have actually detected the same person, resulting in multiple robots offering services to the same person, as shown in the photo. In Fig. 18 (right) one robot has mistaken another for a pedestrian and is trying to initiate a social interaction with it. Since our robots are humanoid in form, they can be mistakenly detected as people by some sensor systems. This has resulted in robots offering services to each other, as shown in the photo. These two problems were common in our early field trials.

Fig. 17. Example of an area in a shopping mall where features change from day to day. Top: photos on two different days. Bottom: laser scan maps of the area on two different days.

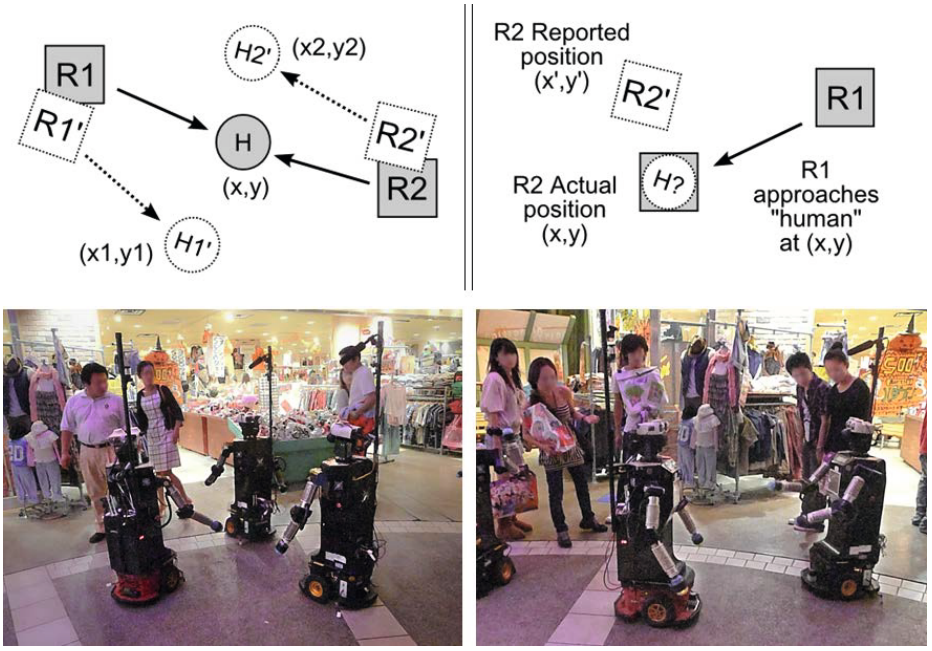

Fig. 18. Social robot failures that can occur due to localization problems. Left: Example of multiple robots approaching the same person. Right: Example of a robot mistaking another robot for a human and talking to that robot instead of an actual customer.

Table 1. Key system elements and functions

System Element	Functionality
Sensing framework	Robust tracking of people
	Recognize and anticipate people's behavior
	Assist in robot localization
	Identify individuals
Information registries	Store information about robots
	Store information about environments
	Store information about customers
Path planning and spatial allocation	Coordinate robot paths to avoid conflicts and deadlock
	Ensure smooth locomotion near people
	Provide paths based on robot type
Service allocation	Coordinate robot services
	Enable users to request services
	Assign services based on anticipated need
Support from a human operator	Support for recognition
	Direct control of robot
	Ability to control multiple robots

4.3 Information Registries

Roughly speaking, three categories of information are needed to support a network robot system, summarized in Table 2.

The *Robot Registry (RR)* includes information about the capabilities of each robot, which can be used by a central planner for path planning within each robot's mobility constraints and appropriate allocation of robots to perform services. This information is used by the planner to allocate robots to services appropriate to their capabilities, e.g. assigning a cart robot to a baggage-carrying task.

The *User Registry (UR)* holds personal information about customers (or other service recipients) and is necessary for applications where personalized services are to be provided. For example, in some of our field experiments, customers provided their shopping list information via smartphones. Such information is stored in the UR together with the customer's name and known device ID.

The *Map Registry (MR)* includes navigation and safety maps of an environment, to be used for localization and path planning. In our implementation, navigation maps are generated through offline SLAM using laser scan and odometry data recorded from robots, and safety zone maps are generated by hand.

The safety zone maps are necessary because public environments often contain dangerous areas that a robot cannot detect with its sensors. Transparent and reflective objects such as glass doors and mirrors, or drop-offs such as downward steps, can be difficult or impossible for robots to detect with laser range finders or cameras. Fig. 19 shows some examples of obstacles that are difficult for robots

Fig. 19. Dangerous areas in a shopping mall. Left: glass walls. Center: movable tables and shelves where only legs are visible to ground-level LRF's. Right: movable clothing rack where only the center pole is visible to ground-level LRF's.

Table 2. Summary of information registries

Registry Name	**Data Provided**
Robot Registry (RR)	Services offered
	Navigable terrain types
	Maximum clearance
	Maximum speed
	Ownership
Map Registry (MR)	Localization map
	Dangerous areas
	Traversability map
User Registry (UR)	Customer name
	Mobile device ID
	Application content
	Personalization data

to detect with ground-level laser range finders (a typical way for robots to detect obstacles). Maps of these invisible obstacles are stored in the MR.

4.4 Coordination Module

The *coordination module* addresses the needs of path planning and of spatial coordination between robots. Access to limited spatial resources is actively managed so as to avoid deadlock between robots which are competing to occupy a critical space, such as advertising robots crowding near an entrance or several robots with low battery attempting to access a charging station. When a robot

requests use of a limited spatial resource, the coordination module will grant permission only if the space is not already in use.

Dynamic path planning is also provided, both to avoid collisions between robots and to ensure smooth movement among pedestrians, based on tracking data from the sensing framework. An example is shown in Figure 20.

Fig. 20. Coordinating multiple robots: (a) Robots are given non-conflicting paths to reach their respective customers, (b) Each robot provides its service

The coordination module can also generate socially-meaningful paths, based on the robot's current service task. For example, approach paths should be computed to approach people from a frontal direction rather than the side or back [32, 26]. A robot can also communicate intention through its locomotion, as illustrated by the example of "friendly patrolling" [12].

The path planner also considers traversability constraints. Some robots can traverse uneven surfaces, slopes, or small steps, while others cannot. These differences are reflected in a traversability map for each robot type, stored in the MR, and are used in path planning.

4.5 Service Allocation

The *service allocator* is the central planning mechanism which assigns services to robots and monitors the execution of those services. It handles service requests, identifies service opportunities, handles reservations for future services, and coordinates service allocation across multiple robots by considering the priorities of services and the capabilities and physical locations of the robots in its allocation algorithm.

In our framework, each service to be provided by robots is comprised of several *service tasks*, which are execution units managed by the server. The server contains logic determining which service tasks should be executed, under which conditions, by which types of robots. Once the server assigns a service task to a robot, the robot itself handles the details of service task execution, reporting back to the server upon success or failure.

On-demand services. For on-demand services, customers need a means to request services directly from the system, e.g. using a smartphone, or from the robots directly. In either case, the requests are sent to the service allocator. Service requests can be for immediate service or reservations for future services.

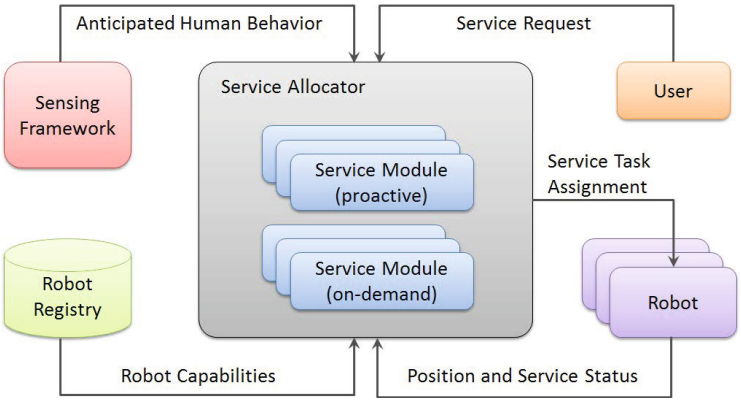

Fig. 21. Basic flow of service task allocation

Proactive services. For "proactive," or "targeted" services, such as giving directions, recommending shops, or advertising services, the robots will approach unknown people to offer their services. In such cases, the service allocator must identify *opportunities* for providing services, rather than responding to requests, and allocation logic must be developed to assign robots to services based on anticipation of who will need or want the service. To do this, it uses the statistical model of pedestrian behavior provided by the *primitive analyzer*, described in Section 3 to target and avoid people performing specific behaviors.

For example, in the case of robots advertising for a shop, the system could be configured to target customers who are exhibiting "stop" or "idle walk" behavior, in the spatial region in front of the shop, and to avoid customers who are performing "busy walk" primitive.

The model of global behaviors can be used to predict customers who are likely to perform this behavior in this area several seconds before they arrive, which gives the system time to allocate a robot and for that robot to move into the appropriate area. The robot is then sent to approach the person and give information about the shop.

4.6 Support from a Human Operator

While robots today have greater capabilities for sensor recognition, dynamic planning, error detection, and error recovery than ever before, they are still far from ready to be deployed autonomously alongside humans in unstructured,

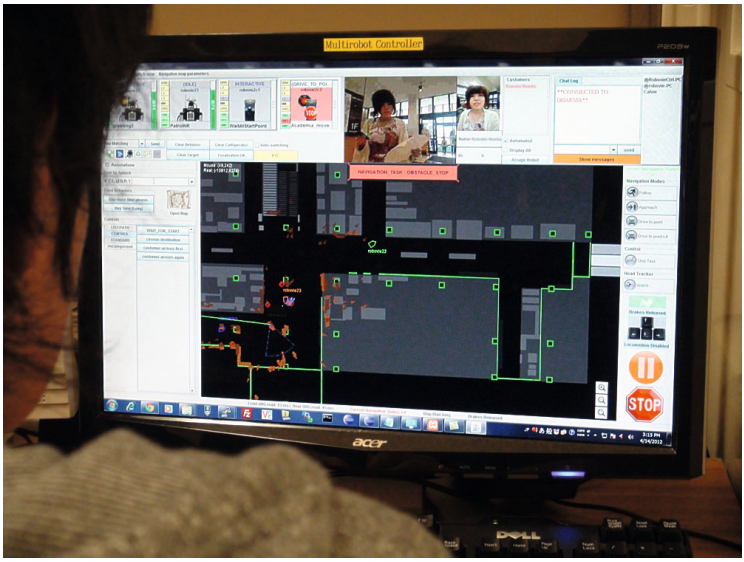

Fig. 22. Operator using a teleoperation console to supervise four robots

public environments. For the foreseeable future, we expect that there will always be a human supervisor present behind the scenes to monitor and assist robots at some level.

In our system, supervisors typically use an interface such as that shown in Fig. 22 to assist the robot's recognition of sensor inputs, e.g. speech recognition or person identification, and to monitor for and correct sensing errors, e.g. identifying dangerous situations or correcting localization. The robot performs its own speech, gesture, and motion planning autonomously, and the role of the human is only to provide occasional sensor inputs.

In rare cases, an operator will need to control the robot directly to handle "uncovered" situations, such as an unexpected question from a customer, or replanning the robot's path to avoid unmodeled obstacles. In these cases, the robot cannot respond autonomously, so the human controls the robot directly.

Finally, some mechanism is needed to enable one operator to manage multiple robots. Techniques such as *proactive timing control* [8] and *conversation fillers* [30] can help improve performance of semi-autonomous robot teams in social interactions.

In the future, as the technology for speech recognition and robot localization improves, the responsibilities of the operator will most likely shift towards handling only rare, exceptional situations and monitoring robots for safety and quality of service. Such a high-level supervisory operator could potentially manage large teams of robots, much like a supervisor at a modern call center.

4.7 Standardization

An open standard for the architecture for robotic services presented here has been formalized and is currently the focus of much standardization work and prototype development. It is known as the Ubiquitous Network Robot Platform (UNR-PF), and its details are introduced in [14].

The common platform architecture was discussed in the International Telecommunication Union Telecommunication Standardization Sector (ITU-T), study group 16 (SG16) as an application of ubiquitous sensor network (USN). The proposal was accepted as a standardization work item in 2011 and was issued as recommendation F.747.3 in March 2013.

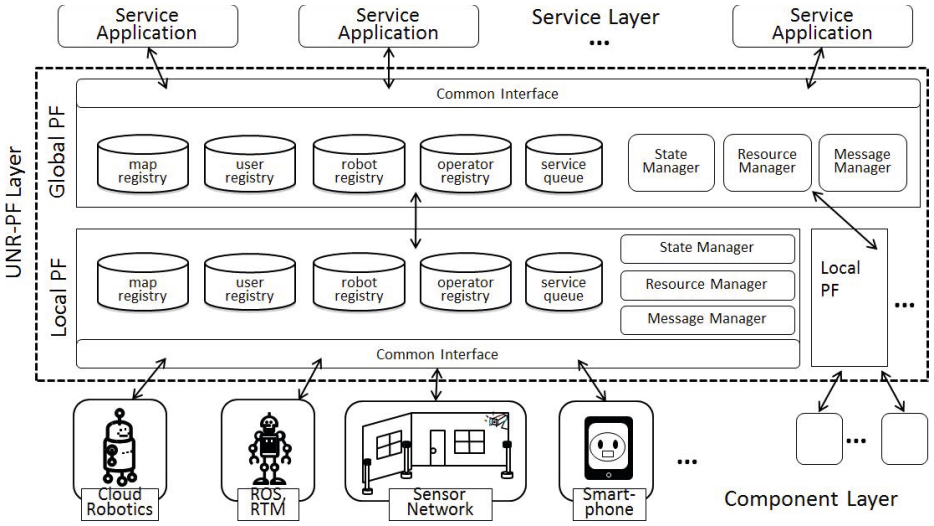

Fig. 23. Overview of the UNR-PF architecture

Figure 23 shows the UNR-PF architecture.

Some extensions in the open platform include an Operator Registry, so that robot operators with varying skills can be accommodated and assigned by the system as human supervisors for specific tasks, and a separation of the platform into local platforms (LPF) and global platforms (GPF), to accommodate deployments in multiple locations.

The standardization of common interfaces between service applications and robotic functional components, that includes robots and sensing framework, is treated in OMG as the Robotic Interaction Service (RoIS) Framework specification, which was issued in Feburary 2013 as RoIS 1.0 specification.

5 Field Deployments

We have deployed the systems described here in several locations, for both short- and long-term field studies as well as experiments for research and many months of development and testing. In this section, we will summarize the kinds of services that were provided in these field trials and how they were supported by the Network Robot System.

Robots. For most of these trials, we used various models of "Robovie," an interactive humanoid robot designed for communication using speech and human-like gesture [17](Figure 24). Robovie has a head with three degrees of freedom (DOF), two arms with four DOF each, and a wheeled differential-drive mobile base. Its height and weight are 120 cm and 40 kg. On its head it has two CCD cameras as eyes and a speaker for a mouth. It is equipped with basic computation resources, and it communicates with the NRS via wireless LAN. We used corpus-based speech synthesis [20] for generating speech. For some applications, we used a shopping-cart robot capable of carrying a shopping basket, shown in Figure 24, with no head or arms but the same speech synthesis and locomotion capabilities.

Fig. 24. Robots used in these studies, left to right: Robovie II, Robovie IIs, shopping-cart robot, Robovie-R3

Environments. Different versions of our system have been used in a variety of locations, including an elderly care home, elementary schools, a train station, and a science museum. However, the field deployments described here were mainly conducted in two locations. The first was the Universal CityWalk Osaka shopping arcade described in Section 3, and the second was APiTA Town Keihanna, a shopping mall near our laboratory which includes a large entry atrium, several aisles between shops with open storefronts, and a supermarket.

5.1 Targeted Services

In many scenarios, we have used the results of the primitive analysis presented in Section 3 to target robot services to people based on the context of their spatial or behavior primitives, rather than responding to explicit requests.

Route Guidance. Figure 25 illustrates an application in which the robot gives people directions. Near a large intersection in a shopping center, a robot is waiting to offer route guidance to customers. A woman stops in front of a map of the mall (Fig. 25 (a)). While looking at the map, she is approached and offered help by the robot: "Are you looking for a particular shop?" (Fig. 25 (b)). The robot then answers any of her questions by giving directions or accompanying her to a destination. This scenario illustrates the need to recognize and anticipate people's needs, and the ability to allocate robot services accordingly.

Fig. 25. An example of a *targeted service*: (a) The sensing framework detects a woman stopping in front of a map, then (b) The robot approaches her to offer information

Entertainment Application. In other trials we have had robots provide entertainment by chatting with people. As mentioned earlier, the shopping arcade is next to an amusement park, so it is a reasonable for the robot to be entertaining people who have free time. We think that such an entertainment service would be reasonable for a robot in other environments as well, as robots today are still an exciting novelty.

In this case the robot approached people and chatted about the attractions in the amusement park. For example, the robot said, "Hi, I'm Robovie. Yesterday, I saw the Terminator at Universal Studios. What a strong robot! I want to be cool like the Terminator. 'I'll be back...' ". We set the target local behavior as *stop*, and non-target as *fast-walk*, in order to serve people who are idle. Overall, people seemed to enjoy seeing a robot that approached them and spoke.

Shop Recommendations. The second example is one in which the robot recommends and invites the customer to visit a shop. In the shopping arcade, attracting people's attention to shops and products is an important task. We believe

that this is also a reasonable service to expect from a robot, as the novelty of robots makes them very effective in attracting people's attention. The contents the robot provided were simple; for example, the robot said, "Hello, I'm Robovie. Do you enjoy shopping? I'd like to recommend this shop, where they sell clothes by the kilogram!" Whenever it mentioned a shop, it pointed the direction of the shop with a reference term "this" or "that" [33].

In the demonstration, many people were interested in the robot and listened to its invitations. Figure 26 shows an impressive example where the robot approached a couple who were performing *idle-walk*. When the robot pointed to the shop and gave its recommendation (Figure 26 (c)), they smiled with surprise to see a robot performing a real business task. After the robot mentioned the shop, the woman walked directly to the shop and entered it (Figure 26 (d)). Observing such behavior indicates that such an invitation task can be a promising application. As indicated above, the robot was able to attract people's attention and redirect their interests to shops and products.

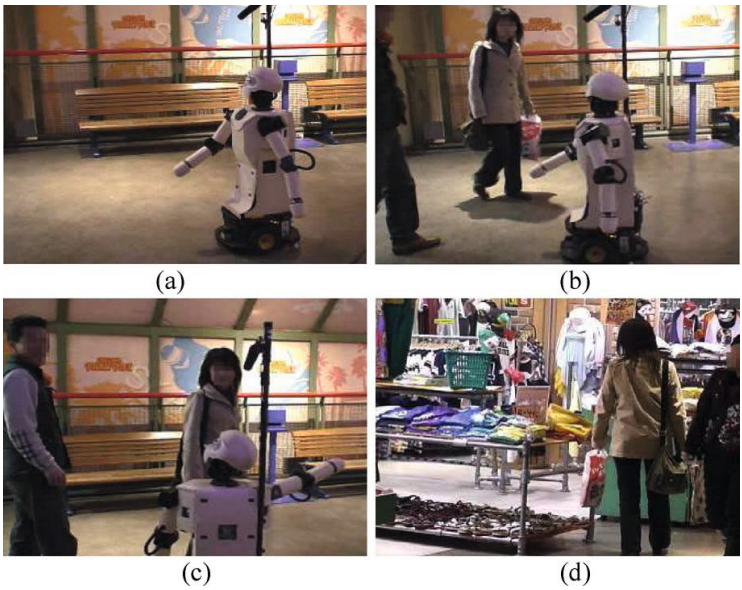

Fig. 26. A robot successfully inviting a person to a shop

5.2 Personalized Services

When personal information for individual customers is registered in the system, the NRS enables personalized services to be provided. In one demonstration we showed a scenario in which a registered customer uses her mobile phone at home to request a robot to help her on her next shopping trip. She enters her shopping

list verbally, using a mobile application which connects to the NRS (Fig. 27 (a)). Upon her arrival at the mall (Fig. 27 (b)), a robot comes to greet her, identifies her via her mobile phone, using wifi fingerprinting, and accompanies her through the supermarket carrying her basket (Fig. 27 (c)). Based on their location in the supermarket, the robot can remind her of items on her shopping list. This scenario illustrates how the personal information can be used in services. It also shows the need for a means of personal identification of the service recipient.

Fig. 27. An example of *personalized service*: (a) requesting a robot from her mobile phone, (b) detecting the customer's arrival, and (c) shopping with the customer

5.3 Shopping Assistance

In a medium-term study, shown in Figure 28, Iwamura et al. used the NRS to provide robotic shopping assistance in a supermarket to 24 senior citizens over a set of four shopping trips each [13]. In that study, humanoid and non-humanoid robots were used to accompany the users through the supermarket, conversing with them during the shopping trip. The dialogue was semi-autonomous, with the timing chosen by the teleoperator and the contents chosen by an autonomous system.

Fig. 28. Robot assisting elderly shoppers in a supermarket

5.4 Mobility Assistance

Although in most of our field trials the objective has been to develop robots which are highly autonomous, requiring a minimum level of intervention by an operator, autonomy is not always the objective. In one project, we demonstrated the possibility of using the NRS to support a robotic wheelchair, as shown in Figure 29. In this scenario, a user reserves a wheelchair using a smartphone. The system can detect when the user arrives at the shopping mall using the smartphone's GPS localization, and the robot goes out to meet the user. Once the user is seated in the wheelchair, they can drive the wheelchair themselves using a joystick, taking advantage of the wheelchair's on-board safety system, or they can request to go to a specific destination, using the path planning functionality of the NRS.

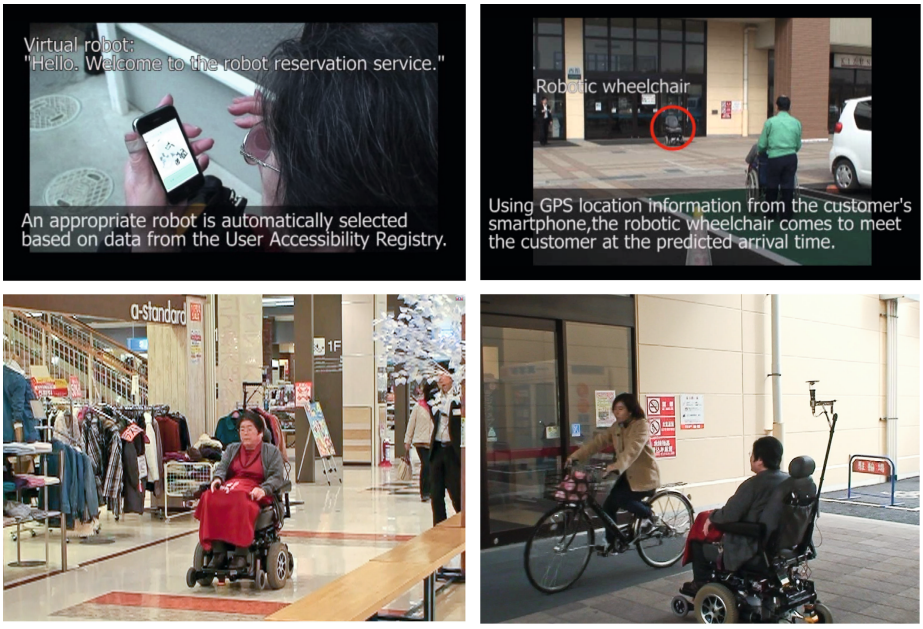

Fig. 29. Robotic wheelchair supported by the Network Robot System. (Top) User reserves the wheelchair robot ahead of time, and robot goes to meet the user as she arrives. (Bottom) Robot guides user safely through shopping mall, avoiding dynamic obstacles.

This scenario is motivated by the fact that many elderly wheelchair users are not comfortable going out alone in their wheelchair, due to safety concerns. This makes them dependent on family members whenever they want to go out. However, by using a robotic wheelchair supported by the NRS, they can take advantage of built-in safety systems, automatic navigation, and most importantly,

they can take comfort in knowing that a remote operator is available if they have any trouble. In this scenario, the operator is not merely a replacement for technologies which are not yet available, but is an essential part of the service.

5.5 Cross-Platform Collaboration

One strength of our NRS framework is the ability to easily integrate new robots, new sensors, or new services to the system. Using simple protocols to connect to the planning, coordination, and localization servers, third-party robots can be integrated easily into the NRS without deep or complex software integration, enabling collaboration between very different kinds of robots.

We have conducted collaborative work with the DustCart robot from the EU Dustbot project (Fig. 30), and with Honda's ASIMO robot (Fig. 2). In these demonstrations, Robovie talked with visitors and initiated a collaborative task, wherein the other robot performed some physical task, e.g. serving a drink or carrying baggage, while Robovie continued talking to the visitor, offering chatting or verbal instruction.

Fig. 30. Collaboration between Robovie and DustCart, supported by the NRS

In each case, only 1-2 weeks of implementation and testing were necessary to integrate the new robots with the NRS platform and prepare a collaborative robot demonstration. We have also conducted other NRS demonstrations with robots such as Mitsubishi's Wakamaru and Toshiba's ApriPoco.

Discussion. Further details about people's responses to robots were examined in more detail in succeeding studies, e.g. a study of social behavior in approaching humans [26] and integration of different capabilities of robots [28], which are based on the techniques and service frameworks reported in this paper.

Practical Considerations. Aside from the target functionalities presented in this paper, our experiences have shown a number of practical benefits provided by the modular design of the NRS framework.

When robots experience hardware problems – hard drive crashes, electrical failures, etc., the modularity of the NRS framework makes it easy to swap a backup robot into the system, enabling the experiment or demonstration to continue in a nearly seamless way. Rather than statically specifying services, paths, etc. within individual robots, the NRS dynamically allocates paths and services, which minimizes the settings or code that need to be modified when the composition of the robot team changes.

We have even replaced robots with different robot models – in one field trial we had some hardware problems with a Robovie-R3 robot, and we were able to seamlessly replace it with a Robovie-R2 (a robot with a very different design) for an important demonstration. This was possible because differences in hardware components and internal implementations of gestures and poses are hidden beneath the abstraction layer of "service tasks," enabling the different robots to operate interchangeably within the network robot system.

The addition of new sensor types is also facilitated by our modular design. We have developed a new version of our human-tracking system using RGBD sensors [3]. Although developed by an independent team, such alternate sensor systems can be seamlessly used with our robots if they support the data protocols in our NRS framework design. This flexibility has been extremely helpful in managing the complexity of heterogeneous robot deployments in multiple environments with different sensor systems.

Finally, the use of the Map Registry makes it possible to easily switch environments. We often move robots between our lab and various field trial environments, and the local NRS at each environment enables the robots to automatically make use of the latest navigation maps and receive path planning and service allocation for that environment.

5.6 Conclusions

We have presented a framework for a Network Robot System, in which mobile robots, planning servers, and sensors embedded in an environment are integrated to provide robot services to people in social contexts. The requirements for this framework, motivated by our experiences in several years of field trials, primarily include the need for recognition and anticipation of people's behavior, identification of individuals, coordination of services and navigation paths between robots, and supervision by a human operator.

We presented a field experiment showcasing the capabilities of this framework by providing services with four robots in a shopping mall, and our results showed that not only was the technical framework successful in supporting the robot services, but that people who used the robots responded in a positive way, with a great majority indicating that they would like to use services like these in the future. This underscores the worth of conducting research and field experiments to investigate and develop social robot services in real-world environments, and we submit that the NRS approach is an effective and practical way to make such robot deployments a reality.

6 Cloud Networked Robotics

Although the NRS architecture has proven to be tremendously useful even with today's technology, the future promises many exciting possibilities for extending this approach.

In particular, the trend towards using cloud-based resources is becoming a popular new direction in robotics, and we believe it represents the natural next step in evolution of the NRS. The technologies of web services and service-oriented architecture (SOA), which form the technical foundation of cloud computing, have also been applied to robotic technologies in three ways.

6.1 Cloud Computing

One of the performance bottlenecks in robotics has always been recognition. Common sensory recognition tasks such as mapping and face and speech recognition require heavy processing and have long been the focus of optimization efforts. Tasks like these are excellent candidates for moving the processing load to networked servers, and eventually remote server farms.

The field of social robotics presents a wide variety of difficult processing tasks - recognition of social relationships and situations, recognition of human intention, and decisions as to how to best interact with people to provide effective services are complex tasks which could perhaps best be relegated to the cloud.

6.2 Sharing Data

Great benefits could be recognized from establishing shared data stores enabling social behavior generation or recognition. Online data exchanges such as RoboEarth[4] are already being developed as a means to provide cloud-based knowledge support for networked robots [38]. We have already conducted a proof-of-concept study demonstrating the integration of the UNR Platform and RoboEarth, combining RoboEarth's cloud-based support for robot recognition and action scripts with the platform-independent service execution architecture provided by the UNR-PF [35].

On the other hand, some knowledge stored in the information registries could be highly proprietary to the owners of a NRS, whereas other knowledge, such as map data, might be shareable or even outsourced to external services. Careful consideration will need to be given to levels of privacy and ownership of information when, for example, one organization licenses robots to multiple businesses.

Recently, several notions of cloud computing have been introduced into robotics that are known as cloud-enabled or cloud robotics.

[4] RoboEarth. `http://www.roboearth.org`

6.3 Service Continuity

Another approach utilizes robotic resources as a cloud to solve the issue of continuous support in robotic services. Since robotic services and robotic components are considered services in SOA, they can cooperate with each other if they are organized appropriately. Du et al. [40] introduced the concept of Robot as a Service and the framework of a Robot Cloud Center. Quintas et al. [23] proposed a service robotic system in which a group of robots and a smart-room share acquired knowledge over an SOA. The above projects rely on both *de facto* and *de jure* standards in the fields of networks, web service, knowledge representation for utilizing the technologies in SOA, and cloud computing. To realize cloud networked robotics, common protocols for robotic services must also be standardized for integration.

7 Conclusion

In this work, we have explored many aspects of the problem of how to enable the deployment of social robots in real-world environments. The essential points that have been presented are as follows:

- The use of external sensors to provide robust, high-precision tracking of people in the environment to assist robots in navigational interactions.
- Development of empirical models of social behavior in a space, to enable anticipation of people's future behavior.
- The use of a human operator to assist a team of robots with difficult recognition problems and unexpected situations.
- A framework for robot coordination, service allocation, and knowledge sharing to support the operation of heterogeneous teams of service robots.
- A set of global standards for a robot service architecture enabling independent application development for a networked ecology of of robots, sensors, data resources, and mobile devices.

We have demonstrated stable implementations of each of the systems presented in this work through a series of robot experiments and long-term deployments in several field environments over a period of about five years. The effectiveness of these systems has been demonstrated in the field, and the field experiences have contributed directly to the direction of this research. All of the systems presented here are still in use as framework elements supporting a variety of research in human-robot interaction.

Thus, this work provides a successful, concrete example of a coherent collection of systems for human tracking, behavior analysis and anticipation, supervisory teleoperation, interaction design, and robot service coordination, which together enable the practical deployment of teams of social robots to provide services in real-world environments.

It is our sincere hope that through our global standardization work for RoIS and the UNR-PF, we can share with the world the practical knowhow gained

through our years of experimentation, and that this contribution will help to bootstrap and accelerate the development of commercial applications for service robots as we enter the fledgling years of a new cloud robotics era.

Finally, beyond the engineering solutions and system design, the development of this system has provided a deeper and more significant contribution - it has enabled us to obtain an early glimpse of what the world will be like when robots eventually work in real social environments.

Without actual, real-world deployment of robots, modeling and laboratory experiments can only take us so far – we can only speculate about how people may theoretically interact with robots and use their services in the future. But the development and deployment of this system has provided a way to truly observe and study real human-robot interactions in social environments, opening the door to a wide variety of academic studies and commercial innovations.

Acknowledgments. We would like to thank Dr. Masahiro Shiomi and Dr. Satoru Satake for their contributions in designing and building this framework, Dr. Satoshi Koizumi for his help in the organization and realization of the field trials, and the many students, interns, engineers, researchers, and assistants who have contributed directly and indirectly to the development of the Network Robot System over the years. We would also like to thank the management and staff of Universal CityWalk Osaka and APiTA Town Keihanna, without whose cooperation this work would not have been possible.

This work was partially supported by the Japanese Ministry of Internal Affairs and Communications, the Grant-in Aid for Scientific Research (A), Kakenhi, under Grant 21680022, the Program for Promoting the Establishment of Strategic Research Centers, and the Special Coordination Funds for Promoting Science and Technology of the Ministry of Education, Culture, Sports, Science and Technology of Japan.

References

[1] Ball, G., Hall, D.: Isodata, a novel method of data analysis and pattern classification. Technical report, DTIC Document (1965)

[2] Brooks, A., Williams, S.: Tracking people with networks of heterogeneous sensors. In: Australasian Conference on Robotics and Automation (ACRA 2003), Brisbane QLD, Australia, December 1-3, pp. 1–7 (2003)

[3] Brščić, D., Kanda, T., Ikeda, T., Miyashita, T.: Person tracking in large public spaces using 3-d range sensors. IEEE Transactions on Human-Machine Systems PP(99), 1–13 (2013)

[4] Burgard, W., Cremers, A.B., Fox, D., Hahnel, D., Lakemeyer, G., Schulz, D., Steiner, W., Thrun, S.: The interactive museum tour-guide robot. In: Proceedings of the Fifteenth National/Tenth Conference on Artificial Intelligence/Innovative Applications of Artificial Intelligence, Madison, Wisconsin, United States, pp. 11–18. American Association for Artificial Intelligence (1998)

[5] Cui, J., Zhao, H., Shibasaki, R.: Fusion of detection and matching based approaches for laser based multiple people tracking. In: Proc. of the IEEE Computer Society Conference on Computer Vision and Pattern Recognition (CVPR 2006), New York, USA, pp. 642–649 (2006)
[6] Garrell, A., Sanfeliu, A.: Model validation: Robot behavior in people guidance mission using dtm model and estimation of human motion behavior. In: 2010 IEEE/RSJ International Conference on Intelligent Robots and Systems (IROS), pp. 5836–5841 (2010)
[7] Glas, D.F., Kanda, T., Ishiguro, H., Hagita, N.: Simultaneous people tracking and localization for social robots using external laser range finders. In: IEEE/RSJ International Conference on Intelligent Robots and Systems, IROS 2009, St. Louis, MO, USA, pp. 846–853. IEEE Press (2009)
[8] Glas, D.F., Kanda, T., Ishiguro, H., Hagita, N.: Teleoperation of multiple social robots. IEEE Transactions on Systems, Man and Cybernetics, Part A: Systems and Humans 42(3), 530–544 (2012)
[9] Glas, D.F., Miyashita, T., Ishiguro, H., Hagita, N.: Laser-based tracking of human position and orientation using parametric shape modeling. Advanced Robotics 23(4), 405–428 (2009)
[10] Glas, D.F., Satake, S., Ferreri, F., Kanda, T., Ishiguro, H., Hagita, N.: The network robot system: Enabling social human-robot interaction in public spaces. Journal of Human-Robot Interaction 1(2), 5–32 (2012)
[11] Gockley, R., Forlizzi, J., Simmons, R.: Interactions with a moody robot. In: Proceedings of the 1st ACM SIGCHI/SIGART Conference on Human-Robot Interaction, Salt Lake City, Utah, USA, pp. 186–193. ACM (2006)
[12] Hayashi, K., Shiomi, M., Kanda, T., Hagita, N.: Friendly patrolling: A model of natural encounters. In: Robotics: Science and Systems VII, Los Angeles, CA. MIT Press (MA) (2012)
[13] Iwamura, Y., Shiomi, M., Kanda, T., Ishiguro, H., Hagita, N.: Do elderly people prefer a conversational humanoid as a shopping assistant partner in supermarkets?. In: Proceedings of the 6th International Conference on Human-Robot Interaction, Lausanne, Switzerland, pp. 449–456. ACM (2011)
[14] Kamei, K., Nishio, S., Hagita, N., Sato, M.: Cloud networked robotics. IEEE Network 26(3), 28–34 (2012)
[15] Kanda, T., Glas, D.F., Shiomi, M., Hagita, N.: Abstracting people's trajectories for social robots to proactively approach customers. IEEE Transactions on Robotics 25(6), 1382–1396 (2009)
[16] Kanda, T., Hirano, T., Eaton, D., Ishiguro, H.: Interactive robots as social partners and peer tutors for children: A field trial. Human-Computer Interaction 19(1), 61–84 (2004)
[17] Kanda, T., Ishiguro, H., Imai, M., Ono, T.: Development and evaluation of interactive humanoid robots. Proceedings of the IEEE 92(11), 1839–1850 (2004)
[18] Kanda, T., Shiomi, M., Miyashita, Z., Ishiguro, H., Hagita, N.: An affective guide robot in a shopping mall. In: Proceedings of the 4th ACM/IEEE International Conference on Human Robot Interaction, La Jolla, California, USA, pp. 173–180. ACM (2009)
[19] Kanda, T., Shiomi, M., Perrin, L., Nomura, T., Ishiguro, H., Hagita, N.: Analysis of people trajectories with ubiquitous sensors in a science museum. In: 2007 IEEE International Conference on Robotics and Automation, pp. 4846–4853. IEEE (2007)
[20] Kawai, H., Toda, T., Ni, J., Tsuzaki, M., Tokuda, K.: Ximera: A new tts from atr based on corpus-based technologies. In: Fifth ISCA Workshop on Speech Synthesis (2004)

[21] Mazzolai, B., Mattoli, V., Laschi, C., Salvini, P., Ferri, G., Ciaravella, G., Dario, P.: Networked and cooperating robots for urban hygiene: The eu funded dustbot project. In: Proceedings of the 5th International Conference on Ubiquitous Robots and Ambient Intelligence, URAI (2008)
[22] Mutlu, B., Forlizzi, J.: Robots in organizations: the role of workflow, social, and environmental factors in human-robot interaction. In: Proceedings of the 3rd ACM/IEEE International Conference on Human Robot Interaction, Amsterdam, The Netherlands, pp. 287–294. ACM (2008)
[23] Quintas, J., Menezes, P., Dias, J.: Cloud robotics: Towards context aware robotic networks. In: Proc. of the 16th IASTED International Conference on Robotics, Pittsburgh, USA
[24] Sakoe, H., Chiba, S.: Dynamic programming algorithm optimization for spoken word recognition. IEEE Transactions on Acoustics, Speech and Signal Processing 26(1), 43–49 (1978)
[25] Sanfeliu, A., Hagita, N., Saffiotti, A.: Special issue: Network robot systems. Robotics and Autonomous Systems 56(10), 791–791 (2008)
[26] Satake, S., Kanda, T., Glas, D.F., Imai, M., Ishiguro, H., Hagita, N.: How to approach humans?: Strategies for social robots to initiate interaction. In: Proceedings of the 4th ACM/IEEE International Conference on Human Robot Interaction, La Jolla, California, USA, pp. 109–116. ACM (2009)
[27] Schulz, D., Burgard, W., Fox, D., Cremens, A.B.: People tracking with mobile robots using sample-based joint probabilistic data association filters. International Journal of Robotics Research (IJRR) 22(2), 99–116 (2003)
[28] Shiomi, M., Kanda, T., Glas, D.F., Satake, S., Ishiguro, H., Hagita, N.: Field trial of networked social robots in a shopping mall. In: IEEE/RSJ International Conference on Intelligent Robots and Systems, IROS 2009, St. Louis, MO, USA, pp. 2846–2853. IEEE Press (2009)
[29] Shiomi, M., Kanda, T., Ishiguro, H., Hagita, N.: Interactive humanoid robots for a science museum. IEEE Intelligent Systems 22(2), 25–32 (2007)
[30] Shiwa, T., Kanda, T., Imai, M., Ishiguro, H., Hagita, N.: How quickly should communication robots respond? In: Proceedings of the 3rd ACM/IEEE International Conference on Human Robot Interaction, Amsterdam, The Netherlands, pp. 153–160. ACM (2008)
[31] Siegwart, R., Arras, K.O., Bouabdallah, S., Burnier, D., Froidevaux, G., Greppin, X., Jensen, B., Lorotte, A., Mayor, L., Meisser, M., Philippsen, R., Piguet, R., Ramel, G., Terrien, G., Tomatis, N.: Robox at expo.02: A large-scale installation of personal robots. Robotics and Autonomous Systems 42(3), 203–222 (2003)
[32] Sisbot, E.A., Alami, R., Simeon, T., Dautenhahn, K., Walters, M., Woods, S.: Navigation in the presence of humans. In: 2005 5th IEEE-RAS International Conference on Humanoid Robots, pp. 181–188 (2005)
[33] Sugiyama, O., Kanda, T., Imai, M., Ishiguro, H., Hagita, N., Anzai, Y.: Humanlike conversation with gestures and verbal cues based on a three-layer attention-drawing model. Connection Science 18(4), 379–402 (2006)
[34] Takayama, L., Marder-Eppstein, E., Harris, H., Beer, J.M.: Assisted driving of a mobile remote presence system: System design and controlled user evaluation. In: 2011 IEEE International Conference on Robotics and Automation (ICRA), pp. 1883–1889 (2011)
[35] Tenorth, M., Kamei, K., Satake, S., Miyashita, T., Hagita, N.: Building knowledge-enabled cloud robotics applications using the ubiquitous network robot platform. In: IEEE/RSJ International Conference on Intelligent Robots and Systems (IROS 2013), pp. 5716–5721 (2013)

[36] Tomizawa, T., Ohya, A., Yuta, S.: Remote shopping robot system - development of a hand mechanism for grasping fresh foods in a supermarket. In: 2006 IEEE/RSJ International Conference on Intelligent Robots and Systems, pp. 4953–4958 (2006)
[37] Villagrasa, A.M.: People tracking for a personal robot. Master's thesis, Royal Institute of Technology, Stockholm, Sweden (August 2005)
[38] Waibel, M., Beetz, M., Civera, J., D'Andrea, R., Elfring, J., Galvez-Lopez, D., Haussermann, K., Janssen, R., Montiel, J., Perzylo, A.: Roboearth. IEEE Robotics and Automation Magazine 18(2), 69–82 (2011)
[39] Zhao, H., Shibasaki, R.: A novel system for tracking pedestrians using multiple singlerow laser-range scanners. IEEE Transactions on Systems, Man, and Cybernetics 35(2), 283–291 (2005)
[40] Zhihui, D., Weiqiang, Y., Yinong, C., Xin, S., Xiaoying, W., Chen, X.: Design of a robot cloud center. In: 2011 10th International Symposium on Autonomous Decentralized Systems (ISADS), pp. 269–275 (2011)

Intelligence Technology for Ubiquitous Robots

Jong-Hwan Kim, Sheir Afgen Zaheer, and Si-Jung Ryu

Department of Electrical Engineering, KAIST,
Guseong-dong, Yuseong-gu, Daejeon, 305-701, Republic of Korea
johkim@rit.kaist.ac.kr
http://rit.kaist.ac.kr/home

The evolution of computer technology, in terms of technology and its interrelationship with humans, inspired the dawn of ubiquitous computing [1]-[2]. This revolutionary concept of ubiquity inspired a new generation of robotics, i.e. ubiquitous robotics. In the second generation of robots, the service robots were characterized by standalone robotic platforms. As such, the capabilities of these service robots were limited to their current location. Even with advancements in the internet network that led to the development of innovative architectures, the interface provided by these robots was spatially restricted to their physical existence. On the other hand, ubiquitous robotics spawn the idea of an omnipresent robot platform. Both the service and interface provided by ubiquitous robots are not spatially limited.

The primary advantage of the ubiquitous robotics, the third generation of robotics, is that it permits the abstraction of intelligence from the real world by decoupling it from perception and action capabilities. In other words, ubiquitous robots can be considered as networked cooperative robot systems that can provide calm and seamless services.

During the past five decades, robots have come a long way from being high precision tools of the modern industrial development to our personal assistants, such as our pet companions and even as artificial body parts. All these applications vary considerably on the scales of precision and cognitive ability. To equip ubiquitous robots with these advancements, we present "intelligence technology (InT) for ubiquitous robots." InT is the application of machines and agents to perceive and process data and information for knowledge-based reasoning and to utilize their own reasoning to execute an appropriate action [3]. InT not only aims for intelligent behavior execution but also for equipping robots with thought mechanisms that lead them to actually manipulate intelligence via different components of ubiquitous robots.

1 Ubiquitous Robotics

Robotics has been defined as the 'intelligent connection of perception to action' [4]. Ubiquitous robotics justifies that definition by allowing us to redefine the interconnection between the three components: intelligence, perception and action. These are manifested individually as the intelligent software robot: Sobot,

S. Mohammed et al. (eds.), *Intelligent Assistive Robots,*
Springer Tracts in Advanced Robotics 106, DOI: 10.1007/978-3-319-12922-8_10

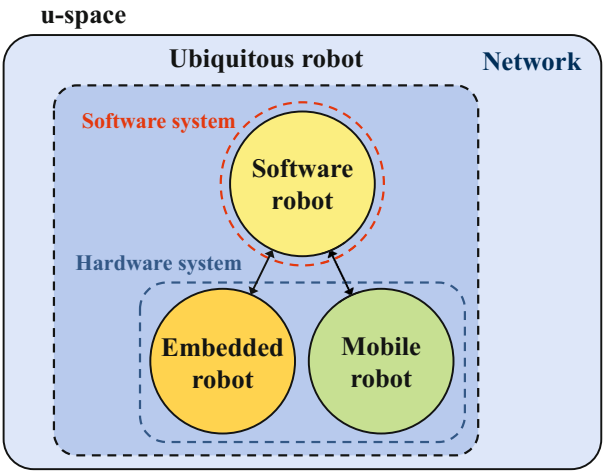

Fig. 1. Ubiquitous robot in ubiquitous space

the perceptive embedded robot: Embot and the physically active mobile robot: Mobot, respectively, as described in [5].

Ubiquitous robotics spawn the idea of an omnipresent robot platform. Both the service and interface provided by ubiquitous robots are not spatially limited. Ubiquitous robot systems enable the abstraction of intelligence from the real world by decoupling it from perception and action capabilities. Inspired from the attributes of ubiquitous computing, this abstraction allows ubiquitous robots to be calm, seamless and context aware.

The ubiquitous robot is created and exists within a u-space (Fig. 1) which consists of both physical and virtual environments. It can be conceptualized as a networked cooperative robot system. Software robots, or Sobots, constitute the core intelligence of the system, and are connected to the distributed Embot sensors in the physical space to ensure context awareness through perceived environmental information. The final outcomes of intelligent processing by Sobots in the virtual space are realized in the physical space by Mobots. Sensory information by Embots is standardized along with motor or action information of Mobots and this permits the abstract intelligence to proceed with the task of providing services in a calm and seamless manner.

Ubiquitous robots provide services through the network in a u-space through the distributed capabilities provided by their constituent Sobot, Embot and Mobot systems. Based on their application domain, each ubiquitous robot has its own specific intelligence and roles, and it can communicate information through networks. Some of the integrated services and solutions offered by the ubiquitous robot technology include ubiquitous home services for smart homes, location based services like GIS, health services in telemedicine, ubiquitous learning systems and ubiquitous commerce services.

The following subsections explain the aforementioned components of the ubiquitous robot system: Sobot, Embot and Mobot, along with Middleware for communications and implemented ubiquitous robot system, called the Ubibot system [6].

1.1 Software Robot: Sobot

Sobots are entirely confined to the virtual space of the network and are able to connect with other systems irrespective of temporal and geographical limitations. Sobots are capable of operating as intelligent entities without any help from other ubiquitous robots and are typically characterized as self-learning, context-aware, intelligent, calm and seamless. Sobots perceive the environmental context within the u-space and often make decisions and execute them without requiring direct supervision from the user. They are proactive and demonstrate rational behavior and show capabilities to learn new skills.

1.2 Embedded Robot: Embot

The embedded robots are implanted within the environment or upon Mobots. Embots sense and monitor the location of a user or a Mobot. They also integrate assorted sensory information to comprehend the current environmental situation in the physical space. Embots are also networked and equipped with processing capabilities. therefore, they may deliver information to the user directly or under the Sobot's instructions. The salient attributes of Embots are their calm sensing, information processing and information communication capabilities.

1.3 Mobile Robot: Mobot

Mobots are the application/service level component of the ubiquitous robot system in the physical space. Mobility is a key property of Mobots, as well as the general capacity to provide services in conjunction with Embots and Sobots. The Mobot remains in continuous communication with the Sobot in order to provide practical services based on information given by the Embot. Moreover, Mobots also serve as a data gathering platform for Embots.

1.4 Middleware

To deliver the required services,ubiquitous robot systems require seamless communication. This calls for Middleware that allows communication within and among ubiquitous robots using a variety of network interfaces and protocols. Middleware usually varies from one vendor to the next depending upon a variety of factors. The selected middleware allows conversion of the constituent entities of the ubiquitous robot system into specific components with respect to the developer, thereby making it convenient to update functions, maintain resources and perform power management. The Middleware structure for a ubiquitous

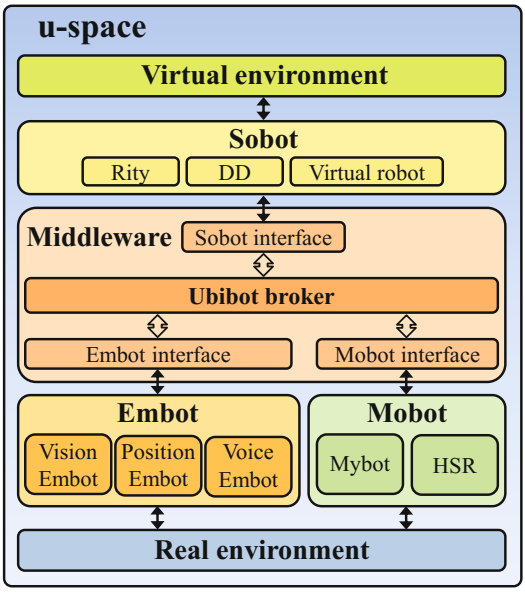

Fig. 2. The Ubibot System Architecture

robot system must contain at least one interface and one broker. The interfaces refer to the hardware level interfaces of the communication protocols such as Bluetooth and Ethernet and the software level interfaces like HTTP and FTP. The broker enables the system to make an offer of service irrespective of the operating structure, position and type of interface. This thus enables Sobots to receive information from a wide variety of Embots and to communicate with the Mobots.

1.5 Ubibot: Implemented Ubiquitous Robot System

Ubibot was developed to demonstrate the functionality and effectiveness of a ubiquitous robot system. Ubibot consists of multiple Embots, two Mobots: Mybot and HSR, and a Sobot: Rity. The overall architecture of the Ubibot system is shown in Fig. 2. Various components of Ubibot are explained in the followings:

Embots. The Ubibot system uses 3 kinds of Embots, Vision Embot, Sound Embot, and Position Embot.

a. ***Vision Embot:*** The Vision Embot, implemented via a USB camera sensor, is used for object detection and facial recognition The face detection algorithm can detect faces within 120 cm of the camera, under various lighting conditions, with an operating time of 50∼100 ms, images being captured at a rate of 16 frame/sec.The face recognition module then acts on the detected

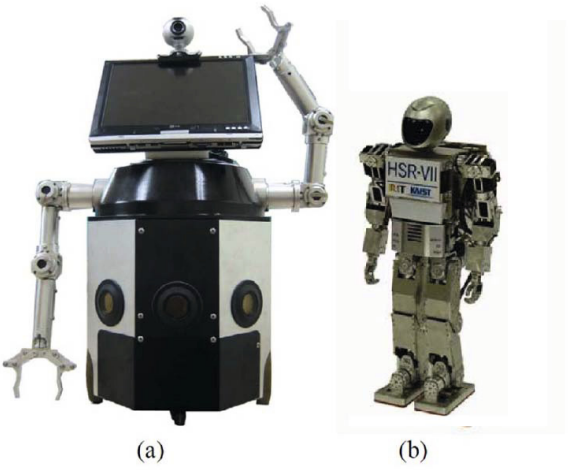

Fig. 3. Mobots: (a) Mybot–Wheeled mobile robot and (b) HSR–Humanoid robot type

face data and transmits the detected results asynchronously to Middleware at periodic intervals.

b. ***Sound Embot:*** The sound Embot employs a preprocessing algorithm to process background noise and categorize it into 5 levels: noisy, normal, calm, sudden loud, and sudden calm. It can also recognize 10 short sentences. The Sound Embot then transmits the detection results asynchronously to Middleware at periodic intervals of once in 4 seconds.
c. ***Position Embot:*** The Position Embot estimates the location of robots, objects, and humans in a 2D Cartesian coordinate system. The detected Cartesian coordinates are transmitted to Middleware at the rate of 10 hertz.

Mobots. The Ubibot system uses 2 Mobots, a wheeled mobile personal robot, Mybot and a small sized humanoid robot HSR.

a. ***MyBot:*** Mybot (Fig. 3(a)) uses a differential drive platform powered by DC motors. It is 31cm x 21cm x 42cm in size and weighs 12 Kg. It has an on-board Pentium III 850Mhz computer handling the drive, control and sensors. It is equipped with six Polaroid 6500 ultrasonic sensors covering 0.15m∼5 m in all directions on the horizontal plane. It has a mount for a Tablet PC which then communicates with the on-board PC to display the Sobot environment in real time apart from handling the wireless network access through a built-in WiFi card. A USB camera is provided for the Vision Embot.
   As it can be seen from Fig. 3(a), it also has 2 arms with grippers at the end, enabling it to provide a wide variety of service. These arms also have additional purpose of serving as the means through which Mybot can emote. Mybot also has an interactive interface in the form of its tablet PC. Once the Sobot downloads itself onto the Mybot, it can be visually seen on the screen.

Fig. 4. The artificial creature Rity, Sobot of the Ubibot system, expressing different emotions

b. ***HSR:*** HSR (HanSaRam) is a small sized humanoid robot developed in the RIT Lab at KAIST. It consists of 13 DC motors in the lower body with 14 RC servomotors in the upper body giving it a total of 27 DOFs. It has a hand with fingers which can flex together. It thus has the ability for fully independent locomotion, sensing and processing, utilizing an on-board Pentium III compatible 666 MHz PC.

Sobot. An artificial creature, Rity, developed as an agent that behaves autonomously driven by its own motivation, homeostasis, and emotion operates as the software robot for the Ubibot system. Rity visually resembles a simulated 12 DOF dog with which users can interact in a number of ways as shown in Fig. 4. Rity has a complex internal architecture with 14 internal states. It has 47 perceptions, exhibits 5 facial expressions, some of which are shown in Fig. 4 and can exhibit a total of 77 behaviors.

Rity is an intelligent software robot that lives inside the virtual world of a computer network, but interfaces with the real world through the peripheral hardware attached to the network: cameras, input devices, screens, and audio systems. The internal architecture of Rity is depicted in Fig. 5.

The general architecture of Rity is composed of 5 primary modules: perception module to perceive the environment with virtual or real sensors, internal state module to defines motivation, homeostasis, and emotion, behavior selection module to select a proper behavior for the perceived information, learning module to learn from interaction with people, and motor module to execute behaviors and express emotions.

Middleware. Since all data communication is based on TCP/IP, the middleware is realized using TCP/IP related components provided by Visual C++

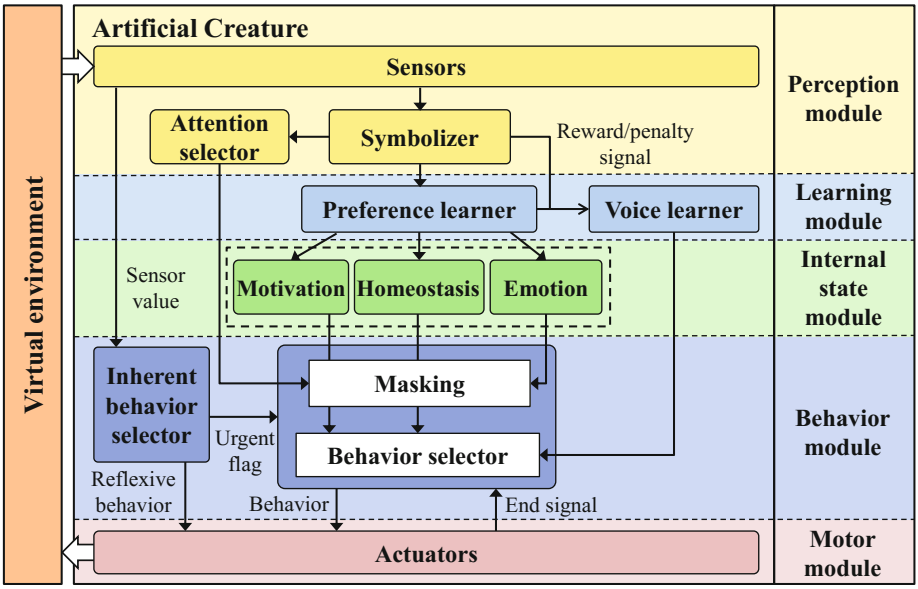

Fig. 5. Internal architecture of Rity

6.0 which is robust in a distributed environment. The Sobot transfer is accomplished through the File Transfer Protocol by using a buffer. The actual data is an abstract arrangement of its individual features encompassing data such as its internal state. The Ubibot broker program handles the transfers. Embot data transfer is done using Server/Client socket programming.

2 Intelligence Technology (InT)

Since Capek's first depiction in 1921 [7], robots have been fantasized as intelligent machines that are subservient to humans. The core issue in realizing this fantasy is to equip robots with human-like intelligence for natural interaction with humans. However, unlike humans, robots do not posses a sophisticated and highly evolved medium to manipulate intelligence. Therefore, to replicate biological intelligence, robots need to be equipped with appropriate technology for intelligent operation. To address this issue, we proposed InT [8]. InT is the application of machines and agents to perceive and process data and information for knowledge- based reasoning and to utilize their own reasoning to execute an appropriate action. InT covers all aspects of intelligence from perception at sensor level to reasoning at cognitive level to behavior planning at execution level for each low level segment of the machine.

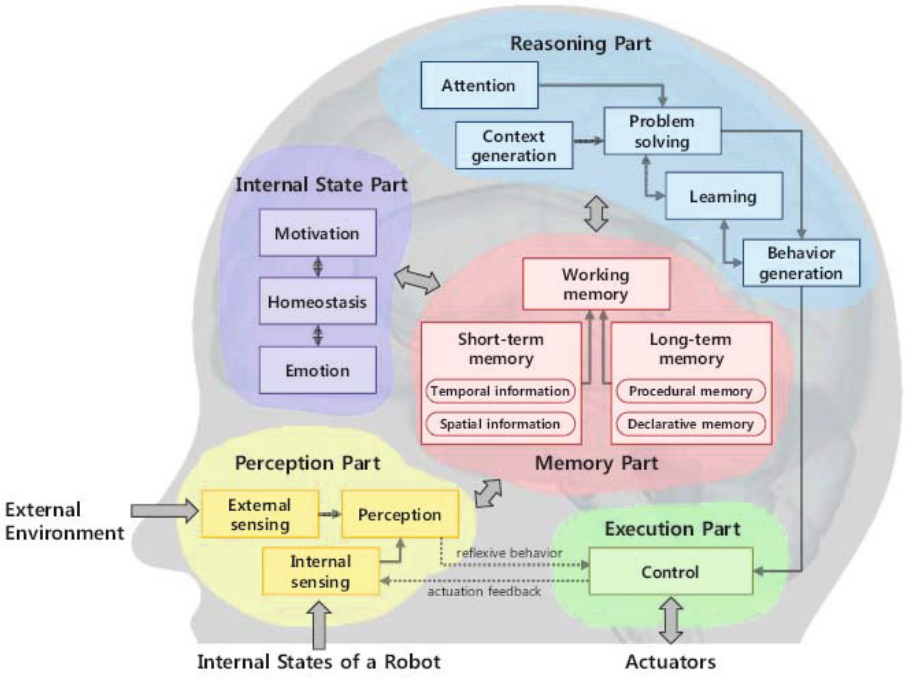

Fig. 6. Intelligence operating architecture (iOA)

2.1 Intelligence Operating Architecture for InT

To realize all aspects of InT, we proposed a modular architecture inspired by human brain functions and capable of implementing all aspects of InT. We named it as intelligence operating architecture (iOA) and it is graphically depicted in Fig. 6. The details about the five parts and 15 modules are described as follows [8].

In perception part, external and internal sensing modules gather sensory data respectively from external environment and internal states of the robot. The perception module converts the sensory data from the two sensing modules to context data and transmits it to other modules such as attention, memory, internal state modules, etc. If the context data requires an urgent response from the robot, it is directly forwarded to the control module in execution part to generate a reflexive behavior. In internal state part, each of the three modules for motivation, homeostasis and emotion controls the corresponding internal state value of the robot based on the context data through memory part. Moreover, all data including the internal state values and the context are shared with other modules through memory part.

There are three kinds of memory modules in memory part. The short-term memory module stores spatial and temporal information from the environment for a short period of time. On the contrary, the long-term memory module

deals with information stored for a long period of time. There are two types of long-term memory: procedural memory and declarative memory. The procedural memory holds information needed to use objects and to execute movements. The declarative memory refers to memories which can be consciously recalled such as facts and knowledge; it can be divided into two categories: episodic memory and semantic memory. The episodic memory stores specific events that happened in the past. The semantic memory contains factual information that is not associated with time and place. Moreover, the long-term memory module enables the robot to improve its behaviors in the future through a learning module in reasoning part. Lastly, the working memory module holds the information needed to perform tasks such as reasoning, memorizing numbers, objects, making a decision, etc., at the working moment.

In reasoning part, the attention module decides which percept has to be focused on by referring to memory part and it allows the robot to gather more useful sensory data in the environment through the gaze control. The context generation module generates a high level and/or complex contexts from the information provided by the perception module through memory part. The problem solving module is responsible for making sense of the context, analyzing all available options and selecting a plausible behavior or a course of behaviors by planning, scheduling, etc. However, the behaviors selected by this module are in a high level or abstract form, e.g. "going to a particular waypoint." To execute the selected behavior through the actuators of a particular robot, such behaviors need to be translated into basic low level tasks, e.g. "going to a particular waypoint" requires a footstep generation algorithm for a humanoid robot but in the case of wheeled robots, a steering algorithm is required. The behavior generation module deals with conversion of the high level behavior, selected by the problem solving module, into low level behaviors by utilizing algorithm(s) to handle actuator level generation of such behaviors. The learning module works in conjunction with the behavior generation module and the problem solving module. It helps both modules to learn from previous experiences stored in the long-term memory by updating the memory contents. The control module in execution part actualizes the selected behaviors through the actuators of the robot. It also sends actuation feedback to the internal sensing module in perception part.

2.2 Taxonomy of Intelligence Technology

InT is used to realize six types of intelligences: cognitive intelligence, social intelligence, behavioral intelligence, ambient intelligence, collective intelligence, and genetic intelligence.

Cognitive Intelligence. Usually, robots utilize a rigid decision process to instantly react upon the perceived information, which is generated from sensory data. However, users often expect robots to act more intelligently, such as being able to adapt to the situation by memorizing and learning. This is where cognitive intelligence steps in to reason complex or unknown context from perceived

information. Cognitive intelligence is closely related to technologies like decision making, task scheduling and memory management.

Related Application: Gaze Control

When a humanoid robot navigates in a complex dynamic environment, it needs to determine the most appropriate gaze direction after gathering useful information in the surrounding environment. It should consider the user's preference for objectives in navigation along with various types of information, such as the distance and velocity of dynamic obstacles, the localization errors of surrounding obstacles and the robot itself, its walking state, etc. For this purpose, the fuzzy integral-based gaze control algorithm was proposed [9]. After receiving the context and user's preference information, the functionality of the gaze control algorithm is mainly distributed among three modules of reasoning part. The attention module chooses the most important object to focus on, the problem solving module computes the corresponding gaze direction for the robot, and finally, the behavior generation module generate the necessary actuator level behaviors to achieve that gaze direction. The proposed algorithm considers a stand-alone robot, with a local vision system based on four criteria (or objectives) and the corresponding partial evaluation functions. The details about this proposed gaze control can be found in [9].

To perform simulations, an OpenInventor-based navigation simulator was developed by using the model of HSR (Fig. 7). The simulations were performed in a dynamic environment with moving obstacles. The robot was able to effectively deal with moving obstacles through the gaze control-based navigation in a dynamic environment.

Social Intelligence. Social intelligence deals with the sociability of robots. While interacting with humans, the robot should be able to empathize towards the interacting humans in order to understand the nature of the interaction. Social intelligence includes both proactive and reactive aspects of sociability. The robot is socially proactive when it seeks the attention of interacting humans, and it is socially reactive when it responds to human attention or commands.

Related Application: Robotic Doll, Gomdoll

A robotic doll, Gomdoll, is a specially designed to manipulate social intelligence through emotional behaviors as shown in Fig. 8 [10]. Gomdoll has emotions and motivations, which are implemented in internal state part, to reflect its internal state. Moreover, to provide natural interaction, it utilizes reasoning part to express its internal state by selecting the most appropriate behavior.

The Big Five framework [11] of personality traits is employed in this research. The framework consists of five basic dimensions of personality, referred to as the Big Five personality dimensions. They are classified as follows: extroverted (as opposed to introverted), agreeable (as opposed to antagonistic), conscientious (as opposed to negligent), openness (as opposed to closedness), and neuroticism (as opposed to emotional stability). Gomdoll evolved in a virtual world by customizing the genetic code satisfying the propensity desired by the user. In this

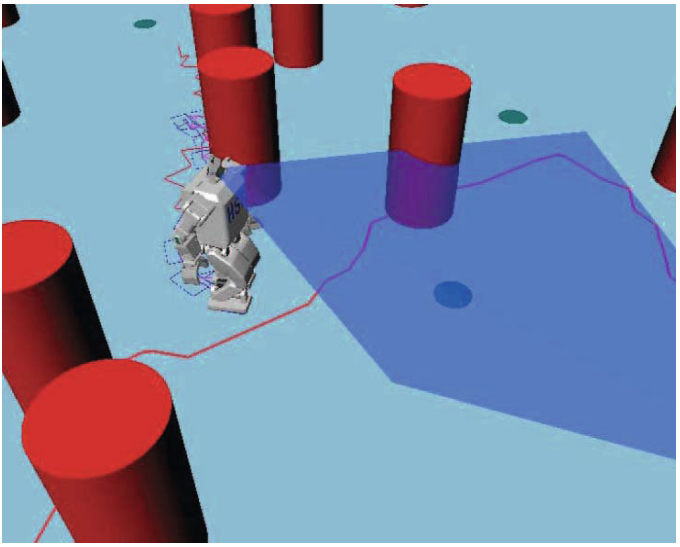

Fig. 7. Humanoid robot simulator for gaze control

(a) Happiness. (b) Sadness. (c) Anger. (d) Fear.

Fig. 8. Emotional behaviors of Gomdoll

way, robots possessing the user desired propensity could be developed for more social interaction with the user.

Behavioral Intelligence. Behavioral intelligence enables the robot to execute behaviors in an appropriate manner. It allows the robot to plan its behavior execution at the actuator level and to alter its discourse if the robot encounters an unwanted object or an obstacle.

Related Application: Walking Pattern Generator for Humanoids

The behavioral intelligence in humanoid robots is manipulated through walking pattern generation algorithms. Walking pattern generator in the behavior generation module and control algorithm in the control module play a significant role in the walking behavior. In order to handle complex navigational commands from the problem solving module in real time, a modifiable walking

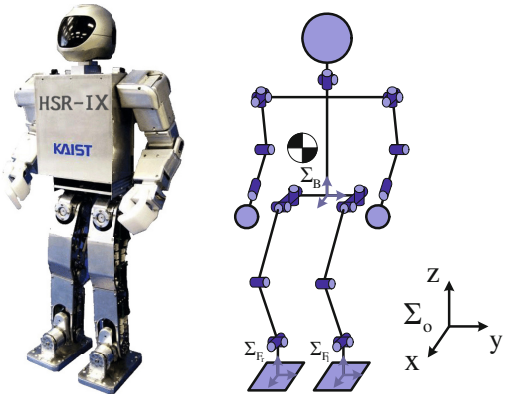

(a) HanSaRam-IX. (b) Configuration.

Fig. 9. Humanoid robot, HanSaRam-IX, and its configuration

pattern generator (MWPG) was proposed [12]. This is implemented in the behavior generation module. The MWPG receives navigational commands from the problem solving module and provides the desired joint angles to ensure the execution in the control module. The MWPG extended a conventional 3-D linear inverted pendulum model (3-D LIPM) in which the primary dynamics of the humanoid robot is modeled as the 3-D LIPM. Moreover, the MWPG enables modification of the walking period and the step length in both sagittal and lateral planes.

The small-sized humanoid robot, HanSaRam-IX, was used for experiments, as shown in Fig. 9. Fig. 10 shows the generated walking pattern on a flat plane using the proposed method. In addition, the robot is able to walk on inclined planes and uneven terrains by using the extended MWPG [13]-[16]. From the viewpoint of behavioral intelligence, the walking pattern generator is useful to generate proper locomotion that consists of repeated actions such as walking.

Ambient Intelligence. Sensory data is meaningful in itself but high level processes, including decision making, usually require high level context information. Therefore, sensory data can be more useful when it is translated into higher level context information. Ambient intelligence recognizes the context from sensory data collected in the environment. It is often realized through a sub-system such as vision-based face recognition system, gesture recognition system, RFID-based object recognition system [17].

Related Application: Interactive Robot-Based Tutoring System

In contrast to the established paradigm of researches focused on robot behaviors and learning under human supervision, the interactive robot-based tutoring system (IRTS) proposed a framework in which a robot was used to provide tutoring service to humans.

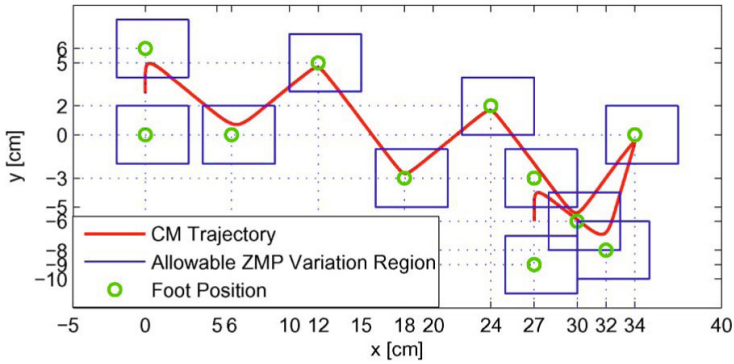

Fig. 10. Generated walking pattern using MWPG

This research proposed IRTS with intelligent tutoring system (ITS) based on the concept of ambient intelligence [20]. ITS is a computer-based expert system to provide customized instruction or feedback to users. The IRTS involves the robot interacting with a user, generating the user model, providing training tasks for guiding the user, and giving feedback on his/her performance. The proposed system is applied to ball-passing training as shown in Fig. 11, where a human trainee passes a ball to a robot tutor and receives feedback from the robot on how to improve kicking, based on the direction and velocity of the ball. The global vision system on the robot is used for ambient intelligence to gather the information about ball position and velocity.

Fig. 11. Snapshot of the ball-passing training

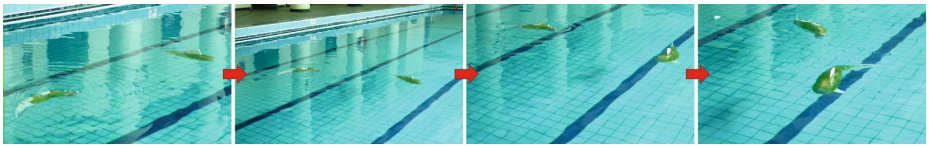

Fig. 12. Schooling behavior of two robotic fishes

Collective Intelligence. Collective intelligence is responsible for enabling cooperative behavior among multiple robots. The key issue to collective intelligence is information sharing; therefore, robots need to have the ability to communicate with each other. Utilizing collective intelligence, robots can carry out tasks that are difficult or impossible for a single robot to do [18]-[19].

Related Application: Schooling Behavior of Fibo

Schooling behavior is a large scale coordinated movement of fish. The schooling behavior consists of three movements: alignment, separation, and cohesion. Alignment is required to follow the same direction as the leading fish, whereas separation is required to avoid crowding and cohesion is required to move toward the leading fish while trying to minimize the distance between the two.

In this research, a camera was installed on the front of the robotic fish head. In this way, the robotic fish can calculate both the angle and distance between its head and the goal. Then, the robotic fish should determine its heading direction with respect to the goal location. To control the steering angle of the robotic fish towards the horizontal component of the heading direction, the line of sight method was used. The vertical component of heading direction was controlled by adjusting the center of the mass and using an artificial bladder.

Using vision and control algorithms, two robotic fishes could perform schooling behavior while swimming like real fishes do. Using color and shape of the robotic fish, the following robotic fish could distinguish the leading robotic fish (Fig. 12) [21]-[22].

Genetic Intelligence. Genetic intelligence relates to the personal traits and knowledge of a robot that it inherited from its parents. These inherited personal aspects define the personality of the robot. The behaviors generated by the robot are dictated by the personality of the robot. The representation of such personal parameters, similar to genes in biological species, constitutes the genetic code in robots and artificial species. Robots and artificial species with diverse personalities can be generated by the genetic code, which represents a specific personality desired by user for more natural HRI.

Related Application: Artificial Genome for Rity

An artificial creature has its own genome in which each chromosome consists of many genes that contribute to defining its personality. The large number of genes makes it a highly complex system. It becomes increasingly difficult and time consuming to ensure reliability, variability and consistency for the artificial creature's personality, if gene values are manually assigned for the individual genome. To solve

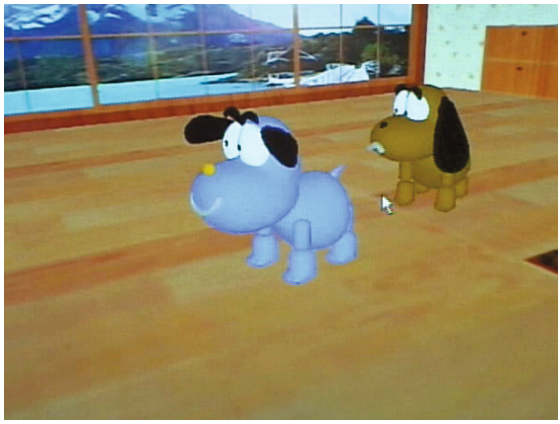

Fig. 13. Agreeable Rity (blue color) and antagonistic Rity (brown color) in a 3D virtual world

this problem, an evolutionary generation process (EGPP) for developing artificial creatures' genomes for specific personalities. Through EGPP, non-dominated genomes having specific personalities can be obtained and they are successfully tested by using an artificial creature, Rity, in the virtual 3D world created in a virtual space [23]. Rity is designed to be a believable interactive software agent for human-robot interaction as shown in Fig. 13.

The agreeable and antagonistic personality models were chosen to validate the proposed EGPP and the obtained fittest genome was implanted to Rity to verify the feasibility of EGPP [24]. The parameter settings of EGPP were applied equally in both the cases of agreeable and antagonistic personalities. The population size was 20 and the number of generations was 1,000. Crossover and mutation operate independently between two arbitrary parents at three different kinds of gene-dependent crossover and mutation rates. Fig. 14 shows generated genomes of an agreeable personality and antagonistic one in gray and red levels, where the grays denote positive values with darker shades representing higher values and the reds denote negative values with darker shades representing lower values. The key objective of this process is to generate an artificial creature with a personality that is both complex and feature rich, but still plausible by human standards for an intelligent life form.

3 Intelligence Technology Manipulation through Ubiquitous Robot System

Ubibot system was developed as a prototype to validate the effectiveness of ubiquitous robotics. Ubibot, through all its components is capable of manipulating all aspects of InT. The following subsections describe how different aspects of InT are manipulated by different components of Ubibot system.

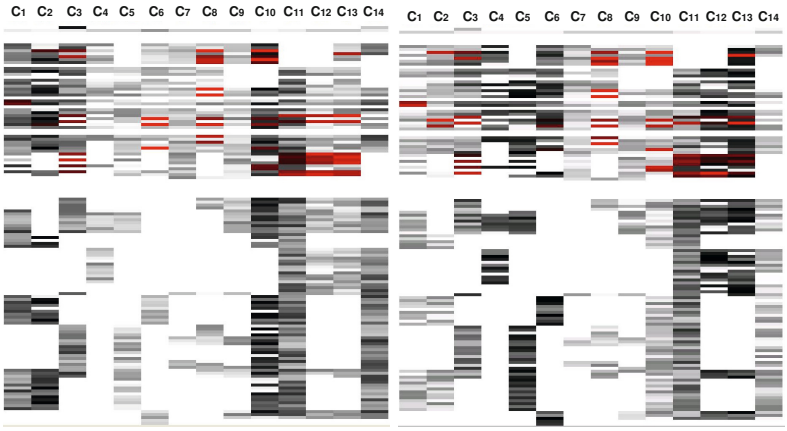

(a) Agreeable genome (b) Antagonistic genome

Fig. 14. Generated genome by using EGPP

3.1 Sobot's Cognitive Intelligence

To make artificial creatures deliberately interact with their environment like living creatures, a cognitive architecture for mimicking living creatures thought mechanism is needed. To equip Sobot with cognitive intelligence, the degree of consideration-based mechanism of thought (DoC-MoT) for Rity was developed. Rity has a human-like thought process which is affected by personal biases and prejudices based on psychological, cognitive or environmental grounds, is used to model the mechanism of thought for artificial creatures. The creatures' degrees of consideration (DoCs) for their internal wills and environmental contexts constitute the basis of the thought mechanism. In the proposed model, the DoCs for input (i.e. wills and contexts) symbols are represented by the fuzzy measures and the fuzzy integral is used for the global evaluation of the target (i.e. behavior) symbol on the basis of the partial evaluations over input symbols and their DoCs [25].

Fig. 6, discussed in the previous section, shows the cognitive architecture for the Sobot. The context generation module identifies a current environmental context using perceptions from the perception module, and the internal state module identifies a current will of an artificial creature. The memory module stores all the necessary memory contents including symbols of wills, contexts and behaviors. It also has the information on the DoCs for input symbols and the knowledge links between input and behavior (target) symbols. The DoCs are represented by the fuzzy measures and the knowledge link strengths are given by the partial evaluation values of behavior symbols over each input symbol. Considering the identified will and context, the behavior selection algorithm in the problem solving module selects a proper deliberative behavior by the fuzzy integral aggregating the partial evaluation values and the DoCs for input symbols.

Fig. 15. Sobot User Interaction through Mobot, the Sobot has downloaded itself onto Mybot to enable monitoring of the user and thus providing anyplace and anytime service

Reflexive behaviors are generated using sensor information from the perception module. The learning algorithm to change the characteristics of artificial creatures is executed in the learning module. The key modules for behavior selection, namely internal state, behavior selection, learning and memory modules, are described in [26].

3.2 Social Intelligence via Embots and Mobots

In the Ubibot system, the aim is for the Sobot to actuate the Mobot to continually monitor and provide services to the human user. After initiating the Sobot's attention, the user proceeds to move away. The Sobot perceives this and decides to follow the user. This setup portrays a real world situation where the user might dynamically engage and disengage various Embots, leading the Sobot to physically follow him/her by actually moving onto the Mobot. This is depicted in Fig. 15, where the Sobot has downloaded itself via Middleware from the remote site, onto the Tablet PC of the Mybot, thus enabling it to monitor the user in real time irrespective of his actual location. This verified the seamless integration of the Ubibot system transcending spatial limitations in its ability to provide services.

3.3 Behavioral Intelligence in Mobots

The Ubibot system consists of various Mobots, both wheeled and humanoid. Therefore, Mobots require behavioral intelligence to execute motion and other behaviors in accordance with their hardware resources. the humanoid Mobot, HSR, has MWPG (discussed in the previous section) to walk from one point to another, while the wheeled Mobot is equipped with a navigation algorithm for differential wheeled robots. A non-singleton interval type-2 fuzzy logic controller for Xbot (a cleaning robot platform that can be used as a Mobot) was developed

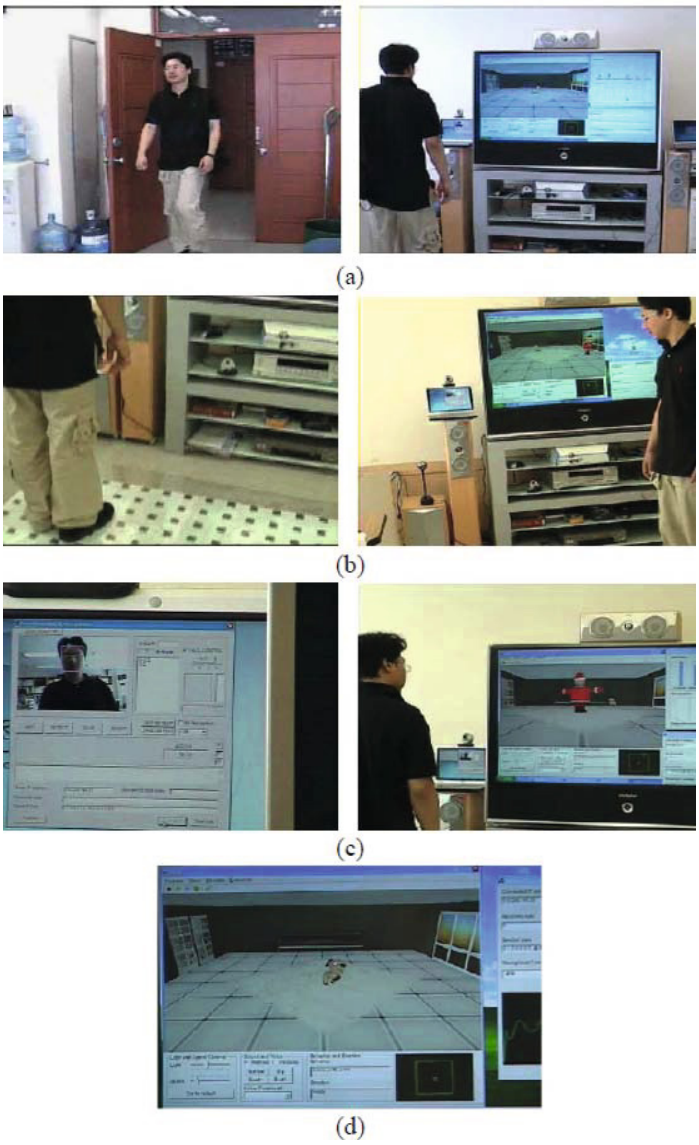

Fig. 16. Sobot-user interaction, (a) a subject enters the u-space, (b) position Embot senses the subject's location and transmits information to Sobot, symbolically resembling the appearance of Santa-Claus figure in the world; (c) Vision Embot performs face recognition and Sobot exhibits happiness upon perceiving its master, which (d) Sound Embot indicates that Dance command has been spoken, causing Sobot to comply and dance

to enable mobile robot to navigate in real world environments with measurement uncertainties. In [27], we demonstrated the effectiveness of such interval type-2 fuzzy logic controllers for systems with uncertainties. Such controllers enable the robot to autonomously take care of the navigation behavior in real environments with high uncertainties.

3.4 Ambient Intelligence via Embots

The Sobot interacts with a user actively since it is designed as a synthetic pet. In a complex scenario where a subject moves around in a home environment, the Sobot needs to access and exchange information from a number of Embots and Mobots. In the image sequence shown in Fig. 16, a demonstration was carried out, where the subject walked into the u-space simulated home environment with a TV with attached computers, upon which the Ubibot became immediately aware through the position Embot and Vision Embot. The latter then performed face recognition to identity the subject. Once the identification was established, Rity proceeded to react with joy and happiness and the user might transmit commands through voice or using keyboard and mouse.

This setup demonstrated the calm-sensing and context aware capabilities of the Ubibot allowing it to monitor its ambience, including the users and objects within the u-space.

3.5 Collective Intelligence

As the Ubibot system comprises of various components, some of which can function as standalone robots as well, collective intelligence is inevitable for the operation of ubiquitous robots. For seamless and calm operation of ubiquitous robots, all the Mobots, Embots and Sobot work in cohesion with each other. Sobot connects seamlessly and transmits itself to any location via Mobots. Moreover, different Sobots can co-operate with other Sobots (Ritys) by downloading themselves in the virtual spaces of each other and then proceed to interact with each other based on their internal states.

3.6 Sobot's Genetic Intelligence

Rity (Sobot) also has an artificial genome that was used for the realization of the concept of genetic robot wherein robotic genomes encode the artificial creature's personality, as in [23]. Its personality is dictated by the artificial evolution process of robotic chromosomes, which is a set of computerized DNA (Deoxyribonucleic acid) code, for the creation of artificial creatures that can think, feel, express intention and desire, and could ultimately reproduce their kind and evolve their species. The details about the artificial genome has been summarized in the previous section and Fig. 14.

4 Summary

In this chapter, the third generation of robotics, ubiquitous robotics, was introduced. Ubiquitous robots integrates three forms of robots: Sobot, Embot and Mobot. Sobots, which are software-based virtual robots in virtual environments, can traverse space through physical networks. Embots, the embedded robots, are implanted in the environment or embedded in Mobot, for sensing, detecting, recognizing, and verifying the objects or the situation. The processed information is to be transferred to Sobot or Mobot. Mobots provide integrated mobile services that Sobots and Embots cannot. Sobots and Embots can work individually or within Mobots. The Ubibot system is seamless, calm, context aware in its ability to provide integrated services. Rity, a 3D character and a Sobot, was introduced and implemented using two scenarios to demonstrate the possibility of realizing Ubibot.

We also presented InT for ubiquitous robots. The iOA was presented for intelligence technology to implement robot intelligence. Robot intelligence was classified into six categories: cognitive intelligence, social intelligence, behavioral intelligence, ambient intelligence, collective intelligence and genetic intelligence. Implementations, using software and hardware robots, demonstrated the significance of each category of robot intelligence.

References

1. Weiser, M.: The computer for the 21st century. Scientific American 265(3), 94–104 (1991)
2. Weiser, M.: Some computer science problems in ubiquitous computing. Communications of ACM 36(7), 75–84 (1993)
3. Kim, J.-H., Zaheer, S.A., Choi, S.-H.: The Next Technological Wave: Intelligence Technology for Intelligence Super Agent. IEEE Computational Intelligence Magazine 9(3), 54–64 (2014)
4. Brady, M.: Artificial Intelligence and Robotics. Artificial Intelligence 26, 79–121 (1985)
5. Kim, J.-H., Kim, Y.D., Lee, K.-H.: The 3rd Generation of Robotics: Ubiquitous Robot (Keynote Speech Paper). In: The Proceedings of International Conference on Autonomous Robots and Agents (2004)
6. Kim, J.-H., Lee, K.-H., Kim, Y.-D., Kuppuswamy, N.S., Jo, J.: Ubiquitous Robot: A New Paradigm for Integrated Services. In: The Proceedings of IEEE International Conference on Robotics and Automation, pp. 2853–2858 (2007)
7. Asimov, I.: The vocabulary of science fiction. Asimov's Science Fiction. Doubleday, New York (1979)
8. Kim, J.-H., Choi, S.-H., Park, I.-W., Zaheer, S.-A.: Intelligence Technology for Robots That Think. IEEE Computational Intelligence Magazine 8(3), 70–84 (2013)
9. Yoo, J.-K., Kim, J.-H.: Fuzzy integral-based gaze control architecture incorporated with modified-univector field navigation for humanoid robots. IEEE Transactions on Systems, Man, and Cybernetics C 42(1), 125–139 (2012)
10. Lee, D.-H., Kim, J.-H.: Evolutionary personalized robotic doll: GomDoll. In: The Proceedings of IEEE Congress on Evolutionary Computation, pp. 30254–33029 (2008)

11. McCrae, R.R., Costa, P.T.: Validation of a five-factor model of personality across instruments and observers. J. Pers. Social Psychol. 52, 81–90 (1987)
12. Lee, B.-J., Stonier, D., Kim, Y.-D., Yoo, J.-K., Kim, J.-H.: Modifiable walking pattern of a humanoid robot by using allowable ZMP variation. IEEE Transactions on Robotics 24(4), 917–923 (2008)
13. Hong, Y.-D., Kim, J.-H.: 3-D command state-based modifiable bipedal walking on uneven terrain. IEEE/ASME Transactions on Mechatronics 18(2), 657–663 (2013)
14. Hong, Y.-D., Lee, B.J., Kim, J.-H.: Command state-based modifiable walking pattern generation on an inclined plane in pitch and roll directions for humanoid robots. IEEE/ASME Transactions on Mechatronics 16(4), 783–789 (2011)
15. Hong, Y.-D., Park, C.-S., Kim, J.-H.: Human-like stable bipedal walking with a large stride by the height variation of the center of mass using an evolutionary optimized central pattern generator. In: Proceedings of Annual Conference on IEEE Industrial Electronics Society, pp. 136–141 (2011)
16. Hong, Y.-D., Kim, Y.-H., Han, J.-H., Yoo, J.-K., Kim, J.-H.: Evolutionary multi-objective footstep planning for humanoid robots. IEEE Transactions on Systems, Man, and Cybernetics C 41(4), 520–532 (2011)
17. Yan, R., Tee, K.P., Chua, Y., Li, H., Tang, H.: Gesture recognition based on localist attractor networks with application to robot control. IEEE Computational Intelligence Magazine 7(1), 64–74 (2012)
18. Lee, D.-H., Han, J.-H., Kim, J.-H.: A preference-based task allocation framework for multi-robot coordination. In: The Proceedings of IEEE International Conference on Robotics and Biomimetics, pp. 2925–2930 (2010)
19. Sayama, H.: Robust morphogenesis of robotic swarms. IEEE Computational Intelligence Magazine 5(3), 43–49 (2010)
20. Lee, D.-H., Kim, J.-H.: A framework for an interactive robot-based tutoring system and its application to ball-passing training. In: The Proceedings of IEEE International Conference on Robotics and Biomimetics, pp. 573–578 (2010)
21. Jeong, I.-B., Park, C.-S., Na, K.I., Han, S.-B., Kim, J.-H.: Particle swarm optimization-based central pattern generator for robotic fish locomotion. In: The Proceedings of IEEE Congress on Evolutionary Computation, pp. 152–157 (2011)
22. Na, K.I., Park, C.-S., Jeong, I.B., Han, S.-B., Kim, J.-H.: Locomotion generator for robotic fish using an evolutionary optimized central pattern generator. In: The Proceedings of IEEE International Conference on Robotics and Biomimetics, pp. 1069–1074 (2010)
23. Kim, J.-H., Lee, C.-H.: Multi-objective evolutionary generation process for specific personalities of artificial creature. IEEE Computational Intelligence Magazine 3, 43–53 (2008)
24. Kim, J.-H., Lee, C.H., Lee, K.-H.: Evolutionary generative process for an artificial creature's personality. IEEE Transactions on Systems, Man, and Cybernetics C 39(3), 331–342 (2009)
25. Kim, J.-H., Ko, W.-R., Han, J.-H., Zaheer, S.-A.: The degree of consideration-based mechanism of thought and its application to artificial creatures for behavior selection. IEEE Computational Intelligence Magazine 7(1), 49–63 (2012)
26. Kim, J.-H., Lee, K.-H., Kim, Y.-D.: The origin of artificial species: Genetic robot. Int. J. Control, Autom., Syst. 3(4), 564–570 (2005)
27. Zaheer, S.A., Kim, J.-H.: Type-2 Fuzzy Airplane Altitude Control: a Comparative Study. In: The Proceedings of IEEE International Conference on Fuzzy Systems, pp. 2170–2176 (2011)

Using Cognitive Ubiquitous Robots for Assisting Dependent People in Smart Spaces

Abdelghani Chibani[1], Antonis Bikakis[3], Theodore Patkos[1,2], Yacine Amirat[1], Sofiane Bouznad[1], Naouel Ayari[1], and Lyazid Sabri[1]

[1] LISSI Laboratory, University Paris Est Crteil, France
[2] FORTH ICS, Greece
[3] University College London, UK
{chibani,amirat,bouznad,naouel.ayari,lyazid.sabri}@u-pec.fr
a.bikakis@ucl.ac.uk, patkos@ics.forth.gr

Abstract. In this chapter we discuss the necessity to move beyond built-in monotonic semantic web based reasoning-architectures for endowing ubiquitous robots with cognitive capabilities, which are strongly required in ambient assistive living, towards new architectures that combine different reasoning mechanisms to achieve better context awareness and adaptability in dynamic environments. We also present practical reasoning approaches that we have developed during the last decade for ambient intelligence and robotics applications. Finally, we discuss future directions that should be investigated to implement high-level cognitive capabilities that can be supported by cloud computing platforms as reasoning backend for robots and connected devices in smart spaces. These will enhance the human-environment interaction using robots, emergency prevention, management and rescue.

1 Introduction

Enhancing the cognitive capabilities of ubiquitous robots, in order to supply users with assistive services and execute complex tasks in dynamic real world domains, requires not only having some semantically rich descriptions of the environment, its objects and the context in which humans and robots evolve, but also powerful reasoning techniques.

Imagine the following scenario. Nathan is an elderly resident of a smart space designed to provide ambient assisted living services to people with certain types of cognitive and physical difficulties. Although Nathan is still at the beginning of his old age and physically capable of accomplishing all daily tasks on his own, he frequently finds himself losing track of the activities he undertakes and forgetting to complete tasks he has initiated (mild attention and memory disorder). An assistant robot, in collaboration with the stationary entities of the smart space, is assigned the task to monitor Nathan's actions, recognize his activities on different levels of abstraction, identify normal as well as potentially hazardous current or future situations and respond by triggering reminders and alerts both reactively and proactively. Since Nathan is not considered disabled, it is important for the robot's intervention to his daily routine to be as less intrusive as possible and only

S. Mohammed et al. (eds.), *Intelligent Assistive Robots*,
Springer Tracts in Advanced Robotics 106, DOI: 10.1007/978-3-319-12922-8_11

take initiatives when truly needed. Activity and situation recognition and context awareness are widely used concepts in the fields of pervasive computing, ambient intelligence and robotics. They provide a better understanding of the needs of persons and their context including their situations, activities and surrounding objects. They also help in adapting the assistive services that are supplied by the smart space or robots operating in it.

The concept of context is usually defined as the observation and interpretation of a set of interrelated physical objects. The most adopted definition is the one given by Dey et al. [1] according to which context refers to any information that can be used to characterize the situation of an entity (e.g a person, place, etc) that is considered relevant to the interaction between a user and an application. A situation is defined by Joelle Coutaz [2] as an external semantic interpretation of context. The meaningful interpretation of context is done from the application point of view or system observer, rather than from sensors or context itself. Information such as location, identity, time, and activity are considered as the primary context types for characterizing the situation of an entity [1].

The current trend of enabling robots with cognitive capabilities of representing, recognizing and reasoning about context and situations relies largely on standard Semantic Web languages, such as OWL and RDF, and also, on reactive rule-based systems. Ontology languages are valuable tools for creating semantic descriptions of the environment, and its associated entities and events. For instance when an event occurs in the environment, such as switching on the light spot or a robot entering into the kitchen, the reasoning system translates these events to ontology management actions.. Subsumption or satisfiability reasoning operations can be used, according to the open world assumption, to address several practical issues that are critical in ubiquitous robotics such as objects anchoring and classification.

Most existing context-aware implementations for Ambient Intelligence (AmI) are based on reactive reasoning procedures to deliberate on high-level context, recognize activities and adapt the system to the user's profile, preferences and needs. Depending on the characteristics of the underlying ontology language they employ AmI systems can benefit from the expressive power of semantic representations. Although mature enough, these technologies do not yet meet many of the challenges of such complex domains [3].

Considering that ubiquitous robots and ambient intelligence artifacts are evolving in highly dynamic real-world environment, their reasoning capabilities should be extended beyond the ontology T-Box/A-Box reasoning operations or their combination with first order logic rules such as SWRL horn like inference rules. Such advanced reasoning capabilities should take into account important aspects and requirements such as: bridging between physical perception and symbolic representation without semantic loss, ramifications, default reasoning, reasoning under constraints partial knowledge description or knowledge imperfection.

In our opinion, commonsense reasoning is a key issue that needs to be encapsulated and demonstrated by entities that inhabit smart spaces, in order to strengthen the reasoning capacity of ubiquitous robots and AmI systems.

It will enable them to deal with different trends of applications fields such as ambient and assisted living applications related to everyday housekeeping activities, healthcare and rehabilitations, entertainment, education and security.

In this chapter we discuss why ontology built-in reasoning tools are insufficient to build context and situation awareness reasoning capabilities in particular for ubiquitous robots in dynamic environments, and present a set of knowledge representation and reasoning tools that can be valuable in developing context aware assistive services in smart spaces using ubiquitous robots. The rest of the chapter is structured as follows. Section 2 provides background information on Ambient Assisted Living and Ubiquitous Robots as well as in context and situation awareness. Section 3 presents ontology-based approaches for reasoning about context in Ambient Intelligence environments. Section 4 discusses more advanced reasoning methodologies based on commonsense reasoning models. Section 5 concludes the chapter and discusses ongoing and future work.

2 Background

2.1 Ambient Assisted Living and Ubiquitous Robots

Ambient Intelligence (AmI) was introduced by the Programme Advisory Groups, the European Community Information Society Technology (ISTAG) in 2001 [4]. The first research projects concerned the concept of smart homes, where the most important issue was the interoperability with hardware, sensors, actuators and devices that are used or installed in different areas. Applications were mainly enhancing the social communication between people that are inside or outside the smart home and/or home automation such as the monitoring of electricity, heating, air-conditioning, ventilation, and fire and intruder alarms and/or the detection and reaction to risk situations, such as a fall of an old person. Today AmI is a well established and active research topic in the field of pervasive and ubiquitous computing that targets the provision of technologies and solutions, which supply intelligent and responsive services not only in smart homes but also in outdoor environments such as shopping malls, bus stops, offices buildings, etc. In this context, ubiquitous robots, as part of ambient intelligence, are considered as the best channel for interacting with humans in several cases instead of smartphones, smart TVs and other smart devices. Moreover, they can enhance the way we can supply ambient assisted living services in a motivating and socially acceptable manner to facilitate independent living at home. Ubiquitous robots can be easily and seamlessly integrated within an ambient intelligence environment to augment their perception and actuation capabilities using sensor networks, RFID, building automation systems and actuators that are disseminated in the environment. [5,6].

2.2 Context and Situation Awareness

Several techniques have been proposed for context and situation awareness. We can classify them into two main categories: quantitative and qualitative methods.

The quantitative approaches use soft computing techniques such as machine learning, situation lattices, Bayesian methods and fuzzy logic to address context classification and cope with imperfections of sensor data. Qualitative approaches are usually based on a symbolic modeling of context by using first order logic axioms and rules. The reasoning is based mostly on a unification process of logical inference rules over statements describing relationships between facts. Most approaches dealing with context awareness are based on ontology based logic programming or events stream processing. The reasoning concerns mainly the detection of ontology inconsistency and the inference of new types or roles for the individuals; for example, the inference of user current activity (e.g. cooking) by using information collected from camera and RFID sensors. Ontology consistency checking can be used during the development or update of the ontology knowledge base to check consistency in the class hierarchy and consistency between instances. For instance, consistency checking allows detecting classification errors, such as a person being in two spatially disjoint locations at the same time. Wang et al [7] proposed to combine a description logics ontology called CONON with Horn like inference rules, while Yau et al. [8] developed a situation ontology, which includes concepts to express time constraints on the logical specifications of situations. They used First Order Logic (FOL) inference rules to support the conversion of situation specifications to FOL representations and a FOL rule-based inference engine to reason with situations. The performance they obtained, concerning the transformation of situations specification, makes their model unusable for time-critical applications. Chen et al [9] proposed an ontology called SOUPA and logic programming in the form of F-logic to allow different agents on the one hand, to share the same consistent interpretation of knowledge and on the other hand, to perform inferences to determine current context in a specific place. However, the failure or unavailability of sensors can cause the overall failure of the inference process. Overcoming such issues by adding more inference rules and new sensors will lead in the most to complex and non-maintainable rule bases. Description logics ontologies have also been used to model complex contexts. In [10] the authors proposed an ontology model of video events, based on Video Event Representation Language, VERL and *Video* Event Markup *Language*, VEML. This model consists of two ontologies. The first ontology provides a semantic description of the classes corresponding to VERL definitions. The second ontology is an event taxonomy, which provides a description of the annotation structures VEML using elements of the VERL event definitions ontology. The VEML model can be used to support tasks such as context understanding in video surveillance, video browsing, and content-based video indexing. The lack of suited reasoning to infer semantics of the possible n-ary relation between events definitions and events taxonomy is the main limitation of this approach.

3 Ontology Based Approaches

The approaches presented above, which use semantic web ontologies, are based on an open world assumption (OWA). The Open world assumption does not

make any hypothesis about the truth or falsity of a fact unless it can be proven. Thus, if the truth or falsity of some statement is unknown, nothing can be inferred about it and both scenarios must be considered [11]. These scenarios may represent contradictory states of the context or lead to conflicting conclusions or decisions for action. Moreover, we cannot assume in OWL the uniqueness of concepts names: i.e., two different instances can refer to the same object. Ambient Intelligence and ubiquitous robots systems that are based on OWL rely on a limited 'inference by inheritance' reasoning paradigm of Description Logics reasoners such as KAON, Pellet, Fact++, or Hoolet. These reasoning engines are more suitable to solve the most common classification ("subsumption") problems than to execute more complex reasoning operations where new knowledge must be produced from the existing one. The recovery proposition of representing Horn like rules as ontologies to deal with this limitations, such as SWRL, RuleML, TRIPLE, does not provide all the reasoning capabilities needed for Ambient Intelligence and remains particularly complicated to be used in rules writing. For instance, the Semantic Web Rule Language SWRL, which relies on the Open World Assumption, does not support 'negation as failure', as well as classical negation, disjunctions and non monotonicity. Moreover, being more 'expressive' than OWL DL, SWRL is not 'decidable'; more precisely, it is 'semi-decidable'. As a consequence, SWRL rules are often written in a decidable subset of SWRL called 'DL-Safe SWRL'. One of the consequences of this restriction is that DL-Safe SWRL variables can only be bound to known individuals in an OWL ontology. This is too restrictive for many applications where variables must also be bound (i.e. when a specific instance is unknown) to the general concept *subsuming* this instance. Executing the SWRL rules is then delegated to external Rete-based and LISP-oriented rule engines. Building context aware ambient intelligent and ubiquitous robots systems based on semantic web rules, leads, in several cases, to complex rule bases to meet the requirements of specific application fields, and are therefore difficult to maintain, evolve and reuse.

3.1 SembySem

On the contrary, a semantic reasoning system based on CWA (Closed World Assumption) such as the SembySem approach proposed in [11] assumes that every fact which cannot be proved as true is implicitly assumed to be false. This requires that the existing facts are assumed to be complete, or that common-sense conclusions can be drawn from existing evidence under incomplete information. Building the cognitive capabilities of ubiquitous robots according to the CWA renders the inference non-monotonic: the presence of new evidence can invalidate previously drawn conclusions, while the name of the concepts must be unique to avoid any possible contradiction. SembySem is used as a semantic model and reference architecture to build reactive context aware ambient intelligence systems and ubiquitous robots [12].

The architecture of SembySem, depicted in Figure 1, is composed of two main layers. The Facade layer is used to capture information sent by real world objects such as sensors and actuators about their description, status and measurements.

The Facade layer allows also capturing the actions that are triggered by the upper layer, which is called the reasoning core. The latter checks the consistency of the data sent by objects and executes queries and productions rules in order to update the semantic knowledge base of the robot or trigger some relevant actions corresponding to a particular context.

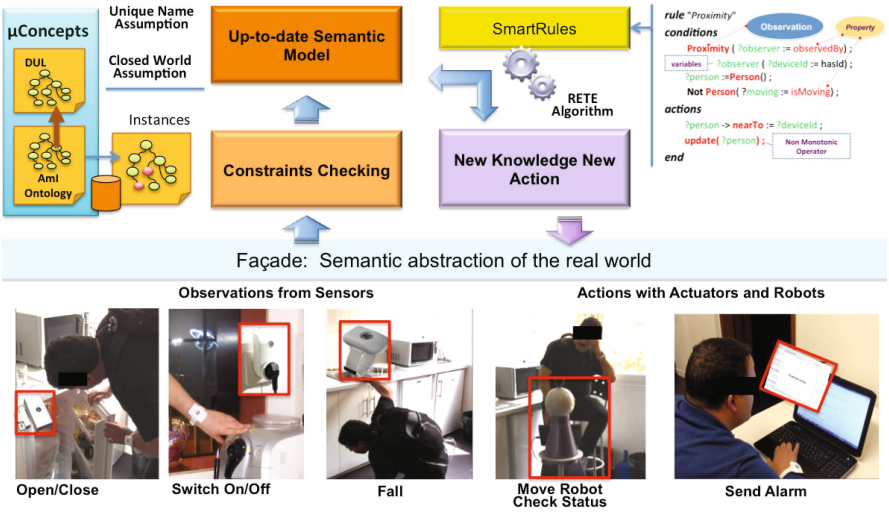

Fig. 1. Architecture of the SemBySem approach

The semantic knowledge base is represented using the CWA μ-concepts ontology and production rules that describe semantically how the context is inferred from the objects that are in the surrounding of the user. In addition, the μ-concepts ontology describes the characteristics of every sensor and actuator and their possible composition to build complex sensors and actuators. The μ-concept ontology language consists of the following conceptual components: concept, property, instance and action [12]. The main similarity of μ-concept with OWL and RDF, lies in the way of defining relations that are represented independently from the concepts, and may then symbolize a relation between any kinds of μ-concept. On the other hand, the multilingual support makes μ-concept ontologies usable in several languages. The first main difference of μ-concept with OWL concerns the fact that each μ-concept is used to describe how each entitiy should behave upon each context. For this purpose, a μ-concept provides "actions" concepts that allow to associate its physical/logical operation with its symbolic instantiation. The action concept description may also include restrictions on properties that are separated in two parts: the first one concerns properties specifying the restrictions when the action is launched (input restrictions), while the second one is related to the restrictions when the action is complete (output and effect restrictions). These restrictions behave exactly like

```
<smc:Action rdf:ID = "move2Kitchen">
  <smc:actionDomain rdf:resource="#MobileRobot"/>
  <rdfs:Label xml:lang="fr">deplacerVersCuisine</rdfs:Label>
  <rdfs:Label xml:lang="en"> move2Kitchen </rdfs:Label>
  <smc:Property rdf:ID = "currentLocation" smc:Input="true">
    <MinCardinality>1</MinCardinality>
  </smc:Property>
  <smc:Property rdf:ID = "ReasonMessage">
    </rdfs:domain rdf:resource = "#presentInside">
    </rdfs:range rdf:dataType = "&xsd;string">
  </smc:Property>
  <smc:Agent rdf:ID = "#MobileRobot">
</smc:Action>
```

Fig. 2. An action description as a μ-concept

```
import ontology "./AmI.smc";

Rule "Rule #3"
priority = 3;
declare noMotionDetected
@role ( event )

Conditions
      ?v_person:= PERSON (?v_person := all(hasID)),
            exists (one in ?v_person (hasID=="MaryRFID");
      ?v_context := exists (COOKER( isRunning(true)),
            PERSONAL_CONTEXT ( IsSleeping(true),
timestamp == datetime("now");

Actions
      createAction(KITCHEN_DEVICE(?turnOff));
      'KITCHEN_DEVICE/TurnOff' ?turnOffAction :=
                        createAction('KITCHEN_DEVICE/TurnOff');
      ?turnOffAction->Reason := 'ActionReason/
SafetyProcedure';
      execute(?turnOffAction);

End
```

Fig. 3. A production rule for switching off kitchen devices

property restrictions on the μ-concept, overriding the default property behaviour on its domain (see Figure 2).

In addition, the action concept is characterized by a set of special properties: Agent, Object, Source, Beneficiary, Modality, Topic and Context; possible extensions concern more general properties like Cause, Goal, Coordination, Alternative. All these properties are optional, with the exception of '*ActionAgent*', whose presence is mandatory in the definition of each of the actions associated with the model and in the description of the corresponding instances. The possibility of defining this sort of actions implies that the μ-concept model can be considered as free from any constraints of the 'binary' way with which OWL or description logics describe relations among μ-concepts. We can consider that the μ-concept is closer to conceptual models in the Entity/Relationship style.

A second main difference of μ-concept with OWL is its inference language called smart rules. This language provides designers with means to set up monitoring rules as simple "if/then" production rules. The condition pattern of a smart rule is characterized by a set of μ-concepts or variables that can be bound

to a μ-concept with the possibility to add a single or a set of constraints. An instance referenced by a variable has a class type that can be automatically deduced from the corresponding matched elements in the ontology. A smart rule expressed without restrictions allows us to match every instance of a given concept. The consequence part represents all the operations to be performed on instances when the rule is triggered. We denote the following operations: create or remove instances in/from the knowledge base, update property values or global variables and multi-cardinality properties. The latter can be associated with actions and can then be considered as another way of overcoming the 'binary' limitations associated with W3C languages. Two other interesting features of the μ-concept smart rules language that are missing from the W3C languages concern the possibility of defining inequality constraints on the properties and, properties calculated as a combination of other ones. Due to space limitations we will not give complex rules that show the potential of the smart rules language to handle complex entities but we present a rule that allows switching off kitchen devices (see Figure 3). Using the ontology the system will identify the cooking devices and execute the operations that turn them off. The designer will not take care of the implementation details of the targeted environment when building this cognitive basic behaviour.

3.2 NKRL

Ontological knowledge representation and reasoning can be successfully applied to real-world human-robot interaction scenarios. In [13], we proposed a narrative-based approach for representing and reasoning about space, changes and events in ambient intelligent environments. This approach, based on the NKRL n-ary ontologies, has proved to be useful to endow ubiquitous robots with the ability to recognize and understand high-level representations of situations [14]. The proposed architecture, depicted in Figure 4, is in line with the ones proposed in SembySem. The facade layer is used for the semantic abstraction of the events, interactions that happen in the real world or the actions that must be executed by the robot or any other actuator. The NKRL facade transforms any captured event or interaction into semantic narratives, called NKRL predicative occurrences. The second layer is composed of reasoning tools, which process the semantic relations that exist among the predicative occurrences in order to infer contexts.

One of the main advantages of NKRL is the possibility to develop a semantic model of a dynamic ambient environment using two ontological components: (i) the HCLass that can imported from any OWL1/2 static real world ontological description, (ii) the HTemp which is an n-ary ontology of events, which are composed using an hierarchy of templates representing dynamic knowledge such as moving a physical object, changing the state, talking to, acting as, etc. These templates are based on the notion of "semantic predicate", which can be understood as the formal representation of generic classes of elementary events. The reasoning process is mainly achieved by linking factual primitives events using

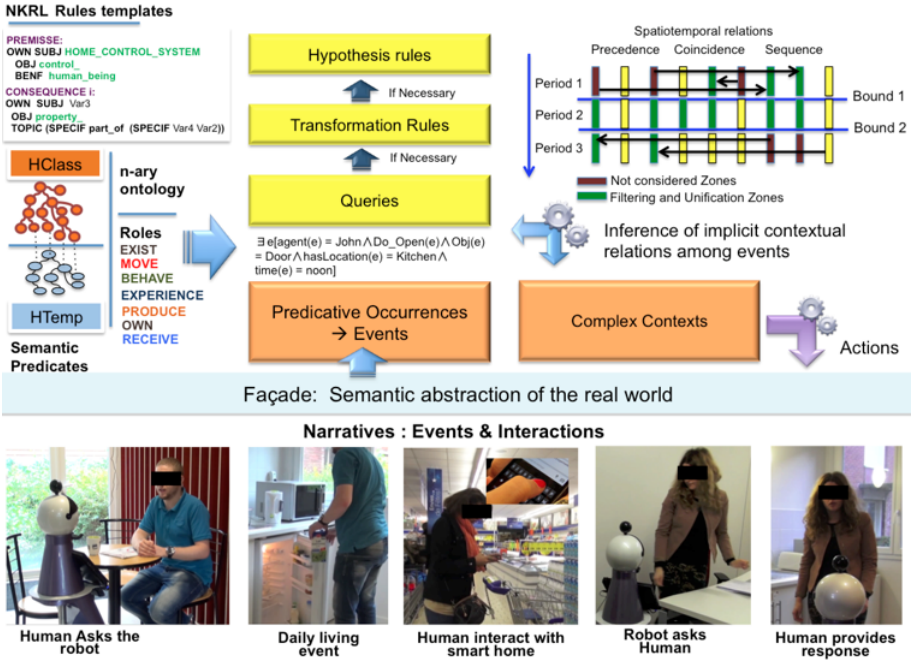

Fig. 4. Architecture of the NKRL approach

semantic correlations of events over time. We have demonstrated how the reasoning system can build up a context for information retrieved within a factual knowledge base automatically. We demonstrated also how NKRL transformation rules, with their corresponding triggering patterns, can generate the context information of a triggering event automatically. The causal explanation of this event can be found easily by the user by interrogating the robot using any human computer interaction functionality, such as speech to text, touch screens and others. The added value of this approach is its capability of driving natural interactions between the Robot and/or the Smart space with the users. The robot can provide in most of the times a plausible explanation of the context of the occurred events, even in the absence of direct facts that correspond to this event in the knowledge. Current attempts concern the transformation of Natural Language Interactions between human into NKRL predicate occurrences [15]. The transformation module is used to build a reasoning procedure that allows the robot to forward a failed NKRL query to the closest human in order to find a response in order to complete in the fly its knowledge base. The failed query is posed to the user in natural language. The reasoning on the context that failed in the first step can be finalized with success and avoid situations of context generation failures due to the absence of relations among facts, which cannot be handled by the hypothesis and transformation rules [15].

4 Commonsense Reasoning Approaches

The limitations of semantic web approaches become more evident when attempting to implement truly applicable context and intention aware robot assistive service that run in a highly dynamic world. To clarify this requirement, let us take the following case. Nathan enters the kitchen in the morning and follows an ordinary pattern of actions for preparing breakfast. He takes the eggs out of the fridge and finds the pot not on the cabinet as usual, but rather on the corner of the table. If requested, the robot could provide some possible locations to look for the pot, given commonsense knowledge and context information (e.g., last known location, places where similar objects are located given the system's sensory abilities etc.). Nathan fills the pot with tap water and places it on the hot plate, after turning the plate on. The system has accurately recognized his intention to prepare a meal, which, considering the time of the day and Nathan's profile, is categorized as breakfast. In addition, it has noticed that the water inside the pot will start to boil in approximately three minutes. Nathan leaves the kitchen and enters the bathroom. The situation is not characterized as critical yet; therefore the robot deliberates that no alert needs to be initiated until it is close to the boiling time. But then Nathan turns on the faucet of the bathtub tap and starts filling it with water. The system now identifies that these two parallel activities will require Nathan's actions at approximately the same time in two different locations, i.e., he should stop the water from reaching the rim of the bathtub while also turn off the hot plate in the kitchen. Although the critical situation refers to a future point in time and it is not certain that it will actually occur, a reminder is more appropriate to be placed in the present situation. In addition, the robot can even offer to perform some action on behalf of Nathan, such as to explain the situation and suggest to turn off the hot plate for him.

A multitude of aspects make the aforementioned and other similar scenarios challenging for current context-aware systems: a. Deliberating in ambient intelligence domains requires *potent cognitive skills*. Recent studies highlight the significance for a system to accomplish effective decision making by coupling expressive context models with commonsense knowledge about the domain, the properties of the entities that comprise it and the properties of the events and actions that occur and modify it (e.g., [16,17,18]). A representation of the causal properties of the domain is required that can capture the context-sensitive direct and indirect effects of actions, their potential ramifications, the non-deterministic nature of occurring events and others. This way, context awareness can benefit from more accurate high-level context knowledge that combines sensor data with inferences about the cause of the narrative of events that are detected, enabling a more thorough comprehension of the situation at hand [13]. b. While most current context-aware systems focus on implementing reactive behavior upon recognized situations, real-world ambient intelligence systems require *more powerful reasoning*. Decision making needs to foresee potential future situations in addition to reacting on current abnormal situations, and also to perform projection on future contingencies that need to be handled in the present. The description of temporal relations in such dynamic domains and the performance

of temporal reasoning is an essential capacity of ambient and ubiquitous systems. c. Information obtained by the environment can by no means be regarded as totally accurate or be readily available whenever needed; still, the entities of an ambient system need to operate effectively under unambiguous conditions. *Reasoning under partial observability* is required, in order to combine the knowledge at hand with the causal description of the domain and the cognitive competency of the reasoner. For instance, if the system is unaware of the state of the hot plate when the pot is placed on it a potential future triggering of the boiling event should also be accounted for. Epistemic reasoning, i.e., reasoning about knowledge and the lack of it, provides the means to perform inferencing in partially observable domains. Ambient intelligence systems often need to combine data from different types of sensors and also other kinds of information sources (e.g. profiles, the Web, etc.). In the example scenario, information about the location of the pot may be derived both from an image processing system that processes images from a camera installed in Nathans flat, but also from an RFID-based localization system; and the data coming from the different sensory systems may lead to conflicting inferences. We therefore need reasoning models that enable integration of information from heterogeneous sources, and reasoning algorithms that resolve conflicts using additional information, such as preferences, priorities, confidence values, etc. Defeasible contextual reasoning [19,20] can provide efficient solutions to such problems. Next we highlight how the domain can benefit from coupling semantic representations with advanced epistemic reasoning models, such as commonsense, defeasible and epistemic reasoning, thus enhancing the predictive behavior of deliberate entities. The proposed approach combines in a unified and efficient manner expressive contextual knowledge representations with powerful reasoning capabilities, integrating progress in a multitude of AI fields, such as the Semantic Web, cognitive robotics, production systems and modal logics.

4.1 Causality-Based Reasoning

Ambient intelligence environments are populated by entities that generate events anywhere and anytime, deeming essential a formal treatment of their properties. Event-based architectures offer opportunities for flexible processing of the information flow and knowledge evolution over time; yet, rule-based languages provide only limited expressiveness to describe certain complex features, such as compound actions, therefore they do not fully exploit the potential of the event-based style to solve challenging event processing tasks raised by ubiquitous computing domains. The Event-Condition-Action (ECA) paradigm that is most frequently applied can be used for reacting to detected events, viewing them as transient atomic instances and consuming them upon detection. They do not consider their duration, how far into the past or future their effects extend nor do they investigate causality issues originating from the fact that other events are known to have occurred or are planned to happen. Paschke [21] has already shown that the ECA treatment may even result in unintended semantics for some compositions of event patterns. However, real-world systems demand for-

mal semantics for verification and traceability purposes. To this end, tools from the field of reasoning about actions and causality provide valuable solutions. Action theories are formal tools, based on the predicate calculus particularly designed for addressing key issues of reasoning in dynamically changing worlds by axiomatizing the specifications of their dynamics and exploiting logic-based techniques in order to draw conclusions. Different formalisms have been developed that model action preconditions and effects and solve both deduction and abduction problems about a multitude of commonsense reasoning phenomena, such as effect ramifications, non-deterministic actions, qualifications and others. One of the most prominent formalisms is the Event Calculus [22,23], which establishes a linear time structure enabling temporal reasoning in order to infer the intervals in which certain world aspects hold. The notion of time, inherently modeled within the Event Calculus, as opposed to other action theories, is a crucial leverage for event-based systems, e.g. to express partial ordering of events or timestamps. In order to promote a high-level description of the specifications of applications and to achieve a high degree of interoperability among services, event ontologies can be designed that capture the notions of atomic and compound events and define operators among event sets, such as sequence, concurrency, disjunction and conjunction (e.g. see Figure 5). An event is further characterized by its initiation and termination occurrence times (for atomic events they coincide), the effect that it causes to context resources, the physical location at which it occurred, the service that detected or triggered it etc.

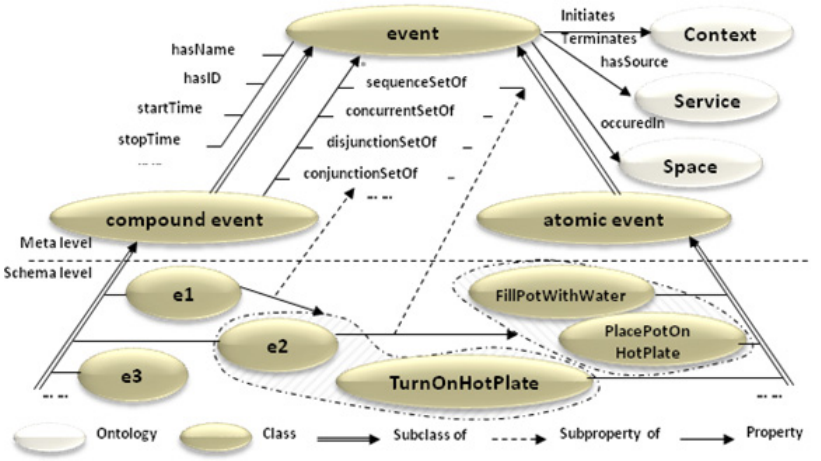

Fig. 5. Event ontology sample

To define formal semantics for the operators, a translation of the upper-level semantic language into Event Calculus axioms can be performed. Let a compound event e_1 in Figure 3 for instance, that expresses the partially ordered event

type $[[FillPotWithWater; PlacePotOnHotPlate] \wedge TurnOnHotPlate]$ where (;) represents the sequence operator. In order to utilize e_1 for reasoning tasks we axiomatize its temporal properties in Event Calculus

$Happens(Start(e_1), t) \equiv$
$Happens(FillWithWater(Pot), t_1) \wedge$
$Happens(PlaceOn(Pot, HotPlate), t_2) \wedge$
$Happens(TurnOn(HotPlate), t_3) \wedge$
$(t_1 < t_2) \wedge (t = min(t_1, t_3))$
(respectively for $Happens(Stop(e_1), t)$), as well as its causal properties:
$Initiates(Start(e_1), PreparingHotDrink(), t) \wedge$
$Terminates(Stop(e_1), Heating(Pot), t)$

This way we can formalize the effects of compound events to act cumulatively or canceling the effects of their atomic components and also we can specify whether certain effects hold at beginning times or at ending times.

Main advantages of the Event Calculus, in comparison to rule-based approaches, are its inherent ability to perform temporal reasoning considering both relative and absolute times of event occurrences and that it can reevaluate different variations of event patterns as time progresses. With ECA style reactive rules events are consumed as they are detected and cannot contribute to the detection of other complex events afterwards.

In [24] we introduced an architecture for online reasoning on smart spaces' events. This architecture, depicted in figure 6, can be used to couple high-level causal and temporal reasoning with multi-modal probabilistic inference for context-aware human support in smart spaces. Its aim is to recognize everyday user activities in indoor domains, monitor their proper execution, and perform assistive actions, in the form of recommendations, warnings, alerts or device handling, in order to facilitate user's domestic tasks and prevent possible incidents.

If needed, the system can control a variety of stationary and mobile robotic entities, in order to promote its perception capacity in understanding occurring situations and to react effectively. The architecture is modular to enable the experimentation with a multitude of reasoning approaches at different levels.

Emphasis has been given in the seamless integration of formal tools with data-driven approaches for activity recognition aiming at completing the loop of knowledge representation, reasoning and decision making in real-world AmI settings.

4.2 Epistemic Reasoning

In the case of partial observability of world aspects, e.g., when mobile devices such as robots or PDAs, need to perform lightweight reasoning tasks having limited access to the full description of the KB due to connection failures or resource constraints, epistemic reasoning is applied. An epistemic extension of the Event

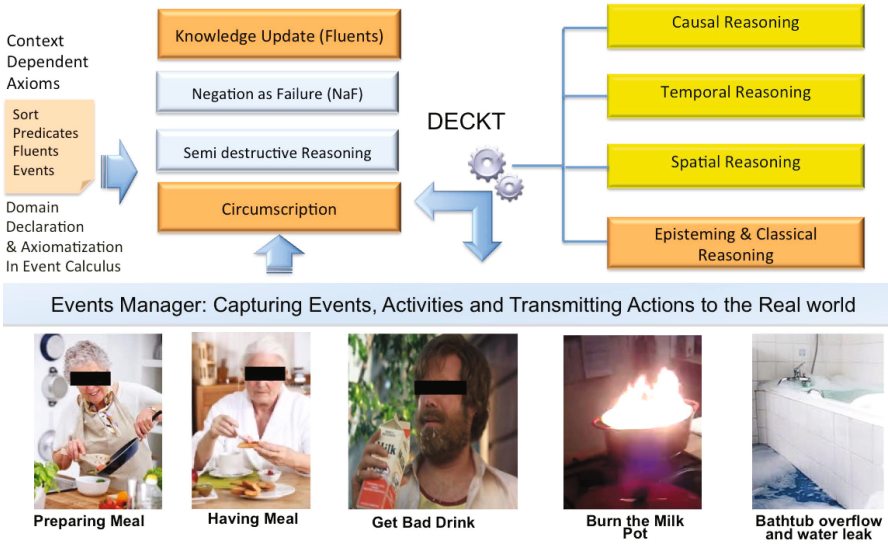

Fig. 6. Event Calculus based online reasoning platform for ambient intelligence

Calculus named Discrete time Event Calculus Knowledge Theory (DECKT) can be employed for that purpose. DECKT [25,26] is a provably sound and complete extension of the Event Calculus that introduces epistemic features enabling reasoning under partial observability about a wide range of commonsense phenomena, such as temporal and delayed knowledge effects, knowledge ramifications, non-determinism and others. It assumes agents acting in dynamic environments having accurate but potentially incomplete knowledge and able to perform sensing and actions with context-dependent effects. DECKT employs an alternative approach for representing knowledge as opposed to the highly expressive, yet computationally intensive, possible worlds structures used by related action theories that implement modal-logic Kripke semantics for reasoning about knowledge (e.g., [27,28,29]). Specifically, DECKT introduces a generic form of temporal implication rules, called *hidden causal dependencies* (HCDs), that capture the causal relation between unknown world aspects and effects of actions and characterize how an agent believes the state of the world has evolved at a particular time instant (in contrast to state constraints, for instance, that prescribe how the world should be at all times). This way, the theory achieves significant computational benefits when applied to real-world implementations in comparison to possible worlds-based implementations. Given the knowledge at hand, the epistemic component of a reasoner can create a partial description of the world state by associating and maintaining causal relations among unknown world parameters that change dynamically and by deliberating about the potential triggering of events. The DECKT axiomatization gives Kripke semantics to the framework and enables sound and complete derivations of knowledge, while adopting a more efficient knowledge representation with respect to possible worlds structures. The causal relations identified provide a valuable source of information, not only for

outlining an agent's epistemic reflection of the world state, but also for the determination of which sense actions to perform and when. A powerful epistemic model can enhance significantly the cognitive skills of deliberating agents; even parameters not directly measurable may be indirectly inferred when studying the epistemic ramifications of actions. Our implementation of the framework uses a forward-chaining rule-based system whose operational semantics achieves run-time execution of Event Calculus theories that have been first compiled into production rules [24]. In contrast with ordinary rule-based systems deployed in context-aware domains, where the actions that lead to the assertion and retraction of facts have no real semantics and high-level structures, our system uses the underlying high-level structures of the Event Calculus and DECKT to define the causal properties of actions and events or to distinguish between ordinary and epistemic facts that are initiated, terminated or triggered based on the given context.

4.3 Defeasible Contextual Reasoning

Our proposed reasoning model for handling conflicts caused by the integration of information from heterogeneous information sources is *Contextual Defeasible Logic* (CDL [20,30,31]). CDL is a distributed rule-based approach, which combines elements from:

- *Defeasible Logic* [32] - it is rule-based, skeptical, and uses priorities to resolve conflicts among rules;
- *Multi-Context Systems* (MCS [33,34]) - logical formalizations of distributed context theories connected through mapping rules, which enable information flow between contexts. In MCS, a *context* can be thought of as a logical theory - a set of axioms and inference rules - that models local knowledge.

CDL extends classical MCS with defeasible bridge rules and a preference ordering on the system contexts, which are used to model and resolve potential conflicts caused by the integration of information from different contexts. For CDL we have already obtained the following theoretical results: an argument-based characterization [20], a proof-theory [30], and four algorithms for distributed query evaluation, each one implementing a different strategy for conflict resolution [31].

In R-CoRe [35], a contextual reasoning platform for Ambient Intelligence environments, we used CDL as the underlying reasoning model and implemented the CDL algorithms on top of Kevoree, a component-based software framework for distributed, dynamically adaptive systems [36]. The deployment of CDL in Ambient Intelligence environments was based on the following ideas: Entities operating in an AmI environment are modeled as autonomous logic-based agents; the knowledge of an agent is represented as a local rule theory (context theory); and bridge rules are used to associate the knowledge of different agents enabling information flow between them. To handle cases of missing or inaccurate local context data, context theories are represented as theories of Defeasible Logic; and

to resolve potential inconsistencies caused by the integration of information from different agents, priorities among conflicting bridge rules are determined based on the agents preferences. Preferences in Ambient Intelligence Systems may represent the relative confidence of an agent in the quality of data imported from other agents.

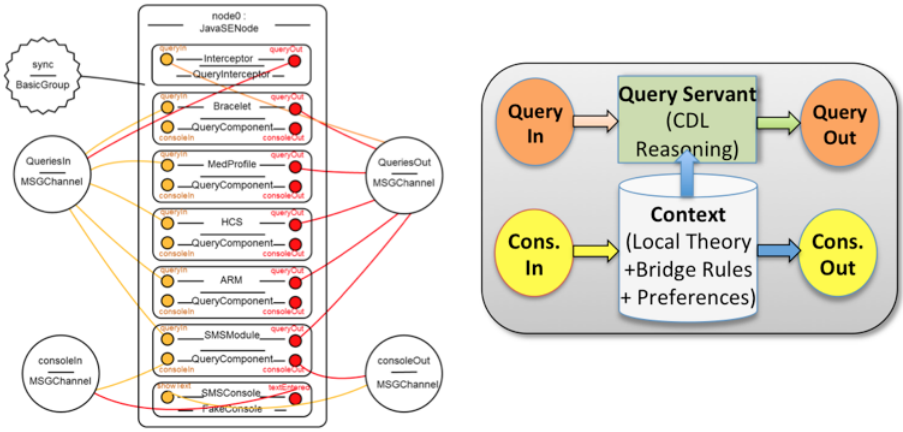

Fig. 7. The architecture of Kevoree components in R-CoRe

Kevoree is an open-source software platform that provides tools for building and synchronizing distributed systems. The most primitive element in Kevoree is that of a component, with which we can represent services, sensors or software applications. The set of services or applications offered by an entity, e.g. a mobile computing device, is represented as a Kevoree node. Components have I/O ports and communicate by exchanging messages through the Kevoree channels, which implement several types of communication, such as emails, sms messages, TCP/IP socket connections and others. We implemented the CDL model and algorithms in Kevoree as follows. Contexts were implemented as Kevoree components (see Figure 7). Specifically, each R-CoRe component consists of: a theory of Defeasible Logic, which encodes the local knowledge of an agent; a set of defeasible bridge rules; an ordering on the system contexts, which represents the preferences of the context; query servant processes, which are used to handle the queries that are posed to the component; and two input and two output ports. The first pair of ports is used for the exchange of queries between the components. The second one is used for communicating with the console, through which users can interact with the component, e.g. to change the knowledge base. Information exchange between contexts was implemented as message exchange between components through the Kevoree channels. Finally, the auto-discovery and adaptive capabilities of Kevoree enable to detect any new entities (e.g. mobile computing devices) that join the environment, and adapt to any changes such as the modification of the local theory of an agent. Figure 8 shows the

setup of R-CoRe for a specific use case scenario: An R-CoRe node here contains seven components: five *Query Components*, each of which represents a different agent in the scenario; one *Console*, which enables interacting with one of the Query Components; and an Interceptor, which visualizes the interaction between the components. The communication between the components is implemented through dedicated Kevoree channels (*MSHChannel*).

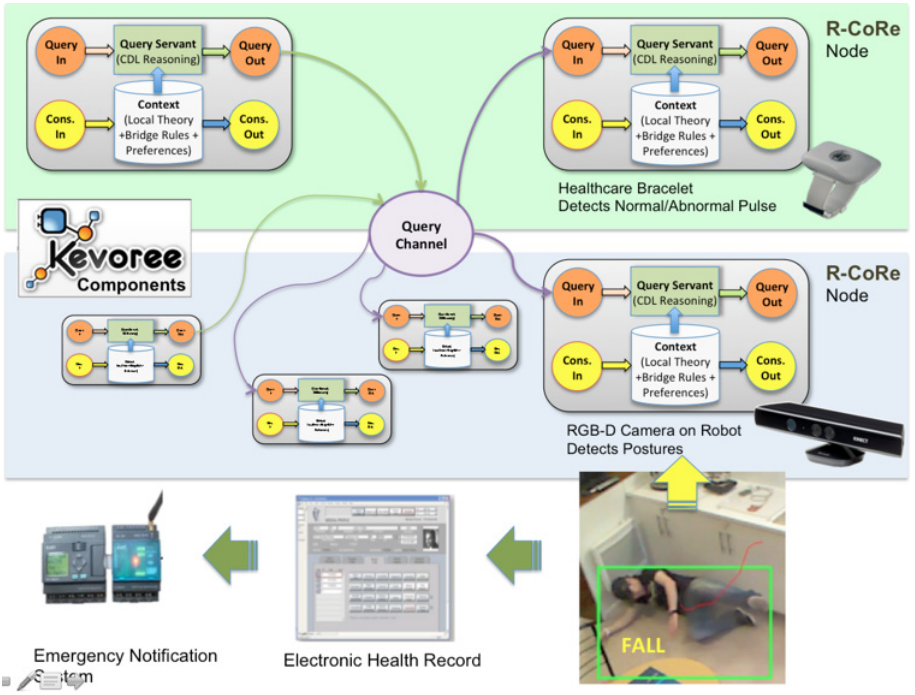

Fig. 8. R-CoRe setup for a use case from Ambient Assisted Living

R-CoRe has been tested in Ambient Assisted Living use cases in the Internet of Things Laboratory of the Interdisciplinary Centre for Security, Reliability and Trust (SnT) in Luxembourg, and was demonstrated at the 7th International Rule Challenge[1]. We are now extending it with new capabilities, such as the ability to handle shared pieces of knowledge, which are directly accessible by all system contexts. This will enable different agents operating in an Ambient Intelligence environment to maintain a common system state. In the future we also plan to: develop forward-chaining reasoning algorithms, which will be triggered by certain events or changes in the environment; integrate Complex Event Processing techniques, which will allow us to reason with low-level sensor data.

[1] `http://2013.ruleml.org/content/7th-international-rule-challenge.html`

5 Conclusion

In this chapter we presented how the current scheme of semantics-based context awareness can significantly benefit from integrating advancements made on the broader field of Knowledge Representation and Reasoning. Motivated by the limitations of existing research trends in implementing truly open context-aware systems, we identified key points that cast ontology built-in reasoning tools insufficient for building context and situation awareness for ubiquitous robots in dynamic environments. To this end, we demonstrated how practical and theoretical reasoning tools, such as reasoning with expressive ontologies under the CWA, using spatial and spatio-temporal reasoning or applying commonsense, defeasible and epistemic reasoning techniques, can be coupled to address the challenges introduced, facing them from the robotics perspective. We expect that this work will provide the substrate to investigate how advantages in fields that range from quantitative approaches to symbolic representations and have evolved in separation can be bridged within the context of robotics for ubiquitous applications. Epistemic reasoning, in particular, can be extended to allow for belief revision techniques when information arriving from the sensors is contradictory or does not match the knowledge stored in the robot's KB. The coupling with quantitative techniques can be achieved my means of tools, such as Markov Logic Networks, which have already demonstrated promising results in real-world implementations. A significant next step will also be the extension of the described frameworks to support in addition to temporal projection also abductive reasoning, in order to solve planning tasks. Determining action sequences that achieve a goal state in the presence of uncertainty and sensing is well studied within the context of conformant and contingency planning; lately, approaches within this field attempt to integrate epistemic structures like the ones presented in this study, in order to exhibit better performance in comparison to existing planners (e.g., [37]). Combining the progress of both fields is expected to result in the inclusion of efficient search components within an online high-level planner that acquires knowledge at runtime through sensing and adapts accordingly to exogenous events that occur in the environment. Finally, we plan to study how the different methodologies from epistemic reasoning and defeasible reasoning can be integrated in a holistic solution for contextual reasoning in Ambient Intelligence environments.

References

1. Dey, A.K.: Understanding and using context. Personal Ubiquitous Computing 5(1), 4–7 (2001)
2. Horrocks, I., Patel-Schneider, P.F.: Knowledge representation and reasoning on the semantic web: Owl. In: Handbook of Semantic Web Technologies, vol. 9 (2010)
3. Riboni, D., Bettini, C.: Owl 2 modeling and reasoning with complex human activities. Perv. and Mob. Computing 7, 379–395 (2011)
4. Ducatel, K., Bogdanowicz, M., Scapolo, F., Leijten, J., Burgelman, J.-C.: Scenarios for ambient intelligence in 2010. IST Programme Advisory Group, ISTAG (2001)

5. Yachir, A., Tari, K., Chibani, A., Amirat, Y.: Toward an Automatic Approach for Ubiquitous Robotic Services Composition. In: IEEE/RSJ International Conference on Intelligent Robots and Systems, pp. 3717–3724 (2008)
6. Yachir, A., Tari, K., Amirat, Y., Chibani, A., Badache, N.: Qos based framework for ubiquitous robotic services composition. In: Proceedings of the 2009 IEEE/RSJ International Conference on Intelligent Robots and Systems, pp. 2019–2026 (2009)
7. Wang, X.H., Zhang, D.Q., Gu, T., Pung, H.K.: Ontology based context modeling and reasoning using owl. In: Proceedings of the Second IEEE Annual Conference on Pervasive Computing and Communications Workshops, pp. 18–22 (2004)
8. Yau, S.S., Liu, J.: Hierarchical situation modeling and reasoning for pervasive computing. In: Proceedings of the Fourth IEEE Workshop on Software Technologies for Future Embedded and Ubiquitous Systems, and the Second International Workshop on Collaborative Computing, Integration, and Assurance (SEUS-WCCIA 2006), pp. 5–10 (2006)
9. Chen, H., Finin, T., Joshi, A.: The soupa ontology for pervasive computing. In: Ontologies for Agents: Theory and Experiences, pp. 233–258 (2005)
10. Francois, A.R.J., Nevatia, R., Hobbs, J., Bolles, R.C.: Verl: An ontology framework for representing and annotating video events. IEEE MultiMedia 12(4), 76–86 (2005)
11. Zarri, G.P., Sabri, L., Chibani, A., Amirat, Y.: Semantic-based industrial engineering: Problems and solutions. In: Proceedings of the 2010 International Conference on Complex, Intelligent and Software Intensive Systems, pp. 1022–1027 (2010)
12. Sabri, L., Chibani, A., Amirat, Y., Zarri, G.-P.: Semantic reasoning framework to supervise and manage contexts and objects in pervasive computing environments. In: Proceedings of the 2011 IEEE Workshops of International Conference on Advanced Information Networking and Applications, pp. 47–52 (2011)
13. Sabri, L., Chibani, A., Amirat, Y., Zarri, G.P.: Narrative reasoning for cognitive ubiquitous robots. In: IROS 2011 Workshop: Knowledge Representation for Autonomous Robots (2011)
14. Zarri, G.P.: Representation and Management of Narrative Information, Theoretical Principles and Implementation. Springer (2009)
15. Ayari, N., Chibani, A., Zarri, G.P., Amirat, Y.: Semi-automatic natural language representation for narrative information. Technical Report, UPEC LISSI Lab
16. Santofimia, M.J., Fahlman, S.E., del Toro, X., Moya, F., Lopez, J.C.: A semantic model for actions and events in ambient intelligence. Journal Engineering Applications of Artificial Intelligence 24, 1432–1445 (2011)
17. Ye, J., Dobson, S.: Exploring semantics in activity recognition using context lattices. Journal of Ambient Intelligence and Smart Environments 2, 389–407 (2010)
18. Chen, L., Nugent, C., Mulvenna, M., Finlay, D., Hong, X., Poland, M.: A logical framework for behaviour reasoning and assistance in a smart home. Int. Journal of Assistive Robotics and Mechatronics 9 (2008)
19. Brewka, G., Eiter, T.: Equilibria in Heterogeneous Nonmonotonic Multi-Context Systems. In: Proceedings of the Twenty-Second AAAI Conference on Artificial Intelligence, Vancouver, British Columbia, Canada, July 22-26, pp. 385–390 (2007)
20. Bikakis, A., Antoniou, G.: Defeasible Contextual Reasoning with Arguments in Ambient Intelligence. IEEE Trans. on Knowledge and Data Engineering 22(11), 1492–1506 (2010)
21. Paschke, A.: ECA-RuleML: An Approach combining ECA Rules with temporal interval-based KR Event/Action Logics and Transactional Update Logics. CoRR, vol. abs/cs/0610167 (2006)
22. Kowalski, R., Sergot, M.: A Logic-Based Calculus of Events. New Generation Computing 4(1), 67–95 (1986)

23. Miller, R., Shanahan, M.: Some alternative formulations of the event calculus. In: Kakas, A.C., Sadri, F. (eds.) Computational Logic: Logic Programming and Beyond. LNCS (LNAI), vol. 2408, pp. 452–490. Springer, Heidelberg (2002)
24. Patkos, T., Chibani, A., Plexousakis, D., Amirat, Y.: A production rule-based framework for causal and epistemic reasoning. In: Bikakis, A., Giurca, A. (eds.) RuleML 2012. LNCS, vol. 7438, pp. 120–135. Springer, Heidelberg (2012)
25. Patkos, T., Plexousakis, D.: Reasoning with knowledge, action and time in dynamic and uncertain domains. In: IJCAI 2009, pp. 885–890 (2009)
26. Patkos, T., Plexousakiss, D.: Efficient epistemic reasoning in partially observable dynamic domains using hidden causal dependencies. In: The 9th International Workshop on Nonmonotonic Reasoning, Action and Change (NRAC 2011), pp. 55–62 (2011)
27. Moore, R.C.: A formal theory of knowledge and action. In: Formal Theories of the Commonsense World, pp. 319–358 (1985)
28. Scherl, R.: Reasoning about the Interaction of Knowledge, Time and Concurrent Actions in the Situation Calculus. In: IJCAI 2003, pp. 1091–1098 (2003)
29. Thielscher, M.: Representing the Knowledge of a Robot. In: KR 2000, pp. 109–120 (2000)
30. Bikakis, A., Antoniou, G.: Contextual Defeasible Logic and Its Application to Ambient Intelligence. IEEE Transactions on Systems, Man, and Cybernetics, Part A 41(4), 705–716 (2011)
31. Bikakis, A., Antoniou, G., Hassapis, P.: Strategies for contextual reasoning with conflicts in Ambient Intelligence. Knowledge and Information Systems 27(1), 45–84 (2011)
32. Antoniou, G., Billington, D., Governatori, G., Maher, M.J.: Representation results for defeasible logic. ACM Transactions on Computational Logic 2(2), 255–287 (2001)
33. Giunchiglia, F., Serafini, L.: Multilanguage hierarchical logics, or: how we can do without modal logics. Artificial Intelligence 65(1) (1994)
34. Ghidini, C., Giunchiglia, F.: Local Models Semantics, or contextual reasoning=locality+compatibility. Artificial Intelligence 127(2), 221–259 (2001)
35. Moawad, A., Bikakis, A., Caire, P., Nain, G., Le Traon, Y.: A Rule-based Contextual Reasoning Platform for Ambient Intelligence environments. In: Morgenstern, L., Stefaneas, P., Lévy, F., Wyner, A., Paschke, A. (eds.) RuleML 2013. LNCS, vol. 8035, pp. 158–172. Springer, Heidelberg (2013)
36. Fouquet, F., Barais, O., Plouzeau, N., Jézéquel, J.-M., Morin, B., Fleurey, F.: A Dynamic Component Model for Cyber Physical Systems. In: 15th International ACM SIGSOFT Symposium on Component Based Software Engineering (July 2012), http://hal.inria.fr/hal-00713769
37. Palacios, H., Geffner, H.: Compiling uncertainty away in conformant planning problems with bounded width. Journal of Artificial Intelligence Research 35(1), 623–675 (2009)

Motion Control and Fall Detection of Intelligent Cane Robot

Toshio Fukuda, Jian Huang*, Pei Di, and Kosuge Sekiyama

[1] Key Laboratory of Image Processing and Intelligent Control, School of Automation, Huazhong University of Science and Technology, No. 1037, Luoyu Road, 430074 Wuhan, Hubei, China
[2] Department of Micro-Nano Systems Engineering, Nagoya University, Furo-cho, Chikusa-ku, Nagoya 464-8603, Japan
huang_jan@mail.hust.edu.cn

Abstract. An intelligent cane robot was designed for aiding the elderly and handicapped people walking. The robot consists of a stick, a group of sensors and an omni-directional basis driven by three Swedish wheels. Multiple sensors were used to recognize the user's "walking intention", which is quantitatively described by a new concept called intentional direction (ITD). Based on the guidance of filtered ITD, a novel intention-based admittance motion control (IBAC) scheme was proposed for the cane robot. The experiment results demonstrated that the user feels more natural and comfortable when walking with the assistance of cane robot controlled by the IBAC strategy. To detect the fall of user, a detection method based on Dubois possibility theory was proposed using the combined sensor information from force sensors and a laser ranger finder (LRF) fixed on the cane robot. The human fall model was represented in a two-dimensional space, where the relative position between the Zero-Moment-Point (ZMP) and the center of support triangle was utilized as a significant feature. The effectiveness of proposed fall detection method was also confirmed by experiments.

Keywords: Intelligent Cane Robot, Intention Estimation, Admittance Control, Fall Detection, Zero Moment Point (ZMP), Possibility Theory.

1 Introduction

The world is facing challenges of rapid aging population. Elderly people may suffer from low levels of physical strength due to muscle weakness, which affects

* This work was supported by the International Science & Technology Cooperation Program of China "Precision Manufacturing Technology and Equipment for Metal Parts" under Grant No.2012DFG70640, the International Science & Technology Cooperation Program of Hubei Province "Joint Research on Green Smart Walking Assistance Rehabilitant Robot" under Grant No. 2012IHA00601 and was supported by Program for New Century Excellent Talents in University (Grant No.NCET-12-0214).

S. Mohammed et al. (eds.), *Intelligent Assistive Robots*,
Springer Tracts in Advanced Robotics 106, DOI: 10.1007/978-3-319-12922-8_12

their motion ability significantly. Restricted movement lowers the performance of most activities of daily living (ADLs). In addition, the growing elderly population causes the shortage of young people for nursing care. Therefore, walking-aid robots find their application in the nursing and therapy field for these mobility impaired people.

A number of walking-aid robots have been proposed in the last decade, including RT-Walker, PAMM, and so on. So far, the walking-aid robot systems may be mainly classified into two groups according to mobility factor, i.e., the system moving on the ground according to the motion of the subjects and the system giving effects of walking to the subjects. The former system is active-type walker [1] [2] which is driven by servo motor. The latter corresponds to a system driven by servo brakes and is passive-type walker [3] [4]. There is still much space for improvement of the present walker systems. First, most walkers can only be used in the indoor environment. Second, the cumbersome design makes them be difficult to operate by novices. In addition, many old persons are not so weak that they have to be nursed carefully. Moderate support, like a cane or stick, is sufficient to help them go outside and improve their ADL functioning to a great extent. In this sense, a robot cane system may be more useful than walkers due to its flexibility and handiness.

Spenko proposed the well-known PAMM system in [5] together with a Smartcane robot. This cane robot has relative small size but the nonholonomic kinematics reduces its maneuverability. To make the cane robot can be used in most of the living environment (e.g. the narrow corridor, the elevator etc.), an omni-directional moving ability is required. Recently, commercial omni-wheels are available and applied in the area of walker systems[6]. Based on the wheels, small omni-directional platform can be constructed. In this article, an intelligent cane system was proposed and investigated based on a commercially available three-wheeled omni-directional platform.

2 Mechanical Design of Intelligent Cane Robot

The intelligent cane robot system consists of several parts: a tiltable metal stick, an omni-directional base, a control subsystem, and a group of sensors.

The tilt mechanism of metal stick is realized by two servo motors whose rotation axes are perpendicular to each other (see Fig. 1). By rotating the two motor, the stick can tilt to any direction. This may improve the stability of cane robot when a fall event suddenly occurs.

The omni-directional base is comprised of three commercial omni-wheels and the corresponding actuators. The resultant moving velocity is confined less than 1.2m/sec so as to ensure the safety of user. Despite the small size, the load capacity of this mobile base is up to 50 kilograms.

In the sensor group, a six-axis force sensor is mounted at the end of stick to measure the interaction forces between the robot and the user. The walking intention of user can be inferred from the measured forces, which will be illustrated in Section 3. Two laser ranger finders (LRFs) are used to measure the distances

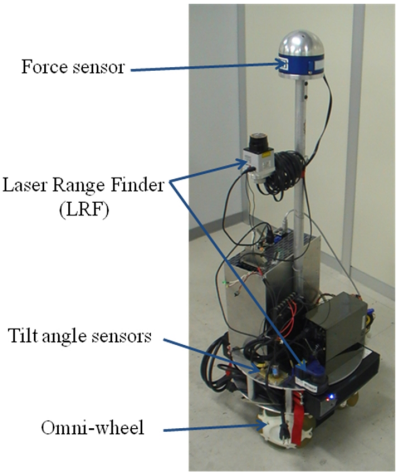

Fig. 1. The intelligent cane robot system

between the stick and the legs, and between the stick and the body, respectively. By online sampling the distance information, fall-prevention function of the cane robot may be implemented as Hirata did in [7].

3 Walking Intention Based Motion Control of Intelligent Cane Robot

3.1 Modeling and Estimation of Human Walking Intention

Preliminary Definitions and Force Analysis. The coordinate definition of human-cane robot system is shown by Fig. 2, in which the coordinate system $O - x_1y_1z_1$ is the reference frame. The local coordinate system $O - x_ry_rz_r$ is fixed on the cane robot and rotates with the yaw angle ψ. The coordinate system $O - x_Iy_Iz_I$ is related to the intentional direction, which is illustrated in the following.

To control the cane robot in accordance with the user's intention, it is necessary to quantify and formulate the human walking intention. Therefore, an important concept called "Intentional Direction (ITD)" is proposed in our previous work [8] to comply with this requirement.

Definition 1. *The direction to which a person intends to move is referred to as intentional direction (ITD).*

As illustrated by Fig. 2, the ITD is not always parallel to the sagittal plane because there are various possible walking modes, including lateral moving, turning around etc.. Note that the ITD can be evaluated by the angle between the forward direction (FW) and the ITD itself. $\rho(n)$ is used to denote the time-variant ITD in the rest of the paper. Here n is the time scale.

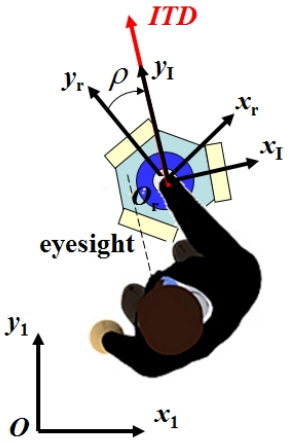

Fig. 2. Quantitative representation of the intentional direction (ITD). The eyesight line is denoted by the broken line, which indicates the direction that the user is intentional to move.

During the user's walking aided by the cane robot, the measured force and torque at time n are denoted by $\mathbf{F}(\mathbf{n})$ and $\mathbf{n}(\mathbf{n})$. The measurement can be represented in different coordinate systems as follows:

$$\begin{cases} \mathbf{F}(n) = \left[{}^{r}F_x(n)\ {}^{r}F_y(n)\ {}^{r}F_z(n)\right]_r^T = \left[{}^{I}F_x(n)\ {}^{I}F_y(n)\ {}^{I}F_z(n)\right]_I^T, \\ \mathbf{n}(n) = \left[{}^{r}n_x(n)\ {}^{r}n_y(n)\ {}^{r}n_z(n)\right]_r^T = \left[{}^{I}n_x(n)\ {}^{I}n_y(n)\ {}^{I}n_z(n)\right]_I^T \end{cases} \tag{1}$$

Except the direction, the quantity of this intention is characterized by the absolute value of measured resultant force ${}^{I}F_y(n)$ along the ITD.

State Model of ITD. The dynamic model of ITD is required to obtain the quantitative formulation of the user's walking intention. Since the dynamics of ITD has different forms in different walking modes, we first enumerate all possible walking modes. Because only several modes are often used in the daily life, the enumeration procedure can be simplified. In this study, we are concerned about five simple walking modes, which are listed in TABLE 1. The transition diagram of the five modes is also illustrated in Fig.3.

To detect the transition between any two walking modes, the following assumptions are concluded from common experiences.

Assumption 1. *In mode I, the ITD is supposed to be always zero.*

Assumption 2. *In mode II, the ITD is supposed to be a constant.*

Assumption 3. *In mode III, the ITD monotone converges to zero from an initial non-zero value.*

Table 1. POSSIBLE WALKING MODES

Mode	Description
I	Stop
IIa	Go straight forward
IIb	Go straight in other directions
IIIa	Turn to the right
IIIb	Turn to the left

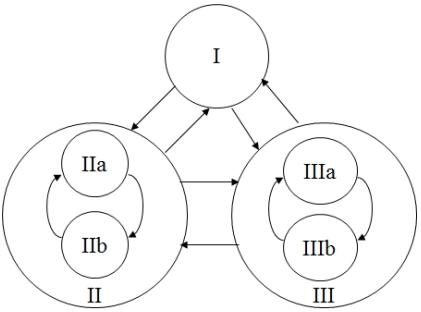

Fig. 3. Transition diagram of possible walking modes

Normally, there is some target one wants to move towards during turning around. Assumption 3 is then proposed based on this fact (see Fig. 4). During the process of turning around, the value of $\rho(n)$ decreases gradually and finally converges to zero, which causes a transition to mode I or II.

According to these assumptions and the proposed walking modes, a hybrid linear state model of ITD can be obtained as follows:

$$\rho(n+1) = A_{\sigma(n)} \cdot \rho(n), \quad \sigma(n) \in \{I, II, III\} \tag{2}$$

where $\sigma(n)$ is used to denote the different walking mode given by TABLE 1. The state transition matrices are given by

$$A_I = 0, A_{II} = 1, A_{III} = a(n) \tag{3}$$

where $a(n)$ satisfies

$$0 < a(n) < 1 \tag{4}$$

Observation Model of ITD. Note that the state variable $\rho(n)$ cannot be directly measured. The interaction forces between the user and cane robot reflect the walking intention. Obviously, the ITD is along the direction of resultant force of F_x and F_y if there are no measurement noises. Thus, the observation model of ITD is described by

$$y(n) = \tan^{-1}\left(\frac{{}^{r}F_x(n)}{{}^{r}F_y(n)}\right) = \rho(n) + \omega(n) \tag{5}$$

$\omega(n)$ is a combination of sensor noises and human gait habit. Normally, different people have different gait habit during walking (e.g., some people unintentionally move laterally even when they walk straight forward). For the sake of simplicity, $\omega(n)$ is assumed as a white noise sequence with a user-dependent covariance $Q(\rho)$. It is observed that the values of $Q(\rho)$ are almost same for the same user. Thus, conventional Kalman filter is very suitable for estimating the ITD in mode II and III.

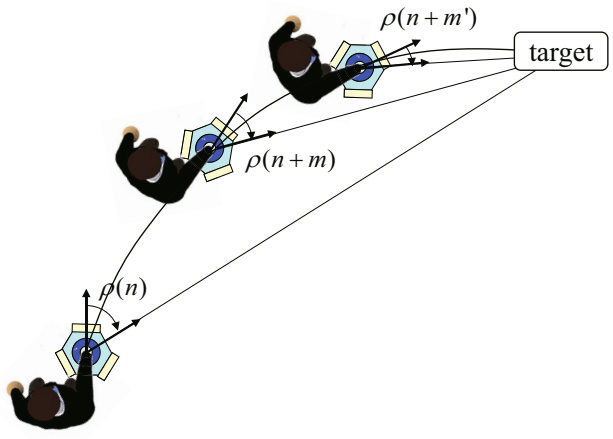

Fig. 4. Typical turning around move mode

Online Estimation of ITD Based on Kalman Filters. In this section, we discuss the approach to online estimate the ITD from measured forces. The first problem that should be solved is how to detect the walking mode transition. In this study, we use a rule-based method to infer current walking mode $\sigma(n)$. Fuzzy threshold detection methods are used to check if some rule is satisfied. These rules are generated from common-sense experiences and described as follows.

Rule set. (Rule-Based Method)

1. IF $\sigma(n-1) \neq$ I AND ${}^{r}F_x(n) \approx 0$ AND ${}^{r}F_y(n) \approx 0$ AND ${}^{r}n_z(n) \approx 0$, THEN $\sigma(n) =$ I.
2. IF $\sigma(n-1) \neq$ IIa AND ${}^{r}F_x(n) \approx 0$ AND $|{}^{r}F_y(n)| > 0$ AND ${}^{r}n_z(n) \approx 0$, THEN $\sigma(n) =$ IIa
3. IF $\sigma(n-1) \neq$ IIb AND $|{}^{r}F_x(n)| > 0$ AND $|{}^{r}F_y(n)| > 0$ AND ${}^{r}n_z(n) \approx 0$, THEN $\sigma(n) =$ IIb
4. IF $\sigma(n-1) \neq$ IIIa AND ${}^{r}n_z(n) > 0$, THEN $\sigma(n) =$ IIIa
5. IF $\sigma(n-1) \neq$ IIIb AND ${}^{r}n_z(n) < 0$, THEN $\sigma(n) =$ IIIb

In mode I and II, the dynamics of ITD is described by a linear state model. Therefore a conventional Kalman filter is suitable to be applied to online estimate the ITD.

In mode III, the state model of ITD can be rewritten as

$$\rho(n+1) = (a_0 + \Delta a(n)) \cdot \rho(n) \tag{6}$$

where a_0 is a constant and satisfies $0 < a_0 < 1$. $\Delta a(n)$ is the model uncertainty. It is well known that normal Kalman filter will generally not guarantee satisfactory performance when uncertainty exists in the system model. Thus, we choose a robust Kalman filter to calculate the estimation of ITD in this case [9].

We conclude the above discussion by proposing the following online ITD estimation algorithm.

Algorithm 1. (Online ITD Estimation Algorithm)
Input: $\mathbf{F}(n-1)$, $\mathbf{n}(n-1)$, $y(n)$, $\rho_e(n-1)$, $\sigma(n-1)$

1. Apply the rule-based method to determine $\sigma(n)$
2. IF $\sigma(n-1) = \sigma(n)$ THEN
3. SWITCH $\sigma(n)$
4. CASE I:Let $\rho_e(n) = 0$
5. CASE II:
6. Use the Kalman filter to infer $\rho_e(n)$
7. IF $\sigma(n) =$ IIa THEN let $\rho_e(n) = 0$
8. CASE III:
9. Use the robust Kalman filter to infer $\rho_e(n)$
10. ELSE
11. Let $\rho_e(n) = y(n)$ to initialize the filter.
12. ENDIF

Output: $\rho_e(n)$, $\sigma(n)$

3.2 Walking Intention Based Admittance Control

The cane robot motion controller uses an admittance control scheme based on the inferred human intention, which is called intention based admittance control (IBAC) scheme. The conventional admittance control uses an admittance model emulates a dynamic system and gives the user a feeling as if he is interacting with the system specified by the model. This model is defined as a transfer function with the users forces and toques, F(s), as the input and the reference velocity of cane robot, V(s), as the output. It is expressed as:

$$G(s) = \frac{V(s)}{F(s)} = \frac{1}{Ms + B} \tag{7}$$

where M and B are the mass and damping parameters respectively.

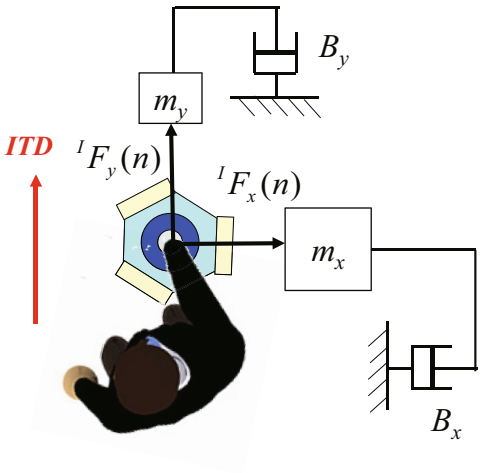

Fig. 5. The principle of IBAC scheme

During walking, people feel comfortable if the cane is easily maneuvered in the ITD and hardly maneuvered in the direction perpendicular to the ITD. To meet the requirement, we propose the IBAC scheme in which two admittance models are used. One model is defined for the motion along the ITD, which has selected mass and damping parameters from the acceptable area presented in [5]. The other model is defined for the motion perpendicular to the ITD, which has much bigger mass and damping parameters. The general idea is shown by Fig. 5. The final three-DOF mass-damping model for our cane robot is defined as:

$$\mathbf{M}^d \cdot \ddot{\mathbf{q}}^d + \mathbf{B}^d \cdot \dot{\mathbf{q}}^d = \mathbf{F} \tag{8}$$

where state $\mathbf{q}^d$ and the measured force $\mathbf{F}$ are represented in the coordinate frame $\{I\}$ based on the current walking intention, satisfying

$$\mathbf{q}^d = \begin{bmatrix} {}^I x^d \\ {}^I y^d \\ {}^I \rho^d \end{bmatrix}_I, \mathbf{F} = \begin{bmatrix} {}^I F_x \\ {}^I F_y \\ n_z \end{bmatrix}_I \tag{9}$$

Matrices $\mathbf{M^d}$ and $\mathbf{B^d}$ are the desired mass and damping coefficients. These coefficients are described by

$$\mathbf{M^d} = \begin{bmatrix} {M_x}^d & 0 & 0 \\ 0 & {M_y}^d & 0 \\ 0 & 0 & {J_z}^d \end{bmatrix}, \mathbf{B^d} = \begin{bmatrix} {B_x}^d & 0 & 0 \\ 0 & {B_y}^d & 0 \\ 0 & 0 & {B_z}^d \end{bmatrix} \tag{10}$$

where ${M_x}^d >> {M_y}^d, {J_z}^d$and ${B_x}^d >> {B_y}^d, {B_z}^d$

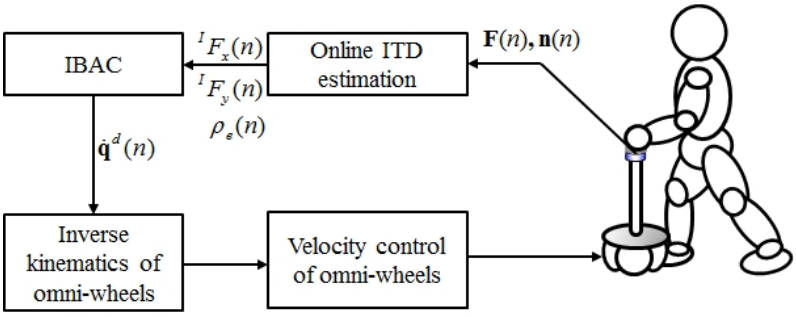

Fig. 6. Control diagram of the whole system

3.3 Experiment Study

Investigating Observation Noise. Three university students (subject A, B and C) utilized the cane robot realizing mode II and III in these experiments. Same experiments were performed by them while wearing the brace to imitate a handicapped people. To verify the white noise assumption of the observation noise, firstly the subjects were requested to intentionally maneuver the robot moving straight along five fixed directions, which is shown by Fig. 7. From these experiments, we can investigate the observation noise characteristics of ITD by applying statistic techniques. For moving-straight experiments (mode II), the observation noise $\omega(n)$ can be easily obtained and analyzed from the observation model (5). For the obtained noise signal of each experiment, we tested both the normality and independence of residuals by applying Jarque Bera and Portmanteau test methods. It was found that more than 80% of the experiment results passed the statistical tests. Thus, a white noise assumption is thought to be acceptable in our study.

Further, the results of evaluated covariance Q of the white observation noise $\omega(n)$ are also depicted in Fig. 7. For each subject, the direction-dependent Q of this subject can be thought as a random variable. Coefficients of variation (cv) of these random variables were calculated and found to be less than 10%. Therefore, it is reasonable to assume that values of Q are almost the same in different directions for the same person, as pointed out in subsection B of section III. Another interesting phenomenon that should be pointed out is that the covariance Q of the subject wearing a brace is higher than that of the subject performing a normal walking. This proves the fact that the observation noise of a handicapped peoples walking is usually bigger than that of a normal people.

Motion Control on Flat Ground. In the experiments for illustrating the validity of the IBAC control strategy, subject A utilized the cane robot to implement two series of walking modes.

The inferred ITDs and their observations based on force signals are shown in Fig. 8(a) and Fig. 9(a). Trajectories of estimated mode are also shown in

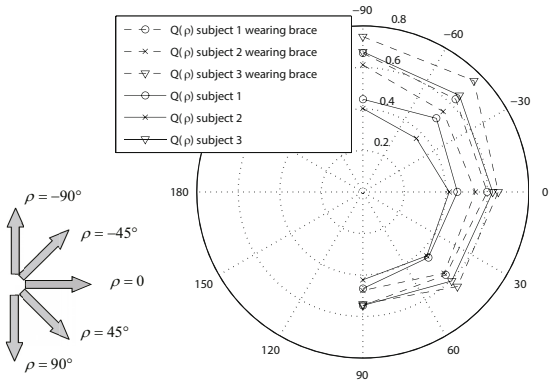

Fig. 7. The covariance of noise when a person moves straight

these figures, where we use integers from 1 to 5 to denote the five walking modes sequentially (see the value of mode trajectory depicted by the dot-dash line). Note that even if there are some fault recognitions of mode transition, the performance of rule-based mode transition function is sufficiently satisfactory in the practice. In the experiment results, the main fault recognitions of mode transitions are mistaking mode IIa for mode IIb. This will not affect the system performance much because mode IIa is actually a special case of mode IIb. The advantage of fast detection of mode IIa is to quickly get an accurate ITD estimation ($\rho_e(n) = 0$), which can be used to guide the motion control very clearly. However, even mode IIa is mistaken for mode IIb, the ITD which is estimated by Kalman filter is nearly equal to zero and smooth enough to obtain a satisfactory intention-based motion control.

As mentioned above, Kalman filter and robust Kalman filter are used in mode II and III respectively. Coefficient $a(n)$ in model (3) satisfies $a(n) = a_0 + \Delta a(n)$ with $a_0 = 0.93$, $|\Delta a(n)| < 0.3$. Comparing with the observation $y(k)$ from the noisy force signals, the online estimated ITD $\rho_e(n)$ reflects the human intention smoothly and distinctly, which provides explicit guidance to the IBAC controller. In particular, when the subject moves straight forward, which is the walking mode in most of the time, the inferred ITD is exactly the forward direction. This reduces meaningless lateral movements of the cane robot to a great extent. In addition, typical force responses are shown in Fig. 8(b) and Fig. 9(b) of the walking experiments.

Comparison Experiment Study. As illustrated in section V.A, observation noise of the ITD always exists while the cane robot is operated by either a normal user or an imitated disabled user. If a conventional force control approach is applied, the cane robot will move unexpectedly due to the effect of noise. This unexpected motion makes the user feel uncomfortable and deteriorates

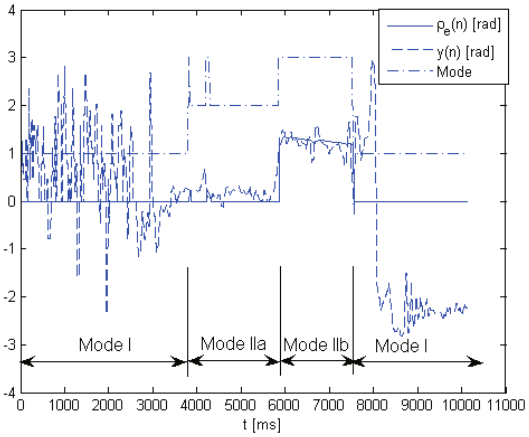

(a) Observed and inferred ITD vs Time (ms)

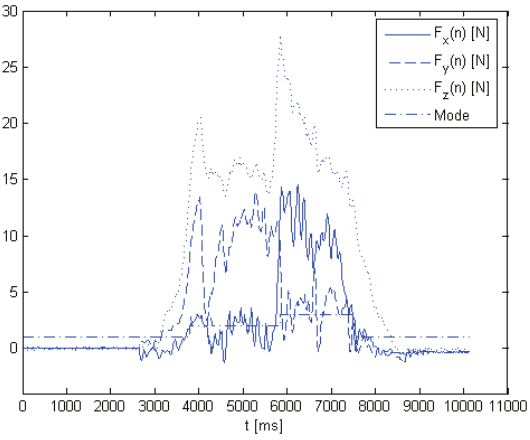

(b) Force signals vs Time (ms)

Fig. 8. Experiment 1 on the flat ground (I→IIa→IIb→I)

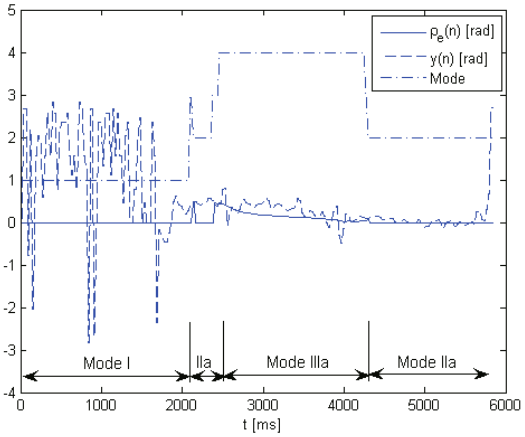

(a) Observed and inferred ITD vs Time (ms)

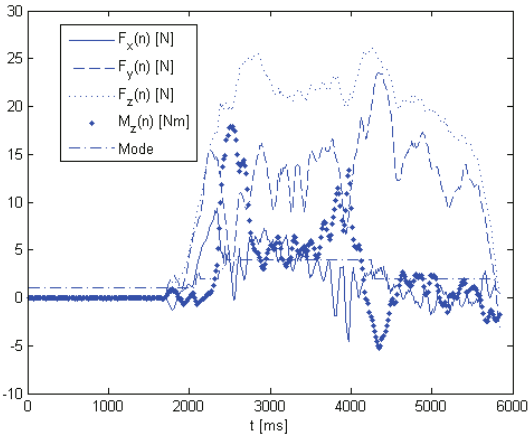

(b) Force signals vs Time (ms)

Fig. 9. Experiment 2 on the flat ground (I→IIa→IIIa→IIa)

the maneuverability of robot. To safely assist the elderly or disabled walking, the proposed IBAC approach overcomes the disadvantage of conventional force control to a great extent. The validity of IBAC approach is further illustrated by the following experimental comparison study.

In this experiment, a subject was asked to perform two series of walking modes depicted by Fig. 10. A conventional admittance control (CAC) strategy which is often used in [5] was tested first and the motion trajectories of cane robot were recorded. The same experiments were conducted on the cane robot controlled by the IBAC strategy.

To quantitatively evaluate the coincidence between the motion of cane robot and the users walking intention, we assume a metric which is given by

$$D(cane, ITD) = \frac{1}{N} \sum_{i=1}^{N} \sqrt{(x_c(i) - x_{fit}(i))^2 + (y_c(i) - y_{fit}(i))^2} \qquad (11)$$

where N is the data number of a motion trajectory of cane robot. $(x_c(i), y_c(i))$ is the i-th point in the motion trajectory. $(x_{fit}(i), y_{fit}(i))$ is the i-th point of the best-fit line through the point set of the motion trajectory. Note that the best-fit line should be obtained according to the given walking mode series, which reflect the users walking intention. For instance, the best-fit line of walking experiment A (see Fig. 10(a) consists of two straight lines representing the walking mode IIa and IIb respectively. The best-fit line of walking experiment B (see Fig. 10-(b) is composed of two straight lines (representing mode IIa at the beginning and end of the walking mode series) and an arc (representing mode IIIa).

Fig. 11 shows two comparison results of walking experiments on flat ground using the IBAC strategy and the conventional admittance control strategy. The difference between the robot motion trajectory in the case of using the IBAC strategy and its best-fit line is much smaller than that in the case of using normal admittance control. This fact was further proven by calculating the average values of *D(cane,ITD)* after conducting a number of comparison experiments in different cases illustrated in the above subsections (see Table 2). As a conclusion, smaller values of *D(cane,ITD)* are obtained when the IBAC strategy is applied to our cane robot. That is, there are less unexpected motions of the cane robot if the IBAC strategy is employed. This is very important in the sense of making the user feel safe and comfortable while operating the cane robot.

Table 2. Comparison of $D(cane, ITD)$ using different control strategies

Subject	Experiment number	Average Value of D (CAC)	Average Value of D (IBAC)
A	50	0.0129	0.006
B	50	0.0117	0.006

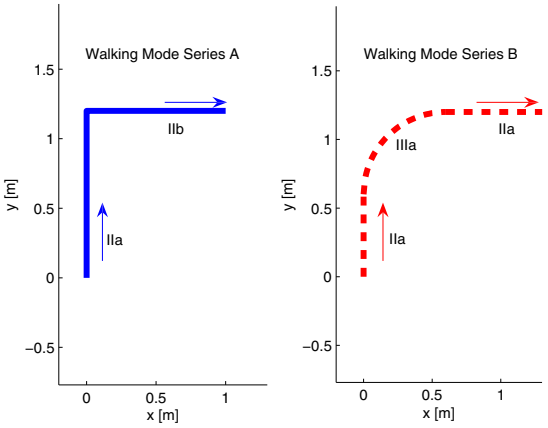

(a) (b)

Fig. 10. Two walking mode series used in the comparison study

4 Fall Detection Using Intelligent Cane Robot

4.1 ZMP Estimation

In this study, a novel method is proposed to detect the risk of falling in the elderly based on Zero-Moment-Point (ZMP) estimation. The ZMP is a very important concept of the motion planning for biped robots, and also can be applied in the area of tripedal or multiped robot. There are two walking modes of legged robot from a stability viewpoint; one is statically stable walking and the other is dynamically stable walking. For dynamically stable walking robot, the ZMP can be computed using the equations (12), (13). The stability can be achieved by controlling the position of ZMP of the robot to be inside the support polygon.

$$x_{zmp} = \frac{\sum_{i=1}^{n} m_i x_i \left(\ddot{z}_i + g\right) - \sum_{i=1}^{n} m_i \ddot{x}_i z_i - \sum_{i=1}^{n} I_{iy} \ddot{\theta}_{iy}}{\sum_{i=1}^{n} m_i \left(\ddot{z}_i + g\right)} \tag{12}$$

$$y_{zmp} = \frac{\sum_{i=1}^{n} m_i y_i \left(\ddot{z}_i + g\right) - \sum_{i=1}^{n} m_i \ddot{y}_i z_i - \sum_{i=1}^{n} I_{ix} \ddot{\theta}_{ix}}{\sum_{i=1}^{n} m_i \left(\ddot{z}_i + g\right)} \tag{13}$$

where m_i is the mass of link, I_{ix}, I_{iy} are the inertial components, θ_{ix}, θ_{iy} are the acceleration of link (as shown in Fig. 12).

Unfortunately, these equations can only be used to compute the ZMP for a robot system, not for a human. Since the human is an uncontrollable factor in

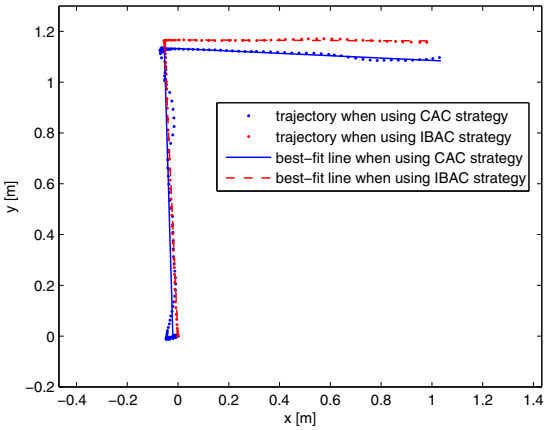

(a) A comparison of experiment results for walking mode series A

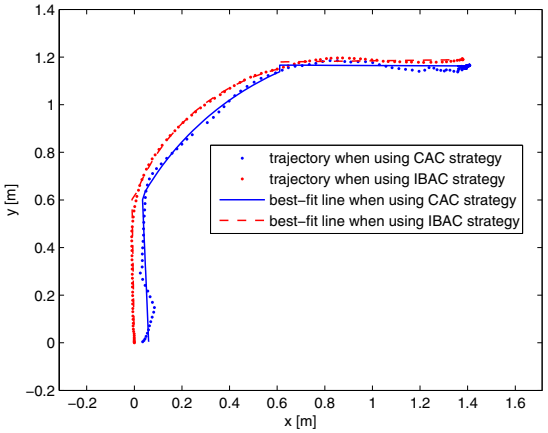

(b) A comparison of experiment results for walking mode series B

Fig. 11. Comparisons of experiment results using the IBAC strategy and the CAC strategy

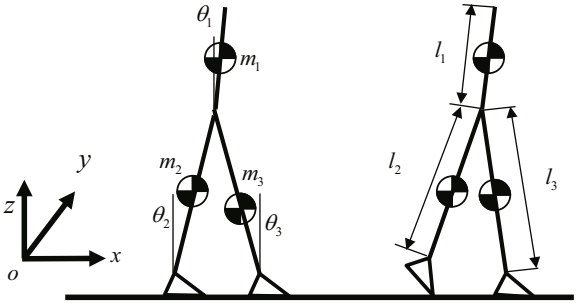

Fig. 12. The simplified link model of human walking

our human-cane system, we cannot control the movement and rotation of each part of human body. Furthermore, the position of each link (x_i, y_i, z_i) cannot be obtained by the existing sensors of the cane robot system. Therefore, we cannot control or even estimate the ZMP of user by using Eq. (12), (13).

Thus, the statically stable walking model is applied to estimate the users ZMP. The static model can remain statically stable if and only if its center of gravity (COG) projects vertically inside the support polygon. In a quasi-static case, the ZMP is proved be equivalent to the projection of COG. According to this principle, the falling risk can be detected by the statically walking model given by

$$x_{cog} = \frac{\sum_{i=1}^{n} x_i f_i}{\sum_{i=1}^{n} f_i}, \; y_{cog} = \frac{\sum_{i=1}^{n} y_i f_i}{\sum_{i=1}^{n} f_i} \tag{14}$$

where x_i, y_i (n=1, 2, 3) denote the position of ground reaction force (the LRF is origin of the coordinate system). f_i denotes the magnitude of ground reaction force measured by the 6-axis force sensor and on-shoe load sensor that will be illustrated as follows.

4.2 Sensor Configuration

To apply the statically mode model (14), a wearable load sensor system was proposed to obtain the dynamical ground reaction force. This system includes four parts which is shown in Fig. 13-(A).

As shown in Fig. 14, the ground reaction forces f_1, f_2 and f_3 are measured by the 6-axis force sensor and on-shoe load sensors respectively. The three contact points are denoted by P_1, P_2 and P_3. The coordinate value of point P_1, is easily obtained for it is just the position of cane robot. By using a laser ranger finder, the coordinate values of point P_2 and P_3 can be approximately calculated (see the two yellow scanned segments on the legs in Fig. 14).

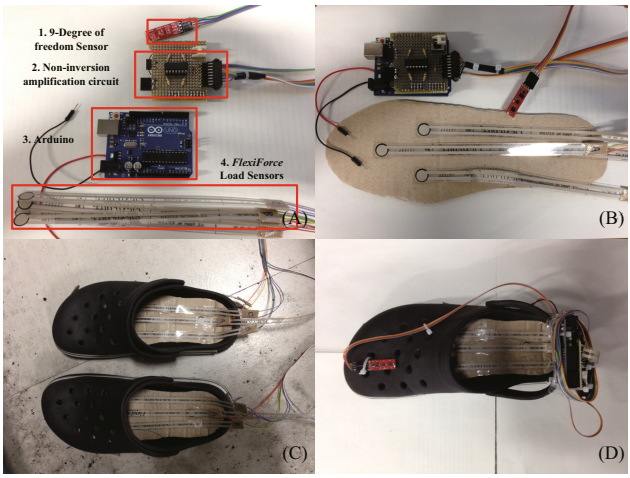

Fig. 13. On-shoe load sensor system

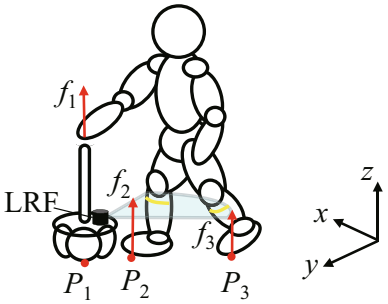

Fig. 14. Sensory data required in ZMP estimation

4.3 Fall Detection Method Based on Fuzzy Theory

As shown in Fig. 15-(a), possible falling states include 'forward falling', 'backward falling' and 'sideward falling'. Here state 'sideward falling' consists of all falling cases except forward and backward falling. In Fig. 15-(b), the positions of point P_1, P_2, P_3 and ZMP are depicted for all possible falling cases.

Obviously, an important feature indicating the user's falling state is the relative position between the ZMP and point P_0, which is the center of support triangle with vertices P_1, P_2 and P_3 (see Fig. 16). This relative position can be described by a two-dimensional vector $(\Delta x, \Delta y)^T$. While the user is walking normally, the ZMP should fluctuate around P_0 in a small area. This area differs from different people. When the user is falling down, the distance between ZMP and P_0 will increase suddenly. And the falling direction can also be easily obtained by observing vector $(\Delta x, \Delta y)^T$.

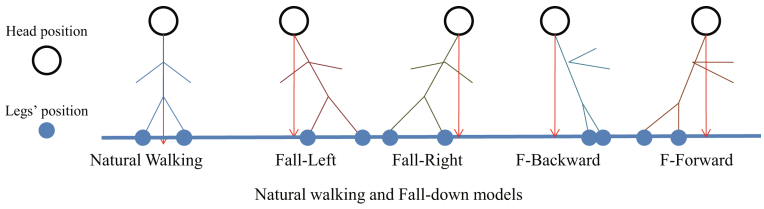

(a) Normal walking and possible falling states

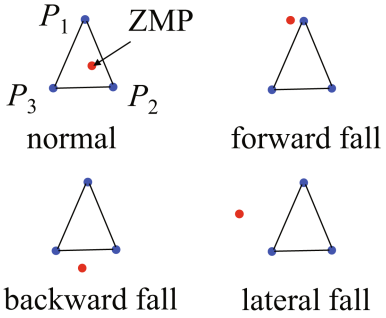

(b) Point positions of different falling cases

Fig. 15. Walking states analysis

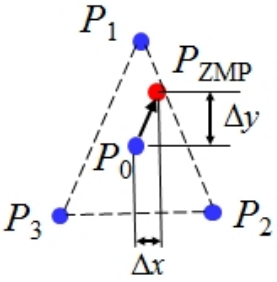

Fig. 16. The feature $(\Delta x, \Delta y)^T$ of fall detection

The distribution of feature during normal walking is analyzed similar to [7]. Dubois possibility theory is applied to describe the distribution of vector $\overrightarrow{P_0 P_{ZMP}} = [\Delta x, \Delta y]^T$ during the normal walking state [10].

The procedure starts by constructing the data histograms for Δx and Δy^T during normal walking state. The number of bins h for a histogram is experimentally determined. Each bin is represented by the center of the interval denoted by y_j. The height of each bar is the number of learning points, located in this bin.

The probability distribution $\{p(y_j) : \ j = 1, 2, \cdots, h\}$ is calculated by dividing the height of each bin by the total number of learning points belonging to the

same class. The possibility distribution $\{\pi(y_j) : \ j = 1, 2, \cdots, h\}$ is deduced from the probability distribution by the bijective transformation of Dubois and Prade defined by

$$\pi(y_k) = \sum_{j=1}^{h} \min\left[p(y_k), p(y_j)\right] \tag{15}$$

The membership functions $\mu(\cdot)$ that characterize the fuzzy set "normal walking", is finally calculated from the corresponding possibility distributions by linear interpolation.

The fall detection is implemented by a very simple algorithm, which is illustrated as follows: (assuming the human walking behavior is monitored at discrete times, n denotes the current time)

IF $\mu(\Delta x(n), \Delta y(n)) < c$ *and* $\mu(\Delta x(n-1), \Delta y(n-1)) < c$, *THEN a fall is detected.*

Constant c is a small positive number which indicates a very low possibility of "normal walking" state.

4.4 Experiment Study

We experimented with the cane robot to illustrate the effectiveness of the proposed methods. First, the possibility distribution of "normal walking" state is investigated. Then the validity of fall detection method is verified by experiments.

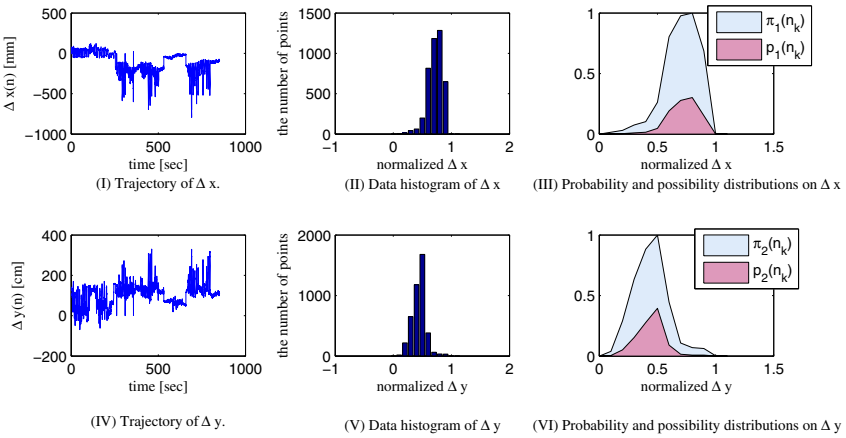

Fig. 17. Trajectories, data histagrams, probability and possibility distributions of "normal walking

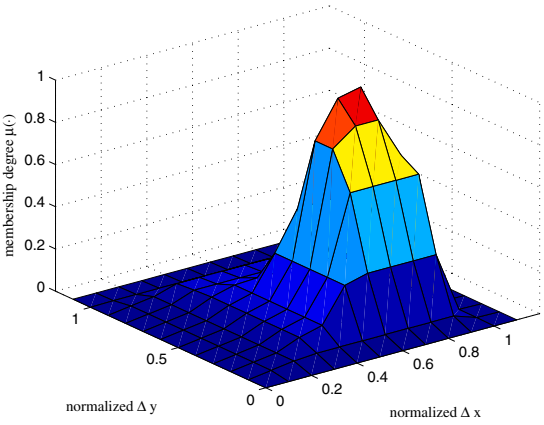

Fig. 18. The membership degree function of "normal walking"

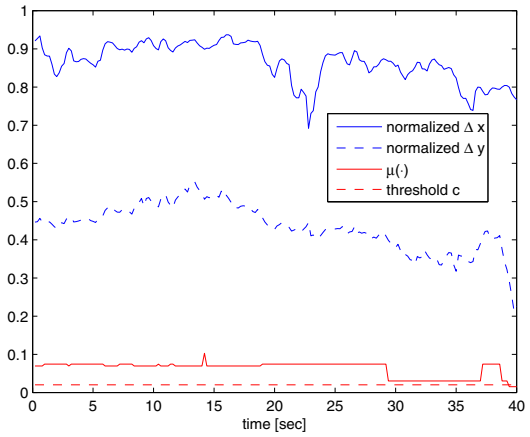

Fig. 19. Fall detection experiment

Experiments of "Normal Walking". A university students were requested to operate the cane robot to conduct "normal walking" experiments. From the experimental data, the possibility distributions of "normal walking" were obtained as well as the membership degree function. The original trajectories and corresponding data histograms of $\Delta x(n)$ and $\Delta y(n)$ are shown in Fig. 17 (I) and (IV). The constant h is assumed to be 10. The probability distribution $p(n_k)$, possibility distribution $\pi(n_k)$ are depicted in Fig. 17 (II), (III), (V) and (VI). The obtained membership function $\mu(\Delta x(n), \Delta y(n))$ is given in Fig. 18

Experiments of "Fall Detection". In this experiment, the subject pretended to fall down during walking. The fall detection rule described in section 4.3 was

applied in the experiment. Constant c was chosen as 0.02. The fall was detected promptly as shown by Fig. 19.

4.5 Conclusion

A new omni-directional type intelligent cane robot is developed for the elderly and handicapped. Motion control and fall detection of this robot are studied based on online estimating human walking intention and the position of ZMP.

The main contribution of this study lies in: 1) presenting dynamic models and online inference algorithm for the human walking intention, which is significant to lead the user walking in a natural and comfortable way. 2) proposing practical ZMP based fall detection method during operating the cane robot. An intention based admittance control (IBAC) scheme is also proposed and used to drive cane robot. Experiments were performed on the flat ground to verify the effectiveness of proposed algorithms.

Future work will focus on the investigation of fall prevention measures and plentiful operation experiments by different users.

References

1. Dubowsky, S., Genot, F., Godding, S.K., Skwersky, H.A., et al.: PAMM-a robotic aid to the elderly for mobility assistance and monitoring: A helping-hand for the elderly. In: IEEE International Conference on Robotics and Automation, pp. 570–576. IEEE Press, New York (2000)
2. Hirata, Y., Baba, T., Kosuge, K.: Motion control of omni-directional type walking support system walking helper. In: The 12th IEEE International Workshop on Robot and Human Interactive Communication (RO-MAN), pp. 85–90. IEEE Press, New York (2003)
3. Rentschler, A.J., Cooper, R.A., Blaschm, B., Boninger, M.L.: Intelligent walkers for the elderly performance and safety testing of vapamaid robotic walker. Journal of Rehabilitation Research and Development 40, 423–432 (2003)
4. Hirata, Y., Hara, A., Kosuge, K.: Passive-type intelligent walking support system "RT Walker". In: IEEE International Conference on Intelligent Robots and Systems (IROS), pp. 3871–3876. IEEE Press, New York (2004)
5. Yu, H., Spenko, M., Dubowsky, S.: An Adaptive Shared Control System for an Intelligent Mobility Aid for the Elderly. Auton. Robots 15(1), 53–66 (2003)
6. Soai Co. Ltd., `http://www.soai-net.co.jp/`
7. Hirata, Y., Muraki, A., Kosuge, K.: Motion Control of Intelligent Passive-type Walker for Fall-prevention Function based on Estimation of User State. In: IEEE International Conference on Robotics and Automation (ICRA), pp. 3498–3503. IEEE Press, New York (2006)
8. Wakita, K., Huang, J., Di, P., Fukuda, T., Sekiyama, K.: Human Walking Intention Based Motion Control of Omni-directional Type Cane Robot. IEEE/ASME Trans. Mechtronics 18(1), 285–296 (2013)
9. Xie, L., Soh, Y.C., Souza, C.E.: Robust Kalman Filtering for Uncertain Discrete-time Systems. IEEE Trans. Automat. Contr. 39(6), 1310–1314 (1994)
10. Dubois, S., Prade, H.: Possibility Theory and Its Applications: A Retrospective and Prospective View. In: IEEE International Conference on Fussy Systems, pp. 25–28. IEEE Press, New York (2003)

Human-Friendly Motion Control of Power-Assisted Wheelchair

Sehoon Oh[1] and Yoichi Hori[2]

[1] Robotics Engineering, Daegu Gyeongbuk Institute of Science and Technology (DGIST), Daegu 711-873, Korea
sehoon@dgist.ac.kr
[2] Department of Electrical Engineering and Information Systems, The University of Tokyo, Tokyo 113-8656, Japan
hori@k.u-tokyo.ac.jp

Abstract. Wheelchairs which have enhanced locomotion of people with muscular weakness or paralysis still can be improved using various assistive technologies, e.g., electric wheelchairs have been developed and widely used for enhancement of the maneuverability and safety of people. The power-assisted wheelchair (PAW) is a relatively new type of a wheelchair, which is equipped with torsion sensors to measure force applied on rims by a human and provides the assistive torque based on the measured force. With this propelling process, the user still can involve with the propulsion of the wheelchair while the assistive torque can relieve the user's propulsion effort.

This PAW is a case of human-machine interface and requires an adequate control of assistive torques to interact with a human without confliction. To address this issue, human-friendly motion control of the PAW is introduced in this chapter, which consists of the accurate observation of the physical states of the PAW and the disturbance rejection control based on the observed states to support safe and comfortable operation of the PAW.

Several physical states of the PAW are defined as the operation states, which are associated with the motion of the PAW and the environmental condition, and they are observed utilizing multiple motion sensors (i.e., encoders, gyroscopes, and accelerometers) and an algorithm to fuse them. Then, control algorithms to remove the effect of undesired disturbance on the PAW without perturbing human's operation are developed in a human-friendly way utilizing the observed operation states. The effectiveness of this human-friendly motion control of PAW is verified through various experiments using a commercialized PAW.

Keywords: power-assisted wheelchair, gravity compensation, operation state, state-space-based sensor fusion, two dimensional control, disturbance observer, mode decomposition.

1 Introduction

Recently, with the help of motors and conrollers, significant changes have been made to wheelchairs that have provided mobility solutions to the people with

S. Mohammed et al. (eds.), *Intelligent Assistive Robots*,
Springer Tracts in Advanced Robotics 106, DOI: 10.1007/978-3-319-12922-8_13

muscular weakness or paralysis[8]. Electric wheelchairs that are fully electrically powered and manipulated by a joystick have been widely used and paved the way for people with disabilities to reach any place without a difficulty.

There are other types of wheelchairs such as a power-assisted wheelchairs (PAW's) that measure human's force applied on the rims and provide assistive torque by motors based on the measured force. On this PAW, the user still can be involved with the propulsion of the wheelchair while the assistive torque can relieve the user's propulsion effort.

Various methods have been investigated for improving the maneuverability and the safety of an advanced wheelchair by utilizing various sensors and actuators[5]. The major research issues on the advanced wheelchairs include: 1) wheelchair dynamics and stability analysis[35,25,32], 2) mechanical system designs, 3) user interface designs (i.e., operation method design), 4) human-interactive control algorithms, and 5) the evaluation of wheelchair performance. In particular, the wheelchair dynamics and stability analysis have been intensively studied in terms of stability in the pitch direction (i.e., on the sagittal plane) since the tip-over of a wheelchair is one of the most dangerous motions that threaten the safety of a user[9,3,17]. The planar dynamics of a wheelchair[11] has been actively investigated from the viewpoint of push-rim kinematics[6], motion of caster wheels[4], and rolling resistance[37].

Diverse research has been done also on the controller design for the advanced wheelchairs, however, most of it deals with fully-powered wheelchairs that is controlled using a joystick[10,33] making them very similar to mobile robots[15,36,13]. On the other hand, the control algorithms for the PAWs where the user's force is involved in the dynamics motion of the wheelchair, should be designed differently from the ones for the fully-powered wheelchair, since the user has direct contact with the push-rim on the PAW as on the manual wheelchair.

Cooper's group suggested a shared control to provide adequate assistance torque sufficient for the PAW focusing on each wheel's assistance[7], Seki developed a fuzzy algorithm which helps user steering ability[31], and we also developed an integrated control algorithm that enhances the wheelchair's safety in three dimensions[27]. Much of the other research on control algorithm using the PAW focuses on development of the interface to ascertain the user's intent. Katsura[19], Chen[30] and our group[28] suggested assisting controllers that do not use any force sensor. They utilized the disturbance observer[34] to estimate the human force, designed controllers using the estimated force, and analyzed the stability and performance of the controllers.

Most of this research discusses how to generate assistive torques to support human, but less discussion has been conducted on the rejection of the disturbance, which gives a significant problem to the PAW on slopes. Since the effect of gravity cannot be removed from the conventional PAW unless the user applies forces[26], the wheelchair is pulled downhill by gravity even though the motors can compensate for it. An appropriate selection of sensors and feedback control design can address this problem. To this end, this chapter introduces a human-friendly motion control which consists of feedback control algorithms to

attenuate the external force while keeping the controllability for the user based on the accurate observation of the operation states of the wheelchair.

In addition to this disturbance attenuation control, the observation of the physical states and environmental condition improves the stability and performance of the human-friendly motion control. In this chapter, the wheel speed (or the longitudinal speed of the center of wheels of the wheelchair), the pitch angle and the external forces including the gravitational force are selected as the necessary operation states for the control of the PAW. A sensor fusion algorithm is introduced to accurately estimate these states, since there is no sensing method that directly measures such information, which is the other topic of this chapter. As a power-assisted wheelchair, YAMAHA JWII shown in Fig. 1 is utilized for the analysis and the design of human-friendly motion control in this chapter.

Fig. 1. Power-assisted wheelchair used in this research (YAMAHA JW II)

In the following, the overall control scheme and the details of each design will be explained.

2 Human-Friendly Motion Control of Power-Assisted Wheelchair (PAW) System Considering Human Interaction and External Environments

2.1 Experimental Apparatus

Table 1 is the specification of the wheelchair used here. A commercialized pushrim-activated PAW (YAMAHA JWII,[1]) is used in the following experiments. This PAW has two torsion sensors to measure human torques on both wheels and two electric motors to provide assistive torques based on the measured human torques. The assistance from the motors relieves the necessary power[23] to operate the wheelchair[7], but there still are problems that cause difficulty in operating the wheelchair. For example, the PAW does not compensate for gravity, which can accelerate or decelerate the wheelchair on hills against the user's will.

In order to improve the performance and safety of the assistance, multiple sensors are utilized to measure accurate states of the wheelchair; an encoder is installed in each of the back wheels, and a gyroscope and a triaxial accelerometer are installed on the PAW body. Figure 2 shows the configuration of these motors and sensors.

Table 1. Specification of a PAW used in this chapter

Wheelchair power unit	YAMAHA JW II
Motor	DC motor (24V 90W × 2)
Encoder resolution	960 ppr
Wheel radius	0.3 m
Weight	40 kg (including motors and controllers)
Track / Wheelbase	0.47 m / 0.4 m

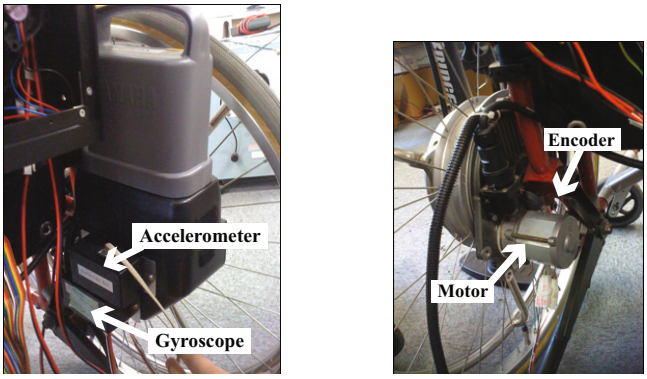

Fig. 2. Motor and sensors installed in the wheelchair

2.2 Overall Scheme of Human-Friendly Motion Control for Power-Assisted Wheelchair

Figure 3 shows the whole schematic of the wheelchair observation and control system that will be introduced here. The controller consists of three sections: assistive control algorithm, operation state observer and operation condition detection. This chapter explains the assistive control algorithm and operation state observer, and the readers are referred to our previous work[26,27] for further information of this schematic.

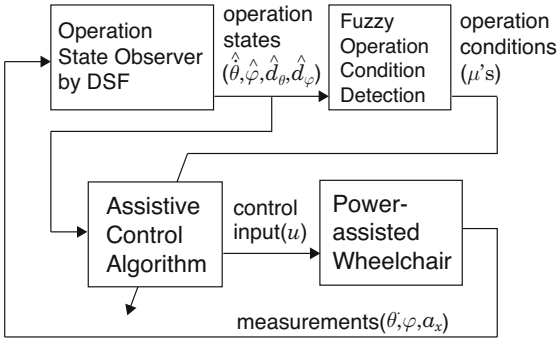

Fig. 3. Overall scheme of human-friendly motion control for a PAW

The operation state observer in Fig. 3 observes the accurate physical quantities that are fed back to the assistive controller and also sent to the operation condition detection algorithm. Based on the observed operation states, the operation detection algorithm calculates the likelihood of each condition using the fuzzy algorithm, which can be used for the control of a PAW.

The operation state observer estimates the important physical quantities (i.e., the wheel speed ($\hat{\dot{\theta}}$), the pitch angle ($\hat{\varphi}$) and the external forces ($\hat{d}_\theta, \hat{d}_\varphi$) which are described in Fig. 5) from the redundant measurements by encoders (θ), a gyroscope ($\dot{\varphi}$), and an accelerometer (a_x). In addition to this operation state observation, an operation condition detection algorithm based on fuzzy logic can be designed to detect the environmental states of the overall wheelchair system. For example, in the cases of uphill and wheelie, the wheel speed and the pitch angle are similar, while their environmental states are completely different. The operation state observer and operation condition detection algorithm can distinguish these dynamic difference caused by environmental differences calculating the likelihoods (μ's) of four physical conditions (i.e., level ground, uphill, downhill and wheelie which are described in Fig. 4) in real-time[29].

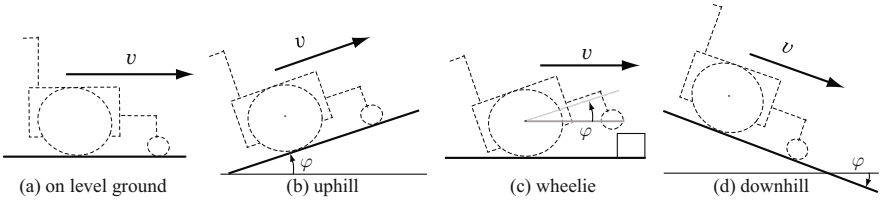

Fig. 4. Important operating conditions of wheelchair

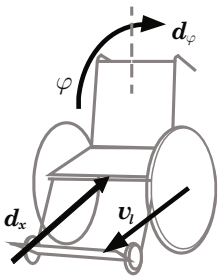

Fig. 5. Operation states of the wheelchair

Then the assistive control algorithm provides the required control input u to the PAW based on the estimated operation states $(\hat{\dot{\theta}}, \hat{\varphi}, \hat{d}_\theta, \hat{d}_\varphi)$ and condition (μ's). The control input u generated by the assistive control algorithm includes the assistive torques which are associated with the applied human torque and resistive torques which suppress the effect of the external force according to the direction of the wheelchair motion.

2.3 Organization of the Chapter

This chapter is organized as follows. In Sec. 3, a dynamic model of the wheelchair is derived in order to be utilized in the observer design. Based on the equation of motion, the operation state observer is designed for a PAW, and its performance is verified by experiments in Sec's 4 and 5. In Sec. 6, the modes of two dimensional motion of a wheelchair defined based on the direction of the motions, and a dynamic model of the wheelchair is derived based on the modes. Using this model, control algorithms to attenuate the external force on a wheelchair are designed in Sec. 7 and verified through experimental results in Sec. 8.

3 Dynamic Modeling of Wheelchair for Dynamic Sensor Fusion

A sensor fusion method named as dynamic sensor fusion (DSF) is designed here as a method to design the operation state observer necessary to estimate operation state and operation condition. Since the DSF utilizes the dynamics of a PAW taking the external forces into consideration, a dynamic model of a PAW is derived here.

3.1 Definition and Dynamics of Operation States of a PAW

Although a PAW has four wheels and exhibits three-dimensional motion, this chapter focuses mainly on its sagittal plane motions, as shown in Figs 4 and 5.

The sagittal motion of the wheelchair can be modeled as a wheeled inverted pendulum. Figure 6 shows the analogy between a wheelchair and an inverted pendulum, where θ is the wheel angle, and ω is the wheel speed ($\omega = \dot{\theta}$). When the front caster wheels of the wheelchair are lifted, the dynamics of the wheelchair becomes that of an inverted pendulum[33]. Moreover, in a normal operation condition, a user puts the center of pressure at the position of the large rear wheels. Considering this aspect, the equations of motion are derived in terms of θ, φ as an inverted pendulum for the sake of simplicity.

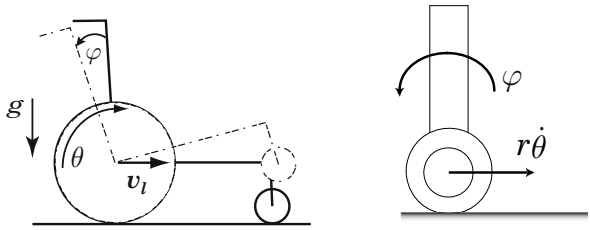

(a) a wheelchair with pitch motion (b) an inverted pendulum

Fig. 6. Analogy between a wheelchair and an inverted pendulum

Equations (1) and (2) are the equations of motion of the wheelchair, where τ is the torque input to the rear wheel. It should be noticed that the motion of the wheelchair user on the PAW is not taken into consideration, and the user's body is assumed to be fixed to the wheelchair frame.

$$(m+M)\, r^2\ddot{\theta} - mlr\ddot{\varphi}\cos\varphi + mlr\dot{\varphi}^2\sin\varphi + B_w\dot{\theta} = \tau \tag{1}$$

$$ml^2\ddot{\varphi} - mlr\ddot{\theta}\cos\varphi - mgl\sin\varphi + B_p\dot{\varphi} = 0 \tag{2}$$

Figure 7 illustrates all the parameters used in this model: l is the distance from the wheel axis to the center of mass of the pendulum, m is the mass of the pendulum, M is the mass of the wheel, J_M is the inertia of the wheel, and r is the radius of the wheel. B_w and B_p are the dampings for the two states.

Since the wheel speed $\dot{\theta}$ is slow in typical operation conditions for user's safety, it is reasonable to assume that there is no slip between the wheel and the ground. With this assumption, the longitudinal velocity v_l is equivalent to $r\dot{\theta}$. In the rest of the chapter, $\dot{\theta}$ is considered as the required operation state instead of v_l, since it is (inaccurately, but) directly measurable by sensors (e.g., encoders). The external torque d_θ that affects the motion of θ is also regarded as the external force d_x in the longitudinal direction.

3.2 Simplified Dynamics of Wheelchair with External Force Inputs

The dynamics in (1) and (2) can be linearized as (3) and (4) by the small angle approximation; the pitch angle φ can be assumed to be small, and the pitch angle velocity $\dot{\varphi}$ is small enough, i.e.,

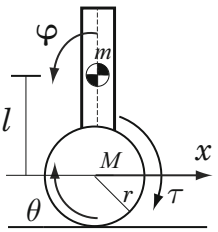

Fig. 7. Variables of an inverted pendulum's dynamic model

$$(M+m)\,r^2\ddot{\theta} - mlr\ddot{\varphi} + B_w\dot{\theta} = \tau \tag{3}$$
$$ml^2\ddot{\varphi} - mlr\ddot{\theta} - mgl\varphi + B_p\dot{\varphi} = 0 \tag{4}$$

As stated in Sec. 2.2, the external forces are the important operation states to provide information on the conditions of the PAW, and thus they need to be included in the dynamics. Equations (5) and (6) are the final dynamic model of the wheelchair that is to be utilized in the operation state observer design.

$$(M+m)\,r^2\ddot{\theta} - mlr\ddot{\varphi} + B_w\dot{\theta} = \tau + d_\theta \tag{5}$$
$$ml^2\ddot{\varphi} - mlr\ddot{\theta} + B_p\dot{\varphi} - mgl\varphi = d_\varphi, \tag{6}$$

where d_θ is the external force in the wheel motion and d_φ is the external force in the pitch direction.

The dynamics may be subjected to modeling errors; however, the affluent sensor measurement allows for this simplification and makes the observation precise and robust enough, which will be shown in the following experiments.

4 Design of Operation State Observer by Dynamic Sensor Fusion

4.1 Definition of States and Description of Dynamics

By decoupling the inertias in (5) and (6), the dynamics of the wheelchair can be re-organized as

$$\ddot{\theta} = \frac{ml^2(-B_w\dot{\theta} + d_\theta + \tau) + mlr(-B_p\dot{\varphi} + mgl\varphi + d_\varphi)}{Mml^2r^2} \tag{7}$$
$$\ddot{\varphi} = \frac{mlr(-B_w\dot{\theta} + d_\theta + \tau) + (M+m)r^2(-B_p\dot{\varphi} + mgl\varphi + d_\varphi)}{Mml^2r^2} \tag{8}$$

With this dynamics, the whole states and their dynamics can be described in the state-space form, i.e.,

$$\begin{aligned}\dot{\boldsymbol{x}} &= \begin{bmatrix} -\frac{B_w}{Mr^2} & 0 & -\frac{B_p}{Mlr} & \frac{mg}{Mr} & \frac{1}{Mr^2} & \frac{1}{Mlr} \\ 1 & 0 & 0 & 0 & 0 & 0 \\ -\frac{B_w}{Mlr} & 0 & -\frac{(M+m)B_p}{Mml^2} & \frac{(M+m)g}{Ml} & \frac{1}{Mlr} & \frac{M+m}{Mml^2} \\ 0 & 0 & 1 & 0 & 0 & 0 \\ 0 & 0 & 0 & 0 & 0 & 0 \\ 0 & 0 & 0 & 0 & 0 & 0 \end{bmatrix} \boldsymbol{x} + \begin{bmatrix} \frac{1}{Mr^2} \\ 0 \\ \frac{1}{Mlr} \\ 0 \\ 0 \\ 0 \end{bmatrix} \tau \\ &=: \mathbf{A}\boldsymbol{x} + \mathbf{B}\tau, \end{aligned} \tag{9}$$

where $\boldsymbol{x}$ is the system states to be observed, i.e.

$$\boldsymbol{x} = \begin{bmatrix} \dot{\theta} & \theta & \dot{\varphi} & \varphi & d_\theta & d_\varphi \end{bmatrix}^T \in \mathcal{R}^6, \tag{10}$$

τ is the torque input to the wheels that is a sum of human torques and the assistive torques by electric motors. This value can be measured using torque sensors or estimated using a current sensors or estimation algorithm such as disturbance observer. The unknown external forces d_θ and d_φ are assumed to be constant and modeled as a first-order dynamics $\dot{d}_\theta = 0$ and $\dot{d}_\varphi = 0$.

4.2 Kinematics of Sensor Output

The most important point of the operation state observation is that sensors measure the required physical quantities in a redundant manner; one physical quantity is measured by multiple sensors. For example, the wheel speed $\dot{\theta}$ is measured by an encoder and an accelerometer, and the pitch angle is measured by a gyroscope and an accelerometer. The output equations of three sensors described in Table 2 explain this point.

Table 2. Output equation of each sensor

Encoder	$y_{\text{enc}} = \theta$
Gyroscope	$y_{\text{gyro}} = \dot{\varphi}$
Accelerometer	$y_{\text{acc}_x} = a_x = r\ddot{\theta}\cos\varphi + g\sin\varphi$
	$y_{\text{acc}_y} = a_y = g\cos\varphi - r\theta\sin\varphi$

The use of the accelerometer is the key in the operation state observation. Figure 8 shows the orientations of the accelerometer axes. The longitudinal acceleration measurement, a_x, contains information related to the longitudinal wheelchair velocity (i.e., the derivative of v_l) and the pitch angle coupled with the gravity (i.e., $g\sin\varphi$).

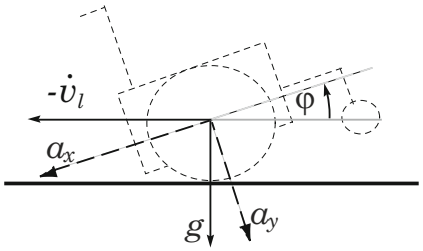

Fig. 8. Accelerations measured by accelerometer

The output equations in Table 2 can be linearized as (11) under the same small angle approximation.

$$\begin{aligned}\boldsymbol{y} &= \begin{bmatrix} 0 & 0 & 1 & 0 & 0 & 0 \\ 0 & 1 & 0 & 0 & 0 & 0 \\ -\frac{B_w}{Mr} & 0 & -\frac{B_p}{Ml}\left(\frac{m}{M}+1\right)g & \frac{1}{Mr} & \frac{1}{Ml} \end{bmatrix} \boldsymbol{x} + \begin{bmatrix} 0 \\ 0 \\ \frac{1}{Mr} \end{bmatrix} \tau \\ &=: \mathbf{C}\boldsymbol{x} + \mathbf{D}\tau, \end{aligned} \tag{11}$$

where $\boldsymbol{y} = \begin{bmatrix} \dot{\varphi} & \theta & a_x \end{bmatrix}^T \in \mathcal{R}^3$ is the output vector.

4.3 Optimal Observer Gain Design Using Least Square Gaussian Design

Since the proposed state observer is to be implemented in a microprocessor, the dynamics in (9) and (11) are discretized, and the observer is designed in the discrete-time domain as

$$\hat{\boldsymbol{x}}[k+1] = \mathbf{A}_d\hat{\boldsymbol{x}}[k] + \mathbf{B}_d\tau[k] + \mathbf{L}\left(\boldsymbol{y}[k] - \mathbf{C}\hat{\boldsymbol{x}}[k] - \mathbf{D}\tau[k]\right), \tag{12}$$

where k is each sampling instance, and $\mathbf{A}_d$ and $\mathbf{B}_d$ are system matrices describing the discretized wheelchair dynamics[24]. The sampling period is set to 1ms here.

The gain $\mathbf{L}$ can be designed in various ways such as the Luenberger method and the steady-state Kalman filter. The steady-state Kalman filter method[14] is adopted here, since it can utilize the sensor and dynamics characteristics by specifying their covariance matrices.

The noise covariance parameters for the determination of the observer gain are set as below.

$$\mathbf{Q}_x = \mathrm{diag}\left(Q_{\dot{\theta}}, Q_{\theta}, Q_{\dot{\varphi}}, Q_{\varphi}, Q_{d_\theta}, Q_{d_\varphi}\right) \tag{13}$$

$$\mathbf{R}_y = \mathrm{diag}\left(R_{\mathrm{gyro}}, R_{\mathrm{enc}}, R_{\mathrm{acc}}\right) \tag{14}$$

Notice that the external forces are included as the dynamic states, which tells that the Kalman filter designed in this way is different from the conventional kinematic sensor fusion; it is a dynamic sensor fusion which utilizes the dynamics of a wheelchair considering the external forces.

5 Experimental Verification of the Operation State Observer

Experiments were carried out to verify the effectiveness and the advantages of the operation state observer design; the operation state observer is verified on several conditions and compared with the conventional measurements. By this comparison, the advantage of this kind of operation state observer is revealed.

A user with the bodyweight of 65kg participated in the experiments. Parameters used for the observer were M = 30kg, B_w =3.33 Nms, m = 45kg, B_p =3.125Nms, r = 0.3m, and l = 0.5m. The noise/error covariance matrix was set as $\left(Q_{\dot{\theta}}, Q_{\theta}, Q_{\dot{\varphi}}, Q_{\varphi}, Q_{d_\theta}, Q_{d_\varphi}\right)$ = (0.1,0.1,0.0001,0.001,100,10), and $\left(R_{\text{gyro}}, R_{\text{enc}}, R_{\text{acc}}\right)$ = (0.1,0.1,10000).

5.1 Comparison with Conventional Measurements

First, an experiment was conducted on a level ground. Figure 9 shows the observation of the wheel speed $\dot{\theta} = \omega$, where the output of the operation state observer is compared with the differentiation of the encoder output with a low-pass filter of the 15 rad/s cut-off frequency. The dotted line is the observation through the operation state observer, while the solid line is the encoder measurement. They are very close to each other as shown in the figure.

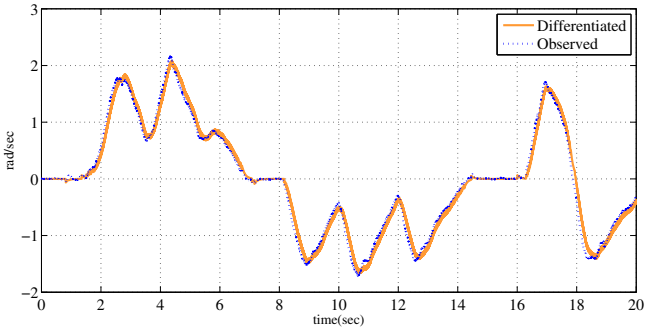

Fig. 9. Comparison of observation with conventional measurements - Angular velocity $\hat{\dot{\theta}}$ on level ground

Figure 10 is a zoomed-in plot of Fig. 9, where two differentiated encoder signals with different cut-off frequencies of the low-pass filter are shown for better comparison. The operation state observer output (i.e., the black line) is smoother than the differentiated measurement with high cut-off frequency filtering (i.e. the thin dotted gray line) and faster than the differentiated measurement with low cut-off frequency filtering (i.e., the thick dashed gray line). This smooth, accurate, and fast observation of velocity, in particular at low velocities, is important

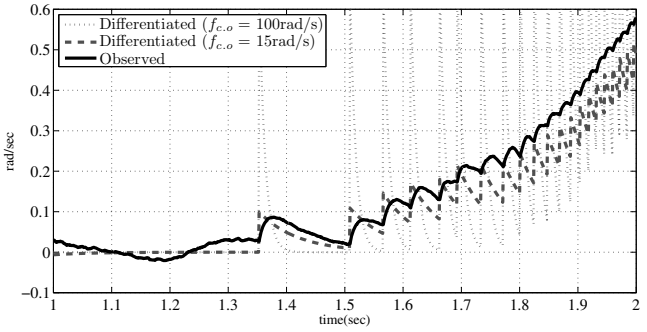

Fig. 10. Fast and correct estimation of velocity by the operation state observer

in the control of a PAW, because a PAW usually moves at slow velocities and frequently decelerates to stop. Moreover, if the velocity measurement is noisy, the control performance is deteriorated because the design of the feedback gains are restricted by the noise. Notice that by using the operation state observer, even low-resolution encoders can provide accurate estimate of the driving velocity, which gives economical advantages.

This velocity observation performance is verified in several different situations such as driving on level ground, on an uphill, and during a wheelie. The result in Fig. 11 verifies that the operation state observer can provide more precise and faster velocity observation in any situation.

Pitch angle observation experiment was conducted on an uphill. The wheelchair started on level ground, and went up a hill and stopped at the next plateau. Figure 12 compares the observation result with the measurement - the integration of the gyro output. The dotted line is the operation state observer output and the solid line represents the integration. The results are very close for most of the time. However, the estimation by integrating the gyroscope measurement is subjected to a drift caused by the sensor noise, while the observer output is free from the drift problem. In order to highlight the robustness of the operation state observer, an artificial noise was added to the gyroscope measurement deliberately at 10 seconds in each experiment, as shown in Fig. 13. Figure 14 shows the result, where the dotted lines represent observation of φ, and the solid lines represent integration of the gyroscope. In the conventional method, the drift caused by the integration of the sensor noise led to a large estimation error in the pitch angle that was not recovered. On the other hand, the operation state observer recovered from the error and converged to the original value. All the three experiments showed the robustness of the operation state observer to the noise in the measurements in various practical conditions. The operation states estimated accurately by the proposed observer will be utilized as the feedback information for control in the following sections.

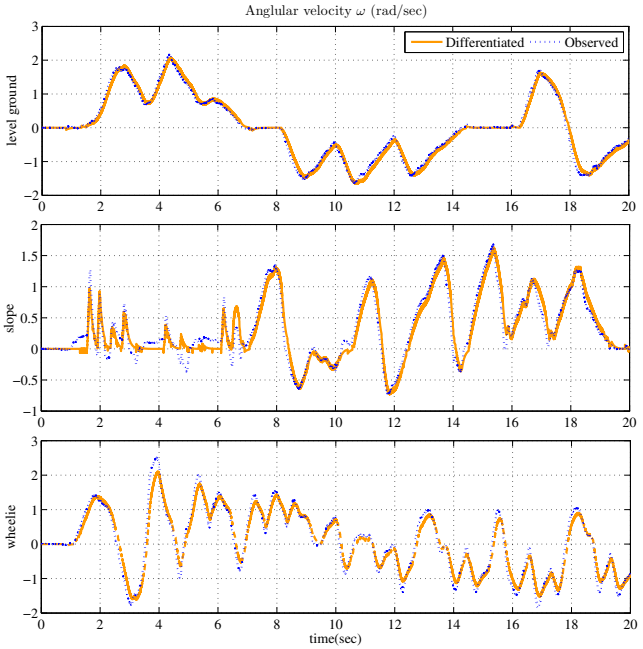

Fig. 11. Angular velocity estimation ($\hat{\omega}$) in various environments

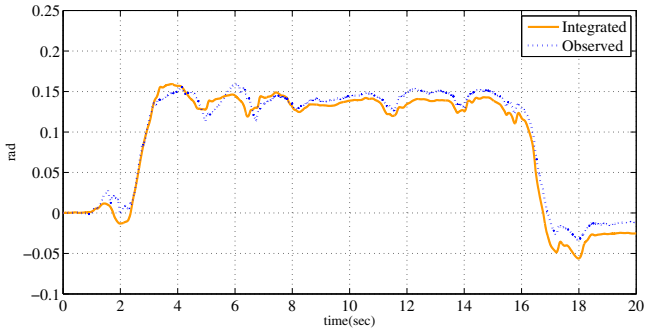

Fig. 12. Comparison of observation with conventional measurements - Pitch angle $\hat{\varphi}$ on slope

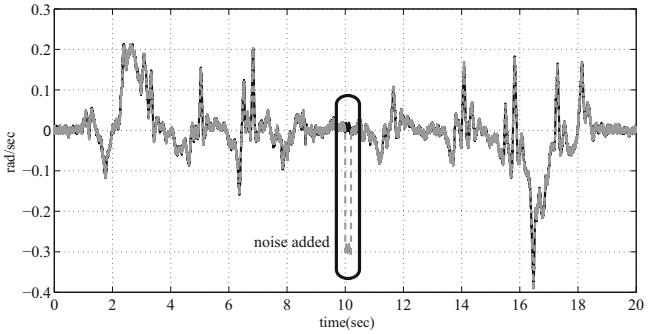

Fig. 13. Noise added to the measurement of the gyroscope

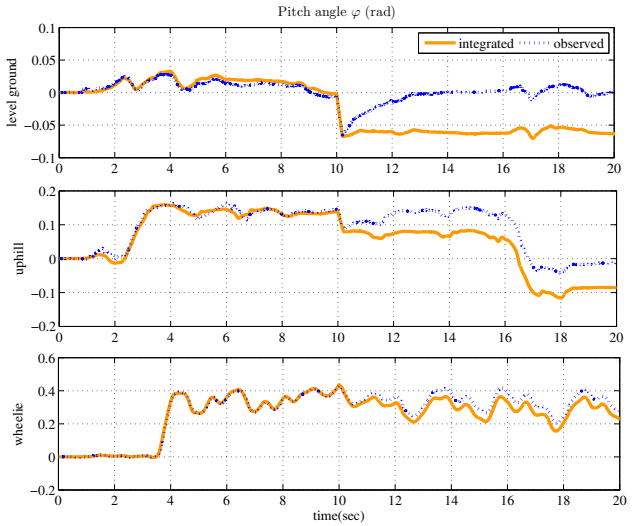

Fig. 14. Pitch angle estimation ($\hat{\varphi}$) with additional noises in various environments

6 Decomposition of Motion Modes and Two Dimensional Dynamic Model of Wheelchair

6.1 Description of Two Dimensional Wheelchair Motion

Since a wheelchair has two wheels to be controlled, two controllers for each wheel are required to be designed. Even though the controllers can be designed to control each motor individually[27] from the perspective of the actuators, it is better to design the controllers from the perspective of the whole motion dynamics of the wheelchair.

This difference in the design perspectives can be better explained when it comes to the dynamic model which the controller design takes into consideration; the controller design for two independent wheels needs to consider the dynamics

of each wheel. This may not be appropriate to describe the whole dynamics of the wheelchair since two wheels are constrained aligned in a wheelchair, and therefore their dynamics are not independent. On the other hand, the control can be designed taking into consideration the dynamics of the whole wheelchair, which describes the longitudinal motion and rotational motion of the wheelchair. For this reason, the controller design introduced here utilizes the dynamics of the whole wheelchair motion.

The whole dynamics of the two dimensional motion of the wheelchair can be described using the common and difference modes of the two wheels' motion[20]. The common mode of the two wheels' motion is associated with the longitudinal motion of the wheelchair, while the difference mode generates the rotation of the wheelchair in the yaw direction. Figure 15 describes this motion decomposition.

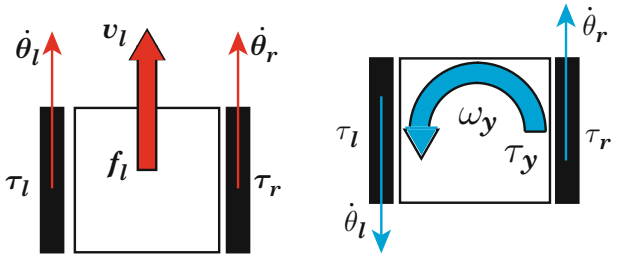

(a) Longitudinal motion (b) Rotational motion

Fig. 15. Decomposition of wheelchair motion

Equations (15) and (16) describe the relationship; $\dot{\theta}_{l,r}$ are the angular velocity, and $\tau_{l,r}$ are the torques of the left and right wheel, v_l is the longitudinal velocity, ω_y is the yaw rate, f_l is the longitudinal driving force, τ_y is the yawing torque, W is the track of the wheelchair. R is the radius of the wheel and the superscript $-T$ represents the inverse of the transpose.

$$\begin{pmatrix} v_l \\ \omega_y \end{pmatrix} = R \begin{pmatrix} \frac{1}{2} & \frac{1}{2} \\ \frac{1}{W} & -\frac{1}{W} \end{pmatrix} \begin{pmatrix} \dot{\theta}_r \\ \dot{\theta}_l \end{pmatrix} = \boldsymbol{J}_m \begin{pmatrix} \dot{\theta}_r \\ \dot{\theta}_l \end{pmatrix} \tag{15}$$

$$\begin{pmatrix} f_l \\ \tau_y \end{pmatrix} = \frac{1}{R} \begin{pmatrix} 1 & 1 \\ \frac{W}{2} & -\frac{W}{2} \end{pmatrix} \begin{pmatrix} \tau_r \\ \tau_l \end{pmatrix} = \boldsymbol{J}_m^{-T} \begin{pmatrix} \tau_r \\ \tau_l \end{pmatrix} \tag{16}$$

6.2 Dynamics Identification of Wheelchair Based on Decomposed Motion

The dynamics of a wheelchair is identified in this section based on the modes introduced in the previous section. The detailed specifications of the wheelchair used here are given in Table 1.

Four types of sinusoidal input (0.4Hz, 0.5Hz, 0.8Hz, 1Hz) were given as input torque $\tau_{l,r}$ and the velocity ($\dot{\theta}_{l,r}$) were measured based on the modes. Although it

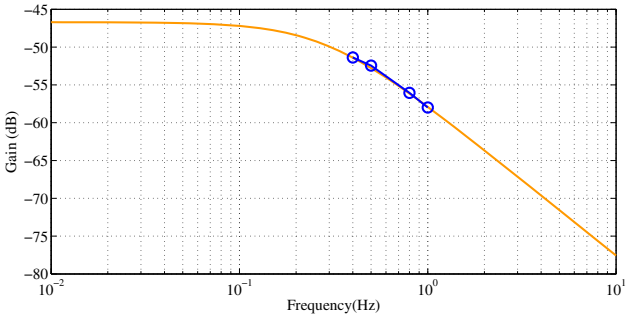

Fig. 16. Frequency characteristic of longitudinal dynamics

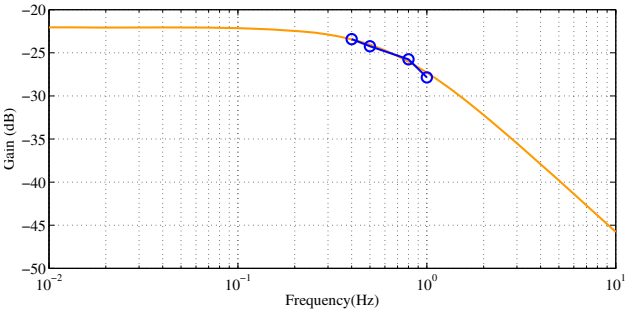

Fig. 17. Frequency characteristic of lateral dynamics

is better to use as many and wide frequencies as possible for the identification, it is practically impossible to use too high frequencies or too low frequencies in the actual experiments; the effect of friction is very obvious in the low frequencies, and the high frequency torque input, with the magnitude high enough to generate the motion, can break down the experimental apparatus. The chosen frequency bandwidth here is the bandwidth of the human operation which is said to be less than several Hz.

To measure the longitudinal motion dynamics, the same torques were given to two wheels to generate only f_l, and the longitudinal velocity v_l in (15) was measured. Since the experiments are to derive the dynamic model of the wheelchair, any external factors should be excluded, so the experiments were conducted on a level ground in the lab. Figure 16 is the frequency characteristic of the dynamic model from the velocity v_l to the input f_l as defined in (15) and (16). The circles in the figure are the responses measured by the experiments. This frequency characteristic can be modeled as (17) where the cut-off frequency is found to be around 0.3Hz.

$$P_{\text{longi}}(s) = \frac{1}{120.2s + 216.4} = \frac{1}{M_n s + D_n}, \tag{17}$$

where M_n and D_n are the estimated mass and damping of the PAW with a user.

Another experiment was conducted without any human user on the wheelchair, and the dynamics is modeled from the experimental results as

$$P_{\text{longi}}^{noH}(s) = \frac{1}{49.09s + 196.4} = \frac{1}{M_n^{noH}s + D_n^{noH}}, \tag{18}$$

where M_n^{noH} and D_n^{noH} are the estimated mass and damping of the PAW by itself. The difference between two masses (M_n and M_n^{noH}) is 120.2 - 49.09 $\simeq$ 70(kg), which is the mass of the user.

The rotational dynamics is derived from the experiments, and Fig. 17 is the derived frequency characteristic where the four circles are the measurements from the experiment. The derived linear dynamic model from τ_y to ω_y is

$$P_{\text{rot}}(s) = \frac{1}{3.088s + 12.66} = \frac{1}{J_n s + B_n}, \tag{19}$$

where the cut-off frequency is around 0.65Hz. Also the rotational dynamics without a user is modeled as

$$P_{\text{rot}}(s) = \frac{1}{1.263s + 6.315} = \frac{1}{J_n^{noH}s + B_n^{noH}}. \tag{20}$$

Even though it is true that the models derived here are approximated models and subject to change by various factors such as friction and road conditions, the derived model can give some hints to model setting for the controller design: the user's weight can be reflected in the nominal values of M_n and J_n, and the frequency bandwidth of the wheelchair is up to several Hz.

The experiments also show that the longitudinal dynamics and rotational dynamics are different in the wheelchair motion, i.e., they have different frequency characteristics such as the response time and the magnitude. The two dynamics are not totally independent and the coupling is variable based on the location of the center of mass and the condition of the front casters. These details will not be discussed in this chapter since the feedback control design can cope with this variation and unmodeled dynamics.

7 Design of Disturbance Attenuation Control for Wheelchair Based on Motion Decomposition

7.1 Two Dimensional Control Design Based on Motion Modes

In this section, a feedback controller for a wheelchair that suppresses external force such as gravity is explained. The disturbance rejection should be designed differently based on the mode or direction of wheelchair. For longitudinal motion, humans are familiar with velocity control [18], i.e., the wheelchair user will generally want to control velocity rather than be concerned with position error, whereas humans are sensitive to angle error for rotational motion, i.e., the user will want to control the heading angle so that they move in the desired direction.

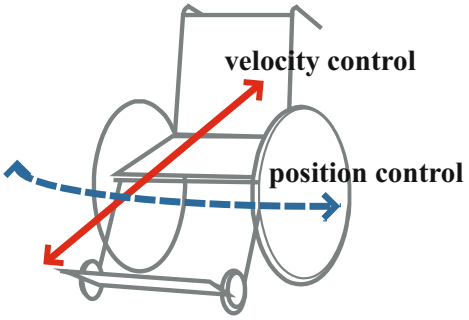

Fig. 18. Necessary control in each direction

Drawing conclusions from the different dynamics of the wheelchair motion and the different sensitivity of the users with respect to the modes, the controller for the wheelchair should also be designed based on the modes as described in Fig. 18. To this end, the following issues are to be addressed.

1. The measurement (encoder outputs) and control inputs (torque inputs) are given in terms of each wheel.
2. The controller should be designed based on the dynamics of the whole motion of the wheelchair.
3. Transformations are necessary between the controllers and their interface with the wheelchair measurements and torque inputs.

The control design illustrated in Fig. 19 is the solution to these issues that will be explained here. Equations (15) and (16) are used for the transformation of the measurements and control inputs. The control design consists of three sections: power-assistive control, longitudinal disturbance attenuation control, and the rotational disturbance rejection control.

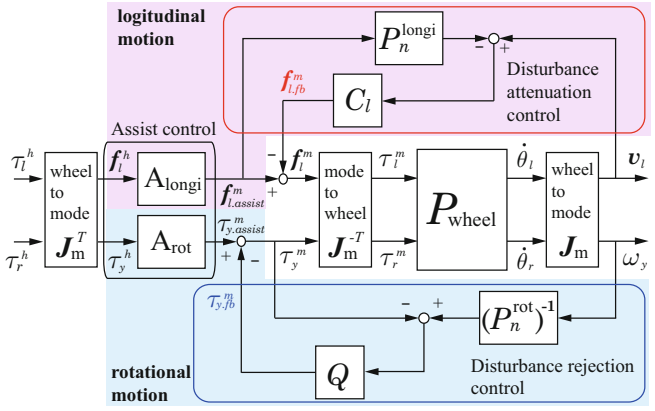

Fig. 19. Overall control design for safe disturbance attenuation of a PAW

7.2 Power-Assistive Control Based on Motion Modes

The blocks A_{longi} and A_{rot} in Fig. 19 represent power-assistive controllers that amplify the measured human torque (τ_l^h, τ_r^h) applied to the left and the right wheels. The amplification process is designed as (21).

$$A_{[longi,rot]} = \frac{\alpha_{[longi,rot]}}{\tau_{[longi,rot]}s + 1}, \tag{21}$$

where $\alpha_{[longi,rot]}$ is the assisting ratio and $\tau_{[longi,rot]}$ is the time constant of first order delay.

By introducing the idea of mode decomposition, power-assistive control can also be designed independently based on the mode; the assist ratio and the time constant can be set independently for each of the modes. The details of this motion mode-based power-assistive control is discussed in [21].

This power-assistive controller requires the precise information on the operation condition of the wheelchair; the assistive torque should be modified depending on the condition the wheelchair is located. For example, when the wheelchair is on a slope or during a wheelie, the assisting ratio $\alpha_{[longi,rot]}$ should be modified to guarantee the safety of the user[27]. The operation condition detection algorithm[29] in Fig. 3 can be utilized to this end. For the details, readers are referred to our previous works[27,29].

7.3 Longitudinal Disturbance Attenuation Control

The objective of the longitudinal disturbance attenuation control is to attenuate the effect of external disturbances while providing the feeling of natural operation to the user. The strategy employed here is to adopt the dynamics derived in Fig. 16 to generate the velocity reference.

The upper section of the controller in Fig. 19 is the longitudinal disturbance attenuation control, where P_n^{longi} represents a nominal dynamic model of the wheelchair derived in Fig. 16.

When there is no external force and no error between the nominal model P_n^{longi} and the wheelchair dynamics P_{wheel}, the real velocity v_l and the output from P_n^{longi} are equal, and there will be no feedback control input to attenuate the disturbance.

When a longitudinal disturbance is present, a velocity error appears, and then the feedback controller C_l generates the torque to attenuate the effect of the disturbance. C_l controller consists of the usual PD controller.

$$C_l(s) = M_d s + D_d \tag{22}$$

Notice that P_n^{longi} works as a velocity reference generator and this makes the whole longitudinal direction feedback control into a velocity control. The gains M_d and D_d change the dynamics or compliance of the wheelchair against the external disturbance as (23). Experimental results in Sec. 8.1 explain how the gains M_d and D_d attenuate the disturbance.

$$\frac{1}{M_n s + D_n} \rightarrow \frac{1}{(M_n + M_d)\, s + D_n + D_d} \tag{23}$$

This change of the dynamics can be derived from Fig. 20 assuming the plant to be the same as the nominal model in the controller. The robustness issue is addressed in our previous work[26].

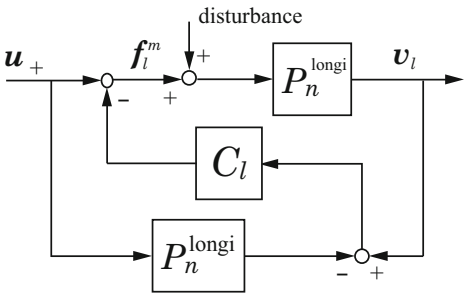

Fig. 20. Dynamics modification by the feedback control of $C_l(s)$

The performance of disturbance rejection of this control is less strong than the disturbance observer or PI controller. Strong disturbance rejection that makes the wheelchair stop on a slope can cause output torque saturation which is dangerous for the users. The disturbance attenuation in (23) which does not make the wheelchair stop on a slope, can provide natural gravity compensation and is less subject to the output torque saturation.

7.4 Rotational Disturbance Rejection Control

As explained in Sec. 7.1, the rotational motion requires position control to keep the heading angle. To apply a strategy similar to the previous longitudinal control for controlling angular position, the dynamic model for rotational motion that will work as a reference generator requires an integrator as described in (24)

$$P_n^{rot.to.angle} = P_n^{rot} \frac{1}{s} = \frac{1}{J_n s + B_n} \frac{1}{s} \tag{24}$$

This integrator in the model can cause integrator windup which is dangerous in wheelchair operation; when there is any obstacle to the rotational motion of the wheelchair and the user continues to apply rotational torque, the reference generated from the dynamic model described as (24) keeps increasing. This causes a large and abrupt motor torque immediately after the obstacle disappears, which exposes the user to danger.

In order to avoid this problem, a disturbance observer[34] can be employed. The disturbance observer is a kind of acceleration controller which eliminates external force other than applied motor torque so that the output is not affected

by the external force[2,22]. Since it does not have any integrator in the loop, the disturbance observer avoids the windup problem while showing similar performance to position control with an integrator. Dynamic model as described in (19) is used for the nominal model P_n^{rot} in Fig. 19.

Q filter in Fig. 19 is the control parameter of the disturbance observer to design the disturbance response; $1 - Q(s)$ is the sensitivity function under the control of the disturbance observer[34]. In this application, the cut-off frequency of the Q filter is set higher than the frequency bandwidth of the P_n^{rot} in (19)[16]. The higher the cut-off frequency of the Q filter is set, the better disturbance rejection performance can be achieved. However, there is a noise problem in the rotational velocity measurement, and it will deteriorate the performance of the disturbance observer when the cut-off frequency of the Q filter is set too high. Here, τ_q in (25) is set to $\frac{1}{2\pi}$ to make the cut-off frequency 1Hz.

$$Q(s) = \frac{1}{\tau_q s + 1} \tag{25}$$

8 Experimental Verification of the Disturbance Attenuation Control Design

8.1 Longitudinal Control Performance with Various Control Parameters

In order to evaluate the longitudinal disturbance attenuation control designed here, several experiments were conducted on a level ground; a pattern of longitudinal disturbance was applied by motors and the velocity of wheels were measured to evaluate the disturbance attenuation performance. M_n and D_n in (17) were used for the nominal model in these experiments.

The applied longitudinal disturbance was a step-wise disturbance with the magnitude of 5.4N that held for 2 seconds and as low-pass-filtered with the 0.5Hz cut-off frequency. Experiments were conducted with several sets of gains M_d and D_d. Figures 21 and 22 show results with constant M_d and varying D_d. The disturbance input is represented as a thick solid line.

Since the disturbance attenuation control is a regulation problem, smaller velocity deviation indicates better control performance. Figure 21 and 22 imply that larger D_d decreases the peak value of deviated wheel velocity more, which can be expected from (23).

Figures 23 and 24 are the results with constant D_d and varying M_d with the same disturbance force. Unlikely in the case of varying D_d, M_d is more related to the rising time; the larger M_d the slower the rising time becomes.

8.2 Incorporation with Power-Assistive Control

In the controller in Fig. 19, the disturbance attenuation control is combined with the power-assistive control, and thus the two controllers should not interfere with

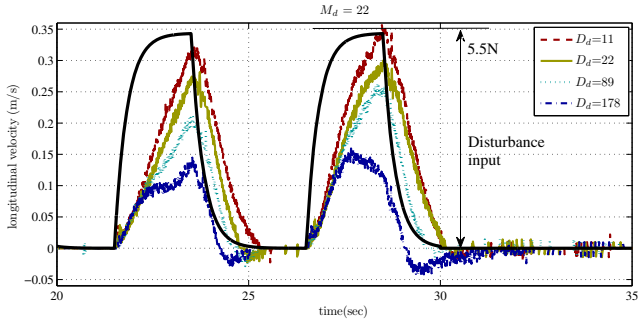

Fig. 21. Longitudinal disturbance responses with varying $D_d(M_d = 22)$

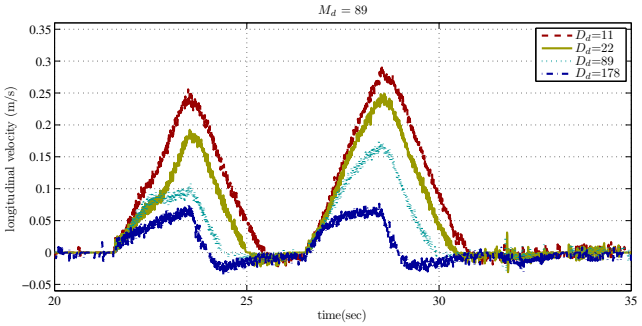

Fig. 22. Longitudinal disturbance responses with varying $D_d(M_d = 89)$

each other in order to provide human-friendly motion control. Experiments were conducted to evaluate this independence.

The amount of torque that the user applies was measured by the torsion sensor installed on two wheels, and the measured torques on the left and right wheels (τ_l^h and τ_r^h) are transformed into f_l^h and τ_y^h as in Fig. 19. Figure 25 shows the longitudinal forces applied to the wheelchair during level ground operation. When the human applied forces f_l^h, the feedback motor torque $f_{l.fb}^m$ and the assisting motor torque $f_{l.assist}^m$ were as illustrated in Fig. 19. The assisting force from the motors amplified the human force while the feedback force to attenuate external disturbances is so small that it can be ignored. This verifies that the longitudinal disturbance attenuation control does not deteriorate the assistance performance.

Figure 26 shows the forces for the 8.6-degree uphill experiment. The feedback force that counteracts the effect of gravity became larger than the assisting force. Figure 27 is a graph of the force on the same slope without feedback control. Notice that in this case without feedback control, the required human force was larger than that was shown in Fig. 26, and more frequent propulsion as necessary to maintain the position of the wheelchair.

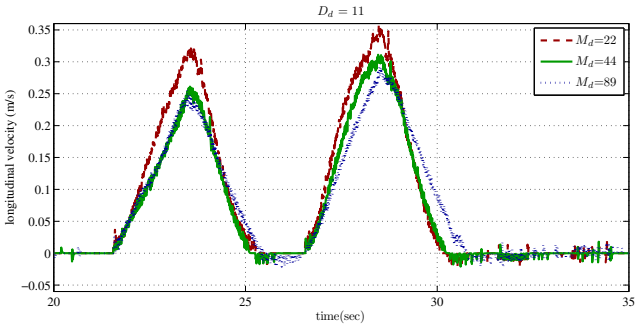

Fig. 23. Longitudinal disturbance responses with varying $M_d (D_d = 11)$

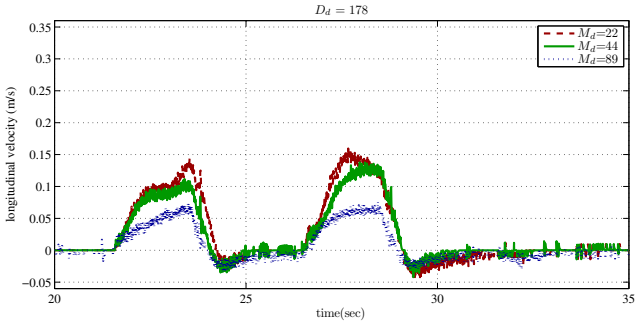

Fig. 24. Longitudinal disturbance responses with varying $M_d (D_d = 178)$

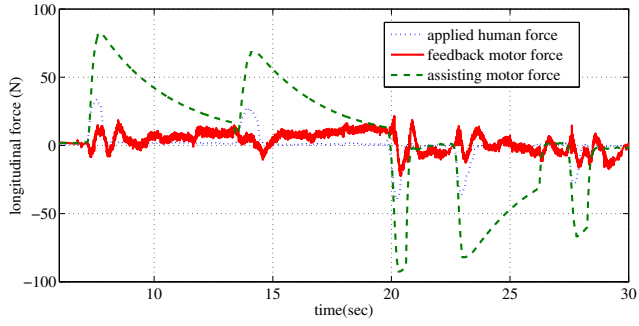

Fig. 25. Forces applied to the wheelchair (level ground)

Figure 28 shows the longitudinal velocities with and without control. One interesting point that can be derived from Fig. 28 is that the disturbance attenuation control improves the smoothness of the velocity rather than the mag-

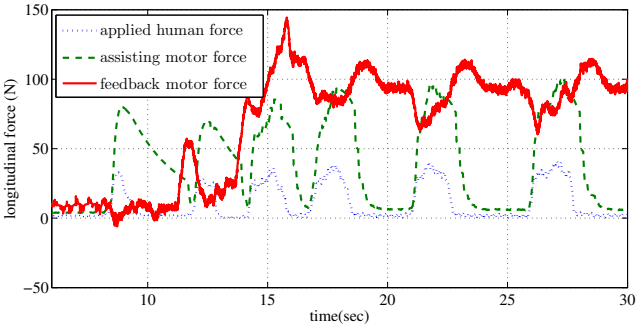

Fig. 26. Forces applied to the wheelchair (uphill with control)

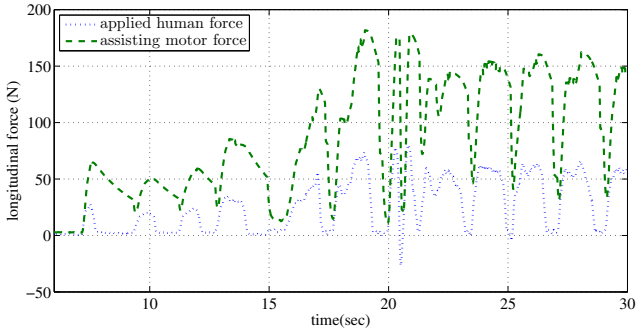

Fig. 27. Forces applied to the wheelchair (uphill w/o control)

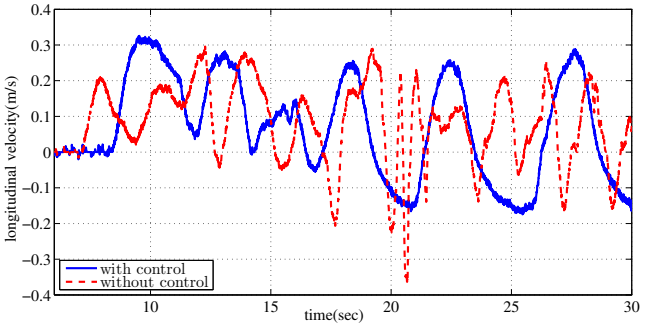

Fig. 28. Longitudinal velocity of the wheelchair on uphill

nitude of the velocity, which implies that the feedback control provides safety and comfort to the user so that the user can operate the wheelchair better while applying a certain pattern of propulsion. Conversely, without the feedback control, the user feels uncomfortable due to abrupt backward acceleration of the

wheelchair, and the user keeps applying force frequently, which is illustrated as the dashed line in Fig. 27.

8.3 Outdoor Experiment on Various Slope Conditions

Three outdoor experiments were conducted to evaluate the effectiveness of the control, i.e., operating the wheelchair along the slope's lateral direction 1) with the disturbance rejection control and 2) without any feedback control, and 3) driving the wheelchair downhill in the diagonal direction with the feedback control.

Figure 29 shows the snapshots of the experimental results, where downhill with the angle of around 3 degrees is to the right. Without control, the wheelchair turns to the downhill due to gravity (Fig. 29(a)). Meanwhile the control rejected the effect of gravity, keeping the heading angle (Fig. 29(b)). When the wheelchair ran down the slope diagonally, the two dimensional feedback controller worked collaboratively; the longitudinal controller reduced acceleration caused by gravity while the rotational controller kept the wheelchair's heading angle (Fig. 29 (c)).

Figure 30 is the experimental results in the case of Fig. 29 (b). Since the wheelchair moved along the slope's lateral direction, there was little longitudinal disturbance, and therefore the feedback motor force to reduce the longitudinal disturbance was very small. On the other hand, due to the large lateral disturbance caused by gravity, the rotational disturbance rejection controller generated large feedback motor torque ($\tau^m_{y.fb}$ in Fig. 19) in the yaw direction (Fig. 30 (b)). Due to this control, the yaw rate was kept small (Fig. 30 (d)) and the heading angle of the wheelchair did not change as in Fig. 29 (b).

Figure 31 is the result in the case of Fig. 29 (c). When the wheelchair went downhill diagonally, gravity worked on the wheelchair in two dimensions. The longitudinal forces in Fig. 31 (a) and the rotational torques in Fig. 31 (b) show the controller suppressed both components' gravity as designed. Compared to Fig. 30 (a), there was constant level of feedback motor force $f^m_{l.fb}$ to suppress the longitudinal gravity. For the rotational torque, there was also constant level of feedback torque $\tau^m_{y.fb}$ in Fig. 31 (b).

The velocities in Fig. 31 (c) and (d) show how the controller worked under the two dimensional disturbance. The longitudinal velocity in this case had a bias velocity compared to the Fig. 30 (c) that was caused by gravity. This shows that the feedback force $f^m_{l.fb}$ in Fig. 31 (a) did not eliminate the effect of gravity. Meanwhile the rotational velocity in (d) reverted to 0 while there was no human torque. This shows that the rotational controller regulated the rotational velocity successfully so that the desired heading angle could be maintained.

9 Conclusions

Human-friendly motion control for a PAW which consists of an operation state observer and a two dimensional disturbance attenuation controller were introduced in this chapter. The operation state observer introduced here was simple

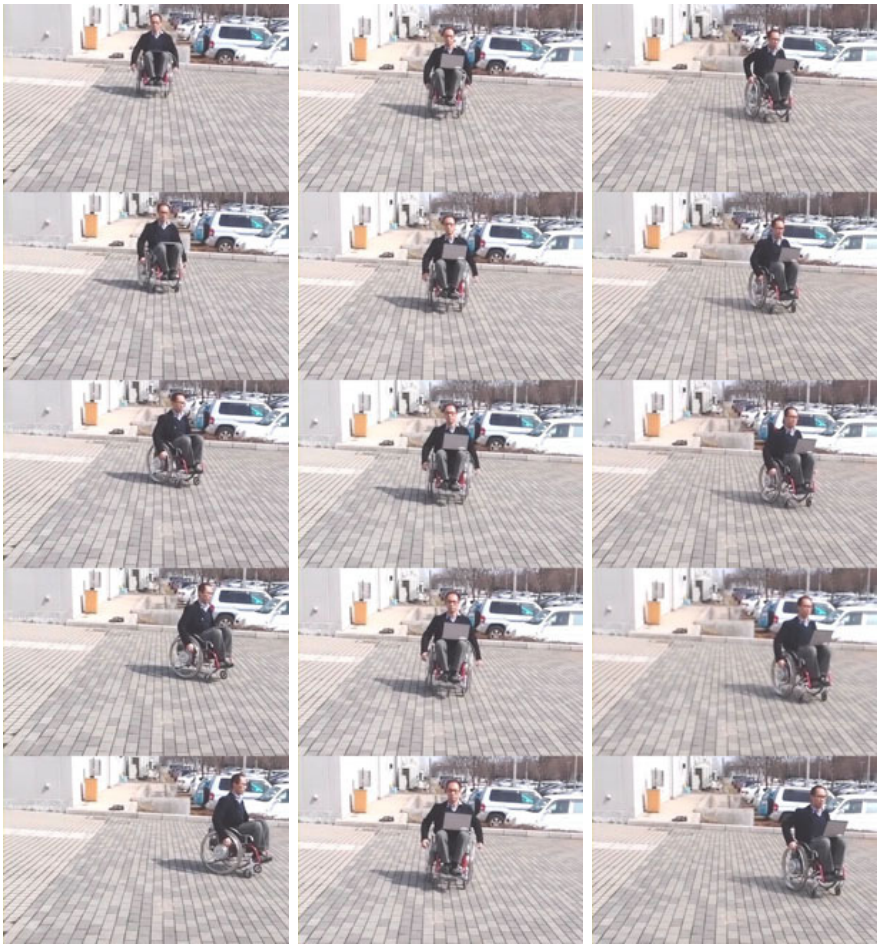

(a) (b) (c)

Fig. 29. Outdoor experiments on a sidehill: (a) without rotational disturbance rejection control (b) with rotational disturbance control (c) driving the wheelchair downhill diagonally with the control

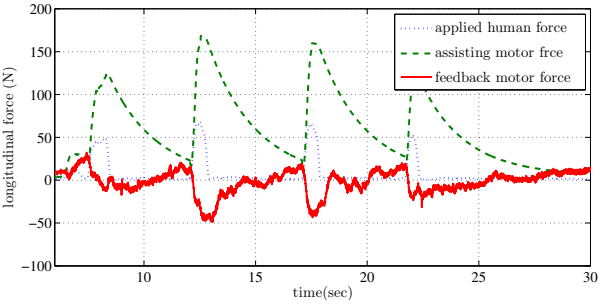

(a) Longitudinal forces

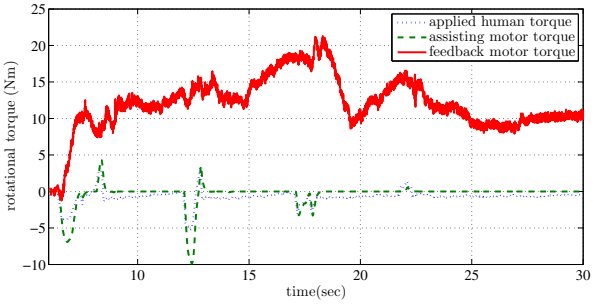

(b) Rotational torques

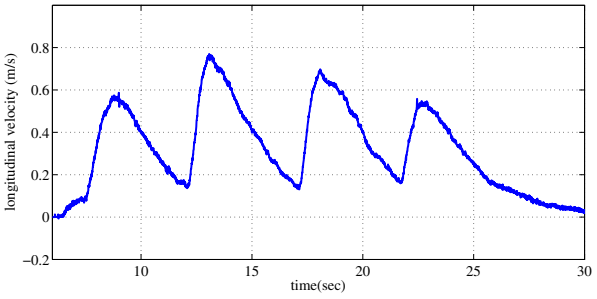

(c) Longitudinal velocity of the wheelchair

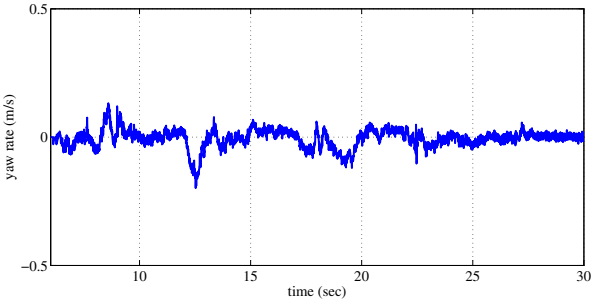

(d) Rotational velocity of the wheelchair

Fig. 30. Experimental results when driving the wheelchair downhill

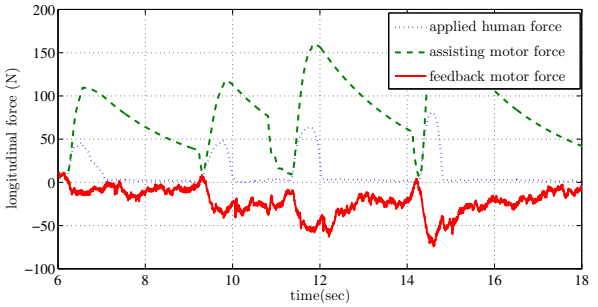

(a) Longitudinal forces

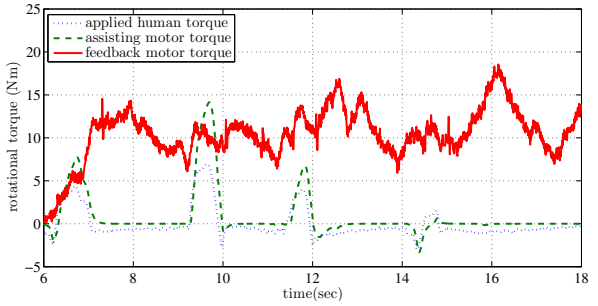

(b) Rotational torques

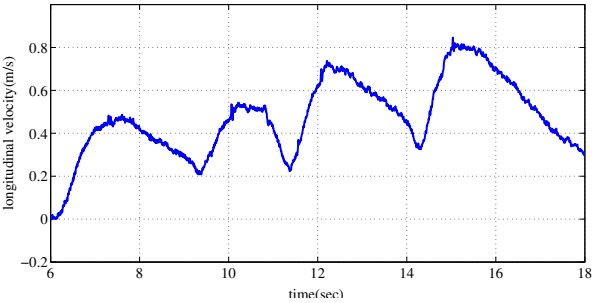

(c) Longitudinal velocity of the wheelchair

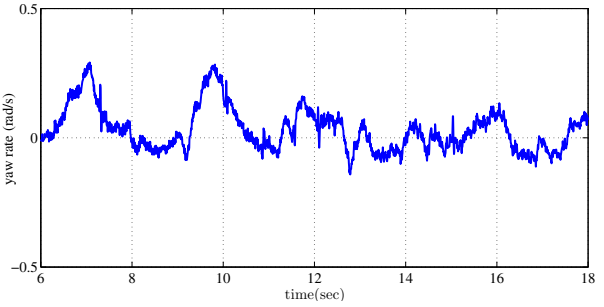

(d) Rotational velocity of the wheelchair

Fig. 31. Experimental results when driving the wheelchair downhill diagonally

enough to be implemented in a microprocessor, while it provided the wheel speed and pitch angle information with high precision. Utilizing the observed operation states, two different types of feedback controllers were designed based on the human's intuition so that the PAW can exhibit familiar motion according to its direction. The experimental results verified that the controller is effective, robust and practical.

The main idea of the human-friendly motion control which was applied for the PAW in this chapter is not restricted only to the PAW but can be extended to other human-machine interface applications.

References

1. YAMAHA JWII (2013), `http://www.yamaha-motor.co.jp/wheelchair/lineup/jw2` (in Japanese)
2. Åkesson, J., Hagander, P.: Integral Action – {A} Disturbance Observer Approach. In: Proceedings of European Control Conference, Cambridge, UK (2003)
3. Ahmad, S., Tokhi, M.O.: Forward and backward motion control of wheelchair on two wheels. In: 2008 3rd IEEE Conference on Industrial Electronics and Applications, pp. 461–466 (June 2008)
4. Chenier, F., Bigras, P., Aissaoui, R.: An Orientation Estimator for the Wheelchair's Caster Wheels. IEEE Transactions on Control Systems Technology 19(6), 1317–1326 (2011)
5. Cooper, R.A.: Intelligent control of power wheelchairs. IEEE Engineering in Medicine and Biology Magazine 14(4), 423–431 (1995)
6. Cooper, R.A., Boninger, M.L., VanSickle, D., Robertson, R., Shimada, S.: Uncertainty analysis for wheelchair propulsion dynamics. IEEE Transactions on Rehabilitation Engineering 5(2), 130–139 (1997)

7. Cooper, R.A., Corfman, T.A., Fitzgerald, S.G., Boninger, M.L., Spaeth, D., Ammer, W., Arva, J.: Performance assessment of a pushrim-activated power-assisted wheelchair control system. IEEE Transactions on Control Systems Technology 10(1), 121–126 (2002)
8. Cooper, R.A., Ding, D., Kwarciak, A.M., Cooper, R., Guo, S., Spaeth, D.M., Zipfel, E., Kelleher, A., Boninger, M.L.: Wheelchair Engineering (2006)
9. Cooper, R.A., Stewart, K.J., VanSickle, D.P.: Evaluation of methods for determining rearward static stability of manual wheelchairs. Journal of Rehabilitation Research and Development 31(2), 144–147 (1994)
10. Ding, D., Cooper, R.A.: Electric powered wheelchairs. IEEE Control Systems Magazine 25(2), 22–34 (2005)
11. Ding, D., Cooper, R.A., Guo, S., Corfman, T.A.: Analysis of Driving Backward in an Electric-Powered Wheelchair. IEEE Transactions on Control Systems Technology 12(6), 934–943 (2004)
12. Doyle, J.C., Francis, B.A., Tannenbaum, A.: Feedback Ccontrol Theory, vol. 134. Macmillan, New York (1992)
13. Fujimoto, Y., Murakami, T.: A realization of wheelchair pushing operation considering high tracking performance and ride quality improvement by mobile manipulator. In: 2010 11th IEEE International Workshop on Advanced Motion Control, pp. 732–737. IEEE (2010)
14. Grewal, M.S., Andrews, A.P.: Kalman filtering: theory and practice using MATLAB, vol. 2. Wiley Online Library (2001)
15. Gulati, S., Kuipers, B.: High performance control for graceful motion of an intelligent wheelchair. In: IEEE International Conference on Robotics and Automation, ICRA 2008, pp. 3932–3938. IEEE (2008)
16. Guvenc, B.A., Guvenc, L., Karaman, S.: Robust Yaw Stability Controller Design and Hardware-in-the-Loop Testing for a Road Vehicle. IEEE Transactions on Vehicular Technology 58(2), 555–571 (2009)
17. Hata, N., Koyasu, Y., Seki, H., Hori, Y.: Backward tumbling control for power-assisted wheelchair based on phase plane analysis. In: Proceedings of the 25th Annual International Conference of the IEEE Engineering in Medicine and Biology Society, vol. 2, pp. 1594–1597 (2003)
18. Hess, R., Modjtahedzadeh, A.: A control theoretic model of driver steering behavior. IEEE Control Systems Magazine 10(5), 3–8 (1990)
19. Katsura, S., Ohnishi, K.: Human Cooperative Wheelchair for Haptic Interaction Based on Dual Compliance Control. IEEE Transactions on Industrial Electronics 51(1), 221–228 (2004)
20. Katsura, S., Ohnishi, K.: Advanced Motion Control for Wheelchair in Unknown Environment. In: 2006 IEEE International Conference on Systems, Man and Cybernetics, pp. 4926–4931. IEEE (October 2006)
21. Kim, K., Nam, K., Oh, S., Fujimoto, H., Hori, Y.: Two-dimensional assist control for power-assisted wheelchair considering straight and rotational motion decomposition. In: IECON 2012 - 38th Annual Conference on IEEE Industrial Electronics Society, pp. 4436–4441 (2012)
22. Lee, H.S.: Robust digital tracking controller for high-speed/high-accuracy positioning systems. Dissertation, Department of Mechanical Engineering, Univ. California, Berkeley (2004)
23. Lombardi Jr., A.D.B., Dedini, F.G.: Biomechanical model for the determination of forces on upper-extremity members during standard wheelchair propulsion. Mathematical and Computer Modelling 49(7-8), 1288–1294 (2009)

24. Luenberger, D.: An introduction to observers. IEEE Transactions on Automatic Control 16(6), 596–602 (1971)
25. Morrow, D., Guo, L., Zhao, K., Su, F., An, K.: A 2-D model of wheelchair propulsion. Disability & Rehabilitation 25(4-5), 192–196 (2003)
26. Oh, S., Hori, Y.: Disturbance Attenuation Control for Power-Assist Wheelchair Operation on Slopes. IEEE Transactions on Control Systems Technology 22(3), 828–837 (2014), doi:10.1109/TCST.2013.226539
27. Oh, S., Hata, N., Hori, Y.: Integrated Motion Control of a Wheelchair in the Longitudinal, Lateral, and Pitch Directions. IEEE Transactions on Industrial Electronics 55(4), 1855–1862 (2008)
28. Oh, S., Hori, Y.: Sensor Free Power Assisting Control Based on Velocity Control and Disturbance Observer. In: Proceedings of the IEEE International Symposium on Industrial Electronics, ISIE 2005, vol. 4, pp. 1709–1714. IEEE (2005)
29. Oh, S., Kong, K., Hori, Y.: Operation state observation and condition recognition for the control of power-assisted wheelchair. Mechatronics 24(8), 1101–1111 (2014)
30. Ou, C., Chen, C., Chen, T.: Modelling and design a power assisted wheelchair used torque observer. In: 2010 International Symposium on Computer Communication Control and Automation (3CA), vol. 2, pp. 63–66. IEEE (2010)
31. Seki, H., Tadakuma, S.: Novel straight and circular road driving control of electric power assisted wheelchair based on fuzzy algorithm. Electrical Engineering in Japan 170(1), 36–44 (2010)
32. Shino, M., Yamakawa, Y., Inoue, T., Kamata, M.: Longitudinal stability control of electric wheelchairs for persons with severe disability. Vehicle System Dynamics 46(suppl. 1), 389–402 (2008)
33. Takahashi, Y., Takagaki, T., Kishi, J., Ishii, Y.: Back and forward moving scheme of front wheel raising for inverse pendulum control wheel chair robot. In: Proceedings of the IEEE International Conference on Robotics and Automation, ICRA 2001, vol. 4, pp. 3189–3194 (2001)
34. Umeno, T., Hori, Y.: Robust speed control of DC servomotors using modern two degrees-of-freedom controller design. IEEE Transactions on Industrial Electronics 38(5), 363–368 (1991)
35. de Vries, T., Heteren, C., Huttenhuis, L.: Modeling and control of a fast moving, highly maneuverable wheelchair. In: Proceedings of the International Biomechatronics Workshop, pp. 110–115 (April 1999)
36. Wang, H., Salatin, B., Grindle, G.G., Ding, D., Cooper, R.A.: Real-time model based electrical powered wheelchair control. Medical Engineering & Physics 31(10), 1244–1254 (2009)
37. van der Woude, L.H.V., Geurts, C., Winkelman, H., Veeger, H.E.J.: Measurement of wheelchair rolling resistance with a handle bar push technique. Journal of Medical Engineering & Technology 27(6), 249–258 (2003)

EMG-Based Control of a Lower-Limb Power-Assist Robot

Kazuo Kiguchi[1] and Yoshiaki Hayashi[2]

[1] Kyushu University, Japan
[2] Saga University, Japan

Abstract. Power-assist robots are expected to work in many fields such as industry, military, medicine, etc. A lower-limb power-assist robot for physically weak persons is supposed to be used for self-rehabilitation or daily motion assist. In order to assist daily motion of the physically weak persons, the robot must estimate the motion intention of the user in real-time. Although there are several kinds of method to estimate the motion intention of the user in real-time, Electromyogram (EMG) signals are often used to estimate that since they reflect the users muscle activities. However, EMG-based real-time motion estimation is not very easy because of several reasons. In this chapter, an EMG-based control method is introduced to control the power-assist lower-limb exoskeleton robot in accordance with users motion intention. A neuro-fuzzy modifier is applied to deal with those problems. The problems of EMG-based motion estimation are cleared by applying the neuro-fuzzy modifier.

Sometimes there is a problem in the users motion even though the users motion is assisted, if the user misunderstands interaction between the users motion and a surrounding environment. In that case, the users motion should be modified to avoid an accident. In this chapter, a method of perception-assist is also introduced to automatically modify the users motion properly.

Keywords: EMG signal, Motion estimation, Intention estimation.

1 Introduction

Many studies on power-assist robots have been carried out up to the present since they are expected to work in many fields such as industry, military, medicine, etc.[1]-[15]. A lower-limb power-assist robot is especially important for physically weak persons to make daily living motion or to perform self-rehabilitation. In order to assist daily motion of the physically weak persons, the robot must estimate the motion intention of the user and assist the estimated users motion in real-time. Although there are several kinds of method to estimate the motion intention of the user in real-time [9]-[11], Electromyogram (EMG) signals are often used to estimate that since they reflect the users muscle activities. The magnitude of the EMG signal is almost proportional to the activity level of the muscle. However, EMG-based real-time motion estimation is not very easy to

S. Mohammed et al. (eds.), *Intelligent Assistive Robots,*
Springer Tracts in Advanced Robotics 106, DOI: 10.1007/978-3-319-12922-8_14

be realized for multi-DOF power-assist exoskeletons because 1: obtaining the same EMG signals for the same motion is difficult even with the same person, 2: activity level of each muscle and the way of using each muscle for a certain motion is different between persons, 3: one muscle is not only concerned with one motion but also another kinds of motion, 4: activity of antagonist muscles affects the generated joint torque, 5: the role of each muscle for a certain motion varies in accordance with joint angles (i.e., the posture change affects the role of each muscle for a certain motion), 6: the activity level of some muscles such as bi-articular muscles are affected by the motion of the other joint, and 7: the effect of antagonist muscle must be taken into account. Therefore, these problems must be cleared in order to apply an EMG-based control method to activate the power-assist robot. In this chapter, an EMG-based control method that can deal with above mentioned problems is introduced to control the power-assist lower-limb exoskeleton robot in accordance with users motion intention.

In the case of the power-assist robots which assist daily motion of physically weak persons, it is important to assist the users motion automatically according to the users intention. However, sometimes there is a problem in the users motion even though the users motion is assisted, if the user misunderstands interaction between the users motion and a surrounding environment. Since not only the motor ability but also the sensory ability is deteriorated in the case of some physically weak persons, the user tends to misunderstand interaction between the users motion and a surrounding environment. In that case, even though the user expands the motor activity with the power-assist robot, the user might not be able to perceive the risks associated with users motions correctly and be involved in an unexpected accident such as tumbling or falling. Therefore, the users motion should be modified to avoid the unexpected accident. In this chapter, a method of perception-assist is also introduced to automatically modify the users motion properly [18]. In the perception-assist, the robot monitors the interaction between the user and the environment using some sensors, and tries to modify the users motion automatically by adding additional force only if certain problems are found in the users motion. Furthermore, ZMP (Zero Moment Point) should be taken into account in order to make the stable lower-limb motion.

2 EMG-Based Motion Estimation

2.1 EMG

Skin surface electromyogram (EMG) is an electric signal generated when the muscle is activated. Since the EMG signals directory reflect the muscle activity levels, they are used as main input signals to estimate the generating lower-limb motion and control the lower-limb exoskeleton in accordance with the users motion intention. Since raw EMG signals are not suitable as input signals to the controller, feature of the raw signal must be extracted. There are many kinds of feature extraction methods, e.g., Root Mean Square, Mean Absolute Value, Mean Absolute Value Slope, Zero Crossings, Slope Sign Changes, or Waveform

Length [19]. One of the most effective feature extraction methods for the real-time human motion estimation is the root mean square (RMS). The RMS of EMG signal is calculated with the equation written below:

$$RMS = \sqrt{\frac{1}{N}\sum_{i=1}^{N} v_i^2} \tag{1}$$

where N is the number of the segments ($N = 400$), v_i is the voltage at ith sampling. Figure 1 shows how the feature of the row EMG signal is extracted with the RMS calculation. The amount of the RMS shows the activity level of the muscle.

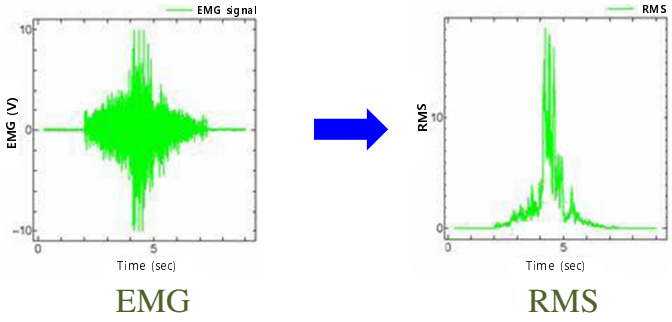

Fig. 1. RMS of EMG signal

2.2 Motion Estimation

When certain motion is performed, the EMG signals of the related multiple muscles show the unique patterns. Therefore, human lower-limb motion can be estimated by monitoring EMG signals of certain muscles of the user since the magnitude of the RMS of the EMG signal indicates the activity level of the muscles. The lower-limb motion (i.e., hip joint flexion/extension motion, knee joint flexion/extension motion, and ankle joint flexion/extension motion) can be estimated by monitoring eight channels of EMG signals per leg. The locations of EMG electrodes are shown in Fig. 2. The relationship between the eight RMS values and the generated vector of joint torques is implemented as shown in eq. (2).

$$\begin{bmatrix} \tau_h \\ \tau_k \\ \tau_a \end{bmatrix} = \begin{bmatrix} w_{h1} & w_{h2} & \cdots & w_{h7} & w_{h8} \\ w_{k1} & w_{k2} & \cdots & w_{k7} & w_{k8} \\ w_{a1} & w_{a2} & \cdots & w_{a7} & w_{a8} \end{bmatrix} \begin{bmatrix} ch_1 \\ ch_2 \\ \vdots \\ ch_7 \\ ch_8 \end{bmatrix} \tag{2}$$

where τ_h, τ_k, and τ_a are torques for hip flexion/extension, knee flexion/extension, and ankle flexion/extension, respectively. ch_j represents the RMS value of the

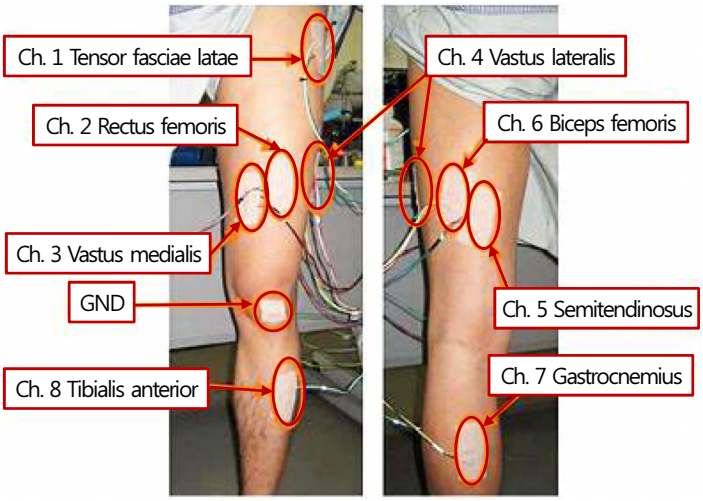

Fig. 2. Location of each electrode

EMG signal measured in channel i. w_{hj} is the weight value for j^{th} EMG signal to estimate the hip flexion/extension motion, w_{kj} is the weight value for j^{th} EMG signal to estimate the knee flexion/extension motion, and w_{aj} is the weight value for j^{th} EMG signal to estimate the ankle flexion/extension motion.

Practically, it is not easy to define the proper weight matrix from the beginning even with the knowledge of human anatomy or the experimental results. Furthermore, the posture of the lower-limb affects the relationship between the EMG signals and the generated joint torques because of anatomical reasons such as change of the moment arm. In other words, the role of each muscle for a certain motion varies in accordance with joint angles. Consequently, the effect of the posture difference of the lower-limb must be taken into account to estimate the correct lower-limb motion for the power assist.

2.3 Neuro-fuzzy Modifier

The neuro-fuzzy modifier has been proposed in order to take into account the effect of the posture difference for the motion estimation [12]. The neuro-fuzzy modifier is used to adjust the weight matrix in eq. (2) by multiplying the coefficients in accordance with the lower-limb posture of the user, so that the effect of lower-limb posture difference can be compensated effectively. It also makes the same effect of adjusting the weight matrix (i.e., the muscle-model matrix) itself to be suitable for each person. The structure of the neuro-fuzzy modifier is the same as a neural network and the process of the signal flow in the neuro-fuzzy modifier is the same as that in fuzzy reasoning.

The architecture of the neuro-fuzzy muscle-model modifier is depicted in Fig. 3. Here, Σ means the summation of the inputs and Π means the multiplica-

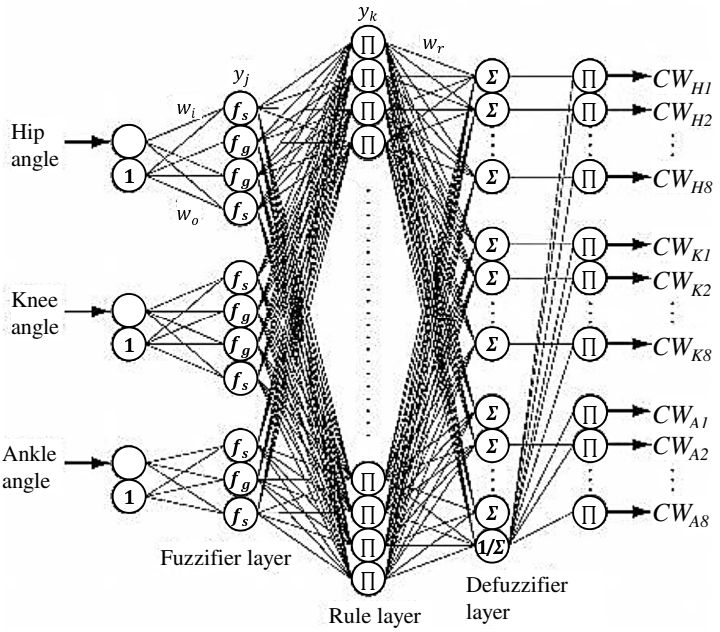

Fig. 3. Nuero-fuzzy modifier

tion of the inputs. The neuro-fuzzy modifier consists of five layers (input layer, fuzzifier layer, rule layer, defuzzifier layer, and output layer). Two joint angles (hip flexion/extension angle and knee flexion/extension angle) are used as inputs for the neuro-fuzzy modifier. Each joint angle is divided into three regions (i.e., FL: flexed region, IM: intermediate region, and EX: extended region for hip flexion/extension angle and knee flexion/extension angle. The output form the neuro-fuzzy modifier is used as a coefficient for each weight of the muscle-model matrix in eq. (2). Consequently, the weight matrix in eq. (2) is adjusted by the neuro-fuzzy method according to the user's lower-limb posture at every sampling time during the control.

In the fuzzifier layer, the degree of fitness of each joint angle is sent to the rule layer. Two kinds of nonlinear functions (f_G: Gaussian function and f_S: Sigmoidal function) are used as the membership functions of the neuro-fuzzy modifier.

$$f_s(u_s) = \frac{1}{1 + e^{-u_s}} \tag{3}$$

$$u_s(x) = w_0 + w_i x \tag{4}$$

$$f_G(u_G) = e^{-u_G^2} \tag{5}$$

$$u_G(x) = \frac{w_0 + x}{w_i} \tag{6}$$

where x is the input signal, w_0 is a threshold value and w_i is a weight. The rules for every combination of the joint angle are prepared in the rule layer. The output of the neuro-fuzzy modifier is calculated by dividing the weighted summation of the degree of fitness of each rule (i.e., the output from the rule layer) by the summation of the degree of fitness of each rule. The initial weight for each rule is set to be 1.0, so that the coefficient for every weight in eq. (2) is 1.0 at first.

The neuro-fuzzy muscle-model modifier adapts itself to each user by performing the training with the information of the force sensors. If there is motion difference between the user's lower-limb motion and the exoskeleton's motion, the force sensors detect the force between them. If the weight matrix is perfectly defined, there is no motion difference between the user's lower-limb motion and the exoskeletons motion. Therefore, if the neuro-fuzzy muscle-model modifier is trained to eliminate the force between the users lower-limb and the exoskeleton, the weight matrix becomes perfect even though the initially defined values are not correct. The error back-propagation learning algorithm is applied to minimize the force between the users lower-limb and the exoskeleton. The equation of the evaluation function is written as:

$$E = \frac{1}{2} f_{err}^2 \tag{7}$$

where E is the error function to be minimized and f_{err} is the measured force/torque between the user and the exoskeleton robot. The lower-limb motion of the user would be properly estimated in real-time after the training the neuro-fuzzy muscle-model modifier.

By the effect of the neuro-fuzzy modifier, w_{hj}, w_k, and w_{aj} are adjusted as follows:

$$\begin{aligned} w_{hj} &= w_{h0,j} \times CW_{Hj} \\ w_{kj} &= w_{k0,j} \times CW_{Kj} \\ w_{aj} &= w_{a0,j} \times CW_{Aj} \end{aligned} \tag{8}$$

where w_{h0j}, w_{k0j}, and w_{a0j} are the initial weight values. CW_{Hj}, CW_{Kj}, and CW_{Aj} are the output from the neuro-fuzzy modifier which are changed according to the users lower-limb posture in order to adjust the relationship between each joint torque and the RMS values in real-time.

3 Power-Assist

3.1 Lower-Limb Power-Assist Robot

The architecture of the exoskeleton robot is shown in Fig. 4. The exoskeleton robot consists of a waist holder, a thigh holder, a lower leg holder, two DC motors

(Maxon DC Motors), two links, a footrest and two force sensors (hip and knee force sensors) in one leg. Locations of force sensors are shown in Fig. 1. There is a passive DOF (dorsiflexion/ planterflexion) in ankle joint and two active DOF (flexion/extension) in hip and knee joints. Each DC motor generates the assist torque at each joint.

Usually, the limitation of human knee movable range is 150 degrees in flexion and 0 degree in extension, and the limitation of human hip movable range is 110 degrees in flexion and 30 degrees in extension. Considering the practical application to everyday life and safety of users, the hip motion limitation of the exoskeleton robot is 110 degrees in flexion and 20 degrees in extension, and the knee motion limitation of the proposed robot is 150 degrees in flexion and 0 degree in extension. The stopper is attached for each joint motion to prevent the exceeding of the movable range. Furthermore, maximum torque of the robot is limited by the hardware and the software for safety.

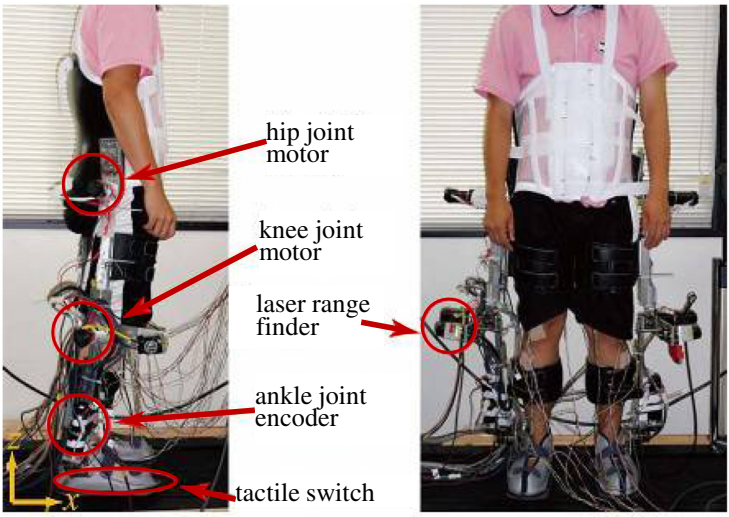

Fig. 4. Lower-limb power-assist exoskeleton robot

3.2 Robot Controller

The controller of the robot consists of the power-assist part and the perception-assist part. Each motor torque is the sum of calculated torques in each part. In this section, the power-assist part is explained in detail. In the power-assist part, the robot is controlled based on two kinds of controller: the force sensor based controller and the EMB-based controller. When the amount of the EMG signals of the user is small, the force sensor based controller is applied to avoid disturbing the users motion. When the amount of the EMG signals of the user is increased, the controller is gradually switched from the force sensor based controller to

the EMG-based controller. An example of the membership functions used to switch the signals is shown in Fig. 5. Thus, as a monitored muscle increases the activity level, the controllers are gradually switched from the force sensor based controller to the EMG-based controller.

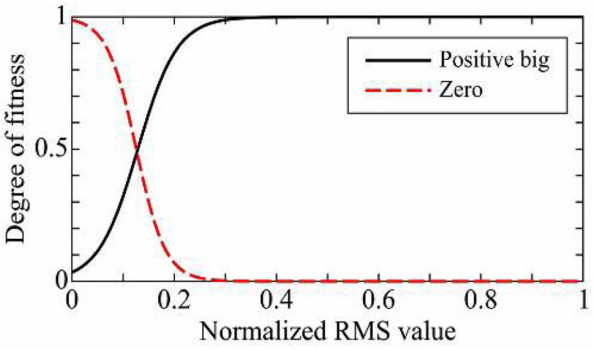

Fig. 5. Membership functions

3.3 EMG-Based Control

The lower-limb motion of the user can be estimated based on the EMG signals as explained in Section 2. Then proper power-assist level can be set by the user to realize the power-assist in accordance with the motion intention of the user.

In order to estimate users motion intention, hand force vector calculation is carried out based on the estimated joint torque vector. The estimated joint torque vector is transferred to the hand force vector of the user using the Jacobian matrix as follows:

$$F_{foot} = J^{-T}\tau_{est} \tag{9}$$

$$F_{f,avg} = \frac{1}{N}\Sigma_{k=1}^{N_f} F_{foot}(k) \tag{10}$$

where F_{foot} is the foot force vector of the user, J is the Jacobian matrix, $F_{f,avg}$ is the average of F_{foot} in N_f number of samples. Then, the desired foot acceleration vector is calculated from eq. (10).

$$\ddot{X}_d = M^{-1}F_{f,avg} \tag{11}$$

where $\ddot{X}_d$ is the desired foot acceleration vector, M is the mass matrix of the robot and the user's lower-limb. To realize the user's intended motion, the following impedance control is applied to obtain the resultant foot force vector F.

$$F = M\ddot{X}_d + B(\dot{X}_d - \dot{X}) + K(X_d - X) \tag{12}$$

where $\dot{X}_d$ d and X_d are the desired hand velocity vector and position vector which are calculated from eq. (11), respectively. B and K are the viscous coefficient matrix and the spring coefficient matrix, respectively. Since impedance parameters of human lower-limb are changed based on the lower-limb posture and the relationship between agonist and antagonist muscles, impedance parameters of the exoskeleton robot are also changed based on them in order to realize natural and comfortable power-assist. Therefore, the impedance parameter matrix B and K in eq. (12) are changed depend on the lower-limb posture and activity levels of activated lower-limb antagonist muscles in real time. Consequently, the joint torque command vector for the joint DC motors is calculated as follows:

$$\tau_{motor} = \kappa J^T F \tag{13}$$

where τ_{motor} is the joint torque command vector, and κ is the power-assist rate.

4 Perception-Assist

4.1 Motion Modification

In the perception-assist part, the robot monitors whether the users motion is in danger or not. Basically the users motion is assisted according to his/her motion intention by the robot. However, if the user has problems in the sensory ability to perceive the environment, the user might not be able to recognize the danger in his/her motion properly. Therefore, if the robot judges the users motion is dangerous, the robot needs to modify the users motion automatically in real-time. This kind of automatic motion modification based on the interaction between the user and the environment is defined as perception-assist. In order to realize the perception-assist, the robot is required to understand not only the motion of the user but also the interaction between the user and the surrounding environment. In the case of lower-limb power-assist robots, the robot needs to prevent the user from falling down during walking, ascending, descending, or standing up. Especially, a user who has problems in the sensory ability to perceive the environment might overlook or misunderstand a bump and stumble on it. Although a healthy person might be able to recover the balance, a user who needs the help of the power-assist robot might fall down. For this reason, the perception-assist is important for the user to avoid an unexpected accident as well as the power-assist.

When the robot detects a the users foot is going to collide with a bump in front of the user, the robot automatically tries to prevent the user from stumbling and falling down by the perception-assist during walking. In this case, the robot tries to modify the users motion by adding the additional modification force in addition to the ordinary power-assist force. Thus, the motion modification is automatically generated regardless of the users intention. For this reason, the user might lose his/her balance and fall down by the effect of the additional modification force of the perception-assist. To prevent such case, the robot takes into account ZMP in the perception-assist algorithm.

A stereo camera or a laser range finder can be used to recognize the environment in front of the user. After a bump in front of the user is detected by the laser range finder or the stereo camera, the distances from the users toe to the bump and the height of the bump are calculated. The robot judge the users toe is going to collide with the bump or not. If the robot find out the users toe is going to collide with the bump, the foot trajectory of the user is automatically modified by adding the additional modification force as well as the power-assist force.

4.2 Examples

In order to prevent the user from losing his/her balance and falling down by the effect of the additional modification force by the perception-assist which is given regardless of the users intention, the robot takes into account ZMP. The supporting leg is found by tactile switches located on both soles. Then, the posture of the users body region is calculated using the joint angles of the supporting leg. ZMP is calculated is written as:

$$x_{zmp} = \frac{\Sigma_{i=1}^{n} m_i(\ddot{z}_i + g)x_i - \Sigma_{i=1}^{n} m_i \ddot{x}_i z_i}{\Sigma_{i=1}^{n} m_i(\ddot{z}_i + g)} \tag{14}$$

where x_{zmp} is the coordinate of ZMP in the horizontal direction, m_i is the mass of each human body part and robot, x_i is the position of the center of gravity (COG) of each part in the horizontal direction, z_i is the position of the COG of each part in the vertical direction and g is the acceleration of gravity. The perception-assist is performed considering x_{zmp}.

When the robot finds out there is no bump in front of the user, the robot evaluates the user's walking based on x_{zmp} in order to prevent the user from falling down in addition to the ordinary power-assist. If x_{zmp} is located in an undesired area, the robot automatically generates additional hip joint torque to change the location of x_{zmp} to the safe area by activating the upper body of the user. The area in which the robot generates the additional hip joint torque in addition to the power-assist is defined as shown in Fig. 6, so that x_{zmp} is moved to center of the support polygon. Since the mass of the upper body region is larger than other regions and the movement of the mass of the upper body is the most effective way to change ZMP, the additional hip joint torque (i.e., the perception-assist torque) is generated at the hip joint motor of the support leg. In Fig. 6, τ_{max} is the amount of the maximum hip joint torque which is defined to protect the user from the injury. The perception-assist torque for walking-assist is calculated using eq. (16).

$$\tau_{walk} = \begin{cases} 0, \ (|\Delta x_{zmp}| < d_{safe}) \\ \frac{\tau_{max}}{d_{cri}}(\Delta x_{zmp} - Sgn \times d_{safe}), \ (d_{safe} \leq |\Delta x_{zmp}| \leq d_{safe} + d_{cri}) \\ Sgn \times \tau_{max}, \ (|\Delta x_{zmp}| \leq d_{safe} + d_{cri}) \end{cases} \tag{15}$$

$$\Delta x_{zmp} = x_{c,ZMP} - x_{zmp}$$

$$Sgn = \mathrm{sgn}(\Delta x_{zmp})$$

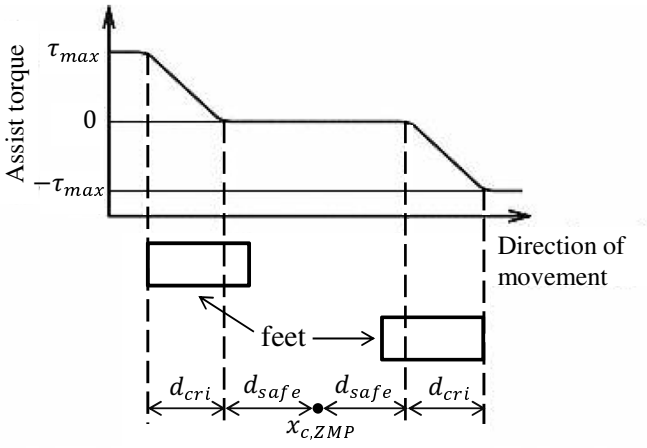

Fig. 6. Perception-assist area based on ZMP

where $x_{c,ZMP}$ is the center position of the support polygon, d_{safe} and d_{cri} are shown in Fig. 6. τ_{max}, d_{safe} and d_{cri} are experimentally defined. When the robot detects a bump, a virtual wall area is generated in front of the bump as shown in Fig. 7(a). The virtual wall area is shown by the trapezoid represented by Δl, Δh and H in Fig. 7 (a). Here, H means the height of the bump, Δl, Δh are the experimentally defined parameters as shown in Fig. 7(a). In the experiments to define Δl and Δh, some subjects walk at normal speed (about $1.4m/sec$). Then, Δl and Δh are defined as minimum values in which the subjects could overcome the bump. If the user's foot enters the virtual wall area as shown in Fig. 7(a), the robot judges the user might stumble on the bump and generates the additional motion modification force along the virtual wall in addition to the power-assist force to avoid the collision with the bump. The additional motor torque generated by the effect of the additional motion modification force (i.e., the perception-assist torque) is written as:

$$\begin{bmatrix} \tau_{h,add} \\ \tau_{k,add} \end{bmatrix} = J^{-T} f_{add} \tag{16}$$

where $\tau_{h,add}$ is the additional hip joint torque, $\tau_{k,add}$ is the additional knee joint torque, J is Jacobian matrix and f_{add} is the additional motion modification force generated along the virtual wall. The amount of f_{add} is related with Δl and Δh. The amount of f_{add} was defined based on the change of ZMP and the feeling of the subjects at the same time when Δl and Δh are defined. Note that $\tau_{h,add}$ and $\tau_{k,add}$ are generated without the user's intention. Therefore, another hip joint torque must be added to compensate for the undesired effect of the ZMP change caused by the additional force, so that the user does not lose his/her balance and fall down by the effect of the perception-assist. Based on eq. (14), τ_{cancel} which is the torque to cancel the effect of the change of ZMP is calculated as:

$$f_{body} = \frac{\tau_{h,add}}{d_{t,cog}} \cdot \frac{x_{t,cog}\sin\theta_{sw,H} - z_{t,cog}\cos\theta_{sw,H}}{x_{b,cog}\sin\theta_b - z_{b,cog}\cos\theta_b} - \frac{\tau_{k,add}}{d_{l,cog}} \cdot \frac{x_{l,cog}\sin(\theta_{sw,k} - \theta_{sw,H}) - z_{l,cog}\cos(\theta_{sw,k} - \theta_{sw,H})}{x_{b,cog}\sin\theta_b - z_{b,cog}\cos\theta_b} \quad (17)$$

$$\tau_{cancel} = f_{body} \times d_{b,cog} \quad (18)$$

where $d_{t,cog}$ is the length between hip joint and the COG of the femoral part, $d_{l,cog}$ is the length between knee joint and the COG of the leg part, and $d_{b,cog}$ are the length between hip joint and the COG of the body part. $x_{p,cog}$ and $z_{p,cog}$ are the position of each body part ($p = t$: femoral part, l: leg part, b: body part).

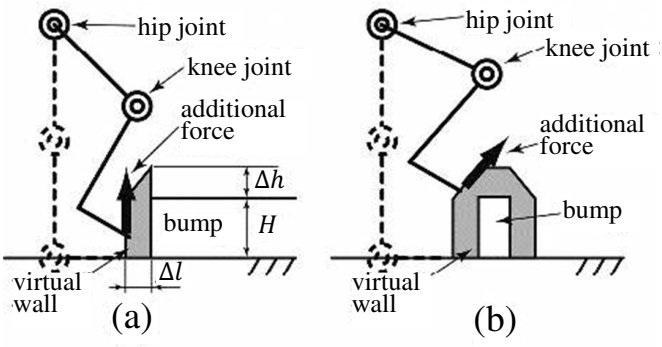

Fig. 7. Virtual wall

After the users foot is lifted over the bump, the robot estimates whether the top surface of the bump has enough space to place the users foot on it. If the top surface of the bump has enough space to place the users foot on it, the robot takes the additional perception-assist torque away from the user and performs the ordinal power-assist. In the case that the top surface of the bump is too narrow, if the robot recognizes the ground ahead on the bump, the robot performs another perception-assist to overcome the bump as shown in Fig. 7(b). Meanwhile, if the robot cannot recognize the ground ahead on the bump, the robot tries to turn back the users foot because the robot cannot find the space to place the users foot on it safety. Thus, the robot takes into account ZMP to prevent the user from losing his/her balance and falling down in any case.

5 Conclusions

In this chapter, an EMG-based control method and a perception-assist method are introduced for the lower-limb power-assist exoskeleton robot. The EMG-based control method is effective method to activate the power-assist robot based

on the users motion intention. The perception-assist is also important especially for the user whose sensory ability is deteriorated to secure the safety.

References

1. Guizzo, E., Goldstein, H.: The Rise of the Body Bots. IEEE Spectrum 42(10), 42–48 (2005)
2. Dollar, A.M., Herr, H.: Lower Extremity Exoskeletons and Active Orthoses: Challenges and State-of-the-Art. IEEE Trans. on Robotics 24(1), 144–158 (2008)
3. Yang, C.J., Zhang, J.F., Chen, Y., Dong, Y.M., Zhang, Y.: A Review of Exoskeleton-type Systems and Their Key Technologies. Proc. of IMechE, Journal of Mechanical Engineering Science, Part C 222, 1599–1612 (2008)
4. Rosen, J., Brand, M., Fuchs, M., Arcan, M.: A Myosignal-Based Powered Exoskeleton System. IEEE Trans. on System Man and Cybernetics, Part A 31(3), 210–222 (2001)
5. Kiguchi, K., Kariya, S., Watanabe, K., Izumi, K., Fukuda, T.: An Exoskeletal Robot for Human Elbow Motion Support. Sensor Fusion, Adaptation, and Control. IEEE Trans. on Systems, Man, and Cybernetics, Part B 31(3), 353–361 (2001)
6. Kiguchi, K., Tanaka, T., Fukuda, T.: Neuro-Fuzzy Control of a Robotic Exoskeleton with EMG Signals. IEEE Trans. on Fuzzy Systems 12(4), 481–490 (2004)
7. Kiguchi, K., Esaki, R., Fukuda, T.: Development of a Wearable Exoskeleton for Daily Forearm Motion Assist. Advanced Robotics 19(7), 751–771 (2005)
8. Cavallaro, E.E., Rosen, J., Perry, J.C., Burns, S.: Gravity-balancing leg orthosis and its performance evaluation. IEEE Trans. Robotics 22(6), 1228–1239 (2006)
9. Riener, R., Lünenburger, L., Jezernik, S., Anderschitz, M., Colombo, G., Dietz, V.: Patient-cooperative strategies for robot-aided treadmill training: first experimental results. IEEE Trans. Neural Syst. Rehabil. Eng. 13(3), 380–394 (2005)
10. Hogan, N.: Impedance control: an approach to manipulation, parts I, II, III. J. Dyn. Syst., Meas. Control 107, 1–23 (1985)
11. Blaya, J., Herr, H.: Adaptive control of a variable-impedance ankle-foot orthosis to assist drop-foot gait. IEEE Trans. Rehabil. Eng. 12(1), 24–31 (2004)
12. Bar-Cohen, Y.: Electroactive Polymer (EAP) Actuators as Artificial Muscles - Reality, Potential and Challenges. SPIE Press (2004)
13. Noritsugu, T., Tanaka, T.: Application of rubber artificial muscle manipulator as a rehabilitation robot. IEEE/ASME Trans. Mechatronics 2(4), 259–267 (1997)
14. Buerger, S.P., Hogan, N.: Complementary stability and loop shaping for improved human-robot interaction. IEEE Trans. Robotics 23(2), 232–244 (2007)
15. Paluska, D., Herr, H.: Series elasticity and actuator power output. In: Proc. IEEE Int. Conf. Robotics Autom.: ICRA 2006, pp. 1830–1833 (2006)
16. Kong, K., Tomizuka, M.: Flexible joint actuator for patient's rehabilitation device. In: Proc. IEEE Int. Symp. Robot Human Interactive Commun.: ROMAN 2007, pp. 1179–1184 (2007)
17. Pratt, J., Krupp, B., Morse, C.: Series elastic actuators for high fidelity force control. Int. J. Ind. Robot 29(3), 234–241 (2002)
18. Low, K.H.: Initial experiments of a leg mechanism with a flexible geared joint and footpad. Adv. Robotics 19(4), 373–399 (2005)
19. Pratt, G.A., Williamson, M.W.: Series elastic actuators. In: Proc. IEEE/RSJ Int. Conf. Intell. Robotics Syst.: IROS 1995, Pittsburgh, PA, pp. 399–406 (1995)

Robust Control of an Actuated Orthosis for Lower Limb Movement Restoration

Samer Mohammed, Weiguang Huo, Hala Rifaï,
Walid Hassani, and Yacine Amirat

LISSI Laboratory, University of Paris-Est Créteil, 122 Rue Paul Armangot,
94400, Vitry Sur Seine, France
samer.mohammed@u-pec.fr

Abstract. The present chapter deals with the development of two rehabilitation approaches of the lower limb by means of the knee joint exoskeleton EICOSI. The model of the exoskeleton is presented as well as a modified Hill-type muscular model of the wearer's lower limb. The parameters of the shank-foot-exoskeleton and the muscles are identified based on a least square optimization algorithm. Two control techniques are proposed: the first one ensures the passive rehabilitation of the lower limb by means of bounded control laws and the second ensures the assistance-as-need of the wearer based on the human intention estimated by means of EMG electrodes fixed at some particular muscles. Experimental tests are performed on healthy subjects and show the efficiency of the proposed strategies.

1 Introduction

Wearable robots, such as orthoses and exoskeletons, are widely used in medical and military fields. For the former purpose, they are usually developed to help patients who have lost or have a weak motor ability, because of spinal cord injuries or weakness of the crucial muscles, to perform rehabilitation training or daily activities. For the latter purpose, they are designed mainly for augmenting the wearer's performance. From the human-robot interface view, the wearable robots introduced in the literature can be divided into two types: the first does not consider the human intention while the second takes it into account. During some medical rehabilitation trainings, the wearable robots only assist the human limbs to accomplish flexion and extension movements or to track a desired trajectory designed by the therapists. In this case, the human intention is not taken into account in the control strategies. On the other hand, the human intention plays an important role in the wearer's assistance during daily activities and/or for performance increase.

To estimate the human intention, muscular or brain activities, limbs developed torque and/or velocity, etc. should be studied. Three main types of interfaces are developed by the researchers and used during the last decades: physical, cognitive interfaces or ideally a combination of them [1]. Physical interfaces have been widely used in the developed exoskeletons such as the force interface which

S. Mohammed et al. (eds.), *Intelligent Assistive Robots,*
Springer Tracts in Advanced Robotics 106, DOI: 10.1007/978-3-319-12922-8_15

utilizes the forces acting on the orthoses/exoskeletons by the human limbs, to estimate the wearer's motion intention. However, there is an inherent drawback of this type of interface related to the time delay. This is because the estimation of the intention occurs after a relatively evident human movement is implemented. In this case, dependent people are easily tired when they are performing rehabilitation training or daily activities with the wearable robots. Another critical challenge for this interactive mode is the differentiation of voluntary human efforts from the external disturbances [2]. Compared to the physical interface, the cognitive one can cover these drawbacks and takes certain advantages for inferring the human intention because it is biologically inspired and the signals are obtained directly from the human body. Electroencephalographic (EEG) and electromyographic (EMG) signals are two common and effective means to estimate the human intention. In comparison, EMG interfaces are more widely used in the researches on wearable robots although the Brain-Machine Interface (BMI) technology has been improved dramatically in the last decade [3]. However, there are also some challenges for employing the EMG signals to estimate the human intention. Firstly, the EMG signals are usually noisy which necessitates the implementation of efficient processing methods. Secondly, in order to estimate the human intention accurately, precise and realistic musculoskeletal model usually needs to be built and studied. Finally, a balancing strategy between the wearer's contribution and the robot's one is usually necessary, which is important for the assistance-as-needed control strategies [1].

In terms of lower limb orthoses or exoskeletons, most of the works found in the literature mainly focus on the following three aspects: i) sophisticated robotic mechanisms that can enable the complex human movements and improve the portability of the robots, ii) intelligent control strategies that can guarantee the effectiveness and the stability of the wearer-robot system, and iii) accurate performance assessment methods [4]. As mentioned above, the lower limb orthoses/exoskeletons can be divided into two types: orthoses/exoskeletons that only focus on the movement rehabilitation of dependent people without taking into consideration the wearer's intention and those that take this parameter into account. For the first type, lower limb orthoses/exoskeletons are mainly used to train the wearer's paralyzed limb during the execution of repetitive motions described by a desired trajectory and to allow relaxing the therapists. They are able to help the patients strengthen their muscles, reduce the joints stiffness and increase the lower limbs range of motion [5,6]. For the second type, the human walking intention is estimated by means of some sensor measurements like the ground reaction force, the EMG signals obtained from the several critical muscles in lower limbs, inertial measurements of the upper body, etc.

De Rossi et al. [7] have presented a distributed-pressure human-robot interface which can provide an accurate walking intention based on the measurements of the interaction force between the wearer's lower limb and the human-robot interface. The orthosis Roboknee also employs a physical interface, based on the vertical ground reaction force, to infer the user's intention [8]. During the guidance of the walking intention, Roboknee can assist the user's thigh muscles to

drive the flexion and extension of the knee joints. Meanwhile, EMG interfaces have also been used in many researches. Their application methods can be classified as: physical-based methods [9,10] and non-physical-based methods [11,12]. The so-called physical-based methods combine the EMG signals and the human musculoskeletal model to estimate the user's walking intention. For example, Rosen et al. [13] have employed the EMG signals and the Hill muscle model as inputs of a neural network to estimate the wearer's muscular force. Fleischer et al. [10] have used a musculoskeletal-knee model combined with EMG signals to improve the precision of the wearer's torque estimation in their researches on a knee joint exoskeleton. On the other hand, non-physical-based methods are usually based on the raw EMG signals without the human body model. In [14], Khokhar et al. have estimated the human intention by using raw EMG signals which are classified by means of a support vector machine, and have employed the intention to control a wrist exoskeleton effectively.

Concerning the control strategies, some special algorithms have been presented according to the feature of the lower limb orthoses/exoskeletons. Nikitczuk et al. [15] have presented a proportional integral (PI) control for an Electro-Rheological Fluid (ERF)-based actuator in the exoskeleton KO-PAR, which is used for the rehabilitation of the knee joint. An EMG-based controller has been developed by Fleischer et al. [10] for a powered orthosis, which is used to assist the wearer during walking. The control of the Hybrid Assistive Limb (HAL)-5 [16] exoskeleton has combined a proportional derivative (PD) controller and an EMG-based controller to assist the wearer during daily activities based on the motion intention. Some other control methods, such as neural-network-based, fuzzy logic and sliding mode control methods are developed as well [17,18,19].

Within the researches conducted in LISSI-Lab, an exoskeleton intelligently communicating and sensitive to intention (EICOSI) has been developed. It has one degree of freedom at the knee joint level and is used to strengthen thigh muscles and to accomplish rehabilitation training. The previous works can be divided into two phases. During the first phase, the main works concentrated on the control strategies of the EICOSI and did not take into account the human intention. Different control methods were developed: a bounded control method, a model reference adaptive control and some sliding mode based control methods [4,17,20,21]. In the second phase, the human intention was employed in the control strategies [1,2]. A modified Hill-type muscle model was developed and the parameters were identified. For both two phases, experiments were performed to verify the effectiveness of the presented control strategies and models. Additionally, some robustness tests were presented concerning the uncertainties of the model parameters and the external disturbances.

The chapter is structured as follows. Section 2 presents the models developed and the associated identification of the parameters: the lower-limb-orthosis model and the modified Hill-type muscular model. Section 3 presents the control strategies and the results of experiments. Finally, in section 4, some conclusions are addressed and future works are introduced.

2 Modeling and Identification

2.1 Lower-Limb-Orthosis Model and Parametric Identification

Modeling of the Lower-Limb-Orthosis System. The lower limb-orthosis system consists of the human shank-foot and the actuated orthosis that includes an upper segment and a lower one. There is one rotational degree of freedom at the knee joint level. The wearer's leg is fixed to the orthosis by means of straps and the orthosis can fit the wearer's leg perfectly. Hence, the wearer's leg and the orthosis are considered moving synchronously during rehabilitation training and walking. For different rehabilitation purposes, two different situations have been discussed in the authors' previous researches [4], [20,21]. In one situation, the wearer does not exert any muscular effort, which means that the rehabilitation situation is totally passive. In the other one, the wearer is able to develop a certain torque at the knee joint level; hence the wearer's torque is taken into account in the training process. Note that the wearer is in a seated position performing flexion and extension movements of the knee joint. The associated different models are given as follows. First, the coordinate frames of the lower limb orthosis system are designed as shown in Fig.1. Denote by $\mathcal{F}(\boldsymbol{x}^f, \boldsymbol{y}^f, \boldsymbol{z}^f)$ a fixed frame in the space and by $\mathcal{S}(\boldsymbol{x}^s, \boldsymbol{y}^s, \boldsymbol{z}^s)$ a frame attached to the shank at the knee joint defined such that the direction of $\boldsymbol{y}^f$ and $\boldsymbol{y}^s$ coincide (Figure 1). The knee, and therefore the orthosis, are in rotation about the pitch axis $\boldsymbol{y}^s$ of the angle θ. The angular velocity $\dot{\theta}$ is equal to the derivative of the rotational position. In the following, the subscripts s and o refer to the shank and orthosis respectively.

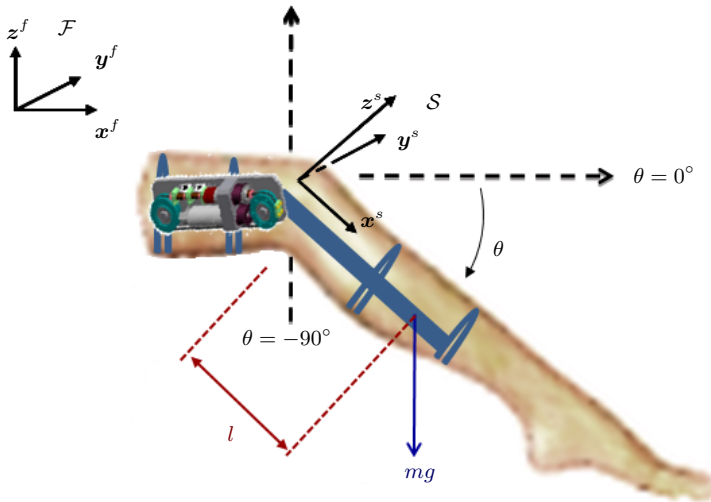

Fig. 1. Human leg embodying the orthosis: Fixed and Shank frames [21]

To model the system, the Lagrangian equation is employed, which is defined as $L_i = E_{ki} - E_{gi}$, where E_{ki} and E_{gi} are the kinetic and the gravitational energies of the human shank and the orthosis respectively, $i \in \{s, o\}$. E_{ki} and E_{gi} are given as follows:

$$E_{ki} = \frac{1}{2} J_i \dot{\theta}^2 \tag{1}$$

$$E_{gi} = m_i g l_i (1 - \sin\theta) \tag{2}$$

Where J_i, $i \in \{s, o\}$, are the moments of inertia of the shank and the orthosis in the frame $\mathcal{S}$. m_i represent the masses of each component (the shank and the orthosis) and g is the gravity acceleration. l_i show the distances from the knee joint to each component's center of mass.

$$J\ddot{\theta} + \tau_g \cos\theta = \tau_{fr} + \tau_{st} + \tau + \tau_h \tag{3}$$

Where:
$J = J_s + J_o$ and $\tau_g = \tau_{gs} + \tau_{go} = m_s g l_s + m_o g l_o$. τ_{fr} is the friction torque which is composed of the solid and viscous terms: $\tau_{fr} = -A\text{sign}\dot{\theta} - B\dot{\theta}$ where A and B are the solid and viscous coefficients respectively. They are computed as: $A = A_s + A_o$, $B = B_s + B_o$. sign() shows the sign function. τ_{st} is the stiffness torque of the human knee joint, which can be described as: $\tau_{st} = -C(\theta - \theta_r)$, where C is the stiffness coefficient of the knee joint and θ_r is the rest angular position of the shank. τ denotes the control torque developed by the orthosis' actuator and τ_h shows the human muscular torque.
Hence, the final lower-limb-orthosis dynamical model can be expressed as follows:

$$J\ddot{\theta} = -\tau_g \cos\theta - C(\theta - \theta_r) - A\text{sign}\dot{\theta} - B\dot{\theta} + \tau + \tau_h, \tag{4}$$

Parameters Identification. As mentioned above, the shank-foot-orthosis system has two components: the human shank-foot (referred in the remaining of the chapter as shank) and the orthosis. The parameters of each component have been identified separately in this study. For the shank component, the equation (4) can be written as:

$$-m_s g l_s \cos\theta = J_s\ddot{\theta} + A_s\text{sign}\dot{\theta} + B_s\dot{\theta} + C_s(\theta - \theta_r) \tag{5}$$

Where the rest position θ_r and the current position θ are measured by means of the orthosis incremental encoder. The angular velocity and the acceleration of the knee joint, $\dot{\theta}$ and $\ddot{\theta}$ respectively, are calculated by derivation of the variable θ. The mass of the shank m_s and the position of its center of gravity l_s can be computed by using the regression equations of Winter [22], based on the given values of the subject's height and weight. In this case, the remaining parameters: J_s, A_s, B_s and C_s can be identified by using the passive pendulum test [23]. Moreover, the EMG signals of the quadriceps muscles are measured and analyzed to identify and reject any undesired muscle contraction.

In terms of the orthosis component, the equation (4) can be rewritten as follows:

$$\tau = m_o g l_o \cos\theta + A_o \text{sign}\dot{\theta} + B_o\dot{\theta} + J_o\ddot{\theta} \tag{6}$$

Where the torque τ developed by the actuator can be computed by using the measurements delivered by the current sensor. The remaining parameters: J_o, A_o and B_o need to be identified.

All the parameters of the shank and orthosis system which need to be identified can be obtained by using the weighted least square optimization [24]. The identified model parameters and their standard deviations are shown in Table 1 and Table 2.

Table 1. Shank parameters identification [21] (Subject: sex=male, age= 35 years old, weight=97Kg, height=1.82m)

Parameter	Symbol	Value ± S.D. (%)
Moment of inertia	J_s	1.5383 ± 0.7052 $Kg \cdot m^2$
Solid friction coefficient	A_s	0.3975 ± 1.3265 $N \cdot m$
Viscous friction coefficient	B_s	4.7528 ± 2.4557 $N \cdot m \cdot s \cdot rad^{-1}$
Stiffness coefficient	C_s	0.45 ± 0.5476 $N \cdot m \cdot rad^{-1}$
Gravity torque	τ_{g_s}	17.4576 $N \cdot m$

Table 2. Orthosis parameters identification [21] (Subject: sex=male, age= 35 years old, weight=97Kg, height=1.82m)

Parameter	Symbol	Value ± S.D. (%)
Moment of inertia	J_o	0.0117 ± 3.5238 $Kg \cdot m^2$
Solid friction coefficient	A_o	0.3525 ± 0.2491 $N \cdot m$
Viscous friction coefficient	B_o	0.6928 ± 0.3811 $N \cdot m \cdot s \cdot rad^{-1}$
Gravity torque	τ_{g_o}	0.2424 ± 0.5518 $N \cdot m$

2.2 Muscle Force Modeling and Identification of the Parameters

Modeling of the Lower-Limb-Muscles Force and the Knee Joint Torque. To estimate the human knee torque, eight associated muscles are used. Four quadriceps are used for the knee joint extension: rectus femoris (RF), vastus lateralis (VL), vastus medialis (VM) and vastus intermedius (VI); the others are the hamstrings for the knee joint flexion: semi-tendinous (ST), semi-membranous (SM) and biceps femoris long head (BL)/short head (BS). In this study, the wearer is considered in a sitting position without taking into account the ground contact. A modified Hill-type muscle modeling method [25] is employed. The human knee torque is expressed by:

$$\tau_h = \sum_{i=1}^{N} F_i^{mt} m a_i \tag{7}$$

where F_i^{mt} is the force generated by the associated i^{th} muscle and ma_i is the moment arm of the i^{th} muscle, $i \in \{1 \dots N\}$ ($N = 8$ in this case). F_i^{mt} can be obtained by the modified Hill-type muscle modeling method as shown in the following:

$$F^{mt}(t) = F_{max}\left[a(t) f_l(\bar{l}^m(t)) f_v(\bar{v}^m(t)) + \bar{b}^m \bar{v}^m(t)\right] \tag{8}$$

Where:

$$\dot{a}(t) + \frac{1}{\tau_{act}}\left[\frac{\tau_{act}}{\tau_{deact}} + (1 - \frac{\tau_{act}}{\tau_{deact}})c(t)\right] a(t) = \frac{1}{\tau_{act}} c(t) \tag{9}$$

$$f_l(\bar{l}_m(t)) = \mathrm{e}^{\dfrac{-(\bar{l}^m(t)-1)^2}{\gamma}}$$

$$f_v(\bar{v}^m(t)) = \begin{cases} \dfrac{k_v\left[\bar{v}^m(t)+1\right]}{-\bar{v}^m(t)+k_v} & \bar{v}^m(t) \le 0 \\ \dfrac{1.8\left[k_v+1\right]\bar{v}^m(t)+0.13k_v}{\left[k_v+1\right]\bar{v}^m(t)+0.13k_v} & \bar{v}^m(t) > 0 \end{cases} \tag{10}$$

F_{max} is the maximum isometric muscle force, $f_l(\bar{l}_m(t))$ is the force-length relationship [26], $f_v(\bar{v}^m(t))$ is the force-velocity relationship [27], $\bar{b}^m$ is the normalized damping coefficient, $\bar{v}^m(t)$ is the instantaneous normalized muscle's velocity. $a(t)$ is the muscle activation [28], τ_{act} and τ_{deact} are the activation and deactivation time constants. k_v is a shape factor. $l^m(t)$ is the instantaneous muscle's length, $\bar{l}^m(t)$ is the normalized value with respect to the optimal muscle's length l_0^m, $l^t(t)$ is the instantaneous musculotendon length and l_s^t is the musculotendon length at rest. Note that the numerical values used in (10) are chosen based on the features of the force-velocity relationship such as curvature, maximum normalized force, etc. Additionally, all muscle tendons are assumed sufficiently stiff in this study. The muscle length $l^t(t)$ is computed as follows [29]:

$$l^m(t) = l^{mt}(t) - l_s^t \tag{11}$$

where l_s^t and $l^{mt}(t)$ are respectively the muscle tendon slack length and the instantaneous muscle tendon length that can be calculated by using the musculoskeletal model based on the anatomical data reported in [30,31].

Parametric Identification. From equations (7)-(11), the parameters F_{max}, l_0^m, l_s^t and ma_i need to be identified because they are characteristic variables of each wearer. Additionally, they need to be identified for all the muscles involved in the knee joint flexion and extension separately. Moreover, the muscle-tendon length l^{mt} and the moment arm ma_i are dependant of the knee joint angle θ. ma_i can be obtained from its relation with l^{mt}: $ma_i = \partial l^{mt}/\partial\theta$. A variable S_c

is used to scale these two parameters. A parameter's vector X is used to denote the parameters that need to be identified, as follows:

$$X_j = [l^t_{s_j},\ l^m_{0_j},\ F_{max_j},\ S_{c_j}], \quad j \in \{1, 2, 3, 4\} \tag{12}$$

Where j is the number of the muscle generating the knee joint flexion or extension.

The optimization formulation used to identify the parameters' vector is given by:

$$\text{minimize}(X) \quad \frac{1}{N_u}\sum_{i=1}^{N_u}(\tau_{he}(i) - \sum_{j=1}^{4} F_j^{mt}(i) r_j^{mt}(i))^2 \tag{13}$$

where τ_{he} is the torque generated by the wearer's lower limb estimated using (4) and N_u presents the number of the data group.

In the experiments, four EMG sensors from Delsys^{TM} are used to measure the muscular activities of the associated muscles. In order to process the raw EMG signals, a fourth-order recursive Butterworth filter with a cutoff frequency equal to 30 Hz is employed. After that, the full-wave rectified signals are filtered by a Butterworth low-pass filter with a 2 Hz cutoff frequency. At last, the parameters are optimized by the nonlinear least squares "Levenberg Marquardt" based algorithm offline. Concerning the other parameters, the activation muscular dynamics parameters τ_{act} and τ_{deact} are set to 0.02s and 0.06s respectively, v_{max} is set to $10l^m_0$, the muscle damping B^m is set to 0.1. A young healthy subject (Height=1.85 m, Weight=92 Kg, Sex=Male, Age=29 years old) was taken part in the experiment. The identified parameters' vector is given in Table 3. One can note that the identified parameters are close to those taken from the literature [30]. To verify the accuracy of the identified parameters, an experiment was performed to compare the estimated torque and the measured one. The compared results are shown in Fig. 2 and Fig. 3. One can note that the estimated torques coincide with the measured ones.

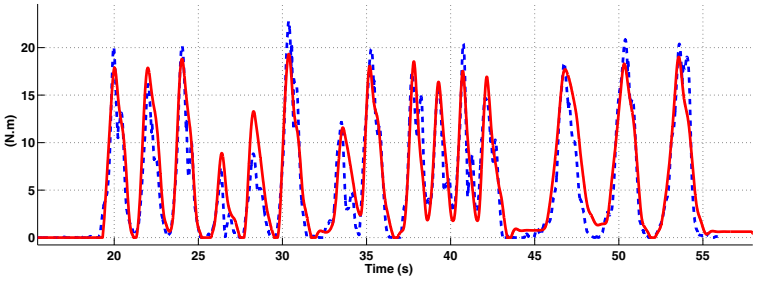

Fig. 2. Compared results of the quadriceps muscular torques: measured (continuous red line) and computed over the estimated quadriceps muscles parameters (dashed blue line) [1]

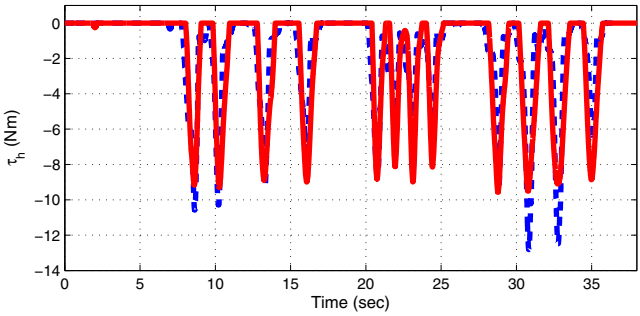

Fig. 3. Compared results of the quadriceps muscular torques: measured (continuous red line) and computed over the estimated quadriceps muscles parameters (dashed blue line) [1].

Table 3. Lower limb musculoskeletal parameters (−: Identified, ∗: [30]) [1]

Muscle		$l_0^m(cm)$	$l_s^t(cm)$	$F_{max}(N)$	S_c
RF	−	10	45.2	1314	1.33
	∗	8.4	34.6	780	1
VL	−	8.4	17.2	2050	1.02
	∗	8.2	15.7	1870	1
VM	−	8.24	12.3	1381	1.15
	∗	8.9	12.6	1295	1
VI	−	8.2	13.3	1318	1.14
	∗	8.7	13.6	1235	1
SM	−	7.2	37.9	1090	1.1
	∗	8	35.9	1030	1
ST	−	18.1	24.3	324	1.08
	∗	20.1	26.2	330	1
BL	−	10.7	30.7	694	1.07
	∗	10.9	34.1	720	1
BS	−	17.1	9.9	400	1.04
	∗	17.3	10	413	1

3 Control Strategies and Experimental Results

The passive rehabilitation consists of performing repetitive flexion and extension movements of the knee joint by a therapist or by means of a mechatronic device, without any intervention of the wearer. This kind of rehabilitation concerns people having been subjected to articular tissue injuries/surgical operations, spinal cord injuries or total knee arthroplasty. It can be performed as well for muscles strengthening. Its main advantages are the increase of the articulation range of motion, the reduction of its stiffness and the reinforcement of the muscles. The use of exoskeletons for this kind of applications can relax the therapist of hard repetitive motions and guarantees the execution of the rehabilitation sequences

in identical conditions. The passive rehabilitation is performed by driving the exoskeleton according to a desired trajectory considered defined by a therapist.

In [4,21], bounded control torques are developed by the exoskeleton's actuator. The bounded control avoids the saturation of the actuator and guarantees its functioning in linear regime. Therefore, the stability conditions are guaranteed for trajectories going sufficiently far from the equilibrium or when some external disturbances intervene which demands high power and torque to ensure the movement. In [21], the control is computed using the measurement of the knee joint angle delivered by the incremental encoder and the angular velocity derived numerically. The control torque bounded between $\pm\bar{\tau}$ is based on nested saturations and defined as:

$$\tau = -\text{sat}_{N_1}[k_1\dot{\theta} + \text{sat}_{N_2}(k_2\tilde{\theta})] + \tau_g \cos\theta + C(\theta_d - \theta_r), \tag{14}$$

Where $\text{sat}_{N_i}(\cdot)$, $i \in \{1, 2\}$, are classical saturation functions with N_i the saturation bounds chosen such that $N_1 > 2N_2 > 2A$. θ_d is the desired orientation and $\tilde{\theta} = \theta - \theta_d$ the orientation error. θ_r is the shank angle relative the horizontal axis at the rest position. k_1 and k_2 are positive scalar parameters. The saturation bound of the control torque (14) is $\bar{\tau} = N_1 + \tau_g + C\frac{\pi}{2}$. This control law ensures the asymptotic stability of the shank exoskeleton when the wearer does not deliver any complementary effort. Experimental tests have been performed on a healthy subject showing a good trajectory tracking with low values of angular velocity for flexion and extension movements defined by step functions (Fig. 4). The control law remains within the saturation bound fixed to 54 Nm. The absence of quadriceps (Rectus Femoris) and hamstrings (Biceps Femoris) muscle activities is plotted only to show the passivity of the user.

In [4], a bounded control torque based on the sum of saturation functions has been developed to ensure the passive rehabilitation. It is given by:

$$\tau = J\ddot{\theta}_d + A\text{sign}\dot{\theta}_d + B\dot{\theta}_d + C(\theta_d - \theta_r) + \tau_g \cos\theta - N_1 \tanh(k_1\vartheta) - N_2 \tanh(k_2\tilde{\theta}), \tag{15}$$

where N_1 and N_2 are saturation bounds, k_1 and k_2 are positive scalar parameters, ϑ is the filtered estimation of the angular velocity error $\tilde{\theta}$ of the knee joint defined by:

$$\vartheta = x + H\theta \tag{16}$$

$$\dot{x} = -H\vartheta - H\dot{\theta}_d \tag{17}$$

where x is an auxiliary variable and H is a positive scalar parameter. The control torque (15)-(17) ensures the asymptotic stability of the shank-exoskeleton system with a passive wearer. Experimental tests performed on a healthy subject are presented in Fig. 5 for a sine desired trajectory. Results show a good convergence of the knee joint angle with an accurate estimation of the angular velocity. The control law remains within the bounds. As for the previous case, the Rectus Femoris (quadriceps muscle) electromyographical activity is plotted only to show the passivity of the wearer.

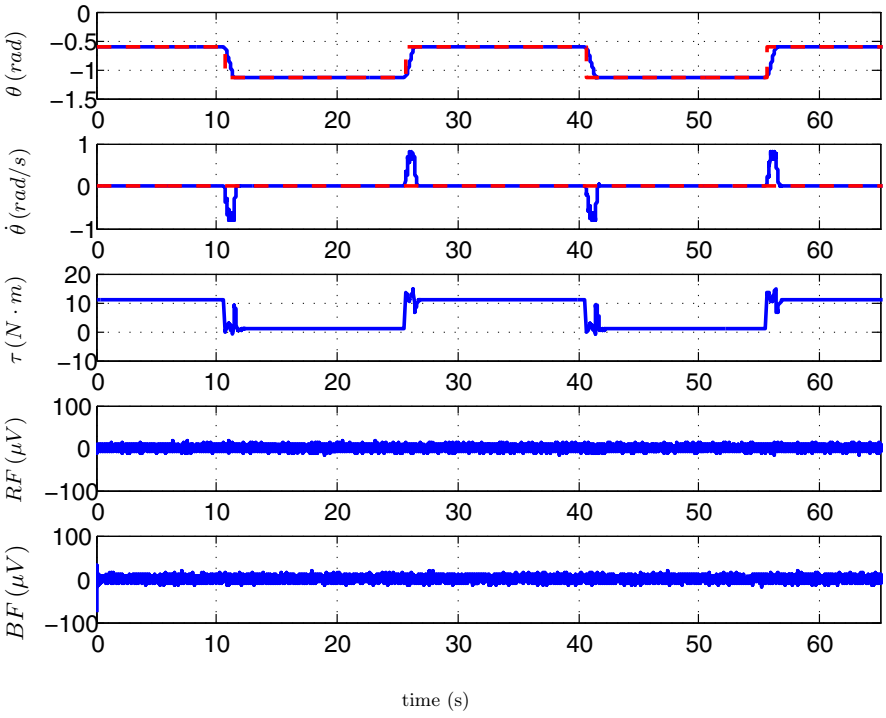

Fig. 4. Flexions and extensions using control law (14): The knee-joint angle, angular velocity, control torque, RF and BF muscle electromyographical activities. The current values are plotted in blue, the desired values in dashed red lines. No electromyographical activity of the Rectus Femoris (quadriceps muscle) and Biceps Femoris (hamstrings) is detectable [21].

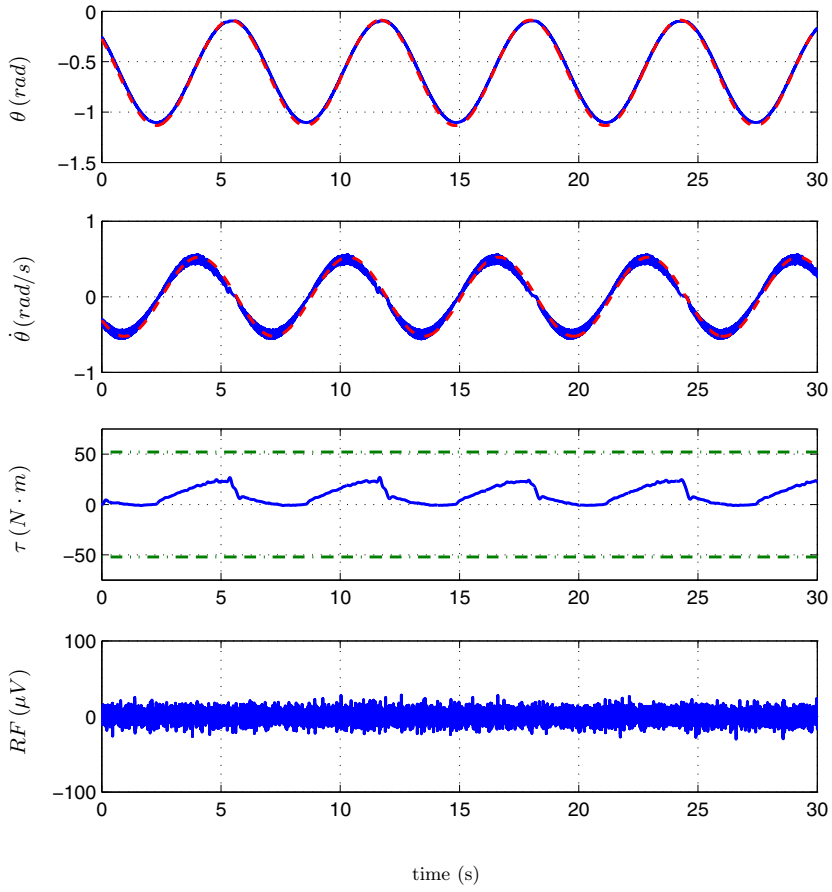

Fig. 5. Sine trajectory of the knee joint using control law (15)-(17): The knee-joint angle, estimated angular velocity, control torque and RF muscle electromyographical activity. The current values are plotted in blue, the desired values in dashed red lines. No electromyographical activity of the Rectus Femoris (quadriceps muscle) is detectable [4].

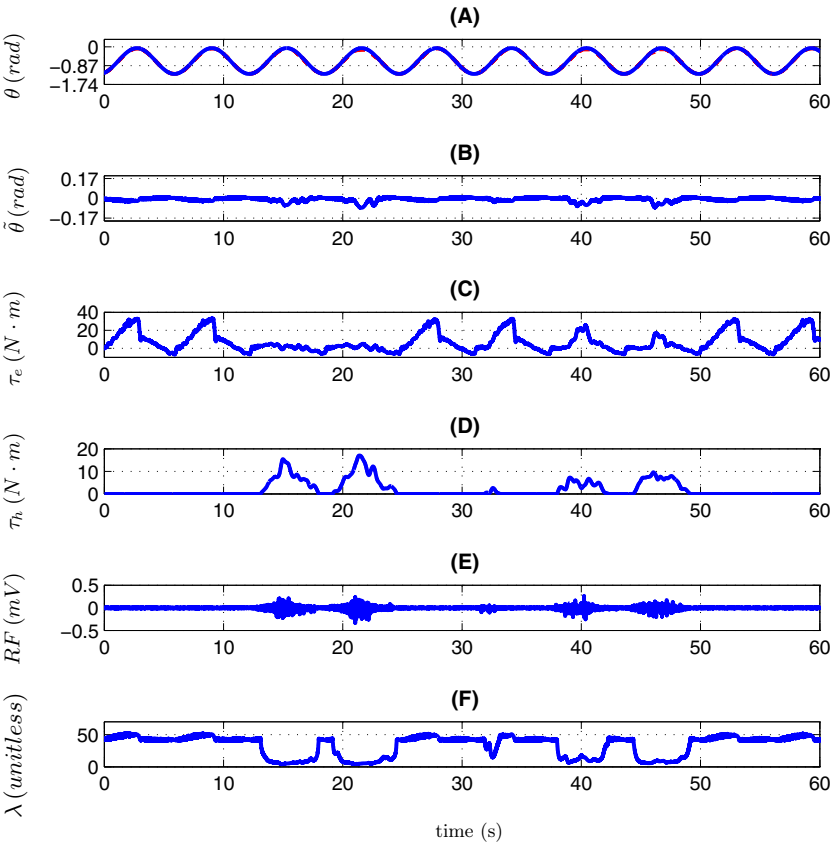

Fig. 6. Knee joint position (A), position tracking error (B), exoskeleton's torque (C), wearer's torque (D), rectus femoris EMG (E) and controller's gain parameter (F). In plot (A) current position value is plotted in blue line while the desired one is plotted in continuous red line.

In [1], an "assistance-as-needed" control strategy based on the human intention, estimated by means of EMG signals and a modified Hill muscular model, is developed. This strategy particularly applies to rehabilitation processes, since the assistance of the orthosis can be decreased with the improvement of the wearer's performance. In this paper, a passivity-based "assistance-as-needed" approach used particularly for nonlinear time-varying systems is employed [32]. A virtual error: $s = \dot{\tilde{\theta}} + \lambda\tilde{\theta}$, with $\tilde{\theta} = \theta - \theta_d$, $\dot{\tilde{\theta}} = \dot{\theta} - \dot{\theta}_d$, is introduced in this control strategy. θ and θ_d denote the current knee joint angle and desired one respectively, $\dot{\theta}$ and $\dot{\theta}_d$ the current and desired velocities. The control torque is defined as:

$$\tau_e = J(\ddot{\theta}_d - \dot{\lambda}\tilde{\theta} - \lambda\dot{\tilde{\theta}}) + B(\theta_d - \lambda\tilde{\theta}) + \frac{\partial E_p}{\partial\theta} - K_d s - \tau_h \tag{18}$$

Where

$$\lambda = \lambda_0 \frac{1 + K_1\|\tilde{\theta}\|}{1 + K_2\|\tau_h - \tau_{h,d}\|}$$

$$E_p = \frac{1}{2}C(\theta - \theta_r)^2 - \tau_g \cos(\theta - \theta_r)$$

Where θ_r is the knee joint angle at the shank rest position. $\tau_{h,d} = \sum_{j=1}^{8} F_{max,j} f_{d,j} r_j^{mt}$ is the wearer's passive damping torque and λ_0, K_d, K_1 and K_2 are the positive scalar parameters. Note that subtracting $\tau_{h,d}$ from τ_h in the expression of λ allows to account for the wearer's active efforts only. To verify the effectiveness of this control method, three main cases are tested in the experiments, as shown in Fig. 6. In the first one (0s–12s, 25s–32s), the subject is in a passive mode; a good trajectory tracking is shown. In the second one (12s–24s), the subject develops an important torque of 17Nm; the orthosis assistance torque is about 5Nm. In the third case (32s–49s), the subject develops a less important torque that does not exceed 9.5Nm; the orthosis assistance torque reaches 24Nm. The results show that this control strategy has high efficiency with different contributions of the wearer during the rehabilitation process.

4 Conclusions and Future Work

The chapter presents control strategies for the rehabilitation of the lower limb using an exoskeleton acting at the knee joint level. The models of i) the shank-foot-exoskeleton based on the system's Lagrangian and ii) the quadriceps/hamstrings muscles based on Hill-model have been presented. The parameters of the models have been identified using least square optimization. Two cases of rehabilitation have been studied: the first one concerns the passive rehabilitation without taking into account the user's intention and the second concerns the assistance-as-needed based on the user's intention determined by means of the EMG signal measurements. Experiments have been performed on a healthy subject. They have showed a good trajectory tracking for both cases of rehabilitation. They

have also showed the efficiency of the assistance-as-needed strategy by adapting the control developed by the exoskeleton function of the torque developed by the wearer.

Ongoing works concern the development of a model of a wearer-full lower limb exoskeleton during the performance of daily living activities, i.e. standing, standing-up, sitting down, walking, climbing stairs. The development of control laws allowing the assistance of the wearer will be also studied. The exoskeleton control will consider the wearer's intention to execute a task using some sensor measurements.

References

1. Hassani, W., Mohammed, S., Amirat, Y.: Real-time emg driven lower limb actuated orthosis for assistance as needed movement strategy. In: The 2013 Robotics: Science and Systems Conference, Berlin, Germany (2013)
2. Hassani, W., Mohammed, S., Rifai, H., Amirat, Y.: Emg based approach for wearer-centered control of a knee joint actuated orthosis. In: 2013 IEEE/RSJ International Conference on Intelligent Robots and Systems (IROS), pp. 990–995 (2013)
3. Pons, J.: Rehabilitation exoskeletal robotics. IEEE Engineering in Medicine and Biology Magazine 29(3), 57–63 (2010)
4. Lalami, M., Rifaï, H., Mohammed, S., Hassani, W., Fried, G., Amirat, Y.: Output feedback control of an actuated lower limb orthosis with bounded input. Industrial Robot: An International Journal 40(6), 541–549 (2013)
5. Jansen, C., Windau, J., Bonutti, P., Brillhart, M.: Treatment of a knee contracture using a knee orthosis incorporating stress-relaxation techniques. Physical Therapy 76(2), 182–186 (1996)
6. UHC: Mechanical stretching and continuous passive motion devices. Technical report, United Health Care Services, Inc. (2011)
7. De Rossi, S., Vitiello, N., Lenzi, T., Ronsse, R., Koopman, B., Persichetti, A., Vecchi, F., Ijspeert, A., Van der Kooij, H., Carrozza, M.: Sensing pressure distribution on a lower-limb exoskeleton physical human-machine interface. Sensors 11(1), 207–227 (2010)
8. Pratt, J., Krupp, B., Morse, C., Collins, S.: The roboknee: an exoskeleton for enhancing strength and endurance during walking. In: 2004 IEEE International Conference on Robotics and Automation, vol. 3, pp. 2430–2435 (2004)
9. Rosen, J., Brand, M., Fuchs, M., Arcan, M.: A myosignal-based powered exoskeleton system. IEEE Transactions on Systems, Man, and Cybernetics 31(3), 210–222 (2001)
10. Fleischer, C., Hommel, G.: A human-exeskeleton interface utilizing electromyography. IEEE Transactions on Robotics 24(4), 872–882 (2008)
11. Sawicki, G., Gordon, K., Ferris, D.: Powered lower limb orthoses: applications in motor adaptation and rehabilitation. In: 9th International Conference on Rehabilitation Robotics (ICORR), pp. 206–211 (2005)
12. Kiguchi, K., Iwami, K., Yasuda, M., Watanabe, K., Fukuda, T.: An exoskeletal robot for human shoulder joint motion assist. IEEE/ASME Transactions on Mechatronics 8(1), 125–135 (2003)
13. Rosen, J., Fuchs, M., Arcan, M.: Performances of hill-type and neural network muscle models - toward a myosignal-based exoskeleton. Computers and Biomedical Research 32(5), 415–439 (1999)

14. Khokhar, Z., Xiao, Z., Menon, C.: Surface emg pattern recognition for real-time control of a wrist exoskeleton. Biomedical Engineering Online 9(1), 41 (2010)
15. Nikitczuk, J., Weinberg, B., Mavroidis, C.: Control of electro-rheological fluid based resistive torque elements for use in active rehabilitation devices. Smart Materials and Structures 16(2), 418 (2007)
16. Suzuki, K., Mito, G., Kawamoto, H., Hasegawa, Y., Sankai, Y.: Intention-based walking support for paraplegia patients with robot suit hal. Advanced Robotics 21(12), 1441–1469 (2007)
17. Mefoued, S., Mohammed, S., Amirat, Y.: Toward movement restoration of knee joint using robust control of powered orthosis. IEEE Transactions on Control Systems Technology 21(6), 2156–2168 (2013)
18. Kiguchi, K., Tanaka, T., Fukuda, T.: Neuro-fuzzy control of a robotic exoskeleton with emg signals. IEEE Transactions on Fuzzy Systems 12(4), 481–490 (2004)
19. Zhang, J., Yang, C.J., Chen, Y., Zhang, Y., Dong, Y.: Modeling and control of a curved pneumatic muscle actuator for wearable elbow exoskeleton. Mechatronics 18(8), 448–457 (2008)
20. Rifai, H., Mohammed, S., Daachi, B., Amirat, Y.: Adaptive control of a human-driven knee joint orthosis. In: 2012 IEEE International Conference on Robotics and Automation (ICRA), pp. 2486–2491 (2012)
21. Rifai, H., Mohammed, S., Hassani, W., Amirat, Y.: Nested saturation based control of an actuated knee joint orthosis. Mechatronics 23(8), 1141–1149 (2013)
22. Winter, D.: Biomechanics and motor control of human movement. John Wiley & Sons (2009)
23. Damiano, D., Laws, E., Carmines, D., Abel, M.: Relationship of spasticity to knee angular velocity and motion during gait in cerebral palsy. Gait & Posture 23(1), 1–8 (2006)
24. Swevers, J., Ganseman, C., Tukel, D.B., De Schutter, J., Van Brussel, H.: Optimal robot excitation and identification. IEEE Transactions on Robotics and Automation 13(5), 730–740 (1997)
25. Sartori, M., Lloyd, D.G., Reggiani, M., Pagello, E.: A stiff tendon neuromusculoskeletal model of the knee. In: 2009 IEEE Workshop on Advanced Robotics and its Social Impacts (ARSO), pp. 132–138 (2009)
26. Thelen, D.: Adjustment of muscle mechanics model parameters to simulate dynamic contractions in older adults. Journal of Biomechanical Engineering 125(1), 70–77 (2003)
27. Schutte, L.: Using musculoskeletal models to explore strategies for improving performance in electrical stimulation-induced leg cycle ergometry. PhD thesis, Stanford University (1992)
28. Yamaguchi, G.: Dynamic modeling of musculoskeletal motion: a vectorized approach for biomechanical analysis in three dimensions. Springer (2005)
29. Zajac, F.: Muscle and tendon: properties, models, scaling, and application to biomechanics and motor control. Critical Reviews in Biomedical Engineering 17(4), 359–411 (1988)
30. Arnold, E., Ward, S., Lieber, R., Delp, S.: A model of the lower limb for analysis of human movement. Annals of Biomedical Engineering 38(2), 269–279 (2010)
31. Delp, S., Loan, J., Hoy, M., Zajac, F., Topp, E., Rosen, J.: An interactive graphics-based model of the lower extremity to study orthopaedic surgical procedures. IEEE Transactions on Biomedical Engineering 37(8), 757–767 (1990)
32. Ortega, R., Loria, A., Nicklasson, P., Sira-Ramirez, H.: Passivity-based con-trol of Euler-Lagrange systems: mechanical, electrical and electromechanical applications. Springer London Ltd. (1998)

Mechatronic Considerations for Actuation of Human Assistive Wearable Robotics: Robust Control of a Series Elastic Actuator

Kyoungchul Kong[1], Joonbum Bae[2], and Masayoshi Tomizuka[3]

[1] Department of Mechanical Engineering, Sogang University, Korea
[2] School of Mechanical and Advanced Materials Engineering, UNIST, Korea
[3] Department of Mechanical Engineering,
University of California, Berkeley, CA, USA

Abstract. To realize ideal force control of robots that interact with a human, a very precise actuating system with zero impedance is desired. For such applications, a rotary series elastic actuator (RSEA) has been introduced recently. This chapter presents the design of RSEA and the associated control algorithms. To generate joint torque as desired, a torsional spring is installed between a motor and a human joint, and the motor is controlled to produce a proper spring deflection for torque generation. When the desired torque is zero, the motor must follow the human joint motion, which requires that the friction and the inertia of the motor be compensated. The human joint and the body part impose the load on the RSEA. They interact with uncertain environments and their physical properties vary with time. In this chapter, the disturbance observer method is applied to make the RSEA precisely generate the desired torque under such time-varying conditions. Based on the nominal model preserved by the disturbance observer, feedback and feedforward controllers are optimally designed for the desired performance: i.e. the RSEA 1) exhibits very low impedance and 2) generates the desired torque precisely while interacting with a human. The effectiveness of the proposed design is verified by experiments.

Keywords: Rotary series elastic actuator, Disturbance observer, Force mode control, Human-robot interaction, Motor impedance.

1 Introduction

Mechatronics technologies play significant roles in applications that improve quality of life. Active assistive devices, such as motorized wheel chairs or active prosthetics, are some of examples. They have improved the mobility of many people with disabilities, which allowed them to engage their everyday lives with much less difficulties. In the last decade, power assistive devices based on mechatronic technologies are being developed in the form of wearable robots for assisting physically impaired people or for augmenting human power.

Fig. 1 shows the basic structure of an assistive robot interacting with a human. The human body ((a) in the figure) is the plant to be controlled. The

S. Mohammed et al. (eds.), *Intelligent Assistive Robots,*
Springer Tracts in Advanced Robotics 106, DOI: 10.1007/978-3-319-12922-8_16

body is actuated by the muscles which are controlled by the brain. Since the desired motion is intrinsically generated in the brain by intention or reflex, the human has a fully closed control loop with no external input. If a human has either nervous or muscular disorders, or needs extra forces to perform demanding work, an assistive robot ((d) in Fig. 1) may provide additional forces (τ_A) to the human body. Recently, various assistive robots have been developed: Sankai developed HAL (Hybrid Assistive Limb) for augmenting power of normal persons [1], [2], and Kazerooni introduced BLEEX (Berkeley Lower Extremity Exoskeleton) for military applications [3], [4]. Yamamoto developed Power Assist Suit to assist nurses lifting heavy patients [5], and Kong and Jeon introduced EXPOS (Exoskeleton for Patients and Old people by Sogang University) for weakened persons [6], [7].

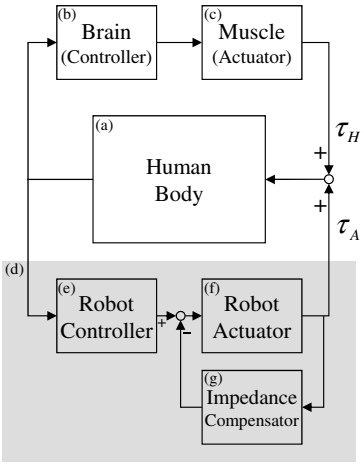

Fig. 1. Conceptual structure of an assistive robot interacting with a human

Many approaches also have been proposed for the controller ((e) in Fig. 1) and the actuator ((f) in the figure). The main role of the controller in this application is to determine the magnitude and the direction of forces for interacting with a human (e.g. assistive forces or feedback forces for rehabilitation). Since it is impossible to directly detect the human intention, the controller usually sets the references for the assistive forces based on the estimated values obtained by the biological sensors [1], [5], [7] or the dynamical properties [3], [8]. For examples, HAL applies EMG (electromyography) sensors to measure muscular efforts [1], and BLEEX calculates the required forces based on the inverse dynamics method [3]. Power Assist Suit applies a novel sensor called the muscle hardness sensor [5]. Since these methods are for estimation of human joint torques during motions, they are usually utilized for assisting healthy/intact people. In applications for patients, an impedance control method [9], [10], [29] is often used. In this case,

a motion trajectory for a patient is predefined for the purpose of rehabilitation [9], and a robot assists the patient to follow the desired motion [9]-[11].

Controllers for human-robot interaction may assume that actuators are operated in an ideal force (or torque) mode control. The ideal force mode implies: 1) the actuator has (output shaft) zero impedance so that it is perfectly backdrivable, and 2) the force (torque) output is exactly proportional to the control input. Researchers have tried to find such actuators for human-robot interaction. For examples, HAL applies DC motors [1], [2], and BLEEX utilizes hydraulic actuators [4]. Power Assist Suit uses pneumatic actuators [5]. EAP (Electroactive Polymer) and rubber-muscle actuators also have been developed recently [12], [13]. In spite of these efforts, lack of a suitable actuator is still evident in the applications involving human-robot interaction. Recently, progresses have been made to overcome the problems encountered in actuators such as friction and rotor inertia by applying an algorithmic compensator [see (g) in Fig. 1]. For example, Buerger and Hogan introduced the complimentary stability and loop shaping method to design the compensator computationally [14]. From the viewpoint of hardware as well as controller designs, series elastic actuators are noteworthy [15]-[21]. In these cases, a spring is installed between an actuator and a human joint and plays the role of an energy buffer as well as a force sensor. The force is generated from the differential position or the deflection of the spring, which is controlled by a position controller [15], [16]. This implies that the impedance compensator in Fig. 1 is accomplished based on a position control method. The spring isolates the human joint from undesired factors of the motor including rotor inertia and nonlinearities. However, it also introduces challenges to the design of a control algorithm. For example, mechanical compliance in the actuation does not offer only advantages without costs. Also, the lower the stiffness, the lower the frequency with which larger output forces can be modulated. Due to the interaction with a human, dynamic characteristics of the whole system is time varying. Therefore, the performance of such actuators is determined by how the control algorithm robustly controls the spring deflection under the time-varying conditions. Namely, the controller of actuators for human-robot interaction should meet the following performance objectives:

1. it reduces mechanical impedance of the actuator by compensating for the inertia and the friction of the actuator,
2. it makes the actuator precisely generate the torque as desired, and
3. it guarantees the robust performance of the actuator while interacting with a human.

In this chapter, the design of controllers for a rotary series elastic actuator (RSEA) is discussed. To assure the robust performance of the RSEA, a disturbance observer is utilized as well as the feedback and feedforward controllers.

This chapter is organized as follows. The basic properties and problems of a geared motor are reviewed in section 2. Hardware design of a RSEA is discussed in section 3. In section 4, a robust control algorithm for the RSEA is designed and its properties are analyzed. The designed control algorithm is evaluated by experiments in section 5. Summary and conclusions are given in section 6.

2 Open Loop Torque Mode Control of Geared DC Motor

Motors have been widely used in applications involving human-robot interaction due to their superior controllability and flexibility. The capacity of a motor is defined by the maximum allowable power, i.e. a multiplication of the angular velocity and the generated torque. Since a motor has physical limitations on the maximum velocity and the maximum torque, the operation range is adjusted by a reduction ratio. The use of reducers introduces various nonlinearities such as friction and backlash. The generated torque is magnified by the reduction ratio, but the rotor inertia and the friction force are also amplified significantly.

Motor impedance, or mechanical impedance, represents a measure of how much the motor resists motion when subjected to a given force. Mathematically, it is defined as the ratio of the force applied to the mechanical system to the resulting velocity of the system, i.e.

$$Z(\omega) = \frac{f(\omega)}{v(\omega)} \tag{1}$$

where $Z(\omega)$ is the motor impedance, $f(\omega)$ is the resistive force, and $v(\omega)$ is the velocity. $f(\omega)$ consists of the following terms:

$$f(\omega) = f_{friction}(\omega) + f_{damping}(\omega) + f_{inertia}(\omega) + f_{bias}(\omega) + \Delta f(\omega) \tag{2}$$

where $f_{friction}(\omega)$ is the coulomb friction force which increases the motor impedance in the low frequency range. $f_{damping}(\omega)$ represents the linear damping force and increases the motor impedance over the entire frequency range. $f_{inertia}(\omega)$ is resulted from Newton's second law, and increases the impedance in the high frequency range. $f_{bias}(\omega)$ is the bias value of force output and $\Delta f(\omega)$ represents forces due to other factors.

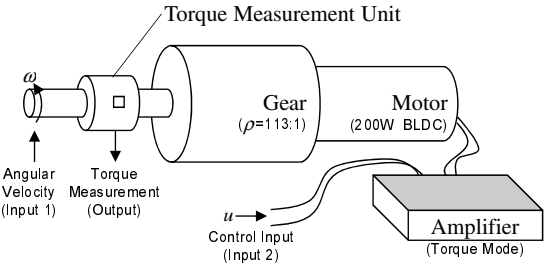

Fig. 2. Experimental setup for motor impedance test

For most dynamic systems such as industrial robots and machining tools, the mechanical impedance of an actuator should be sufficiently large for a large frequency bandwidth and effective rejection of disturbances [22]. For example, an actuator for a machine tool must be insensitive to any applied disturbance forces

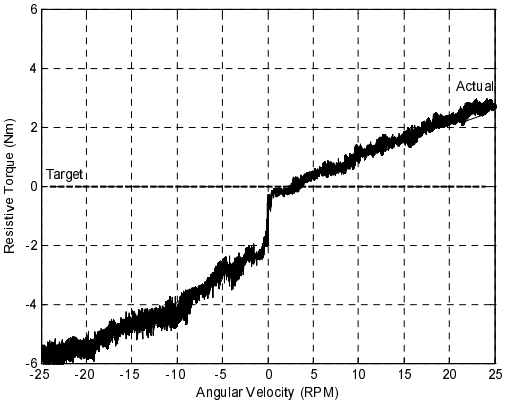

Fig. 3. Motor impedance test: the control input is fixed to zero

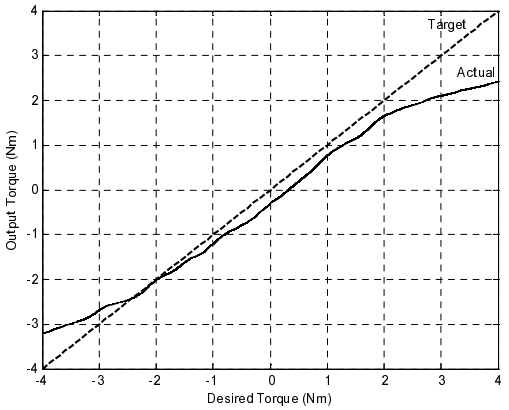

Fig. 4. Linearity test: the angular velocity is fixed to zero

for the best quality of products. However, this paradigm is no longer applied to applications interacting with a human. The most important factor of actuators in such applications may be the comfort of a human, i.e. the actuator should not resist the human motion and generate only the desired force. In other words, the actuators for human-robot interaction must have low mechanical impedance [9], [14]. This requirement creates challenges to the selection of actuators. To realize the ideal actuator, every term in (2) should be eliminated. Also, the large frequency bandwidth is no longer an issue as long as they have the bandwidth up to the frequency range of human motions which is about $4 \sim 8Hz$.

Fig. 2 shows an experimental setup for testing the mechanical impedance of a DC motor. The output torque was measured by a torsional spring. The detailed information on the spring used in this chapter will be discussed in section 3. Ideally, the torque sensor in Fig. 2 should read zero regardless of the angular velocity when the control input is zero [see Target line in Fig. 3]. However, due to the friction force and the rotor inertia of the actual device, the torque sensor reads the resistive torque in actual experiments [see Actual line in Fig. 3]. The experiment in Fig. 3 was performed for testing the relationship between the resistive torque and the angular velocity while the control input is zero. Note that the magnitude of the bias force was so large that the motor rotates even with zero input. This phenomenon often occurs in the applications of DC motors. This problem can be solved by fine tuning the amplifier. However, the default setting was used in the experiment to test in normal conditions. The discontinuity at $\omega = 0$ represents the static friction force. In addition, the motor has nonlinearities related to the control input. Fig. 4 shows the result of the linearity test about the control input u when the rotor was fixed mechanically (i.e. $\omega = 0$). To observe the linearity excluding the static friction effects, the curve in Fig. 4 was obtained by taking the average of many experimental data. In the ideal case, the curve in Fig. 4 should be a straight line which passes through the origin [see Target line in the figure]. However, the actual profile obtained is a nonlinear curve which does not pass through the origin [see Actual line in the figure]. The undesired characteristics (i.e., the damping, Coulomb friction, and input-output nonlinearity) discussed with Figs. 3 and 4 should be eliminated to realize the ideal human-robot interaction.

3 Rotary Series Elastic Actuator

3.1 Hardware Configuration

An actuator interacting with a human may be a burden to the human body because of its mass and friction. For ideal human -robot interaction, the actuator should be controlled in the force (or torque) mode [9], [10], [17], [19]. In reality, however, most actuation systems do not generate the desired torque precisely as discussed in the previous section. Another problem occurs when the desired force is less than the friction of the actuator.

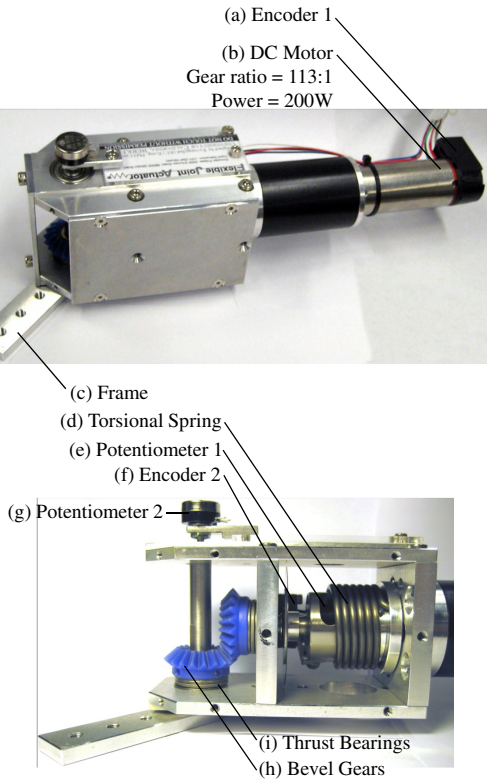

Fig. 5. Rotary series elastic actuator

To compensate for the resistive forces, force sensors such as a loadcell and a strain-gauge are often installed at the load side of a rigid reducer [23], [24]. The motor is feedback controlled by the force measurements. This method has shown good performances in industrial applications involving force mode actuation [23], [24]. However, it is not suitable for the applications of human-robot interaction, since the rigidity of the reducer may cause discomfort or even damage to the user. For such applications, it may be better to have compliance in the reducer such that a human does not feel the resistance when he/she initiates motions.

A solution to this problem is to utilize a mechanism which may serve as a buffer between the actuator and the human joint. For example, in power management of an automobile a clutch mechanism serves as the buffer to connect the engine and varying load due to vehicle motion and environment. Similarly, in actuators of robots interacting with human, a spring serves as the buffer. The actuator is controlled such that the spring between a human joint and the actuator has proper deflection. Now we have two sub-systems: the human body and the actuation system, where the mechanical power for interacting with the human is transferred through a spring.

An actuating system with a torsional spring is called a rotary series elastic actuator (RSEA). The similar approach is shown in [15], [17]-[21] where it applies a linear spring for the same purpose. If the linear spring is used, the structure of the actuator system is similar to that of a muscle. However, it requires torque arms for generating the joint torque. In the design of RSEA, a torsional spring is directly installed between a human joint and a motor such that it can generate the joint torque uniformly over the entire angular range. A RSEA consists of a DC motor, a spring and two encoders as shown in Fig. 5. The position of the DC motor is controlled to have the desired spring deflection such that the RSEA generates the desired torque precisely. Since the human joint angle is required to determine the desired spring deflection or the reference position of the motor, an additional encoder ((f) in Fig. 5) is installed. The joint angle is limited by the angle limiter to protect the patient in case of a malfunction. The overall design is shown in Fig. 5.

3.2 Spring Selection

Since the spring is utilized as a torque sensor as well as a torque generator, the performance of RSEA depends on characteristics of the spring. For example, the maximum torque of RSEA is determined by stiffness of the spring. If the spring is too stiff, however, a human may feel discomfort. Therefore, the spring should be optimally designed considering both the maximum torque and the control performance of the motor.

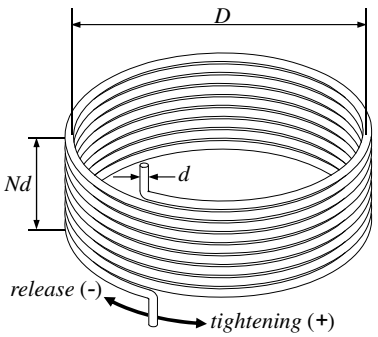

Fig. 6. Design of a torsional spring

Fig. 6 shows the mechanical design of a torsional spring installed in the RSEA ((d) in Fig. 5). The spring constant is determined by D, d, N in Fig. 6 and the elastic modulus of the material [25]. The specific parameters are shown in Table. 1. The desired maximum deflection was determined by considering the encoder resolutions.

Table 1. Specification of a torsional spring

Specification	Values
Encoder resolution of motor side	56500 counts/rev. (encoder resolution: 500 counts/rev. gear ratio: 113:1)
Encoder resolution of human side	2000 counts/rev.
Desired maximum deflection	±25 degrees
Desired maximum torque	±6 Nm
Mean diameter of spring D	33 mm
Wire diameter d	5 mm
Number of turns N	6
Measured spring constant k	0.32 Nm/deg

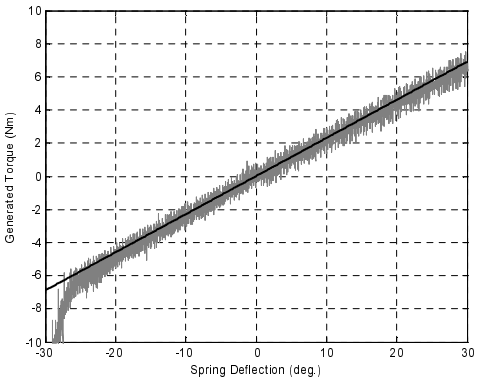

Fig. 7. Experimental result of deflection angle of the spring and generated torque

In general, a spring is a nonlinear element: i.e. the spring force is a nonlinear function of the spring deflection. Since the generated torque is estimated by the spring deflection in this application, the nonlinearity may affect the control performance, i.e. the generated force may be different from the estimated torque. To check the nonlinearity of the spring, an experiment was performed. The body of RSEA was fixed on the ground such that the frame ((c) in Fig. 5) presses a loadcell for measurement of the generated force. The force is converted into the torque by multiplying the torque arm, i.e. the length of the frame. Fig. 7 shows the experimental results of the relation between the spring deflection and the measured torque. It is desired that the curve is a straight line that passes through the origin. As shown in the figure, the spring used in the experiment shows very good linearity in the desired deflection range. The stiffness blows up at a certain deflection angle [see -25 degrees in the figure] because the spring is mechanically constrained. Since the relation shown in the figure is close to linear in the desired deflection range, the spring is regarded as a linear element in this chapter.

4 Controller Design for Rotary Series Elastic Actuator

4.1 System Modeling

A RSEA installed on a human joint is depicted in Fig. 8, where I_H and C_H are the inertia and the damping coefficient of human joint, and I_M and C_M are those of the geared motor, respectively. Since I_H and C_H are different from person to person and from segment to segment, they are treated as unknown parameters in this chapter. The motor and the human joint are connected via a torsional spring with spring constant k. τ_H and τ_M represent the human muscular torque and the motor torque, and θ_H and θ_M are the angle of the human joint from the neutral position and that of the motor respectively. The neutral position of a human body segment is not necessarily the vertical axis (e.g. feet). A RSEA can be modeled as a multi-input and multi-output system where inputs are the actuator torque and the muscular torque, and outputs are the actuator angle and the human joint angle. The controlled output is the spring torque which is proportional to the spring deflection, i.e. the difference between the actuator and the human joint angle.

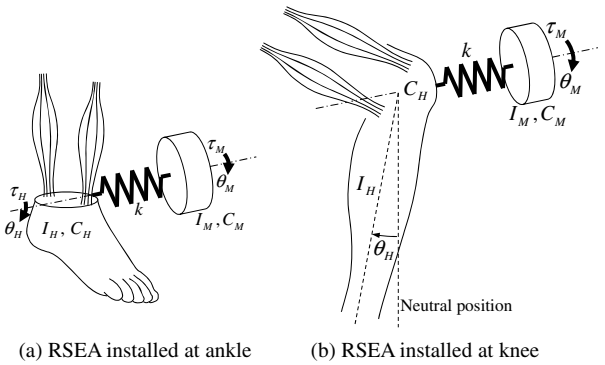

(a) RSEA installed at ankle (b) RSEA installed at knee

Fig. 8. Schematic plots of human joints and rotary series elastic actuators

By Hooke's law, the torque output, τ_A, of the RSEA is

$$\tau_A = k(\theta_M - \theta_H) \tag{3}$$

Subscript A denotes that the quantity represents the assistive torque to human. Based on (3), the desired position of the motor is expressed as a function of the desired torque, i.e.

$$\theta_{M,Desired} = \theta_H + \frac{\tau_{A,Desired}}{k} \tag{4}$$

Note that if the motor tracks the desired position exactly, i.e., $\theta_M = \theta_{M,Desired}$, then the RSEA exactly generates the desired torque rejecting every undesired factor such as friction. Therefore, a precision control algorithm may improve the

performance of RSEA. In (3) and (4), the spring is assumed to be linear. In the case of a nonlinear spring, the inverse of the describing function should be used in (4) instead of the use of the inverse of the spring constant.

The governing equation for the system in Fig. 8 is

$$\begin{bmatrix} I_M & 0 \\ 0 & I_H \end{bmatrix} \ddot{\Theta} + \begin{bmatrix} C_M & 0 \\ 0 & C_H \end{bmatrix} \dot{\Theta} + \begin{bmatrix} k & -k \\ -k & k \end{bmatrix} \Theta = \begin{bmatrix} \tau_M \\ \tau_H - mgl\sin(\theta_H) \end{bmatrix} \tag{5}$$

where, Θ is $[\theta_M \ \theta_H]^T$, m is the mass of human body segment, g is the gravity constant, and l is the distance between joint and center of mass of body segment. The dynamic equation assumes that there is no constraint imposed on either the motor or the human joint. However, the joint is subjected to constraints during some motion phases. For example, if the foot is touching the ground, it may be reasonable to assume that the human side of the spring is grounded as shown in Fig. 9(b). In this case, (5) no longer applies. Thus the human joint actuation system requires multiple dynamic models for complete description of its dynamic behavior. A possible approach to handle such a system is the discrete event system approach. In this chapter, we explore an approach to design a controller for a nominal model. Actual dynamics is regarded as perturbed dynamics.

Assume that there is a relation between the motor angle and the spring deflection, i.e.

$$\frac{E(s)}{\theta_M(s)} = \alpha(s) \tag{6}$$

where $E(s) = [\theta_M(s) - \theta_H(s)]$. $\alpha(s)$ is obtained by setting $\tau_H = 0$ in (5) which assumes that the human force is an external disturbance, i.e.

$$\alpha(s) = \frac{I_H s^2 + C_H s + mgl}{I_H s^2 + C_H s + k + mgl} \tag{7}$$

where $\sin(\theta)$ has been approximated by θ for simple analysis. If τ_H controls the human joint motion, the inertia that the motor sees, I_H, is increased significantly. If actual external forces are imposed on the human body (e.g. ground contact forces in feet), the effective inertia is also increased. In these cases, I_H in (7) is not the pure inertia of the human body segment, but the effective inertia imposed on the RSEA. Namely, $\alpha(s)$ is a transfer function resulted from human-robot interaction which is unknown and time-varying. By multiplying the spring constant k on both sides of (6), the relation between the motor angle and the spring torque is obtained from (3) as

$$\tau_A(s) = kE(s) = k\alpha(s)\theta_M(s) \tag{8}$$

By Newton's third law, the spring torque is exerted to the motor system as well as the human body. Therefore, the dynamics of the motor part is

$$I_M\ddot{\Theta}_M + C_M\dot{\Theta}_M = \tau_M(t) - \tau_A(t) \tag{9}$$

Combining (8) and (9), a transfer function from τ_M to θ_M is obtained as

$$\Psi(s) = \frac{1}{I_M s^2 + C_M s + \alpha(s)k} \tag{10}$$

$\Psi(s)$ represents a possible model set of the RSEA. Note that the model is time-varying as $\alpha(s)$ changes due to human-robot interaction. Fig. 9 shows two extreme cases.

Case 1

Case 1 in Fig. 9 applies during swinging of a leg. During the swing motion of the normal gait, the movements of ankle and knee joints are large. In this case, it is a reasonable assumption that the joint motion is mainly resulted from the gravity and the assistive torque, and the transfer function from $\tau_M(s)$ to $\theta_M(s)$ is

$$P_1(s) = \frac{1}{I_M s^2 + C_M s + \alpha(s)k} \in \Psi(s) \tag{11}$$

where $\alpha(s)$ is given by (7) and its magnitude depends on the physical properties of human body segments. In this case, I_H in $\alpha(s)$ represents the pure inertia of a human body segment.

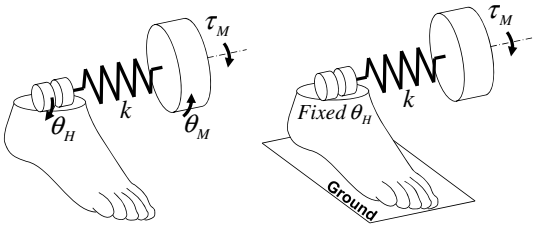

(a) *Case 1* (b) *Case 2*

Fig. 9. Two possible cases of human joint

Case 2

During the stance phase of the normal gait and standing up motion, the movements of ankle and knee joints are slow while the required joint torque is large. Therefore, the motion of the actuator is much larger than that of the human joint. Moreover, since the body segment is grounded, a constraint is imposed on the human joint. This may be regarded as a significant increase of I_H in (7), i.e. $I_H \gg 1$, which results in $\alpha(s) \approx 1$, i.e.

$$P_2(s) = \frac{1}{I_M s^2 + C_M s + k} \in \Psi(s) \tag{12}$$

Fig. 10 shows the frequency responses of the two cases mentioned above with reasonable physical values of the ankle joint. Since P_2(s) in (12) has the minimum order in the possible model set and does not require properties of human body which are usually difficult to measure, the transfer function of (12) is used as a nominal model in this chapter.

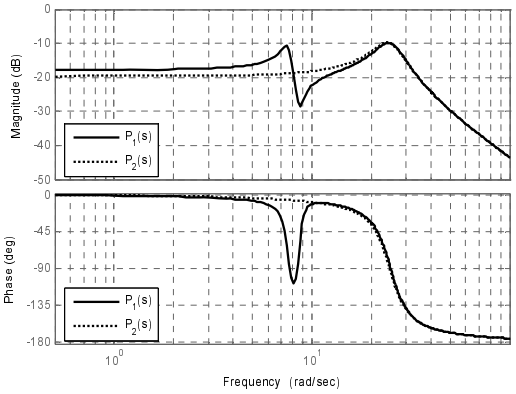

Fig. 10. Frequency responses of *Case 1* and *Case 2*: $P_1(s)$ and $P_2(s)$ are as defined by (11) and (12).

4.2 Force Feedback Control

To improve the tracking performance, a feedback control algorithm is required. For the design of the controller, the control loop is reconfigured as shown in Fig. 11. In the figure, E_D represents the desired spring deflection calculated by (3). The aim of the controller ($C(s)$ in the figure) is to maintain the desired spring deflection regardless of the variations of the system model. Since the spring deflection is directly related to the generated force (torque), the control system in Fig. 11 can be regarded as a force feedback system where the force is estimated by the spring deflection.

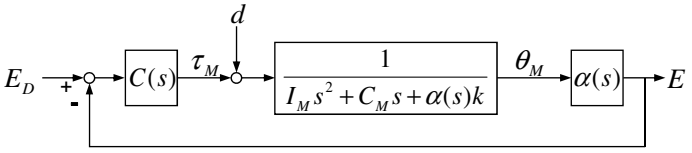

Fig. 11. Block diagram of the Joint Controller: The desired deflection E_D is obtained by (3) and d represents the exogenous disturbances.

Fig. 12 shows the location of poles and zeros of the open loop transfer function from τ_M to E in Fig. 11. By increasing I_H in $\alpha(s)$, poles and zeros converge to the points labeled (d) in Fig. 12. Note that there is a weakly damped complex pole-zero pair and the pair moves towards the imaginary axis as I_H is increased. As I_H approaches infinity, they asymptotically cancel each other, and the open loop transfer function is asymptotic to (12).

A simple and effective controller is a PD (Proportional- Derivative) controller. If the zero of the PD controller is fixed, the closed loop poles shift as shown in

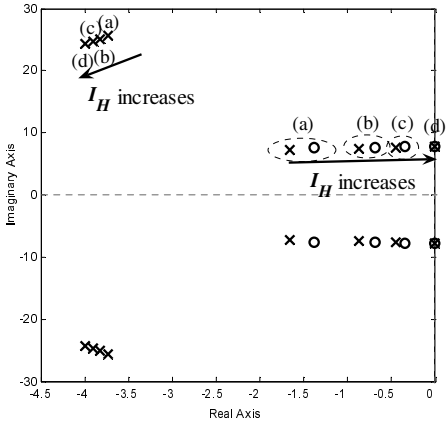

Fig. 12. Poles and zeros of the open loop transfer function: (a), (b), (c) and (d) apply for the ankle joint of the $50\%^{ile}$ female, the knee joint of the $50\%^{ile}$ female, the knee joint of the $50\%^{ile}$ male and the constrained joint respectively.

Table 2. Properties of human body segments used in Fig. 12 [26]

Human Body Segment	Moment of Inertia I_H (kgm^2)
Foot of the $50\%^{ile}$ female	0.027
Foot and shank of the $50\%^{ile}$ female	0.459
Foot and shank of the $50\%^{ile}$ male	0.660

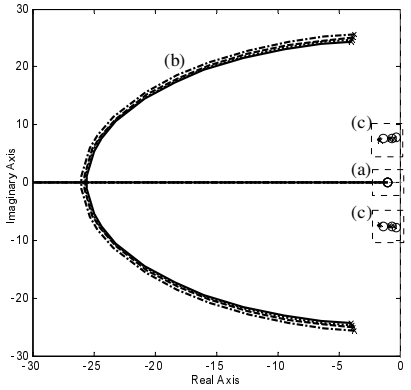

Fig. 13. Root loci applying the PD controller: Arrows indicate increasing control gains for a fixed P-D gain ratio

Fig. 13 for the varying control gain from 0 to ∞. As the gain of the PD controller is increased from zero, the closed loop poles on the branch (b) in Fig. 13 move away from the imaginary axis and move toward the real axis which means that the response becomes faster and less vibratory. If the gain is excessively large, a real pole moving toward the origin will slow down the response speed. As mentioned already, the open loop poles and zeros defining branch (c) in Fig. 13 are very close to each other, and they minimally influence the closed loop transfer function.

More quantitative way to tune the PD control gains is to apply the LQ (Linear Quadratic) method. The LQ method is applicable when the nominal model in (12) is expressed in the state space. Moreover, if the state consists of position and velocity in the second order model case, the LQ method provides the optimal PD gains. In the case of $P_2(s)$ in (12), the state space model is expressed as

$$\begin{bmatrix} \ddot{\theta} \\ \dot{\theta} \\ \theta_M \end{bmatrix} = \left[\begin{array}{cc|c} -\frac{C_M}{I_M} & -\frac{k}{I_M} & \frac{1}{I_M} \\ 1 & 0 & 0 \\ \hline 0 & 1 & 0 \end{array}\right] \begin{bmatrix} \dot{\theta} \\ \theta \\ \tau_M \end{bmatrix} \tag{13}$$

where $\dot{\theta}$ and θ define the state, τ_M is the input, and θ_M is the output.

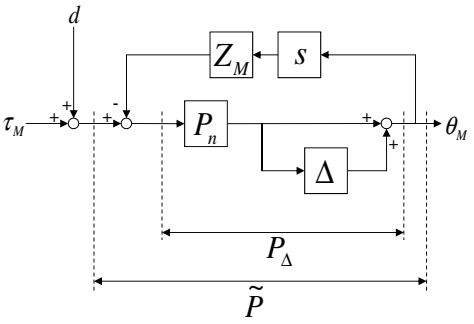

Fig. 14. Representation of actual actuator

The LQ performance index is

$$J = \int_0^\infty \left[\theta_M^2(t) + R\tau_M^2(t)\right] dt = \int_0^\infty \left[\begin{bmatrix} \dot{\theta} \\ \theta \end{bmatrix}^T C^T C \begin{bmatrix} \dot{\theta} \\ \theta \end{bmatrix} + R\tau_M^2(t) \right] dt \tag{14}$$

where R is the weighting factor to determine the relative importance between θ_M and τ_M. The control law for τ_M to minimize (14) is given by

$$\tau_M(t) = -K \begin{bmatrix} \dot{\theta} \\ \theta \end{bmatrix}, \text{ where } K = R^{-1}B^T P \tag{15}$$

In (15), P is the positive definite solution of the Riccati equation,

$$0 = A^T P + PA - PBR^{-1}B^T P + C^T C \tag{16}$$

where A, B, and C are as defined in (13). Since R is scalar, we have only one degree of freedom for designing the feedback controller. R should be sufficiently small to realize a high gain control law.

To analyze the performance of the closed loop system, the actuator model is reconfigured as shown in Fig. 14. It is assumed that the nominal plant P_n (i.e. P_2 in (12)) is subject to three undesired factors: the model variation Δ due to the interaction with a human, the unmodeled motor impedance Z_M (e.g. friction force), and the exogenous disturbance d. Since the resistive force due to the motor impedance is related to the velocity, a differential operator, s, appears in front of Z_M in Fig. 14. The perturbed system is expressed as

$$\tilde{P}(s) = \frac{P_\Delta(s)}{1 + sZ_M(s)P_\Delta(s)} \tag{17}$$

where

$$P_\Delta(s) = P_n(s)[1 + \Delta(s)] \tag{18}$$

Applying the feedback controller, $C(s)$, the perturbed closed loop control system in Fig. 11 is expressed as

$$E(s) = \left[\frac{\alpha(s)\tilde{P}(s)C(s)}{1 + \alpha(s)\tilde{P}(s)C(s)}\right] E_D(s) + \left[\frac{\alpha(s)\tilde{P}(s)}{1 + \alpha(s)\tilde{P}(s)C(s)}\right] d(s) \tag{19}$$

where $E_D(s)$ is the desired spring deflection. Note that the model variation is attenuated when control gains in $C(s)$ increases as long as the closed loop system remains asymptotically stable. As $|C(j\omega)| \to \infty$, $E(j\omega)$ is asymptotic to $E_D(j\omega)$ and is not influenced by $d(j\omega)$.

4.3 Robustness Enhancement

Since the PD control gains may be increased only in a limited range due to practical problems such as noise and instability caused by discretization, a better robust control method may be required to achieve the desired performance objectives. It is desirable to make the magnitude of the closed loop frequency response close to one over a sufficiently large frequency range.

The bandwidth of the human joint is about $4 \sim 8Hz$ [26] and the frequency response should be flat at least over this frequency range. Note that the closed loop transfer function significantly depends on $\alpha(s)$, which makes the dynamic transient vary significantly. In order to overcome this problem, the DOB (Disturbance Observer) may be introduced as shown in Fig. 15.

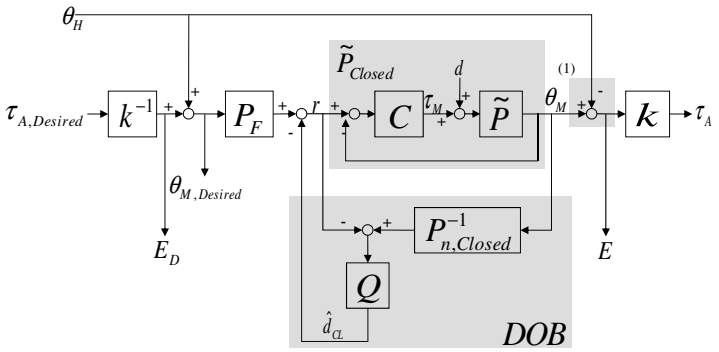

Fig. 15. Block diagram of the overall joint control system: The overall control method corresponds to Impedance Compensator in Fig. 1.

In general, the DOB may be used to:

1. estimate and cancel disturbance, and
2. compensate for the variation of plant dynamics by treating the variation as an equivalent disturbance.

In this application, the DOB is used more to the second objective although the disturbance cancellation is taking place also. For the basic properties of DOB, see [27].

It should be noted that the DOB is applied for the motor part only, i.e. the human joint angle is not fed into the DOB as shown in Fig. 15. Since the DOB is capable of rejecting exogenous disturbances, it increases the motor impedance significantly. Moreover, if E is fed back into the DOB, the human joint motion θ_H may be regarded as a disturbance [see (1) in Fig. 15] and rejected (or resisted) by the DOB. Since this is undesirable for human-robot interaction, the human joint angle should not be fed into the DOB.

The overall control scheme in Fig. 15 is as follows:

1. First, the desired spring deflection (E_D) is obtained from (3) on-line. Adding the human joint angle (θ_H) the desired position of the motor ($\theta_{M,Desired}$) is obtained as in (4). Note that if the desired torque is zero, then $\theta_{M,Desired}$ is the same as θ_H.
2. Second, the feedforward filter (P_F) is applied for compensation of the closed loop dynamics. P_F is designed based on the nominal closed loop model. In fact, the tracking performance of the motor is significantly improved by this feedforward filter.
3. Third, the PD controller (C in Fig. 15) is applied to attenuate the model variation. It allows increasing the bandwidth of DOB so that the performance of the overall system is improved significantly. The PD control gains are optimally obtained from (15) and (16) based on the nominal model in (12).
4. Finally, the DOB compensates for model variations resulted from human-robot interaction, and rejects undesired disturbances such as the friction

force. It makes the motor behave as the nominal model. Therefore, the feedforward filter (P_F) remains effective.

It is assumed that the closed loop transfer function, $\tilde{P}_{Closed}(s)$, in Fig. 15 is expressed as

$$\tilde{P}_{Closed}(s) = P_{n,Closed}(s)\,[1 + \Delta_{Closed}(s)] \tag{20}$$

where $P_{n,Closed}(s)$ is the nominal closed loop dynamics obtained from $P_2(s)$ in (12) under PD control, i.e.

$$P_{n,Closed}(s) = \frac{P_2(s)C(s)}{1 + P_2(s)C(s)} \tag{21}$$

and $\Delta_{Closed}(s)$ is

$$\Delta_{Closed}(s) = \frac{(1-\alpha(s))k}{I_M s^2 + C_M s + \alpha(s)k + C(s)} \tag{22}$$

Note that the closed loop transfer function in (21) is used as a nominal model in the design of DOB.

In the design of DOB, the selection of the filter labeled Q in Fig. 15 is important. The first requirement is that the order of $Q(s)$ must be such that $Q(s)P^{-1}_{2,Closed}(s)$ is realizable. The remaining two conditions ((23) and (24) below) make the closed loop system with DOB robust in terms of performance and stability. Namely, the DOB is effective at frequencies where

$$|Q(j\omega)| \approx 1 \tag{23}$$

The stability condition introduces another constraint, i.e.

$$|Q(j\omega)| < |\Delta_{Closed}(j\omega)|^{-1} \tag{24}$$

Notice that (23) and (24) require the magnitude of the model uncertainty to be less than one over a sufficiently large frequency range. Since the magnitude of the model uncertainty in (22) decreases as the PD control gains increase, the Q filter can be designed to have a sufficiently large bandwidth.

Even though the proposed controller stably controls the RSEA for every possible model in Fig. 9, a question arises that drastic changes of dynamic characteristics may introduce instability to the system. However, since phases of a human motion change smoothly and continuously [28] in normal conditions, the dynamic characteristics also change smoothly and continuously. When the dynamic model drastically changes (e.g., falling), however, stability may become a critical issue. In fact, simulations did not suggest such a stability problem even in the extreme cases.

The feedforward filter, P_F, may be determined by applying the pole-zero cancellation method, i.e.

$$P_F(s) = P^{-1}_{n,Closed}(s)P^*(s) \tag{25}$$

where $P_{n,Closed}(s)$ is as defined in (21). Since the inverse of the transfer function is usually unrealizable, $P^*(s)$ has been introduced to make the feedforward filter realizable. Also the magnitude of $P^*(j\omega)$ should be close to one over a sufficiently large frequency range. Note that the functions of $P^*(s)$ are the same as those of $Q(s)$ in DOB. For the simple design of the controllers, it is assumed that $P^*(s) = Q(s)$.

Arranging (18), (21), and (25) based on the control structure in Fig. 15, we obtain the transfer function of the motor part as follows

$$\begin{aligned}\theta_M(s) = &\frac{Q(s)a(s)}{a(s)Q(s) + b(s)[1 - Q(S)]}\left[\theta_H(s) + \frac{\tau_{A,Desired}}{k}\right] \\ &+ \frac{b(s)[1 - Q(s)]}{a(s)Q(s) + b(s)[1 - Q(s)]}\frac{\tilde{P}(s)}{1 + \tilde{P}(s)C(s)}d(s)\end{aligned} \tag{26}$$

where

$$a(s) = \frac{\tilde{P}(s)}{P_n(s)},\ b(s) = \frac{1 + \tilde{P}(s)C(s)}{1 + P_n(s)C(s)} \tag{27}$$

By applying (3) to (26), the transfer function of the overall system is obtained as follows

$$\begin{aligned}\tau_A(s) &= k\left[\theta_M(s) - \theta_H(s)\right] \\ &= Z_H(s)\theta_H(s) + Z_r(s)\tau_{A,Desired}(s) + Z_d(s)d(s)\end{aligned} \tag{28}$$

where

$$Z_H(s) = k\left[\frac{a(s)Q(s)}{a(s)Q(S) + b(s)[1 - Q(s)]} - 1\right] \tag{29}$$

$$Z_r(s) = \frac{a(s)Q(s)}{a(s)Q(s) + b(S)[1 - Q(s)]} \tag{30}$$

$$Z_d(s) = k\frac{b(s)[1 - Q(s)]}{a(s)Q(s) + b(S)[1 - Q(s)]}\frac{\tilde{P}(s)}{1 + \tilde{P}(s)C(s)} \tag{31}$$

$Z_H(s)$, $Z_\tau(s)$, and $Z_d(s)$ represent transfer functions to the torque output from the human joint angle $\theta_H(s)$, the desired output $\tau_{A,Desired}(s)$ and the exogenous disturbance input $d(s)$, respectively. According to the performance objectives, it is ideal to have $Z_H(s) = 0$, $Z_\tau(s) = 1$, and $Z_d(s) = 0$, which are not possible due to stability among other reasons. Note that when $Q(s)$ is close to one, (29),(30), and (31) are asymptotic to

$$Z_H(s) \approx 0,\ Z_r(s) \approx 1, Z_d(s) \approx 0 \tag{32}$$

$Z_H(s) \approx 0$ implies that the RSEA does not generate any resistive torque to the human joint motion, i.e. motor impedance is decreased. $Z_\tau(s) \approx 1$ represents that the actuator generates the torque as desired precisely. Finally, $Z_d(s) \approx 0$ means that the exogenous disturbance does not affect the torque output.

4.4 Reformulation into Force Feedback Loop

Since the spring plays a role of a torque sensor as well as an energy buffer, it may be reasonable to control the RSEA by feeding back the torque estimated from the spring deflection. The proposed control system in Fig. 15 also can be represented in the force feedback configuration. The control law in by Fig. 15 implies

$$\tau_M(s) = C(s)\left[\frac{P_{n,Closed}^{-1}(s)Q(s)}{k(1-Q(s))}(\tau_{A,Desired} - \tau_A) - \frac{\tau_A}{k} - \theta_H\right] \tag{33}$$

where $P_{n,Closed}(s)$, $Q(s)$, $C(s)$, θ_H are as defined above. τ_A and $\tau_{A,Desired}$ are the estimated and the desired torques, respectively.

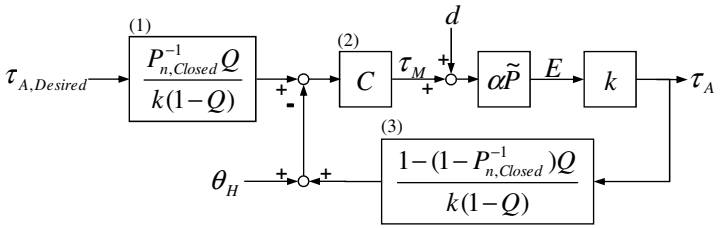

Fig. 16. Block diagram of the controllers in Fig. 15 reformulated into a simple feedback loop: k is a spring constant, and α and $\tilde{P}$ are as defined in (6) and (18), respectively.

Equation (33) is realized in a block diagram shown in Fig. 16. Noting (8) and Fig. 14, $\tau_A = k\alpha\tilde{P}(\tau_M + d)$, which means that the control system shown in Fig. 16 is equivalent to that in Fig. 15. Note that the new block diagram includes a feedforward filter ((1) in the figure) and feedback controllers ((2) and (3) in the figure). The generated torque τ_A is estimated by multiplying k to the spring deflection E. It also should be noted that the human joint angle, θ_H, is included in the feedback loop. This is not shown in the fundamental force feedback systems shown in Fig. 11. It acts as a feedforward signal such that the control system considers the human motion. The controllers in Fig. 16 do not include human factors (e.g., physical properties of body segments, etc.) and are designed based on the nominal model of the motor part. Therefore, the proposed control system can be applied to human-robot interaction applications for different people without measuring the properties of body segments.

5 Performance Analysis by Experiments

Once a RSEA is stabilized by applying the overall control system in Fig. 15, it is desired to verify the following performance objectives by experiments:

1. Capability of rejecting the undesired disturbances including the rotor inertia and any disturbances, i.e., the controlled RSEA should exhibit low impedance,
2. Capability of generating the desired torque precisely, and
3. Capability of generating the desired torque with a sufficient frequency bandwidth.

5.1 Experimental Setup

A RSEA shown in Fig. 5 was used to verify the proposed systems. For the design of the controllers, the nominal model of the motor should be obtained first, i.e. I_M and C_M are to be identified. Note that the spring constant, k, is known as shown in Table. 1. The motor used in the RSEA is an EC-powermax30 motor of Maxon Motor Company. The reduction ratio is 113:1 and the maximum power of the motor is $200W$. The system model obtained by sinusoidal excitations is

$$P(s) = \frac{4.463}{s^2 + 9.821s + 22.31} \tag{34}$$

The model in (34) includes a torque constant of the servo amplifier.

The PD controller, $C(s)$, was designed by the LQ method as discussed. R in (14) was set to 0.0001. $P_{n,Closed}(s)$ was obtained by (21) with the designed $C(s)$ and $P(s)$. The Q filter in DOB was a lowpass filter with the cut-off frequency of $20Hz$. Since the frequency range of the human motion is about $4 \sim 8Hz$, $20Hz$ is enough for the frequency bandwidth of actuation. Since $P_{n,Closed}(s)$, $C(s)$, $Q(s)$, and k are known, the control law in (33) is realizable.

5.2 Motor Impedance Test

As mentioned already, actuators for human-robot interaction should have low mechanical impedance. Otherwise, human has to make an additional effort to overcome the resistive forces. Fig. 17 shows the relation between the actual resistive torques and the angular velocities under the proposed control system when the desired torque output was zero. To exert the precise angular velocity to the RSEA from the load side, i.e. the human joint in case of assistive device applications, an additional motor, which has large mechanical impedance, was used. For comparison of the performance, the figure also shows the results under PD control (i.e. $C(s)$ without DOB) and open loop control. By applying the proposed control system, the measured torque was close to zero [see "Proposed Control" line in Fig. 17], which means no resistive torque is generated regardless of motion of the rotor. For more quantitative comparison, the curve fits were obtained (continuous lines in the figure) with the following fitting function,

$$f(\omega) = a_1 + a_2 \mathrm{sgn}(\omega) + a_3\omega \tag{35}$$

where a_1, a_2, and a_3 represent terms due to bias, nonlinear friction, and linear damping, respectively. For the desired performance, i.e. to have low motor

impedance, all parameters in (35) should be zero. Table. 3 shows the obtained parameters for each control method. Note that the magnitude of each parameter significantly decreases under the proposed control system. For example, the magnitudes of the bias, the friction, and the linear damping forces are decreased by 99.13%, 99.85%, and 99.79% from the open loop performance, respectively. Comparing with the PD control, they are reduced by 86.2%, 85.9%, and 98.18%, respectively. Note that the proposed controller effectively reduces the linear damping effects, which means the proposed one shows a good performance over the enough frequency bandwidth.

Table 3. Coefficients of motor impedance

Control Method	a_1 Bias[3)]	a_2 Friction[4)]	a_3 Linear Damping[5)]
No Control	-1.509×10^{0}	9.572×10^{-1}	1.414×10^{-1}
PD Control[1)]	-9.534×10^{-2}	1.040×10^{-1}	1.614×10^{-2}
Proposed Control[2)]	1.311×10^{-2}	1.464×10^{-3}	-2.941×10^{-4}

Each number shows the coefficient obtained by the curve fit based on (31).
[1,2)] See block diagrams in Fig. 11 and Fig. 15, respectively.
[3,4,5)] use the units of $[Nm]$, $[Nm]$ and $[Nm/(rad/s)]$, respectively.

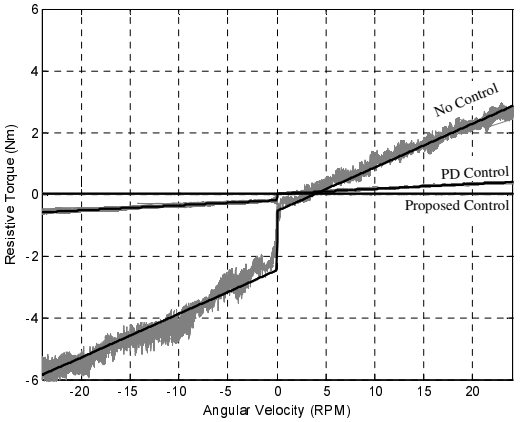

Fig. 17. Motor impedance test about angular velocity: the desired torque is zero

Fig. 18 shows the relation between the generated torques and the desired torques under the proposed control method when the angular velocity was fixed

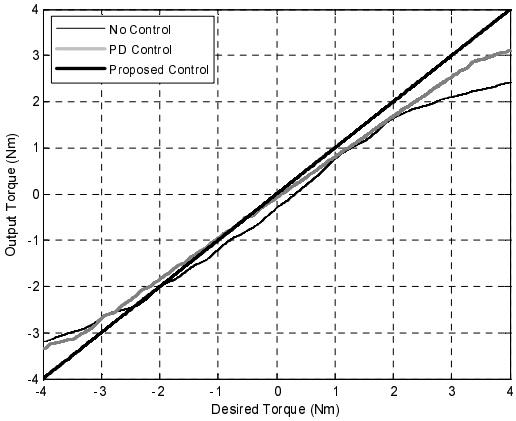

Fig. 18. Linearity test about control input: the angular velocity of rotor is fixed to zero

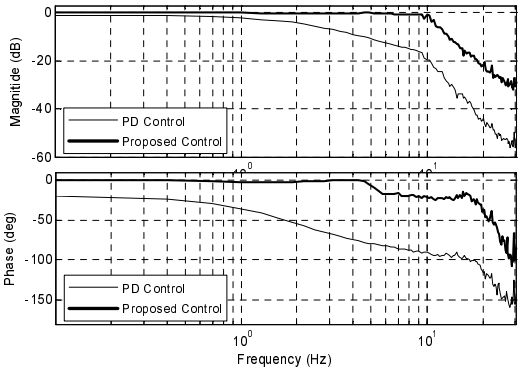

Fig. 19. Frequency response of each control scheme

to zero, i.e. the frame ((c) in Fig. 5) was fixed mechanically. This setup is as defined in *Case 2* in Fig. 9. Fig. 18 verifies that a RSEA controlled by the proposed control system generates torques as desired precisely. The output torque was estimated by multiplying the spring constant to the deflection. In the linear-region shown in Fig. 7, the torque estimation is reliable. Applying the proposed control system, the nonlinearities were compensated.

5.3 Frequency Response Analysis

It is also required that the RSEA generates the desired torque over a sufficiently large frequency range. Fig. 19 shows the frequency responses of the RSEA controlled by the proposed controller. The experimental setup for frequency response analysis was the same as in Fig. 17 except for a mass attached to the

load side of the RSEA. Otherwise, the output velocity of the RSEA easily saturates to the maximum, which implies that the inertia of the RSEA is eliminated effectively. This setup may correspond to *Case 1* in Fig. 9. It is known that the human motion contains frequency components up to $4 \sim 8Hz$ [26]. Note that the RSEA with the proposed control algorithm generates the desired torque properly up to about $10Hz$.

5.4 Verification by Human Walking Experiments

Experiments shown in Figs. 17, 18, and 19 verified the performances of RSEA without human factors. Therefore, they did not verify if the proposed control system robustly rejects the undesired disturbances and reduces the actuator impedance in the environments interacting with a human. To verify the robustness of the control system, RSEAs were installed at an active orthosis system as shown in Fig. 20. Two actuators were attached to each knee and ankle joint and controlled by the proposed control algorithm without change of parameters. The human factors of the knee and ankle joints (e.g. the inertia and the damping coefficient) are different so that the robustness may be verified if both actuators show the same performances.

Setting the desired torque to zero, a subject wearing the active orthosis was walking on a treadmill as shown in Fig. 20(b). It is desired that the subject does not feel any resistance from the actuators. Fig. 21 shows the ankle joint motion and the torque generated by the RSEA. As shown in Fig. 21(a), the motor followed the human joint motion to keep zero spring deflection. However, it was delayed by a few samples due to the phase delay of $P^*(s)$ in the feedforward filter

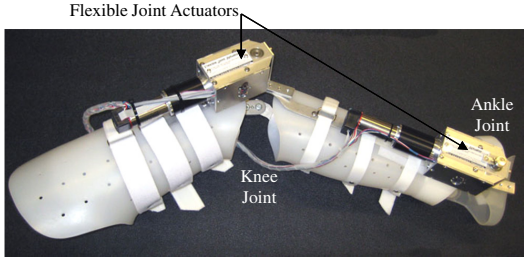

(a) Active orthosis system actuated by rotary series elastic actuators

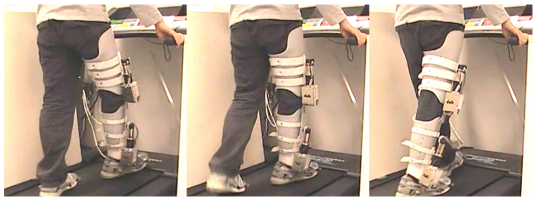

(b) Walking experiments

Fig. 20. Application of rotary series elastic actuator

[see (25)]. In this experiment, $P^*(s)$ was the same as the Q filter in DOB for the simple design of controllers. If the cut-off frequency of $P^*(s)$ is increased, the resistive torque shown in Fig. 21(b) is decreased significantly, but a human feels a high frequency vibration, which makes the human uncomfortable. Therefore, the filter should be selected considering the human comfort as well as the control performance. Even though the resistive torque was generated due to the time delay, the magnitude of the resistive torque was small ($4.25 \times 10^{-6} Nm$ in root-mean-square, $9.44 \times 10^{-2} Nm$ in peak-to-peak) so that the subject did not feel any resistance. The resistive torque was calculated from the spring deflection measured by encoders.

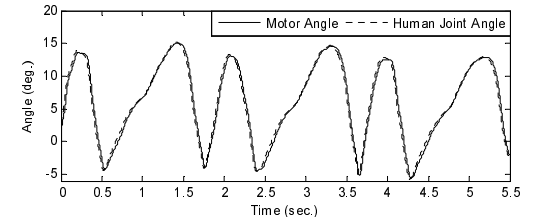

(a) Motor angle θ_M and human joint angle θ_H

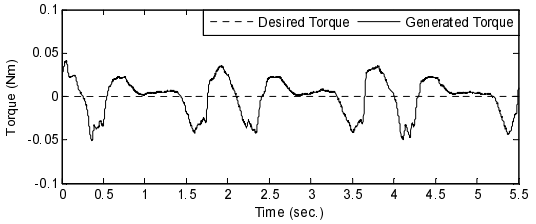

(b) Desired and generated torques

Fig. 21. Experimental data on ankle joint during walking: the desired assistive torque was zero

It is also desired that the RSEA installed at the knee joint shows the same performance without changing the control parameters. Fig. 22 shows data on the knee joint during the same experiment. Similarly, the motor followed the human joint motion with a time delay of a few samples as shown in Fig. 22(a). Since the maximum angular velocity of the knee joint was greater than that of the ankle joint, the resistive torque of the knee actuator was larger. Fig. 22(b) shows the resistive torque generated by the actuator. The resistive torque is large at high angular velocities (e.g. see about 0.9 seconds). The generated resistive torque was $3.33 \times 10^{-4} Nm$ in root-mean-square and $1.49 \times 10^{-1} Nm$ in peak-to-peak. Even though the magnitude of the resistive torque is slightly increased compared with the ankle joint, the RSEA showed the similar performance for a different joint without changing the control parameters. The increased resistive torque may be because of relatively higher angular velocity of knee joint motions while the control performance can be affected by the human motions (i.e. $Z_H(s)$ in

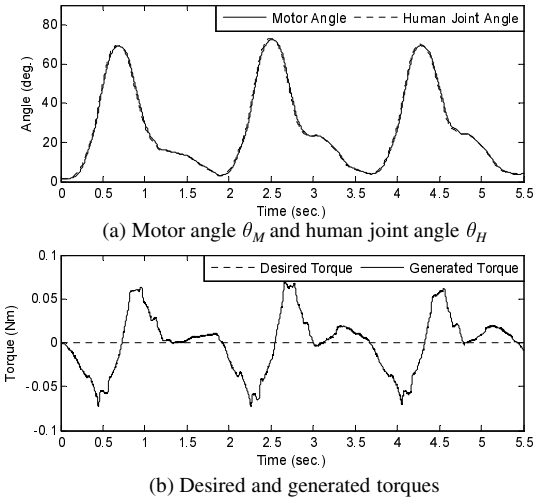

(a) Motor angle θ_M and human joint angle θ_H

(b) Desired and generated torques

Fig. 22. Experimental data on knee joint during walking: the desired assistive torque was zero

(29) is not zero in reality). However, it should be noted that the stability was not affected by the human motions or the different human factors. Therefore, the experiment in Fig. 22 verified that the proposed method can be applied to systems that physically interact with a human without considering the human factors.

An experiment in Fig. 23 was performed to check if the RESA with the proposed control algorithm generates the desired torque precisely. In the actual cases, the desired torque should be determined for particular purposes, e.g. rehabilitation or human power augmentation. Since this chapter focuses on how to control an actuator for the force mode actuation, the desired torque was simply set as a sinusoidal wave as shown in Fig. 23(b). For examples of the higher level control algorithms that determine the desired torque, see [3], [6], [9]-[11]. The subject was resisting the generated torque for the first 11 seconds and started the walking motion. Note that the human joint motion shown in Fig. 23(a) is slightly different for each stride because the human motion was affected by the generated torque. Fig. 23(a) also shows the motor angle as well as the knee joint angle. The motor followed the human joint motion with a certain offset such that the spring has a proper deflection. Since the motor angle was precisely controlled to have the desired spring deflection, the generated torque matched the desired torque, as shown in Fig. 23(b). The magnitude of the torque error shown in Fig. 23(c) was slightly increased when the human motion was active but the system was still stable and generated the desired torque successfully.

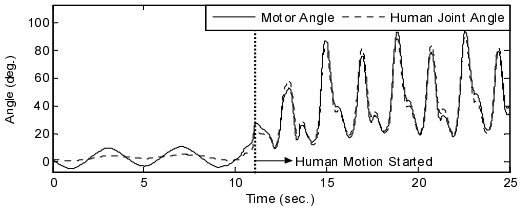

(a) Motor angle θ_M and human joint angle θ_H

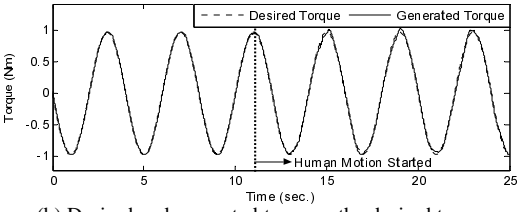

(b) Desired and generated torques: the desired torque was sinusoidal wave

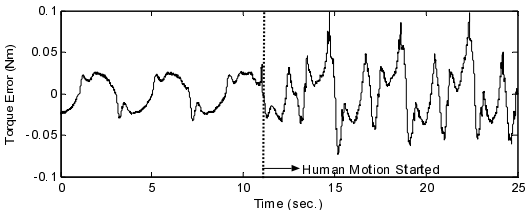

(c) Error between desired and generated torques

Fig. 23. Experimental data on knee joint when the desired torque varies

6 Conclusions

In applications involving human-robot interaction, actuators should have zero impedance for precise force control. In spite of numerous efforts, the actuator design is still one of the most evident problems in this field. In this chapter, a rotary series elastic actuator (RSEA) was designed and its control method was proposed for improved human-robot interaction.

In the RSEA, a torsional spring was installed between a human joint and a motor as the energy buffer. By controlling the motor part with a position control method, the torque was precisely generated via the spring deflection.

The use of spring introduced challenges to the design of controllers. In this chapter, the optimal PD control, the feedforward control, and the disturbance observer were applied to robustly control the RSEA under the environments interacting with a human. It was shown that the proposed control method meets the desired performances: the RSEA precisely generated the torque as desired, and its impedance has been decreased significantly. In this chapter, the performance was verified by experiments.

The RSEA and its control algorithm proposed in this chapter may provide a good solution for actuation methods in applications of human-robot interaction, in particular wearable robots. Since the control method does not require any physical properties of the human body, it is unnecessary to design the controllers for each individual. It allows precise force (or torque) mode control, and it provides the foundation to the design of higher level controls for human-robot interaction.

Series elastic actuators, including RSEA, provide both advantages and disadvantages for human assistive robots. The reduced mechanical impedance and improved torque precision make the robots able to assist people with light impairments including the elderly and patients with progressive muscular weakness. Most of the target users of the assistive robots are such people, and thus the series elastic actuators can contribute to realization of an effective assistive robot for a number of potential users. However, due to the use of additional mechanical peripherals, such as a spring, the power density, i.e., the power-to-weight ratio, becomes low. This is a clear disadvantage of the series elastic actuators for application to mobile systems. These factors should be considered in selection of an actuation system for assistive robots.

References

1. Hayashi, T., Kawamoto, H., Sankai, Y.: Control method of robot suit HAL working as operator's muscle using biological and dynamical information. In: Proc. IEEE/RSJ Int. Conf. Intell. Robots Syst.: IROS 2005, pp. 3063–3068 (2005)
2. HAL-5, Cyberdyne Co., `http://www.cyberdyne.jp`
3. Kazerooni, H., Racine, J., Huang, L., Steger, R.: On the control of the berkeley lower extremity exoskeleton (BLEEX). In: Proc. IEEE Int. Conf. Robotics Autom.: ICRA 2005, pp. 4353–4360 (2005)
4. Zoss, Kazerooni, H., Chu, A.: Biomechanical design of the berkeley lower extremity exoskeleton (BLEEX). IEEE/ASME Trans. Mechatronics 11(2), 128–138 (2006)
5. Yamamoto, K., Ishii, M., Noborisaka, H., Hyodo, K.: Stand alone wearable power assisting suit-sensing and control systems. In: Proc. IEEE Int. Workshop Robot Human Interactive Commun.: ROMAN 2004, pp. 661–666.
6. Kong, K., Jeon, D.: Design and control of an exoskeleton for the elderly and patients. IEEE/ASME Trans. Mechatronics 11(4), 428–432 (2006)
7. Kong, K., Jeon, D.: Fuzzy control of a new tendon-driven exoskeletal power assistive device. In: Proc. IEEE/ASME Int. Conf. Adv. Intell. Mech.: AIM 2005, pp. 146–151 (2005)
8. Banala, S.K., Agrawal, S.K., Fattah, A., Krishnamoorthy, V., Hsu, W., Scholz, J., Rudolph, K.: Gravity-balancing leg orthosis and its performance evaluation. IEEE Trans. Robotics 22(6), 1228–1239 (2006)
9. Riener, R., Lünenburger, L., Jezernik, S., Anderschitz, M., Colombo, G., Dietz, V.: Patient-cooperative strategies for robot-aided treadmill training: first experimental results. IEEE Trans. Neural Syst. Rehabil. Eng. 13(3), 380–394 (2005)
10. Hogan, N.: Impedance control: an approach to manipulation, parts I, II, III. J. Dyn. Syst., Meas. Control 107, 1–23 (1985)

11. Blaya, J., Herr, H.: Adaptive control of a variable-impedance ankle-foot orthosis to assist drop-foot gait. IEEE Trans. Rehabil. Eng. 12(1), 24–31 (2004)
12. Bar-Cohen, Y.: Electroactive Polymer (EAP) Actuators as Artificial Muscles - Reality, Potential and Challenges. SPIE Press (2004)
13. Noritsugu, T., Tanaka, T.: Application of rubber artificial muscle manipulator as a rehabilitation robot. IEEE/ASME Trans. Mechatronics 2(4), 259–267 (1997)
14. Buerger, S.P., Hogan, N.: Complementary stability and loop shaping for improved human-robot interaction. IEEE Trans. Robotics 23(2), 232–244 (2007)
15. Paluska, D., Herr, H.: Series elasticity and actuator power output. In: Proc. IEEE Int. Conf. Robotics Autom.: ICRA 2006, pp. 1830–1833 (2006)
16. Kong, K., Tomizuka, M.: Flexible joint actuator for patient's rehabilitation device. In: Proc. IEEE Int. Symp. Robot Human Interactive Commun.: ROMAN 2007, pp. 1179–1184 (2007)
17. Pratt, J., Krupp, B., Morse, C.: Series elastic actuators for high fidelity force control. Int. J. Ind. Robot 29(3), 234–241 (2002)
18. Low, K.H.: Initial experiments of a leg mechanism with a flexible geared joint and footpad. Adv. Robotics 19(4), 373–399 (2005)
19. Pratt, G.A., Williamson, M.W.: Series elastic actuators. In: Proc. IEEE/RSJ Int. Conf. Intell. Robotics Syst.: IROS, Pittsburgh, PA, pp. 399–406 (1995)
20. Robinson, D.W., Pratt, J.E., Paluska, D.J., Pratt, G.A.: Series elastic actuator development for a biomimetic walking robot. In: Proc. IEEE/ASME Int. Conf. Adv. Intell. Mech.: AIM 1999, Atlanta, GA, pp. 561–568 (1999)
21. Williamson, M.M.: Series Elastic Actuators. M.S. Thesis, Massachusetts Institute of Technology (June 1995)
22. Alter, D.M., Tsao, T.C.: Dynamic stiffness enhancement of direct linear motor feed drives for machining. In: Proc. American Cont. Conf.: ACC 1994, vol. 3, pp. 3303–3307 (1994)
23. Katsura, S., Matsumoto, Y., Ohnishi, K.: Analysis and experimental validation of force bandwidth for force control. IEEE Trans. Ind. Electronics 53(3), 922–928 (2006)
24. McKnight, E.: Control of Joint Forces: a New Perspective. Afcea International Press (1989)
25. Shigley, J., Mischke, C., Budynas, R.: Mechanical Engineering Design, ch. 10. McGraw-Hill (2004)
26. Winter, D.: Biomechanical Motor Control and Human Movement. Wiley-Interscience Publication (1990)
27. Lee, H., Tomizuka, M.: Robust motion controller design for high-accuracy positioning systems. IEEE Trans. Ind. Electronics 43(1), 48–55 (1996)
28. Kong, K., Tomizuka, M.: Smooth and continuous human gait phase detection based on foot pressure patterns. In: Proc. IEEE Int. Conf. Robotics Autom.: ICRA 2008, pp. 3678–3683 (2008)
29. Masia, L., Krebs, H., Cappa, P., Hogan, N.: Design and characterization of hand module for whole-arm rehabilitation following stroke. IEEE/ASME Trans. Mechatronics 12(4), 399–407 (2007)

On Ethical, Legal and Social Issues of Care Robots

Pericle Salvini

The BioRobotics Institute
Scuola Superiore Sant'Anna, Pisa, Italy
p.salvini@sssup.it

Abstract. According to recent figures, in the next years, Western developed societies will be supposed to face the "aging problem". The population aged 60 will surpass that of younger people and, to make things even worst, current trends in social relations indicate that family carers are no more willing to look after their older relatives. Such a situation has given more emphasis to the rise of robotics as a possible solution to deal with the demographic change and the new social norms in the care of elderly and disabled people. The ways in which robotics has been proposed to address the "aging problem" are manifold: ranging from humanoids, general purpose robots, to less invasive, distributed and task-specific systems. This chapter intends to provide the reader with an overview of the main ethical, legal and societal challenges concerning the use of care robots.

Keywords: Ethical issues, legal issues, social issues, care robots, robotics.

1 Introduction

"Assistive robots", "care robots" and "personal robots" are labels commonly used in the related literature to indicate different kinds of robots and different types of applications. In this chapter, I will use the expression "care robots" and will refer mainly to robots designed for the care of the elderly and disabled people (although I am aware that old age should not be considered as a form of disability). Care robots can be described as robots 'designed for use in home, hospital, or other settings to assist in, support, or provide care for the sick, disabled, young, elderly or otherwise vulnerable persons' [1]. Recently, the International Standard Organisation (ISO) released a definition of personal care robots as: 'robots that typically perform tasks to improve the quality of life of intended users, irrespective of age or capability, excluding medical applications' [2].

There are many arguments made by several stakeholders in support of designing and developing care robots. Among the most widespread motivations is the demographic shift, that is, the increase of the elderly population and the corresponding decrease of younger people. According to several statistics [3-4], the world population is growing older and therefore more people will need assistance during old age; however, the number of younger people will hold steady due to low fertility rates and therefore, in the next coming years, there will be a shortage of workforce, including care-givers [5]. The Global watch index points out that in Europe there are currently

S. Mohammed et al. (eds.), *Intelligent Assistive Robots*,
Springer Tracts in Advanced Robotics 106, DOI: 10.1007/978-3-319-12922-8_17

172.6m people over 60 and according to estimations there will be 233.1m in 2050, corresponding to 33.6% of the total regional population [3]. According to the World Health Organisation 'this population ageing can be seen as a success story for public health policies and for socioeconomic development, but it also challenges society to adapt, in order to maximize the health and functional capacity of older people as well as their social participation and security' [4]. Hence, many scholars claim that care robots can offer a valid solution to deal with the changes in demography and social norms.

Another of the main arguments used to support the development of care robots is the need to improve the quality of care. Such a need reflects a non ideal situation in the current practice of care. Improving the quality of care it means providing better working conditions for care-givers as well as better care for care-receivers. On the one hand, care robots could be a tool for empowering care-receivers. As a matter of fact, care robots could make elderly or disabled people more independent from the need to receive help from others by reducing physical or mental impairments and thus favouring aging at home.

On the other hand, robots could contribute to improve the quality of care. Indeed, the quality and quantity of assistance provided by care-givers is not always of the highest professional standards [6]. It is well know that in many countries live-in care-givers are migrant workers recruited from the black market [7]. The use of immigrants can be detrimental to the quality of care for the elderly, who are often unable to accept cultural differences and are attended by people lacking the professional skills needed. As rightly noted by scholars, this is a societal as well as humanitarian problem [8]. Moreover, it is well-know that the work of care-givers is hard, stressful (physically and psychologically demanding and with tight schedules), and economically unattractive (low rates and therefore a low social status). Robots could be designed to reduce the cognitive and physical stress of care-givers, which should result in better quality and quantity of human care.

Finally, last but not least, among the strongest motivations for introducing care robots is to reduce the cost of healthcare, even though, a great deal of the care provided comes from voluntary and non formal care-givers (i.e. family members or voluntaries). Moreover, the financial costs of care, in many countries, are mainly on the shoulders of families.

All these arguments could be considered as good motivations for introducing robots in care and assistance scenarios. In fact, they could potentially satisfy the needs and desires of many of the stakeholders involved in the field of care. However, the introduction of care robots cannot be considered as a neutral solution to fix the serious problem of care in the ageing society.

The goal of this chapter is to provide an overview of the main ethical and legal implications, positive as well as negative, emerging from the application of robots designed to care and assist elderly and disabled people. The overall goal is to increase the stakeholders' awareness on the ethical, legal and societal issues. The ambition is to turn such awareness into design requirements (e.g. "ELS specifications", equal to safety and usability standards), which, coupled with a careful design process, may contribute to develop better robots applications.

Indeed, the role of research in the fields of ethics, law and society should not be understood as a way to hinder scientific and technological developments, but rather as a way to steer advances in the "right direction" [9]. The right direction generally means responsible innovation and sustainable developments for human beings (including next generations) and for the natural environment [10].

2 Designing Care Robots

Drawing on Vallor's definition (quoted in section 1), it is possible to highlight three main aspects common to all robots, which should be taken into account in the design process: the kind of operative environment (e.g. private or public?), the typology of users (e.g. healthy or disabled? Youngster or adults?), and the nature of the task (e.g. lifting a person or handling a bottle?). In the specific case of care robots, there can be different kinds of potential users, namely the persons that may directly or indirectly benefit from the services carried out by the robot and those who directly or indirectly enter into contact with it. A first macro distinction applicable to care robots is that between care-receivers and care-givers (both formal and informal). To whom is the robot designed for? Such a question is determinant since there are clear differences in terms of needs and desires between care-receivers and care-givers. For instance, Jennifer A. Parks and colleagues point out that while a technology for lifting may be deemed desirable by care givers because it relieves them from hard-physical work, the same technology may appear unacceptable by elderly [11]. To make things even more complex, the vision of care-givers and that of care-receivers are often in contrast with that of the designers, that is, the engineers working on the robot. As reported in the study by Arjanna van der Plas and colleagues, the assumptions concerning the robot tasks of roboticists were in contrast with those of care-givers and care-receivers, who were against the idea that the robot could be a companion or a communication medium since they were afraid that such functionalities could create isolation and loss of human contact [12].

However, distinctions should be made also within each category of users. For instance, within the category of care-givers, there might be differences between formal and informal assistants. Likewise, within the category of care-receivers it is widely known that disabled people have different requirements with respect to the elderlies. Moreover, the physical and cognitive levels of the designated users are a matter of differences too. As pointed out by Jeson Borenstein and Yvette Pearson it is necessary to distinguish between different levels of age (e.g. infants, from adults) and capabilities of users (i.e. healthy or physical or cognitive impairments) [13]. Moreover, users may have different levels of expertise and different attitudes towards technology and to consider all these aspects during the design phase is important for improving the robot social acceptance and the degree of usability.

In particular, these issues can be determinant for the design of the interaction between the robot and the user. As pointed out by Tracy Mitzner and colleagues, one of the considerations to take into account in the design of a care robot is 'who would be interacting with it and in which roles' [14]. As a matter of fact, the difference between

the potential users of a care robot are many and they may have different levels of expertise or familiarity with technology (e.g. professional users such as nurses vs. non professional users, such elderly people for whom easier and simpler interfaces may be necessary) and roles (e.g. clinicians vs. relatives). Therefore, interaction modalities and interfaces should be designed by keeping in mind all possible users and all possible physical, cognitive and subjective differences among them.

As far as the operative environment is concerned, that is, the context – physical, structural and cultural – in which the technologies will be used, Mitzner and colleagues identify three main contexts for which a care robot can be developed: private homes, assisted living, skilled nursing [14]. As pointed out by the authors, 'the environmental differences between private homes and assisted living or skilled nursing facilities could have distinct implications for the design of robots. For example, long-term care residences tend to have wider open hallways than private homes, which allow for easier autonomous robotic navigation' [14]. To take into account the requirements of the environment is therefore crucial to solve not only technical difficulties, but to avoid ethical (e.g. tasks), social (e.g. robot appearance), economic (e.g. costs), and legal problems (e.g. privacy and liability).

Finally, with respect to the tasks, care robots are usually meant to carry out three main activities: daily tasks for assistance; monitor health and behaviour and companionship or entertainment [8]. However, it seems difficult to separate the activities carried out by robots in rigid categories. As a matter of fact, the ideal robot would be one that possesses multiple functions: for instance, to assist you in daily tasks and personal hygiene, but also to monitor your health and your safety, and, maybe, to entertain you and be of company. However, the choice of tasks should be the result of empirical evaluations of the users' requirements and needs.

As pointed out earlier, care can mean different things to different people, for instance, it depends on the users' perspective: the needs and desires of care-givers and care-receivers are different and may be different from those of the engineers designing and developing the robot. In the interviews made by [12], the differences between the needs and desires of care-givers and care-receivers are very well illustrated: dehydration, that is, the impossibility to raise and drink a cup of tea or water was pointed out by a care-giver, putting the shoes by a care-receiver, pushing beds in halls by a hospital nurse.

Therefore, an adequate design process should be the result of the interaction among designated users, context of use and tasks. In order to clearly identify the users, the operative environment and the tasks, it should be bore in mind that there exist differences among users, specific constraints for each type of environment as well as the fact that not all tasks can be automatized or performed by a robot. Furthermore, the operative environment, the user and the task, combined together, may be determinant for making other relevant design decisions, such as the definition of the shape or morphologies of the robot (e.g. humanoid or appliance-like?), its capabilities or functions (e.g. mobile or fixed?), and the level of autonomy (e.g. tele-operated or autonomous). Altogether, such considerations are fundamental in order maximize the robot performance, and, at the same time, minimize possible resistances deriving from ethical, legal and social implications.

3 Ethical and Societal Issues of Care Robots

The goal of this section is to provide the reader with an overview of the main arguments in favour and against care robots based on ethical, legal or societal issues. However, before entering into details, I believe necessary to address a few issues, which are preliminary to the phase of evaluations, namely the methods used in the identification and analysis of ethical and social issues.

3.1 Which Ethical Framework and Which Methods?

Which ethical framework should be used in the analysis of the ethical issues surrounding care robots? In other words, what are the values that should be taken into account when talking about care? And from which perspective: care-receivers, caregivers, parents, or the national health system? Moreover, which methods should be used to identify and analyse the ethical issues of care robots? Finally, is it possible to implement ethics into the design of a robot and which are the most appropriate legal instruments to regulate the design, development and use of robots?

These are among the main questions, still partly unanswered, concerning the so called areas of "roboethics" and "robolaw", that is, the theoretical and empirical research in the ethical, legal and social issues of robotics. These questions pertain to robotics in general, let alone care robots.

As far as the ethical framework is concerned, a few scholars propose to draw on the capability approach [13], [15]. The capability approach is based on the theories of philosophers Amartya Sen and Marta Nussbaum and its main principle is to promote and preserve human flourishing: 'Certain technological interventions expand people's opportunities by improving their ability to interface with their environment and helping them build or maintain relationships with others' [16]. According to the capability approach, therefore, care robots should be evaluated on the basis of their ability to promote human capabilities and its primary concern should be the care-receiver: 'if the use of robot caregivers is also efficient and convenient for professional and "informal" human caregivers, those are acceptable side effects, but having them as the sole or main impetus for using robot caregivers is likely to produce undesirable ethical and social outcomes' [16].

Another solution proposed by scholars to frame the ethical, legal and social debate is to draw on the principles contained in 'national and international charters and treaties concerning the promotion and protection of fundamental rights. These documents often include sections and articles specifically concerned with healthcare and medicine' [17]. For instance, article 35 of the European Union Charter of Fundamental Rights states that: 'Everyone has the right of access to preventive health care and the right to benefit from medical treatment under the conditions established by national laws and practices. A high level of human health protection shall be ensured in the definition and implementation of all Union policies and activities' [18].

In their analysis of the ethical issues related to socially assistive robots, David Feil-Seifer and Maja J Matarić propose an ethical framework based on medical ethics. In particular, they draw on Beauchamp and Childress's model based on four principles:

'beneficence – caregivers should act in the best interest of the patient; Non-maleficence – the doctrine, "first, do no harm," that caregivers should not harm a patient; autonomy – the capacity to make an informed, un-coerced decision about care; and justice - fair distribution of scarce health resources' [19].

However, as point out by Aimee van Wynsberghe, the attempts made by scholars to frame the ethical analysis fall short in their objectives. Indeed, it seems that the problem is not the ethical framework selected, but how it is applied to robots. In other words, it is necessary to combine and implement the ethical, legal, and societal frameworks with the common features characterizing each robot, that is, its designated users, its operative environment and the tasks, otherwise the risk is to remain at an abstract and theoretical level. Wynsberghe proposes a holistic and practical methodology for ethical identification, analysis and implementation. Indeed, according to her: 'A framework for the ethical evaluation of care robots requires recognition of the specific context of use, the unique needs of users, the tasks for which the robot will be used, as well as the technical capabilities of the robot. Above and beyond a retrospective evaluation of robots, however, what is needed is a framework to be used as a tool in the design process of future care robots to ensure the inclusion of ethics in this process. What's more, given the lack of standards provided by the International Organization for Standardization (ISO 2011), there exists an opportunity at this time to incorporate ethics into the actual design processes for these kinds of robots' [20].

As to the research method, there are neither standards nor validated procedures currently in use for identifying and analysing ethical, legal and social issues. For instance, scholars point out the need to distinguish between speculative ethics vs. pragmatic ethics, that is, factual from fictional problems. As point out by a few scholars, many studies about robotics and ethics are speculative since they deal with fictional issues, such as robot rights, robots taking over human beings, etc. [12], [21]. The risk is that theoretical discussion may overlook a number of ethical issues that emerge only in practical deployments. In contrast to speculative thinking, pragmatic or grounded ethics starts from what is technologically feasible and it is the result of users' involvement in discussions and interviews. According to Stina Nylander, grounded ethics should be complementary to theoretical speculations concerning ethics in care. As a matter of fact, it contributes to better focus on practical and scenarios oriented ethical issues: 'We believe that framing robots and robotic products in real-life use and real-life settings help developers, potential users, as well as researchers to create images of robots that balance the ones from fiction. This will shed important light on user needs, ethical issues, and design challenges within the field of robotics' [21].

In the method proposed by Arjanna van der Peas and colleagues, called "Visions Assessment" (VA), they propose to bring together the vision of the experts, i.e. roboticists, and the vision of the designated users, i.e. elderly. The authors point out that in their method 'the technological knowledge of the robot experts and the contextual knowledge of the designated users is married in a design, which is able to solve actual needs and seems technically feasible as well' [12]. The approach proposed by Van der Peas and colleagues is not exclusively aimed at the identification of ethical issues, but it is meant to co-construct moral vision and guidelines in the process of designing a

robot. In this method, the ethical analysis is not kept apart from the design of technology and vice versa.

However, among the main obstacles to ethical analysis one should mention also the methodological difficulties in assessing the safety of the robot with respect to the so called "soft" threats. With respect to "hard threats", which are related to the physical damages and can be easily quantified via empirical studies, "soft threats", which derive from prolonged interactions with care robots and affect the user's cognitive and emotional levels, are more difficult to be evaluated. For instance, it will be very difficult to study and assess the effects of "nursery robots" on babies.

Finally, and to sum up, there are many proposals, but not unanimous agreement among the experts concerning frameworks and methods for ELS analysis. It seems that the ethical discourse of robotics is still stuck in a "brainstorming phase", which has started more than a decade ago and is characterised by many attempts to identify and analyse ethical issues, but it is still far away from delivering sound scientific results. In addition, as to the "normative phase", which should naturally follow the ethical and societal analyses, there is still research to do on how to implement ethics into binding requirements for improving the design process and regulate the deployment of robots. Which are the legal instruments that can best translate ethical and societal "specifications" into binding requirements for robot designers and developers?

In the next subsections, a non exhaustive overview of the main ethical, legal and social issues voiced by scholars, researchers and experts in care, ethics and robotics is provided.

3.2 Positive Ethical and Social Aspects of Care Robots

In general, it is argued that care robots can contribute to improve dignity via empowerment of people in need, such as elderly and disabled. As a matter of fact, by providing physical or cognitive support, robots can improve people's autonomy and relieve them from dependence on the help of others, such as toileting or bathing, which may be caused of embarrassment or distress. According to Borenstein and Pearson, care-receivers are liberated from 'the frustration, awkwardness, and sense of dependence associated with requesting assistance from other persons' [13]. Moreover, according to the empirical study carried out by Nylander and colleagues on the effects of an eating-assistance device, robotic technologies can have positive effects not just on independence and autonomy but also on privacy and identity. The authors report on the story of Carl, a disabled person who, for a period of time accepted to use Bestic, an eat-aid device. The authors point out that thanks to Bestic 'Carl can have a meal with his wife without having an assistant present and not have his wife feed him. Bestic allows them both to have a social experience since they both feed themselves and no one has to help the other. They can talk to each other without having Carl's assistant listening and they do not have to include the assistant in the social conversation' [21]. According to the authors the device 'will not replace Carl's assistant, or create a situation where he never needs help from his wife, but it creates a more private and independent eating situation. Finally, by favouring autonomy and independence, robotic assistive devices may delay the move to skilled nursing home and, on

the contrary, favour aging in place, with great financial benefits for families or the healthcare system as well as psychological benefits for care-receivers. As pointed out by Mitzner and colleagues, move to higher level of care may be detrimental to the health and quality of life of elderly people. As a matter of fact, studies suggest that the development of depression and suicide in older adults is correlated to move from home to assisted living or other facilities [14].

From the standpoint of care-givers, the introduction of care robots can improve the quality of their job by alleviating the burden of care, that is, making less tight their schedules and reducing the physical effort needed in many activities, such as in toileting or bathing. Moreover, it is believed that in providing care-givers with more time and less physical stress, robot could favour human physical contact and communication with care-receivers.

Finally, for parents as well as physicians, care robots could be a way to have immediate access, via the robot cameras, to what a person is doing (care-receiver or care-giver). Monitoring their relatives, patients and the people looking after them as well as having a means to directly interact with the person in need (via audio and video implemented in a mobile base) can also contribute to parents' peace of mind and improve the effectiveness of therapies. Sharkey and Sharkey believe that robots could be used to monitor care givers to ensure they do not violate the rights of care receivers and thus be a way to improve the standard of care [8].

3.3 Negative Ethical and Social Aspects of Care Robots

One of the main perceived problems with respect to care robots is that they will lead to a deterioration of care. Such an opposing attitude is confirmed by the survey on robotics requested by the Directorate-General for Information Society and Media (INSFO) of the European Commission. The results show that only 4% of EU citizens believe that robots should be used in activities concerning the care of children, elderly or disabled. Moreover, 60% of interviewed consider care robots should be banned [22].

Among the main arguments against care robots pointed out in the literature by almost all stakeholders, including roboticists, is the problem of social isolation and loss of human contact. Indeed, social isolation is often already a problem for elderly and disabled people, independently from the environment or context in which they live. The most widespread feeling is that the use of robots may make the problem worse.

It is possible to identify two main fears supporting such a widespread feeling: 1) robots will replace human carers (completely or partially) and this will eliminate or reduce the time spent with human beings, and 2) robots will offer more possibilities for remote presence at the expense of in-presence situations, such as visits paid by relatives and friends [8], [23]. Concerning fear no. 1, it seems that nobody is interested in building robots that will replace human care givers anymore, not even roboticsts. In the Europ Strategic Research Agenda, it argued that: 'Particular care must be taken with the elderly and children. Robots should support, but not replace, human carers or teachers and should not imitate human form or behaviour. Further ethical issues can be derived from the European Charter of Fundamental Rights.' [24].

The fear to loose human contact and socialisation is usually targeted towards humanoid, general purpose robots, since they can, if ever realized, replace a human being in the accomplishment of many complex tasks. However, also robots designed for specific tasks (trivial or intimate activities) may raise the same concerns. As a matter of fact, care-givers and experts point out that the tasks that are most embarrassing, such as toileting or personal hygiene, or non social tasks, such as vacuum cleaning the floor, are often offering the occasion to be with another person and trigger social interactions [25], [16]. Moreover, scholars have argued that it is very unlikely that with the automation of some care tasks the number of human beings employed in care activities will remain the same. As pointed out by Jennifer Parks: 'The likely consequence of a technology boom in aged care is that the number of human caretakers will be seriously reduced; the net result will be a further reduction in the amount of human contact to which our elderly citizens will have access' [11]. Therefore, if on the one hand (general purpose or specific tasks) robots may contribute to improve dignity, autonomy, independence and privacy, on the other hand, it seems likely that they may reduce social interactions and human contact.

Deception is another widespread ethical issue identified by scholars. It concerns in particular the robots that show a high level of similarity with human beings or animal behaviour and/or morphologies. Some of these robots are currently used in therapeutic applications with patients affected by autism or senile dementia, such as the seal robot Paro [26]. According to Robert Sparrow, the therapeutic effect depends upon "deception". In other words, the working of these robots is based on the pretence that the robot can interact and behave like a human person or a real animal (i.e. having feelings and inners states): 'for an individual to benefit significantly from ownership of a robot pet they must systematically delude themselves regarding the real nature of their relation with the animal. It requires sentimentality of a morally deplorable sort. Indulging in such sentimentality violates a (weak) duty that we have to ourselves to apprehend the world accurately' [25]. Is this pretence problematic in itself, even if none wishes to deceive anybody? According to Jeason Borenstein and Yvette Pearson 'as long as there is no intention to deliberately deceive or neglect dementia patients through the use of a robot, the fact that some patients may form erroneous beliefs about a robot caregiver – a process over which other agents may have little control – does not necessarily amount to being disrespectful to a care recipients' [13].

For some people, the idea of having a robot with which they can interact at different levels, physical, cognitive as well as emotional, may be very appealing. Indeed, as pointed out by Byron Reeves and Clifford Nass, human beings, including healthy subjects, tend to behave socially with technological artefacts, such as computers and robots [27]. However, even if we were perfectly aware that the robot is not a 'real living entity', and therefore neither "authenticity" nor "deception" were a problem anymore, there could be another risk to take into account. Psychologist Sherry Turkle points out that interacting with "nurturing machines" – as she calls them – that is objects that simulate the mutual relations occurring among living beings can be a matter of concerns since 'a robot that demands attention by playing off of our natural responses may cause a subconscious engagement that is less voluntary' with respect to traditional liminal objects (e.g. a doll or teddy bear) [28]. Indeed, according to Turkle,

with "nurturing machines" – as she calls them – we are no more in control of our engagement and therefore are less free to step back from it.

Another critical issue pointed out by a few scholars is that care robots could imply a loss of freedom for care-receivers. A reduction of freedom could occur especially with robots designed to suggest or even impose a specific behaviour on people for their own benefit. For instance, if a robot is meant to monitor the activities of a person affected by dementia during the day there might be occasions in which the robot will have to necessarily limit (as much as possible) the will or freedom of the person for preserving that person's health. However, there might be occasions in which the restriction is not grounded on a real danger and, as pointed out by Sharkey and Sharkey 'restraining a person to avoid harm could be a slippery slope towards authoritarian robotics' [8]. Moreover, although up to now monitoring and assistance are related to the robot verbal, rather than physical, capabilities, it is likely that with further progress in physical interaction, robots with more effective coercive measures could be designed.

Finally, scholars point out that dependence and lack of competencies can be consequences of robots that provide too much help or assistance. As pointed out by Oppenaur-Meerskraut 'it could be that robots remove the need to do things that older people can still do and thus accelerate the process of forgiveness and therefore create a situation of dependence on the technology and a lack of skill…' [23]. Due to the lack of training a person may unlearn how to do things and therefore increase the dependence from other people and technology.

4 Legal Challenges for Care Robots

With respect to the ethical and social analysis, the study of the legal implications of robotics has a younger history. The growing attention to legal issues of the last decade is probably a result of the more realistic possibilities to turn robots from research prototypes into commercial products. The main motivation for developing a legal framework for robots is twofold: on the one hand to pave the way to the development of a market for robotic products and on the other to protect users from the consequences of new accidents.

Among the questions currently debated by scholars and experts in law is whether the current legal framework will be adequate to address the issues emerging from the deployment of robotic products and services. As a matter of fact, it is still a matter of concern whether robots, at least in its current state of development, will bring about new problems and therefore produce "legal gaps" in the current legal frameworks. Moreover, if new laws were to be designed, another relevant issue would be to determine the most appropriate legal tool (i.e. soft or hard laws?) for regulating the new robotic applications.

In what follows, I will present a non exhaustive list of general legal issues concerning robotics, which could be relevant for care robots too. As we shall see, most of the legal implications of robots are determined by what robots can do and by what they are [29].

Many of the care robots currently tested or used in private homes or public institutions are endowed with cameras and other recording devices to monitor the user and store different kinds of data, besides physiological parameters, such as user's preferences, habits, and wishes. With such capabilities a robot may offer very useful functionalities to care-givers, care-receivers and relatives. For instance, it could issue warning messages to prevent a fall, suggestions for cocking, reminders, or telepresence services. However, such capabilities may also cause a privacy problem, as illustrated by Sharkey and Sharkey: 'An elderly person might not like to find that an operator could remote control a robot to peer round their apartment before they are dressed, or when they are taking a bath. They might prefer the robot to have to do the equivalent of knocking on the door and waiting to be invited in. The issue becomes more complex if an elderly person's mental state deteriorates further and they become confused. A person with Alzheimer's would probably forget that the robot was monitoring them, and could perform acts or say things thinking that they are in the privacy of their own home' [8]. As a possible solution the Sharkeys propose that the robot should make its presence always detectable and before entering a room should ask permission and provide clear indications when recording or monitoring [8]. According to Feil-Seifer and Mataric, a further solution could be to distinguish between confidential and non confidential information. However, the authors wonder whether a robot could ever be capable of making such a distinction [19].

Monitoring and recording capabilities may also generate a breach in data protection. As a matter of fact, it is legitimate to wonder how safe will be and who will have the right to access and handle the files containing images and sounds recordings taken from the robot, which may be very appealing to the market [29].

Who is going to be responsible for the damages caused by an autonomous robot? This is one of the most recurring questions in discussions of robots and law by experts and non experts. However, the answer seems to be quite simple. As pointed out by Lehman-Wilzig, 'as long as robots continue to be merely sophisticated automata, many injuries stemming from their actions would fall into the broad category of product liability' [30]. A different scenario would emerge if robots could be considered as if human agents. As to current issues concerning liability, scholars point out that in case of damages caused by an autonomous robot it might be more difficult to identify a responsible due to the increased complexity of the causal chain [30]. As a matter of fact, to turn a robot into a market product involves many actors: manufacturer, importers, wholesalers, retailers, repairers, installers, inspectors, and the users. Moreover, as pointed out by Lehman-Wilzig, the manufacturer has now doubled into the hardware and the software manufacturers. Therefore, it could be more difficult to attribute or share the responsibility for a defect or a fault and in many cases there might be 'no one at fault!' [30]. The issue of the indeterminacy of liability is related to robot autonomy, but also to share control robot: who is responsible for a damage caused by an elderly person while using (i.e. controlling) a robot? According to Sharkey and Sharkey, in case of a care robot, the level of control should be related the user's state of mind [8].

If one day autonomous robots will enter into basic, economic transactions, by performing legal acts, and even being accountable for the damages caused to their users and to third parties, they should be granted the status of legal subjects. As point out by Elettra Stradella and colleagues, endowing robots with legal capacity it is not a matter of ontology, that is, granting robots the status of "sentient beings", but it could be a way to solve practical problems. As a matter of fact, to enter into a contract could allow a robot, for instance, to purchase goods, such as food, drugs, newspapers, etc. Therefore, turning a robot into a legal subject could be a way to solve the problem of having a centre of imputation for the effects deriving from the agreement and avoiding the contract to be considered void [31].

Some law scholars have proposed to create a new legal category for this kind of robots, i.e. "e-person" (electronic persons), by analogy with that category of "legal subjects", in use for corporations, foundations, and companies, which have legal rights and duties even though they are not physical persons [32]. However, it seems that legal scholars agree that without assets to compensate for the damages caused by a robot, to hold them liable will not make sense. Indeed, the supplier would not get paid and the victims could not recover damages. Therefore, a few scholars propose to entrust robots, previously entered in a public register, with a certain financial basis, according to the area of application, hazard, and degree of autonomy [32].

Finally, the legal status or classification of autonomous robots deserves some consideration. As illustrated by the numerous experiments with autonomous robots operating on public roads (e.g. Google car), in the sea or in the air, there is currently no category for classifying self-driving cars, AUV (Autonomous Underwater Vehicles) or drones according to existing laws. Special permissions [33] and, in some cases, modifications of the law [34] have been necessary to allow autonomous robots to be deployed on public roads [33], [34], in the air [34] or water [35]. Given their flexible nature, there might be cases of robots operating in mixed environments, that is, private and public areas [37] or ground, air and water and this may complicate things from the legal perspective.

5 Conclusions

According to Joan Tronto care should be distinguished into care *for* and care *about* [38]. To *care for* somebody means to provide help or try to alleviate the physical and cognitive impairment of people, while to *care about* somebody means to provide a person with love, attention and social exchanges. This distinction is important because it points out that hidden in the generic term "care" there are very important meanings, which are determinant both for robots and human beings. Care does not mean only physically assisting someone, but also establishing a human relation with another human being. Such a distinction is useful since it helps to better understand what care really means and also to evaluate the potential role of robots in practices of care.

As a matter of fact, as one of the most advanced technologies, robotics can contribute to care and assist people in need. The question is: how? Among the solutions proposed it is possible to distinguish two main trends: on the one hand general

purpose, mobile robots, such as a humanoids, theoretically capable of replacing human beings at almost all levels, from physical to emotional interaction; on the other, there are distributed robotic devices, which perform specific tasks, such as automated wheel-chairs. At least in the next decades, robotics does not seem capable of *caring about* human beings and, perhaps, it should be better not to use it in such a way. The widespread fear that care robot may determine a loss of human contact and socialisation is a significant warning in this respect.

On the contrary, robotics could be a solution for many tasks belonging to the practice of *caring for*. Among the benefits that could derive from the introduction of robots in the care of elderly and disabled, there is the improvement of the quality of care both for care-receivers (e.g. independence, autonomy, dignity, privacy, etc.) and care-givers (reduction of physical and cognitive burden).

However, *care for* and *care about* should never be separated in care practices. Therefore, care robots should be understood as a tool in the hands of care-receivers and care-givers and not as a replacement of the latter or a companion for the former.

Nevertheless, the de-humanisation of care and the objectification of care-receivers are not just problems brought about by robots, but they can emerge also when care is provided by other human beings. The need to improve the quality of care, both of care-givers and care-receivers, also in view of the incumbent demographic shift, is of paramount importance, but the solution cannot be only one and that one cannot be only robots. The hype always surrounding new technologies such as care robots may conceal the drawbacks and make people think that technology can solve all the problems; in so doing we tend to forget that there might be alternative solutions based on human beings. In the specific case of care, an alternative solution could be to make the job more appealing by proposing better working conditions, such as better economic remuneration, improved professional quality of care-givers and by granting equal rights and duties to immigrant workers. Robotics alone cannot be the solution for all the problems affecting care: from the demographic shift, the low quality of care, to the demanding working conditions of care givers and the high-costs of care. A combined solution is needed, brining together robotics technologies and human beings.

References

1. Vallor, S.: Carebots and Caregivers: Sustaining the Ethical Ideal of Care in the Twenty-First Century. Philosophy & Technology 24(3), 251–268 (2011)
2. ISO 13482 (2014)
3. Global watch index 2013 by ONU and Help age international (2013), http://www.helpage.org/global-agewatch/ (accessed December 10, 2013)
4. WHO 2013 World Health Organisation, http://www.who.int/topics/ageing/en (accessed December 10, 2013)
5. Graham, J.: A shortage of caregivers. The New York Times (February 26, 2014)
6. Beckford, M.: Elderly suffer poor care in half of NHS hospitals. The Telegraph (October 2011)

7. Atanackovic, J., Bourgeault, I.L.: Economic and Social integration of immigrant live-in.caregivers in Canada, IRPP Study, No 46 (April 2014)
8. Sharkey, A., Sharkey, N.: Granny and the robots: Ethical issues in robot care for the elderly. Ethics and Information Technology 14, 27–40 (2012)
9. Verruggio, G.: The birth of roboethics. In: IEEE International Conference on Robotics and Automation Workshop on Robo-Ethics, ICRA 2005, Barcelona, Spain, April 18 (2005)
10. Von Schomberg, R.: A vision of responsible innovation. In: Owen, R., Heintz, M., Bessant, J. (eds.) Responsible Innovation. John Wiley, London (2013) (forthcoming)
11. Parks, J.A.: Lifting the Burden of Women's Care Work: Should Robots Replace the "Human Touch"? Hypatia 25(1), 100–120 (2010)
12. van der Plas, A., Smitsb, M., Wehrmannc, C.: Beyond Speculative Robot Ethics: A Vision Assessment Study on the Future of the Robotic Caretaker. Accountability in Research: Policies and Quality Assurance 17(6) (2010)
13. Borenstein, J., Pearson, Y.: Robot caregivers: harbingers of expanded freedom for all? Ethics and Information Technology archive 12(3), 277–288 (2010)
14. Mitzner, T.L., Chen, T.L., Kemp, C.C., Rogers, W.A.: Identifying the Potential for Robotics to Assist Older Adults in Different Living Environments. International Journal of Social Robotics (November 2013)
15. Coeckelbergh, M.: Human development or human enhancement? A methodological reflection on capabilities and the evaluation of information technologies. Ethics of Information Technologies 13, 81–92 (2011)
16. Borenstein, J., Pearson, Y.: Robot Caregivers: Ethical Issues across the Human Lifespan. In: Lin, P., Abney, K., Bekey, G.A. (eds.) Robot Ethics. MIT Press (2012)
17. Datteri, E., Tamburrini, G.: Ethical Reflections on Health Care Robotics. In: Ethics and Robotics. IOS Pres (2009)
18. Charter of Fundamental Rights of The European Union (2000/C 364/01)
19. Feil-Seifer, D.J., Matarić, M.J.: Ethical Principles for Socially Assistive Robotics. IEEE Robotics & Automation Magazine 18(1), 24–31 (2011); Special issue on Roboethics, Veruggio, J.S., Van der loos, M.
20. van Wynsberghe, A.: Designing Robots for Care: Care Centered Value-Sensitive Design. Sci. Eng. Ethics 19, 407–433 (2013)
21. Nylander, S., Ljungblad, S., Jiménez Villarreal, J.: A complementing approach for identifying ethical issues in care robotics - grounding ethics in practical use. In: RO-MAN 2012, pp. 797–802 (2012)
22. Special Eurobarometer 382. Public Attitudes Towards Robots Report. Fieldwork: February - March 2012 Publication (September 2012)
23. Oppenauer-Meerskraut, C.: Would a Virtual Butler Do a Good Job for Old People? Psychological Considerations about Benefits and Risks of Technological Assistance. In: Trappl, R. (ed.) Your Virtual Butler. LNCS, vol. 7407, pp. 11–15. Springer, Heidelberg (2013)
24. EUROP (European Robotics Technology Platform). Robotic Visions. To 2020 and Beyond, The Strategic Research Agenda for Robotics in Europe (July 2009)
25. Sparrow, R.: The March of the Robot Dogs. Journal Ethics and Information Technology Archive 4(4) (2002)
26. Shibata, T., Kawaguchi, Y., Wada, K.: Investigation on People Living with Paro at Home. Effects of Sex Difference and Owners' Animal Preference. In: The 18th IEEE International Symposium on Robot and Human Interactive Communication, Toyama, Japan, September 27-October 2 (2009)

27. Reeves, B., Nass, C.: The Media Equation: How People Treat Computers, Television, and New Media Like Real People and Places (Center for the Study of Language and Information Publication Lecture Notes) (2003)
28. Turkle, S.: Authenticity in the age of digital companions. Interaction Studies. Social Behaviour and Communication in Biological and Artificial Systems 8(3) (2007)
29. Sanfeliu, A., Punsola, A., Yoshimura, Y., Llácer, M.D., Gramunt, M.R.: Legal Challenges for Networking Robots Deployment in European Urban Areas: The Privacy Issue. In: Workshop on Network Robots Systems, IEEE International Conference on Robotics and Automation (ICRA 2009), Kobe (Japan), May 12 (2009)
30. Lehman-Wilzig, S.N.: Frankenstein Unbound: Toward a Legal Definition of Artificial Intelligence. Futures: The Journal of Forecasting and Planning 13 (1981)
31. Stradella, E., Salvini, P., Pirni, A., Di Carlo, A., Oddo, C.M., Dario, P., Palmerini, E.: Robot Companions as Case-Scenario for Assessing the "Subjectivity" of Autonomous Agents. Some Philosophical and Legal Remarks. In: 1st Workshop on Rights and Duties of Autonomous Agents (RDA2) ECAI, The Biennial European Conference in Artificial Intelligence, Montpellier, France, August 28 (2012)
32. Beck, S.: Legal Liability of Machines. In: Flagship RoboCom - Rise of Sentient Machines? Robot, 2012 Companions for Citizens, May 22. Diaconis Tagungszentrum Blumenberg, Bern (2012)
33. Salvini, P., Teti, G., Spadoni, E., Frediani, E., Boccalatte, S., Nocco, L., Mazzolai, B., Laschi, C., Comandé, G., Rossi, E., Carrozza, P., Dario, P.: An investigation on legal implications of service robots deployment in urban areas. Advanced Robotics 24(13) (October 2012)
34. Markoff, J.: Google cars drive themselves, in traffic. The New York Times (2010)
35. Showalter, S.: The Legal Status of Autonomous Underwater Vehicles. The Marine Technology Society Journal Spring 38(1) (2004)
36. Leroux, C., Labruto, R. (eds.): Proposals for a Green Book on the Legal Regulation of the Production and Application of Robots, Draft version 2.0 – January 5th 2012, euRobotics (FP7-ICT-2009-4, Grant Agreement Number 248552) (2012)
37. Robot-Era, European Funded project FP72007-201, GA 288899, http://www.robot-era.eu/robotera/
38. Tronto, J.: Moral boundaries: A political argument for an ethic of care. Routledge, New York (1993)

Author Index